

Preface

This publication is the result of the fourth TRACE (**T**ree **R**ings in **A**rchaeology, **C**limatology and **E**cology) conference held between April 21st and 23rd 2005 in Fribourg, Switzerland. The meeting was hosted by the Department of Geosciences, Unit Geography, University of Fribourg. TRACE seeks to strengthen the network and scientific exchange of scientists and students involved in the study of tree rings. About 100 scientists from 25 countries attended the meeting. The authors of talks and posters took the chance to display a wide range of topics in form of 32 oral presentations and 30 posters, covering the topics (1) Climatology - Southern Hemisphere, (2) Climatology - Northern Hemisphere, (3) Ecology, (4) Geomorphology, (5) Archaeology, (6) Isotopes, and (7) New Applications. The contributions clearly documented the progress that has been accomplished in recent years. Some of the studies originated from extra-European parts of the World such as Iran or Australia and enriched the contents of the conference which is usually centred on European topics. This current volume contains 36 extended abstracts based on the conference presentations.

The invited speaker Erica Hendy, a Comer Abrupt Climate Change Post Doctoral Research Fellow at the Lamont-Doherty Earth Observatory (USA), came from a related field outside the dendrochronology community. She spoke about her work on corals from the Great Barrier Reef used for palaeoclimatology. It was very interesting to learn that she was the first to apply our dendrochronology methods to corals, hence the title of her talk "Dendroclimatology underwater: Australian coral records from 1565AD" (first contribution in this volume, page 8-15) was very appropriate.

We want to thank all participants of TRACE 2005 for the rewarding discussions and for contributing to this volume. We wish to acknowledge the assistance of Kathryn Allen, Martin Bridge, David Frank, Karl-Uwe Heussner, Hans-Peter Kahle, Klaus-Felix Kaiser, David Rose, Constantin Sander, Matthias Saurer, Uwe Treter, Kerstin Treydte, and Vanessa Winchester for their help with the review of the manuscripts. In addition, we would like to say thank you to our sponsors Credit Suisse, Regent Instruments, Interprofession du Gruyère, Kantonale Gebäudeversicherung Fribourg and Banque Raiffeisen de Marly.

Ingo Heinrich
Holger Gärtner
Michel Monbaron
Gerhard H. Schleser

CONTENTS

SECTION 1 CLIMATOLOGY - SOUTHERN HEMISPHERE

<i>E.J. Hendy:</i>	8
Dendroclimatology underwater: Australian coral records from 1565AD	
<i>M.T. Brookhouse:</i>	16
Crossdating of terminal and reverse-latewood eucalypt tree-rings	
<i>A. Fowler:</i>	23
Mean sea level pressure composite mapping as an exploratory tool in dendroclimatology	
<i>A. Verheyden, G. Helle, G.H. Schleser & H. Beeckman:</i>	31
High-resolution carbon and oxygen isotope profiles of tropical and temperate liana species	

SECTION 2 CLIMATOLOGY - NORTHERN HEMISPHERE

<i>U. Büntgen, D. C. Frank, R. Böhm & J. Esper:</i>	38
Effect of uncertainty in instrumental data on reconstructed temperature amplitude for the European Alps	
<i>J. Esper, U. Büntgen, D.C. Frank, D. Nievergelt, K. Treydte & A. Verstege:</i>	46
Multiple tree-ring parameters from Atlas cedar (Morocco) and their climatic signal	
<i>D. Frank, J. Esper & E. Cook:</i>	56
Effect of uncertainty in instrumental data on reconstructed temperature amplitude for the European Alps	
<i>B. Neuwirth, F.H. Schweingruber & M. Winiger:</i>	67
Interannual climate/growth-relations of Central European tree rings - A dendro-ecological network analysis	
<i>D. Ogrin:</i>	77
Tree rings and climate in sub-mediterranean Slovenia	
<i>O.V. Sidorova, M.M. Naurzbaev & E.A. Vaganov:</i>	84
An integral estimation of tree-ring chronologies from subarctic regions of Eurasia	
<i>M. Sigl, H. Strunk & H.-J. Barth:</i>	92
Dendroclimatic Investigations in Asir Mountains – Saudi Arabia. Preliminary Report	

M. Staudinger & H. Strunk:	99
Dendroclimatic research in Western Siberia – The reconstruction of temperature and precipitation since the 16 th century	
G. Weber & K.F. Kaiser:	107
Dendrochronological records of late Holocene and recent glacier fluctuations of Eagle, Herbert, and Mendenhall Glaciers, Southeast Alaska	

SECTION 3 ECOLOGY

A. Bär, J. Löffler & A. Bräuning:	114
Methodological approach for dendroecological analysis of dwarf shrubs - A contribution to ecosystem reconstructions in the Norwegian Scandes	
B.A. Black & M.D. Abrams:	120
An evaluation of boundary-line release criteria for eleven North American tree species	
A. Bräuning & I. Burchardt:	127
Detection of growth dynamics in tree species of a tropical mountain rain forest in southern Ecuador	
A. Cedro:	132
Influence of thermic and pluvial conditions on the radial increments of <i>Pseudotsuga menziesii</i> Franco from Western Pomerania, Poland	
N.M. Devi:	141
Climate driven height growth change of multistem trees of Siberian larch in the Polar Ural mountains	
D. Friedrichs, B. Neuwirth & H. Gottschling:	145
Dendroecological Analysis of Growth Anomalies in Walnut Forests in Southern Kyrgyzstan	
H.P. Kahle:	152
Impact of the drought in 2003 on intra- and inter-annual stem radial growth of beech and spruce along an altitudinal gradient in the Black Forest, Germany	
M. Panayotov & S. Yurukov:	165
Dendroecological analysis of the influence of strong winds and snow accumulation on the growth of trees at the treeline in Vitosha Mountain, Bulgaria	
O. Rößler, J. Löffler & A. Bräuning:	175
The use of dendroecological methods in a landscape-ecological approach on upper treeline fluctuations	

N. Schmitz, A. Verheyden, F. De Ridder, H. Beeckman & N. Koedam:	180
Hydraulic architecture of the mangrove <i>Rhizophora mucronata</i> under different salinity and flooding conditions	
N. Zafirov:	188
Dendroecological analysis of Scots pine (<i>Pinus sylvestris</i> L.) stands in Vitosha Mountain, Bulgaria	

SECTION 4 GEOMORPHOLOGY

O. Hitz, H. Gärtner, I. Heinrich. & M. Monbaron:	196
Reconstruction of Erosion Rates in Swiss Mountain Torrents	
I. Malik:	203
Extreme rainfall events as a triggering mechanism for erosion analysed by means of anatomical changes in exposed roots in permanent gullies (southern Poland)	
M. Matyja:	213
The role of flood events in mid-mountain river-bed transformation dated by anatomical changes in exposed roots	
M. Santilli & M. Pelfini:	223
Debris flow activity and relevant effects on the tree radial growth - An example from the Central Italian Alps	

SECTION 5 ARCHAEOLOGY

M. Gurskaya:	236
Preliminary tree-ring dating of historical wood from Ust-Voykar settlement (15 th -20 th Century), Northwestern Siberia	
G. Lambert, S. Durost & J. Cuaz:	244
2500 years from dendrochronology back to ancient French human biotopes. Trees studied: low altitude oaks	

SECTION 6 ISOTOPES

O. Planells, L. Andreu, O. Bosch, E. Gutiérrez, M. Filot, M. Leuenberger, G. Helle & G.H. Schleser:	266
The potential of stable isotopes to record aridity conditions in a forest with low-sensitive ring widths from the eastern Pre-Pyrenees	

<i>K. Treydte et al. (corresponding author, list suppressed):</i>	273
The European Isotope Network ISONET: First Results	
<i>K. Weidner, G. Helle, J. Löffler, B. Neuwirth & G. H. Schleser:</i>	281
The reaction of $\delta^{13}\text{C}$, $\delta^{18}\text{O}$ and ring width on Larch Budmoth (<i>Zeiraphera diniana</i> Gn.) outbreaks in the European Larch (<i>Larix decidua</i> Mill.) – A case study in the Lötschental, Switzerland	

SECTION 7 NEW APPLICATIONS

<i>H. Gärtner & C. Denier:</i>	288
Application of a 3D Laser scanning device to acquire the structure of whole root systems- A pilot study	
<i>I. Heinrich, H. Gärtner & M. Monbaron:</i>	295
Different forms of tension wood in alder and beech in relation to mechanical stress - Preliminary results	
<i>I. Heinrich:</i>	300
Higher nutrient-levels in tree rings of <i>Eucalyptus grandis</i> following a wildfire	
<i>List of participants</i>	308
TRACE 2005 Conference, April 21 st – 23 rd 2005, Department of Geosciences, Geography, University of Fribourg, Switzerland	
<i>List of sponsors</i>	313

SECTION 1

CLIMATOLOGY - SOUTHERN HEMISPHERE

Dendroclimatology underwater: Australian coral records from 1565AD

E.J. Hendy

Lamont Doherty Earth Observatory, Columbia University, Palisades NY 10964, USA

Email: ejhendy@ldeo.columbia.edu

Introduction

Replication of records from within individual trees, between multiple trees, and between sites, is fundamental to dendroclimatology because it allows explicit quantification of the strength of common growth forcing and chronology confidence (Fritts 1976). The same approach is applied in this study of multi-century records replicated between coral colonies, which demonstrates the reproducibility of coral-based tracers and reveals the common environmental signals on decadal to century timescales. The massive aragonitic skeleton formed by coral colonies of *Porites* sp. accumulates at ~1 cm/year and archives physiological, isotopic and elemental tracers that vary with changes in sea surface temperature (SST), salinity, rainfall and river runoff, sediment input, upwelling and/or shifts in water mass circulation. Sub-annual sampling also allows the reconstruction of short-term events e.g. individual river floods, in continuous records that can span many centuries. The development of such high resolution, multi-century, tropical ocean surface climate reconstructions is critical to understanding the role of the tropical ocean and atmosphere in global climate variability. Global climate anomalies originating from the tropics include high frequency perturbations like the El Niño Southern Oscillation (Allan et al. 1996), to the Pacific Decadal Oscillation (Latif and Barnett 1994, Trenberth and Hurrell 1994, Power et al. 1999) and millennial scale impacts (Cane and Clement 1999, Clark et al. 2002).

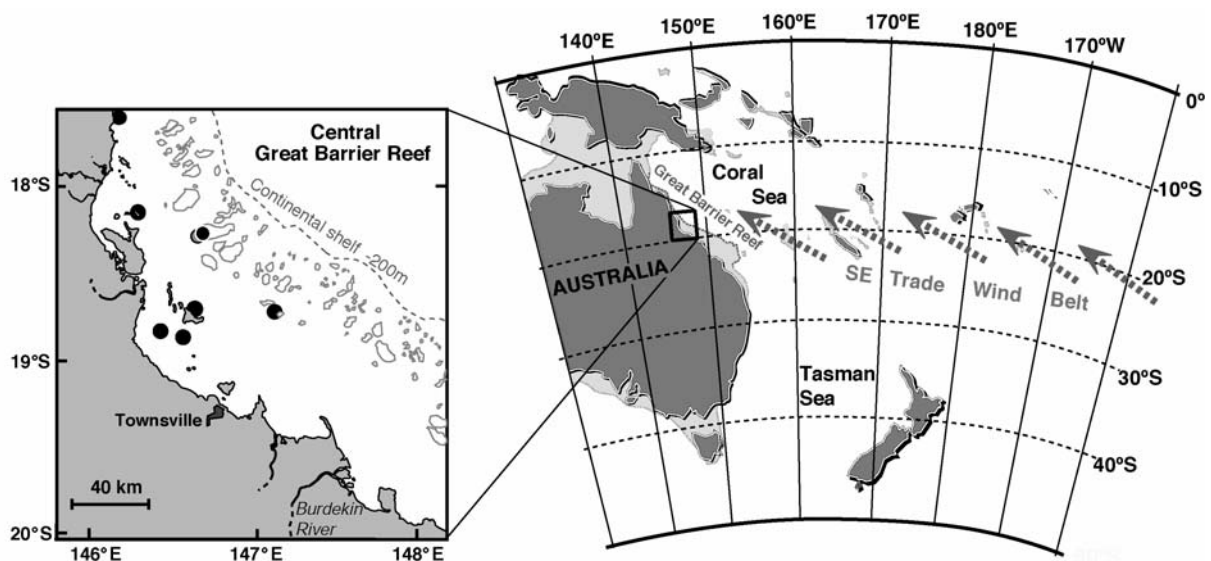


Figure 1: The reef locations of the eight coral cores used in this study, from the Central Great Barrier Reef, Australia.

Study outline

Accurate error estimates need to be established for coral-based climate reconstructions, and to do this requires the examination of fundamental issues including:

- (1) age control
- (2) signal reproducibility, and
- (3) tracer behaviour, and therefore interpretation, over the timescale to be reconstructed.

This study addressed all of these issues by adapting dendroclimatological approaches to coral reconstructions with particular attention to low frequency variability. The study used eight cores taken from *Porites* sp. colonies growing within a 60km radius in the Great Barrier Reef, Australia (Fig. 1). The coral cores spanned the period 1565 to 1985 AD (Fig. 3A).

Age control of coral records: cross-dating, historical die-offs and rainfall extremes.

Absolute age control was critical for parts 2 and 3 of this study. The accuracy of traditional methods of assigning years to coral proxy-climate records, such as counting skeletal density bands, had not been previously established, but typical error estimates are quoted as 1-2 years per century. In this study, UV luminescent lines caused by annual river floods and associated with the Australian summer monsoon, were used as a second marker to assign years to the eight multi-century coral cores. Cross-dating techniques were adapted from dendrochronology and applied to characteristic patterns of luminescent lines visible in the coral skeleton under UV light (e.g. Fig. 2, full details in Hendy et al. 2003a). The timing, width and intensity of the luminescent bands correlate strongly with summer monsoonal rainfall and the magnitude of coastal discharge from Queensland's largest river, the Burdekin (Isdale 1984, Lough 1997, Isdale et al. 1998).

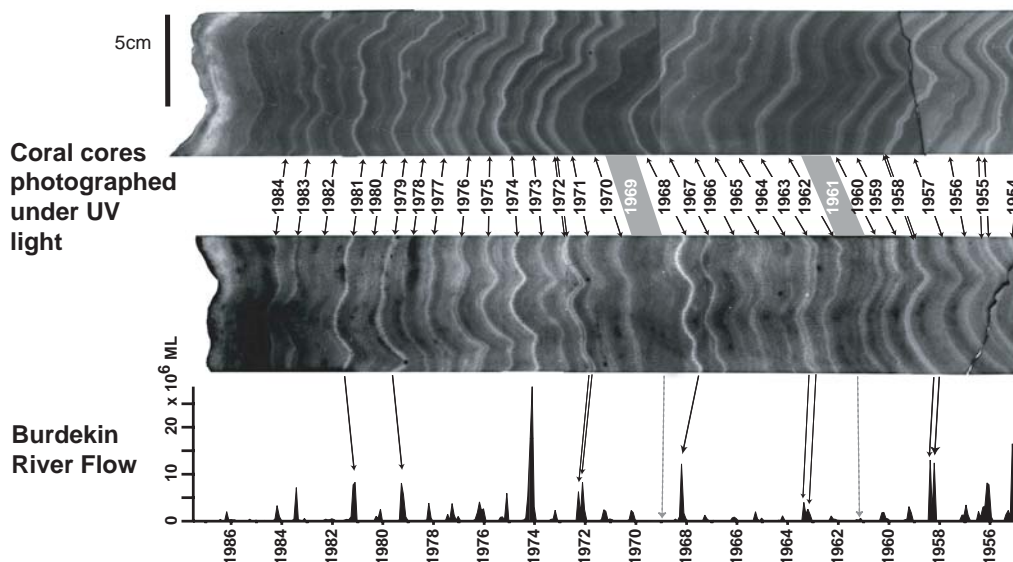


Figure 2: Black and white photomontage of luminescent lines in two coral core slabs under UV light, compared with the Burdekin River discharge record (1955-1985). The two cores were collected from inshore central GBR reefs, 120 km (top core) and 170 km (lower core) north of the Burdekin River mouth (Fig. 1).

Following methods developed in tree-ring studies, skeleton-plots of luminescent banding were produced for each core and combined into a master luminescence chronology giving annual and absolute precision back to 1615 AD. A 373-year cross-dated chronology was developed (Fig. 3B), despite gaps between core sections, growth hiatuses and patches of complex growth orientation within individual cores. Discrepancies of up to 15 years relative to previously published chronologies for these cores (e.g. Lough and Barnes, 1997, Isdale et al. 1998) demonstrate the need for a more rigorous dating approach in coral research. Cross-dating also highlighted sampling errors where a core section had been inverted before labeling. Problems inherent in dating a single coral core, such as difficult growth orientation, skeletal discontinuities and breaks between core sections, were also resolved by cross-dating, for example a 3-year gap was identified between two sections of one core.

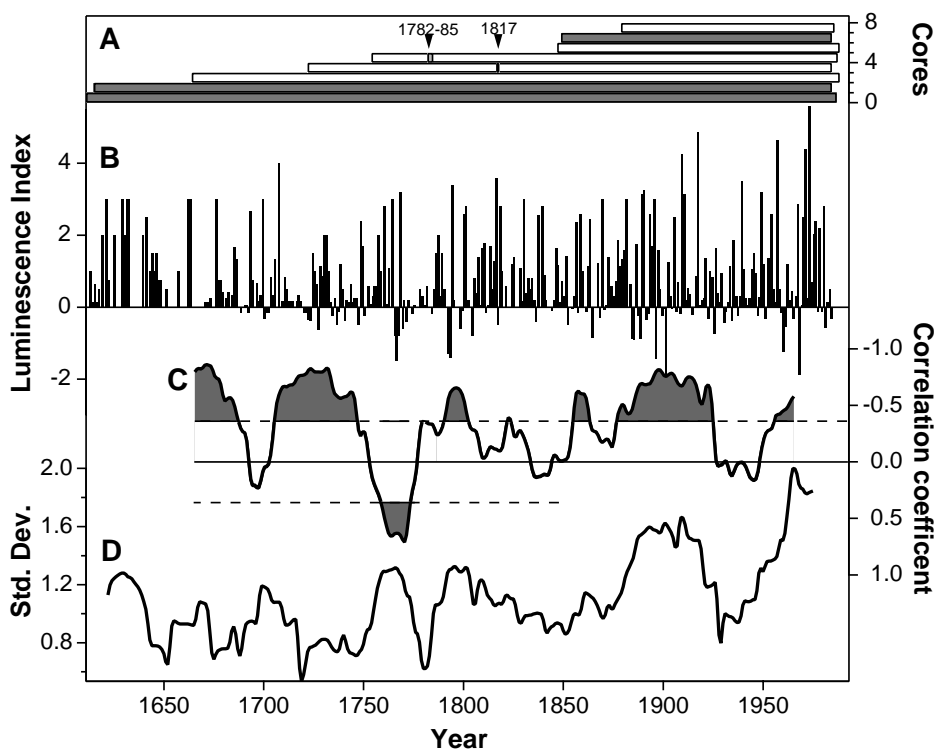


Figure 3: (A) The number of coral cores contributing to the study through time separated into inshore reef locations (white) and midshelf reefs (shaded dark grey). Growth hiatus scars are also marked. (B) Luminescence master chronology for the central Great Barrier Reef, 1612-1985 AD. (C) Cross correlations between the luminescence master series and NINO3 SST reconstruction (Mann et al., 2000) for 30-year sliding windows (shaded areas are where the relationship is significance at 0.05 level). (D) Interannual variability of the luminescence master series expressed as the standard deviation of the series calculated over a 20-year sliding window. Further details are given in Hendy et al. 2003a and 2003b.

The luminescent master chronology provides a reconstruction of regional rainfall and river runoff. It was significantly correlated with the instrumental record of Burdekin River flow ($r=0.82$, 1894-1985 extended using rainfall records, Isdale et al. 1998), and Lough's (1997) index of Queensland summer rainfall ($r=0.65$, 1891-1985). The master luminescence chronology also provides evidence for the non-stationary nature of ENSO teleconnections

with the Australian Monsoon (Hendy et al. 2003a). Years with a marked absence of luminescence coincide with many historical drought records from the western Pacific and these often occur during ENSO events. However, the relationship between ENSO events occurring in the equatorial Pacific and climatic anomalies in ENSO-sensitive regions, like NE Australia, is non-stationary. For example, during the 1920s to 1950s ENSO activity was reduced, ENSO teleconnections with sensitive regions were weak to non-existent, and Australia experienced prolonged drought conditions with reduced interannual rainfall variability (Allan et al. 1996). The off-on relationship between NE Australian rainfall and ENSO can be observed in the shifting correlation between the luminescence master chronology and the Mann et al. (2000) NINO3 reconstruction (Fig. 3C). For much of the period from the 1650s to 1800s, 1870s to 1920s and 1950s onwards ENSO-related teleconnections were a dominant factor in NE Australian rainfall variability. The relationship breakdown recognized in the instrumental record for the 1920s-50s is reproduced, and an analogous period is highlighted from the 1800s to 1870s (Fig. 3C). As in the 1920s-1950s, there is a reduction in interannual and interdecadal variability between 1800 and 1870 (Fig. 3D). The positive trend in interannual variability towards the present suggests an increasing number and amplitude of extreme rainfall events. This long-term trend, however, is biased prior to 1750 because the earlier period is dominated by less sensitive records from midshelf sites, which only experience the more extreme river floods.

Reproducibility of low frequency variability in multi-century coral records

A suite of geochemical tracers was measured from each of the eight cores, including oxygen ($\delta^{18}\text{O}$) and carbon ($\delta^{13}\text{C}$) isotopes, and trace element ratios, strontium/calcium, uranium/calcium and barium/calcium (Hendy 2003). Measurements were made in 5-year increments, and where possible samples of the same time period were duplicated within cores by taking contemporaneous samples from different growth axes. A basic principle of dendroclimatology, the aggregation of a number of records into one common master series to enhance common environmental signals (Cook and Kairiukstis 1989), was applied in the construction of master records for each coral geochemical tracer (e.g. Sr/Ca and $\delta^{18}\text{O}$ records in Fig. 4). This was the first quantitative analysis of coral tracer reliability over decadal-to-centennial timescales, and the results highlight that it is critical to replicate information from multiple coral colonies in order to reliably reconstruct the paleoclimate signal (Hendy et al. 2002). For example, the variability between individual Sr/Ca records was large in comparison to the desired signal on interdecadal to century timescales, and for this reason a single core on average accounted for only a third of the variance contained in the master Sr/Ca record. The $\delta^{18}\text{O}$ records were more consistent between cores in terms of relative trends on both decadal and century scales, and on average a single record reconstructed over 70% of the composite record. Anomalous periods when $\delta^{18}\text{O}$ records did not reproduce were valuable markers of artifacts (e.g. skeletal diagenesis or unusual growth). Confidence estimates for each of the composite records were used to demonstrate the reproducibility of coral tracer signals over multi-decadal to century timescales and show that coherent regional-scale information is being replicated between coral colonies (Fig. 4).

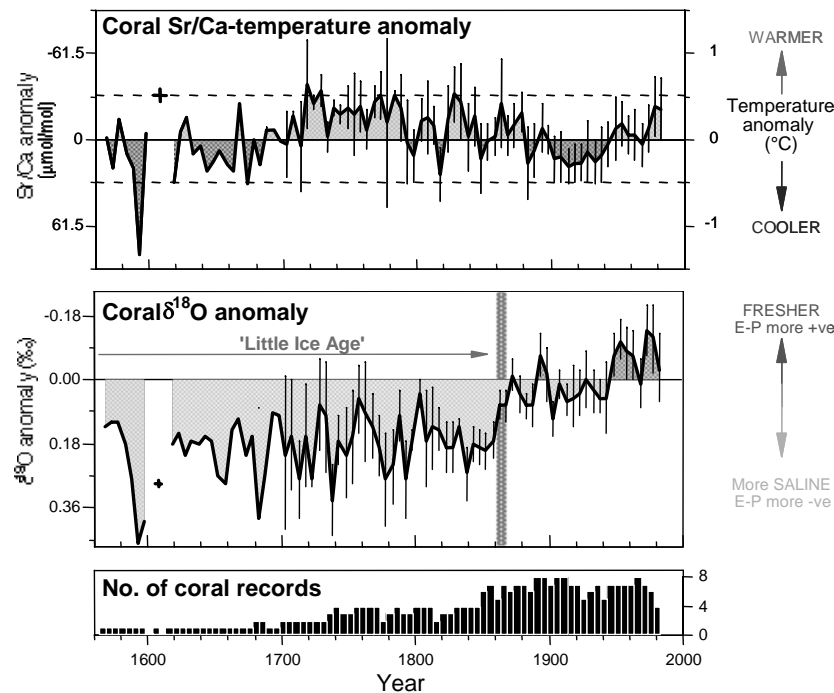


Figure 4: The Sr/Ca (upper panel) and $\delta^{18}\text{O}$ (middle panel) composite master records with 95% confidence envelope. A temperature slope calibration of $-62 \mu\text{mol/mol Sr/Ca per } ^\circ\text{C}$ (Alibert and McCulloch 1997, Gagan et al. 1998) is used to convert Sr/Ca anomalies (left axis) to sea surface temperature anomalies (right axis). The number of coral cores contributing to each 5-year average are given in the lower panel. More details are provided in Hendy et al. 2002.

Verification of the coral palaeo-environmental reconstructions on decadal to century timescales

The interpretation of proxy records is complicated because tracers can respond to a number of environmental variables, and different variables can dominate over different timescales. In addition, the climate-related mechanism that produces the coral geochemical signal is often uncertain. The master records for each geochemical tracer were verified against local and regional-scale instrumental records using previously published calibrations developed from short high-resolution records. For example, the Sr/Ca record (Fig. 4 upper panel) successfully reconstructs the 0.7°C warming (1905-1985) observed in the local ($146^\circ\text{E } 18^\circ\text{S}$) GISST2.2 series (Rayner et al. 1996, $r=0.68$, $p<0.005$).

Through the measurement of multiple geochemical tracers it is possible to separate competing environmental influences on tracer variability. For example, coral $\delta^{18}\text{O}$ records are difficult to interpret because $\delta^{18}\text{O}$ is influenced by both salinity and SST, but the replication of multiple tracers allows a comparison of the proposed sea surface temperature-tracers (Sr/Ca, U/Ca, $\delta^{18}\text{O}$) and the freshwater flux tracers ($\delta^{18}\text{O}$, Ba/Ca and luminescence). The similarity of the freshwater flux signals between $\delta^{18}\text{O}$, Ba/Ca and luminescence, and the poor correlation between parallel Sr/Ca and $\delta^{18}\text{O}$ records (Fig. 4) demonstrated that the $\delta^{18}\text{O}$ was dominated by changes in the evaporation-precipitation balance on decadal-century timescales, not by temperature.

The last five centuries: the demise of the 'Little Ice Age' and the 20th century warming

In global and hemispheric-scale composite reconstructions of palaeotemperature the anomalous warmth of the 20th century contrasts dramatically with the millennium-scale cooling trend that culminated in the 'Little Ice Age' (LIA) between the 15th and late 19th centuries (Bradley, 2000, Jones et al., 2001, Mann et al. 2000). Glacial advances in both hemispheres (Grove, 1988) and enhanced polar atmospheric circulation (Kreutz et al., 1997) suggest that the LIA was a global-scale event, though cooler conditions were possibly restricted to higher latitudes (Rind, 1998, 2000). Coral provide one of the few tropical climate reconstructions of this period.

The GBR coral proxy records of SST anomalies (from Sr/Ca, Fig. 4 top panel) and sea surface salinity anomalies ($\delta^{18}\text{O}$, Fig. 4 middle panel) suggest that a dramatic shift occurred in the tropical ocean-atmosphere system at the end of the LIA (Hendy et al., 2002). The striking 0.2‰ shift in $\delta^{18}\text{O}$ from the 1850s to modern values in the 1870s indicates an abrupt shift to lower salinities, and this signal is seen simultaneously in coral $\delta^{18}\text{O}$ records across the Pacific and Indian Oceans from latitudes within the trade wind belts (e.g. Druffel and Griffin 1993, Quinn et al. 1993, Linsley et al. 1994, Quinn et al. 1998, Kuhnert et al. 1999). The late 19th century abrupt transition in the ocean-atmosphere freshwater flux coincides with a sudden weakening of atmospheric circulation, including the trade winds, and surface driven ocean currents. At the same time, the glacial retreat signaling the end of the LIA occurs during a recovery to warmer conditions at the higher latitudes, but tropical cooling according to coral SST records (Linsley et al. 2000, Hendy et al. 2002). These results support the scenario that a stronger latitudinal temperature gradient and intensified Hadley circulation occurred during the LIA. Evaporation and condensation processes are extremely effective mechanisms for transporting and redistributing energy on all scales. Increased salinities from 1565 to 1870 in sites within the trade-wind belt are consistent with an intensified Hadley circulation impacting E-P and enhancing poleward moisture transport. More tropical palaeoclimate reconstructions are required to improve our understanding of the nature of the LIA and possible role of the tropics. This study shows how a replicated coral-based multi-tracer approach, and the application of lessons learnt from dendroclimatology, can provide paleoclimate information on multiple components of the tropical ocean-atmosphere system.

Acknowledgements

Thank you to Ingo Heinrich and Michel Monbaron for the invitation to present this research at the TRACES 2005 meeting. This work was the basis of my PhD at the Australian National University, Canberra, which was funded by an Australian Postgraduate Award, and I thank my supervisory panel; Michael Gagan, Malcolm McCulloch, Janice Lough, Chantal Alibert and John Chappell for their input and collaboration.

References

- Alibert, C., McCulloch, M.T. (1997): Strontium/calcium ratios in modern Porites corals from the Great Barrier Reef as a proxy for sea surface temperature: calibration of the thermometer and monitoring of ENSO. *Paleoceanography* 12: 345-365.
- Allan, R.J., Lindesay, J., Parker, D. (1996): El Niño Southern Oscillation and climate variability. Collingwood, Australia, CSIRO Publishing. 405 pgs.
- Bradley, R.S. (2000) 1000 years of climate change. *Science* 288: 1353-1354.
- Cane, M.A., Clement, A.C. (1999): A role for the tropical Pacific coupled ocean-atmosphere system in Milankovitch and millennial timescales. Part II. Global impacts. *Geophysical Monographs* 112: 373-384.
- Clark, P.U., Pisias, N.G., Stocker, T.F., Weaver, A.J. (2002): The role of the thermohaline circulation in abrupt climate change. *Nature* 415: 863-869.
- Cook, E.R., Kairiukstis, L.A., (Eds.) (1989): Methods of dendrochronology: applications in the environmental science. International Institute for Applied Systems Analysis. Dordrecht, The Netherlands, Kluwer Academic Publishers. 394 pgs.
- Druffel, E.R.M., Griffin, S. (1993): Large variations of surface ocean radiocarbon: evidence of circulation changes in the Southwestern Pacific. *Journal of Geophysical Research* 98(C11): 20249-20259.
- Fritts, H.C. (1976): Tree Rings and Climate. London, Academic press. 567 pgs.
- Gagan, M.K., Ayliffe, L.K., Hopley, D., Cali, J.A., Mortimer, G.E., Chappell, J., McCulloch, M., Head, M.J. (1998): Temperature and surface-ocean water balance of the mid-Holocene Tropical Western Pacific. *Science* 279: 1014-1018.
- Hendy, E.J., Gagan, M.K., Alibert, C.A., McCulloch, M.T., Lough, J.M., Isdale, P.J. (2002): Abrupt decrease in tropical Pacific sea surface salinity at end of Little Ice Age. *Science* 295: 1511-1514.
- Hendy (2003): Decadal-to-Centennial Climate Variability from Great Barrier Reef Coral. PhD Thesis, Australian National University, Canberra. 337pg.
- Hendy, E.J., Gagan, M.K., Lough, J.M. (2003a): Chronological control of coral records using luminescent lines and evidence for non-stationary ENSO teleconnections in northeast Australia. *The Holocene* 13 (2): 187-199.
- Hendy, E.J., Lough, J.M., Gagan, M.K. (2003b): Historical die-offs in massive Porites from the central Great Barrier Reef, Australia: evidence of past environmental stress? *Coral Reefs* 22: 207-215.
- Isdale, P. (1984): Fluorescent bands in massive corals record centuries of coastal rainfall. *Nature* 310: 578-579.
- Isdale, P.J., Stewart, B.J., Tickle, K.S., Lough, J.M. (1998): Palaeohydrological variation in a tropical river catchment - a reconstruction using fluorescent bands in corals of the Great Barrier Reef, Australia. *The Holocene* 8: 1-8.
- Jones, P.D., Osborn, T.J., Briffa, K.R. (2001): The evolution of climate over the last millennium. *Science* 292: 662-667.

- Kreutz, K.J., Mayewski, P.A., Meeker, L.D., Twicker, M.S., Whitlow, S.I., Pittalwala, I.I. (1997): Bipolar changes in atmospheric circulation during the Little ice Age. *Science* 277: 1294-1296.
- Kuhnert, H., J., Patzold, B., Hatcher, K.-H., Wyrwoll, A., Eisenhauer, L.B., Collins, Z.R., Zhu, Wefer, G. (1999): A 200-year coral stable oxygen isotope record from a high-latitude reef off Western Australia. *Coral Reefs* 18: 1-12.
- Latif, M., Barnett, T.P. (1994): Causes of decadal climate variability over the North Pacific and North America. *Science* 266: 634-637.
- Linsley, B.K., Dunbar, R.B., Wellington, G., Mucciarone, D.A. (1994): A coral-based reconstruction of Intertropical Convergence Zone variability over Central America since 1707. *Journal of Geophysical Research* 99(C5): 9977-9994.
- Linsley, B.K., Wellington, G.M., Schrag, D.P. (2000): Decadal sea surface temperature variability in the subtropical South Pacific from 1726 to 1997 A.D. *Science* 290: 1145-1148.
- Lough, J.M. (1997): Regional indices of climate variation: temperature and rainfall in Queensland, Australia. *International Journal of Climatology* 17: 55-66.
- Lough, J.M., Barnes, D.J. (1997): Several centuries of variation in skeletal extension, density and calcification in massive Porites colonies from the Great Barrier Reef: A proxy from seawater temperature and a background of variability against which to identify unnatural change. *Journal of Experimental Marine Biology and Ecology* 211: 29-67.
- Mann, M.E., Gille, E., Overpeck, J., Gross, W., Bradley, R.S., Keimig, F.T., Hughes, M.K. (2000): Global temperature patterns in past centuries: an interactive presentation. *Earth Interactions* 4: 1-29.
- Power, S., Casey, T., Folland, C.K., Colman, A., Mehta, V. (1999): Inter-decadal modulation of the impact of ENSO in Australia. *Climate Dynamics* 15: 319-324.
- Quinn, T.M., Taylor, F.W., Crowley, T.J. (1993): A 173 year stable isotope record from a tropical south Pacific coral. *Quaternary Science Reviews* 12: 407-418.
- Quinn, T.M., Crowley, T.J., Taylor, F.W., Henin, C., Joannot, P., Join, Y. (1998): A multicentury stable isotope record from a New Caledonia coral: Interannual and decadal sea surface temperature variability in the southwest Pacific since 1657 A.D. *Paleoceanography* 13: 412-426.
- Rayner, N.A., Horton, E.B., Parker, D.E., Folland, C.K., Hackett, K.B. (1996): Version 2.2 of the Global Sea-Ice and Sea Surface Temperature data set, 1903-1994. CRTN 74. Hadley Centre for Climate Prediction and Research, Meteorological Office, Bracknell, Berkshire, U.K. 21 p.
- Rind, D. (1998): Latitudinal temperature gradients and climate change. *Journal of Geophysical Research* 103(D6): 5943-5971.
- Rind, D. (2000): Relating paleoclimate data and past temperature gradients: Some suggestive rules. *Quaternary Science Reviews* 19: 381-390.
- Trenberth, K.E., Hurrell, J.W. (1994): Decadal atmosphere-ocean variations in the Pacific. *Climate Dynamics* 9: 303-319.

Crossdating of terminal and reverse-latewood eucalypt tree-rings

M.T. Brookhouse

School of Resources, Environment and Society, The Australian National University, Canberra, ACT, Australia

Email: matthew.brookhouse@anu.edu.au

Introduction

Crossdating is a fundamental dendrochronological principle. However, despite its importance, crossdating has been applied infrequently in the eucalypt dendrochronological literature. One factor limiting crossdating in previous eucalypt tree-ring studies has been the difficulty associated with objective tree-ring identification and measurement, particularly in samples from lower montane (500-800m) sites (Bi 1994). To overcome this problem Brookhouse (1997) proposed the 'reverse-latewood' identification technique. In contrast to the terminal form, reverse-latewood occurs at the start of the eucalypt tree-ring (Fig. 1). Whilst tree-ring counts indicate that both terminal and reverse-latewood may indicate truly annual tree-ring boundaries (Brookhouse 1997, Green 1967) crossdating has not been quantitatively demonstrated for either type in eucalypts.

The present study was undertaken using samples of known age to investigate the potential of eucalypts to preserve common environmental signals by quantitatively demonstrating crossdating within and between two eucalypt species – one characterised by terminal latewood and the other reverse-latewood – and identifying the climatological source of common signals preserved within the derived tree-ring chronologies.

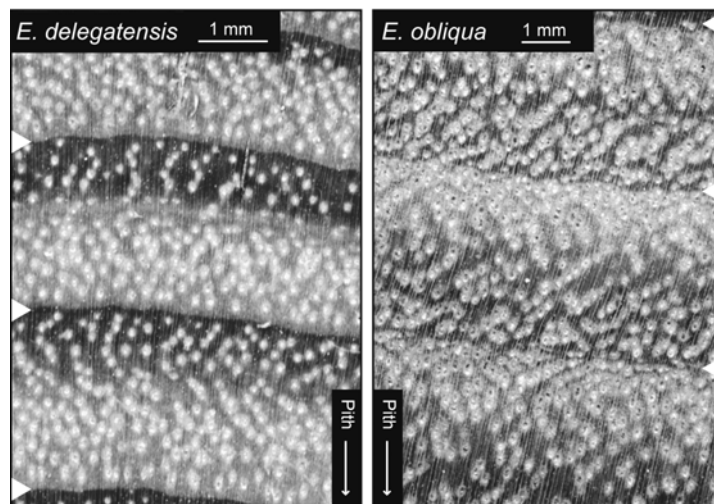


Figure 1: Terminal and reverse-latewood tree-ring structure. Dark latewood can be easily identified at the terminal boundary of *Eucalyptus delegatensis* tree-rings. Latewood type fibres in *E. obliqua* are formed at the start of the tree-ring. In tree rings exhibiting this structure, the clear boundary between earlywood and latewood type fibres is defined as the boundary. Tree-ring boundaries and the direction of the pith are indicated.

Methods

Samples used in this study were collected from the Black and Federation Ranges in Victoria's central highlands (Fig. 2) by the Department of Sustainability and Environment, Victoria as part of regional timber resource surveys (Hamilton, 1999) and stem analysis sampling in forest stands of known age. Throughout the study area cold winter temperatures limit cambial activity leading to the formation of annual rings. Two species, one exhibiting terminal latewood (*Eucalyptus delegatensis* Baker, R.T.) the other exhibiting reverse-latewood (*E. obliqua* L'Herit), were selected for analysis.

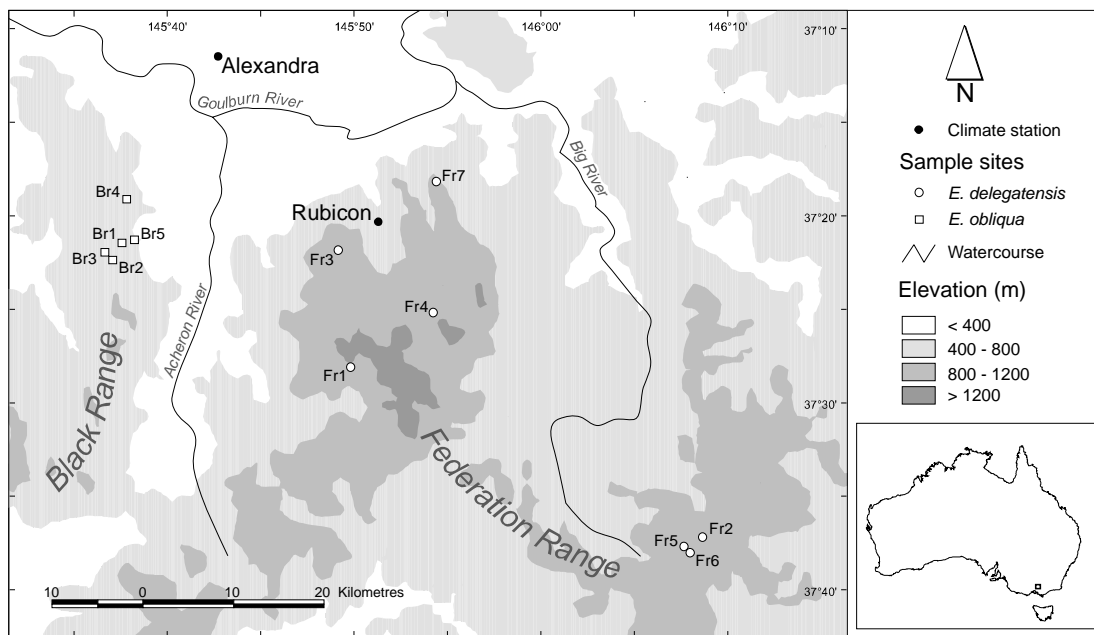


Figure 2: Location of sample sites and climate stations.

Sample disks were stored, allowed to air-dry and then sanded. Up to four radii, evenly spaced around each sample disk, were selected for identification and measurement on each sample. In many instances fewer than four radii were selected due to sample deformities. Tree-ring structure of all samples was examined under stereo-microscope. Tree-rings were identified on each radius and calibrated against other radii on the same sample. Radii were then visually crossdated with samples from the same site. Tree-ring widths were measured to the nearest 0.01 mm using Henson and LINTAB tree-ring measurement stages and TRIMS and TSAP software.

Verification of visual crossdating was conducted in Xmatch (Fowler 1998). Although the outermost ring year of each sample was known, Xmatch was permitted to conduct a 'best-fit' search. Only samples for which the Xmatch best-fit was consistent with visual crossdating were retained for further analysis. COFECHA (Holmes 1983) was used to assess the placement of missing rings. Product moment correlation coefficient significance testing was conducted between crossdated radii. Only radii with highly significant ($p < 0.0001$) inter-tree radial correlation were retained for chronology development.

A two-stage detrending approach within ARSTAN was used for standardisation using a negative exponential or simple linear function followed by a cubic smoothing spline. Mean individual species chronologies were calculated using an arithmetic mean. Autoregression of each chronology was conducted to remove serial correlation. The Expressed Population Signal (EPS) statistic (Briffa and Jones 1990) and Mean Sensitivity (MS) were calculated for each chronology. The Gleichläufigkeit (GLK) was also calculated between the species' chronologies.

Climatological analysis was based upon monthly mean maximum temperature and total monthly precipitation data from the Rubicon (838 m) climate station (Fig. 2). Analysis was restricted to a time period common to both tree-ring chronologies (1952-1998). The influence of both the current and previous season's climate conditions were analysed using 24 months of mean temperature and precipitation data (September_{n-1}-August_n). Seasonal (three-month) temperature means and precipitation totals were calculated and included in analysis. Correlation between climate and each species' chronology was evaluated using the product moment correlation coefficient.

Results

Crossdating results are summarised in table 1. Only nine missing rings, constituting 0.002% of the entire crossdated dataset, were identified. Each of these missing rings was identified during visual crossdating. Although achieved intra-specifically, inter-specific radial crossdating was not achieved. The crossdated proportion of the original sample varied markedly between species – 76% and 40% of *E. obliqua* and *E. delegatensis* radii, respectively.

Table 1: Full and crossdated sample summary

Species	Sample radii (trees)		Missing rings	
	All	Crossdated	Visual	Xmatch
<i>E. delegatensis</i>	60 (19)	24 (15)	1	0
<i>E. obliqua</i>	41 (14)	31 (13)	8	0

Chronology statistics are presented in table 2. Mean sensitivity and within and between tree correlations indicate that both chronologies hold relatively equal dendroclimatological potential. Autocorrelation is relatively low and non-significant and the EPS exceeds 0.85 in both instances.

Table 2: Species chronology statistics. Reported statistics are autocorrelation (AC), mean sensitivity (MS), correlation within (W_t) and between (B_t) trees and expressed population signal (EPS).

Species	n (years)	AC	MS	W_t	B_t	EPS
<i>E. delegatensis</i>	47	0.11	0.22	0.57	0.34	0.87
<i>E. obliqua</i>	58	0.06	0.27	0.51	0.38	0.90

Correlation between the two chronologies is highly significant (Fig. 3). This apparent potential for interspecific chronology crossdating potential is also indicated by the relatively high inter-specific GLK.

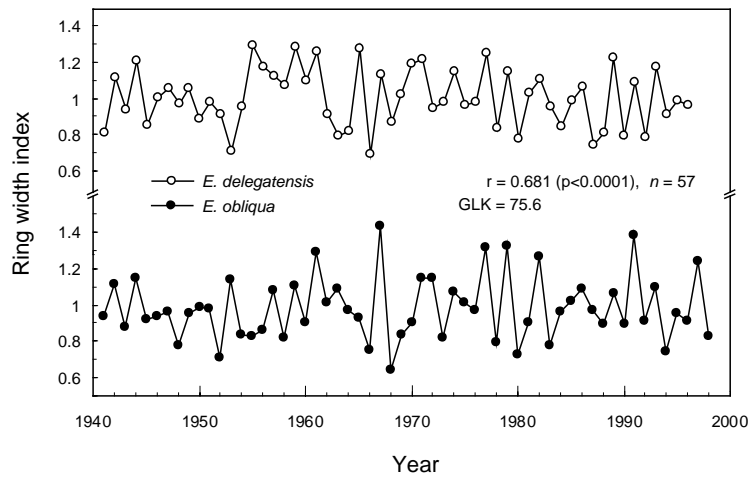


Figure 3: Standardised tree-ring chronologies for *E. delegatensis* and *E. obliqua*. Inter-chronology correlation and Gleichläufigkeit (GLK), or absolute first order concordance, is reported.

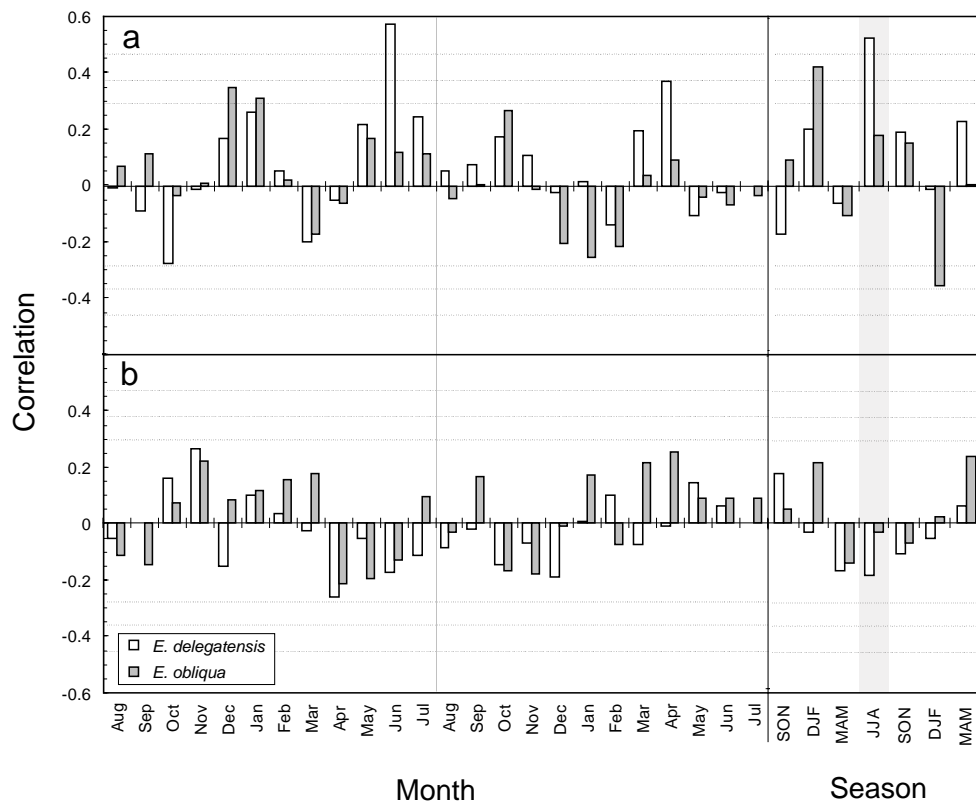


Figure 4: Climate response graphs for *E. delegatensis* and *E. obliqua*. Response graphs summarise correlation between 24 months of monthly and seasonal temperature (a) and precipitation (b) each species chronology. Dashed horizontal lines indicate 0.05, 0.01 and 0.001 significance levels. The boundary of the preceding and current growing season is indicated for monthly (line) and seasonal (shaded).

Climatological results are presented in figure 4. No significant correlations were observed between precipitation and either chronology. Significant correlations were identified between each chronology and temperature. Significant positive correlation between the *E. delegatensis* chronology and mean temperatures was identified for the preceding June ($r=0.573$, $p<0.0001$), current April ($r=0.370$, $p<0.05$) and preceding winter (June-August, $r=0.533$, $p<0.001$). Significant positive and negative correlations were identified between the *E. obliqua* chronology and temperature during the preceding December ($r=0.348$, $p<0.05$). Similarly, significant correlation was identified between seasonal mean temperature during the preceding ($r=0.420$, $p<0.01$) and current summers ($r=-0.351$, $p<0.05$).

Discussion

Crossdating

Correlation analysis of visually crossdated eucalypt tree-ring series – independently confirmed in Xmatch – verified crossdating within separate species exhibiting terminal and reverse-latewood. The capacity for intra-specific crossdating of eucalypt samples collected over a broad geographic area indicates that macro-scale environmental signals are preserved within eucalypt tree-ring data and provides an important validation of the reverse-latewood identification technique. Similarly inter-specific chronology crossdating indicates that new chronologies from separate species may be used for cross-verification.

Climate analysis

Analysis of temperature data revealed significant correlation with tree-ring widths. Whilst, positive correlation between *E. delegatensis* ring-width and April temperatures of the current season may express the extension of the growing season during a warm autumn, correlation between preceding winter temperature and *E. delegatensis* ring width indices may be due to lag effects of frost injury and cold induced photoinhibition of overwintering foliage (Holly et al. 1994, King and Ball 1998, Rolland et al. 1999, Butterworth 2000, Thomson et al. 2001, Davidson et al. 2004).

In contrast to *E. delegatensis*, standardised *E. obliqua* ring widths were positively correlated with temperature during the previous summer and negatively correlated with temperature during the current summer. Negative correlation between summer temperature has been reported relatively frequently in the dendroclimatological literature (Cregg and Dougherty 1988, Richter et al. 1991, Pan et al. 1997, Rubino and McCarthy 2000, Yeh and Wensel 2000, Peterson et al. 2002) and has been interpreted as a result of increased evaporation and transpiration depleting soil moisture. However, high summer temperatures may affect carbon assimilation, and hence growth, of eucalypts independently of soil moisture by regulating transpiration and carbon assimilation through stomatal control (Wong et al. 1978, Körner and Cochrane 1985) and by inducing thermodormancy (Blake 1976).

Positive correlation between *E. obliqua* ring width and previous summer temperature may correspond with the long-term tree level carbohydrate budget. Stored carbohydrates during a previous season may provide an important basis for later growth (Kozłowski 1971). In eucalypts stored carbohydrates may be critical for eucalypt survival and recovery following drought and disturbance (Fensham and Bowman 1992, Walters et al. 2005). Hence,

carbohydrates that remain unused during the current growth season, due to thermodormancy or stomatal closure may remain available for leaf, canopy and stem diameter growth during the following season (Fritts 1976).

Whilst this study has demonstrated that crossdating between samples and identification of potential climatological influences on eucalypt growth from tree-ring data are possible it has also presented a problem. Approximately half of all radii were not crossdated and the proportion of crossdated radii varied dramatically between the two species. Hence, the question of how the efficiency of eucalypt dendrochronological sampling be improved, must be addressed.

Acknowledgements

I wish to acknowledge the assistance of Dr Cris Brack, Dr Janette Lindesay, Mr Ken Johnson, Dr John Ogden and Dr Anthony Fowler for their analytical assistance and advice. This study was supported by the Co-operative Research Centre for Greenhouse Accounting and Department of Sustainability and Environment.

References

- Bi, H. (1994): South-east regrowth forest growth and yield modelling: design, methods and progress. State Forests of New South Wales, Sydney.
- Blake, T.J. (1976): Thermodormancy in seedlings of *Eucalyptus obliqua* L'Herit. *Australian Journal of Plant Physiology* 3, 269-273.
- Briffa, K.R., Jones, P.D. (1990): Basic chronology statistics and assessment. In 'Methods of dendrochronology: applications in the environmental sciences'. (Eds ER Cook and LA Kairiukstis) pp. 1-8. (Kluwer Academic Publishers: Dordrecht)
- Brookhouse, M.T. (1997): Identification and analysis of growth rings in *Eucalyptus obliqua* L'Herit. and *E. cypellocarpa* L.Johnson. Honours thesis, Australian National University.
- Brubaker, L.B. (1980): Spatial patterns of tree growth anomalies in the Pacific Northwest. *Ecology* 61, 798-807.
- Butterworth, J.A. (2000): Low-temperature photoinhibition and the growth of *Eucalyptus pauciflora* sieber ex sprengel seedlings. PhD thesis, ANU.
- Cregg, B.M., Dougherty, P.M. (1988): Growth and wood quality of young loblolly pine trees in relation to stand density and climatic factors. *Canadian Journal of Forest Research* 18, 851-858.
- Davidson, N.J., Battaglia, M., Close, D.C. (2004): Photosynthetic responses to overnight frost in *Eucalyptus nitens* and *E. globulus*. *Trees* 18, 245-252.
- Fensham, R.J., Bowman, D. (1992): Stand Structure and the Influence of Overwood on Regeneration in Tropical Eucalypt Forest on Melville-Island. *Australian Journal of Botany* 40, 335-352.
- Fowler, A. (1998): 'XMATCH98: an interactive tree-ring crossdating program. Occasional Paper 38.' Department of Geography, University of Auckland, Auckland.
- Fritts, H.C. (1976): 'Tree Rings and Climate.' (Academic Press: London)

- Green, J.W. (1967): A study of altitudinal variation in *Eucalyptus pauciflora* Sieb. ex Spreng. Ph.D. thesis, Australian National University.
- Hamilton, F., Penny, R., Black, P., Cumming, F., Irvine, M. (1999): Victoria's Statewide Forest Resource Inventory: an outline of methods. *Australian Forestry* 62, 353-359.
- Holly, C., Laughlin, G.P., Ball, M. (1994): Cold induced photoinhibition and design of shelters for establishment of eucalypts in pasture. *Australian Journal of Botany* 42, 139-147.
- Holmes, R.L. (1983): Computer-assisted quality control in tree-ring dating and measurement. *Tree-Ring Bulletin* 43, 69-75.
- King, D.A., Ball, M.C. (1998): A model of frost impacts on seasonal photosynthesis of *Eucalyptus pauciflora*. *Australian Journal of Plant Physiology* 25, 27-37.
- Körner, C., Cochrane, P.M. (1985): Stomatal responses and water relations of *Eucalyptus pauciflora* in summer along an elevational gradient. *Oecologia* 66, 443-455.
- Kozlowski, T.T. (1971): 'Growth and Development of Trees. Volume II: Cambial growth, root growth and reproductive growth.' (Academic Press: London)
- Pan, C., Tajchman, S.J., Kochenderfer, J.N. (1997): Dendroclimatological analysis of major forest species of the central Appalachians. *Forest Ecology and Management* 98, 77-87.
- Peterson, D.W., Peterson, D.L., Ettl, G.J. (2002): Growth responses of subalpine fir (*Abies lasiocarpa*) to climatic variability in the Pacific Northwest. *Canadian Journal of Forest Research* 32, 1503-1517.
- Richter, K., Eckstein, D., Holmes, R.L. (1991): The dendrochronological signal of pine trees (*Pinus* spp.) in Spain. *Tree-Ring Bulletin* 51, 1-13.
- Rolland, C., Michalet, R., Desplanque, C., Petetin, A., Aime, S. (1999): Ecological requirements of *Abies alba* in the French Alps derived from dendro-ecological analysis. *Journal of Vegetation Science* 10, 297-306.
- Rubino, D.L., McCarthy, B.C. (2000): Dendroclimatological analysis of White Oak (*Quercus alba* L., Fagaceae) from an old-growth forest of southeastern Ohio, USA. *Journal of the Torrey Botanical Society* 127, 240-250.
- Thomson, V.P., Nicotra, A.B., Steinbauer, M.J. (2001): Influence of previous frost damage on tree growth and insect herbivory of *Eucalyptus globulus globulus*. *Austral Ecology* 26, 489-499.
- Walters, J.R., Bell, T.L., Read, S. (2005): Intra-specific variation in carbohydrate reserves and sprouting ability in *Eucalyptus obliqua* seedlings. *Australian Journal of Botany* 53, 195-203.
- Wong, S.C., Cowan, I.R., Farquhar, G.D. (1978): Leaf Conductance in Relation to Assimilation in *Eucalyptus pauciflora* Sieb Ex Spreng - Influence of Irradiance and Partial-Pressure of Carbon-Dioxide. *Plant Physiology* 62, 670-674.
- Yeh, H.-Y., Wensel, L.C. (2000): The relationship between tree diameter growth and climate for coniferous species in northern California. *Canadian Journal of Forest Research* 30, 1463-1471.

Mean sea level pressure composite mapping as an exploratory tool in dendroclimatology

A. Fowler

School of Geography and Environmental Science, The University of Auckland, Private Bag 92019, Auckland New Zealand. Email: a.fowler@auckland.ac.nz

Introduction

A typical starting point in dendroclimatological research is to statistically relate tree-ring growth indices to local or regional climate variables (response function analysis). This sometimes leads to identification of links between tree growth and perturbations in atmospheric circulation, the latter often oscillatory in nature, such as the El Niño - Southern Oscillation (ENSO) phenomenon. This approach relies on the researcher linking the (hopefully known) local-scale climate impacts of an oscillatory phenomenon with the response function results. An alternative is to directly investigate relationships between tree growth and atmospheric circulation using composite mapping techniques. Here I explain and demonstrate composite mapping, using the United Kingdom Meteorological Office gridded global monthly mean sea level pressure data set (GMSLP2.1f) and *Agathis australis* (kauri) tree rings.

Data

Gridded Pressure

Although the mapping of global MSLP has a long history, digital gridded MSLP data sets covering significant portions of the globe (required for the compositing analysis presented here) are a relatively recent development (Barnett et al. 1984; Harnack and Harnack 1984; Jones and Wigley 1988; Jones et al. 1987; Jones 1991). The methods used to develop these have evolved considerably over the last twenty years (e.g. establishing background climatology, spatial interpolation techniques, error detection and correction), but the basic requirement of reconstructing a spatial grid from incomplete point data is common.

By the mid-1990s, attempts were being made to combine regional gridded data sets, such as that of Jones (1991), to produce a full global domain. One result of these activities was the United Kingdom Meteorological Office GMSLP2 data set used by Allan et al. (1996) to investigate global MSLP patterns associated with the El Niño – Southern Oscillation (ENSO) phenomenon. Blending diverse regional gridded data sets was a complex exercise, having to deal with a myriad of additional problems, such as: differences in grids and time periods; differences in how missing data was dealt with; and spatial inhomogeneities between data sets (Basnett and Parker 1997). Several versions of GMSLP2 were produced as methods developed, including the direct incorporation of observed data to supplement the blended gridded data (Basnett and Parker 1997). GMSLP2.1f is the version of the data set used here.

GMSLP2.1f is a gridded 5° latitude by 5° longitude fully global monthly MSLP data set for the period 1871 to 1994. Basnett and Parker (1997) evaluated GMSLP2.1f. They note that the inclusion of quality-controlled observed data (since GMSLP2.1a) has improved reliability, but they also identify several weaknesses. These include the need to resort to climatology in data sparse regions, especially in the Southern Hemisphere prior to 1951, and a lack of reliability in earlier decades.

Kauri tree rings

The proxy data used here is the modern kauri master chronology (AGAUM04a) built by Fowler et al. (2004). Fowler et al. provided details of kauri, the data used to build the chronology, and the chronology construction method. For the 1871-1994 period (corresponding to GMSLP2.1f), the kauri master was built from at least 145 trees from 15 sites, growing throughout kauri's natural growth range in the far north of New Zealand (north of 38S). Fowler et al. standardised the kauri tree ring width time series used to build the master using very flexible smoothing splines (50% variance cut-off at 20 years). The standardisation maximised the climate signal in kauri by removing radii- and tree-specific "noise", resulting in a master tree-ring chronology with utility for investigating high frequency climate forcing, but lacking multi-decadal to century scale information.

Southern Oscillation Index (SOI)

The ENSO component of this research was limited to the most commonly used index of the SO, the normalised pressure difference between Tahiti and Darwin. These are relatively long-term surface air pressure recording sites, near the respective poles of the SO across the equatorial Pacific Ocean. Specifically, monthly SOI values (1871–1994) published on the Internet by CSIRO Division of Atmospheric Research were used. These values are relative to a 1933–1992 base period.

Auckland Drought Index

Fowler and Adams (2004) modelled soil water for Auckland using a daily soil water balance model. Model details were presented by Fowler (1999) and application for long-term soil water modelling was described by Fowler (2002). Fowler and Adams (2004) computed monthly mean soil water deficits and used a 1900–1994 subset for MSLP composite mapping. The same data set is used here.

Composite Mapping

Composite mapping is a technique used by climatologists to identify consistent spatial patterns in relationships. For example, Allan et al. (1996) investigated the global-scale fingerprint of ENSO by mapping common responses (frosts, fires, temperature, precipitation, etc) to past El Niño and La Niña events. When applied to gridded MSLP data, compositing involves looking for patterns within the MSLP fields, typically expressed in terms of anomalies relative to some reference period. These anomaly fields are then interpreted in

terms of associated impacts on the frequency and/or strength of prevailing winds, which in turn may help explain observed statistical relationships.

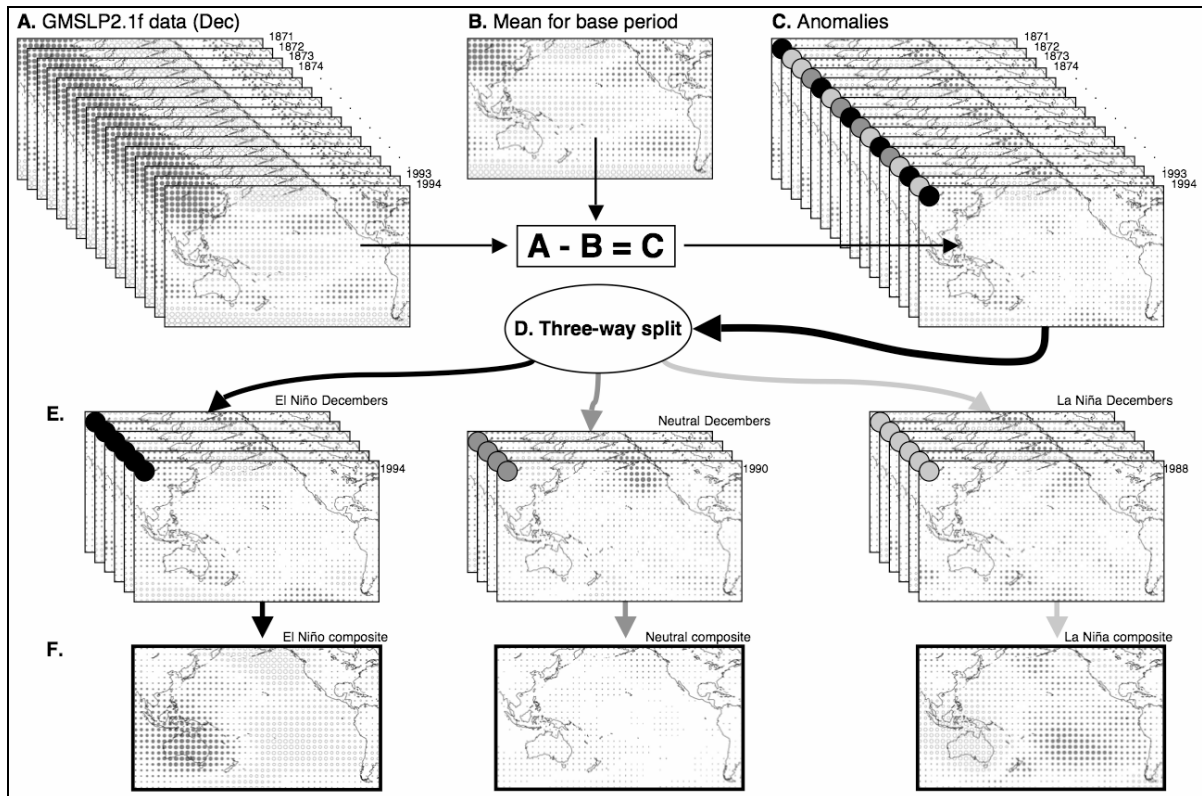


Figure 1: Schematic representation of composite mapping using a card stack analogy. Solid (open) dots indicate MSLP above (below) standard atmospheric pressure at sea level (A, B), or positive (negative) MSLP anomalies (C, E, F). Dot area indicates magnitude (± 30 hPa for A, B, C, E; ± 3 hPa for F). Shaded dots in the top left corners of stacks in C and E indicate the way cards are split (based on a compositing key variable).

Figure 1 is a schematic representation of composite mapping, as applied to the GMSLP2.1f data set, using the analogy of a stack of cards. December is used here to demonstrate the method for a subset of the global domain, centred on the Pacific Ocean. The same method would be repeated for other months and results subsequently combined into time periods of interest (e.g. seasons or longer multi-month blocks). Starting from the 1488 monthly cards in the GMSLP2.1f data set, through to interpretation of the composite spatial anomaly fields, can be viewed as the nine-step process outlined below.

Figure 1A represents the full set of GMSLP2.1f data for December (124 cards). The dots on the top card show the data grid. Solid (open) dots indicate MSLP above (below) standard atmospheric pressure at sea level (1013.25 hPa), with the area of the dots indicating the magnitude of the departure (ca. ± 30 hPa). For the purpose of this demonstration the full set of cards is used for compositing. However, because of the quality issues previously outlined, it may be appropriate to limit analysis to a high quality period (e.g. 1951-1994). Some research questions may also require the use of temporal subsets, or even multiple subsets where evolving patterns are being investigated. Splitting the pressure data into monthly sub-

stacks is the first step in composite mapping. Determining the temporal subset(s) to use is the second.

Several broad scale features are apparent in Figure 1A which characterise the atmospheric circulation in December. These include the Siberian High in the northwest corner, the Aleutian Low in the north Pacific, equatorial low pressure, high pressure ridges either side of the equator, and the low pressure band in the south. These features are a function of the annual cycle and are therefore common to all cards in the December stack. Differences between Decembers are subtle changes in the relative strength of the features and small shifts in position. Consequently, when an average is computed for the stack (Fig. 1B), the common features come through strongly. Computation of this gridded mean field is the third compositing step, calculated over the entire temporal subset, or for a more restricted base period (e.g. 1961-90). The latter is particularly appropriate where a comparison is being made with other data sets where a reference base line period has been used, such as the SOI.

The fourth step is the calculation of gridded pressure anomaly fields (Fig. 1C). This is simply the mean fields subtracted from the original pressure data for each month. This generates a new stack of gridded pressure field “anomalies” relative to normal conditions which shows the magnitude and spatial extent of anomalous MSLP features. Solid (open) dots now indicate positive (negative) pressure anomalies. In the case of December 1994, the anomaly field (Fig. 1C) shows a strengthening of both the Siberian High and the Aleutian Low, with much of the eastern Pacific rim experiencing higher than normal pressure. All subsequent analyses use the anomalies data set.

The primary purpose of composite mapping is to investigate if there are consistent patterns in MSLP anomaly fields associated with potential forcing factors or some consequent impact. For example, compositing based on sea-surface temperatures in the NINO3.4 region of the equatorial Pacific could reveal MSLP anomalies (which may or may not be forced) associated with ENSO events. Conversely, compositing based on local drought may indicate persistent pressure anomalies forcing local climate variation. To do the compositing, a relevant “compositing key” variable is used to make a three-way split of the gridded anomalies stack (Fig. 1D). Monthly or annually resolved compositing keys can be used and the three-way split can be into equal or unequal sub-stacks (Fig. 1E). Three-way splitting of the data is the fifth compositing step.

The sixth step is calculation of mean gridded MSLP for each of the three composites (Fig. 1F). This is intended to bring out any common spatial pattern associated with the compositing key. The example shown in Figure 1 is for ENSO-based compositing. Cards in the left stack of Figure 1E are Decembers during El Niño years (including December 1994), cards in the right stack are Decembers during La Niña years (including December 1988), and the middle stack is for all other Decembers (including December 1990). Averaging through the El Niño composite cards gives the characteristic MSLP anomaly pattern for El Niños of high pressure over Australia, extending into Southeast Asia and the Indian Ocean, with a boomerang-shaped low pressure anomaly field in the eastern Pacific. The La Niña composite shows a near-opposite pattern, and no significant anomaly pattern is associated with the

ENSO-neutral composite. Note though that there is an order of magnitude change in the scale of the anomalies plotted in Figure 1F. Whereas December anomalies for 1988 (La Niña), 1990 (ENSO-neutral) and 1994 (El Niño) are ± 21 hPa, the mean anomalies for the El Niño and La Niña composites are less than 2 hPa. Clearly the patterns emerging from the compositing analysis are subtle relative to inter-annual variability, at least in terms of monthly data.

The seventh step is to numerically combine (e.g. by averaging) monthly plots, such as those shown in Figure 1F, into multi-month blocks of interest (e.g. seasons). These are then plotted (Step 8, Fig. 1F). If spatial patterns in the composite maps are apparent, these are then interpreted in terms of altered wind fields and associated local climate effects (Step 9). For example, in the case of the El Niño composite, the positive pressure anomalies over Australia indicate more frequent and/or more intense high pressure systems, bringing an increased chance of drought. They also indicate more frequent and/or stronger southerly quarter winds over New Zealand, resulting in cooler conditions, but a complex precipitation response (due to interactions with New Zealand's complex topography).

A Kauri Example

The discussion to this point has systematically summarised a standard climatological analysis technique. This section is a novel application of that technique to a high resolution climate proxy. The intention is to demonstrate how composite mapping can be used to identify the climate reconstruction potential of a proxy.

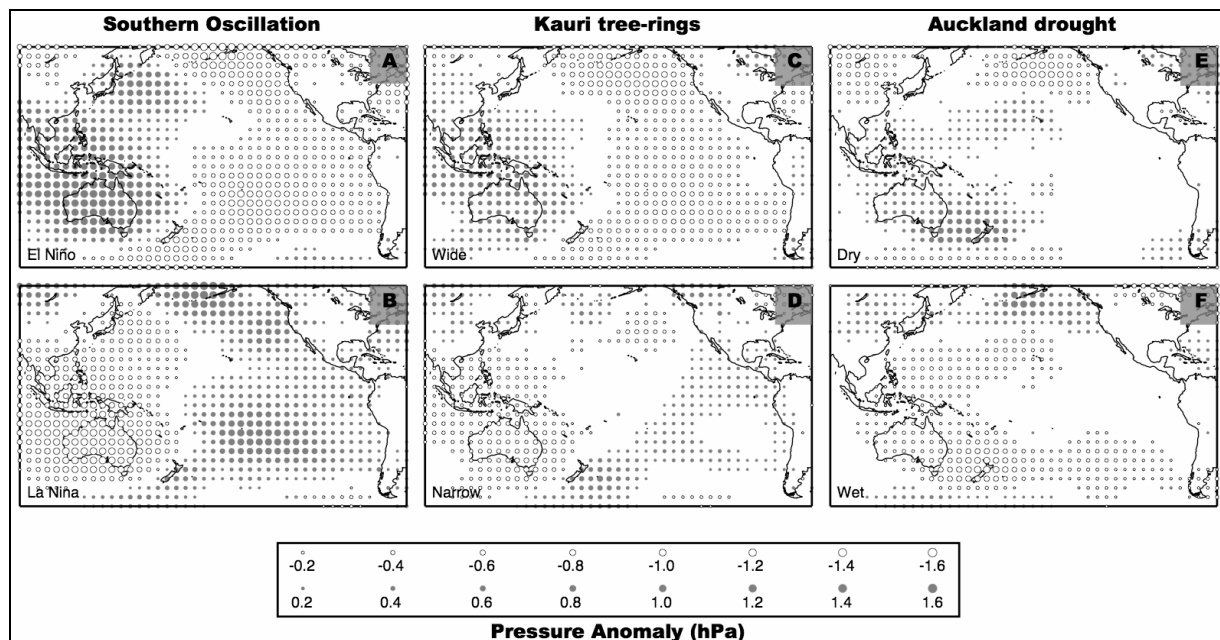


Figure 2: September to February MSLP anomaly composite maps for three compositing key variables (SOI, kauri tree-ring indices, Auckland drought). Composites were calculated for the common period 1901-1994 with equal three-way splits into composite stacks (only high and low composites shown).

Figure 2 shows compositing results derived from a 1901-1994 subset of GMSLP2.1f for three compositing key variables (SOI, kauri tree-ring indices, Auckland drought). The analyses were limited to the six month window from September to February, based on known persistent negative correlations between kauri tree-ring indices and local monthly precipitation and surface air temperature over this interval (Buckley et al. 2000). The 1901-1994 time period was determined by the limit of the available drought index data (Fowler and Adams 2004). Auckland has the longest record of climate data within kauri's growth range, and is conveniently close to the middle of that range (see Fowler et al. (2004) for details).

The SOI and drought analyses were based on monthly compositing, in which each month was separated into three stacks based on the composite key value for that specific month. This is as described in Section 3. For kauri, however, there was only one index value for each year, so the compositing was done based on whole six month blocks. For example, if the tree-ring index for a given year corresponded to a high composite (wide ring), then each month from September to February was allotted to a high composite stack. Equal three-way splitting of the months was done for each compositing key.

MSLP composite maps for wide and narrow kauri tree rings (Fig. 2C, D) indicate Pacific Basin wide relationships. Wide rings are associated with positive anomalies over South-east Asia and Australia; and also with negative anomalies extending in a boomerang shape from the northern central, through the eastern, to the southern central Pacific (south and east of New Zealand). Narrow rings show close to a near-reversal of the anomaly patterns in a band extending from the South-east Asian archipelago to the southern ocean, southeast of New Zealand. A weaker reversal to positive pressure anomalies is also apparent in the eastern Pacific, but this breaks down in the northern Pacific.

The kauri growth region in the far north of New Zealand lies between the pressure anomaly features centred over Australia and Indonesia, and those (of opposite sign) to the southeast of New Zealand. This means that wide and narrow kauri tree rings are associated with significant and opposite wind field perturbations. For example, in the case of wide rings, the pressure anomaly fields shown in Fig. 2C would be expected to cause an increase in the frequency and/or strength of south-westerly winds, bringing relatively cool and dry conditions. The associated pressure anomaly fields for narrow rings would be expected to result in warmer and wetter conditions.

The MSLP composite maps for kauri contrast with those for Auckland dry and wet phases (Fig. 2E, F). The latter demonstrate some spatially extensive anomaly patterns, but the most obvious features are synoptic-scale patterns straddling New Zealand. In contrast, the kauri composite maps exhibit strong similarity to those corresponding to ENSO phases (Fig. 2A, B). The agreement between the El Niño composite map (Fig. 2A) and that for kauri wide rings (Fig. 2C) is particularly striking. The kauri wide-ring anomalies are weaker and there is no significant high pressure anomaly east of Japan, but the patterns are otherwise nearly identical, especially in the Australasian region (including the demarcation between positive and negative anomalies). Anomaly patterns associated with narrow rings (Fig. 2D) agree well with the La Niña composite (Fig. 2B) in a band from Indonesian extending through to the

southeast of New Zealand, but the representation of the La Niña phase positive eastern Pacific anomaly pattern is weaker, especially in the north Pacific.

Clearly, kauri has rather more potential as an ENSO proxy than as a drought proxy. The fact that the best agreement is between wide rings and El Niño suggests that kauri may have greater value as an El Niño than a La Niña proxy. It may also provide a better representation of the western than eastern pole of the SO.

Conclusions

The results show that composite mapping is a powerful tool for tree-ring research, capable of identifying atmospheric circulation characteristics associated with wide and narrow tree rings, and helping to determine the potential of tree rings for reconstructing atmospheric circulation features. Note though that the example presented here is very limited. A more detailed compositing-based analysis of the relationship between kauri growth and ENSO in Fowler (2005) shows additional applications in stationarity and sensitivity analyses, and to refining understanding of tree growth response to forcing. Fowler (2005) also discusses some of the pitfalls of composite mapping.

References

- Allan, R.J., Lindesay, J.A., Parker, D.E. (1996): El Niño Southern Oscillation and Climatic Variability. CSIRO Publications, Melbourne. pp. 405.
- Barnett, T.P., Brennecke, K., Limm, J., Tubbs, A.M. (1984): Construction of a near-global sea-level pressure field. Scripps Institute of Oceanography, La Jolla, CA, *SIO Reference Series* 84-7.
- Basnett, T., Parker, D. (1997): Development of the Global Mean Sea Level Pressure Data Set GMSLP2, *Climate Research Technical Note 79*, Hadley Centre, United Kingdom Meteorological Office.
- Buckley, B., Ogden, J., Palmer, J., Fowler, A., Salinger, J. (2000): Dendroclimatic interpretation of tree-rings in *Agathis australis* (kauri). 1. climate correlation functions and master chronology. *J Roy Soc NZ* 30: 263-275.
- Fowler, A.M. (1999): Potential climate change impacts on water resources in the Auckland Region (New Zealand). *Clim Res* 11, 221-245.
- Fowler, A.M. (2002): Assessment of the validity of using mean potential evaporation in computations of the long-term soil water balance. *J Hydrol* 256, 248-263.
- Fowler, A.M. (2005): Sea-level pressure composite mapping in dendroclimatology: advocacy and an *Agathis australis* (kauri) case study. *Clim Res* 29, 73-84.
- Fowler, A., Adams, K. (2004): Twentieth century droughts and wet periods in Auckland (New Zealand) and their relationship to ENSO. *Int J Climatol* 24: 1947–1961.
- Fowler, A., Boswijk, G., Ogden, J. (2004): Tree-ring studies on *Agathis australis* (kauri): a synthesis of development work on Late Holocene chronologies. *Tree-Ring Res* 60:15-29.
- Harnack, J., Harnack, R.P. (1984): A Southern Hemisphere sea level pressure data set for use in climate studies. *J Climatol* 4: 187-204.

- Jones, P.D. (1991): Southern Hemisphere sea level pressure data: an analysis and reconstructions back to 1951 and 1911. *Int J Climatol* 11: 585-607.
- Jones, P.D., Wigley, T.M.L. (1988): Antarctic gridded sea level pressure data: an analysis and reconstruction back to 1957. *J Clim* 1: 1199–1220.
- Jones, P.D., Wigley, T.M.L., Briffa, K.R. (1987): Monthly mean pressure reconstructions for Europe (to 1780) and North America (to 1858). US Department of Energy Carbon Dioxide Research Division, Washington DC *DoE Technical Report TR037*, p 99.

High-resolution carbon and oxygen isotope profiles of tropical and temperate liana species

A. Verheyden^{1,2}, G. Helle¹, G.H. Schleser¹ & H. Beeckman²

¹ Forschungszentrum Jülich GmbH, Institut für Chemie und Dynamik der Geosphäre, ICG-V Sedimentäre Systeme, Leo-Brandt Strasse, 52425 Jülich, Germany

² Laboratory of Wood Biology and Xylarium, Royal Museum of Central Africa (RMCA), Leuvensesteenweg 13, 3080, Tervuren, Belgium.

Email: anouk.verheyden@africamuseum.be

Introduction

Previous studies on high-resolution isotope measurements in wood have found a remarkable annual cyclicity in the isotope profile and this for temperate as well as tropical tree species (Schleser et al. 1999, Helle and Schleser 2004, Helle et al. 2004, Verheyden et al. 2004). The presence of this annual cyclicity offers great potential for tropical dendrochronology in general. Indeed, if these results can be confirmed in other tropical tree species, the annual isotope signal can be used to identify annual tree ring boundaries in trees that do not produce anatomical tree ring boundaries (a problem commonly encountered in tropical trees) (Verheyden et al. 2004). However, the high-resolution isotope profiles could not entirely be explained by changes in environmental conditions. Previous investigations suggested that the isotope signal is probably the result of a post-photosynthetic signal on which the environmental signal is superimposed (Helle and Schleser 2004, Verheyden et al. 2004). In this context, the post-photosynthetic signal is defined as the signal resulting from additional fractionations occurring after leaf sugar synthesis, such as fractionations involved in the storage and remobilization of starches. If high-resolution isotope profiles are to be used for dendrochronological purposes, two fundamental questions need to be answered: 1) is the annual cyclicity in the isotope profile a universal pattern and 2) can the environmental signal be separated from the post-photosynthetic signal(s)?

In this study, the high-resolution stable carbon and oxygen isotope profiles of three liana species were investigated to contribute to the growing knowledge on changes in the intra-annual isotopic composition of tree rings. More specifically, the aim of this study was to 1) investigate whether there is a periodicity in the high-resolution stable isotope profiles in tropical and temperate liana species, 2) compare the isotope profiles of a tropical evergreen, a temperate evergreen and a temperate deciduous species, 3) compare the oxygen and carbon isotope profiles.

Materials and Methods

Three liana species were investigated: the temperate evergreen *Hedera helix* (Fam. Araliaceae), the temperate deciduous *Clematis vitalba* (Fam. Ranunculaceae) and the tropical evergreen *Tetracera alnifolia* (Fam. Dilleniaceae). *H. helix* and *C. vitalba* were collected on 14 November 2004 in Zavelenberg, Sint-Agatha-Berchem, Belgium. *T. alnifolia* was collected

in 1989 from the Kouilou region, Republic of Congo. All samples are now part of the Royal Museum for Central Africa, Tervuren, Belgium. From each sample, a series of tangential wood slices of 20 to 40 μm thickness were obtained for isotope measurements using a fixed-blade sledge microtome (Polycut E, LEICA Microsystems, Bensheim, Germany). No cellulose extraction of the samples was performed, since many studies have reported a constant offset between the isotopic composition of bulk wood and cellulose (e.g. Livingston and Spittlehouse, 1996, Saurer et al., 2000, Helle and Schleser, 2004).

Results and Discussion

Hedera helix

Both, the stable carbon and oxygen isotope profiles of *H. helix* show an annual cyclicity (Fig. 1). The lowest $\delta^{13}\text{C}$ value occurs at the tree ring boundary, after which a gradual increase takes place. The decrease in $\delta^{13}\text{C}$ begins in the late stage of the growth ring formation (at approximately 2/3 of the ring width). The $\delta^{18}\text{O}$ also shows a lowest value at the tree ring boundary, however, the highest value precedes the maximum of the $\delta^{13}\text{C}$ value. In the year 2003, $\delta^{13}\text{C}$ and $\delta^{18}\text{O}$ show higher values than in the two other years (Fig. 1). These higher values are most likely caused by the severe drought that occurred in that year (Trigo et al., 2005). Furthermore, it is interesting to note that the $\delta^{13}\text{C}$ and $\delta^{18}\text{O}$ pattern look very similar in 2002 and 2003, which indicates that both signals detain similar information during this time period, however the signals differ in 2004.

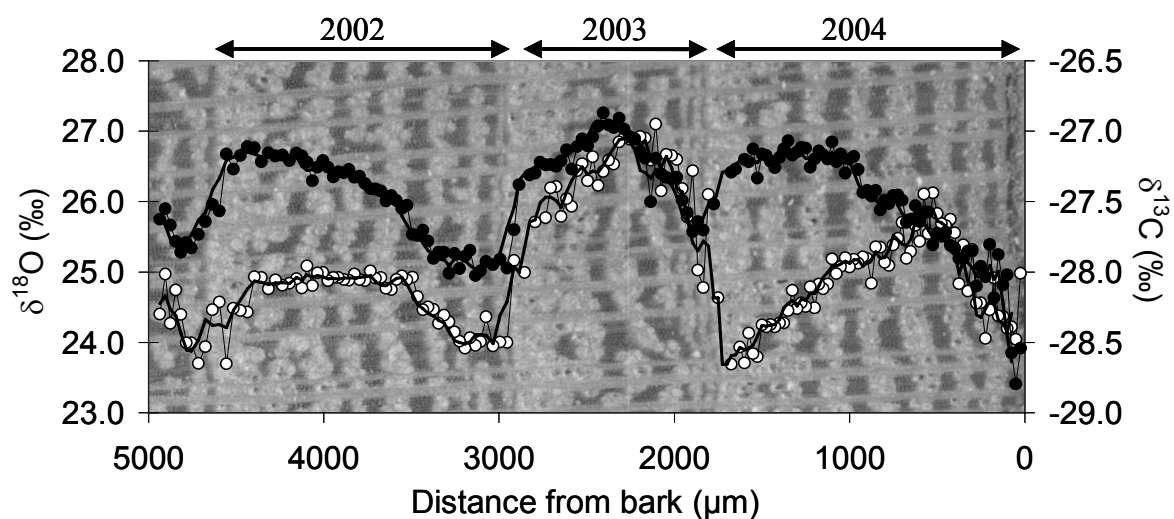


Figure 1: High-resolution stable oxygen (solid symbols) and carbon (open symbols) isotope profiles of *Hedera helix*.

Clematis vitalba

Similar to the profiles of *H. helix*, the $\delta^{13}\text{C}$ and $\delta^{18}\text{O}$ profiles of *C. vitalba* also show an annual cyclicity (Fig. 2). However, the annual $\delta^{13}\text{C}$ signal is strongly influenced by the 2003 drought, which probably also affected the year 2004. The $\delta^{13}\text{C}$ pattern under more 'normal' environmental conditions is therefore, implied from the year 2002. The $\delta^{13}\text{C}$ pattern of *C. vitalba* differs from *H. helix* in that the highest value and the consequent decrease in $\delta^{13}\text{C}$ occurs in the earlywood and therefore, in an early stage of the growth ring formation, while a

more or less stable value is obtained in the latewood. Interestingly, this pattern has also been observed in *Quercus* spp. (Helle and Schleser, 2004). Both *C. vitalba* and *Quercus* spp. are ring porous and characterized by an abrupt difference between small vessels in the latewood and large vessels in the earlywood. Ring porous species are known to use stored carbohydrates to develop their earlywood vessels, prior to leaf emergence and therefore, prior to the production of new photosynthetic material (Aloni, 2004). This affects the $\delta^{13}\text{C}$ profile in particular, as indicated by the high $\delta^{13}\text{C}$ value in the earlywood of 2004, but not the $\delta^{18}\text{O}$ profile, which is consistent with the results from Hill et al. (1995). Indeed, these authors found that the $\delta^{13}\text{C}$ value of the earlywood was influenced by the previous year carbohydrates, while the $\delta^{18}\text{O}$ value was not, due to exchange with current-year xylem water. The similarity in the isotope profiles of *C. vitalba* and *Quercus* spp. offers additional evidence that the shape of the $\delta^{13}\text{C}$ profile is probably mainly controlled by post-photosynthetic processes. The $\delta^{18}\text{O}$ signal has a lowest value in the vicinity of the tree ring boundary, while the highest value occurs in the latewood and therefore, is considerably different from the $\delta^{13}\text{C}$ profile (Fig. 2).

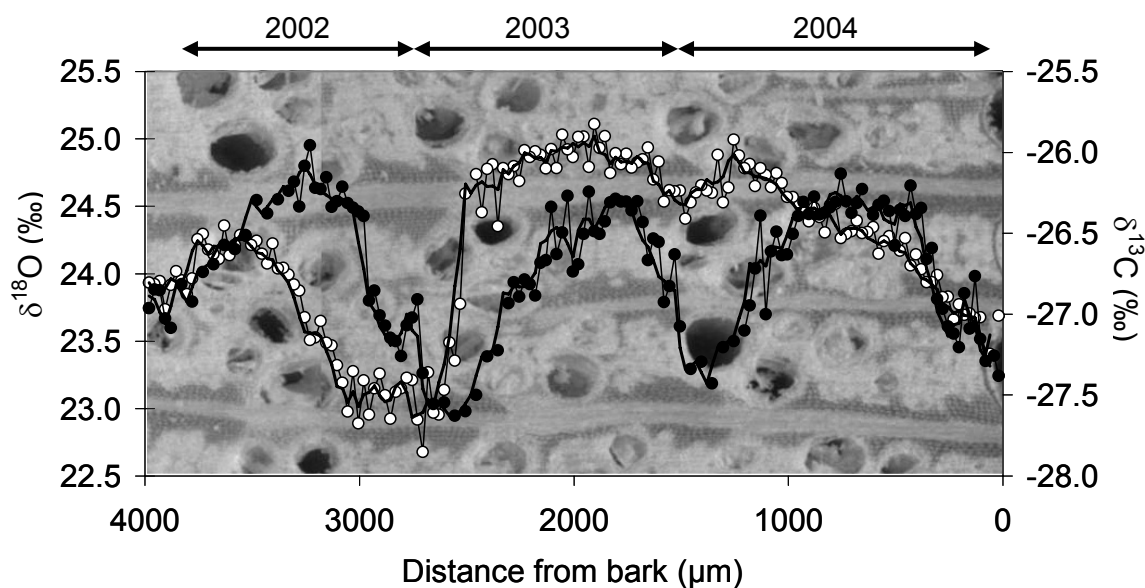


Figure 2: High-resolution stable oxygen (solid symbols) and carbon (open symbols) isotope profiles of *Clematis vitalba*.

Tetracera alnifolia

Similar to the temperate liana species, the isotope signal in this tropical species also shows considerable variation in the high-resolution profile (Fig. 3), with peak amplitudes (2 ‰) exceeding those observed in the temperate liana species (1.5 ‰). However, the isotopic composition of *T. alnifolia* was measured over a larger wood section (by a factor of about 3) as compared to the temperate liana species.

Although the *T. alnifolia* sample originated from a region with a distinct dry season of four months, no distinct growth ring boundaries could be identified, nor does the $\delta^{13}\text{C}$ profile present the typical periodicity observed in other temperate and tropical trees (e.g. Helle and Schleser 2004, Helle et al. 2004, Verheyden et al. 2004). Due to the absence of distinct

growth ring boundaries, we can at this moment, not confirm whether the observed peaks are annual, nor can we exclude the possibility that the peaks reflect severe droughts which are known to occur in the region sporadically. Comparison of the peaks with particular anatomical features (Fig. 3) reveals only partial association of peaks with indistinct anatomical structures in the wood. These results illustrate that the use of high-resolution profiles for identification of growth ring boundaries in tropical woody plants is not straightforward and needs to be further confirmed in different species.

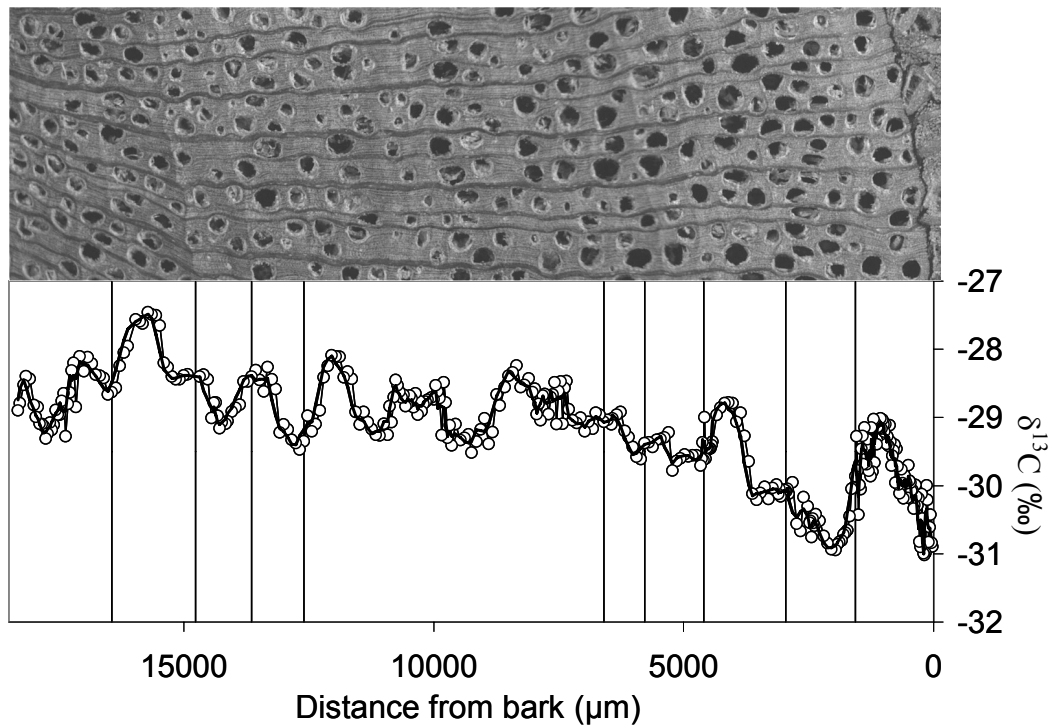


Figure 3: High-resolution stable carbon isotope profiles of *Tetracera alnifolia*. Vertical lines indicate position of observed indistinct anatomical features.

Conclusions

The results from this study add evidence for the presence of an annual cyclicity in the isotope profiles of temperate woody plants. Although the annual cyclicity could not be proven in the evergreen tropical liana species, the considerable variation in the high-resolution isotope profile is remarkable for this species which shows relatively little variation in wood anatomical features. Furthermore, the results obtained here suggest that the shape of the profiles are species specific, but that they can be classified according to similarities in the pattern. Comparison of the profiles of different species, can then further give insight in the processes involved in the shaping of the profile as was observed here for *C. vitalba* and *Quercus* spp. Finally, the study clearly showed that, unlike the results obtained in other studies (Barbour et al. 2002, Verheyden et al. 2004), the $\delta^{18}\text{O}$ and $\delta^{13}\text{C}$ values do not give similar signals in the two temperate liana species, pointing to different causes of their formation.

Acknowledgements

The authors would like to thank Dr. S. Godefroid from the Vrije Universiteit Brussel for collecting the temperate liana samples, W. Laumer, M. Schrimpf and G. Reiss of the Forschungszentrum Jülich, Germany, for their assistance during this work.

References

- Aloni, R. (2004): The Induction of Vascular Tissues by Auxin. In: Davies, P.J. (Ed.), *Plant Hormones. Biosynthesis, Signal Transduction, Action!* Kluwer Academic Publisher: 471-492.
- Barbour, M.M., Walcroft, A.S., Farquhar, G.D. (2002): Seasonal variation in $\delta^{13}\text{C}$ and $\delta^{18}\text{O}$ of cellulose from growth rings of *Pinus radiata*. *Plant, Cell and Environment* 25: 1483–1499.
- Helle, G., Schleser, G.H. (2004): Beyond CO_2 -fixation by Rubisco – An interpretation of $^{13}\text{C}/^{12}\text{C}$ variations in tree rings from novel intra-seasonal studies on broadleaf trees. *Plant, Cell and Environment* 27: 367–380.
- Helle, G., Treydte, K.S., Verheyden, A. (2004): Tropical *Swietenia macrophylla* wood reveals a systematic recurring carbon isotope pattern. In: Jansma, E., Bräuning, A., Gärtner, H., Schleser, G.H. (Eds), *Tree Rings in Archaeology, Climatology and Ecology, Volume 2 Proceedings of the DENDROSYMPOSIUM 2003, May 1st – 3rd 2003, Utrecht, The Netherlands*: 107 – 109.
- Hill, S.A., Waterhouse, J.S., Field, E.M., Switsur, V.R., Aprees, T. (1995): Rapid recycling of triose phosphates in oak stem tissue. *Plant Cell and Environment* 18: 931-936.
- Livingston, N.J., Spittlehouse, D.L. (1996): Carbon isotope fractionation in tree ring early and late wood in relation to intragrowing season water balance. *Plant, Cell and Environment* 19: 768–744.
- Saurer, M., Cherubini, P., Siegwolf, R. (2000): Oxygen isotopes in tree rings of *Abies alba*: The climatic significance of interdecadal variations. *Journal of Geophysical Research – Atmospheres* 105: 12461–12470.
- Schleser, G.H., Helle, G., Lücke, A., Vos, H. (1999): Isotope signals as climate proxies: the role of transfer functions in the study of terrestrial archives. *Quaternary Science Reviews* 18: 927-943.
- Verheyden, A., Helle, G., Schleser, G.H., Dehairs, F., Beeckman, H., Koedam, N. (2004): Annual cyclicity in high-resolution stable carbon and oxygen isotope ratios in the wood of the mangrove tree *Rhizophora mucronata*. *Plant, Cell and Environment* 27: 1525-1536.

SECTION 2

CLIMATOLOGY - NORTHERN HEMISPHERE

Effect of uncertainty in instrumental data on reconstructed temperature amplitude for the European Alps

U. Büntgen¹, D.C. Frank¹, R. Böhm² & J. Esper¹

¹Swiss Federal Research Institute WSL, Zürcherstrasse 111, 8903 Birmensdorf, Switzerland

Email: buentgen@wsl.ch

²Central Institute for Meteorology and Geodynamics, Hohe Warte 38, 1190 Vienna, Austria

Introduction

We compiled two recent high-resolution climate reconstructions (Büntgen et al. 2005a, b) estimating millennial-long temperature variations in the European Alps. These records show similar long-term behavior including the Medieval Warm Period (MWP), Little Ice Age (LIA), and recent warmth (Grove 1988, IPCC 2002, Lamb 1965), however, vary in their estimates of the absolute reconstructed temperature amplitude. Reasons for these amplitude ranges are manifold, including the utilization of differing tree-ring parameters (ring width and maximum latewood density), slightly varying instrumental targets, and differing calibration methods. This regional-scale finding is even more striking for the Northern Hemisphere, where uncertainty in reconstructed amplitudes is in the order of the total variance estimated over the last millennium (Esper et al. 2005a, b).

Herein, we more systematically study the effect of utilizing instrumental target data on the reconstructed Alpine temperature amplitude. We re-calibrate the two temperature reconstructions (Büntgen et al. 2005a, b) against two differing 20th century instrumental datasets representing the same area in the Alps, and test the effect of changing calibration periods and seasonal means on the obtained amplitude. We show that reconstructed amplitude ranges in the order of $\sim 1\text{-}1.4^\circ\text{C}$ solely result from scaling against different instrumental target datasets. Further amplitude variations are quantified and their relevance for the 'true' long-term course of Alpine temperature variability discussed.

Data and methods

Two Alpine datasets of 1527 tree-ring width (TRW; 951-2002 period) and 180 maximum latewood density (MXD; 755-2004 period) measurement series were used for chronology development (Büntgen et al. 2005a, b). Sub-alpine larch (*Larix decidua* Mill.) samples were collected from living trees and historic material (Büntgen et al. 2006), all from elevations $>1,500$ m asl. The TRW dataset additionally includes 417 pine (*Pinus cembra*) samples (Nicolussi and Schiessling 2002). The MXD chronology compiles larch samples only. No data overlap between the MXD and the TRW chronologies exists, although, 120 out of 180 MXD measurements derive from the >1500 TRW dataset. To preserve high to low frequency variation from the measurement series, data were detrended using regional curve standardization (RCS; Briffa et al. 1992, Esper et al. 2003). Key distinctions between the TRW and MXD data are the larch bud moth correction performed on the MXD measurements (Esper et al. 2005c), and the differing seasonal signal captured (TRW=JJA, MXD=JJAS). For details, e.g., site ecology, growth/climate response, detrending, and reconstruction

development, see Büntgen et al. (2005a) and (2005b) for the TRW and MXD data, respectively.

The TRW and MXD based JJA and JJAS temperature reconstructions correlate at 0.55 over the 951-2002 common period. Correlations increase to 0.61-0.66 after 10-60-year low-pass filtering. Both records provide evidence for a pronounced MWP, LIA and recent warmth (Fig. 3). Key differences include higher temperatures in the 960–80s and 1200–20s as indicated by the MXD record, and higher temperatures prior to AD 1000, and slightly cooler conditions in the early 13th century as indicated by the TRW record. The MXD reconstruction captures a distinct cold period ~1040-60s that is less pronounced in the TRW data. Both parameters reveal generally cool conditions between ~1350-1850, accompanied by inter-decadal fluctuations, i.e., low temperatures during 1580-1710, and relatively high temperatures ~1500 and ~1800. Temperatures discontinuously increase since ~1710. A remarkable cold period is seen ~1810-20, and 20th century warming is indicated from the early 1910s to the end of the 1940s, and from the late 1960s to present.

For calibration, two instrumental grids of monthly temperature anomalies with respect to the 20th century (spanning 1901-2000) are used. These include nine 1°x1° (updated 2004-11-release of Böhm et al. 2001) and 42 0.5°x0.5° (Mitchell and Jones 2005) grid-points, hereafter referred to as HISTALP and CRU, respectively. Both grids cover the same region in the western-central Alps (45°-47°N and 6°-9°E). Key distinctions between the regional-scale HISTALP and large-scale CRU compilations include the homogenization, gridding, and clustering procedure, and consideration of altitudinal effects in the HISTALP network (>1,400 m asl). For details see Böhm et al. (2001), Auer et al. (2005) and Mitchell and Jones (2005).

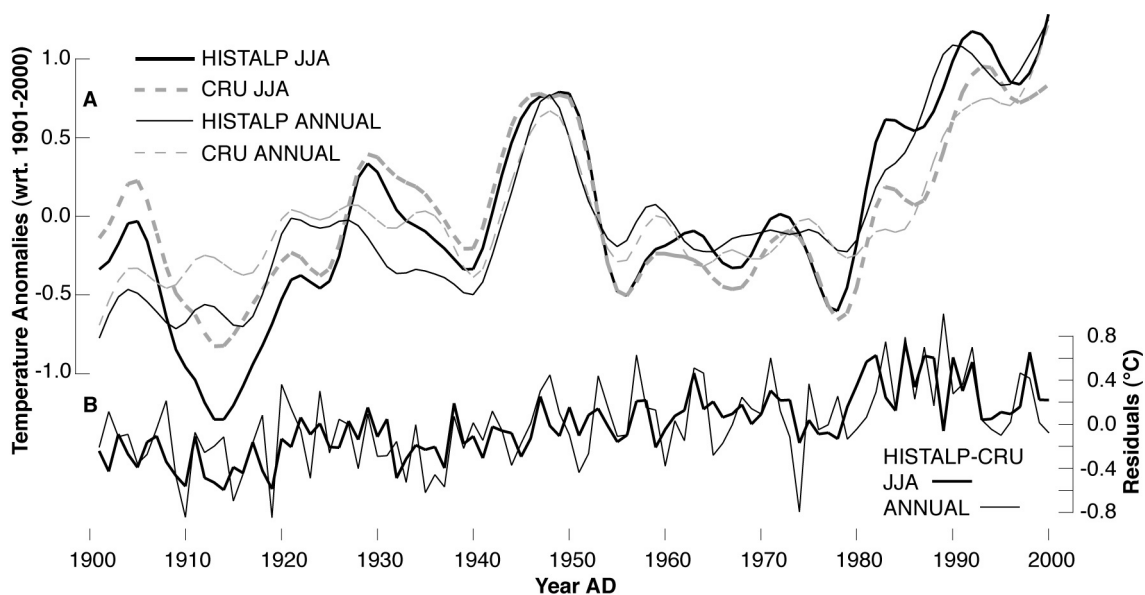


Figure 1: **A** Comparison of the (JJA and annual) HISTALP and CRU data after 10-yr low-pass filtering (1901-2000). **B** Residuals (HISTALP minus CRU) computed from the unsmoothed records.

After decadal smoothing, the HISTALP grid shows more, and the CRU grid less 20th century warming (Fig. 1A). This trend difference is stronger during summer, but also visible for annual means. Notable offset between the (colder) HISTALP and (warmer) CRU data is seen

before ~1940 and *vice versa* after ~1980. Constantly increasing residuals between the annually resolved grids (HISTALP minus CRU) highlight these longer-term discrepancies. Maximum residuals approach $\pm 1.0^\circ\text{K}$ seen in 1910, 1919, 1974, and 1989, for example (Fig. 1B).

Variability changes within the four instrumental targets, HISTALP/JJA, CRU/JJA, HISTALP/annual, CRU/annual, are indicated by 31-year moving standard deviations computed over the 1901-2000 period (Fig. 2). Similar periods of decreased and increased variability are revealed for all records. Annual values remain below those of the summer season, and CRU values tend to be lower than those of the HISTALP data. High summer variability is computed before 1920, between 1940-1960, and after 1980. Low variability occurred ~1930 and 1970. Variability of the annual means fluctuates less than those of the summer month. These temporal and seasonal differences in the target variability affect the reconstructed amplitude (see below).

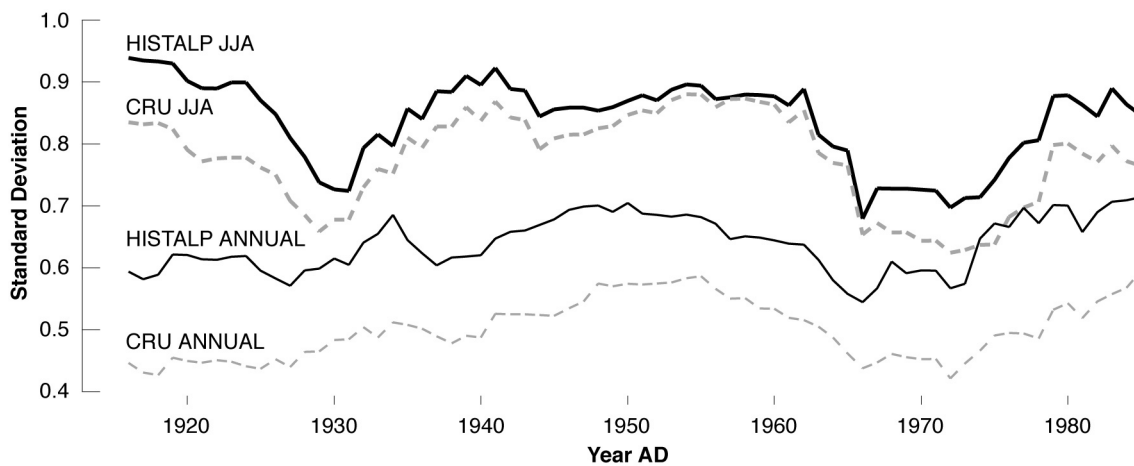


Figure 2: Moving 31-yr standard deviations of the unsmoothed June-August (bold) and annual (thin) mean temperature anomalies from the 20th century, calculated for the HISTALP (black) and CRU (grey) instrumental datasets over the 1901-2000 common period.

Since larger-scale analyses indicate an underestimation of the reconstructed temperature amplitude when using linear regression (Esper et al. 2005a, von Storch et al. 2004), simple scaling, i.e., adjusting the variance and mean is applied. Doing so, the TRW and MXD chronologies are calibrated against June-August (JJA) and annual mean instrumental temperatures. Scaling is performed over the 1901-2000 period of overlap, and additionally over three split periods (1901-1933, 1934-1966, 1967-1999). To assess the model's skill, the explained variance (R^2), and Durbin-Watson index (DW) are computed. The DW statistic tests for lag-1 autocorrelation in the model residuals (Durbin and Watson 1951).

Results

Correlations between the TRW chronology and the HISTALP and CRU instrumental summer temperatures are 0.59 and 0.54. Correlations between the MXD chronology and the HISTALP and CRU instrumental summer temperatures are 0.66 and 0.72. All correlations reach the 99.9% significance level after correction for lag-1 autocorrelation. Correlations with annual mean temperatures are significantly lower (0.42-0.51 for MXD and 0.44-0.46 for

TRW), but slightly higher when using the CRU instead of the HISTALP data. The *DW* index ranges between 1.52 and 1.75 for the TRW reconstruction, and decreases to 1.15-1.46 for the MXD reconstruction, indicating more (less) lag-1 autocorrelation for the MXD (TRW) model residuals. These results lead to the assumption that enhanced high frequency calibration skill exists for the MXD chronology, whereas the TRW chronology performs better in the lower frequency domain.

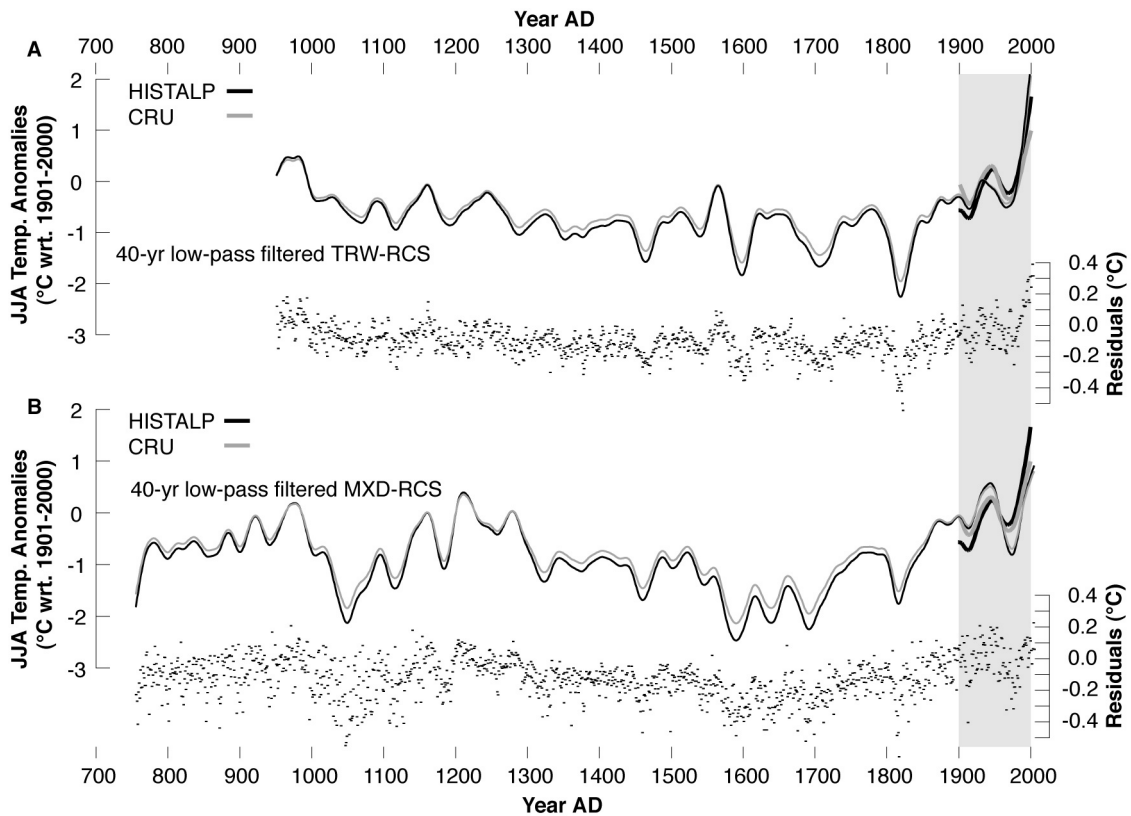


Figure 3: Millennial-long **A**, TRW and **B**, MXD RCS chronologies after scaling against JJA mean temperatures derived from the HISTALP (black) and CRU (grey) grids (1901-2000, grey box). Records are 40-yr low-pass filtered (without padding towards the ends) using a cubic smoothing spline. Annual residuals between the (unsmoothed) reconstructions are shown at the bottom.

After scaling against JJA mean temperatures (HISTALP/CRU), the TRW chronology reveals warmest summers in 2001 (+3.1°C/+2.7°C) and, 2002 (+2.5°C/+2.2°C), and coldest summers in 1821 (-4.1°C/-3.6°C), and 1820 (-3.8°C/-3.3°C). The MXD chronology reveals warmest summers in 2003 (+1.8°C/+1.6°C), 970 and 1928 (both +1.7°C/+1.5°C), and coldest summers in 1816 (-4.7°C/-4.1°C), and 1046 (-4.1°C/-3.6°C). Simple calibration against instrumental data (here scaling) does not change the long-term course of a reconstruction, but rather only determines the variance of the modeled temperature variability. This amplitude is higher when scaling against summer temperatures rather than annual means (Tab. 1A, B). The difference in amplitude between the temperature reconstructions scaled against HISTALP or CRU data is in the order of ~1°C when modeling summer, and ~1.4°C when modeling annual temperatures. This uncertainty range solely results from the difference in the instrumental target's variability and trend. In other words, uncertainty during the instrumental period propagates into the pre-instrumental period.

Table 1: **A** Calibration statistics (R^2) and (DW) computed over the 1901-2000 period. **B** Annual- and decadal-scale temperature amplitudes of the TRW (1821-2001 and 1810s-1990s) and MXD (1816-2003 and 1810s-1940s) chronologies after scaling against HISTALP and CRU instrumental data.

A	JJA HISTALP		JJA CRU		annual HISTALP		annual CRU		B	
	R^2	DW	R^2	DW	R^2	DW	R^2	DW	JJA HISTALP	JJA CRU
TRW annual	.35	1.52	.29	1.60	.19	1.75	.21	1.67	7.18°C	6.25°C
TRW decadal									4.23°C	3.68°C
MXD annual	.44	1.15	.52	1.46	.18	1.33	.26	1.29	6.49°C	5.64°C
MXD decadal									3.15°C	2.74°C
STDEV target	0.94		0.82		0.74		0.56			

The three split calibration periods (1901-1933, 1934-1966, 1967-1999) result in further amplitude modifications (Fig. 4). The amplitude of the MXD based JJA reconstruction after scaling against the three HISTALP grids ranges from 5.93-6.23°C, with the full 20th century calibration period amplitude being 6.49°C. Scaling against CRU data results in a range from 5.42-5.80°C, with the full calibration period amplitude being 5.64°C. Even wider amplitude ranges are obtained for the TRW based summer temperature reconstruction (5.72-8.90°C/HISTALP, and 5.35-8.70°C/CRU). The calibration period-effect on the reconstructed amplitude using annual mean values shows similar results, with the amplitude of the MXD based annual temperature reconstruction after scaling against the HISTALP grid ranging from 4.18-4.91°C compared with 5.10°C for the full calibration period. After scaling against CRU data, amplitudes range from 2.98-4.13°C, with the full calibration period amplitude being 3.87°C. Even wider amplitude ranges are obtained for the TRW based annual mean temperature reconstruction (4.64-7.25°C/HISTALP, and 3.90-5.96°C/CRU) (Fig. 4).

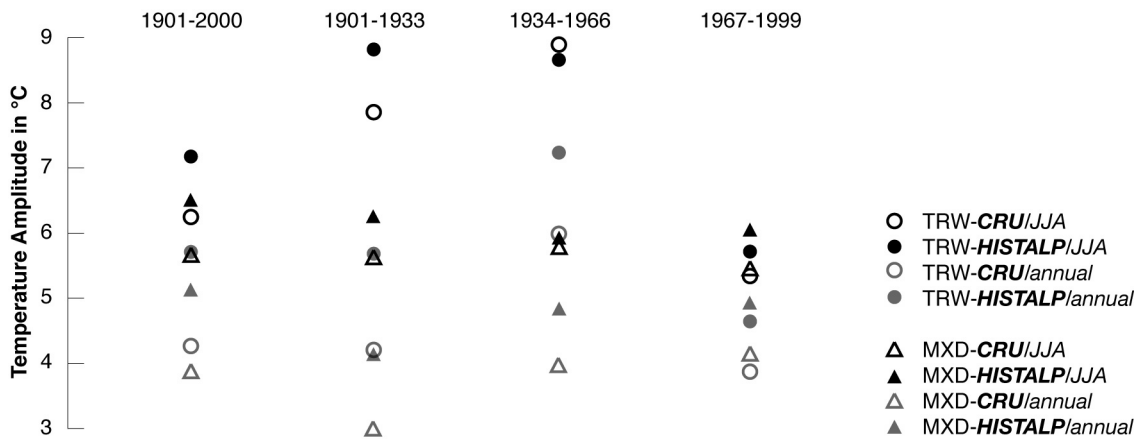


Figure 4: Reconstructed temperature amplitudes after scaling the TRW and MXD chronologies against differing combinations of JJA and annual mean temperatures derived from the HISTALP and CRU grids over differing calibration periods.

JJA and annual mean temperatures (951-2002) after scaling the TRW chronology against HISTALP (CRU) data are -0.68°C (-0.58°C) and -0.53°C (-0.40°C) colder than the 1901-2000 instrumental reference periods. JJA and annual mean temperatures (755-2004) after scaling the MXD chronology against HISTALP (CRU) data are -0.87°C (-0.75°C) and -0.68°C (-0.51°C) colder than the 1901-2000 instrumental reference periods.

Discussion

Two instrumental grids show differing temperature trends and variability over the 20th century. Böhm et al. (2001, p. 1779) already reported characteristic differences between the CRU and HISTALP data: 'The mean annual temperature increase since 1890 in the Alps is 1.1 K, which is twice as much as the 0.55 K in the respective grid-boxes of the most frequently used global dataset of the Climatic Research Unit (CRU; Jones and Moberg 2003).' Trend dissimilarities originate from differing homogenization procedures applied to individual station records. These are performed to reduce the influence of urban artificial heating (Jones et al. 1990), for example. Variability dissimilarities could result from the number of stations included as well as their weightings in the gridding procedure.

We showed that these variations in the instrumental data (increased trend and variability in the HISTALP data) influence the reconstructed pre-observational amplitude. Since HISTALP utilizes a denser network of stations including a more detailed examination of the station metadata (Auer et al. 2005, Böhm et al. 2001), we believe that this dataset is a more precise representation of surface temperature variations of the European Alps, whereas, the CRU grid is more large-scale in nature.

Besides this variation from using differing instrumental targets, uncertainty is large in long-term temperature reconstructions, and includes those within the proxy developed, and the calibration method applied (Esper et al. 2005a). Uncertainty within the tree-ring proxy, such as sample reduction back in time (Frank and Esper, this issue), trees responding rather to maximum than mean temperatures (Wilson and Luckman 2005), changes in the growing season length, slow ecological response shifts (Büntgen et al. 2005c), reduced site control of historic material (Büntgen et al. 2006), and methodological detrending uncertainties (Cook et al. 1995, Esper et al. 2003) cannot be discounted. A possible change in the annual cycle of temperatures would further affect the relationship between predictor and predictand (Jones et al. 2003). Since a vertical component in Alpine climate diminishes correlation between instrumental stations more than horizontal separation does (Böhm et al. 2001), uncertainty exists, if predictor and predictand originate from differing altitudinal belts. Methodological uncertainty additionally emerges from the differing calibration approaches including scaling or regression (Esper et al. 2005a), which is statistical in nature.

Reconstructed amplitudes of the TRW and MXD records, even though, they show no overall linear trend after simple scaling, i.e., $r^2=0.0$ for the 951-2002 and 755-2004 periods, respectively (Fig. 3A, B), vary from 2.98-8.90°C, solely depending on the instrumental calibration target data, season, and period used. The upper part of this wide amplitude spectrum is dominated by TRW based summer temperature reconstructions whereas the lower end of the spectrum is dominated by MXD based annual temperature reconstructions. The smallest (largest) amplitude spectrum results from the calibration period 1967-1999 (1901-1933).

Our results indicate that amplitude differences in the order of ~1-1.4°C solely result from scaling against HISTALP or CRU data (Tab. 1). The uncertainty derived here in the relatively short period of instrumental observations affects the reconstructed millennial-long Alpine temperature amplitude in the order of the total warming trend measured for the 20th century. These regional-scale results further diminish, when extended networks of larger-scale are

compiled (Esper et al. 2005b).

We herein suggest to (i) scale instead of regress (ii) over the maximal period of instrumental/proxy overlap, which best captures the full range of temperature variability without underestimations, such as those resulting from regression, (iii) apply the HISTALP grid that is more regional in scope, (iv) use summer instead of annual temperature means, since the proxy is dominantly weighted towards growing season, and (v) perform MXD measurements that reveal slightly more stable growth/climate response patterns.

Acknowledgements

Supported by the EC project ALP-IMP (BBW 01.0498-1) and SNSF (NCCR Climate). U.B. supported by the SNSF project Euro-Trans (#200021-105663).

References

- Auer I, and 31 co-authors (2005): HISTALP – Historical instrumental climatological surface time series of the greater Alpine region 1760-2003. *Int J Climatol* in review.
- Böhm R, Auer I, Brunetti M, Maugeri M, Nanni T, Schöner W (2001): Regional temperature variability in the European Alps: 1760-1998 from homogenized instrumental time series. *Int J Climatol* 21:1779-1801.
- Briffa KR, Jones PD, Bartholin TS, Eckstein D, Schweingruber FH, Karlen W, Zetterberg P, Eronen M (1992): Fennoscandian summers from AD 500: temperature changes on short and long timescales. *Clim Dyn* 7:111-119.
- Büntgen U, Esper J, Frank DC, Nicolussi K, Schmidhalter M (2005a): A 1052-year tree-ring proxy for Alpine summer temperatures. *Clim Dyn* 25:141-153.
- Büntgen U, Frank DC, Nievergelt D, Esper J (2005b): Summer temperature variations for the European Alps, AD 755-2004. *J Clim* in press.
- Büntgen U, Frank DC, Schmidhalter M, Neuwirth B, Seifert M, Esper J (2005c): Growth/climate response shift in a long subalpine spruce chronology. *Trees* doi: 10.1007/s00468-005-0017-3.
- Büntgen U, Frank DC, Bellwald I, Kalbermatten H, Freund H, Schmidhalter M, Bellwald W, Neuwirth B, Esper J (2006): 700 years of settlement and building history in the Lötschental/Valais. *Erdkunde* in press.
- Cook ER, Briffa KR, Meko DM, Graybill DA, Funkhouser G (1995): The 'segment length curse' in long tree-ring chronology development for palaeoclimatic studies. *The Holocene* 5:229-237.
- Durbin J, Watson GS (1951): Testing for serial correlation in least squares regression. *Biometrika* 38:159-78.
- Esper J, Cook ER, Krusic PJ, Peters K, Schweingruber FH (2003): Tests of the RCS method for preserving low-frequency variability in long tree-ring chronologies. *Tree-Ring Res* 59:81-98.
- Esper J, Frank DC, Wilson RJS (2004): Low frequency ambition, high frequency ratification. *EOS* 85/12:113, 120.

- Esper J, Frank DC, Wilson RJS, Briffa KR (2005a): Effect of scaling and regression on reconstructed temperature amplitude for the past millennium. *Geophys Res Lett* doi:10.1029/2004GL021236.
- Esper J, Wilson RJS, Frank DC, Moberg A, Wanner H, Luterbacher J (2005b): Climate: Past Ranges and Future Changes. *Quat Sci Rev* 24:2164-2166.
- Esper J, Büntgen U, Frank DC, Nievergelt D (2005c): Waiting for the muth. *Nature* in review.
- Grove JM (1988): The Little Ice Age. Methuen & Co., London and New York, pp 498.
- IPCC (2001): Climate Change: The Scientific Basis. Cambridge University Press. Cambridge, 944 pp.
- Jones PD, Groisman PY, Coughlan M, Plummer N, Wang W-C, Karl TR (1990): Assessment of urbanization effects in time series of surface air temperature over land. *Nature* 347:169-172.
- Jones PD, Moberg A (2003): Hemispheric and large-scale surface air temperature variations: an extensive revision and update to 2001. *J Clim* 16:206-223.
- Jones PD, Briffa KR, Osborn TJ (2003): Changes in the Northern Hemisphere annual cycle: implications for paleoclimatology? *J Geophys Res* doi:10.1029/2003JD003695
- Jones PD, Mann ME (2004): Climate over the past millennia. *Rev Geophys* doi:10.1029/2003RG000143.
- Lamb HH (1965): The early medieval warm epoch and its sequel. *Palaeogeogr Palaeoclimatol Palaeoecol* 1:13-37.
- Mitchell TD, Jones PD (2005): An improved method of constructing a database of monthly climate observations and associated high-resolution grids. *Int J Climatol* 25:693-712.
- Moberg A, Sonechkin DM, Holmgren K, Datsenko NM, Karlén W (2005): Highly variable Northern Hemisphere temperatures reconstructed from low- and high-resolution proxy data. *Nature* 433:613-617.
- Nicolussi K, Schiessling P (2002): A 7000-year-long continuous tree-ring chronology from high-elevation sites in the central eastern Alps. In: Dendrochronology, Environmental Change and Human History. 6th International Conference on Dendrochronology, Quebec City, Canada. August 22nd-27th 2002:251-252.
- Wilson RJS, Luckman B (2003): Dendroclimatic reconstruction of maximum summer temperatures from upper treeline sites in Interior British Columbia, Canada. *The Holocene* 13/6:851-861.

Multiple tree-ring parameters from Atlas cedar (Morocco) and their climatic signal

J. Esper, U. Büntgen, D.C. Frank, D. Nievergelt, K. Treydte & A. Verstege

Swiss Federal Research Institute WSL, 8903 Birmensdorf, Switzerland

Email: esper@wsl.ch

Introduction

Cedrus atlantica ring width data from the site 'Col du Zad' southeast of the main range of the High Atlas (Fig. 1) are included in several regional and larger scale palaeoclimatic analyses (e.g. Chbouki et al. 1995, Glueck and Stockton 2001, Mann et al. 1999, Stockton 1988, Verstege et al. 2004). Ring width data recorded at this site – and basically at all cedar sites in Morocco – correlate with precipitation variation during winter and the vegetation period, allowing for reconstructions of the North Atlantic Oscillation via its fingerprint on regional winter rainfall in Morocco (e.g., Cook et al. 2002). Col du Zad is of particular interest, since individual cedar trees reach ages of 1000 years and more, making this site valuable for millennium long reconstructions of precipitation variability, and via synoptic relationships for long-term temperature estimations.

In an effort to survey the potential of using further measurements in addition to 'traditional' ring width data (TRW) for palaeoclimatic studies, we here assess the climatic signal of multiple tree-ring parameters recorded from *Cedrus atlantica* at Col du Zad: maximum latewood density (MXD), minimum density (MID), latewood width (LWW), and earlywood width (EWW). We present a comparison of these parameters and correlate them with regional temperature and precipitation data. The capability of *Cedrus atlantica* TRW measurements for long-term climate reconstructions is demonstrated by estimating October-September precipitation variations over the past 900 years using a combined 150+ core sample dataset integrating series from the sites Col du Zad and a nearby cedar site Tizi n' Tarhzeft, hereafter referred to as Col and Tiz, respectively.

Material and Methods

Col (32°58'N, 5°04'W) and Tiz (33°06'N, 4°54'W) are located in the Middle Atlas at ~2,150 m a.s.l. (Fig. 1). Tree coverage, influenced by the dry climate in the rain shadow of the first Middle Atlas ranges north of the sampling sites, ranges from 35% at Col to less than 10% at Tiz. 106 core samples from about 70 trees and 57 core samples from about 40 trees were taken at Col and Tiz, respectively. Maximum and mean lengths of the tree-ring series are 1024 and 299 years for Col, and 848 and 371 years for Tiz (Verstege et al. 2004).

We selected 20 core samples from 10 trees in Col to measure high resolution (10 µm) density variations over the past ~200 years using a Walesch-2003 X-ray densitometer (Schweingruber et al. 1978). Selected trees represent different age classes, i.e. young and old cedars were considered. High resolution density profiles were then utilized to derive five

tree-ring parameters TRW, MXD, MID, LWW, and EWW (Schweingruber 1983) for comparison with regional climate data.

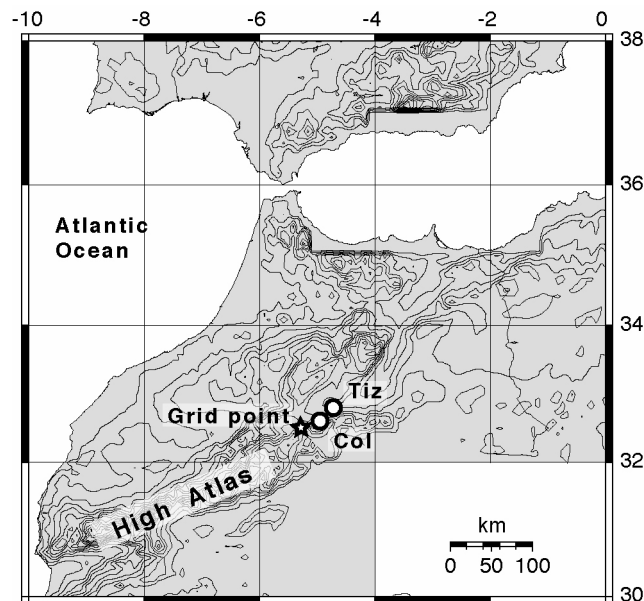


Figure 1: Map showing the tree-ring sampling sites Col and Tiz (circles), and the instrumental climate grid point location (star) in the Middle Atlas, Morocco.

Tree-ring data were standardized by calculating residuals from 300-year fixed splines (Cook 1985), after stabilizing the ‘spread-versus-level relationship’ of individual measurements using a data adaptive power transformation to avoid potential end-effect problems in resulting chronologies (Cook and Peters 1997). Since little to no power was found for the MXD and MID density parameters, effectively no transformation occurred in these measurements. Chronologies were calculated using the arithmetic mean, and the chronologies’ variance stabilized using a method outlined by Osborn et al. (1997). See also Frank et al. (2005), this volume. Signal strength of the arithmetic mean timeseries was estimated by calculating interseries correlations (RBAR) over 50-year intervals lagged by 25 years along the chronologies (Wigley et al. 1984).

To estimate the climatic signal in the proxy data, we correlated each parameter chronology with gridded observational temperature and precipitation data over the 1901-2000 period (Mitchell et al. 2004). The grid-point closest to the tree-ring sites at 32°50’N/5°50’W was considered (Fig. 1).

Results

Long-term negative trends in fitted growth curves (Fig. 2, 300-year splines), likely related to the aging of cedar trees, are similar between TRW, LWW and EWW. They, however, appear on differing levels related to the varying mean widths recorded for these parameters (Tab. 1, 0,73 mm for TRW, 0.13 mm for LWW, 0.60 for EWW). Visual inspection of the detrended measurement series indicates high common variance in TRW and EWW, and less common

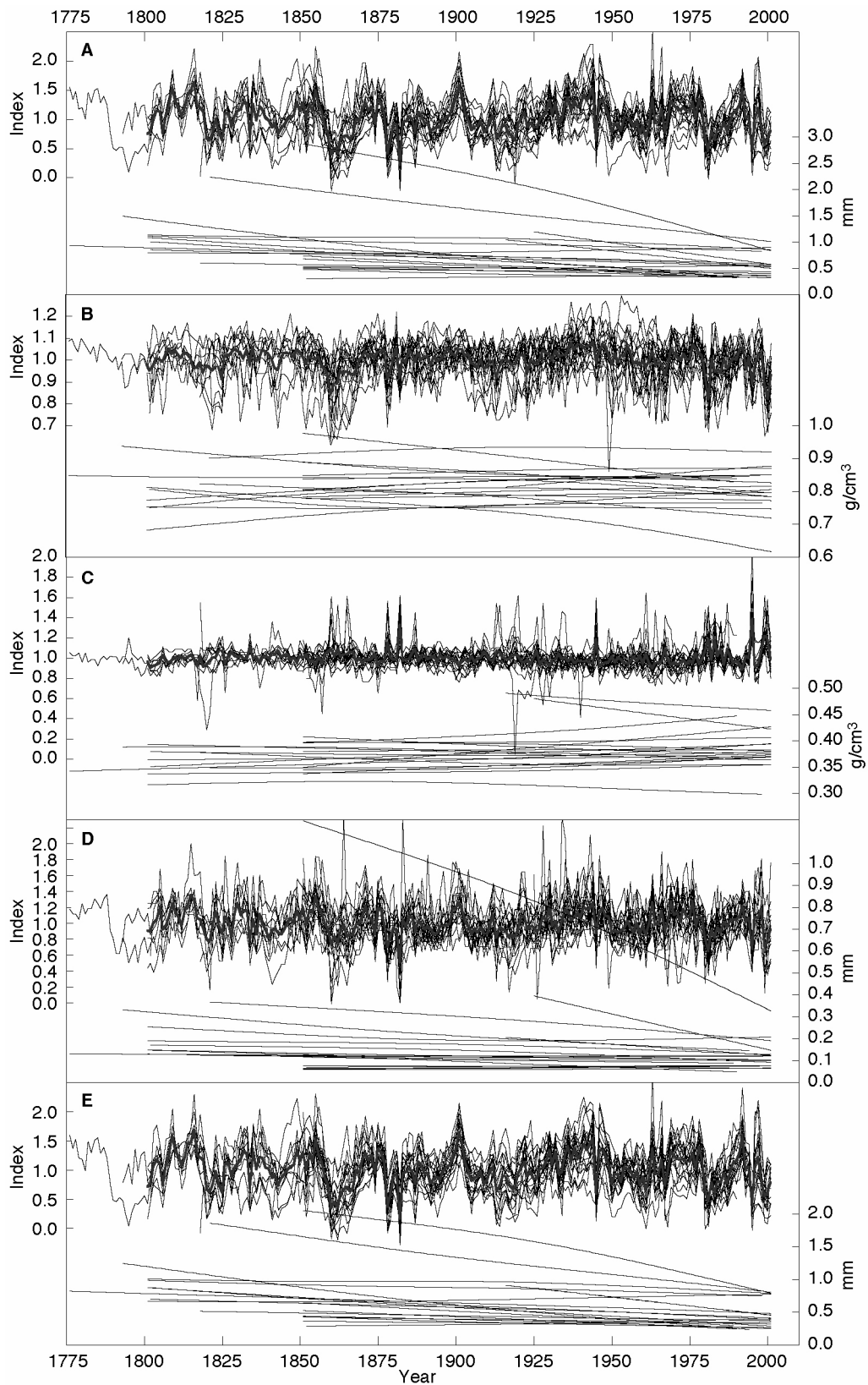


Figure 2: Standardized tree-ring series and 300-year fixed spline growth curves used for detrending. Shown are the results for the 20 core samples from Col for A, TRW, B, MXD, C, MID, D, LWW, and E, EWW.

variation in LWW (Fig. 2), with rich inter-annual to inter-decadal variability seen in all three width parameters.

Table 1: Col multiple tree-ring parameter growth statistics from 20 core samples (10 trees) spanning 1776-2001. 'Mean' is the arithmetic mean over all 3,341 tree-rings. AC (raw) and AC (detr) are the first order autocorrelations of the raw and 300-year spline detrended data, respectively. RBAR (raw) and RBAR (detr) are the interseries correlation of the raw and detrended data, respectively. AC (chron) is the first order autocorrelation of the spline detrended chronology calculated over the 1901-2000 period of overlap with instrumental data.

Parameter	Mean	AC (raw)	AC (detr)	RBAR (raw)	RBAR (detr)	AC (chron)
TRW	0.73 mm	0.70	0.63	0.43	0.41	0.49
MXD	0.82 g/cm ³	0.59	0.53	0.17	0.19	0.52
MID	0.31 g/cm ³	0.32	0.30	0.26	0.28	0.11
LWW	0.13 mm	0.54	0.44	0.24	0.24	0.35
EWW	0.60 mm	0.70	0.63	0.43	0.41	0.48

In comparison, the 300-year splines fitted to the density data indicate positive (MID) and no long-term trends (MXD). Detrended MXD data exhibit high variance between single series relative to the variations of the mean curve, i.e. increased spread between detrended measurements. The detrended MID data, however, behave different from all other parameters. These data show less decadal scale variation, accompanied by remarkably positive extreme values (pointer years). These findings, i.e., the differing low frequency biases in raw measurements (removed by 300-year spline fits), the higher low frequency loading of the standardized width parameters TRW and EWW, and the reduced common variance in the density parameters and LWW, are confirmed by the first order autocorrelations and RBAR statistics averaged over the individual measurement series (Tab. 1).

Interestingly, the chronologies of the width parameters TRW, EWW, LWW correlate >0.90 over the well-replicated 1801-2001 period (Fig. 3a), indicating little independence between these measurements. These high inter-parameter correlations occur even though the common variance in the detrended LWW data is lower than in the TRW and EWW data (Fig. 3b). The width parameter chronologies (TRW, EWW, LWW) are also similar to the MXD results (Fig. 3a) with correlations over the 1801-2001 period all >0.65. The comparison of multiple parameters further reveals that only the MID data shows somehow different information. MID variations correlate negatively with all other parameters. The lowest but still significant correlation (-0.50) is found between the MID and MXD chronologies (1801-2001 period). Common variance in the MID data is higher than in the MXD data (except for one segment centered around 1860, Fig. 3b).

With respect to the limited independence between these various tree-ring parameters, it is not surprising that the correlations with monthly and seasonal temperature and precipitation data show similar patterns (Fig. 4a). Overall, temperature has no significant impact on any of the considered parameters. February precipitation sums correlate significantly with all parameters, and May and June sums with MID. MID correlations are opposite to the results

obtained from all other parameters. These patterns are also valid for the seasonal precipitation records (Oct-Sep, Feb-Apr, Dec-Jul) that overall indicate the highest diagnostic skill of the tree-ring parameters (with the sign of the MID correlation again reversed). Highest correlations are found between MID and October-September (-0.54) and December-July (-0.55) precipitation sums. Visual inspection of the fit with October-September precipitation (Fig. 4b) indicates that both inter-annual and decadal scale variations are well captured in the MID data. This seems surprising, since MID generally appeared to possess lowered loading in the decadal scale frequency domain (Fig. 2).

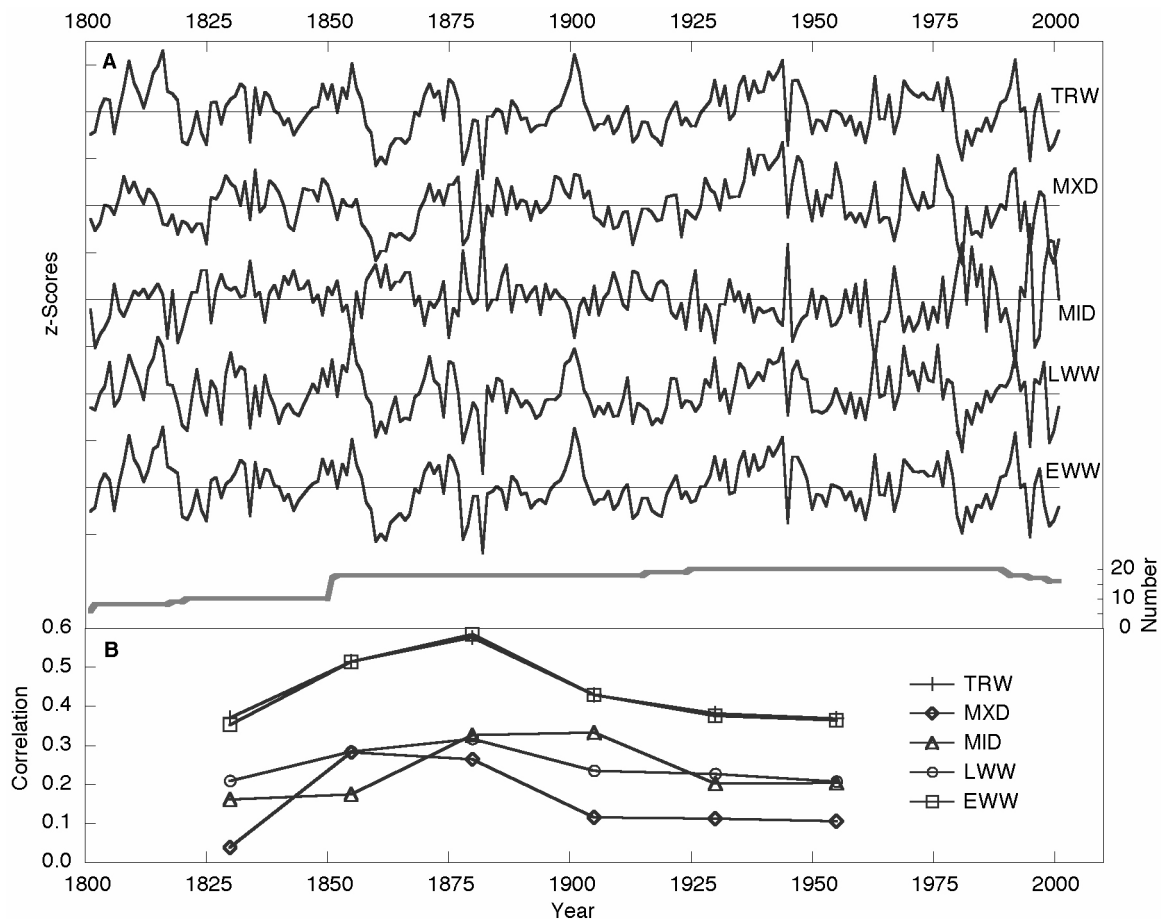


Figure 3: Tree-ring chronologies and common variance statistics. **A**, 300-year spline detrended TRW, MXD, MID, LWW, and EWW tree-ring chronologies and sample replication (bottom). **B**, Interseries correlations (RBAR) calculated for 50-year segments lagged by 25 years.

The correlation between MID and MXD data ($r = -0.50$, 1801-2001 period; Fig. 5) was rather unexpected, since no such relationship is reported for tree-ring data from high latitude, temperature sensitive sites (Briffa et al. 1998, Schweingruber et al. 1996). For the Moroccan data, it basically indicates that low MID values, seemingly caused by high precipitation sums (Fig. 4), are linked with high MXD values. The relationship is stronger in the higher frequency than in the lower frequency domains, i.e. is -0.59 for 10-year high-pass and -0.45 for 10-year low-pass filtered data, both calculated over the 1801-2001 period.

Since low MID values are indicative for wide earlywood cells, the MID data significantly correlate with the TRW (-0.64) and EWW (-0.64) chronologies, calculated over the 1801-2001 period. This dependency is again well known from high latitude tree sites (Schweingruber et al. 1996).

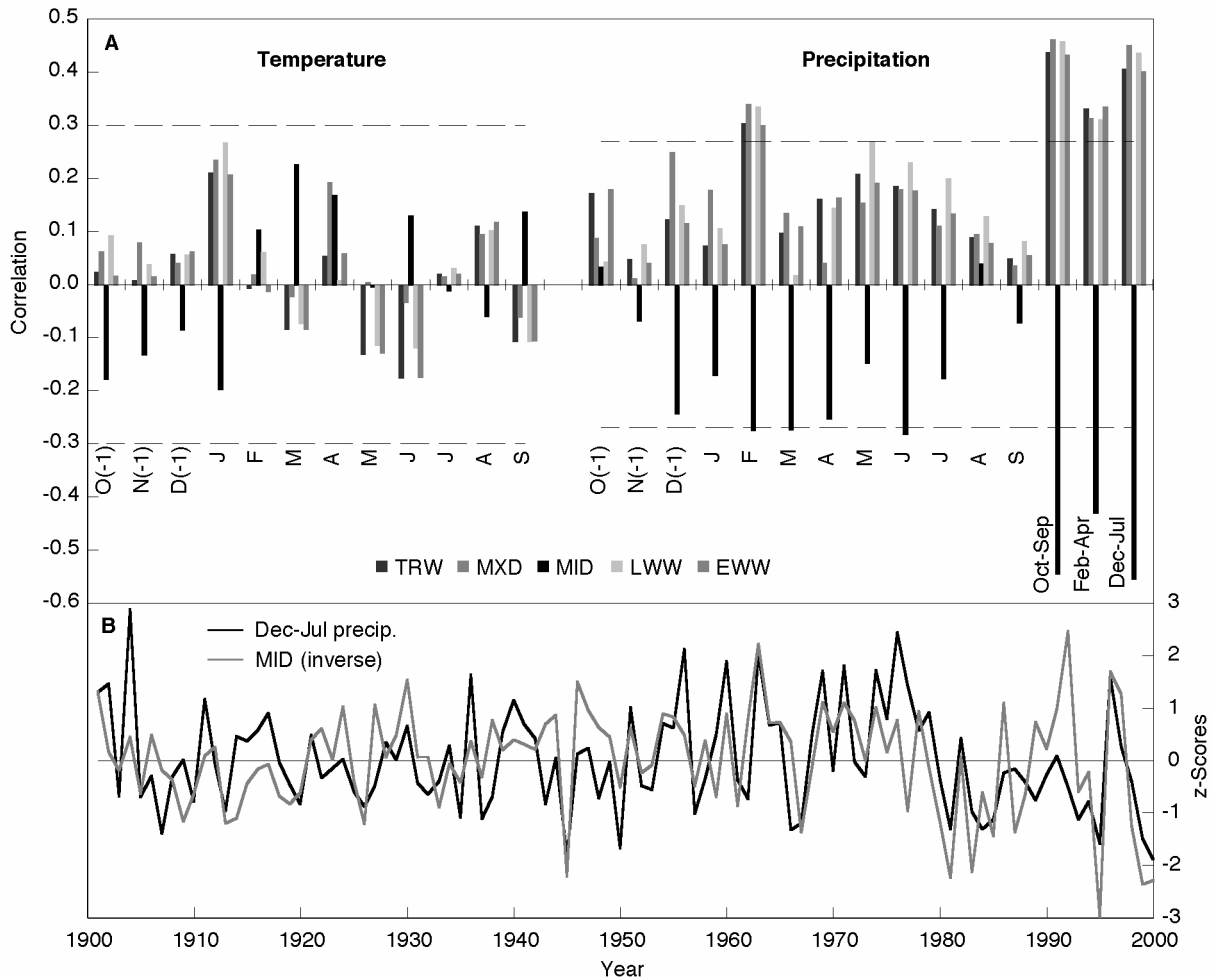


Figure 4: Climate signal of multiple tree-ring parameters, and MID versus precipitation comparison. A, Pearson correlation coefficients between Col tree-ring parameters (TRW, MXD, MID, LWW, EWW) and temperature and precipitation data. Climate data represent the closest grid point provided by the Climatic Research Unit (Mitchell et al. 2004). Temperatures are monthly mean values, and precipitation monthly and seasonal sums. Horizontal lines indicate (maximum) $p < 0.01$ significance levels, corrected for lag-1 autocorrelation considering the October-September climate data. For tree site and grid point locations see figure 1. **B,** Visualization of the fit between December-July precipitation and (inverse) MID data.

To demonstrate the potential of these additional tree-ring parameters (particularly MID), for estimating past climate variability, a long-term reconstruction of October-September precipitation sums back to AD 1100 is shown (Fig. 6a). This record represents a combination of 157 TRW series from Col and Tiz, regressed against observational grid point data (Mitchell et al. 2004). The model explains 36% of the variance of instrumental data during the 1902-2000 period of overlap ($r = 0.60$). Linear regression, as applied here to transfer the proxy data into precipitation estimates, reduces the models' variance in the order of the un-

explained variance (Fig. 6b), i.e. there is a tendency that the model underestimates the ‘true’ variance of precipitation sums over the past 900 years (Esper et al. 2005).

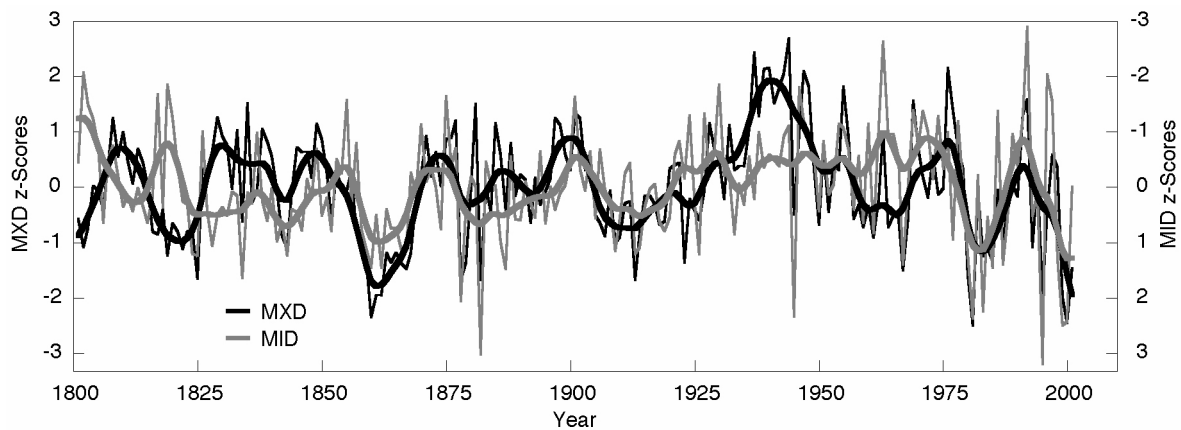


Figure 5: Comparison of the 300-year spline detrended MXD and MID chronologies. Data are normalized over the 1801-2001 period (correlation is -0.50). Bold curves are 10-year smoothed values. MID is inverted.

The precipitation reconstruction also seems to be biased by an increase in variance back in time. This change in variability appears, even though the variance of the TRW chronology was stabilized using the method outlined by Osborn et al. (1997). These variance changes are in part related to the decrease in sample replication back in time (minimum replication in AD 1100 is 3 core samples), accompanied by an increase in interseries correlation as expressed by the RBAR measurements (Fig. 6a). For details on this issue see Frank et al. in this volume.

Conclusions

The analysis of multiple tree-ring parameters from Moroccan *Cedrus atlantica* trees, including TRW, MXD, MID, LWW, and EWW, revealed little additional potential to estimate long-term climate variations that would exceed the existing evidence based on TRW only. This conclusion largely stems from the limited independence between several of the tested parameters, namely TRW, LWW, and EWW. For MXD, common variance is much lower than reported from temperature sensitive high latitude sites (e.g. Briffa et al. 1998). Also, the climatic signal (here only significant with precipitation) does not reach the strength as found in TRW data. The MID data, however, seems to provide additional information on past precipitation variations. This occurs despite the fact that the standardized MID series show little lower frequency variability, and reduced signal strength statistics in comparison to TRW and EWW. Due to the nature of MID data, the correlation with precipitation is opposite to TRW measurements. To robustly estimate the potential of MID for climate reconstructions, more data from ecologically differing sampling sites in the Middle and High Atlas would need to be measured. This current analysis suggests that such an effort would be worthwhile.

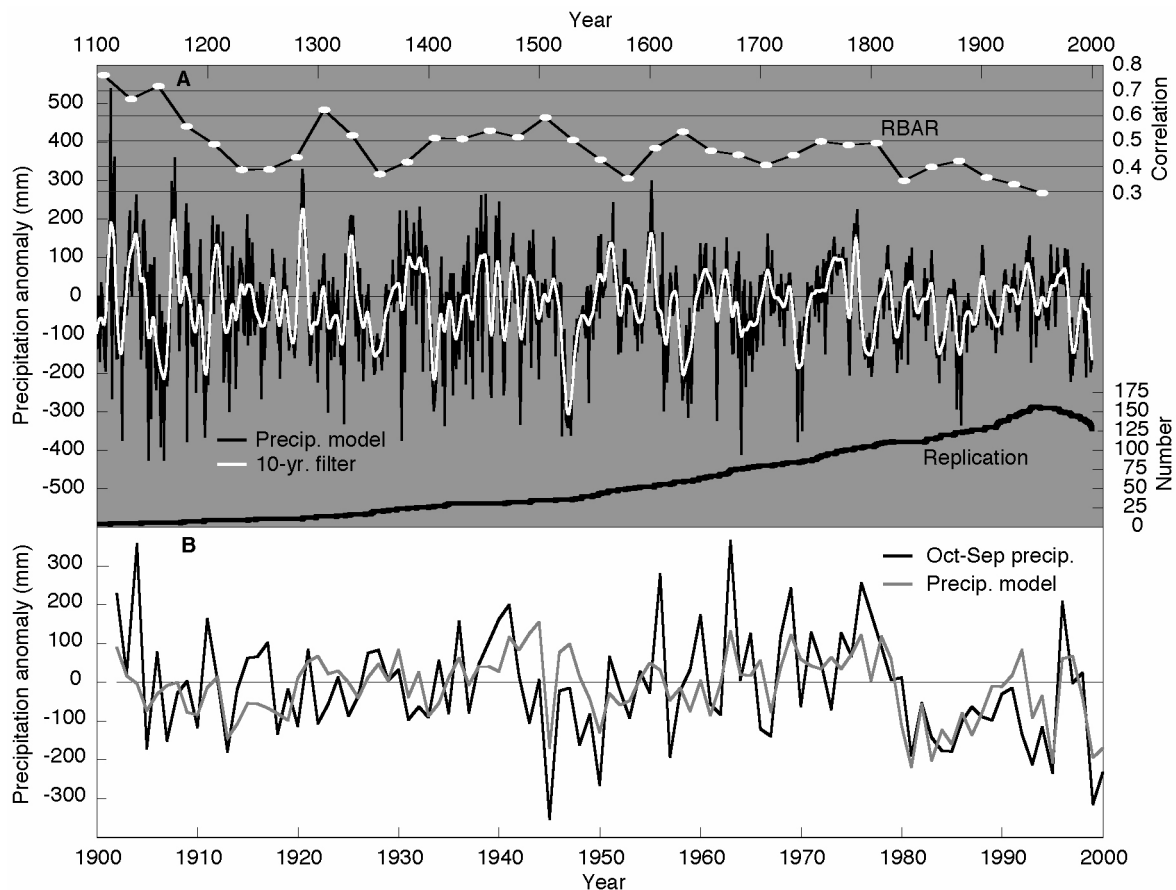


Figure 6: Long-term precipitation model. A, October (previous year) to September precipitation reconstruction back to AD 1100 utilizing 157 ring width measurements from Col and Tiz. Measurements were detrended using a data adaptive power transform, and residuals from 300-year fixed splines calculated. The precipitation model is the variance corrected arithmetic mean of these index series regressed to grid point precipitation data over the 1902-2000 period, with 1902 considering the October to December rainfall sums recorded in 1901. Interseries correlation (RBAR) calculated over 50-year segments lagged by 25 years, and core sample replication are shown at the top and bottom, respectively. **B**, Visualization of the fit between the model and observational data in the 20th century. Correlation is 0.604.

MID data also seem to be related to MXD data, a novel finding not reported from other density analysis (Schweingruber, pers. comm.). While this seems to be an interesting feature, we do not have a physical explanation for this dependency. The association between MID and MXD is mainly driven by the higher frequency, inter-annual component, and the level of correlation (-0.50 over the 1801-2001 period) seems to be robust enough to further investigate the association between these parameters.

The capability of cedar trees for climate reconstruction is revealed by a long-term precipitation model using TRW data. Artifacts resulting from changes in sample replication, inter-sample cross-correlation, and variance changes in the detrended single measurements, make this reconstruction to indicate an increase in precipitation variability back to AD 1100 (see Frank et al., this volume). The model also indicates that no long-term, centennial-scale precipitation variation is reconstructed over the past 900 years. This characteristic is likely related to the individual spline detrending procedure that removes lower frequency variation from the TRW data (Cook et al. 1995, Esper et al. 2003), i.e., the model as presented here

does not allow for an evaluation of potential centennial scale variation, as, for example, recently reconstructed in Europe, the US, and Central Asia (Cook et al. 2004, Treydte et al. 2005, Wilson et al. 2005). These issues demonstrate the profound impacts that methodology can have on resulting reconstructions. More data and tests using differing detrending methods would be necessary to explore the low frequency spectrum of long-term precipitation variability in Morocco.

Acknowledgements

Supported by the Swiss National Science Foundation (Grants # 2100-066628, 'Millennia', # 200021-105663, 'EuroTrans'), and the European Community (Grant # EVK2-CT-2002-00147, 'Isonet').

References

- Briffa, K.R., Schweingruber, F.H., Jones, P.D., Osborn, T.J., Shiyatov, S.G., Vaganov, E.A. (1998): Reduced sensitivity of recent tree-growth to temperature at high northern latitudes. *Nature* 391: 678-682.
- Chbouki, N., Stockton, C.W., Myers, D.E. (1995): Spatio-temporal patterns of drought in Morocco. *International Journal of Climatology* 15: 187-205.
- Cook, E.R. (1985): *A time series analysis approach to tree-ring standardization*. Lamont-Doherty Geological Observatory, New York, 171 pp.
- Cook, E.R., Briffa, K.R., Meko, D.M., Graybill, D.A., Funkhouser, G. (1995): The 'segment length curse' in long tree-ring chronology development for palaeoclimatic studies. *The Holocene* 5: 229-237.
- Cook, E.R., Peters, K. (1997): Calculating unbiased tree-ring indices for the study of climatic and environmental change. *The Holocene* 7: 361-370.
- Cook, E.R., D'Arrigo, R., Mann, M.E. (2002): A well-verified multiproxy reconstruction of the winter North Atlantic Oscillation index since AD 1400. *Journal of Climate* 15: 1754-1764.
- Cook, E.R., Woodhouse, C., Eakin, C.M., Meko, D.M., Stahle, D.W. (2004): Long-term aridity changes in the Western United States. *Science* 306: 1015-1018.
- Esper, J., Cook, E.R., Krusic, P.J., Peters, K., Schweingruber, F.H. (2003): Tests of the RCS method for preserving low-frequency variability in long tree-ring chronologies. *Tree-Ring Research* 59: 81-98.
- Esper, J., Frank, D.C., Wilson, R.J.S., Briffa, K.R. (2005): Effect of scaling and regression on reconstructed temperature amplitude for the past millennium. *Geophysical Research Letters* 32, doi: 10.1029/2004GL021236.
- Glueck, M.F., Stockton, C.W. (2001): Reconstruction of the North Atlantic Oscillation, 1429-1983. *International Journal of Climatology* 21: 1453-1465.
- Mann, M.E., Bradley, R.S., Hughes, M.K. (1999): Northern Hemisphere temperatures during the past millennium – inferences, uncertainties, and limitations. *Geophysical Research Letters* 26: 759-762.

- Mitchell, D.T., Carter, T.R., Jones, P.D., Hulme, M. New, M. (2004) A comprehensive set of high-resolution grids of monthly climate for Europe and the globe. *Tyndall Center Working Paper 55*, 30 pp.
- Osborn, T.J., Briffa, K.R., Jones, P.D. (1997): Adjusting variance for sample-size in tree-ring chronologies and other regional-mean time-series. *Dendrochronologia 15*: 89-99.
- Schweingruber, F.H. (1983): *Der Jahrring – Standort, Methodik, Zeit und Klima in der Dendrochronologie*. Haupt, Bern.276 pp.
- Schweingruber, F.H., Fritts, H.C., Bräker, O.U., Drew, L.G., Schär, E. (1978): Dendroclimatic studies on conifers from central Europe and Great Britain. *Tree-Ring Bulletin 38*: 61-91.
- Schweingruber, F.H., Briffa, K.R. (1996): Tree-ring density networks for climate reconstruction. In: Jones P.D. et al. (Eds.) *Climatic Variations and Forcing Mechanisms of the Last 2000 Years*. NATO ASI Series I41: 43-66.
- Stockton, C.W. (1988): Current research progress toward understanding drought. In Conference Proceedings: *Drought, Water Management and Food Production*, November 21-24, Imprimerie de Fedala, Mohammedia, 21-35.
- Treydte, K.S., Schleser, G.H., Helle, G., Haug, G.H., Winiger, M., Frank, D.C., Esper, J. (2005): 20th-century precipitation maximum In Western Central Asia from 1000-year tree-ring $\delta^{18}\text{O}$. *In prep.*
- Verstege, A., Esper, J., Neuwirth, B., Alifriqui, M., Frank, D. (2004): On the potential of cedar forests in the Middle Atlas (Morocco) for climate reconstructions. In: Jansma E et al. (Eds.) *Proceedings International Conference TRACE* (Utrecht, May 1-3, 2003), 78-84.
- Wigley, T.M.L., Briffa K.R., Jones, P.D. (1984): On the average of correlated time series, with applications in dendroclimatology and hydrometeorology. *Journal of Climate and Applied Meteorology 23*: 201-213.
- Wilson, R.J.S., Luckman, B.H., Esper, J. (2005): A 500-year dendroclimatic reconstruction of spring-summer precipitation from the lower Bavarian forest region, Germany. *International Journal of Climatology 25*: 611-630.

On Variance Adjustments in Tree-Ring Chronology Development

D. Frank¹, J. Esper¹ & E. Cook²

¹ Swiss Federal Research Institute WSL, 8903 Birmensdorf, Switzerland

² Tree-Ring Laboratory, Lamont-Doherty Earth Observatory, Palisades NY, 10964, USA

Email: frank@wsl.ch

Introduction

In dendrochronology it is common practice to create a mean-value function as the best estimate of the trees' signal at a site. This averaging process helps eliminate noise particular to individual trees and cores thereby increasing the signal quality. The variance of the mean-value function, however, depends upon the number of series averaged together and their interseries correlation (Wigley et al. 1984). As the number of single series rarely remains constant in dendrochronological or more generally climatic investigations, simple averaging routinely produces changes in variance that are solely a by-product of changes in the number of series. This issue extends into a wide variety of fields; relevant examples from global change studies include the construction of instrumental averages with diminishing numbers of stations and spatial representativity back in time (Jones et al. 1999), averages of proxy networks for climate reconstruction (Esper et al. 2002), and in the construction of individual tree-ring chronologies (e.g., Esper et al. 2005, this volume).

Osborn et al. (1997) theoretically provided and experimentally tested a correction procedure to eliminate variance changes resulting from changing sample replication. The basic correction centers around the use of the effective independent sample size, N_{eff} , which considers the sample replication at every time and the mean interseries correlation (hereafter, r_{bar}) between the samples. This is defined as:

$$N_{\text{eff}} = \frac{n(t)}{1 + (n(t) - 1)r}$$

where $n(t)$ is the number of series at time t , and r is r_{bar} . Multiplication of the mean timeseries with the square root of N_{eff} at every time t theoretically results in variance that is independent of sample size. This result can then be further scaled by the square root of $1/r_{\text{bar}}$ to yield an estimate of the mean series in the original units. In the limiting cases, when the r_{bar} is zero or unity, N_{eff} obtains values of the true sample size and unity, respectively. Osborn et al. (1997) extend this basic correction procedure with examples showing possibilities and methods to account for temporal and frequency dependence in r_{bar} . Temporal dependence in r_{bar} may arise from changes in the spatial density of series being averaged together, for example.

In this paper we intend to revisit this topic from a more applied perspective. Specifically, our motivation comes from evaluating the final chronology for the Morocco dataset (see Esper et al. 2005, this volume) corrected with the commonly applied variance stabilization routine incorporated into the program ARSTAN (Cook 1985). After the application of the

“Briffa/Osborn” correction, the variance of this chronology was observed to still increase back in time (Esper et al. 2005, this volume). Corresponding to this increase in variance is an increase in the r_{bar} , which is to a large extent a likely consequence of the higher percentage of correlations computed between cores collected from the same trees (see figure 6 in Esper et al. 2005, this volume). We hypothesize that the correction procedure used in ARSTAN, which does not consider time-dependent changes in the r_{bar} , is limited by this trend in correlation. To more completely assess and potentially improve upon this situation, we developed a routine, following the guidelines of Osborn et al. (1997), to allow for time dependent changes in correlation to be considered in the variance stabilization. We test and compare this time dependent r_{bar} correction method, with the uncorrected average and the sample size correction method that uses a single time independent r_{bar} value (as in ARSTAN).

This paper contains two major themes. In part 1, synthetic datasets are introduced to demonstrate the effects of changing sample size and correlation on the computation of mean chronologies. For each dataset, three mean-value functions and running standard deviations of these mean-value functions are presented. In the second part, we look at the Morocco dataset and evaluate its characteristics with the same array of computations. Results lead us to explore some of the characteristics of the basic tree-ring data from Morocco. We close with a brief discussion and conclusion.

Data

For this study we utilize a set of three synthetic datasets composed of white noise. These datasets possess varying correlation structures and varying sample replication (Fig.1) to allow evaluation of the influence of these features on computation and correction of mean-value functions. The individual series within these datasets have constant variance and no autocorrelation apart from that resulting from chance alone. These three “Cases” should a) illustrate how and when variance inflation occurs and b) how the different variance corrections can or cannot account for the time dependent changes in sample replication and correlation. In Case 1, a dataset with nearly time stable correlations, yet decreasing sample size is studied. In Case 2, a dataset with constant sample replication and increasing r_{bar} back in time is studied. For Case 3, the two basic characteristics of Cases 1 & 2 are combined, for a synthetic dataset that possesses diminishing sample replication and increasing r_{bar} values back in time. This third case most closely mimics the sample replication and r_{bar} characteristics of the Morocco dataset. It should be noted however that as these datasets are generated from a random normal distribution with independence between neighboring observations, they do not fully capture the characteristics of real tree-ring data. Nevertheless, we do believe they represent a good basis for demonstrating and testing some of the features relevant to the computation and variance correction of a mean-value function.

The Morocco dataset is a collection of *Cedrus atlantica* samples taken from living trees in 2002. The individual series, after applying an adaptive power-transformation (Cook and Peters, 1997) and detrending with a 300-year spline, are the basic data utilized in the

calculations herein. These data and their treatments are the same as those used for the final chronology shown in Esper et al. 2005 (this volume), although in closing we briefly detail some of the attributes of the raw and ratio detrended Morocco data. The reader is referred to the Esper et al. 2005 publication (this volume) for more details and information about these data.

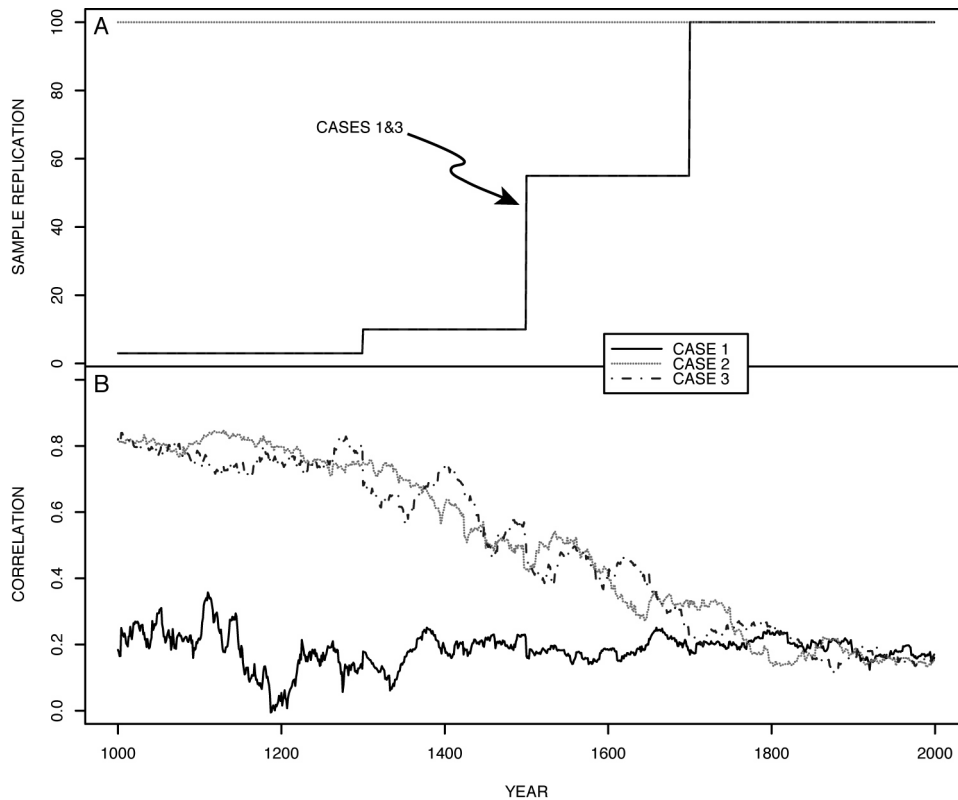


Figure 1: Sample replication (A) and r_{bar} computed in 50-year running windows (B) for the three synthetic datasets. Case 1: stable r_{bar} , decreasing n ; Case 2: increasing r_{bar} , constant n ; Case 3: increasing r_{bar} , decreasing n .

Methods

For all datasets we computed mean time series with a) no sample size correction, b) with the basic correction for sample size that utilizes a single mean estimate of the r_{bar} , and c) a correction that considers both the sample size and temporal dependence of r_{bar} . Herein, we refer to these chronologies as: UNCORRECTED, MEANr corrected, and RUNNINGr corrected. The MEANr corrected version, following Osborn et al. (1997) should be rather similar to that used in ARSTAN, although there is a range of possibilities in exactly how r_{bar} is determined. For the RUNNINGr correction, we utilized a 50-year window to estimate the r_{bar} at every time t . R_{bar} is computed as the average Pearson correlation, of all pairs that share at least 25 years of data, within a given window. This diverges from the Osborn et al. (1997) approach, wherein for every time t , the r_{bar} was determined as the average correlation among all data pairs with data during time t , computed over their maximum period of overlap. That is, in the Osborn et al. (1997) approach, the r_{bar} only changes when sample replication changes, and the period of r_{bar} estimation occurs over the period of maximum

common overlap and not confined within a running window as in our approach. With the RUNNINGr correction, additional ambiguity exists in the window size used for computation. The final UNCORRECTED, MEANr, and RUNNINGr corrected series are evaluated by simply plotting the resulting chronologies, and by plotting running standard deviations of the mean-value functions computed within 50-year windows.

Results

Variance adjustments in synthetic datasets

Figure 2 shows the final chronologies and running standard deviation for Case 1 which has a decreasing sample replication and a nearly constant r_{bar} of about 0.2. A clear increase in variance is observed in the UNCORRECTED mean, when the sample replication drops from 50 to 10 and then again from 10 to 3. The UNCORRECTED mean is rather insensitive to the change from 100 to 50 series and reflects the asymptotic nature of N_{eff} for larger sample sizes. The MEANr and RUNNINGr chronologies are quite similar and neither shows an increase in variance. Periods when the MEANr chronology has greater variance than the RUNNINGr chronology, correspond to time periods when the running r_{bar} is greater than the mean r_{bar} (Fig. 1b).

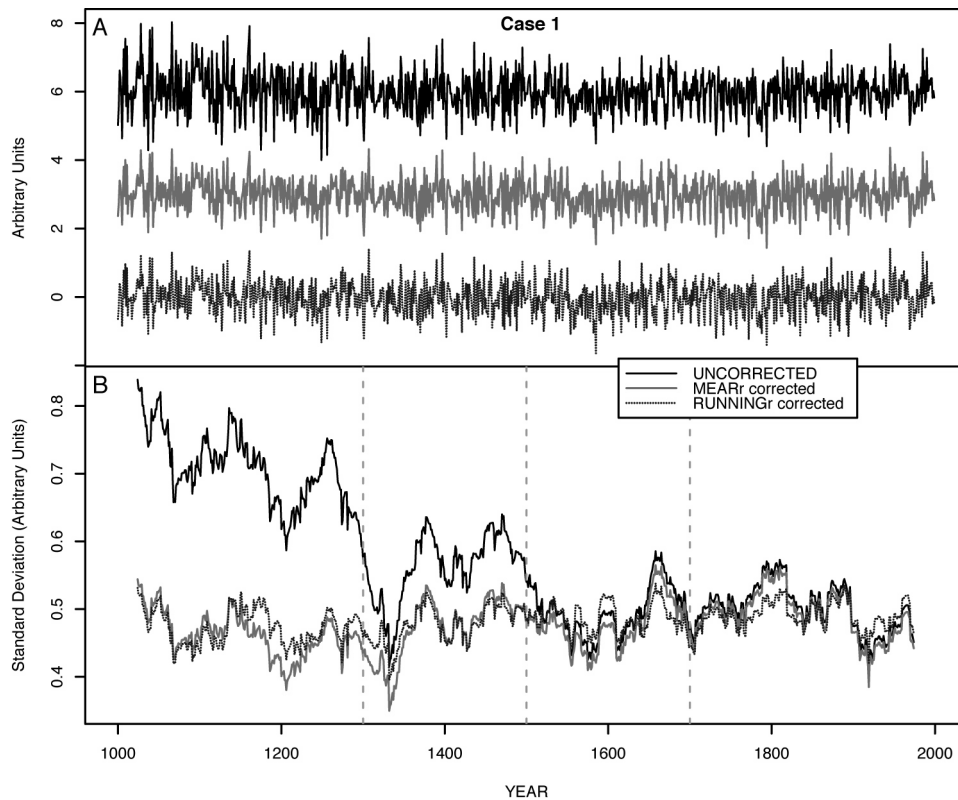


Figure 2: Mean value functions (A) and their running standard deviation (B) computed for the Case 1 synthetic dataset. The times corresponding to replication changes are indicated as vertical dashed lines in B.

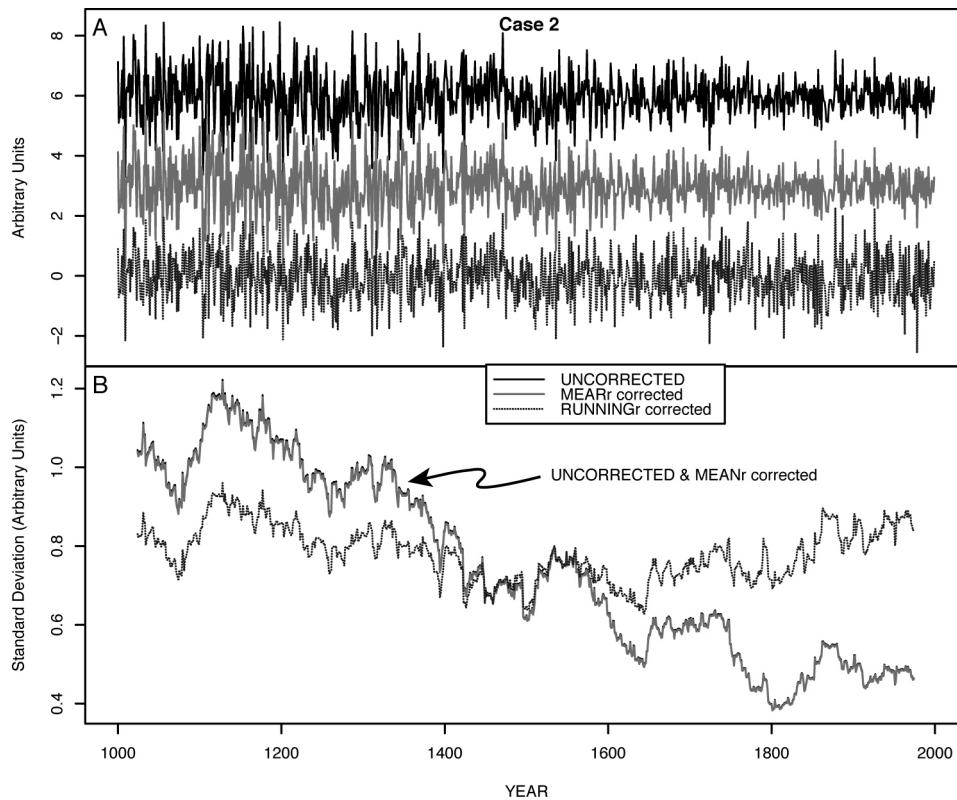


Figure 3: Mean value functions (A) and their running standard deviation (B) computed for the Case 2 synthetic dataset.

For the Case 2 dataset (Fig 3.), where sample size remains constant and r_{bar} essentially increases monotonically (Fig. 1b), the UNCORRECTED and MEANr corrected chronologies are identical, with both possessing substantially greater variance towards the higher r_{bar} values back in time. In contrast, the variance of the RUNNINGr chronology remains reasonably stable over the entire chronology, with deviations representing only the stochastic nature of this dataset. This demonstrates the ability of the RUNNINGr correction to “follow” changes in the underlying correlation structure and subsequently mitigate or eliminate these biases during the computation of the mean-value function. It should be noted, that the time dependent correlation demonstrated by Osborn et al. (1997) would produce the same results as the UNCORRECTED and MEANr corrected versions here, because using their methodology the correlations are computed over the period of individual series overlap, which in this case does not change. However, Case 2 (constant replication, increasing r_{bar}) is perhaps not very realistic for real data characteristics and is used here primarily to illustrate the systematic changes that result from changes in r_{bar} alone.

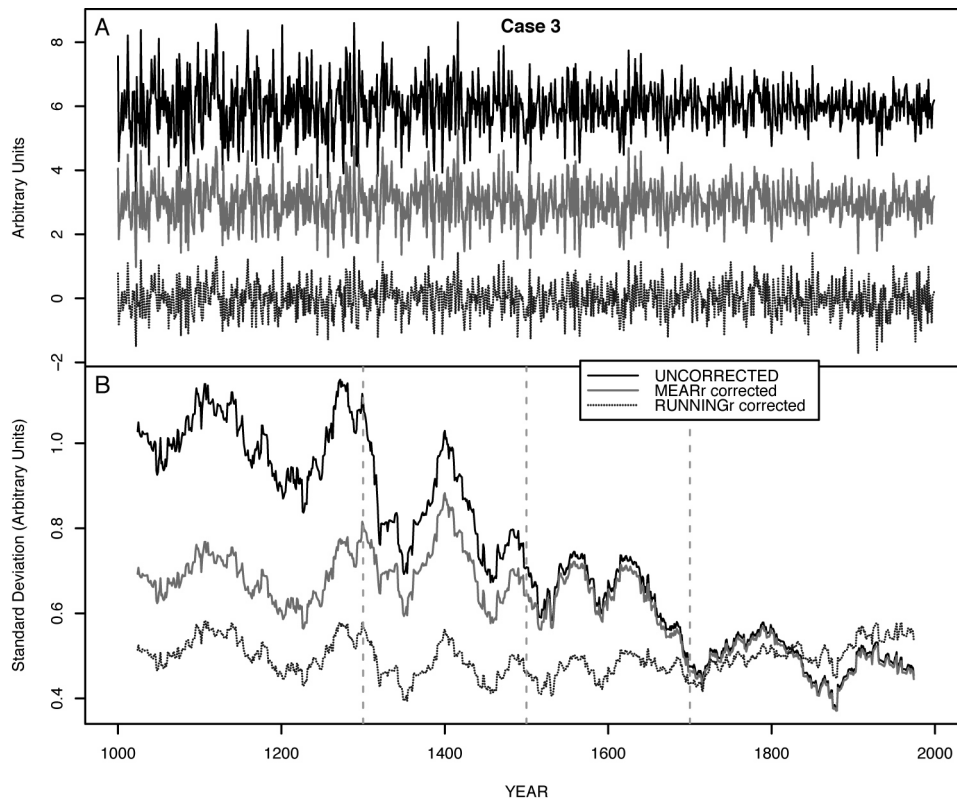


Figure 4: Mean value functions (A) and their running standard deviation (B) computed for the Case 3 synthetic dataset. The times corresponding to replication changes are indicated as vertical dashed lines in B.

In Case 3, as could be inferred, a mixture of the attributes of the mean value functions from Cases 1 and 2 are observed (Fig.4). The variance of the RUNNINGr corrected chronology remains rather stable, as this method successfully considered the time dependent changes in \bar{r} and sample replication. Both the UNCORRECTED and MEANr corrected chronologies show a noticeable increase in variance roughly corresponding to the time when replication drops from 100 to 50 series. It is however likely that the majority of this increase in both series is due to the somewhat steeper increase in correlation at about this time, rather than the decrease in sample replication. In comparison to Case 1, the difference between the variances of the UNCORRECTED and MEANr corrected chronologies in Case 3 is smaller between 1300 and 2000. This is a result of the greater insensitivity to changes in sample replication for higher \bar{r} values (Osborn et al. 1997), which are on average higher for Case 3 than for Case 1. During the earliest period, the variance of the UNCORRECTED chronology shows substantially inflated values, in comparison to the MEANr and RUNNINGr corrected chronologies. In this example, based on the differences between the standard deviation for the different computations during the early portion of the record, it can be estimated that during this early time period, about one third of the standard deviation increase in the UNCORRECTED chronology results from the increase in correlation over the course of this series, and about two-thirds from sample replication changes. Interestingly at around 1400 where the difference in variance between the MEANr corrected and RUNNINGr corrected chronologies is greatest, \bar{r} reaches a local maximum value (Fig. 1b), which

results in a decrease in N_{eff} , and hence also the standard deviation for the RUNNINGr corrected series.

Variance adjustments in *Cedrus atlantica* (Morocco)

We applied the same basic procedure as described above to the *Cedrus atlantica* dataset (see Esper et al. 2005, this volume), with results shown in Figure 5. The raw tree-ring data were subjected to a power-transform to eliminate the heteroscedastic behavior of the raw ring width series (Cook and Peters, 1997) and detrended by taking residuals between the power-transformed data and 300-year-spline fits to eliminate the age-trend. As is conventional for tree-ring indices, the detrended series were rescaled automatically in ARSTAN to have a means near unity. However, it is important to note the variance corrections outlined here assume the individual series to have a mean of zero. To approach this condition, we simply subtracted 1 from all series, resulting in series that are centered approximately around zero. Also included for comparison is the “Briffa/Osborn” variance adjusted version of the Morocco dataset as computed in ARSTAN. To account for the different scalings applied in our calculations and those from ARSTAN, all series were normalized with respect to the 20th century.

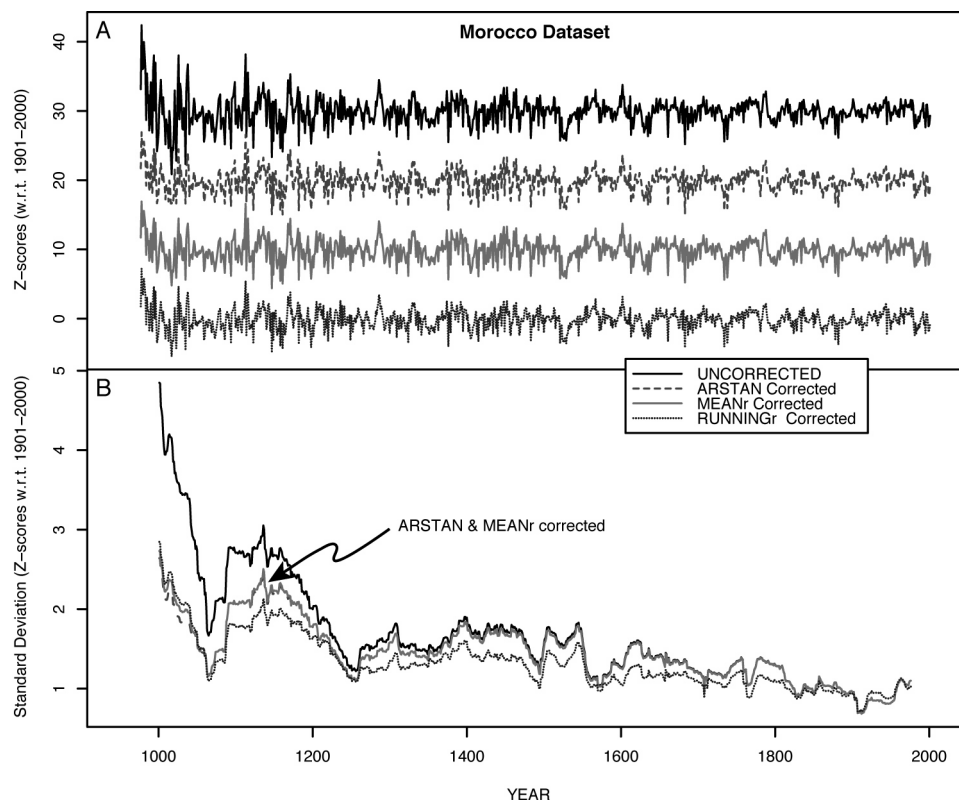


Figure 5: Mean value functions (A) and their running standard deviation (B) computed for the Morocco dataset. Also included is the ARSTAN computed correction. For more details and plots showing sample size and interseries correlations, the reader is referred to Esper et al. (this volume).

The UNCORRECTED, ARSTAN and MEANr corrected versions are nearly identical back to 1400. Prior to this time the UNCORRECTED variance splays apart from the other series,

with substantial differences during the first hundred or so years. The ARSTAN and MEANr corrected chronologies are nearly identical, with only slight computational differences present during the early portion of the records. The RUNNINGr corrected chronology possesses the smallest trend in variance, indicating the utility of this method for consideration of the increase in r_{bar} (and decrease in replication) back in time. However, in contrast to the synthetic dataset cases shown above, even the RUNNINGr chronology possesses a noticeable trend in the variance. Although mitigating the variance increase, this result largely refutes our initial hypothesis that the RUNNINGr correction procedure would eliminate the variance trend in the final Morocco chronology, which we assumed was primarily a consequence of the r_{bar} increase towards the early portion of this dataset.

In an attempt to understand the source of this variance increase, we computed running standard deviations for the individual series of the Morocco dataset (Fig. 6). It is evident that the average of the individual standard deviations increases back in time. In all likelihood, this tendency explains most of the variance increase still present in the RUNNINGr computed version of the Morocco chronology. None of the correction methods applied are able to “see” or cope with this apparent variance nonstationarity of the individual series.

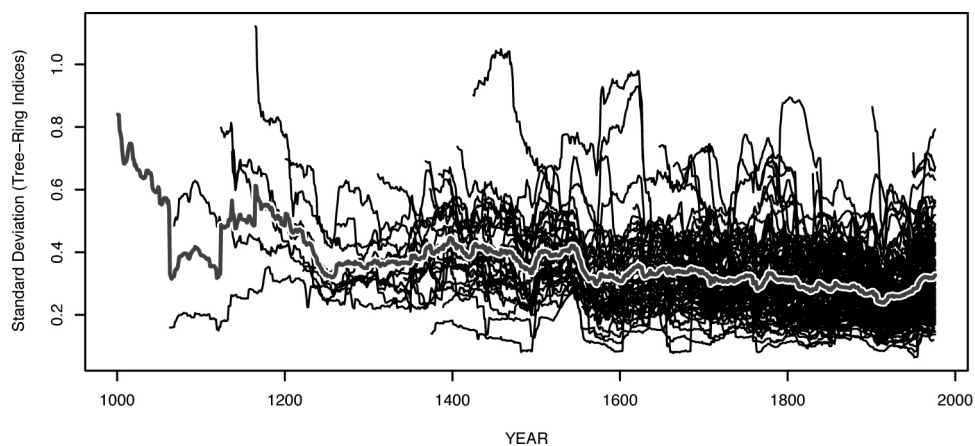


Figure 6: 50-year running standard deviations for the individual series from the Morocco dataset, along with their mean.

To explore if the variance of the individual series may increase with decreasing biological age, as is done for Regional Curve Standardization (Briffa et al. 1992, Esper et al. 2003), we aligned the data by cambial age (although pith-offset data were not used) and again computed the running standard deviations and their mean (Fig. 7). To test the influence of the detrending method, we also detrended the raw tree-ring series using ratios from 300-year-splines instead of power-transformation with residuals. The means from the age-aligned raw and ratio detrended running standard deviations are also shown in figure 7. The standard deviation of the raw series shows the most pronounced trend with biological age. This tendency diminishes with the power-transformed series, and is essentially non-existent with the ratio detrended series. It appears from these results, that these age-related tendencies in variance, as measured here, are not fully removed by the spread versus level calculations used in the adaptive power transformation, yet are removed by the ratio

detrending. It thus seems likely, that the biological age-related tendencies in the variance structure of the power-transformed/residual detrended tree-ring data play a central role in the variance increase found even in the RUNNINGr corrected Morocco mean-value function.

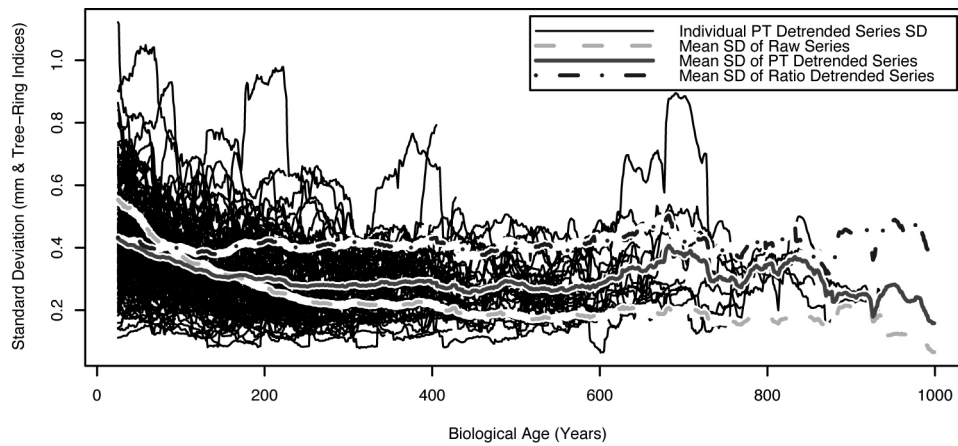


Figure 7: 50-year running standard deviations for the age-aligned individual series from the Morocco dataset, along with their mean. Also shown are mean standard deviations for the age-aligned raw data, and 300-year-spline ratio detrended data.

Discussion and conclusions

Using the synthetic data we demonstrated how an increase in variance can occur from both decreasing sample replication or increasing r_{bar} . Both the MEANr and RUNNINGr variance stabilization methods mitigated variance inflation due to changing sample size, however only the RUNNINGr method can eliminate variance changes resulting from fluctuations in the interseries correlation.

However, with the real dataset, the situation turned out to be more complicated. Although we hypothesized, due to increasing interseries correlations back in time, that the RUNNINGr correction would eliminate the increase in variance found in the Morocco dataset after using the “Briffa/Osborn” correction method in ARSTAN, this was not the case. The RUNNINGr correction mitigated this variance inflation in comparison to the MEANr correction, however, the final RUNNINGr corrected chronology still showed a variance increase. This result was unexpected after tests with the synthetic data. The primary source of this variance increase appears to be that after detrending with a power-transformation and a 300-year spline the variance of the single series (as measured by 50-year running standard deviations) showed a biological age-related component. The greater variance at younger biological ages and the underlying age-structure of this dataset are likely to contribute to the variance trend for all computations and corrections of the mean chronology. Further exploration of this issue is required to more completely understand the origin of this tendency, and to determine if it is unique to this perhaps unusual dataset composed of multi-centennial to millennial length tree-ring series. More efforts to understand the characteristics of ring-width series that make them more or less susceptible to variance nonstationarities in general or after power-transformation are also required.

For brevity we have not digressed even further by showing figures for the Morocco dataset detrended with the ratios method. However, these results (not shown), indicate that the uncorrected chronology possesses a strong increase in variance back in time, which is greatly reduced if the MEANr correction is applied and essentially eliminated if the RUNNINGr correction is performed. If the only criteria for chronology development were the presence of a relatively constant variance, we could suggest at this point that the ratios detrending might be more suitable for this dataset. However, this dataset, with long-lived trees that often possess exceptionally narrow outer rings, is particularly susceptible to index value inflation from detrending curves that enter “the danger zone” (Cook and Peters, 1997). More efforts are needed to untangle costs and benefits in detrending with the power-transformation in comparison to ratios for this dataset, and to understand more generally if other tree-ring sites share these same attributes. For the Morocco dataset presented, with the methods tested, it appears that while the RUNNINGr correction perhaps performed best, the variance structure of the final chronology is still not completely optimal. Exploration of other variance stabilization methods, including an empirically based spline correction (which is also an option in ARSTAN) could be considered. In any case, we can recommend inspection of the individual series variances (perhaps after age-aligning) to determine if there are trends or artifacts that will influence the variance of the underlying chronology. More generally these same issues were seen to effect the variance corrections applied in developing regional means of tree-ring data, when the chronologies themselves were not computed with sample size corrections (Osborn et al. 1997). Similar considerations are easily relevant for the computation of hemispheric-scale temperature reconstructions.

From the synthetic cases, with more stable individual variances, the RUNNINGr correction produced results most consistent with the expectation of constant variance in the mean-value function. Only RUNNINGr types of corrections can mitigate variance artifacts resulting from temporally changing interseries correlations. However, when \bar{r} fluctuates randomly, as in Case 1 presented above, it is possible “overkill” to apply the RUNNINGr correction, when the MEANr correction would perhaps be justified. Variance corrections similar to the RUNNINGr approach used here might be helpful in the computation of gridded or large scale instrumental mean datasets. These datasets not only rely upon fewer and fewer stations back in time, but the locations of the earliest remaining stations tend to be more concentrated in certain areas such as Central Europe or Eastern North America. The RUNNINGr correction applied herein seems to have an additional interesting attribute: during times with greater correlation the variance is diminished. This has implications for the reconstruction of climatologically extreme periods (e.g. the early 19th century in Europe), which are probably not only imprinted on proxy series themselves, but also on the correlation of the individual series. This correction might help mitigate non-linearities resulting from strong pointer years. It is an objective in dendroclimatology for the variance properties of the mean-value function to most closely represent those of the instrumental target data. In this regard, some success was met using a network to look at the variability of extreme events in the Alps (Frank et al. 2005). To better approach this condition, following the work of Osborn et al. (1997), we have shown herein that corrections for sample size are often needed. Additionally, we have shown

examples in which the correction methods routinely applied are additionally complicated by time dependence of \bar{r} and by variance non-stationarity of the raw data. The application or omission of variance adjustments to the mean-value function of time series often has non-negligible consequences. These considerations become critically important in paleoclimatology during the early periods of instrumental or proxy records when sample replication is lowest and spatial, biological, ecological, and sampling representativity are most likely to be unique.

ACKNOWLEDGEMENTS

We thank Kerstin Treydte for helpful suggestions and the Swiss National Science Foundation, Grant # 2100-066628 'Millennia' and NCCR-Climat for support.

REFERENCES

- Briffa, K.R., Jones, P.D., Bartholin, T.S., Eckstein, D., Schweingruber, F.H., Karlen, W., Zetterberg, P., Eronen, M. (1992): Fennoscandian summers from AD 500: temperature changes on short and long timescales. *Climate Dynamics* 7: 111-119.
- Cook, E.R. (1985): A time series analysis approach to tree-ring standardization. PhD dissertation, University of Arizona, Tucson, AZ.
- Cook, E.R., Peters, K. (1997): Calculating unbiased tree-ring indices for the study of climatic and environmental change. *The Holocene* 7: 361-370.
- Esper, J., Büntgen, U., Frank, D.C., Nievergelt, D., Treydte, K., Verstege, A. (in review) Multiple tree-ring parameters from Atlas cedar (Morocco) and their climatic signal. In: Heinrich I (Ed.) Tree rings in archaeology, climatology and ecology, TRACE, Vol. 4.
- Esper, J., Cook, E.R., Schweingruber, F.H. (2002): Low-frequency signals in long tree-ring chronologies for reconstructing of past temperature variability. *Science* 295: 2250–2253.
- Esper, J., Cook, E.R., Krusic, P.J., Peters, K., Schweingruber, F.H. (2003): Tests of the RCS method for preserving low-frequency variability in long tree-ring chronologies. *Tree-Ring Research* 59: 81-98.
- Frank, D., Wilson, R.J.S, Esper, J. (2005): Synchronous variability changes in Alpine temperature and tree-ring data over the last two centuries. *Boreas*, in press.
- Jones, P.D., New, M., Parker, D.E., Martin, S., Rigor, I.G. (1999): Surface air temperature and its changes over the past 150 years. *Reviews of Geophysics* 37: 173-199.
- Osborn, T.J., Briffa, K.R., Jones, P.D. (1997): Adjusting variance for sample-size in tree-ring chronologies and other regional-mean time-series. *Dendrochronologia* 15: 89-99.
- Wigley, T.M.L., Briffa K.R., Jones, P.D. (1984): On the average of correlated time series, with applications in dendroclimatology and hydrometeorology. *Journal of Climate and Applied Meteorology* 23: 201-213.

Interannual climate/growth-relations of Central European tree rings - A dendroecological network analysis

B. Neuwirth¹, F.H. Schweingruber² & M. Winiger¹

¹*Department of Geography, University of Bonn, Meckenheimer Allee 166, 53115 Bonn, Germany*

Email: b.neuwirth@giub.uni-bonn.de

²*Swiss Federal Research Institute WSL, Zürcherstrasse 111, 8903 Birmensdorf, Switzerland*

Introduction

A comparison of dendrochronological data from different sources mostly deals with various problems. Due to missing standards in respect to sampling strategies, ecological site conditions, statistical and indexation methods, etc., interregional differences in tree-ring chronologies need not be the results of changing ecological or climatological forcings. This problem can be solved by excluding all the aspects influenced by varying strategies and methods. Additionally, more than one tree species should be investigated to find out their common/true climatological signals. By using a unique statistical homogenization and a biogeographical stratification of all data big datasets make it possible to reconstruct climatic influences as well in temperate zones (Schweingruber and Nogler 2003).

The main objective of this network analysis is the evaluation of the potentials of tree-ring analytical investigations in the temperate midlatitudes of Europe for reconstructing the climate conditions of historical time periods. Therefore we analyse the interannual climate/growth-relations of Central European tree rings in a dendroclimatological network combining tree-ring data from 377 sites with climatological data. Additionally the network includes modules to edit and to analyse the data, and to present the results.

Data and methods

This dendroclimatological network includes more than 1.25 million values of tree-ring width of the principal forest tree species (see Tab. 1) in Central Europe (defined as the area from 5° to 15°E and 42.5° to 52.5°N) from 377 sites (Fig. 1).

The network combines the tree-ring data with climatological data (temperature, precipitation, and air pressure expressed by the North Atlantic Oscillation (NAO)). Temperature and precipitation values are gridded data in a spatial resolution of 10 minutes for the time period from ad1901 to 2000 (Mitchell et al. 2003).

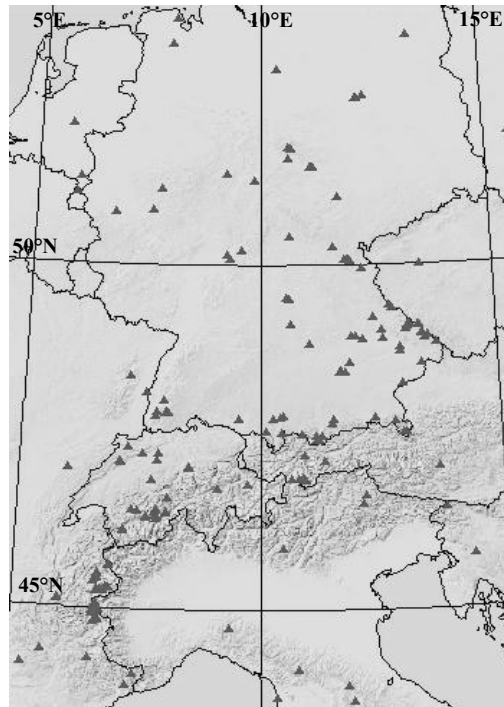


Figure 1: Sites of tree-ring width chronologies in Central Europe.

The NAO is represented by three indices: PON and GIB for the air pressure gradients between the Icelandic climatic stations [Akureyri (65.7°N/18.1°W) or Stykkisholmur (65.0°N/22.8°W)], and Ponta Delgada (37.7°N/25.7°W) at the Azores (van Loon and Rogers 1978, Rogers 1990) and Gibraltar (36.1°N/5.1°W) in Southern Spain (Jones et al. 1997), respectively (Neuwirth et al. 2004). The third NAO index is called PAE and describes the minima and maxima in the air pressure field between 70° and 20°N as zonal mean values (Glowienka-Hense 1990, Paeth 2000). The PAE-index takes into account the spatial movements of the air-pressure centres. The common overlap of all datasets determines the investigation period of this study from ad1901 to 1971.

The raw tree-ring widths of all dendrochronological sites were checked for their suitability by the dendrostatistical parameters like Gleichläufigkeit GLK (Schweingruber 1983), interseries correlation r_{xy} (Fritts 1976), and signal strength parameter NET (Esper et al. 2001). After building sitewise mean curves for the 377 sites the calculation of pointer values expressed by z-transformations according to Cropper (1979) leads to time series illustrating the anomalies against the mean radial growth for every site. The resulting z-transformed Cropper values C_z are grouped into weak ($C_z > 1$), strong ($C_z > 1.28$), and extreme ($C_z > 1.645$) pointer values. The chosen thresholds correspond to the probability, that the pointer year event is rarer than 33%, 20%, or 10% respectively.

Using the multivariate techniques factor-, cluster-, and discriminance analysis the 377 sites were reduced to 59 clusters combining all sites with similar growth anomalies over the investigation period.

Temperature and precipitation anomalies were derived from the long time mean of the period ad1901 to 1971 for every month from September of the year before to August of the year of tree-ring growth. The NAO indices represent anomalies and will be used after a z-

transformation. The synthesis of the climatological interpretation of extreme growth values with the results of correlations between climatological and tree-ring datasets is the base of the analysis of climate/growth-relations follows from the synthesis of.

Results

Radial growth

The mean radial increment derived from all 7,708 Central European trees during the investigation period is 1.42 mm/a. Fir, spruce, and beech are the fast growing species (Tab. 1). In this dataset three species - larch, mountain pine and stone pine - are only located in high mountain regions above 1500m a.s.l.. Larch and mountain pine grow less than 0.9 mm/a. Additionally, the high mountain species show with more than 0.44 mm/a the largest variances in radial growth while the other species spread with less than 0.4 mm/a around the mean.

Gleichläufigkeit GLK (Schweingruber 1983), signal strength parameter NET combining the variance v with GLK (Esper et al. 2001), and Pearsons coefficient of correlation t -value (Schönwiese 1992) give an impression about the quality of the site chronologies. All values are better than the defined thresholds (GLK > 70%; NET < 0.8, t > 10). Therefore the mean curves represent the common signals of the single tree curves for all species. Regarding the three parameters in detail we find out that the mountain pine chronologies have the lowest and beech the highest common signals.

Table 1: Statistical features of central European tree-ring width from ad1901 to 1971 as mean over all tree sites and separated into species.

Abbreviations:

ABAL = *Abies alba*, fir;

LADE = *Larix decidua*, larch;

PCAB = *Picea abies*, spruce;

PICE = *Pinus cembra*, stone pine;

PISY = *Pinus sylvestris*, Scots pine;

PIUN = *Pinus uncinata*, mountain pine;

FASY = *Fagus sylvatica*, beech;

QUSP = *Quercus petraea* & *Qu. robur*, oak;

YRG = yearly radial growth;

v = variance;

GLK = Gleichläufigkeit;

NET = signal strength parameter;

t -value = coefficient of correlation;
after Pearson

AK 1 = autocorrelation lag 1

	all	tree species							
		ABAL	LADE	PCAB	PICE	PISY	PIUN	FASY	QUSP
number of sites	377	76	17	129	27	22	21	38	47
YRG	1.42	1.82	0.88	1.48	1.16	0.99	0.76	1.63	1.30
v	0.39	0.38	0.44	0.37	0.44	0.43	0.45	0.37	0.35
GLK	0.77	0.78	0.79	0.76	0.78	0.76	0.70	0.80	0.76
NET	0.62	0.60	0.65	0.61	0.67	0.67	0.75	0.57	0.56
t -value	13.2	13.0	16.2	12.4	11.9	15.4	10.1	13.4	13.9
AK 1	0.63	0.68	0.56	0.65	0.62	0.64	0.65	0.57	0.56

The autocorrelation of lag 1 separates the species into two groups. Deciduous species (larch, beech and oak) show significant smaller autocorrelations than the other species. Tree-ring growth of evergreen trees depend more on the conditions during the year before than the others.

Pointer values

Figure 2 shows the masterplot of central European pointer values calculated on the base of 59 dendroclusters (black bars in figure 2).

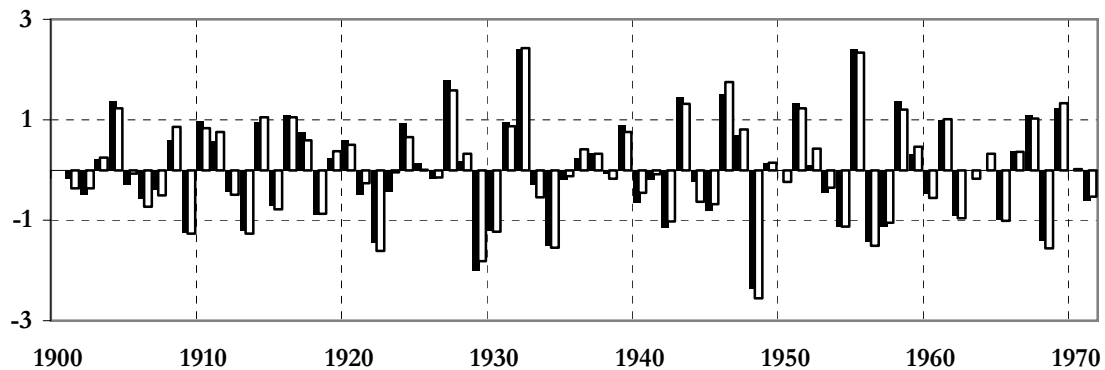


Figure 2: Central European masterplot for the period ad1901 – 1971 derived from 59 dendroclusters (black) and 377 sites (white).

There are 12 years with C_z -values above the threshold 1 and also 13 years with values lower than -1. The positive pointer values are classified into 4 weak (1916, 1961, 1967, and 1969), 6 strong (1904, 1927, 1943, 1946, 1951, and 1958) and 2 extreme (1932 and 1955) pointer years. For the negative growth reactions we can find out 7 weak (1909, 1913, 1930, 1942, 1954, 1957, and 1965), 4 strong (1922, 1934, 1956, and 1968) and 2 extreme (1929 and 1948) pointer years. Comparing this with the masterplot deviated from the 377 sites, (white bars in figure 2) there is no important difference between both plots. In all years the black and white bars tend into the same direction with nearly the same values. Therefore we can conclude that there is no modification by using the dendroclusters as calculation base.

Valuable advices about growth determining factors can be obtained either by differentiating the various ecological sites, in the following expressed by elevation zones, or by regarding the species specific growth reactions (Neuwirth 2005). The subtraction of z-transformed Cropper values C_z averaged over the sites with elevations lower than 750m a.s.l. from the means of the sites above 1500m a.s.l. leads to a modified masterplot (Fig. 3).

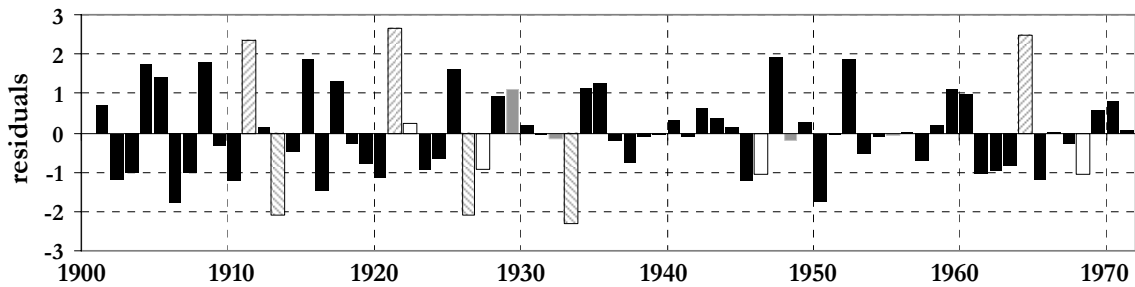


Figure 3: Masterplot for the period ad1901 - 1971 of the residuals from the z-transformed croppervalues of the high- (>1500m a.s.l.) and the low- (<750m a.s.l.) elevated sites in Central Europe. Emphasized are years with extreme pointer values (grey), species specific pointer values (white), and elevation depending pointer values (hatched bars).

Positive pointer years in the highlands and negative pointer values in the lowlands result in positive orientated bars, whereas negative highland values and positive lowland values lead to negative orientated bars. If high and low elevated sites have nearly the same values the residual bars are located nearby the zero line.

In the years ad1911, 1913, 1921, 1926, 1933, and 1964, the strongest differences between low and high elevated sites can be found (hatched bars in figure 3). In these years, the signs of pointer values are changing with the elevation gradient. In 1911 and 1964 the differences are so decisive that in highlands as well as in lowlands, the pointer values are above the thresholds 1 and -1 respectively. The four extreme central European pointer years (1929, 1932, 1948, 1955) show nearly the same values in all elevation zones resulting in bars (grey in figure 3) near by zero. In 1922 and 1946, larch trees show opposite growth in respect to the other species, just as oak in 1927. Because of the small elevational spectrum of larch (only high elevated sites) and oak (mostly in lowlands) in this dataset the individual growth reactions of this species dominate the differences between high and low elevated sites (white bars in figure 3). In 1968 beech, fir, spruce, and larch show negative growth anomalies. Oaks and the pine subspecies have no significant reactions. Therefore the highest Cropper values are located in elevations between 750 and 1500m a.s.l., the main area of fir and spruce. The resulting residual bar is dominated by the negative reactions of low elevated beeches.

For each year pointer values are found which have at least regional and/or species specific relevance. Their spatial distribution is illustrated by yearly maps created by using a GIS with an interpolation between the 8 neighbours of every site. The maps for every year of the investigation period are published on the internet (Neuwirth 2005) and exemplary in Neuwirth et al. 2003. The maps classify the years into four groups: years with (i) positive and (ii) negative growth reactions in nearly the whole investigation area; (iii) years with balanced portions of positive and negative growth anomalies; and (iv) years with growth reactions only in small regions or at several sites. In spite of the similarities in the group internal growth patterns the geographical position, the elevation and the leading species of the dendroclusters are not enough to explain the reasons for the spatial distributions of pointer values. At least we have to take into account the climatological forcings.

Climate/growth relations

The analysis of climate/growth relations consists of a synthesis of the climatological interpretation of pointer values and the results of correlations between climatological and tree-ring datasets, always differentiated in species specific relations. All important individual results are combined in one diagram (figure 4) showing the climatological forcings for positive and negative growth reactions for each tree species in their elevation zones. To demonstrate how to read figure 4, we present the example of fir in their upper elevation zone. Between 1250 and 1750m a.s.l. positive growth reactions result from small winter temperatures above average and strong precipitations in May above average. In contrast, negative growth reactions are caused by cold winter temperatures and/or slightly temperatures in the summer months below average. Regarding the species separately we can summarize the following facts:

- the sensitivity of fir against strong winterly coldness,
- the positive influence of moist summerly conditions for spruce radial growth,
- the positive correlations of beech to increasing summer temperatures, especially above 500m a.s.l.,
- the inferior sensitivity of mountain pine against climatic forcings,
- the high negative influence of temperatures in the autumn of the year before on stone pine,
- the strong sensitivity of scots pine against summerly dryness,
- the high correlation of larch tree-ring growth with summer temperature.

Regarding figure 4 the reciprocal influence of temperature and precipitation on tree-ring growth in nearly all elevations is clearly recognizable. Growth reactions are neither monocausally related to temperature in high elevations nor to precipitations in low elevations.

Elevation	Growth anomaly	ABAL	LADE	PCAB	PICE	PISY	PIUN	FASY	QUSP
1750 m	pos.		Aut _b ☼(+) Su ☼ +	Su ☼ + Wi ♣(+)	Aut _b ☼ - Veg ☼(+)		Sp ☼ +		
	neg.		Su ♣ -	Wi ☼ -	So ♣ - Sp NAO -		Sp ☼ -- Su ☼ +		
1250 m	pos.	Wi ☼(+) May ♣ +		Su ☼(+) Wi ♣ +			Gs ☼(+)		
	neg.	Wi ☼ - Su ☼ (-)		Wi ☼ -			May ♣ -		
750 m	pos.	Wi ☼ + Su ☼ (-)		Su ☼(+)		Aug ☼ +		Su ☼ +	Su ♣ +
	neg.	Wi ☼ -- Su ☼(+)		Gs ♣ -		Sp ☼ - Su ♣ -		Su ☼ -	Su ♣ -
250 m	pos.	Wi ☼ + Su ♣ +		Su ☼ (-) Gs ♣ +		Wi ☼ +		May ♣ +	May ♣ +
	neg.	Wi ☼ -- Su ☼ +		Gs ☼ + Gs ♣ -		Gs ♣ - Sp ☼ -		Gs _b ☼ - Su ☼ -	Aut _b ☼ +
	pos.					Wi ☼ +		Year ♣ +	Sp ♣ + Su ☼ (-)
	neg.					Su ☼ +		Gs ♣ -	Gs ☼ + Gs ♣ -

Figure 4: Schematic illustration of climatic conditions as deviations in respect to the mean from 1901 to 1971 and corresponding growth anomalies of tree species in their elevation zones. Aut_b = Autumn of the year before; Wi = Winter (DJF); Sp = Spring (MAM); Su = Summer (JJA); Gs = growing season; ☼ = temperatur; ♣ = precipitation; +, - = positive, negative anomalies; () = weak; bold = strong; -- = extreme.

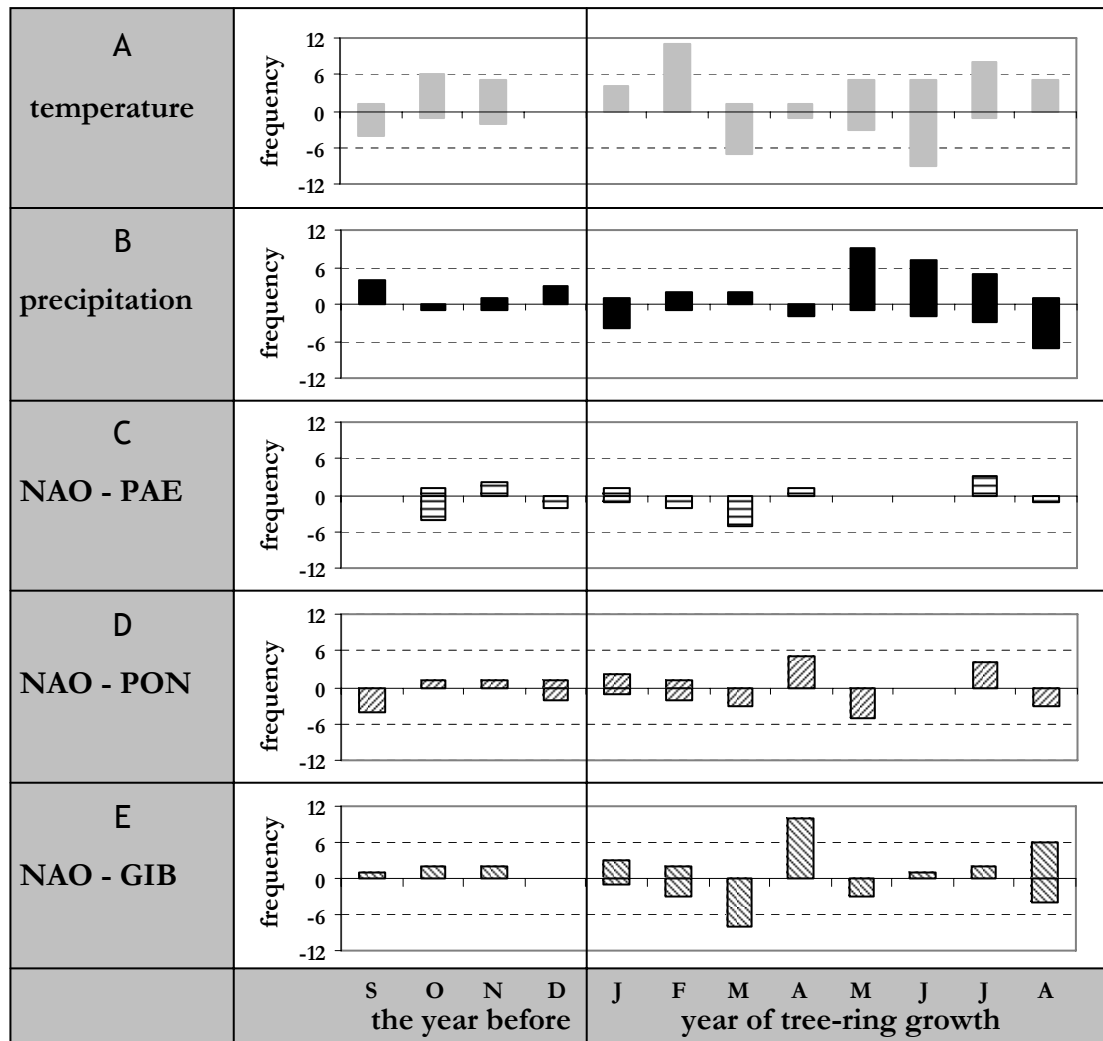


Figure 5: Monthly frequencies of significant correlations between the five climatic indices and the 29 dendrogroups.

Figure 5 illustrates the frequencies of the climate/growth relations in sequences from September of the year before to August in the year of tree-ring building. The frequencies are calculated for dendrogroups defined as the means of species specific means of dendroclusters in the five chosen elevation zones. Precipitation-related influences (Fig. 5B) are mainly concentrated on the months from May to August. They change from positive correlations in May to negative correlations in autumn. In contrast the temperatures correlate in winter exclusively and in summer mostly positive to radial growth. In comparison NAO indices cause less influence on interannual tree-ring growth (5A). For PAE and PON we do not find significant correlations to more than 10 dendrogroups. Only the GIB index, which is derived from the closer to Central Europe located station Gibraltar, correlates in March negative to more than a quarter of the dendrogroups and in April to more than a third of these groups. Additionally, the GIB index is significantly correlated to radial growth of 10 dendrogroups in August, six times positively and four times negatively. Combining a positive NAO index with mostly zonal atmospheric mean streams, we can conclude moist air masses

over Central Europe (Hurrell et al. 2004). In April, these convective air masses are warmer, and in August colder than the surrounding air masses.

Conclusion

Due to the similar editing and preparation of all datasets the presented results demonstrate the suitability of tree-ring widths for comparisons of growth reactions between different tree species and different regions. The results prove that tree-ring widths in the moderate mid-latitudes are also useful for climatological interpretation of pointer values. Growth anomalies are a suitable parameter to explain the relative yearly changing growth patterns related to the modifying influence of climatic forcings. This can be explained by the optimal adaptation of trees to their specific ecological site conditions.

Acknowledgements

We are thankful for providing tree-ring data to the following dendrochronologists:

U. Büntgen, T. Forster, H. Gärtner, F. Kienast, W. Lingg, F. Meyer, P. Nogler, A. Rigling, E. Schär, F.H. Schweingruber, K. Treydte (all Birmensdorf, CH); Ch. Dittmar (Bayreuth, D); E. Gers, D. Friedrichs, H. Gruber, M. Hennen, K. Weidner (all Bonn, D); B. Schmidt (Köln, D); H.H. Leuschner (Göttingen, D); D. Eckstein (Hamburg, D); S. Bonn (Dresden, D); H.P. Kahle, H. Spieker (Freiburg, D); W. Elling (Freising, D); K. Nicolussi (Innsbruck, A); M. Saurer (Bern, CH); C. Desplanque, V. Petitcolas, C. Rolland (all Grenoble, F); E. Jansma (Amersfoort, NL); W. Hüsken (Düsseldorf, D); R. Wilson (Edinburgh, GB). Additionally we would like to thank T. Mitchell (CRU Norwich/GB) for the gridded temperature and precipitation data and H. Paeth (MIUB Bonn, D) for the NAO data.

References

- Cropper, J.P. (1979): Tree-ring skeleton plotting by computer. *Tree-Ring Bulletin* 39: 47-59.
- Esper, J., Neuwirth, B., Treydte, K. (2001): A new parameter to evaluate temporal signal strength of tree-ring chronologies. *Dendrochronologia* 19 (1): 93-102.
- Fritts, H.C. (1976): Tree rings and climate. Academic Press, London. 567 S.
- Glowienka-Hense, R., (1990): The North Atlantic Oscillation in the Atlantic-European SLP. *Tellus* 42A: 497-507.
- Jones, P.D., Jonsson, T., Wheeler, D. (1997): Extension of the North Atlantic Oscillation using early instrumental pressure observations from Gibraltar and South-West Iceland. *International Journal of Climatology* 17 (13-15): 1433-1450.
- Loon, van, H., Rogers, J.C. (1978): The seesaw in winter temperatures between Greenland and Northern Europe. Part I: General Description. *Monthly Weather Review* 106: 296-310.
- Mitchell, T.D., Carter, T.R., Jones, P.D., Hulme, M., New, M. (2003): A comprehensive set of high-resolution grids of monthly climate for Europe and the globe: the observed record (1901-2000) and 16 scenarios (2001-2100). *Journal of Climate*, submitted.

- Neuwirth, B. (2005): Interannuelle Klima/Wachstums-Beziehungen zentraleuropäischer Bäume von ad1901 bis 1971 – eine dendroklimatologische Netzwerkanalyse. Dissertation University of Bonn, 162 pp. (http://hss.ulb.uni-bonn.de/diss_online/math_nat_fak/2005/neuwirth_burkhard/index.htm).
- Neuwirth, B., Winiger, M. (2003): Dendrochronological network analyses of Central European chronologies – a conceptional approach of a new project. In: Schleser, G. et al.: TRACE 1 – Proceedings of the Dendrosymposium 2002, April 11th – 13th 2002, Bonn/Jülich, Germany: 35-39.
- Neuwirth, B., Esper, J., Schweingruber, F.H., Winiger M. (2004): Site ecological differences to the climatic forcing of spruce pointer years from the Lötschental, Switzerland. *Dendrochronologia* 21 (2): 69-78.
- Paeth, H. (2000): Anthropogene Klimaänderungen auf der Nordhemisphäre und die Rolle der Nordatlantik-Oszillation. In: *Bonner Meteorologische Abhandlungen* 51: 168 S.
- Rogers, J.C. (1990): Patterns of low frequency monthly sea level pressure variability (1899-1986) and associated wave cyclone frequencies. *Journal of Climate* 3: 1364-1379.
- Schönwiese, C.D. (1992): Praktische Statistik für Meteorologen und Geowissenschaftler. 2. Aufl., Borntraeger, Stuttgart, 231 p.
- Schweingruber, F.H. (1983): Der Jahrring. Standort, Methodik, Zeit und Klima in der Dendrochronologie. Verlag Paul Haupt, Bern. 234 p.
- Schweingruber, F.H. (1996): Tree rings and environment – Dendroecology. Verlag Paul Haupt, Bern, Stuttgart, Wien. 609 S.
- Schweingruber, F.H., Nogler, P. (2003): Synopsis and climatological interpretation of Central European tree-ring sequences. *Botanica Helvetica* 113 (2): 125-243.

Tree rings and climate in sub-Mediterranean Slovenia

D. Ogrin

University of Ljubljana, Department of Geography, Faculty of Arts, Aškerčeva 2, SI-1000 Ljubljana, Slovenia,
Email: darko.ogrin@ff.uni-lj.si

Introduction

Not many geographical or other studies in Slovenia discuss correlations between the climate and the growth of trees. The problem of establishing the upper tree- and forest-line was studied by Lovrenčak (1977, 1987), Gams (1977), and Plesnik (1971). Levanič (1996) studied the dendroclimatology of European silver fir on the Dinaric high plateau in central Slovenia, and Ogrin (1989, 1991 and 1998) mainly studied dendroclimatology of the Alpine and the sub-Mediterranean regions in Slovenia.

The Sub-Mediterranean and the Alpine regions are most suitable for dendroclimatological investigations in Slovenia since they have certain limiting conditions for the formation of radial increments. Sub-Mediterranean Slovenia is typified by its deficit in humidity in summer months, which is also partly due to prevailing karstic features of the surface. These conditions are more or less clearly reflected in radial increments of trees, confirmed by the previous studies. Thus, the need for further investigations became evident because a climate signal registered in the width of annual rings is indistinct in many places, or deviates from a general scheme of radial increment formation in similar conditions elsewhere in the world (Aloui, 1978, Berger et al., 1979, Seue, 1973, etc.). The formation of radial increments strongly depends on various stress situations, as well as on the local, also non-climatic conditions which cannot be sufficiently comprised in dendroclimatological methodology.

Study area

The term 'sub-Mediterranean Slovenia' denotes the south-west region of Slovenia, which lies under the Alpine-Dinaric barrier and opens towards the Adriatic, from which the mitigated Mediterranean influence spreads. The region is composed of flysch and carbonate rocks in which limestone prevails. The climate becomes more severe the further one gets from the sea. Average temperatures in January are higher than 0 °C (by the sea, > 4 °C), and in July, higher than 20 °C. Annual precipitation by the sea is 1000 mm, and 1600 mm in the foothills of the Dinaric barrier. The majority of precipitation falls in autumn, while the smallest amounts fall in winter and summer when droughts are frequent, owing to high temperatures and the karstic surface. Forest vegetation is thermophillic (submediterranean) and low forests prevail, consisting mainly of oriental hornbeam and oaks (pubescent and durmast oak). Besides, non-autochthonous forests of black pine with which the barren karstic areas were afforested also occur frequently.

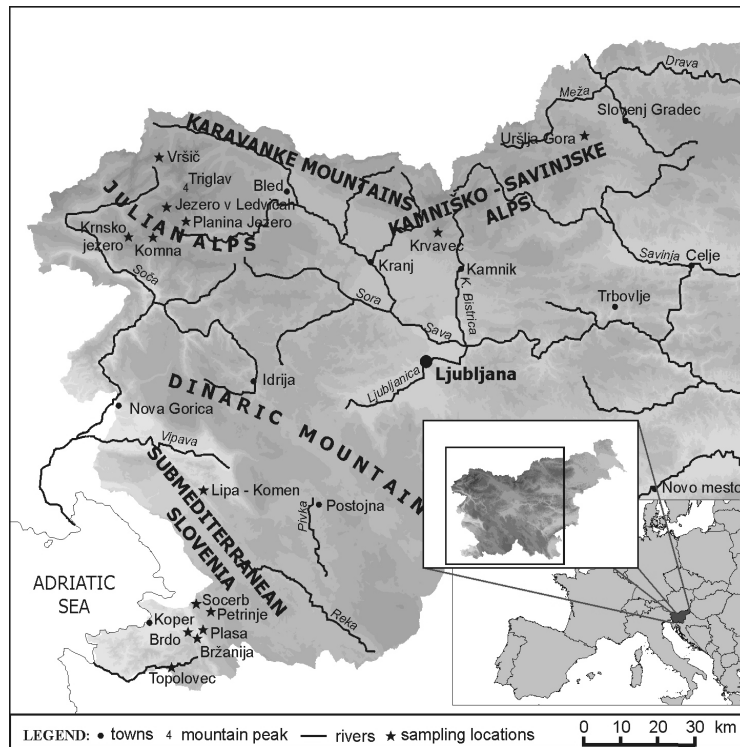


Figure 1: Geographical position of the investigated area with marked sampling locations.

Material and methods

The trees that were sampled for the investigation grow in different growing conditions. In sub-Mediterranean Slovenia, samples were taken from flysch areas (Bržanija, Brdo, Plasa, Topolovec), and also from karstic areas (Socerb, Petrinje, Lipa-Komen). The locations on flysch have better growing conditions; soil is up to 30 cm deep, loamy and not so dry. Bržanija is slightly different; samples here were taken from a marl slope which is exposed to soil solution. On the marl bedrock of the slope, after the afforestation with black pine a hundred years ago, only 10 cm of soil of poorly weathered pine needles accumulated. The sampled trees from the Kras grow on limestone plateau which are covered with up to 10 cm deep non-continuous rendzina, out of which the parent material sometimes protrudes. Samples of oaks (durmast oak and pubescent oak) were taken at the locations of Brdo, Plasa and Topolovec, and samples of black pine at Bržanija, Plasa, Socerb, Petrinje and Lipa-Komen.

Mature trees, with no visible mechanical or other damage and unobstructed crowns were sampled, growing on rather isolated sites (mainly 10 to 20 trees on each location). Most of the samples were taken by means of increment borer. We bored to the center of the trunk at standard breast height, from two opposite sides, parallel with the terrain contours. Trees were felled only at Brdo, Topolovec, Plasa and Lipa-Komen. Air-dried samples were planed, and the width of tree-rings was measured by means of magnifying lens, with the accuracy of 1/100 mm.

Synchronicity of radial increments was established by means of cross-dating, and as a result of anomalies, 6 samples were excluded from further analysis. In making cross-dating we

made use of the so-called leading chronologies. Then followed the dating and standardization by means of which the biological trend of growth was eliminated. Applied was the "corridor method". Local index chronologies were made for each site, and from them, regional chronologies were made for individual tree species.

The tree-ring climate signal for both local and regional chronologies was established by means of correlation. In this process, the 13-month period was made use of, from September of the previous year when the beginning of future increment was formed, to September of the respective vegetation period. Correlations for monthly and seasonal values, for the vegetation period (April - September), and yearly values were calculated separately. Correlations of greater than +0.25, or smaller than - 0.25, were taken as significant. As the source of climatic data, meteorological stations located close to and having similar positions to the sampling locations were used: Kubed (262 m) and Komen na Krasu (289 m).

Results and discussion

Local and regional chronologies

The samples represent all growing conditions of parent material, exposure to sun, and landform features at individual locations. Thus, the average growing conditions of each location are reflected in the local chronologies. Only undamaged and moderately damaged trees were used in making chronologies; the samples of trees with intense decline in increments or missing tree-rings were eliminated. From the samples of sub-Mediterranean Slovenia, four local chronologies for black pine and three for durmast oak were made. The pine chronologies are about 40 years long, mainly comprise the period after the World War II. The oak chronologies are of similar length, with the exception of that from Topolovec, which is almost 100 years long, covering the period 1888 to 1985. The regional chronologies were made for the time for which the climate data were available, so that they are 30 to 40 years long. Thus, the regional chronology for black pine is 38 years long, consisting of the period from 1951 to 1988, and regional chronology for oak is slightly shorter, 31 years, made for the time between 1955 and 1985.

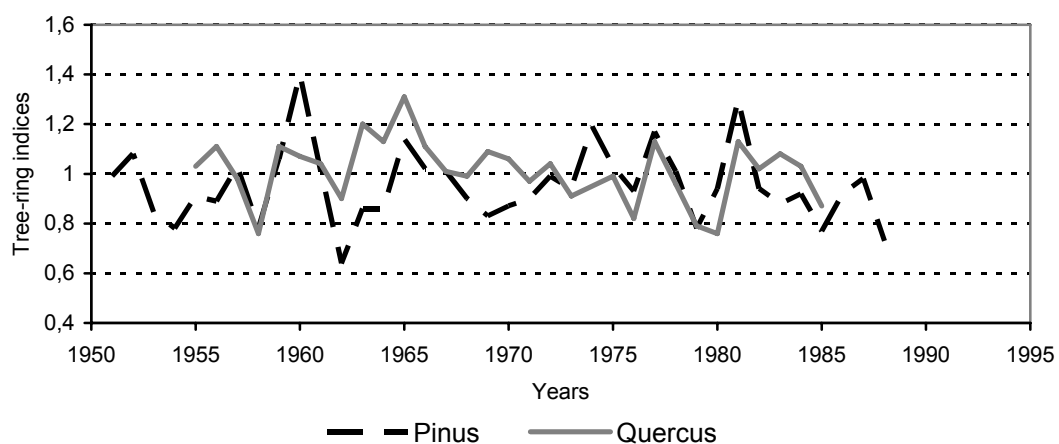


Figure 2: Regional chronologies of tree-rings indexes

Climate dependence of tree-ring width

Correlations between the tree-ring widths and temperature and between the tree-ring widths and precipitation were analyzed for individual local chronologies, as well as for the average regional chronologies, separately for each tree species. The whole complexity of relationships between the factors determining radial increments, and the climatic and non-climatic factors are clearly evident in the local chronologies, so that the climate signal registered in the width of tree-rings is often unclear and concealed. The results of regional chronologies evidently show the influence of the so-called mesoclimate, (which is the outcome that we wished to reach with our investigation). These results are discussed below.

Black pine

It is evident from the results of correlation analysis (Fig. 3) that during the period of winter dormancy and at the beginning of the vegetation period (spring), the formation of radial increments is being stimulated by above-average temperatures (winter: $r = 0.4970$; spring: $r = 0.2846$; March: $r = 0.5544$). Average winter temperature in the area of sampling locations is approx. 3.5°C , and average summer temperature, 10.8°C , which is, according to Fritts (1976), lower than the optimum temperature for photosynthesis, being $15\text{-}20^{\circ}\text{C}$ for the tree species of moderate climate. However, higher-than-average temperatures in the remaining months and seasons impede the formation of radial increments. The negative impact of the above-average temperatures in summer ($r = -0.388$) and during the entire vegetation period, from April through September ($r = -0.4829$) are clear. In the areas where samples were taken, the average summer temperatures are about 20°C , and about 16.5°C in the vegetation period. Higher temperatures in these two periods cause high evapotranspiration, which is "felt" by plants as drought, owing to deficient soil moisture. Potential evapotranspiration in sub-Mediterranean Slovenia is higher than precipitation in July and August, and because of the karstic surface, drought can occur as early as June, and may last until the end of September.

Above-average temperatures in the autumn of the previous vegetation period (September: $r = -0.289$; October: $r = -0.2976$; November: $r = -0.3535$) can be shown to be unfavorable for incremental growth. Firstly, higher autumn temperatures can prolong the formation of tissues which use up the nutrition reserve prepared for the growth in spring; and the second explanation is that higher autumn temperatures postpone the preparation of wood to winter (Fritts, 1976). This increases the sensitivity of tissues to damage caused by cold, and exerts negative influence on the growth in the following season.

A picture of the influence of precipitation is less involved. All statistically relevant correlation coefficients are positive and refer to precipitation in the vegetation period (July: $r = 0.2972$; September: $r = 0.3881$; summer: $r = 0.3225$; vegetation period: $r = 0.3713$). Also statistically relevant is the correlation coefficient referring to the annual amount of precipitation ($r = 0.3413$) which means that black pine in sub-Mediterranean Slovenia forms wider tree-rings in the years with above-average precipitation, especially in the vegetation season.

A cause of the need for more abundant precipitation in sub-Mediterranean Slovenia can not be searched in small amounts of precipitation. This need originates in rather high

temperatures, and even more in karstic features of the surface and shallow soil cover that can only retain little moisture, which eventually causes drought.

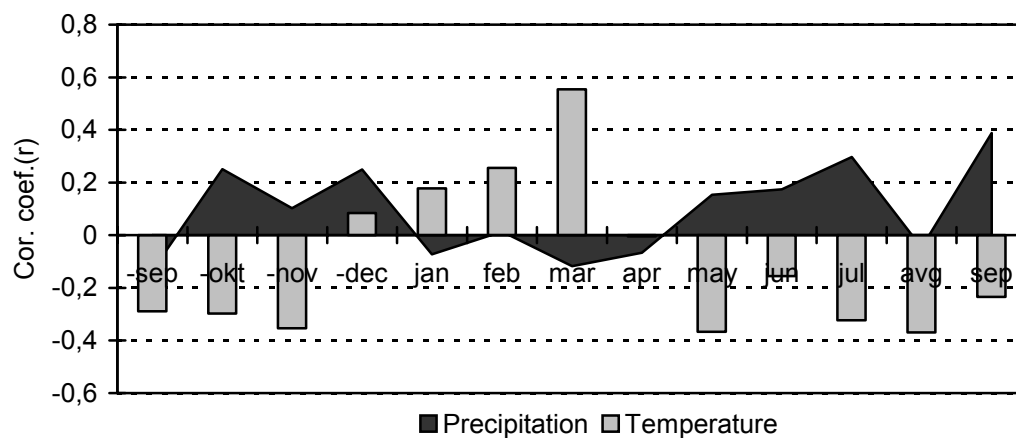


Figure 3: Correlation coefficients of black pine in sub-Mediterranean Slovenia

Oak

The results for the oak chronologies show similar responsiveness to that of black pine, except that the response to precipitation is stronger at oak. The above-average precipitation is stimulative for the formation of radial increments in all seasons (year: $r = 0.2898$). If the influence of precipitation is ranked by correlation coefficients, it becomes evident precipitation in the vegetation period ($r = 0.6654$) and summer (summer: $r = 0.5592$; July: $r = 0.3372$; August: $r = 0.5002$) is most influential on the radial increment. In oak, as in pine, it is important that the above-average precipitation falls during the autumn-winter months of the previous year (October: $r = 0.3193$; November: $r = 0.2207$; December: $r = 0.2956$). Correlation between the precipitation and the width of tree-rings is proportional. The above-average precipitation results in greater soil moisture which reduces the drought stress.

In comparison with black pine, temperature correlations for oak are weaker. The highest values are reached with winter temperatures. Higher temperatures in this season, especially in February, exert negative influence on the formation of radial increments (winter: $r = -0.3003$; February: $r = -0.3371$). This is just the opposite of black pine at which higher winter temperatures have positive influence on the formation of radial increments. One of the possible explanations for this correlation is that winter in sub-Mediterranean Slovenia is the season with the smallest precipitation amount, 250-300 mm, and February with only 80 mm is the driest month. Thus, higher temperatures in this season increase evapotranspiration which, together with deficient soil moisture, results in drought stress. According to Fritts (1976) and Pilcher and Gray (1982), higher temperatures can also directly influence the increased respiration which causes that plant consumes a part of its nutrition reserves as early as winter, which is later manifested in form of reduced increment.

In contrast to winter, a warmer spring or an earlier beginning of the vegetation period is manifested in wider tree-rings (March: $r = 0.2739$; April: $r = 0.2865$; spring: $r = 0.2485$). Except for the August temperatures ($r = -0.2752$), the above-average temperatures in summer do not exert any more significant influence on oak.

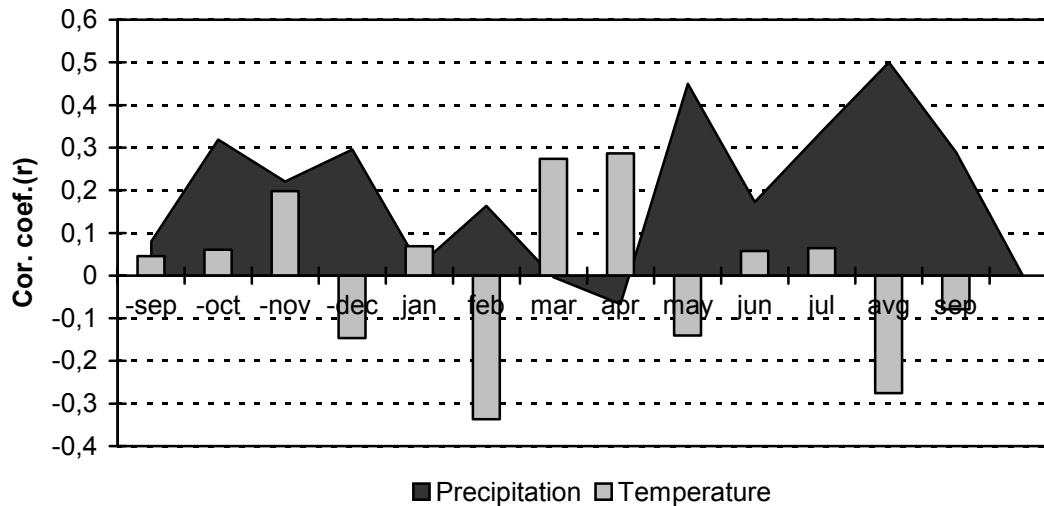


Figure 4: Correlation coefficients of oak in sub-Mediterranean Slovenia

Conclusions

By means of average regional chronologies which were made from local chronologies within an individual climate type, a climate signal registered in the width of tree-rings can adequately be discovered under the condition that trees are climatically sufficiently sensitive, or an element exists within the climatic complex representing the most favorable conditions for the formation of radial increments. Of the three main climate types in Slovenia, the sub-mediterranean, the mountainous and the moderate-continental (Ogrin, 1996), the climate signal recorded in the width of tree-rings is most easily discernible in the sub-mediterranean and also in the mountainous climates.

In sub-Mediterranean Slovenia, the restricting factor of radial increment formation occurs in a form of drought which is further intensified by karstic surface at certain places. Thus, radial increments of oak and black pine are in positive correlation with precipitation, particularly in the vegetation period, and in negative correlation with higher temperatures in the same period. The importance of precipitation in the vegetation period is more explicit in the case of oak, since as much as 44% of radial increment variance can be assigned to it. The conditions at the end of the previous vegetation season are an important influence on growth (preparation for winter), with a wetter than the average autumn with below average temperatures resulting in the largest subsequent rings. In favorable conditions, pine begins to assimilate as early as the end of winter (February), and responds favorably to a warm winter. A warmer spring is favorable for both the tree species studied.

In comparison with the studies which were made in the areas with true Mediterranean climate, where the precipitation amount is smaller, temperature higher and summer drought more explicit, the statistically relevant correlation coefficients for Slovenia are rather low (most of them up to ± 0.4). Also the percentage of variance in radial increment assigned to climate is low. It is slightly higher than 30% for black pine, and 47% for oak. By comparison, Aleppo pine growing in the surroundings of Marseille in southern France, shows as much as 68% of radial increment variance can be accounted for by climate (Munaut, 1982, in: Hughes et al. 1982).

References

- Aloui, A. (1978): Quelques aspects de la dendroclimatologie en Khroumiries. D.E.A. d'Ecologie mediterannee, Universite Aix-Marseille III.
- Berger, A., Guiot, J., Mathieu, L. (1979): Cedar Tree-Rings and Climate in Marroco. *Tree-Ring Bulletin* 39.
- Cook, E.R., Kairiuksis, L.A. (1990): *Methods of Dendrochronology*. Kluwer, 391p.
- Fritr, H.C. (1976): *Tree Rings and Climate*, Academic Press. London, 567p.
- Gams, I. (1977): O zgornji gozdni meji na JV Koroškem. *Geografski zbornik* 16, 151-193.
- Hughes, M.K., Kelly, P.M., Pilchler, J.R., La Marche, V.C. (1982): *Climate from Tree Rings*. Cambridge, 210p.
- Levanič, T. (1996): Dendrokronološka in dendroekološka analiza propadajočih in vladajočih in sovladajočih jelk (*Abies alba* Mill.) v dinarski fitogeografski regiji. dissertation, 163p.
- Lovrenčak, F. (1977): Zgornja gozdna meja v Kamniških Alpah v geografski luči. *Geografski zbornik* 16: 5-150.
- Lovrenčak, F. (1987): Zgornja gozdna meja v Julijskih Alpah in na visokih kraških planotah Slovenije. *Geografski zbornik* 26: 5-58.
- Ogrin, D. (1991): Vpliv padavinskih in temperaturnih razmer na debelinski prirast dreves (na primeru treh pokrajinskih tipov v Sloveniji). *Geografski zbornik* 31: 107-161.
- Ogrin D. (1998): Dendrokronologija in dendroclimatologija Planine pri Jezeru. *Geografski vestnik* 70: 59-73.
- Ogrin, D. (1996): Podnebni tipi v Sloveniji. *Geografski vestnik* 68: 39-56.
- Pilcher, J.R., Gray, B. (1982): The relationships between oak tree growth and climate in Britain. *Journal of Ecology* 70: 297-304.
- Plesnik, M. (1971): O vprašanju zgornje gozdne meje in vegetacijskih pasov v gorovjih JZ in SZ Slovenije. *Gozdarski vestnik* 43: 18-34.
- Seue, F. (1973): *Contributio a l'etude dendroclimatologique du pin d'Alep (Pinus halepensis Mill.)*. These Dr. des Sciences Nat. Marseille.

An integral estimation of tree-ring chronologies from subarctic regions of Eurasia

O.V. Sidorova, M.M. Naurzbaev & E.A. Vaganov

V.N. Sukachev Institute of Forest SB RAS, 660036 Akademgorodok, Krasnoyarsk, Russia

Email: ovsidorova@forest.akadem.ru

Introduction

Using the results of climatic models, some authors state that recorded global warming is directly related to the increased concentration of greenhouse gases in the atmosphere caused by the anthropogenic activity. Quantitative estimations indicate an increase in the average annual temperature in Northern Hemisphere by 0.5-0.6°C (Mann et al. 1998, Jones et al. 2001). According to calculations based on climatic models, the strongest warming should be observed in the high latitudes of the Northern Hemisphere, with an increase of 3-4°C (Kelly et al. 1982, Budyko and Israel, 1987). However, data obtained from analyses of the radial growth of trees from the sub-Arctic area of Eurasia, an area closely tied to strongest temperature changes, do not show significant changes in climatic conditions (Briffa et al. 1998, Naurzbaev and Vaganov 2000). There is also the unresolved issue of the range of natural climate fluctuations, i.e. the amplitude of near-surface air temperature changes in the high latitudes of the Northern Hemisphere during the Holocene. Tree-ring chronologies serve as a reliable instrument for the reconstruction of natural temperature fluctuations in the high latitudes over millennial time scales. Compared to the other indirect sources of climate information, these tree-ring chronologies have important advantages: Firstly, climatic information is distinctly recorded in annual tree-rings (Briffa et al. 1998, Naurzbaev and Vaganov 2000, Naurzbaev et al. 2001). Secondly, at the northern boundary of the Eurasian forests, trees reach a maximum age of 1216 years and the net of dendro-climatic “stations” evenly distributed over a vast territory of Siberia permits spatial and temporal reconstructions of temperature variation (Vaganov et al. 1999, Sidorova and Gerasimova 2005); and finally dead trees, preserved in permafrost, offer the opportunity of obtaining tree-ring chronologies over longer Holocene time scales (Shiyatov 1986, Vaganov et al. 1996, Vaganov and Naurzbaev 1999, Hantemirov 1999, Hughes et al. 1999, Naurzbaev et al. 2002, Sidorova 2001, 2003, Hantemirov and Shiyatov 2002, Grudd et al. 2002).

Materials and methods

We developed 2000-year tree-ring chronologies based on the oldest living trees, dead and sub-fossil wood well preserved in the Eastern Taimyr [72N – 102E] (Naurzbaev and Vaganov 2000, Naurzbaev et al. 2002), North-Eastern Yakutia (Indigirka) [70N – 148E] (Hughes et al. 1999, Sidorova 2001, Sidorova and Naurzbaev 2002) and also used millennia-long chronologies, produced by our colleagues from the Yamal [67N – 70E] (Hantemirov 1999, Hantemirov and Shiyatov 2002), and Sweden [68N – 20E] (Grudd et al. 2002).

To exclude age-dependent variations and to retain the maximally long-term and high frequency climatic signal the raw tree-ring width measurements were standardized by Regional Curve Standardization and corridor methods (Shiyatov 1986, Briffa et al. 1996, Esper et al. 2002).

Results

Main characteristics of these chronologies are given in the table 1.

Table 1: Statistical characteristics of regional long-term tree ring chronologies

Chronologies	Standard deviation	Sensitivity	Correlation coefficient of low pass filtered data ($p < 0.05$)			
			Sweden	Yamal	Taimyr	Indigirka
Sweden	1.28	0.74	1.00			
Yamal	0.73	0.81	0.24	1.00		
Taimyr	1.52	0.80	0.14	0.35	1.00	
Indigirka	1.21	0.80	0.17	0.20	0.25	1.00

All four tree-ring chronologies show a high standard deviation of 0.73 - 1.52 and sensitivity of 0.74 – 0.81. After RCS standardization (Shiyatov 1986, Briffa et al. 1996, Esper et al. 2002) all four tree-ring chronologies are smoothed with a low pass 41-year filter. The chronologies show significant correlation coefficients of low frequency variability (long-term) and insignificant correlation of high (from year to year) variability. It means that summer temperatures on annual basis mainly differ in various sectors of the Subarctic. The more careful analysis indicates that the percentage of years with the same warm or cold calendar years for the whole northern Eurasia does not exceed 20% for the last two millennia (Vaganov et al. 1996, Naurzbaev et al. 2003, Sidorova 2003).

In an earlier part of the analysis of spatio-temporal variability of tree growth in high latitudes of Eurasia it was clearly shown that the local tree-ring chronologies significantly correlate within an area of up to 600-800 km in the west-eastern direction. Thus, millennial chronologies represent various tree-ring growth and climatic variability for large sectors of the Subarctic. Summer temperature variability explains 60-70% of total variability in tree-ring indices.

The combined chronology for Northern Eurasia was calculated as first principal component (Fig. 1).

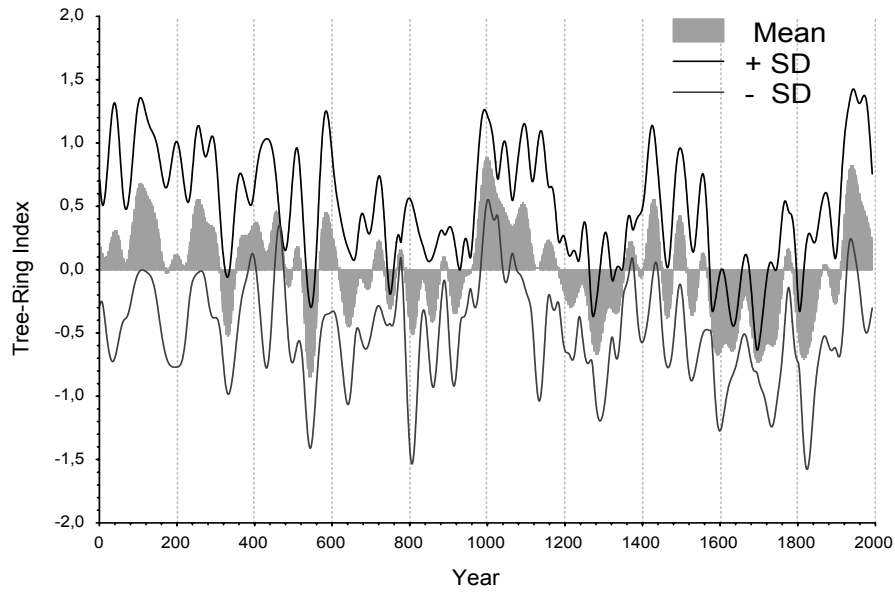


Figure 1: Combined northern Eurasia tree-ring chronology

In figure 1, we can see several warm periods (first to fifth century), the Medieval Warm Period (the maximum increase during the 10th to 12th centuries) and current warming in the middle 20th century and abrupt cooling during the middle of the 16th century and the end of the 19th century. The long-term changes in Northern Eurasia have a similar character during the last 1250 years (Fig. 2).

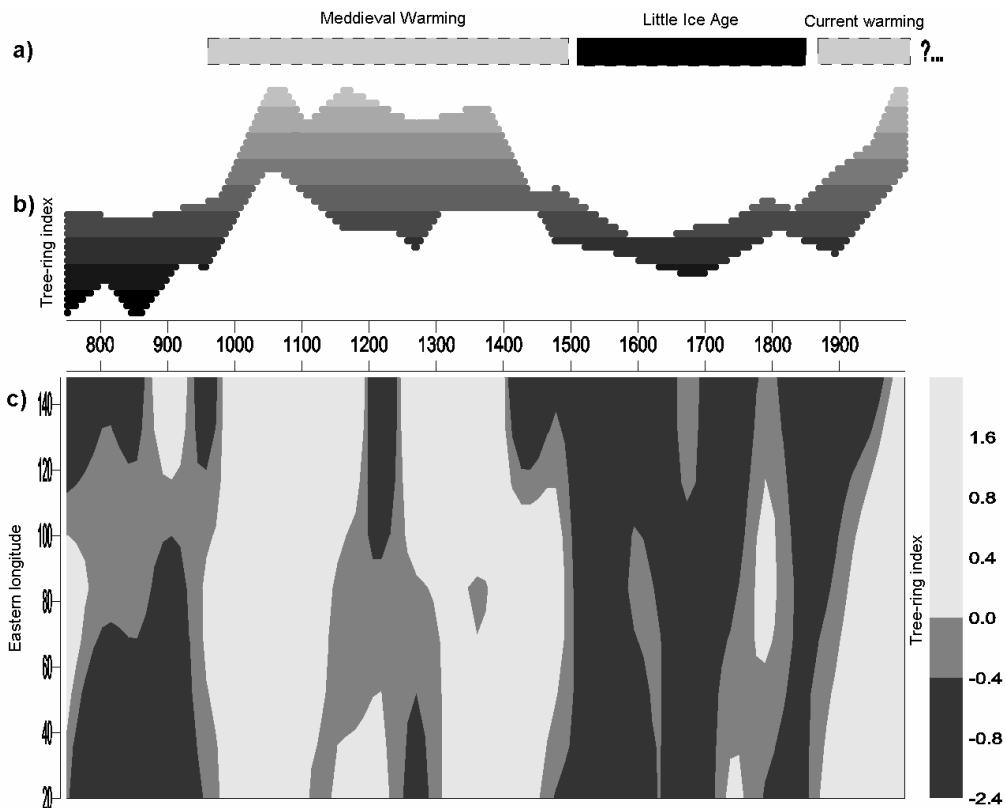


Figure 2: Range of tree-radial growth changes in the millennia chronologies (b) and variability of the tree-ring index chronologies in spatial location (c) for the late Holocene (class. by Lamb 1977) (a)

Medieval warming (MWP) lasted from the 10th to the 12th century and the 15th-century warming was followed by cooler conditions during the Little Ice Age (LIA) with lowest temperatures in the 17th century. The current warming which started at the beginning of the XIX century does not exceed the amplitude of the Medieval Warming. In the last century tree-ring growth is more intensive in the western Subarctic part than in the eastern part. All millennial chronologies fixed Medieval Warming, which has two phases - XI, XII and middle of the XIII, XIV separated by a short period of growth depression (late XII - middle XIII). The radial growth depression was longer in the western part of Eurasia, but more severe in the eastern part. Moreover, all chronologies fixed the radial growth reduction in the LIA (early XVI - XIX) and before MWP.

Let us consider the fragments of the combined tree-ring chronology in the early Medieval Warming and current warming. The estimates (increase by 0.82 and 0.95 for the last 100 years) testify that the mean rate of the long-term growth increase is approximately equal in both periods but the amplitude somewhat disagrees.

For each chronology we calculated the response function and developed a temperature reconstruction for the last 1000 years. We used data of closely located meteorostations for each region. In table 2 the main statistical characteristics of reconstruction models for all four millennia chronologies are shown.

Table 2: Calibration model results of June-July air temperature reconstruction

Chronologies/ meteorostations	Statistics of instrumental series			Statistic of reconstruction models		
	Calibration period, years	Mean temperature, °C	Variance, °C	Correlation coefficient for index chronologies and 5-years moving average series	F- statistics	Synchronism coefficient, %
Sweden/ <u>Karesuando</u>	1830-1838 1951-1980	11.5	1.71	0.48/0.60	F _{1.37} = 11.3; p<0.01	67
Yamal/ <u>Salekhard</u>	1883-1995	11.1	1.80	0.60/0.74	F _{1.111} = 63.4; p<0.01	72
Taimyr/ <u>Katanga</u>	1933-1996	8.8	1.70	0.60/0.66	F _{1.62} = 33.7; p<0.01	63
Indigirka/ <u>Chokurdakh</u>	1945-1989	7.9	1.54	0.61/0.71	F _{1.43} = 25.2; p<0.01	68

The correlation between temperature and tree-ring indices is highly significant and still increases after smoothing. It means that agreements of long changes of radial growth and summer temperature are higher than in the year-to-year variability. Let us compare the quality values of mean summer temperature by results of reconstruction for each century of the last millennia (table 3).

Table 3: Quantitative estimates of mean summer air temperature for the last millennia.

Century	Sweden		Yamal		Taimyr		Indigirka	
	Mean	SD	Mean	SD	Mean	SD	Mean	SD
X	10.2	1.06	10.6	.66	8.6	1.68	8.5	1.38
XI	11.1	.83	10.6	.60	8.9	1.40	9.6	1.96
XII	9.7	.82	10.5	.52	9.0	1.61	9.4	1.44
XIII	9.7	.70	10.4	.44	7.4	1.42	8.4	1.73
XIV	10.3	.84	10.4	.56	8.1	1.74	8.4	1.51
XV	11.0	.75	10.6	.67	8.5	1.25	7.9	1.34
XVI	10.7	1.04	10.3	.45	7.6	1.18	8.1	1.44
XVII	9.3	.90	10.3	.46	7.3	1.18	8.1	1.45
XVIII	9.8	1.04	10.4	.47	8.2	1.23	7.6	1.10
XIX	10.7	1.15	10.1	.49	7.8	1.51	7.4	1.00
XX	11.1	.85	11.0	.78	8.9	1.28	8.0	1.02
Mean	10.2		10.5		8.2		8.3	
(t_{\max} t_{\min})	1.8		0.9		1.7		2.2	

From this table we can see that the range of summer air temperature changes was about 2°C, the only exception being Yamal. For this region there was defined less temperature reduction. The current warming manifests more in the western part of Eurasia and less in the eastern part. The MWP shows higher values of temperatures in the eastern part of Eurasia and approximately equal values in the western part in comparison with the current one. The difference in average temperature of current and Medieval Warming compared to Little Ice Age is not so large -1.5°C and is heterogeneous in space: higher in the eastern part and low in the west.

We compared our Eurasian average chronology with the well-known large-scale Mann's temperature reconstruction from the last IPCC report (Mann et al. 1998) (Fig. 3).

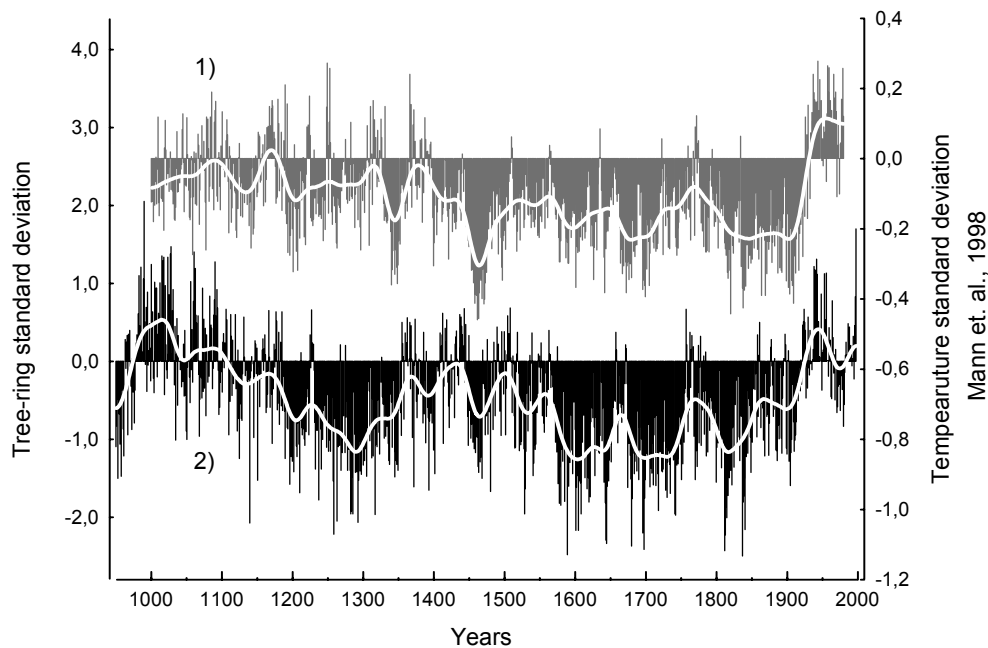


Figure 3: Comparison of Eurasian (1) and large-scale temperature (2) reconstructions

The reconstructions differ markedly in their amplitudes (0.6° - 0.8° C for the Northern Hemisphere and 2.5° - 3.0° C for Northern Eurasia). The curve for Northern Eurasia, however, does not show an abrupt temperature increase in the last century as seen in the hemispheric reconstruction. The significant synchronism between the two curves is noted in decadal to century temperature fluctuation. Also years and periods are revealed indicating synchronous volcanic activity: 1259, 1600, 1641, 1812-1815, 1912, 1960 (Briffa et al. 1996, Sidorova and Naurzbaev 2000).

So, an integral estimation of tree-ring growth spatial-temporal conjugation was carried out based on a tree-ring width network of the subarctic zone of Siberia, Ural and Scandinavia for the last 2000 years. Phase and amplitude disagreements of the annual growth and its decadal fluctuation in different subarctic sectors of Eurasia changed by synchronous fluctuation when century and longer growth cycles were considered. Long-term changes of radial growth indicate common character of global climatic variation in the subarctic zone of Eurasia. Medieval Warming occurred from Xth to XIIth centuries and XVth century warming are changed by Little Ice Age with the cooling culmination taking place in the XVIIth century. Current warming started at the beginning of the XIXth century and presently does not exceed the amplitude of medieval warming. The tree-ring chronologies do not indicate unusually abrupt temperature rise during the last century, which could be reliably associated with greenhouse gas increasing in the atmosphere of our planet. The modern period is characterized by heterogeneous warming effects in the subarctic regions of Eurasia.

Acknowledgements

This work was supported by grants RFBR- 05-04-48069-a, KKFN – 10T09; RFBR-Enisey - 05-05-97708 and Integration Program No 121.

References

- Briffa, K.R., Jones, P.D., Schweingruber, F.H., Karlen, W., Shiyatov, S.G. (1996): Tree-ring variables as proxy indicators: Problems with low-frequency signals. *Climate change and forcing mechanisms of the last 2000 years*. Berlin: Springer, NATO ASI Series 141: 9-41.
- Briffa, K.R., Jones, P.D., Schweingruber, F.H., Karlen, W., Shiyatov, S.G. (1996): Tree-ring variables as a proxy-climate indicators: Problems with low-frequency signals. In: *Climate Change and Forcing Mechanisms of the last 2000 years*, NATO ASI Ser., Ser.1: *Global Change 41*: 9-41.
- Briffa, K.R., Jones, P.D., Schweingruber, F.H., Osborn, T.G. (1998): Influence of volcanic eruptions on Northern Hemisphere summer temperatures over the past 600 years. *Nature* 393: 450-455.
- Briffa, K.R. (2000): Annual climate variability in the Holocene: interpreting the message of ancient trees. *Quaternary Science Reviews* 19: 87-105.
- Briffa, K.R., Osborn, T.J., Schweingruber, F.H., Harris, I.C., Jones, P.D., Shiyatov, S.G., Vaganov, E.A. (2001): Low frequency temperature variations from a northern tree-ring density network. *Journal of Geophysical Research* 106 (D 3): 2929-2941.
- Budyko, M.I., Izrael, Yu.A. (1987): *Anthropogenic Forcing of Climate* (in Russian), Leningrad, Gidrometeoizdat, 476 p.
- Esper, J., Cook, E.R., Schweingruber, F.H. (2002): Low-frequency signals in long tree-ring chronologies for reconstructing past temperature variability. *Science* 295: 2250 -2253.
- Grudd, H., Briffa, K.R., Karlen, W., Bartholin, T.S., Jones, P.D., Kromer, B. (2002): A 7400 year tree-ring chronology in northern Swedish Lapland: natural climatic variability expressed on annual to millennial timescales. *The Holocene* 12.6: 657-665.
- Hantemirov, P.M. (1999): Tree-ring reconstruction of summer temperatures in the North of the West Siberia for the last 3248 years. *Sib. Ecol. Journal* 2: 185-191 (in Russian).
- Hughes, M.K., Diaz, H.F. (1994): Was there a "Medieval Warm Period" and if so, where and when? *Climatic Change* 26: 109-142.
- Hantemirov, R.M., Shiyatov, S.G. (2002): A continuous multimillennial ring-width chronology in Yamal, northwestern Siberia. *The Holocene* 12 (6): 717-727.
- Hughes, M.K., Vaganov, E.A., Shiyatov, S.G., Touchan, R., Funkhouser, G. (1999): Twentieth-century summer warmth in northern Yakutia in a 600-year context. *The Holocene* 9 (5): 603-608.
- Jones, P.D., Osborn, T.J., Briffa, K.R. (2001): The evolution of climate over the last millennium. *Science* 292: 662-667.
- Kelly, P.M., Jones, P.D., Sear, S.B., Cherry, B.S.G., Tavakol, R.K. (1982): Variations in surface air temperature: Part 2. Arctic regions, 1881-1980. *Monthly Weather Reviews* 110: 71-83.
- Lamb, H.H. (1977): *Climate: Present, Past and Future*. Climate History and Future. London, Methuen, 2: 603.
- Mann, M.E., Bradley, R.S., Hughes, M.K. (1998): Global scale temperature patterns and climate forcing over the past six centuries. *Nature* 392/23: 779-787.

- Naurzbaev, M.M., Vaganov, E.A. (2000): Variation of summer and annual temperature in the east Taymir and Putoran (Siberia) over the last two millennia inferred from tree-rings. *Geophys. Res.* 105 (6): 7317-7327.
- Naurzbaev, M.M., Sidorova, O.V., Vaganov E.A. (2001): History of the late Holocene climate of the Eastern Taimyr according to long-term tree-ring chronology. *Archaeology, Ethnology and Anthropology of Eurasia* 3 (7): 17-25.
- Naurzbaev, M.M., Vaganov, E.A., Sidorova, O.V., Schweingruber, F.H. (2002): Summer temperatures in eastern Taimyr inferred from a 2427-year late-Holocene tree-ring chronology and earlier floating series. *The Holocene* 12 (6): 727-736.
- Shiyatov, S.G. (1986): Dendrochronology of upper timberline in Polar Ural Mountain. (in Russian). Moscow, Nauka, 186 p.
- Sidorova, O.V., Naurzbaev, M.M. (2000): Chronology volcanic eruptions fixed in the tree-ring in the Siberian Subarctic. Reports of the All-Russia conference, Tomsk, p. 10.
- Sidorova, O.V. (2001): Climatic response of larch trees growing at the upper timber line and above flood-plain terrace of lower stream Indigirka River. Tree Rings and People. International Conference on the Future of Dendrochronology. Davos, Switzerland. September 22-26, P. 230.
- Sidorova, O.V., Naurzbaev, M.M. (2002): Response of *Larix cajanderi* to climatic changes at the upper timberline and in the Indigirka River valley. *Lesovedenie* 2: 73-75 (in Russian).
- Sidorova O.V. (2003): Long-term climatic changes and the larch radial growth on the northern Taimyr and the North-Eastern Yakutia in the Late Holocene. Abstract of PhD dissertation, 18 (in Russian).
- Sidorova, O.V., Gerasimova, O.V. (2005): The oldest trees on the Earth. Young Scientist conference. Proceedings, Krasnoyarsk, IF SB RAS, 5: 89.
- Vaganov, E.A., Shiyatov, S.G., Mazepa, V.S. (1996): Dendroclimatic study in Ural-Siberian Subarctic. Novosibirsk: Nauka: 246 pp. (in Russian).
- Vaganov, E.A., Naurzbaev, M.M. Eger', I.V. (1999): The age limit of larch in Siberia. *Lesovedenie* 6: 65-75 (in Russian).

Dendroclimatic Investigations in Asir Mountains – Saudi Arabia

Preliminary Report

M. Sigl^{1,2}, H. Strunk¹ & H.-J. Barth¹

¹University of Regensburg, Department of Physical Geography, 93040 Regensburg, Germany

²Paul-Scherrer-Institut, Laboratory for Radio- und Environmental Chemistry, 5232 Villigen, Switzerland

Email: michael.sigl@psi.ch

Introduction

When one thinks of forests or woodlands the Arabian Peninsula is not an area that immediately comes to mind, though in fact the region offers a high variety of botanical landscapes, many of which are wooded. The most spectacular Arabian woodlands are those dominated by species of *Juniperus*, which can be found at the higher altitudes of the northern mountains of Oman (*Juniperus excelsa*) and atop the great mountain spine that runs from the southern Jordanian border to Aden's doorstep. From the border with Jordan at about 29° latitude to Taif at about 22°, *Juniperus phoenicea* can be found and it overlaps along 30 km along the Taif escarpment with *Juniperus procera*, which extends southwards into the mountains of Yemen (Fig. 1).

In the Asir Mountains of Saudi Arabia these juniper woodlands can be found at altitudes as low as 1700 m a.s.l.. There is no upper tree line since the maximum altitude of the Arabian mountains is 3700 m a.s.l.. Elsewhere within their range these junipers grow as high as 4500 m a.s.l. (Esper 2000). The density of the woodlands varies from a maximum of about 200 trees per hectare, in the very open juniper woodlands of Oman, to as high as 4000 per hectare in Asir (Fisher 1997).

Despite their differing densities and species compositions and the fact that in Saudi Arabia and Yemen the woodlands have been heavily impacted by human activities, juniper woodlands throughout the Peninsula have one thing in common: at the lower altitudes they are all exhibiting extensive dieback and there are few signs of regeneration. In some areas this is so extreme that the woodlands look like a cemetery for trees (Fig. 2).



Figure 1: Juniperus procera in healthy condition near Jabal Soudah, 2830 m.



Figure 2: Massive forest decline at Jabal Al Qahar, 1840 m.

The widespread nature of the phenomenon, occurring in both the west and east of the peninsula and affecting three species of *Juniperus*, indicates that localised influences, such as pathogen attack (Hajar 1991) are probably not the ultimate cause of dieback. Available evidence indicates a hydrological and/or climatological cause (Fisher 1997). However our present knowledge of the regional climate is poor, with climate data leading no farther back than to 1978.

Objective

The objective was therefore to identify whether climate could be the ultimate cause of the dieback, which affects juniper communities all over the region, applying tree-ring analysis.

Tree-ring chronologies have rarely been constructed for arid or tropical regions, and except a study by Fisher and Gardener (1998), never for trees on the Arabian Peninsula. This is due to the fact that in most regions there is no climate sufficiently seasonal for the formation of clear annual growth rings. Our study area, the high mountains of Asir and Tihama around Abha in SW Saudi Arabia (Fig. 3), seems to be suitable for dendroclimatological investigations, as winter temperatures fall low enough to ensure a cessation of growth and hence the production of a clear growth ring in the wood (Fig. 4). The rainfall pattern is characterised by a major precipitation maximum during spring months and a minor monsoonal influenced summer maximum with September and October being generally very dry (mean annual precipitation 386 mm).

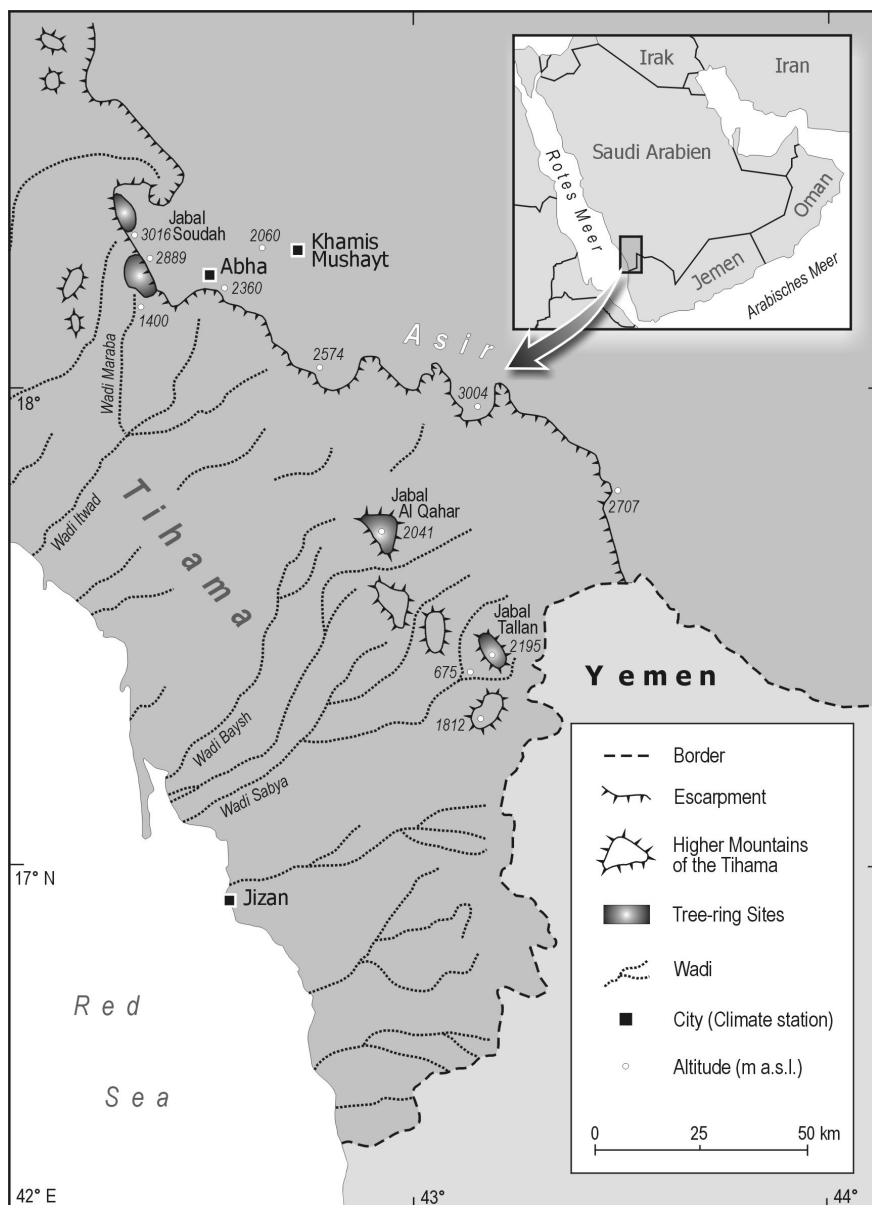


Figure 3: Map of the Asir region with the position of sample sites and climate stations.

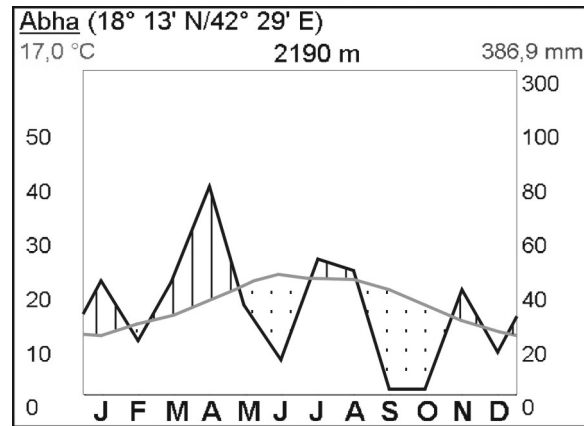


Figure 4: Climogram for the meteorological station at Abha (see figure 3 for location). The black line indicates mean monthly temperature, the grey line mean monthly total precipitation with humid periods indicated by vertical shading and dry periods indicated by point shading. Meteorological data is available only from 1978.

As species of *Juniperus* are known to be difficult subjects for dendrochronology, regarding dating and cross-matching problems (Esper 2000), whole trunk sections rather than cores are required for satisfactory chronology development. With many canopies already being dead a large number of trunk sections could have been taken. Crossmatching with cores obtained from living trees and trunk sections from older buildings should allow the creation of a centennial chronology, on which comparisons with the recent climate can be carried out.

Sampling Sites and Methodology

Four tree-ring sites were sampled. Two of the sites are on the top of Jabal Soudah (3015 m a.s.l.). The other two sites lie on the southern and northern slope of Jabal Tallan in the hilly Tihama (Fig. 3). Elevation of the sampled sites ranges from 1780 to 2940 m a.s.l.. At each tree-ring site a number of samples were taken within a uniform topographic area (Tab. 1).

Table 1: Site data for the sampled tree-ring sites in the Asir region.

Site name	Latitude	Longitude	Elevation (m)	Exp.	Dec.	Time span*	Length	No. of samples	No. of cores	No. of cross-sections
Soudah 2000	18 ° 17' N	42 ° 22' E	2870-2910	Plain	0-8°	1900-2000	101	23	23	0
Soudah 2003	18 ° 17' N	42 ° 22' E	2930-2940	Plain	0-3°	1933-2002	70	23	23	0
Tallan North	17 ° 24' N	43 ° 10' E	1780-1980	NW	10-36°	1850-1994	145	43	0	43
Tallan South	17 ° 24' N	43 ° 10' E	1900-1970	S	14-20°	1950-2002	53	22	22	0

* with at least ten samples

Trunk sections and cores were sanded for microscope examination and measured using standard techniques. Tree ring widths were measured along one to four radii of the trunk sections, depending on the irregularity of the stem. The time series were carefully crossmatched using TSAP[®] crossdate functions. The single tree-ring series were standardized using a unweighted 21-year moving average to remove any age-related trend in the series. By this technique the width of each ring is divided by the value of the regression line for that year, producing a tree ring index, which varies around the value 1 (Cook and Kairiukstis 1990). The standardized single series were then averaged to produce the site

tree-ring chronology. To examine the quality of the site chronology, Pearson correlation coefficient, t-values according to Baillie and Pilcher (1973) and gleichlaeufigkeit were calculated between each single series and the site chronology. Threshold values used for single series elimination are >3 (t-values) and 60% (gleichlaeufigkeit).

To document anatomical features of the sampled juniper wood, anatomical wood preparation techniques according to Schweingruber (2001) were used.

A meteorological station in Abha (2190 m a.s.l.; 18°23' N / 42°60' E) with precipitation records since 1978 was selected to test the climate/tree-ring relations (Fig. 4).

Results and Discussion

Trees of *Juniperus procera* in the Asir mountains have clear rings which can be dated.

The maximum number of tree-rings counted were 260. The average age ranges from 51 years at Tallan South to 138 years at Soudah 2003. Average growth rates are influenced by local site ecology and values vary between 0.99 mm/yr to 1.27 mm/yr.

Unfortunately, juniper trees tend to grow irregularly, often with star shaped and twisted stems as well as strip bark growth forms (Fig. 5). Variability in the formation of rings around the circumference of the trees made cross-matching of cores extremely difficult. As seen in the cross-sections, the amount of locally absent rings was high (up to 18%). Even with cross-sections, cross-matching between trees was difficult because of the occasional formation in juniper wood of a second, relatively narrow growth ring in a single year. More difficulty was found due to the high incidence (up to 12%) of intra-annual boundaries (false rings), which are thought to be built during extreme climate events like droughts.



Figure 5: Cross-section of a sample with typical irregular growth form. The black line indicates the measured radius. Jabal Tallan, 1770 m a.s.l..

Table 2: Chronology data for the tree-ring series of the four sites.

Chronology name	No. of samples	No. of tree-rings	Mean correlation among radii (PEARSON)	Variance (%)
Soudah 2000	18	1518	0,21	64
Soudah 2003	14	1906	0,14	64
Tallan North	20	2773	0,15	76
Tallan South	15	820	0,09	81

The average correlation coefficient between trees for each site demonstrates a low growth signal among trees (Tab. 2). A comparison between the four chronologies is shown in figure 6. The correlation between Tallan North and Tallan South is $r = 0.26$, $N = 100$, $p \leq 0.05$. There was also a significant correlation between Tallan North and Soudah 2000 ($r = 0.18$, $N = 135$, $p \leq 0.05$).

However correlation between the site chronologies was higher between 1980 and 2000. Tallan North and Tallan South correlates significantly with $r = 0.45$, Tallan South and Soudah 2000 with $r = 0.64$ and Tallan North with Soudah 2000 with $r = 0.44$ ($N = 21$; $p \leq 0.05$).

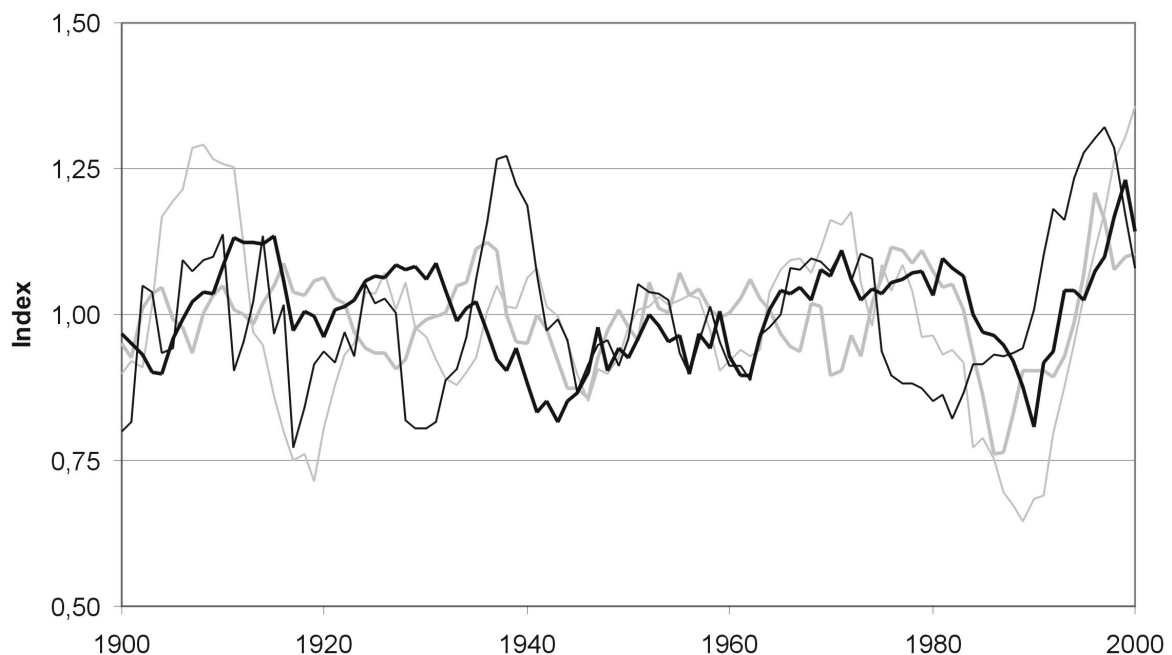


Figure 5: The four site chronologies for 1900-2000, produced by averaging the standardized tree-ring widths of 18 trees from the site 'Soudah 2000' (thin grey line), 14 trees from the site 'Soudah 2003' (bold grey line), 20 trees from the site 'Tallan North' (bold black line) and 15 trees from 'Tallan South' (thin black line). All tree-ring series are smoothed by a unweighted 9-year moving average.

We therefore suggest that there is a common signal in the tree-ring series, but with increasing age the tree rings are not properly dated, due to difficulties in the identification and dating of false and missing rings.

Climatic influence on the growth of trees must be the major focus of future work. Correlations between the tree-ring chronologies of Asir mountains and precipitation data from the weather

station in Abha must be calculated. As variance is high for all of the site-chronologies, new tree-ring series for climate reconstruction should be built, using trunk-sections from living trees of known age. This was not possible in the area of study (Asir Nationalpark) but should be possible in other areas of SW-Arabia, including Yemen.

Acknowledgments

This study would not have been possible without the help of H.E. Prof. Dr. Abdulaziz H. Abuzinada and Tarik Al-Abassi from the National Commission for Wildlife Conservation and Development in Riyadh, Saudi Arabia. I thank Mike Staudinger, Mirko Krabisch, Dr. Oliver Nelle (University of Regensburg), Prof. Dr. Fritz-Hans Schweingruber and Dr. Jan Esper (WSL, Birmensdorf) for their help and support. The work was funded by the DFG.

References

- Baillie, M. G. L., Pilcher, J.R. (1973): A simple cross-dating program for tree-ring research. *Tree Ring Bulletin* 33: 7-14.
- Cook, E. R., Kairiukstis, L. A. (1990): Methods of dendrochronology. Applications in the environmental sciences. Kluwer. 394 pp.
- Esper, J. (2000): Paläoklimatische Untersuchungen an Jahrringen im Karakorum und Tien Shan Gebirge (Zentralasien). Asgard. 126 pp. (Bonner Geographische Abhandlungen, 103), 126 pp.
- Fisher, M. (1997): Decline in the juniper woodlands of Raydah Reserve in south-western Saudi-Arabia. *Global Ecology and Biogeography Letters* 6: 379-386.
- Fisher, M., Gardner, A. S. (1998): The potential of a montane juniper tree-ring chronology for the reconstruction of recent climate in Arabia. Alsharan, A.S.K.W. et al. (Editors): Quaternary Deserts and Climatic Change. Balkema. 273-278.
- Hajar, A.S. et al. (1991): Impact of biological stress on *Juniperus excelsa* M. Bieb. in south-western Saudi Arabia: insect stress. *Journal of Arid Environment* 21: 327-330.
- Schweingruber, F. H. (2001): Dendroökologische Holz Anatomie – Anatomische Grundlagen der Dendrochronologie. Haupt. 472 pp.

Dendroclimatic research in Western Siberia – The reconstruction of temperature and precipitation since the 16th century

M. Staudinger & H. Strunk

University of Regensburg: Dept of Physical Geography, Universitätsstr. 31, 93053 Regensburg, Germany

Email: mike.staudinger@freenet.de

Introduction

The climate of the northern West Siberian Lowlands is influenced by extremely cold winters and short vegetation periods in summer (Franz 1973). The local vegetation grows on permafrost soils with an observed active layer of 40–200 cm. The relief is formed by thermokarst. In summer the formation of thermokarst depressions is initiated by a thawing of the ice-rich upper part of permafrost (Agafanov *et al.* 2004). Hence, at specific ecological sites, temperature seems to be the dominant growth-limiting factor.

The West Siberian Lowlands as a part of Siberia comprise a very large area (Wein 1999), which is relatively unexplored referring to climatic conditions until now.

This is an attempt to find a relation between tree-ring growth of recent *Pinus sibirica* trees and climate data, and to reconstruct the climate of the northern Westsiberian Lowlands back into the 16th century. The prime aim is the analysis of the influence of precipitation and especially temperature on recent trees. The results point to the high potential for climate reconstructions derived from trees of Western Siberia.

Study area

The study sites are located in the northern Taiga of the West Siberian Lowlands near the towns Muzhi and Vanzevat on the banks of the rivers Ob and Synja. At 3 locations named Vanzevat (Ob), Synja (Synja) and ObNord (Little Ob, northern border area of growth of *Pinus sibirica*) 234 cores of *Pinus sibirica* trees have been taken. The study sites Synja and ObNord are about 35–40 km away from Muzhi (65°24'N, 64°00'E). Vanzevat is located 140 km southeast of Muzhi and 250 km south of Salekhard (66°30'N, 66°40'E). The elevation is approximately 20-30 m a.s.l.. The vegetation period at these locations is about 1 to 4 months. The mean annual precipitation in the area ranged between 1933 and 1988 from 300 to 700 mm. Since 1879 the coldest month measured in Salekhard was January in 1885 with a mean of -34.1 degrees centigrade, and the annual average of temperature has been varied between -1 and -8 degrees centigrade. This is the reason why in years with extreme winters and short vegetation periods the trees build tree-rings with only some 1/100 mm.

The water temperature of the 2 rivers is different and influences the air temperature at the study sites. In mid of September 2002 the Ob temperature near Azovy (a village 20 km east of study site Synja) amounted to 8.8 °C, the temperature of the Synja water at study site Synja only 4.6 °C. The cause of this difference is that the river Ob has its origin in the warmer south, while Synja, a tributary of the river Ob, has its origin in the colder Ural mountains.

The predominantly occurring coniferous tree species in the study area are *Pinus sibirica*, *Picea obovata* and *Larix sibirica*.

Methods

The trees

Former examinations showed that *Pinus sibirica* trees are very suitable to reconstruct temperature and precipitation. The local *Pinus sibirica* trees reach a height of about 15 m and a stem diameter of 40 cm. These trees sometimes can either be very young or many hundred years old (for example: location Synja, tree syn36, diameter 35 cm, age: 84 years; location Vanzevat, tree Ob207, diameter 32 cm, age 488 years).

The oldest trees have been found at the southern most location Vanzevat. Most of the samples have been taken at this site (95 cores of 89 trees). The tree-ring statistics for the three study sites derived from MS Excel outputs are listed in table 1.

After preparation and sanding the ring widths of the samples were measured with a precision of 0.01 mm with LINTAB. The tree-ring data series of the three locations have been combined to mean series and related to climate data after finishing crossdating, indexation and elimination of outliers (Cook 1990, Fritts 1976, Schweingruber 1983) with TSAP (Rinn 1996).

Table 1: Statistics for the three site chronologies

	Vanzevat	Synja	ObNord
Number of samples	95	66	73
Number of trees	89	58	39
Average annual increment [1/100 mm/a)	42	69	55
Average age	256	146	162
Standard deviation	19	32	22
Thinnest treering [1/100 mm]	1	4	3
Widest treering [1/100 mm]	419	496	400
Oldest tree	488	282	255
Youngest tree	73	49	81
Period	AD 1512-1999	AD 1721-2004	AD 1748-2002

Meteorological data

The meteorological data are taken from 2 climate stations in Muzhi and Salekhard. The data from Muzhi are monthly temperature data and precipitation data from 1933-1990 or 1933-1988 respectively. The meteorological data from Salekhard are monthly temperature data from 1879-1989. For correlation with the study sites Synja and ObNord the data of the very

close station Muzhi have been used. For correlation with Vanzevat the combination of temperature data from both stations guarantees the proximity to the sampling place.

Climate–Growth relations

The study was focused on the analysis of the interannual relationships between the chronology and the meteorological dataset (monthly, summer periods, annual values). To avoid fluctuations and irregularities the chronologies have been standardized and smoothed by calculating an 11 year moving average. In the same way the temperature and precipitation data of Muzhi and Salekhard have been smoothed.

By means of regression analysis the relation between the chronologies and meteorological dataset can be described. The kind of relation is expressed as an equation. By converting the tree-ring data with this equation it is possible to reconstruct the temperature and the precipitation of the last centuries. The standardised tree-ring series of study site Vanzevat (Fig. 1) have been used to reconstruct the average temperature of the months June, August, September, October, November from 1512-1999 (Fig. 5).

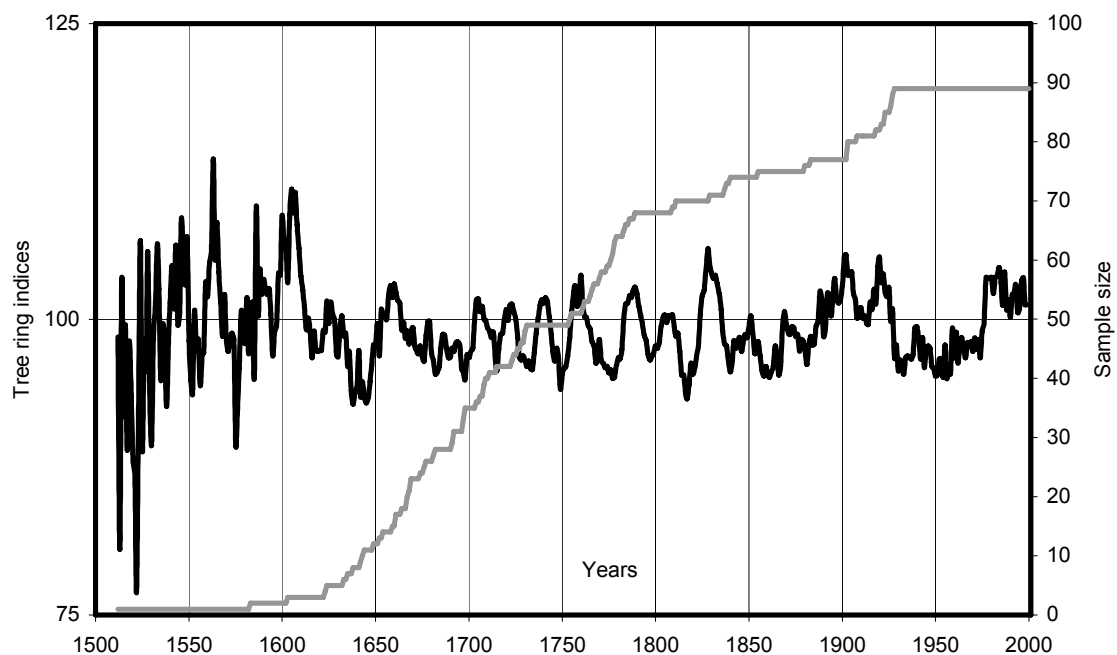


Figure 1: Local Pinus sibirica chronology (black graph, standardised 11-year moving average) and sample size (grey graph) from Vanzevat AD 1512-1999.

Results

The locations ObNord and Synja are situated in a relatively short distance to Muzhi and to each other. There are strong relationships between tree-ring growth and the average temperature of the months April, May, June, July, August and October or April to October respectively. For the location Vanzevat, the most southern and farthest location from Muzhi and Salekhard, a strong relationship between tree-ring growth and the average of the months June, August, September, October and November could be found out (Fig. 2). In figure 1 the

standardised mean Vanzevat-chronology is presented. From the selected cores of 89 trees, a comprehensive local chronology spanning the time period AD 1512-1999 was developed. The low number of single series forming the chronology from AD 1512-1600 is the cause for the unusual and restless course of the graph in the 16th century (Fig. 1).

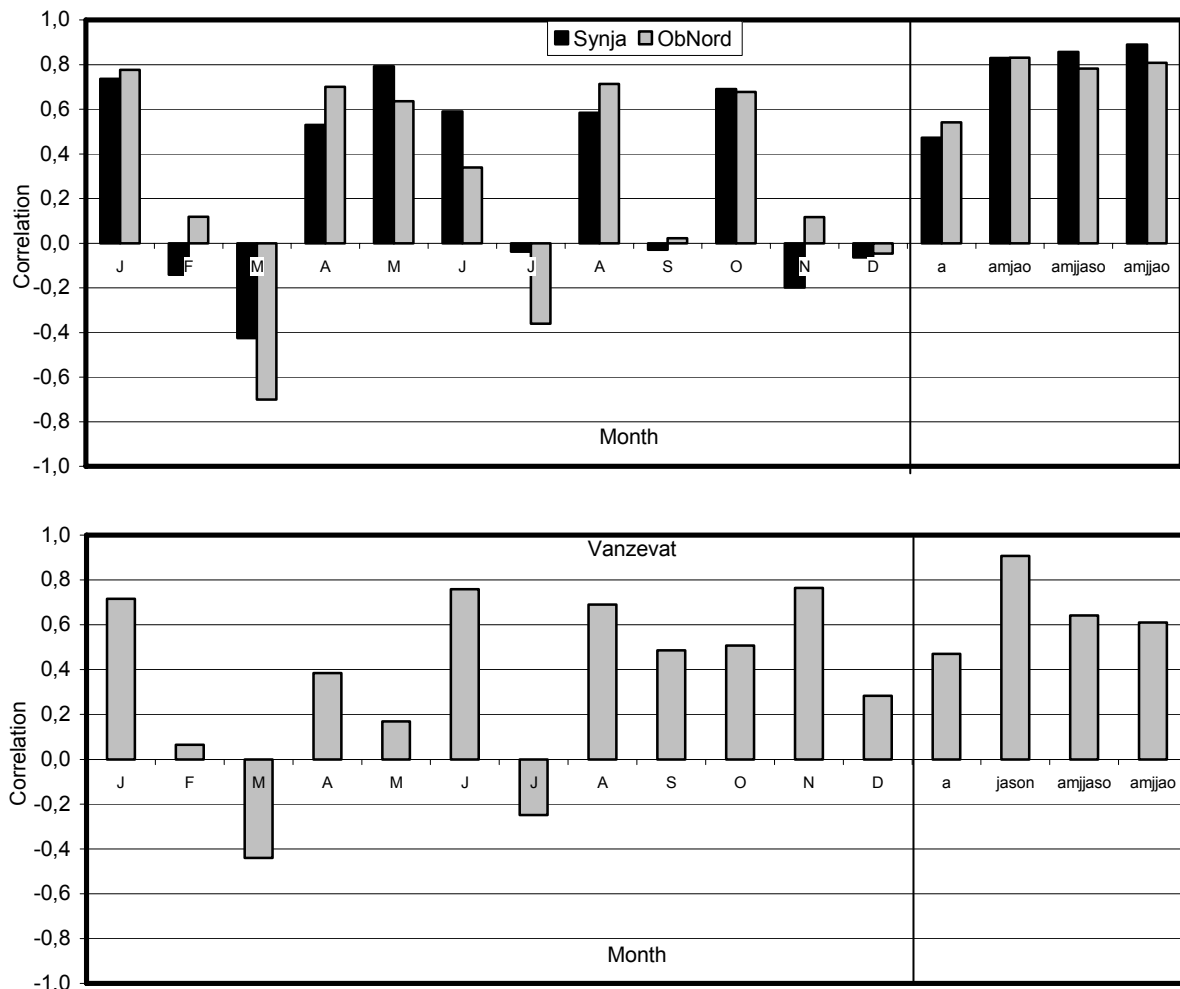


Figure 2: Monthly coefficients of correlation for temperature and tree-ring growth at the three study sites. The left part of the diagrams covers the period January to December. The small letters a, amjao, amjaso and amijao represent the annual value and the averages for the periods April, May, June, August, October and April to October and April to October except September at Synja and ObNord. The only difference at Vanzevat is that "jason" represents the average for the period June, August, September, October, November.

The largest difference between Vanzevat and the other two locations is the low correlation of September and November at Synja and ObNord and the high correlation of September and November at Vanzevat. The reason for an excellent correlation of November is a higher temperature of the Ob water. Besides, Vanzevat is the southern most located study site. Thus the vegetation period of the trees on the Ob bank at Vanzevat takes longer.

As figure 2 illustrates, the highest correlation between tree-ring growth and temperature exists at study site Vanzevat both for single months and for the average for the period June, August to November ($R=0.91$). At the study sites Synja and ObNord the correlations are

high, too, but not as marked as at Vanzevat. In both diagrams of figure 2 the negative correlation of July and especially March is discernible.

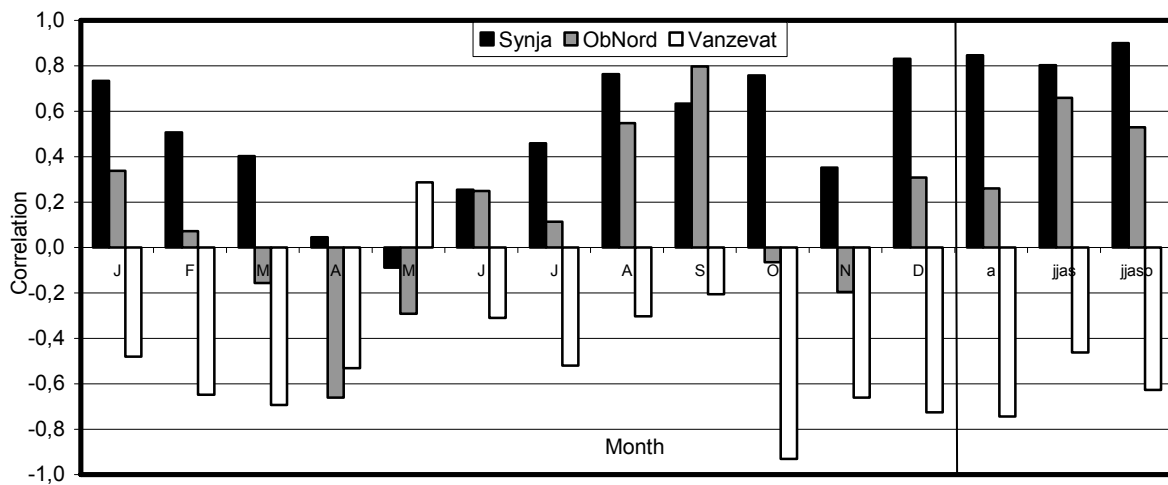


Figure 3: Monthly coefficients of correlation for precipitation and tree-ring growth at the three study sites. The left part of the diagrams covers the period January to December. The small letters a, jjas and jjaso represent the annual value and the averages for the periods June to September and July to October.

Relating to the connections between tree-ring growth and precipitation the situation in Vanzevat is almost vice versa (Fig. 3): The correlation coefficients are predominantly negative. For example for annual precipitation and precipitation in October the correlation is significantly negative ($R=-0.93$; $R=-0.74$). In contrast, the correlation for the other two sites is partly high positive, especially for Synja (period July-October: $R=0.90$). For ObNord the highest correlation is in September and the period June to September ($R=0.80$; $R=0.66$). The reasons for the contradictions of the Vanzevat correlations to the Synja and ObNord correlations relating to precipitation could not be found until now. Besides, the short chronology of precipitation (AD 1933-1988) related to tree growth means a higher probability of error than the chronology of temperature (AD 1879-1989).

Figure 4 illustrates the relation between tree growth and the average of temperature of Muzhi and Salekhard showing the linear regression, the equations of regression and the regression coefficient for the periods 1879-1933, 1934-1989 and 1879-1989. It proves that the high regression coefficient between tree-ring growth and temperature at study site Vanzevat exists not only from 1879-1989 ($R^2=0.82$), but also from 1879-1933 ($R^2=0.85$) and 1934-1989 ($R^2=0.79$).

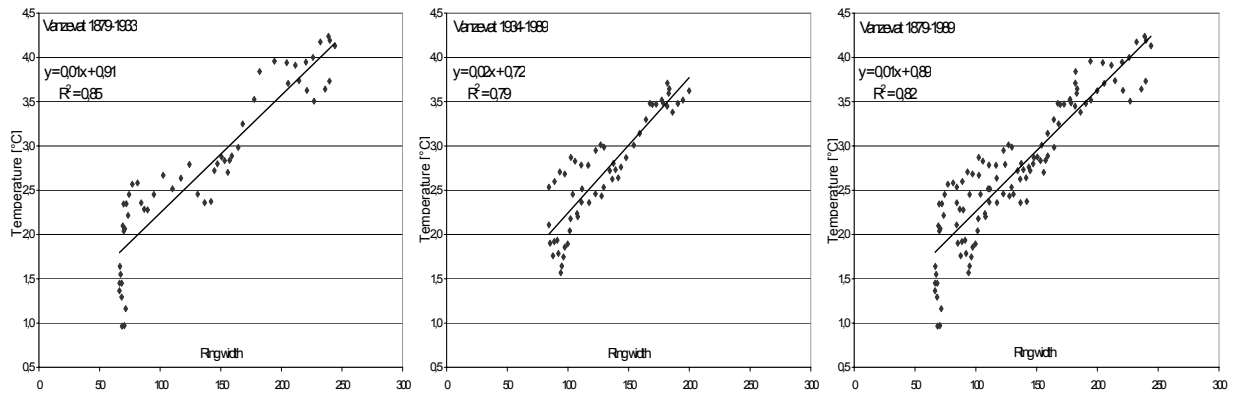


Figure 4: Regression of ring widths of the Vanzevat chronology related to the combined temperature data of Muzhi and Salekhard of the average for the period June, August, September, October, November from 1879-1933, 1934-1989 and 1879-1989.

The equations in the three diagrams are similar. The equation for the regression of 1879-1989 was used to reconstruct the temperature of the average for the period June, August, September, October, November for study site Vanzevat since AD 1512 (figure 5). As the reconstruction shows, the minima in the first half of the 16th, the second half of the 19th and the second half of the 20th, the maxima in the 17th and the first half of the 20th century are discernible.

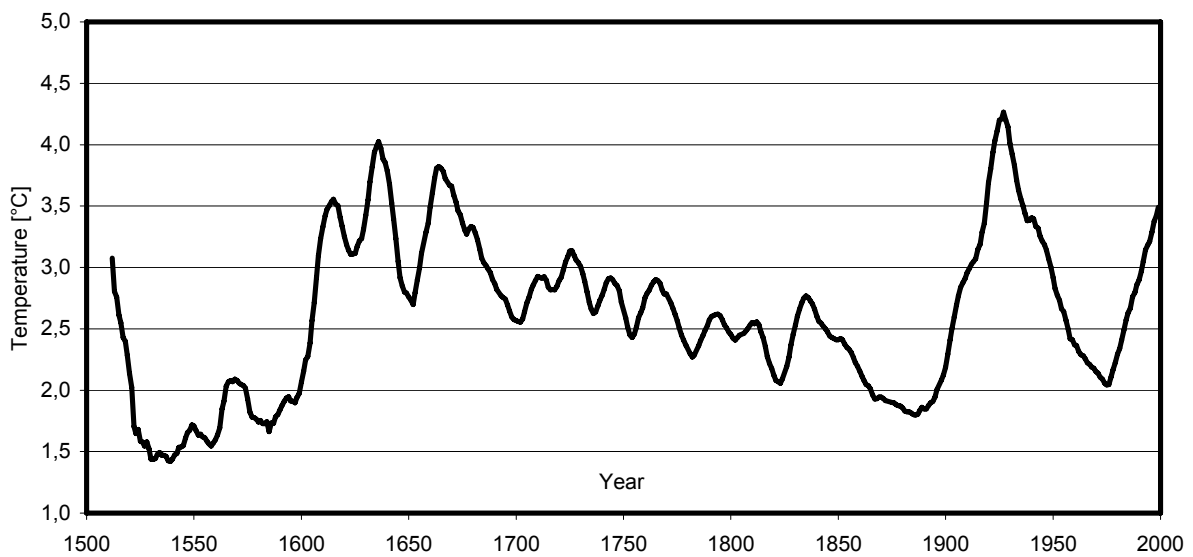


Figure 5: Reconstructed temperature from 1512-1999 for the average of the period June, August, September, October, November for study site Vanzevat.

Anyway there is an evidence for the two minima in the second half of the 19th and the 20th and the maximum in the first half of the 20th century in the temperature recording of the two research stations (Fig. 6).

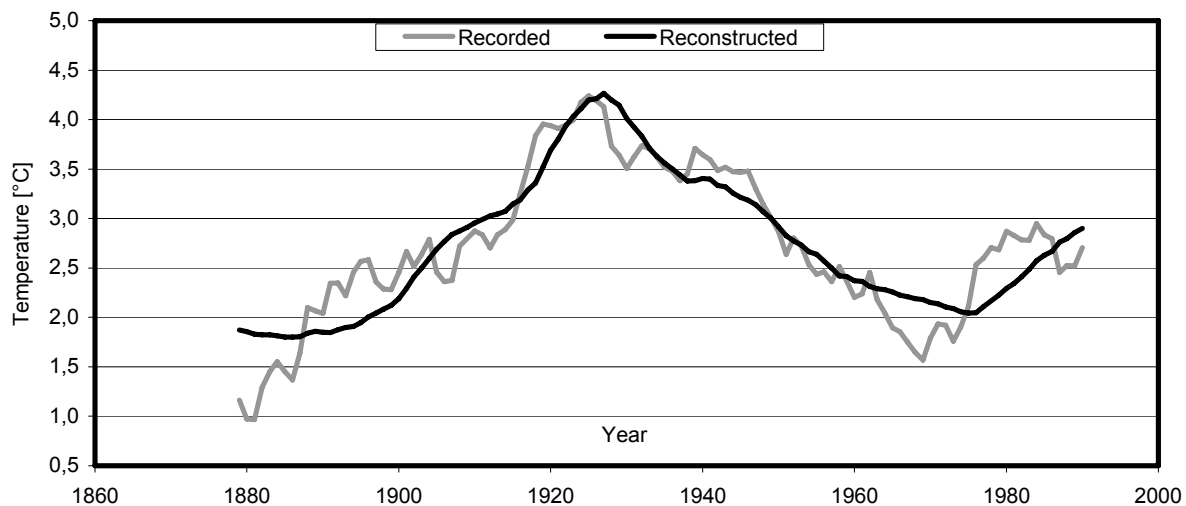


Figure 6: Recorded and reconstructed temperature compared from 1879-1989 for the average of the period June, August, September, Oktober, November.

Conclusion

Our results of dendroclimatological analyses in the West Siberian Lowlands confirm the strong climatological influence on recent tree-ring growth. The study has demonstrated that *Pinus sibirica* can be used for dendroclimatological investigations. While the relation between tree growth and temperature was distinct at all study sites, it was not between tree growth and precipitation. Further studies need to focus on both tree-ring data of other study areas and precipitation data of other climate stations to get a clear idea of the influence of precipitation on recent trees. Thus, a dense network of sites is necessary. However, it was revealed that tree growth at the study sites is influenced more by temperature than by precipitation.

References

- Agafonov, L.J., Strunk, H., Nuber, T. (2004): Thermokarst dynamics in Western Siberia: an experience of dendrochronological research. *Palaeography-Palaeclimatology-Palaeoecology* 209: 183-196.
- Cook, E.R., Kairiukstis, L.A. (eds.) (1990): *Methods of Dendrochronology. Applications in the environmental sciences*. Kluwer. Dordrecht, Boston, London.
- Franz, H.-J. (1973): *Physische Geographie der Sowjetunion*. Gotha, Leipzig.
- Fritts, H.C. (1976): *Tree Rings and climate*. Blackburn Press. Caldwell, New Jersey.
- Jacoby, G.C., Lovelius, N.V., Shumilov, O.I., Raspopov, O.M., Karbainov, J.M., Frank, D.C. (2000): Long-Term Temperature Trends and Tree Growth in the Taymir Region of Northern Siberia. *Quaternary Research* 53: 312-318.
- Rinn, F. (1996): *TSAP – Time Series Analysis and Presentation, Version 3.5 Reference Manual*. Heidelberg.
- Shinkarev, L. (1973): *The land beyond the mountains – Siberia and its people today*. New York.

- Szeicz, J.M., MacDonald, G.M. (1995): Dendroclimatic reconstruction of summer temperatures in northwestern Canada since A.D. 1638 based on age-dependent modelling. *Quaternary Research* 44: 257-266.
- Stokes, M.A., Smiley, T.L. (1968): An introduction to tree ring dating. University of Chicago Press, Chicago.
- Schweingruber, F.H. (1993): Dendroökologie. Birmensdorf.
- Schweingruber, F.H. (1983): Der Jahrring. Standort, Methodik, Zeit und Klima in der Dendrochronologie. Bern, Stuttgart.
- Vaganov, E.A., Hughes, M.K., Kirilyanov, A.V., Schweingruber, F.H., Silkin, P.P. (1999): Influence of snowfall and melt timing on tree growth in subarctic Eurasia. *Nature* 400: 149-151.
- Wein, N. (1999): Sibirien. Gotha.

Dendrochronological records of late Holocene and recent glacier fluctuations of Eagle, Herbert, and Mendenhall Glaciers, Southeast Alaska

G. Weber^{1,2} & K.F. Kaiser^{1,2}

¹ Department of Geography, University of Zurich, Winterthurerstr.190, 8057 Zurich, Switzerland

² Swiss Federal Research Institute WSL, Zürcherstrasse 111, 8903 Birmensdorf, Switzerland

Email: gabrielle.weber@wsl.ch

Introduction

Glaciers play a prominent role in climatic research, since they are important monitoring agents and their fluctuations carry information on past climates. Dendroglaciology allows dendrochronological techniques to be applied to the reconstruction of glacier fluctuations (Schweingruber 1988, 1996, Luckman 1995). In Southeast Alaska, glaciers extended into forested areas enabling dendrochronological techniques to be applied to the reconstruction of glacial dynamics in two ways: (1) Advancing glaciers in the past tilted and overran trees whose remnants, sub-fossil wood, allow former glacial advances to be dated. (2) Retreating glaciers leave bare areas that are rapidly reforested due to the favorable climate. Tree rings provide a precise date for advance or, in this case, for retreat when terminal moraines became ice-free.

The Eagle, Herbert and Mendenhall Glaciers are all part of the Juneau Icefield located in the Juneau area, Southeast Alaska (Fig. 1). In a previous study, Lacher (1999) found that the forefields of the Herbert and Mendenhall Glaciers have several well-developed, densely vegetated terminal moraines dating back to the Little Ice Age ca. 1750 to 1960 AD. He collected subfossil wood and built floating chronologies, but these chronologies could not be linked to recent chronologies and thus they could not be calendar dated. To continue this work, we sampled living trees from different stands near the Eagle Glacier and also subfossil snags in the forefields of all three glaciers. Furthermore, *in situ* stumps that were rooted in a lower soil level were collected in the riverbeds of the Mendenhall and Herbert Rivers. Our objectives are: (1) to reconstruct fluctuations of Eagle glacier, (2) to establish continuous tree-ring chronologies for the last millennium and (3) finally to gain insight into the climatic history of the region. Here, we report the dating of glacial stands in the forefield of Eagle Glacier.

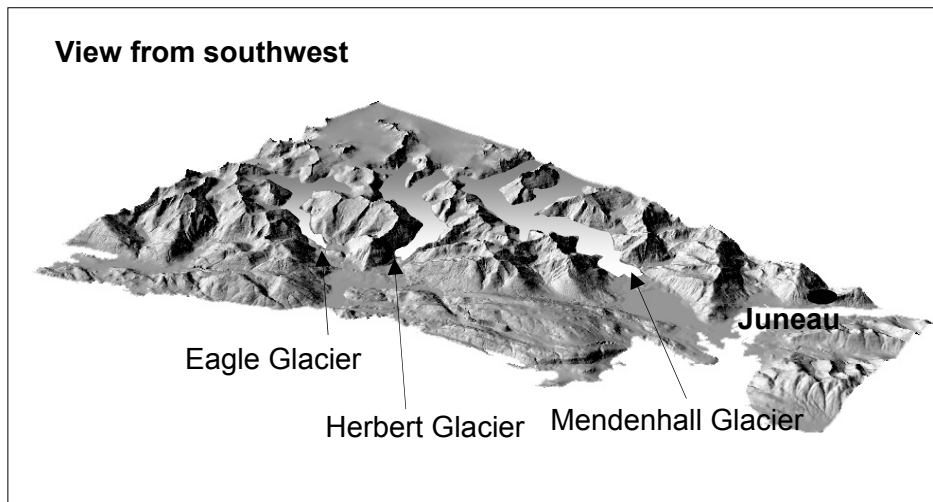
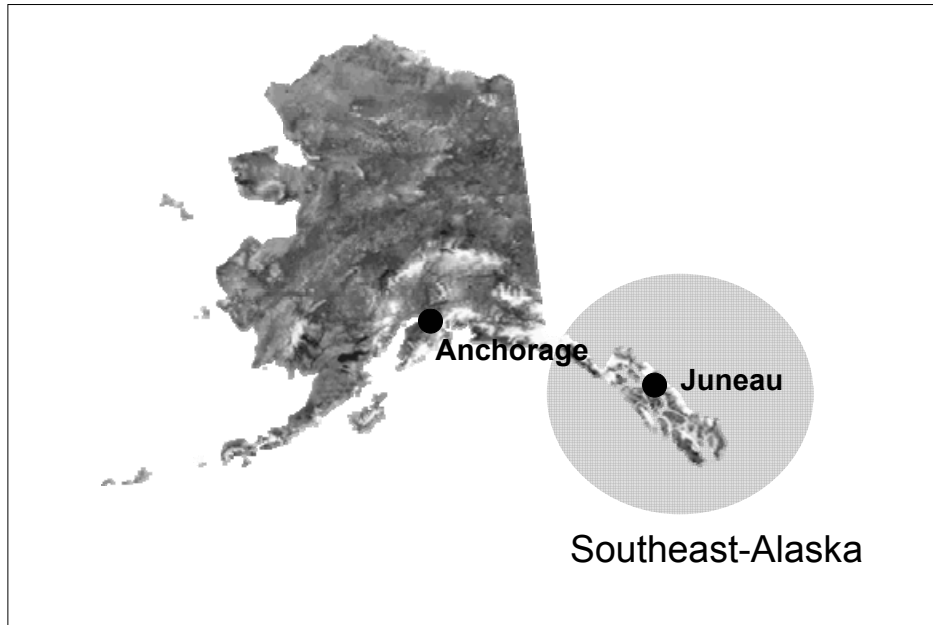


Figure 1: Location of the site.

Material and methods

Mapping: The positions of lateral and terminal moraines were mapped by following the moraine walls with a field GPS. All GPS data were plotted on an orthophoto to determine the exact positions of the moraines. We separated the forefield into three segments suggested by its topography: (A) west of the river, (B) in between river and hill slope, and (C) east of the hill slope (Fig. 2). To reconstruct the retreat of the glacier we estimated the distances between all moraine walls and the oldest terminal moraine (representing the maximum extension of the Little Ice Age) along a line in each of the segments.

Sampling: On 23 different moraines tracts, a total of 370 trees were sampled: in front of, on and behind every moraine wall. Two increment cores (at ca. 180°) from Sitka spruce (*Picea sitchensis*) were taken at a height as close as possible to the germination point, but without root disturbance. After air-drying, the cores were mounted on wooden blocks and polished with progressively finer sandpaper. Annual ring widths were measured to the nearest 1/100

mm using the TSAP tree-ring measurement system (Rinn 1996). The core pairs of every tree were crossdated to detect missing or false rings.

Dates of glacial stands assigned by tree rings remain uncertain until corrections can be made for pith errors, sampling height, and the local ecesis value (Sigafos and Hendricks 1961, Smith et al. 1995, Villalba and Veblen 1997). The ecesis value, or the time lapse between surface stabilization and the germination of the first seedling, was estimated as 5 to 8 years for Sitka spruce in the Juneau area (Lawrence 1950, Lacher 1999). Our own observations confirm this value also for the Eagle Glacier region.

Sampling-height errors arise when the first growth rings are lost due to sampling above rooting system crowns (McCarthy et al. 1991). In order to calibrate the missing years, 12 Sitka spruce saplings of 140 cm height were cut at the germination point level. They were then divided into 10 cm-length segments; ages for all segments were determined by counting the annual rings. Using these results, the ages of all increments cores were corrected for the number of missing years estimated from the coring height and a site chronology was built for every moraine.

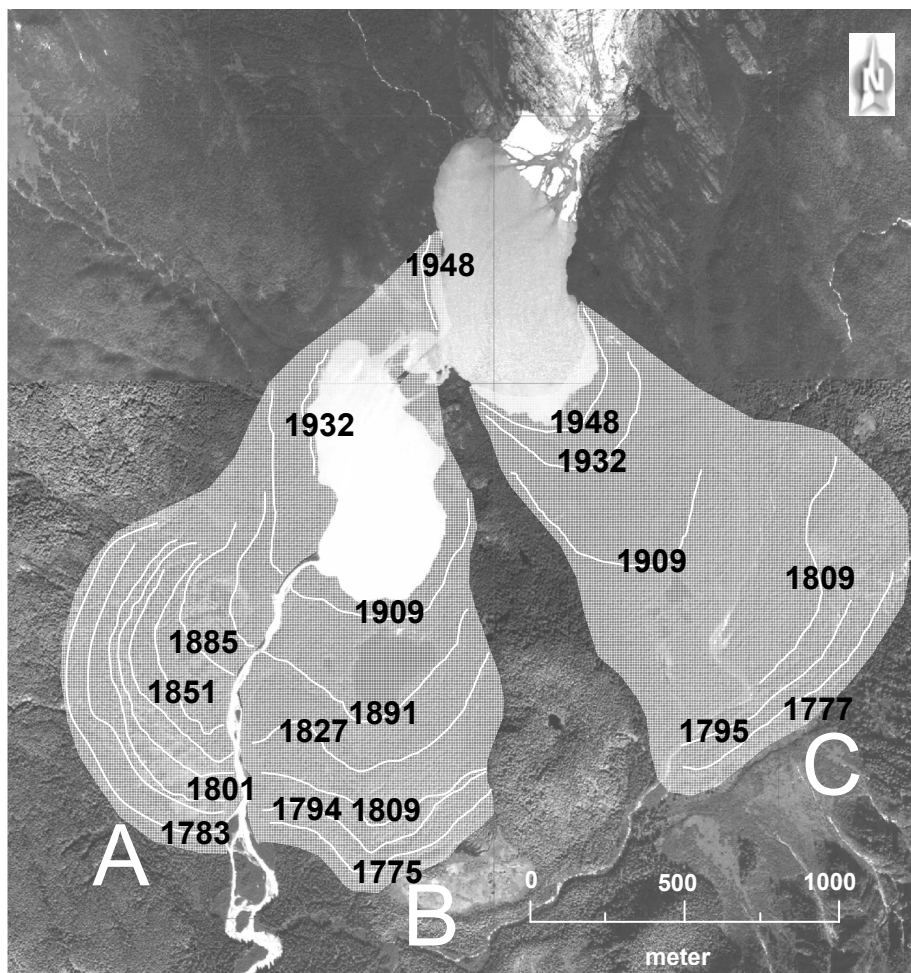


Figure 2: Moraines in the forefield of the Eagle Glacier. The years given are the estimated dates of ice retreat. (Orthophoto USFS, 1996)

Results and discussion

Our results show that the maximum extension of Eagle Glacier in 1775 (Fig. 2) is slightly earlier than the maximum advance in 1785 estimated by Lawrence (1950) in a previous study. However, Lawrence only investigated the west, orographic right side of the river, where we found the oldest tree germinated between 1783 and 1786 (including ecesis value). In our study, the oldest moraine was formed in the intermediate segment only accessible by boat.

The retreating Eagle Glacier provides a series of 11 well-developed stands (Fig. 2). In the 18th century it left two terminal moraines, and in the 19th century six small ones. Three moraines were formed in the 20th century. A lake emerged after 1932, and a second one after 1948. We have two confirmations of our age determinations: a map published by A. Knopf in 1912, showing the ice margin in 1909 and a map published by D.B. Lawrence in 1950, showing the ice margin in 1948.

According to our study, advances among all land-terminating Juneau Icefield glaciers parallel the Neoglacial maximum of Eagle Glacier. The Taku and Herbert Glaciers were the first to retreat after 1750/51, followed by the Mendenhall (1754/55), Twin Lakes (1775/77), and Gilkey Glaciers (1783) (Heusser and Marcus 1964, Lacher 1999, Lawrence 1950). These data illustrate a general condition of recession beginning in the mid 18th century; the high synchronicity between the retreats of the different glaciers implies a major shift in climate affecting the Juneau Icefield at that time (Motyka and Begét 1996).

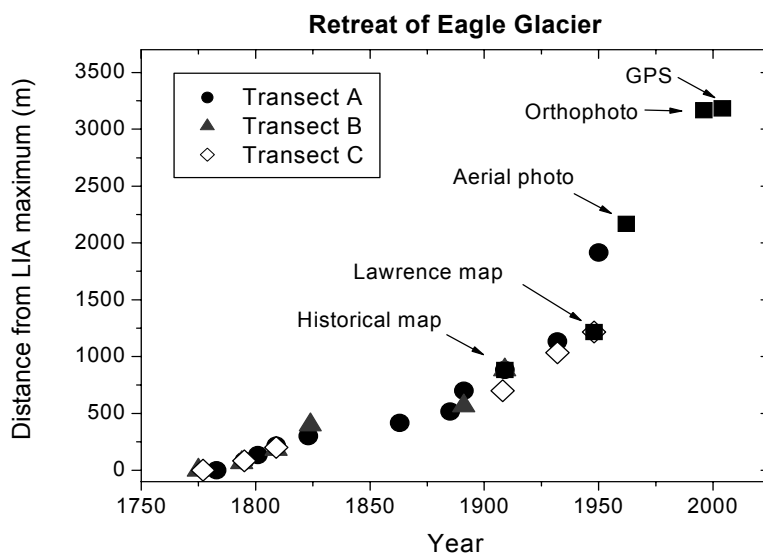


Figure 3: Recession pattern of Eagle Glacier, reconstructed separately for the segments A, B and C. The approximate distance between the dated moraines and maximum extension have been measured on the orthophoto.

Our estimates of moraine ages contain uncertainty because: (1) we cannot exclude not having sampled the oldest tree and (2) the error associated with the increasing 'root-undisturbed' sampling height becomes higher with increasing tree age. However, two aerial

photographs support our findings, one taken by the U.S. Navy in 1929, and the other taken on behalf of the U.S. Forest Service in 1962.

Our reconstruction of the withdrawal of the Eagle Glacier shows that the recession rate has strongly accelerated over time. While the glacier retreated 500 m from 1775 to 1850, by 1950 it had melted another 1250 m thereby losing about 10% of its length. This retreat pattern corresponds with many other land-terminating, maritime influenced glaciers around the Gulf of Alaska (Wiles and Calkin 1994). It in turn suggests that there has been a general warming in this region during the last decades.

Acknowledgements

The authors are very indebted to Mike McClellan, Frances Biles and Ellen Anderson from the Forestry Sciences Lab in Juneau for their kind permission for fieldwork in the National Forest Area, for support with field material and for the orthophotos, as well as to Mike Bartholow, USFS, for general support and permissions. Special thanks go to NorthStar Trekking (Melita Welling, Bob Engelbrecht and their team), Juneau, for the helicopter flights. Furthermore, we would like to thank Steffi and Markus Weber, Patrick Thee and Markus Nater for their essential support in the field.

References

- Heusser, C.J., Marcus, M. G. (1964): Historical Variations of Lemon Creek Glacier, Alaska, and their relationship to the climatic record. *Journal of Glaciology* 5: 77-68
- Knopf, A. (1912): Geology of the Eagle River region, Alaska. *U.S. Geological Survey Bulletin* 502: 61 p.
- Lacher, S. (1999): Dendrochronologische Untersuchungen moderner und historischer Gletscherstände in den Vorfeldern von Mendenhall- und Herbert-Gletscher (Juneau Icefield, Alaska). Diplomarbeit, Universität Zürich.
- Lawrence, D.B. (1950): Estimating dates of recent glacier advances and recession rates by studying tree growth layers. *Transactions of the American Geophysical Union*: 243-248.
- Lawrence, D.B. (1950): Glacier fluctuations for six centuries in southeastern Alaska and its relation to solar activity. *Geographical Review* 40(2): 191-223.
- Luckman, B.H. (1995): Calendar-dated, early 'Little Ice Age' glacier advance at Robson Glacier, British Columbia, Canada. *The Holocene* 5(2): 149-159.
- McCarthy, D.P., Luckman, B.H., Kelly, P.E. (1991): Sampling height-age error correction for spruce seedlings in glacial forefields, Canadian Cordillera. *Arctic and Alpine Research* 23(4): 451-455.
- Motyka, R.J., Begét, J.E. (1996): Taku Glacier, Southeast Alaska, U.S.A.: Late Holocene history of a Tidewater Glacier. *Arctic and Alpine Research* 28(1): 42-51.
- Rinn, F. (1996): TSAP 3.0 Reference Manual. Heidelberg.
- Schweingruber, F.H. (1988): Basics and Applications of Dendrochronology. D. Reidel, Dordrecht.
- Schweingruber, F.H. (1996): Tree rings and environment. Dendroecology. Haupt, Bern.

- Sigafoos, R.S., Hendricks, E.L. (1961): Botanical evidence of the modern history of Nisqually Glacier, Washington. *U.S. Geological Survey Professional Paper 387-A*: 1-20.
- Smith, D.J., Laroque, C.P. (1995): Dendroglaciological dating of a Little Ice Age glacial advance at Moving Glacier, Vancouver Island, British Columbia. *Géographie physique et Quaternaire 50(1)*: 47-55.
- Villalba, R., Veblen, T.T. (1997): Improving estimates of total tree ages based on increment core samples. *Ecoscience 4(4)*: 534-542.
- Wiles, G.C., Calkin, P.E., (1994): Late Holocene, high-resolution glacial chronologies and climate, Kenai Mountains, Alaska. *Geological Society of America Bulletin 106*: 281-303.
- Wiles, G.C., D'Arrigo, R.D., Jacoby, G.C. (1996): Temperature changes along the Gulf of Alaska and the Pacific Northwest coast modeled from coastal tree rings. *Canadian Journal of Forest Research 26(3)*: 474-481.

SECTION 3

ECOLOGY

Methodological approach for dendroecological analysis of dwarf shrubs - A contribution to ecosystem reconstructions in the Norwegian Scandes

A. Bär^{1, 2}, J. Löffler² & A. Bräuning³

¹ University of Oldenburg, Department of Biology and Environmental Sciences, PO Box 2503, D-26111 Oldenburg, Germany

² University of Bonn, Department of Geography, Meckenheimer Allee 166, D-53115 Bonn, Germany
Email: baer@giub.uni-bonn.de; loeffler@giub.uni-bonn.de

³ University of Stuttgart, Department of Geography, Azenbergstr. 12, D-70174 Stuttgart, Germany
Email: achim.braeuning@geographie.uni-stuttgart.de

Introduction

A vast number of dendroecological and dendroclimatological studies have been carried out on tree species close to the upper tree line in many different mountain regions (e. g. Wilson and Luckman 2003, Bräuning and Mantwill 2004). High mountain ecosystems above the upper tree line, however, are still poorly investigated from a dendroecological point of view, although the potential suitability of dwarf shrubs for dendroecological investigations has been demonstrated (Schweingruber 1996, Schweingruber and Dietz 2001). So far, only very few studies exist have been carried out on growth-ring formation of dwarf shrubs (Warren-Wilson 1964, Shaver 1986, Woodcock and Bradley 1994, Petersdorf 1996).

In this study, we aim to verify the variability of growth reactions of dwarf shrubs and the impact of environmental factors on growth and ring widths. The investigations were carried out at multiple spatial scales along micro-topographic, altitudinal, and macro-climatic gradients as part of a long-term project on ecosystem analysis in Central Norway (e.g. Löffler 2003, Löffler and Wundram 2003). In general, micro-topography has significant impact on site conditions in high mountain ecosystems. Vegetation is affected by complex spatio-temporal temperature gradients along micro-topographical gradients (Löffler 2003) mainly depending on relief-related snow cover distribution (Walker et al. 2001). Thus, investigations at a micro-topographic scale are necessary in order to study tree-ring formation in alpine regions.

However, several technical obstacles have to be overcome when measuring dwarf shrub growth rates. Eccentric positions of the pith, extremely asymmetric trunk geometry and many discontinuous rings cause severe problems for proper ring-width series cross-dating.

Study area

Central Norway shows a clearly defined oceanic-continental gradient represented by the western and eastern slopes of the Scandes Mountains. The study area in the Vågå/Oppland region (61° 53' N; 9° 15' E) possesses the most continental climate in Central Norway with annual precipitation totals of 300 – 400 mm/yr. The western study area in Geiranger/Møre og Romsdal (62°03'N; 7°15'E) is climatically characterised by annual precipitation totals of 1500 – 2000 mm/yr. The alpine belt in the study regions stretches from the upper tree line at about

1000 – 1050 m a.s.l. (Vågå) and 840 – 880 m a.s.l. (Geiranger), to the highest peaks, i.e. Blåhø (1618 m a.s.l.) and Dalsnibba (1476 m a.s.l.). The altitudinal zonation of the alpine belt consists of a lower alpine belt dominated by shrub and heath communities, and a middle alpine belt dominated by patchy grass vegetation. The transition zone between the alpine belts is found at 1350 m a.s.l. in the East and 1150 m a.s.l. in the Western region. One study site in each altitudinal belt and climatic zone was chosen as a representative topographic section for Central Norway (Fig. 1).

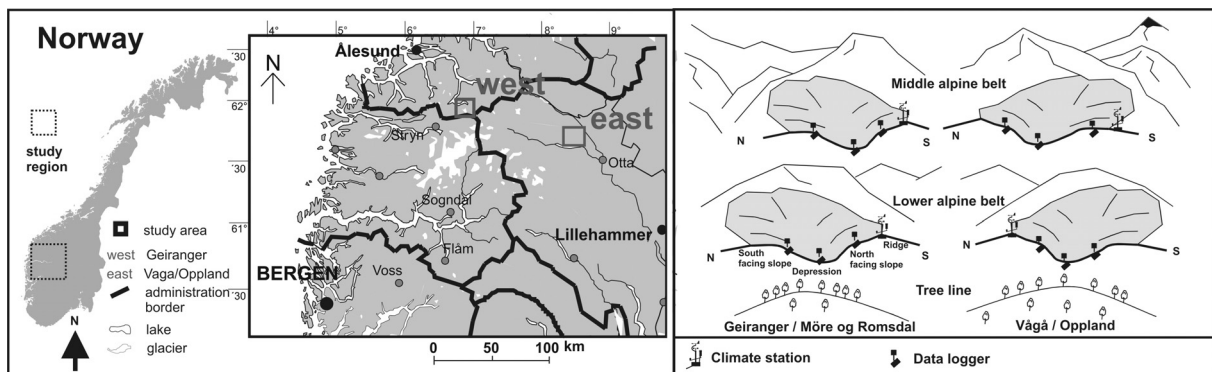


Figure 1: Location of the study area in Central Norway and scheme of investigated altitudinal belts.

Methods and Material

The different dwarf shrub species selected for dendroecological analyses were those that exhibited clearly visible, countable and measurable annual growth rings and occur along all examined gradients. Three species were found to be appropriated: *Empetrum hermaphroditum*, *Loiseleuria procumbens* and *Betula nana*. The maximum age of the analysed individuals was found to reach 85 years. So far, preliminary results were obtained from the continental study area for *Empetrum hermaphroditum*. Within each study site, 12 to 15 individuals of the three indicator species were collected along several north-south exposed transects representing the micro-topographic gradient. Samples were taken from the ridges, the south-facing slopes, the depression between slopes and the north-facing slopes. The four site types represent different snow cover regimes and micro-climatic conditions (Löffler 2003).

Micro-environmental records were collected at each sample site comprising data on relief, soil properties, and vegetation structure. Long-term climate data have been recorded by climate stations on ridges and by data logger in depressions and south-facing and north-facing slopes directly within each study site.

Complete dwarf shrub individuals including their woody root and branch systems were collected in the field. Digital photos were taken of the complete morphological structure before samples were sectioned for laboratory analyses. Altogether, 55 base sections were investigated. Microtome sections of 12 - 15 μm thickness were cut from the whole diameter using a sledge microtome. Digital microphotographs were taken from the stained micro-sections for tree ring detection and measurements. Since the growth rates of the investigated dwarf shrubs are generally very small, magnified prints of the digital wood-anatomy photos

were produced. Manual tracings of tree-ring borders helped to detect discontinuous rings and frost rings. Ring widths were measured on the prints along two radii which showed minimal disturbance by scars and discontinuous rings. The measurement of ring width and the localization of missing rings in the tree-ring curves was accomplished using the LignoVision and TSAPWin (RINNTECH) programs.

Due to obstacles within the synchronisation process calculations of area increments were applied in order to improve chronology building. These determined the area of each growth ring by covering the whole cross-section and thus they integrate asymmetric annual increments and discontinuous rings. Furthermore, the geometrical decrease of ring widths with increasing stem diameter is eliminated and the ecological signal can be strengthened (LeBlanc 1996). This method has so far only been applied to a few samples.

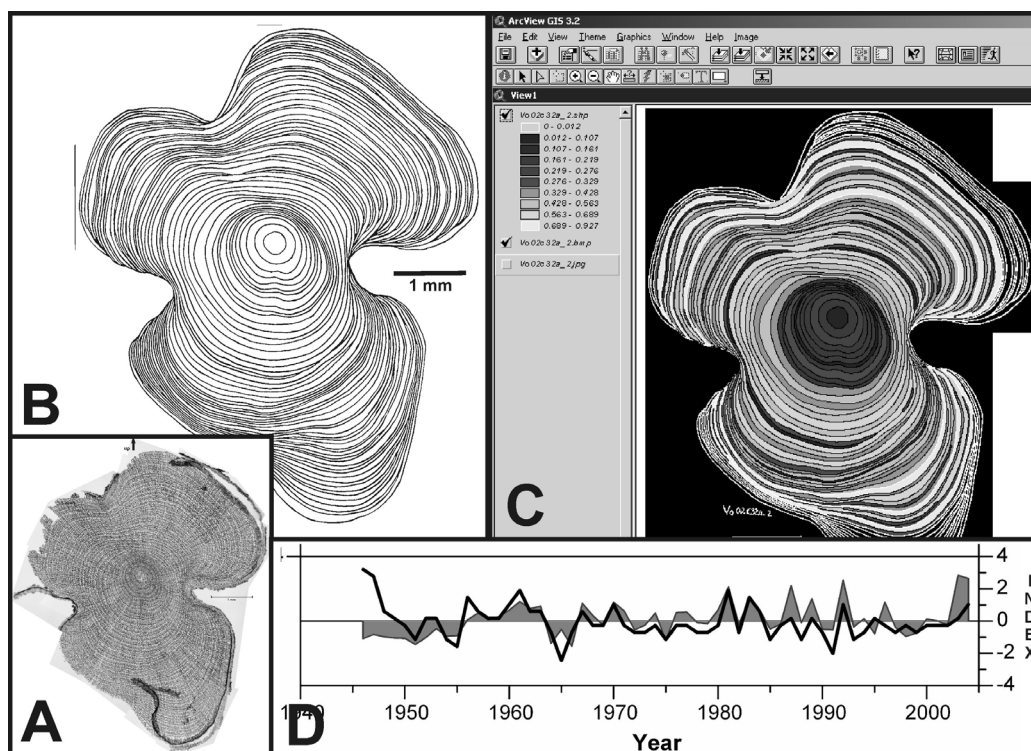


Figure 2: Derivation of area increments calculated by using the real perimeter progression of tree rings. A digital micro-photo; B tracings of tree-ring borders by hand and transformation into vector based polygons; C area calculations using ArcGIS; D area increment curve (shaded area) plotted together with the ring width curve of the same cross-section (black line). Both curves are z-standardised.

The raster-based digital wood-anatomical images were photo-analytically transformed into vector-based polygons by using ERDAS IMAGINE 8.5. The tracings of whole cross-sections were corrected manually. Then, the total areas of all tree-ring polygons were calculated and plotted as a tree-ring curve using ArcGIS. Problems occurred when a cross-section was incomplete or of bad quality due to twisted growth of the stem segment and it was difficult to assign visible ring structures to the correct tree ring in cases of very short diameters resulting from eccentric growth. However, these parts of a growth ring only contribute a very small

portion to the total tree-ring area and are thus negligible. Growth curves were z-standardised for comparison of ring widths and area increments.

Results and Discussion

Asymmetric geometry including lobes and eccentric piths are conspicuous features in most of the *Empetrum hermaphroditum* cross sections (Fig. 3 A). The shortest radius of prostrate stems is always oriented towards the upper side and discontinuous and absent rings are very common occurrences (Fig. 3 C). Kolishchuk (1990) and Woodcock and Bradley (1994) confirm that this is also the case with other dwarf shrub species. No indications of reaction wood occur in any of the analysed cross sections.

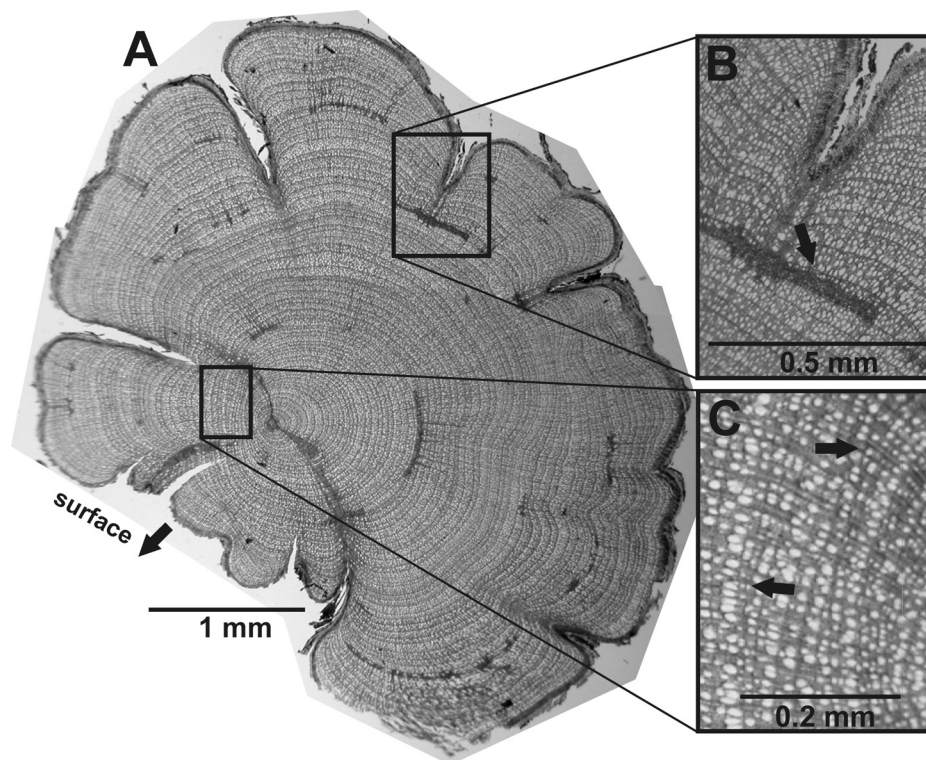


Figure 3: Wood anatomy of *Empetrum hermaphroditum*: **A** lobate growth and eccentric pith; **B** frost ring (black arrow); **C** discontinuous rings (black arrows).

Frost rings are more frequently found on south-facing slopes than on the ridges and thus can be related to micro-site differences (Woodcock and Bradley 1994). The uneven distribution of frost rings at different site types can be an indication of physiological adaptation to seasonal and daily temperature gradients of individuals growing under different ecological conditions (Schweingruber 2001). In general, cell structure damage is mostly restricted to the beginning of a new ring (Fig. 3 B) and can thus be assigned to the occurrence of late frost events after melting of the protective snow cover.

Annual increments are in general very low and vary between 0.08 mm/yr on summer-warm and winter-snow protected south-facing slopes and 0.05 mm/yr on snow-free ridges. *Empetrum* is in general a semi-ring porous species. The latewood often consists of only two

or three rows of wood fibres. When comparing the wood anatomy of individuals from the south-facing slope and ridge we found that the latewood part of the growth rings was often reduced or even absent in the individuals from the ridge. As a consequence, the wood anatomy of individuals from ridge sites appears diffuse porous (Fig. 4).

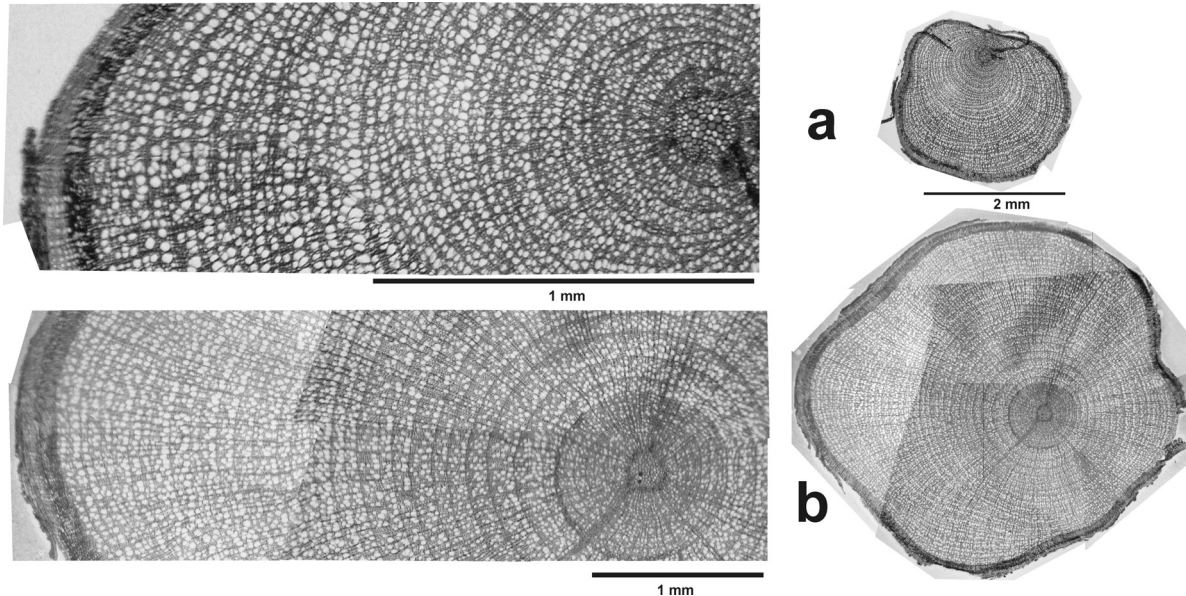


Figure 4: Comparison of wood anatomical features between the ridge (a) and south-facing slope (b) in the lower alpine belt. Differences in diameter (right part of the figure) due to different site conditions are represented by cross sections of two almost even aged individuals.

Our first attempts at chronology building suffered from common wood-anatomical characteristics of dwarf shrubs (including discontinuous rings, complex lobate geometry and minimal ring widths), responsible for highly individualistic growth. Thus, cross dating of ring widths are often only possible within individuals, rarely between neighbouring individuals. Area increment calculations helped to detect discontinuous rings in some cases, but the studied examples show that annual growth variability is similarly reproduced by ring widths and area increments.

Conclusion and Outlook

Different individuals of *Empetrum hermaphroditum* show highly individual growth histories. Thus, cross dating is a challenging task. As preliminary calculations of area increments indicate, individualistic growth forms and growth-ring formation do not only cause dating difficulties. Other cross dating problems are missing rings and growth variability occurring partially or along the entire plant as noted by Kolishchuk (1990) with regard to prostrated shrubs. Thus, serial sectioning will be used in the future as a tool to improve synchronicity. For this purpose, several representative individuals at each site need to be analysed and a greater number of cross-sections made along stems and branches. Highly replicated ring-width curves of these individuals will then be able to serve as reference curves for the remaining individuals in their respective habitats and these should help in the building of site chronologies.

However, despite problems with cross dating, differences in site conditions are reflected in wood anatomy (frost rings, earlywood/latewood portions) and growth rates. Further analyses are required to verify the preliminary results of area increment calculations and to test the serial sectioning method in order to develop local site chronologies.

Acknowledgements

The research work was funded by EU-Marie Curie Scholarship at the University of Bergen, Norway, Heinz-Neumüller Scholarship and the German National Academic Foundation [A. Bär].

References

- Bräuning, A., Mantwill, B. (2004): Increase of Indian Summer Monsoon rainfall on the Tibetan plateau recorded by tree rings. *Geophysical Research Letters* 31: L24205, doi:10.1029/2004GL020793.
- Kolishchuk, V. G. (1990): Dendroclimatological study of prostrate woody plants. In: Cook, E. R., Kairiukstis, L. A., (eds.) *Methods of Dendrochronology. Applications in the environmental sciences.*, Kluwer, Dordrecht, Boston, London. p. 51-55.
- LeBlanc, D. (1996): Using tree rings to study forest decline: an epidemiological approach on estimated annual wood volume increment. In: Dean, J. S., Meko, D. M. and Swetnam, T. W. (eds.): *Tree rings, environment and humanity. Radiocarbon* 437-449.
- Löffler, J. (2003): Micro-climatic determination of vegetation patterns along topographical, altitudinal and continental-oceanic gradients in the central Norwegian high mountains. *Erdkunde* 57: 232–249.
- Löffler, J., Wundram, D. (2003): *Geoökologische Studien zur Prozessdynamik mittelnorwegischer Hochgebirgsökosysteme.* Oldenburger Geoökol. Studien 2; 158 pp.
- Petersdorf, M. (1996): *Dendrochronologische Untersuchungen an Zwergsträuchern.* Diploma thesis, University of Zurich.
- Schweingruber, F. H. (1996): *Tree-Rings and Environment. Dendroecology.* Swiss Federal Institute for Forest, Snow and Landscape Research. Paul Haupt Verlag, Vienna. 609 pp.
- Schweingruber, F. H. (2001): *Dendroökologische Holz Anatomie. Anatomische Grundlagen der Dendrochronologie.* Paul Haupt Verlag, Bern, Stuttgart, Vienna. 472 pp.
- Schweingruber, F. H., Dietz, H. (2001): Annual rings in the xylem of dwarf shrubs and perennial dicotyledonous herbs. *Dendrochronologia* 19 (1): 115-126.
- Shaver, G. R. (1986): Woody stem production in Alaskan tundra shrubs. *Ecology* 56: 401-410.
- Warren-Wilson, J. (1964): Annual growth of *Salix arctica* in the High-Arctic. *Annals of Botany* 28: 71-78.
- Wilson, R. J. S., Luckman, B. H. (2003): Dendroclimatic reconstruction of maximum summer temperatures from upper treeline sites in Interior British Columbia, Canada. *The Holocene* 13 (6): 851-861.
- Woodcock, H., Bradley, R. (1994): *Salix arctica* (Pall.): Its potential for dendroclimatological studies in the high arctic. *Dendrochronologia* 12: 11-22.

An evaluation of boundary-line release criteria for eleven North American tree species

B.A. Black¹ & M.D. Abrams²

¹ Hatfield Marine Science Center, Newport, OR 97365, Email: Bryan.Black@oregonstate.edu

² Corresponding author, 4 Ferguson Building, Penn State University, University Park, PA 16802
Email: agl@psu.edu

Introduction

One of the most fundamental dendroecological techniques for identifying disturbance events in tree ring time series is the analysis of releases (Lorimer and Frelich 1989). Traditionally, a release has been defined as an event where the percent growth change in radial growth exceeds a given minimum threshold, such as 50 or 100 percent, which in some criteria must be maintained for a certain length of time such as five or ten years (Lorimer and Frelich 1989, Nowacki and Abrams 1997). Thus, releases rely on the assumption that the magnitude of percent-growth change corresponds to the magnitude of a canopy disturbance. However, the relationship between percent-growth change and canopy disturbance is complicated by a number of interrelated and confounding variables such as crown size and position; gap proximity, size, and duration; prior growth rate; age and diameter; species, and climate (Nowacki and Abrams 1997).

To better describe the effects of and interactions among variables that could potentially affect the magnitude of a growth pulse following the release of a tree's canopy, Black and Abrams (2003) quantified relationships among tree age, size, canopy class, radial growth rate, and percent growth-change in eastern hemlock (*Tsuga canadensis* L.). A new set of release criteria were developed based on the finding that growth rate prior to a growth pulse was the most fundamental predictor of the maximum possible magnitude of the change pulse, when expressed in terms of percent growth change. In summary, young, small, and suppressed trees were found to be capable of extremely large pulses in percent-growth change in comparison to their older, larger, dominant counterparts. In addition, smaller, younger, and suppressed trees also showed slower radial growth rates. Radial growth rate appeared to be closely related to the magnitude of percent-growth change pulses. Indeed, when percent-growth change is graphed against average radial growth over the past ten years, percent growth-change values extend to a well-defined boundary that declines exponentially across increasing rates of prior growth (Black and Abrams 2003). An important aspect is that eastern hemlock of almost any age, size, and canopy class demonstrates percent growth-change pulses that reach this upper boundary. Slow-growing trees, which tend to be small understory individuals, reach the boundary with large pulses in percent-growth change. Fast-growing trees, which tend to be large dominant individuals, can reach the boundary with only modest pulses in percent-growth change. To incorporate the effects of prior growth into release criteria, each percent growth-change pulse is scaled in terms of its maximum possible value, as predicted by level of prior radial growth. This should better compensate for

differences among age, size, and canopy classes and allow for more direct comparisons of release events across all phases of a tree's lifespan.

In this study, the interactions among prior growth, age, and size are explored in eleven tree species representing a wide variety of ecological strategies and forest types throughout North America. We show that prior growth strongly influences maximum percent-growth change in all eleven species, and that the consistent relationships between prior growth and percent growth change suggest that boundary-line release criteria may be developed in all species. Releases could be better standardized by uniformly expressing them as a percentage of their maximum value predicted by species and prior growth rate. Such standardized releases would facilitate comparisons of disturbance history among species and among stands, increasing the power of release criteria to establish landscape-level patterns of disturbance.

Methods

Species were selected to represent a diversity of habitats in North America, ranging from the boreal forests of Canada to the mountains of the Desert Southwest. In total, nearly 1.3 million growth increments were included from 258 stands from the NOAA International Tree Ring Data Bank (Tab. 1). Eastern species include *Tsuga Canadensis* (hemlock), *Picea glauca* (white spruce), *Picea mariana* (black spruce), *Quercus alba* (white oak), *Quercus prinus* (chestnut oak), *Pinus strobes* (white pine), *Quercus macrocarpa* (bur oak), *Quercus stellata* (post oak), and *Pinus echinata* (shortleaf pine), while western species include *Pinus ponderosa* (ponderosa pine) and *Pseudotsuga menziesii* (Douglas fir). Percent growth change was calculated for each series of tree ring measurements following the technique of Nowacki and Abrams (1997) in which percent growth change for a year is equal to $(M_2 - M_1) / M_1$ where M_1 equals average growth over the prior 10 years and M_2 equals average growth over the subsequent 10 years. The effects of growth history on maximum percent growth change were better quantified for each species by plotting percent growth change against prior growth. Prior growth was defined as the average raw growth over the ten years prior to a given growth increment. Thus, the prior growth value for the 1990 growth increment of a given tree would be the tree's average raw growth between 1980 and 1989. The relationship between prior growth and percent growth change was plotted for every growth increment of every tree, with the exception of the first and last ten years of growth in which percent growth change could not be calculated. The upper threshold of the relationship between prior growth and percent growth change was then quantified by calculating a boundary line. For each species, a boundary line was constructed by first dividing the data set into 0.5 mm segments of prior growth. Then within each segment, the percent growth-change values of the top ten points were averaged. The top ten points in each section ensured an equal sample size across all prior growth classes, and limited the analysis to the few points that represented true maximal releases. To quantify the boundary line linear, power, logarithmic, and exponential curves were fitted to all positive segment averages, and the function that yielded the highest R^2 value was selected (Black and Abrams 2003).

Table 1. Number of sites and total number of growth increments for each species. % of max sites refers to the percentage of sites in which percent growth change values come within at least 90% of the value of the boundary line. Max age indicates the approximate age at which trees consistently fail to reach the boundary line.

Species	N sites	N growth increments	boundary line equation	% of max sites	max age
<i>Pinus echinata</i>	22	74,925	$y = 998.65 e^{-1.0237x}$	33	150
<i>Pinus strobus</i>	12	72,714	$y = 501.96 e^{-0.664x}$	47	250
<i>Pinus ponderosa</i>	23	157,243	$y = 665.97 e^{-0.9354x}$	43	250
<i>Picea glauca</i>	32	102,306	$y = 649.97 e^{-1.0798x}$	17	200
<i>Picea mariana</i>	26	49,007	$y = 407.92 e^{-1.4679x}$	19	250
<i>Tsuga canadensis</i>	25	180,708	$y = 974.54 e^{-1.1202x}$	30	400
<i>Pseudotsuga menziesii</i>	25	172,372	$y = 569.80 e^{-0.928x}$	36	300
<i>Quercus macrocarpa</i>	38	92,092	$y = 511.27 e^{-0.7018x}$	34	50
<i>Quercus stellata</i>	23	169,333	$y = 948.45 e^{-1.6188x}$	39	150
<i>Quercus prinus</i>	8	35,337	$y = 742.83 e^{-0.9445x}$	29	200
<i>Quercus alba</i>	24	164,876	$y = 527.22 e^{-0.787x}$	38	200

Age and size-specific variations in growth rate and percent growth change were explored for each species as a way to validate whether the prior-growth boundary line applies to all phases of a tree's development. Age of each growth increment was estimated by counting all preceding growth rings, while radius was estimated by summing the widths of all preceding growth rings. Growth increments were assigned radius classes in 50 mm increments (0-49.9 mm, 50-99.9 mm, etc.) and age classes in 50 year increments (0-49 years, 50-99 years, etc.). All growth increments were plotted with respect to age or radius class, prior growth, and percent growth change. If all age and radius classes approach the upper threshold of percent growth change values, all classes are capable of maximum percent-growth change as predicted by prior growth. If any age and radius classes fall short of the threshold, the effects of prior growth on maximum percent-growth change do not adequately explain percent growth change differences among age or radius classes.

Results and Discussion

Prior growth is an important determinant of maximum percent-growth change for all surveyed species. In all eleven species, maximum percent-growth change diminishes at a negative

exponential rate with increasing levels of prior growth (Fig. 1). Negative exponential boundary lines appear to be a good fit to the data and all have high R^2 values, ranging from 0.92 to 0.99 (Fig. 1, Tab. 1).

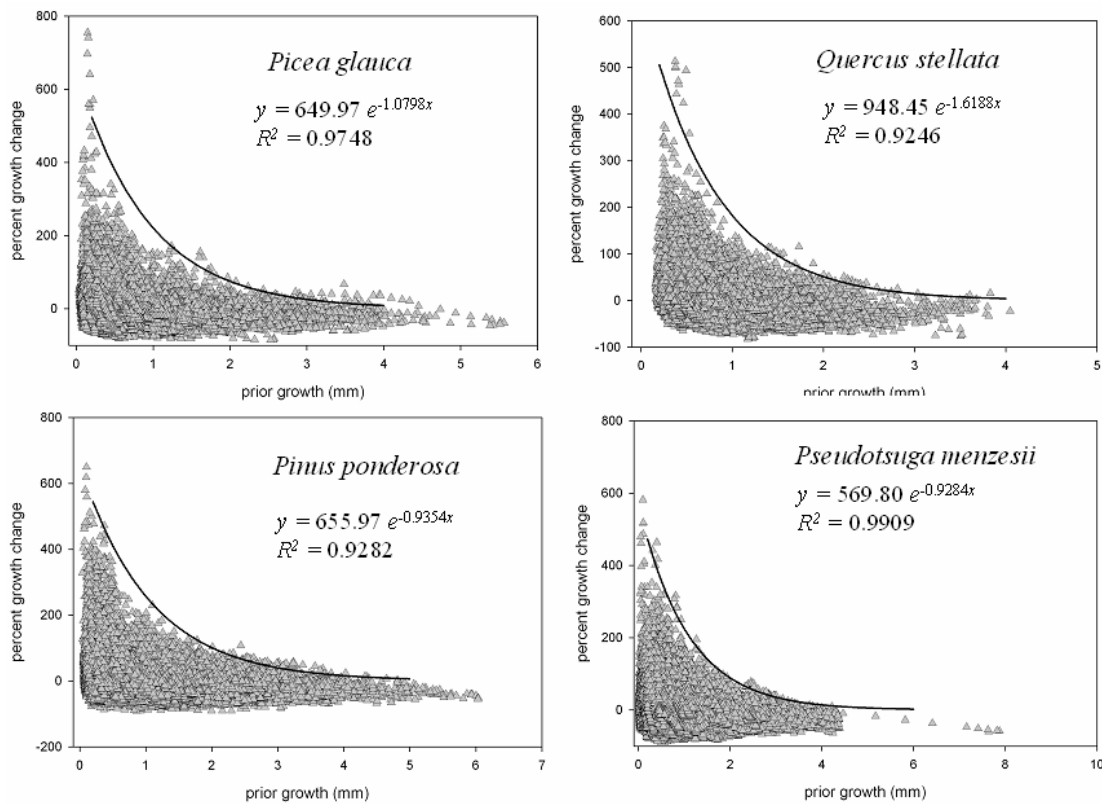


Figure 1: Relationship between percent growth change and prior growth for four North American tree species. A boundary line summarizing maximum values of percent-growth change is also shown.

The only potential exception is shortleaf pine in which a power function of $y = 242.21 x^{-1.2434}$ had an R^2 of 0.97. This is negligibly better than the fit of a negative exponential function ($R^2 = 0.96$), so for consistency the negative exponential function was chosen to represent the boundary line. Overall, the boundary lines closely follow the upper threshold of maximum percent-growth change for all species (Fig. 1). In each case, data from several sites approach the boundary line of each species, ranging from a minimum of 17% of all sites in black spruce to 47% of all sites in white pine (Tab. 1). Furthermore, sites that approach the boundary line occur across very broad geographic regions for many species. For the ponderosa pine these include sites from New Mexico to South Dakota to Oregon and California. Representative trees for Douglas-fir were sampled in New Mexico, Arizona, Wyoming, and Washington. Sites that approach the white oak boundary line are located in Kentucky, Illinois, Pennsylvania, and Minnesota while sites that approach the post oak boundary line are located in Texas, Oklahoma, and Kansas. In a more detailed evaluation, white oak sites from the eastern portion of its range (Pennsylvania, New Jersey, Ohio, and Virginia) approach the boundary line (Fig. 2 A) as do sites from the western portion of its range (Missouri, Iowa, and Minnesota) (Fig. 2 B). Also, Douglas-fir sites from the Cascade Mountains of the Pacific Northwest (Oregon, Washington, and Canada) approach the

boundary line (Fig. 2 C) as do sites from the mountains of Arizona, New Mexico, and Mexico (Fig. 2 D). Site-specific differences may exist, yet on a broad scale, a single boundary line appears to apply to a wide region. More detailed studies in which specific site conditions are known will be required to test whether certain site conditions correspond with failure of trees to attain the boundary line. If indeed site-specific differences are detected, these findings will have implicating for all release criteria, not just the boundary-line approach.

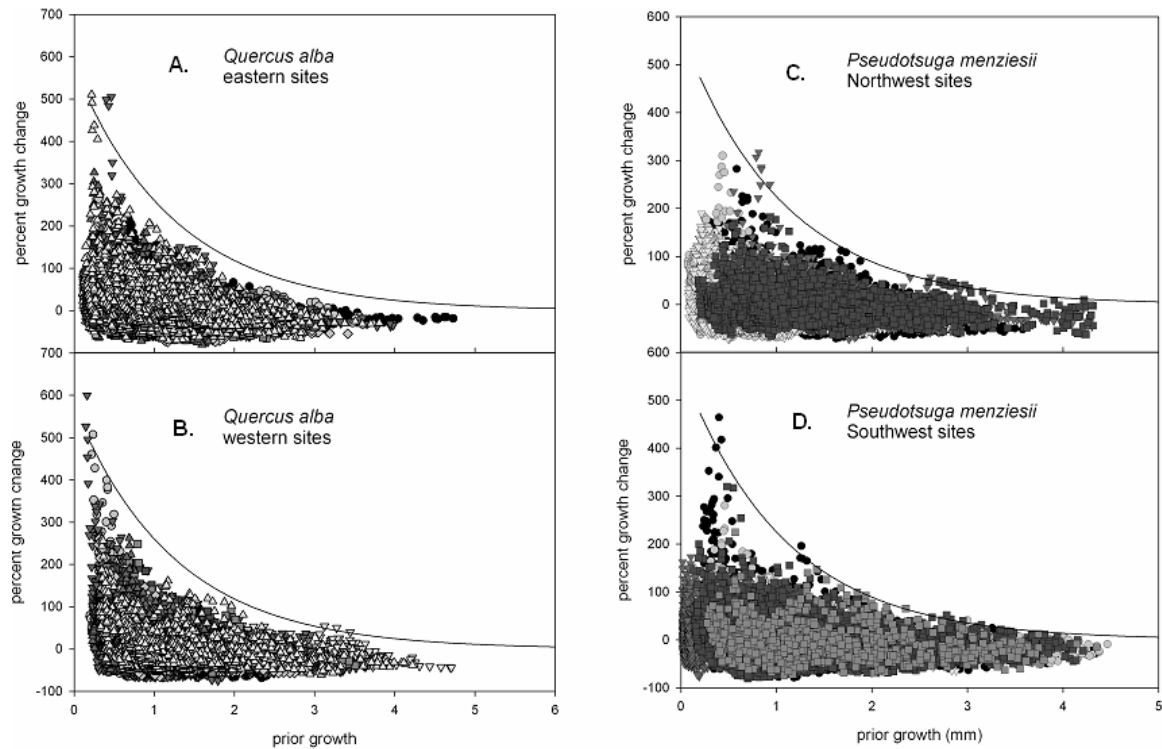


Figure 2: Relationship between prior growth and percent growth change for Douglas-fir and white oak sites. A) Eastern portion of white oak’s range include Ohio, Pennsylvania, and Virginia. B) Western white oak sites include Minnesota, Iowa, and Missouri. C) Northwest Douglas-fir sites are located in the Cascade Mountains or Washington, Oregon, and Canada. D) Southwestern Douglas-fir sites are located in Arizona, New Mexico, and Mexico. The species-specific boundary line is shown for both species.

In many species, declines in raw growth and percent growth change result in the failure of large or old trees to reach the prior-growth boundary line (Tab. 1, Fig. 3). Perhaps the only true exception is eastern hemlock in which almost all age and radius classes approach the upper threshold of maximum percent-growth change as predicted by prior growth. Even trees as large as 80 cm in radius and as old as 400 years can approach this upper boundary of maximum percent-growth change (Tab. 1) (Black and Abrams 2003). Thus eastern hemlock trees of almost any age are capable of showing full releases, and the entire series of tree-ring measurements for each tree may be included in analyses of disturbance history using the boundary-line approach. All other species, however, consistently fail to reach the boundary line after a given age (Tab. 1, Fig. 3). This phenomenon is clearly shown when percent-growth change values of older trees are plotted with respect to the boundary line (Fig. 3). Failure to reach the boundary line often becomes increasingly severe with increasing age, as shown here for shortleaf pine, post oak, eastern white pine, and white spruce (Fig.

3). Overall, approximate age at which trees begin to consistently fail to reach the boundary line varies considerably among species (Tab. 1). Douglas-fir fails to reach the boundary line at the comparatively old age of 300 years. Yet considering the large maximum ages of this species, a substantial proportion of an old-growth tree would not be showing full release. The most extreme example of all species is bur oak, which consistently fails to reach the boundary line by as early as 50 years in age (Tab. 1).

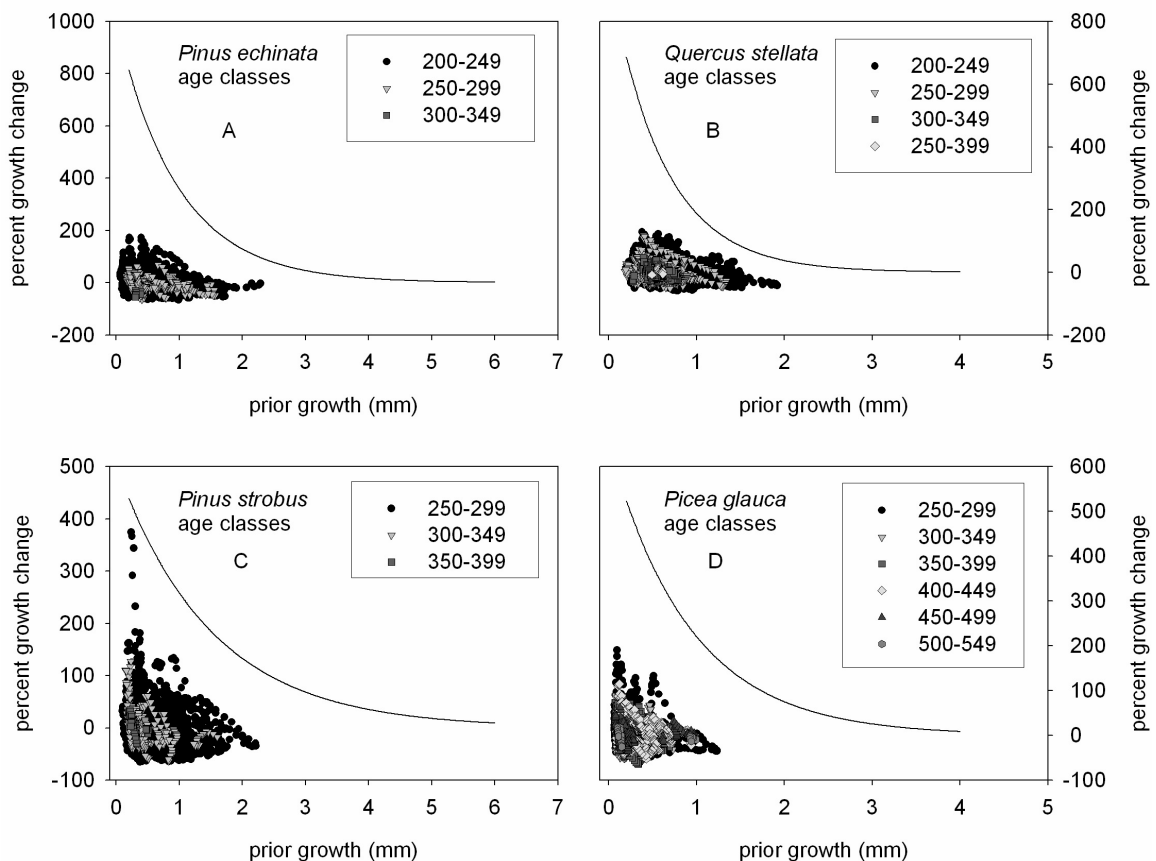


Figure 3: Relationship between prior growth and percent growth change in the oldest 50-year age classes of four species. Each species' boundary line is shown.

The reason as to why older trees fail to reach the boundary line is not immediately clear. These failures could be the result of physiological or morphological factors in which the tree is no longer able to vigorously exploit resources freed by disturbance. Or these older trees simply do not experience such a large increase in resources as compared to their younger counterparts. A disturbance may increase light levels by a factor of ten for a suppressed understory tree, but only expose a relatively small portion of the crown to light in a mature overstory tree. No matter the exact reason for these age-related failures, caution must be used when using older, larger trees. At this time, age or size limits may be necessary for reconstructing disturbance history. In the future, age-specific boundary lines may be developed after more experimental work has been conducted. But for now, growth increments formed after a certain age (or size) should be dropped from analysis. These age restrictions would apply not only to boundary line release criteria, but any release criteria

developed to date. The strength of the boundary-line release criteria is that they can help compensate for many age-related differences in release response, as is shown the most dramatically in eastern hemlock. Before trees reach the age at which they no longer reach the boundary line, releases may be expressed as a fraction of maximum potential value, as predicted by the boundary line. Thus boundary line release criteria will better standardize all releases within and among species and sites.

In conclusion, prior growth is clearly an important factor in determining the potential maximum percent-growth change and should therefore be included in release criteria. The prior-growth boundary-line provides a novel technique that can be applied to a wide range of species, as indicated by the diversity of species in this study. Not only could this provide more accurate estimates of the number and magnitudes of disturbance a tree experienced, but it also serves as a standardized framework of release criteria that can be applied to a wide range of species and forest types. All releases are expressed in terms of maximum potential as predicted by species and level of prior growth. So doing would reduce differences in maximum percent-growth change among individuals growing at different levels of prior growth, and would also standardize among species with different levels of maximum percent-growth change. This standardization would allow for better direct comparisons of disturbance histories among stands, and even for fine-scale studies of disturbance history in multi-species stands. Age and size may still influence maximum percent-growth change in that intolerant species are most likely to have severe reductions while tolerant species may show little or no change. For the present, older and larger trees may have to be eliminated from samples until the mechanisms behind these reductions are experimentally verified. Yet despite these complications, incorporation of prior growth into the release criteria will improve the accuracy of identifying disturbance events and estimating the magnitude of those events. For these reasons we believe the boundary-line technique will serve as a valuable tool for release calculations.

References

- Black, B.A., Abrams, M.D. (2003): A boundary-line approach to establishing release criteria in old-growth hemlock. *Ecological Applications* 13: 1733-1749.
- Black, B.A., Abrams, M.D. (2004): Development and application of boundary-line release criteria. *Dendrochronologia*. 22: 31-42.
- Lorimer, C.G., Frelich, L.E. (1989): A method for estimating canopy disturbance frequency and intensity in dense temperate forests. *Canadian Journal of Forest Research* 19: 651-663.
- Nowacki, G.J., Abrams, M.D. (1997): Radial-growth averaging criteria for reconstructing disturbance histories from presettlement-origin oaks. *Ecological Monographs* 67: 225-249.

Detection of growth dynamics in tree species of a tropical mountain rain forest in southern Ecuador

A. Bräuning & I. Burchardt

Institute of Geography, Azenbergstr. 12, D-70174 Stuttgart, Germany

Email: achim.braeuning@geographie.uni-stuttgart.de

Introduction

Dendrochronology in tropical areas has made substantial progress during the last years, as documented in several overviews (Wimmer and Vetter 1999, Roig, 2000a, Worbes 2002). Several studies reported about occurrence and climatological explanation of annually formed tree rings in neotropical wood species (e.g. Devall et al. 1995, Tomazello Fo et al. 2000, Roig 2000b). Thus, there are new perspectives to close important gaps in paleoclimatic information in the inner tropical regions that exist between tree-ring chronologies in Mexico (Stahle et al. 1998, Biondi 2001, Cleaveland et al. 2003) and the southern Andes (e.g. Villalba et al. 1997, Roig et al. 2001).

The study area is located at ca. 4°S in the province of Loja (southern Ecuador), in the Podocarpus National Park. The climate shows a high spatial variability due to the complex topography of the area that drastically modifies the general climatic conditions (Richter 2003). Along a east-west transect over the eastern Andes (Cordillera Real), the average annual rainfall varies from ca. 2200 mm (Zamorra, 970 m a.s.l.) in the eastern foreland, ca. 2500 mm (San Francisco, 1800 m a.s.l.) in a valley in the central Andes to 835 mm in the intra-andine basin of Vilcabamba (1570 m a.s.l.) to the west of the mountain chain (Hagedorn 1991). In the same direction, the seasonality of the rainfall distribution increases: perhumid conditions prevail on the eastern side of the Andes, whereas in Vilcabamba, which lies on the leeward side of the Andean chain, only 3 months per year (February-April) show humid conditions. Besides an east-west gradient, altitude has a strong impact on average temperature and on the amount of rainfall. At the upper timberline at approx. 3200 m elevation, more than 7500 mm of annual precipitation occur, in addition, approx. 2750 mm of water input by cloud and fog have to be taken into account (Bendix et al., 2004, Fabian et al. 2005).

Detection of growth dynamics

The first task was to realise a wood anatomical screening of approx. 250 different tree species that occur in the area to select some target species which form clear anatomical growth boundaries. As examples of such tree species we show photographs of *Cedrela montana* and *Tabebuia chrysantha* (Fig. 1). Several cores of *Cedrela montana* were measured to compare the inter- and intra-tree variability of these growth zones. Two radii of *Cedrela* allowed crossdating (Fig. 2). The two cores show a Gleichläufigkeit (sign-test) of 94% and a t-value (Baillie and Pilcher) of 8.9. Crossdating was not achieved yet between different trees, although some growth similarity was observed.

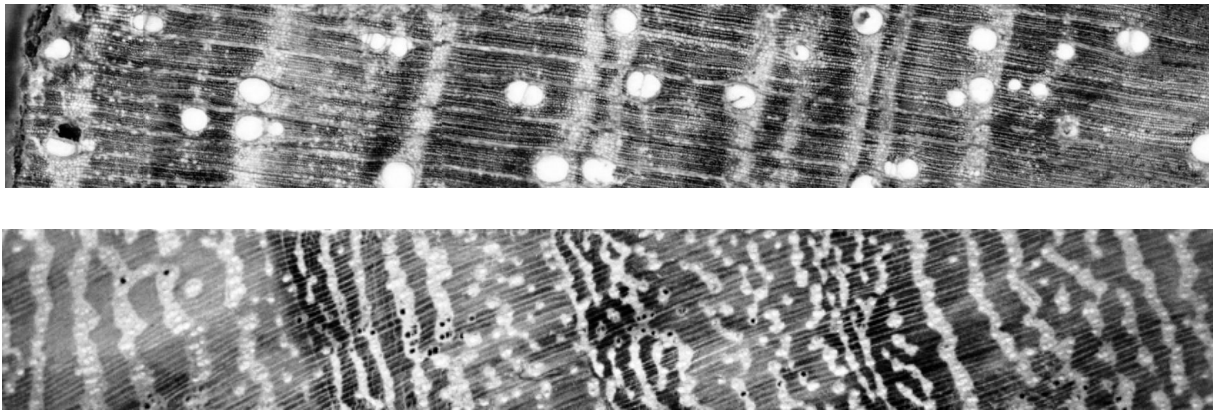


Figure 1: Macroscopic images of *Cedrela montana* (upper photo) and *Tabebuia chrysantha* (lower photo). Both species exhibit clear anatomical growth zones.

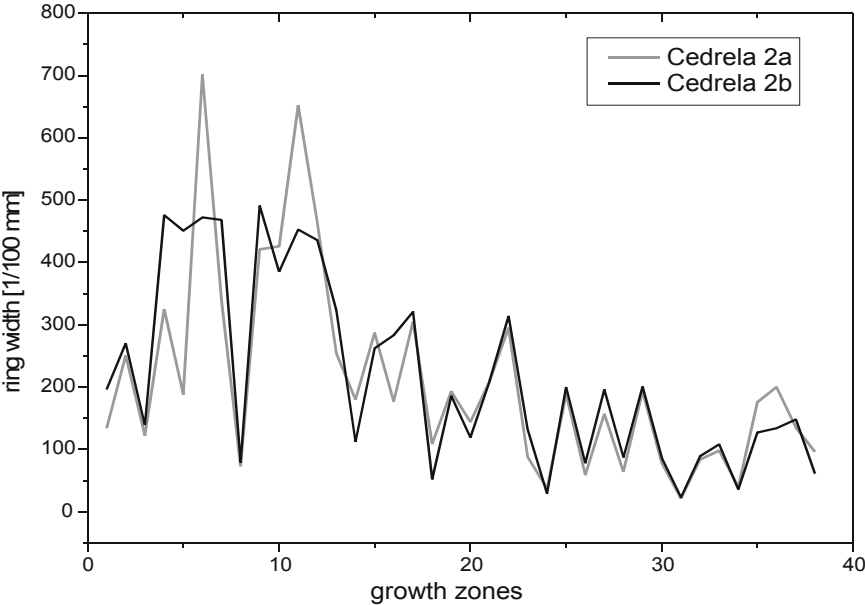


Figure 2: Synchronisation of growth zones within two radii of *Cedrela montana*

One study site where growth dynamics of selected species are studied in detail is located on the western declivity of the Podocarpus plateau at an elevation of 2100 m. The site is located in a transition zone between tropical humid evergreen cloud forest and semi-deciduous forest. Growth dynamics in tree species without distinct ring boundaries has often been studied by the so called ‘pinning-method’, a controlled wounding with needles (e.g. Nobuchi et al. 1995). To achieve a higher temporal resolution and a better control of the seasonal formation of different anatomical types of wood tissues, we collected small wood samples in two-week intervals with an increment puncher (Forster et al. 2000). Microsections with a thickness of 20 μm are produced, stained with solutions of safranin and astrablue and photographed. In addition, we installed dendrometers to register stem swelling and shrinking in 30 min. intervals.

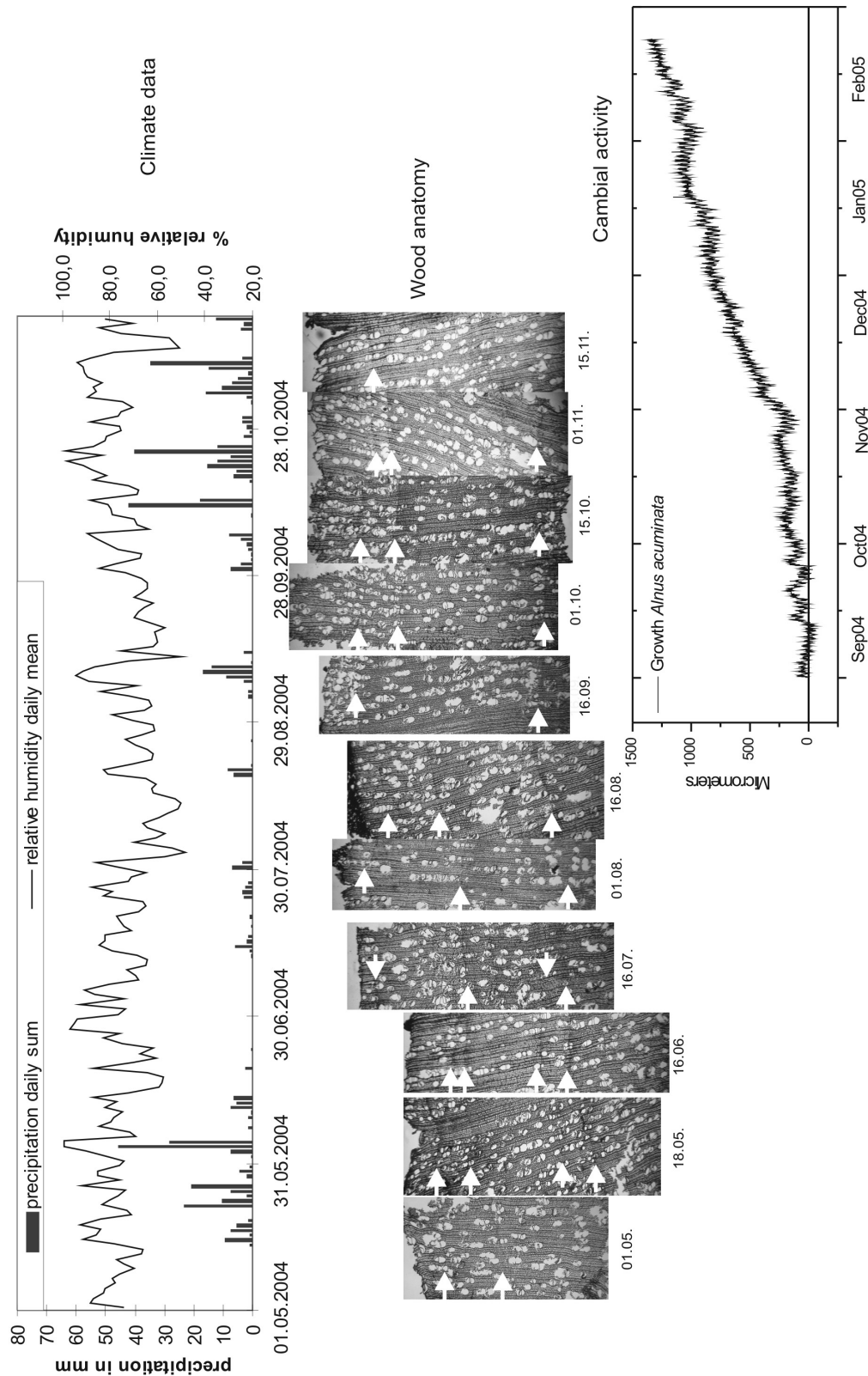


Figure 3: Comparison of climate data (precipitation daily sum and relative humidity daily mean), wood anatomy (microscopic images of biweekly increment puncher samples) and cambial activity (increase of girth recorded by dendrometer) of one *Alnus acuminata* tree in 2004. The white arrows indicate corresponding continuous lines on all samples.

A climate station measuring temperature, relative humidity and precipitation was installed in a distance of ca. 1 km. The pioneer species *Alnus acuminata* has been successfully used for ecological tree-ring studies on fire and landslide dynamics in subtropical Argentina, an area that shows distinct hygric seasonality (Grau et al. 2003).

Three tree species are abundant at the study plot and were selected for dendrometer measurements. The first is the pioneer species *Alnus acuminata* (Alnaceae). Further species are *Cedrela montana* (Meliaceae) and *Prumnopitys montana* (Podocarpaceae). To disentangle wood formation in relation to climate seasonality and girth changes, analyses of micro-sections, growth information from dendrometers and climate data have been combined. An example of this approach for *Alnus acuminata* is shown in Fig. 3 from growth season of 2004.

Alnus did not show formation of new cells during a relatively dry period without rainfall around 1st of May 2004. Probably as a reaction to the early June rainfall, new cells were formed between June 16th and July 16th. The pronounced band of thick-walled wood fibres serves as a marker in the two successive microsections. Between mid June and end of September, almost no rainfall occurred and relative humidity was rather low. *Alnus* did not exhibit formation of new cells. After the rainfalls during October, *Alnus* shows a swelling of the stem which is registered by the dendrometer. Then, according to the dendrometer and climate data, new wood tissue was formed consistently.

To discern seasonality in tropical woods, as many information as possible on the temporal succession of formation of different tissues is necessary. Visual control of the formation of different cells in the increment puncher cores combined with continuous measuring of cambial activity by dendrometer and climate data may help to achieve this goal.

This example illustrates how information about growth seasonality and its relation to local climate can be achieved by a combination of wood anatomy and growth measurements. Unfortunately, it requires regular maintenance of all instruments which is difficult at remote places under humid tropical conditions. Longer periods of overlapping information of all studied parameters are required to fully clarify the seasonality of wood formation at this site. This basic information about tree growth behaviour in a tropical mountain climate may then be used to interpret growth variations found on long increment cores. Finally, we hope to be able to construct tree-ring chronologies that provide new information on climate history in a region that is still largely devoid of high-resolution paleoecological data.

Acknowledgements

The author is indebted to the Deutsche Forschungsgemeinschaft (DFG) for the financial support of the project (BR 1895/8-1-2; FOR 402). Jana Knuth has contributed climate data.

References

Bendix, J., Fabian, P., Rollenbeck, R. (2004): Gradients of fog and rain in a tropical montane cloud forest of southern Ecuador and its chemical composition. Proceedings 3rd Int. Conf. On Fog, Fog Collection and Dew, 11-15. Oct. 2004, Cape Town ZA: H7-1-H7-4

- Biondi, F. (2001): A 400-year tree-ring chronology from the tropical treeline of North America. *Ambio* 30 (3): 162-166
- Cleaveland, M. K., Stahle, D. W., Therrell, M. D., Villanueva-Diaz, J., Burns, B. T. (2003): Tree-ring reconstructed winter precipitation and tropical teleconnections in Durango, Mexico. *Climatic Change* 59: 369-388
- Devall, M. S., Parresol, B. R., Wright, S. J. (1995): Dendroecological analysis of *Cordia alliodora*, *Pseudobombax septenatum* and *Annona spraguei* in central Panama. *IAWA Journal* 16 (4): 411-424
- Fabian, P., Kohlpaintner, M., Rollenbeck, R. (2005): Biomass burning in the Amazon-fertilizer for the mountainous forest in Ecuador. *Environmental Science and Pollution Research: 1-7 (online first)*
- Forster, T., Schweingruber, F. H., Denneler, B. (2000): Increment Puncher: A tool for extracting small cores of wood and bark from living trees. *IAWA Journal* 21 (2): 169-180
- Grau, H. R., Easdale, T. A., Paolini, L. (2003): Subtropical dendroecology - dating disturbances and forest dynamics in northwestern Argentina montane ecosystems. *Forest Ecology and Management* 177: 131-143
- Hagedorn, A. (1991): Extent and significance of soil erosion in southern Ecuador. *Die Erde* 132: 75-92
- Nobuchi, T., Ogata, Y., Siripatanadilok, S. (1995): Seasonal characteristics of wood formation in *Hopea odorata* and *Shorea henryana*. *IAWA Journal* 16 (4): 361-369
- Richter, M. (2003): Using epiphytes and soil temperatures for eco-climatic interpretation in southern Ecuador. *Erdkunde* 57 (3): 161-181
- Roig, F. A. (ed) (2000a): Dendrocronologia en América Latina. EDIUNC, Mendoza, 434 pp.
- Roig, F. A. (2000b): Dendrocronologia en los bosques del Neotropico: revisin y prospeccion futura. In: Roig, F. A. (ed) (2000): Dendrocronologia en América Latina. EDIUNC, Mendoza: 307-355
- Roig, F., Le-Quesne, C., Boninsega, J., Briffa, K., Lara, A., Grudd, H., Jones, P., Villagran, C. (2001): Climate variability 50.000 years ago in mid-latitude Chile as reconstructed from tree rings. *Nature* 410: 567-570
- Stahle, D. W., Cleaveland, M., K., Blanton, D. B., Therrell, M. D., Gay, D. A. (1998): The lost colony and Jamestown droughts. *Science* 280: 564-567
- Tomazello Fo, M., Botosso, P. C., Lisi, C. S. (2000): Potencialidad de familia Meliaceae para dendrocronologia em regioes tropicais e subtropcais. In: Roig, F. A. (ed) (2000): Dendrocronologia en América Latina. EDIUNC, Mendoza: 381-431
- Villalba, R., Boninsegna, J. A., Veblen, T. T., Schmelter, A., Rubulis, S. (1997): Recent trends in tree-ring records from high elevation sites in the Andes of northern Patagonia. *Climatic Change* 36: 425-454
- Wimmer, R., Vetter, R. E. (eds.) (1999): Tree-Ring Analysis. Biological, Methodological and Environmental Aspects. CABI Publishing, 302 pp.
- Worbes, M. (2002): One hundred years of tree-ring research in the tropics: a brief history and an outlook to future challenges. *Dendrochronologia* 20: 217-231.

Influence of thermic and pluvial conditions on the radial increments of *Pseudotsuga menziesii* Franco from Western Pomerania, Poland

A. Cedro

Laboratory of Climatology and Marine Meteorology, Institute of Marine Sciences, Faculty of Natural Science
University of Szczecin, Waska 13, 71-415 Szczecin, Poland
Email: Anna.Cedro@univ.szczecin.pl

Introduction

The Douglas fir (*Pseudotsuga menziesii* Franco) belongs to the most abundant foreign trees planted in Poland. This tree species was introduced to Poland in the 1840s (Szymanowski 1960), and in Western Poland (earlier Prussia) it appeared prior to 1880 (Tumilowicz 1970). The Douglas fir is appreciated for its rapid growth, high productivity (higher than the species naturally occurring in the area), as well as high resistance for pests and diseases (Mejnartowicz 1997).

The first Polish studies on the acclimatisation of Douglas fir in the region date back to the 1920 (works of Tyniecki, Sokołowski, Schappach, see Tumilowicz 1967, Suchocki 1926). These studies focussed on the inventory of existing planted areas, usefulness of seeds from various regions of Northern America to be planted in Poland, and evaluation of the suitability of the timber as a material for sawmills. First attempts to determine the impact of climatic and soil conditions on growth of this tree species were made by Borowiec (1965), Tumilowicz (1967), as well as Birot and Burzynski (1985). These studies demonstrated that the highest negative impact on radial growth of Douglas fir trees was due to low winter temperatures and early-spring frosts. Based on the analysis of the climatic conditions in Poland (the ratio of the total precipitation to the average monthly temperatures), Borowiec (1965) determined the most suitable areas for planting Douglas fir, among others the Pomerania and Baltic Coast regions.

The investigations presented here were based on the fact that various tree species react on changing climatic conditions in different ways. Determination of predominating factors influencing formation of annual growth rings at trees could enable reconstruction of climate beyond the period of instrumental records as well as prediction of dimensions of radial growth in the near future.

Study area

Western Pomerania is located in north-western Poland between Baltic Sea, Szczecin Bay and Odra Valley. All investigated plots are between 53°57' to 52°56' northern latitude and 14°11' to 15°46' eastern longitude, at elevations from 5 to 120 m a. s. l. The prevailing tree species are: *Pinus sylvestris* L., *Quercus robur*, *Q. petraea* and *Fagus sylvatica*. The climate in the area (based on stations: Swinoujscie, Resko, Szczecin and Gorzow Wlk.) can be described as transitional between maritime and continental (with Atlantic Ocean and Baltic

See influence). Mean annual temperatures range between 7,8 to 8,5°C and total precipitation between 532 and 683 mm. Maximum mean temperature is 18°C in July and minimum mean temperature may fall down to -9,7°C. Maximum total precipitation 70 to 80 mm are recorded in July, minima of about 30 mm in February and March (Tab. 1).

Material and methods

Field work was carried out in the forest areas directed by the Regional Direction of National Forests in Szczecin and in the Wolin National Park in the years 1998 to 2002. Altogether 16 research sites were established for *Pseudotsuga menziesii* Franco. The plots that met the methodological criteria were selected for further analyses and the choice had been determined by the existence of long-lived trees of the analysed species. Core samples - the basic research materials were taken from 225 trees.

For every sample tree-ring width were measured with 0.01 mm accuracy. Individual dendrograms were dated a chronology was built following the classical methods of dendrochronological crossdating, presented in numerous publications (Schweingruber 1989, Cook and Kairiukstis 1992, Kaennel and Schweingruber 1995). Thereafter, using Arstan (Holmes 1983, 1994), the chronology was indexed eliminating long-term trends (e.g. age trend) and accentuating the year-to-year variability in widths of the tree rings.

The resulting chronology was used as a basis for dendroclimatological analyses such as response function and pointer years. The response function analyses were based on meteorological data (average monthly air temperatures and total monthly rainfall which was examined for 16-month intervals: from June of the previous year to September of the analysed year in the period of 51 years: 1948-1998) and the indexed values of the tree-ring widths. Except for the current vegetation season, the analyses also included the impact of thermal and pluvial conditions of the preceding summer, autumn, and winter on formation of growth rings at the analysed trees (analysis of periods of 16 months: from July of the previous year to September of the current one (Blasing et al. 1984). The years in which over 90% of the analysed trees exhibited similar growth trends were defined as pointer years. When increments were narrower than the previous year, the pointer years were negative, and contrariwise – positive. Analysis of meteorological conditions and the relationships between the annual increments and climate was carried out for the pointer years, which had been determined with the program TCS (Walanus 2002).

Douglas fir chronologies

16 local chronologies of Douglas fir resulted from various habitats of Western Pomerania. The local chronologies were constructed based on 186 individuals selected from 225 sampled trees (Tab. 2). Average replication of the chronologies was, the highest 15 - for the chronology DG1 from Mysliborz Lakeland - and the least 10 individual trees for the research plots LP2, RY3, WNP4 and WNP5. The longest sequence spans 107-years (chronology WNP2 from a site in the Wolin Island), representing the period 1894-2000, and the shortest 63-years (RY2 from Gryfice Plateau). Average ring width for all local chronologies of Douglas fir (*Pseudotsuga menziesii*) amounts to 3.07 mm, significantly higher than the corresponding

value for Scots pine from Western Pomerania (Cedro 2004). The widest rings (4.04 mm) were noted in trees from site WNP6 (Gryfice Plateau), and the narrowest (1.55 mm) in trees from site DG2 (Mysliborz Lakeland) located southernmost (Tab. 2). No distinct relationship between the average ring widths and the duration of the chronology was observed, which may be due to relatively uniform ages of the analysed trees.

Exceptionally high values of convergence and similarities in local dendrograms for *Pseudotsuga menziesii* indicate predominating influence of environmental factors on the cambial activity and formation of tree rings. The local chronologies established, together with results of convergence, gave rise to construct a standard chronology for Douglas fir from Western Pomerania, labelled PZjedlica. The standard consists of 65 trees (out of 186 investigated trees) displaying the highest similarities of dendrograms (t-values > 6.0, Tab. 3). The regional chronology PZjedlica spans 109 years, between 1894 and 2000.

Results

Analysis of pointer years was carried out for 65 individuals of *Pseudotsuga menziesii* forming the regional chronology (PZjedlica) and for those forming the local chronologies. In case of the regional chronology, 19 pointer years (9 positive and 10 negative, Fig.1) were determined.

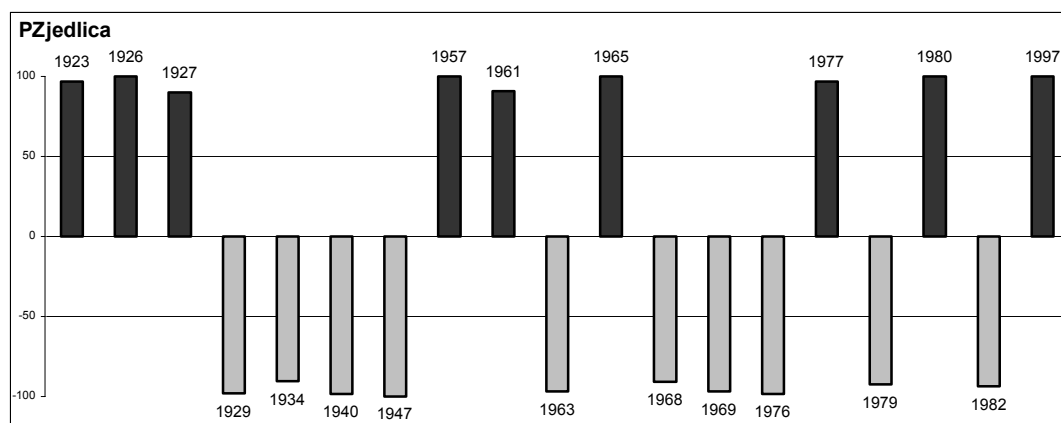


Figure 1: Pointer years determined from growth sequences of regional chronology of Douglas fir for Western Pomerania (PZjedlica).

Negative pointer years occurred in years with frosty and cold winters, with very low values of January and February temperatures. Also temperatures of March were of similar significance for annual growth in the forthcoming vegetation season. Years with cold winters and summer draughts marked deep minima in dendrograms and often continued in the following years. In positive pointer years winter temperatures were predominating; positive temperatures in January and February followed by early spring resulted in formation of wider growth rings. The amount of rainfall in the vegetation season turned out to be of lower importance. In some years (1936, 1948, 1957, 1988, and 1997) decrease of ring widths was noted, in spite of shortage of rainfall in spring and/or summer months.

Table 1: Air temperatures in the period 1948-1998 (in Celsius degree); A – mean monthly temperature, B – minimum monthly temperature, C – maximum monthly temperature. Precipitation in the period 1948-1998 (in mm); A – mean monthly rainfall, B – minimum monthly rainfall, C – maximum monthly rainfall.

TEMPERATURE		I	II	III	IV	V	VI	VII	VIII	IX	X	XI	XII	I-XII
Szczecin	A	-0,6	-0,2	3	7,6	12,8	16,2	17,8	17,1	13,6	9	4,2	1	8,5
	B	-8,8	-7,5	-0,9	3,8	10	13,9	15,2	14,7	11,2	6,2	0,2	-6,3	7,1
	C	4,8	6,4	7,5	10,2	16,4	19,3	22,3	20	16,3	11,7	7,4	4,8	10,1
Swinoujscie	A	-0,2	0,1	2,8	6,5	11,3	15,2	17,2	17,1	13,8	9,4	4	1	8,2
	B	-6,2	-7,5	-1,2	3,8	8,9	13,6	14,5	14,7	11,4	6,7	0,8	-5,2	6,9
	C	4,8	6,1	6,2	9,2	13,9	16,8	19,9	20,6	16,6	11,9	7,2	4,7	9,8
Resko	A	-1,1	-0,7	2,3	6,8	12,1	15,4	17	16,6	12,8	8,5	3,7	0,4	7,8
	B	-9,1	-9,6	-1,7	3,6	9,2	13,5	14,2	13,9	10,1	5,3	-0,3	-6,9	6,3
	C	4,3	5,9	6,9	9,8	15,9	17,9	21,4	19,7	15,4	11,2	6,6	4	9,5
Gorzow Wlk.	A	-1,3	-0,6	3	7,8	13,1	16,4	18	17,6	13,6	8,8	3,6	0,3	8,4
	B	-8,7	-9,7	-1,1	4,4	9,8	14,2	14,8	14,7	10,9	5,6	-0,5	-7,2	6,7
	C	4,2	5,5	7,3	11,4	16,5	19,6	22,3	20,9	16,3	11,4	7,1	3,9	9,9
PRECIPITATION		I	II	III	IV	V	VI	VII	VIII	IX	X	XI	XII	I-XII
Szczecin	A	35	29	32	37	51	60	69	57	43	37	41	41	532
	B	0	4	5	5	12	8	5	7	4	0	9	6	347
	C	83	76	96	106	128	133	137	141	124	90	104	90	716
Swinoujscie	A	41	30	34	39	47	57	57	56	50	44	47	47	551
	B	0	4	4	4	7	9	0	7	2	0	7	8	377
	C	78	66	94	118	120	146	135	106	158	109	128	123	763
Resko	A	51	39	45	45	54	67	82	72	61	53	54	58	683
	B	1	7	6	7	7	16	9	12	6	0	11	8	441
	C	129	85	105	132	122	195	173	173	150	204	121	130	953
Gorzow Wlk.	A	36	30	32	38	51	64	71	56	42	37	41	43	541
	B	1	4	7	6	11	7	2	9	3	1	6	4	337
	C	116	65	81	88	121	134	195	150	114	114	114	104	752

In most cases, however, tree-ring widths were determined by thermal conditions. Results of dendroclimatical analyses (response function) for Douglas fir are presented in Table 3. The coefficients of linear correlation (k) and multiple regression (r) indicate that radial growth were mostly influenced by temperatures of winter months (January, February) and the beginning of spring (March).

Table 2: Statistical data for local measured and index chronologies of Douglas fir from Western Pomerania

No.	Lab. code	No. of years	Time span	No. of samples	Mean RW (mm)	Std. Dev.	Mean sens.	1st order Autocor.	Index Chron.			
									Median	Mean sens.	Std. dev.	1st. order autocor.
1	DG1	78	1922-1999	15	3,87	1,8	0,3	0,67	1,02	0,23	0,2	-0,12
2	DG2	75	1925-1999	11	1,55	0,84	0,28	0,64	1,02	0,21	0,18	0
3	LP2	91	1911-2001	10	1,86	1,04	0,35	0,06	0,99	0,29	0,24	-0,04
4	RES1	68	1934-2001	14	2,48	1,13	0,27	0,64	1,01	0,24	0,22	-0,05
5	RES4	65	1937-2001	11	2,85	1,07	0,27	0,52	1,04	0,24	0,22	0
6	RY2	63	1940-2002	11	3,01	1,16	0,23	0,67	0,97	0,2	0,18	0,09
7	RY3	88	1915-2002	10	2,41	1,03	0,26	0,69	0,99	0,23	0,2	-0,13
8	T1	78	1923-2000	11	3,68	1,62	0,29	0,59	1,01	0,26	0,21	-0,19
9	T2	82	1919-2000	13	3,95	1,75	0,26	0,66	1,03	0,22	0,21	-0,05
10	T5	79	1921-1999	12	2,28	1,13	0,3	0,7	0,97	0,24	0,22	0,02
11	WNP1	98	1903-2000	11	3,68	1,55	0,24	0,72	1	0,21	0,19	0,03
12	WNP2	107	1894-2000	13	3,16	1,2	0,25	0,64	0,99	0,2	0,18	0,01
13	WNP3	101	1900-2000	11	2,82	0,13	0,26	0,71	1	0,22	0,19	-0,07
14	WNP4	89	1912-2000	10	3,92	2,02	0,27	0,73	0,99	0,24	0,2	-0,08
15	WNP5	96	1905-2000	10	3,51	1,52	0,29	0,69	1,02	0,26	0,22	-0,05
16	WNP6	89	1912-2000	13	4,04	2,24	0,3	0,75	1,02	0,26	0,23	-0,07
Mean		84		12	3,07	1,33	0,27	0,63	1	0,23	0,2	-0,04

Table 3: Convergence of Douglas fir local and the regional chronology (PZjedlica) measured with "t" and "GI" value

GI/t	DG1	DG2	LP2	RES1	RES4	RY2	RY3	T1	T2	T5	WNP1	WNP2	WNP3	WNP4	WNP5	WNP6	PZjedlica
DG1	X	10,1	7,7	7,6	5,1	5,4	8,6	8,9	8,8	11,7	7,2	10,1	10,6	10	11,4	9	12,6
DG2	77	X	8,7	4,2	3,7	4	6,1	6,1	4,8	7,4	3,7	5,4	5,6	7,3	5,3	4,9	8
LP2	73	70	X	5,6	3,9	4,9	6,8	8,6	8,1	8,4	5,2	9,7	8	5	8,9	7,3	10,9
RES1	67	59	67	X	10,4	7,5	8	7,5	8	7,2	8,1	12,3	9,1	5,7	9,8	7,9	11,5
RES4	68	63	64	72	X	6,4	5,6	6,9	6,7	6,6	5,8	8,1	6	4,4	7,2	5	9,1
RY2	74	70	71	83	80	X	4,2	5,1	5,9	5	4,3	5,1	4,9	5,6	6	4,5	6,3
RY3	72	68	70	69	63	70	X	10	8,7	9,6	8,4	11	11,5	8,7	10	11	10,8
T1	75	70	77	71	73	73	76	X	15,7	15,3	7,3	10,9	10,3	8,9	9	7	15,4
T2	74	74	77	73	76	73	69	82	X	14	9,8	11,9	11,5	7,9	13	9,7	16,5
T5	76	75	78	69	72	71	69	82	85	X	7,1	11,6	10,6	8,9	10,3	9,4	20,2
WNP1	68	64	70	74	66	67	75	73	77	70	X	12,7	11,7	8	12,2	8	7,9
WNP2	71	61	76	83	71	74	74	81	73	74	78	X	16,8	7,9	15,5	11,7	15,2
WNP3	73	65	74	73	64	68	74	74	76	73	78	81	X	9,9	11,6	13,7	12,9
WNP4	75	77	73	72	69	80	76	79	75	75	74	78	77	X	8,6	8,1	9,1
WNP5	73	65	71	77	70	73	68	73	77	75	81	78	75	72	X	11,2	12,7
WNP6	74	70	75	71	66	75	75	73	77	71	73	78	80	80	80	X	12,5
PZjedlica	77	72	86	79	80	80	70	86	84	88	75	84	76	77	81	79	X

rainfall in February and March are connected with predomination of western circulation pattern in the region. Frequent atmospheric low pressure systems, bringing humid and mild Atlantic air masses, result in an increase of both air temperatures and rainfall, which in turn leads to higher cambial activity in the forthcoming vegetation season. On the other hand, rainfall in summer months of a current growth season seems to have no significant influence on tree growth.

The high values of determination coefficient ($r^2 = 63\%$ in average, minimum 50% in the plot WNP4, maximum 75% in the site WNP6) indicate significant influence of the climatic factors on annual growth of Douglas fir in Western Pomerania.

Discussion

Dendroclimatological studies on the Douglas fir in Poland performed by Feliksik and Wilczynski (1997, 1998a, 1998b, 1999, 2001, 2004a, 2004b) revealed similar relations between climatic factors and annual increment as of the Douglass fir from the Western Pomerania; predominating impact of winter thermal conditions, particularly February. Tree growth positively correlates with temperatures of February (Feliksik and Wilczynski 1997, 2004a, 2004b), and of January, February, and March in the vicinity of Bielsko-Biala (Feliksik 1999). Except for the response function analysis these authors also compared average indexed dendrochronological curves of the analysed sites (including the research plot near Gryfice) with average temperatures for the period December-April, and noted almost total convergence of both (Feliksik and Wilczynski 1997, 2004a). Similar results were obtained for the Karkonosze Mts, NE Poland (Feliksik and Wilczynski 1998a, b), as well as for the Silesian Beskid Mts (Feliksik and Wilczynski 2001). In the last region the authors analysed annual growth rings of several species of foreign and native coniferous trees with response functions. Three of the analysed species: *Picea abies* L., *Pseudotsuga menziesii*, and *Chamaecyparis lawsoniana* revealed high sensitivity on the temperatures of winter and early spring (January, February and March), *Larix kaempferi* did not. Douglas fir, similarly to *Picea abies* L. and *Chamaecyparis lawsoniana*, reacted positively on high rainfall in the summer season (June, July).

Dendroclimatological studies on the Douglas fir growing in natural habitats in North America have been led by numerous researchers, which may be related to the wide range of this tree species. The relationships determined between ring width and climatic factors mostly depend on climate and habitat type; for example growth of *Pseudotsuga menziesii* in New Mexico and Colorado (steppe habitats) mostly depends on the amount of rainfall during vegetation season (Cleaveland 1986). In SW Canada the correlation of climatic parameters and ring widths of earlywood, and latewood, based on 40 chronologies for Douglas fir, demonstrated the predominating role of the atmospheric precipitation for tree-ring formation. Development of earlywood depends on the rainfall in the previous summer, while latewood formation depends on the rainfall in June and July of the current vegetation season. Air temperatures are of lesser importance – correlation coefficient values are negative, especially between May and July, when high temperatures enlarge the evapotranspiration and water stress (Watson and Luckman 2002).

References

- Birot, Y., Burzynski, G. (1985): Analiza próby proveniencyjnej daglezi w Polsce i we Francji (Analysis of provenance trials of Douglas fir in Poland and France). [In Polish, with English summary] *Sylwan* 6: 35-47.
- Blasing, T.J., Solomon, A.M., Duvick, D.N. (1984): Response functions revisited. *Tree-Ring Bulletin* 44: 1-15.
- Borowiec S, 1965. Ocena warunków makroklimatycznych i glebowych w Polsce do hodowli daglezi (*Pseudotsuga taxifolia* Britton), (The evaluation of macroclimatic and soil conditions in Poland for a cultivation of Douglas fir (*Pseudotsuga taxifolia* Britton)). [In Polish, with English summary] *Sylwan* 1: 27-34.
- Cedro, A. (2001): Influence of thermic and pluvial conditions on the radial increments of *Pseudotsuga menziesii* Franco from Western Pomerania. *Tree Rings and People*, Davos: 115.
- Cedro, A. (2004): Zmiany klimatyczne na Pomorzu Zachodnim w świetle analizy sekwencji przyrostów rocznych sosny zwyczajnej, daglezi zielonej i rodzimych gatunków dębów (Climatic changes in Western Pomerania in the light of analysis of tree-ring sequences of Scots Pine, Douglas Fir and native species of Oak). [In Polish, with English summary] *Oficyna In Plus*: 30-36.
- Cleaveland, M. (1986): Climatic response of densitometric properties in semiarid site tree rings. *Tree-Ring Bulletin* 46: 13-23.
- Cook, E.R., Kairiukstis, A. (1992): *Methods of dendrochronology*. Kluwer Academic Publishers: 97-162.
- Feliksik, E., Wilczynski, S. (1997): Klimatyczne uwarunkowania przyrostów rocznych drewna jedlicy zielonej (*Pseudotsuga Menziesii* Franco) z wybranych stanowisk w Polsce {Climatic conditioning of Douglas fir tree ring (*Pseudotsuga Menziesii* Franco)}. [In Polish] *Acta Agraria et Silvicultura, seria Silvestris XXXV*: 1-15.
- Feliksik, E., Wilczynski, S. (1998a): Wpływ temperatury powietrza oraz opadów atmosferycznych na przyrost drewna jedlicy zielonej (*Pseudotsuga menziesii* Franco) z Karkonoszy (Influence of temperature and rainfall on tree ring of Douglas fir (*Pseudotsuga menziesii* Franco) from Karkonosze). [In Polish, with English summary] *Sylwan* 4: 55-62.
- Feliksik, E., Wilczynski, S. (1998b): Dendroclimatological research on the Douglas fir (*Pseudotsuga Menziesii* Franco) from northeastern Poland. *Zesz. Nauk. AR w Krakowie*, 344: 49-57.
- Feliksik, E. (1999): Klimatyczne uwarunkowania przyrostów radialnych jedlicy zielonej (*Pseudotsuga menziesii* Franco), sosny wejmutki (*Pinus strobus* L.) i sosny czarnej (*Pinus nigra* Arnold). [Climatic conditioning of the radial growth of *Pseudotsuga menziesii* (Franco), *Pinus strobus* (L.), *Pinus nigra* (Arnold)]. [In Polish] *Klimatyczne uwarunkowania życia lasu*: 87-94.
- Feliksik, E., Wilczynski, S. (2001): The influence of temperature and rainfall on the increment width of native and foreign tree species from the Istebna Forest District. *Folia Forestalia Polonica, series A - Forestry* 43: 103-114.

- Feliksik, E., Wilczynski S. (2004a): Klimatyczne uwarunkowania przyrostu radialnego daglezi zielonej (*Pseudotsuga menziesii* (Mirb.) Franco) rosnacej na obszarze Polski (Climatic conditions of the radial increment of Douglas fir (*Pseudotsuga menziesii* (Mirb.) Franco) in Poland. [In Polish, with English summary] *Sylwan* 12: 31-38.
- Feliksik, E., Wilczynski S. (2004b): Lata wskaźnikowe daglezi zielonej (*Pseudotsuga menziesii* (Mirb.) Franco) na obszarze Polski (Pointer years of Douglas fir (*Pseudotsuga menziesii* (Mirb.) Franco) in Poland). [In Polish, with English summary] *Sylwan* 12: 39-47.
- Holmes, R.J. (1983) Computer-assisted quality control in tree-ring dating and measurement. *Tree-Ring Bull.* 43: 69-78.
- Holmes, R.J. (1994): Dendrochronology Program Library. Users Manual. University of Arizona, Tucson.
- Kaennel, M., Schweingruber, F.H. (1995): Multilingual glossary of dendrochronology. WSL FNP, Haupt: 133, 162, 184, 292, 331.
- Mejnartowicz, L. (1997): Rozmnazanie generatywne daglezi zielonej (*Pseudotsuga menziesii* [Mirb.] Franco), (Generative propagation of Douglas-fir). [In Polish, with English summary] *Sylwan* 12: 33-45.
- Schweingruber, F.H. (1989): Tree rings. Basics and applications of dendrochronology. Kluwer Academic Publishers.
- Suchocki, S. (1926): Kilka uwag o zarastaniu scietych pni u daglezi zielonej (*Pseudotsuga Douglasii*), {Few remarks about scar of trunk felled of Douglas fir (*Pseudotsuga Douglasii*)}. [In Polish] *Rocznik Polskiego Towarzystwa Dendrologicznego*: 111-112, Lwow.
- Szymanowski, T. (1960): Kiedy wprowadzone zostały obce gatunki drzew do uprawy w Polsce? (When foreign species of trees were introduced for cultivation in Poland?) [In Polish] *Rocz. Sekc. Dendr.* 14: 81-99.
- Tumilowicz, J. (1967): Ocena wyników wprowadzania niektórych obcych gatunków drzew w lasach krainy Mazursko-Podlaskiej (Estimation of results introducing some foreign species of trees in forests of Mazury and Podlasie). [In Polish] *Rocznik Dendrologiczny* XXI: 147-166.
- Tumilowicz, J. (1970): Obce gatunki drzew w naszych lasach (Non-native tree species in our forest). [In Polish] *Sylwan* 8-9: 60-65.
- Walanus, A. (2002): Instrukcja obsługi programu TCS. Program TCS do obliczania lat wskaźnikowych (User's manual of TCS software. TCS software for calculation of pointer years). [In Polish] Kraków: 1-13.
- Watson, E., Luckman, B. (2002): The dendroclimatic signal in Douglas-fir and ponderosa pine tree-ring chronologies from the southern Canadian Cordillera. *Can. J. For. Res.* 32: 1858-1874.

Climate driven height growth change of multistem trees of Siberian larch in the Polar Ural mountains

N.M. Devi

Institute of Plant and Animal Ecology. 8 Marta, 202, Ekaterinburg, Russia, 620144

Email: nadya@ipae.uran.ru

Introduction

Siberian larch growing at the edge of its proliferation possesses various adaptive properties that allow it to exist successfully in the extreme natural and climatic conditions (Gorchakovskiy and Shiyatov, 1985). Quite successive existence of larch at the Polar Urals is possible because of several biological and morphological adaptations. Biological adaptations include the short period of auxiblasts growth (14-28 days), dominant development and substantial life duration of brachiblasts (up to 100 years), and the high content of protective metabolites (Iroshnikov, 1984). Morphological features of coniferous species growing in boreal areas (including Siberian larch) are the ability to exist in a number of life forms (stem, bush, creeping) and to change the growth form under the change of environmental conditions (Gorochkevich and Kustova, 2002).

There is large number of trees that changed several growth forms in the course of their lifetime in the ecotone of the upper forest bound at Polar Urals. Most often, these are the multistem trees that are generated by forming several vertical stems from the creeping form. Such trees can serve as climate change indicators.

The purpose of this paper is to study the effect climate has on form genesis and growth characteristics of the multistem Siberian larch trees.

Major research goals:

- reveal the dates of forming stems and changing growth form;
- examine, whether the growth form change causes a change of tree growth characteristics (axial and radial growth).

Materials and methods

The research is performed in the forest-tundra area (100-300 meters above sea level) at the eastern macroslope of Polar Urals.

The selection of model trees was performed based on a route method. Individual trees of a group of several stems which originate from a single base, which first grew plagiotropically and then orthotropically were selected as model trees.

The cross-sections of 35 Siberian larch (*Larix sibirica* Ledeb.) stems, belonging to six multistem trees are used for analysis. For each stem the morphological parameters are described, including growth form, vitality, stem height and diameter, crown shape and size. Average stem height was 3 meters, diameter at base was 15 cm.

Cuts were made at three main levels (Fig.1) – at the base of a horizontal stem (O), in the point of transfer to vertical growth (A), and at the height of a vertical stem equal to OA.

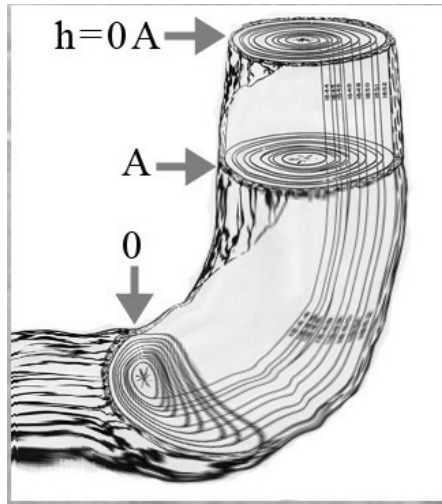


Figure 1: Illustration of levels at which cross-sections have been taken for growth analysis

Specimen dating and growth analysis were performed using dendrochronological methods.

Results and discussion

Figure 2 illustrates the dates of appearance and of life form change of the larch model trees over time. For convenience of analysis growth start dates are smoothed by decades. The smoothed curve demonstrating dynamics of summer months' thermal mode for the analyzed period is also drawn.

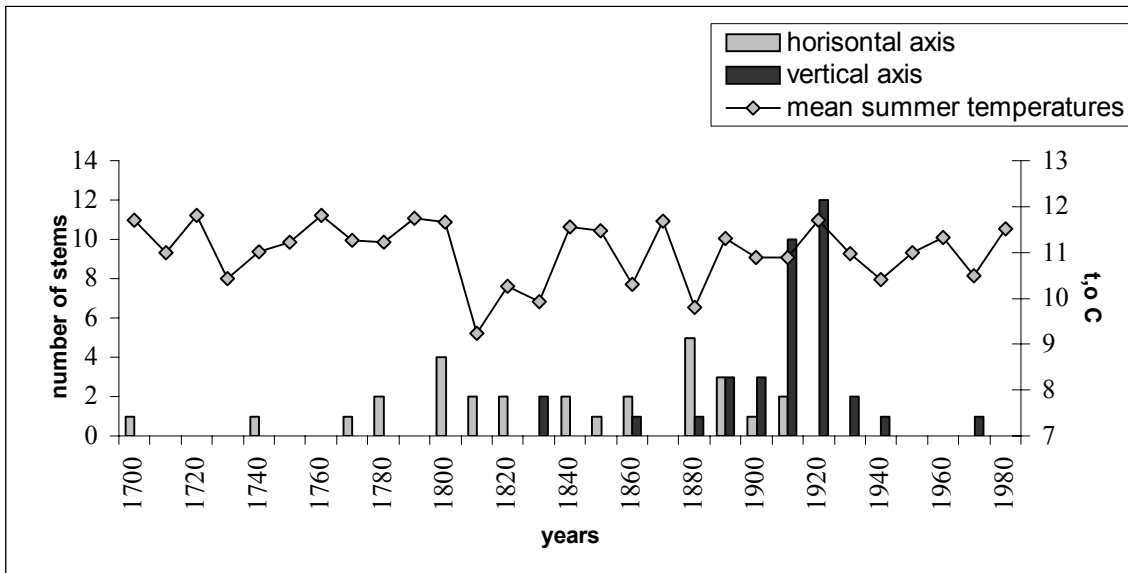


Figure 2: Dates of appearance of the life form change for the Siberian larch model trees and changes of summer months' thermal mode

The growth of horizontal stems started in 18th and 19th centuries. Before the beginning of the 20th century most trees were creeping. In the 1920s the growth form for the majority of studied trees became multistem.

To reveal dendroclimatic relations the analysis of summer months' thermal mode effect on the frequency of tree growth start and life form change dates is undertaken. Analysis does not demonstrate a relation between the frequencies of horizontal stem growth start dates and average summer temperatures of vegetation season. It is possible that the appearance of such trees was affected by other climatic factors, such as the amount of precipitation or the snow accumulation conditions. Regretfully, there is no reconstruction of these factors for the examined period. Nevertheless, a direct statistical relation exists between the dynamics of average summer temperature, and the frequency of years with growth form change for the trees ($r=0.68$).

According to literature data the 18th and 19th centuries at the Urals are characterized by adverse thermal conditions (Graybill and Shiyatov, 1992) and humidity (Mazepa, 1999). In the early 20th century a substantial thermal mode improvement occurred.

The obtained results demonstrate that the change of larch growth form occurred because of the improvement of the environmental conditions and is probably related to climate warming in the beginning of the 20th century. The transition to orthotropic growth form caused a change in stem characteristics, including axial and radial growth. Average axial growth of orthotropic stem parts substantially increased compared to plagiotropic parts (see figure 3) – from 1 to 4 centimeters per year. Obtained differences are statistically significant ($T=5,2$; $p=0,000003\%$).

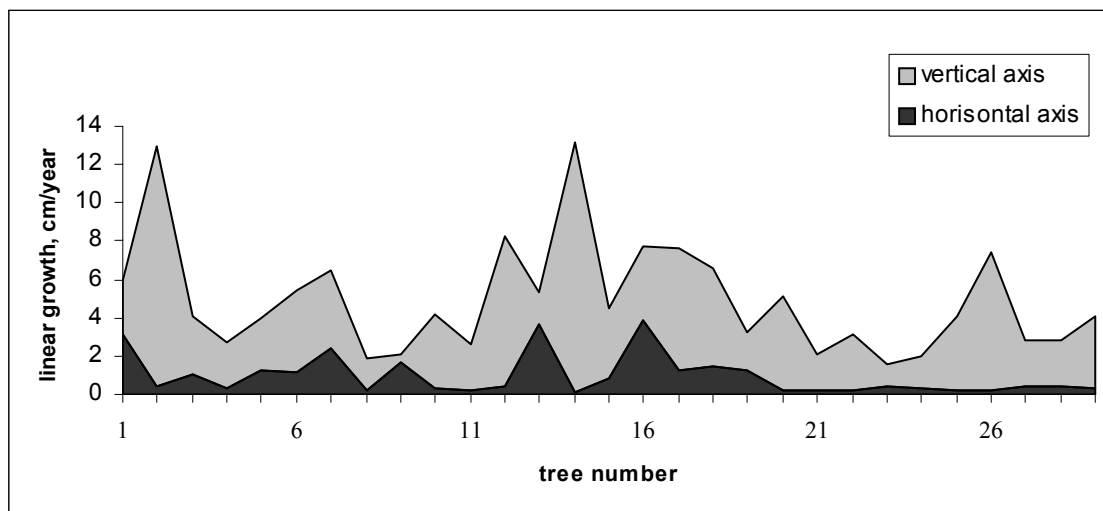


Figure 3: Average axial growth of horizontal (plagiotropic) and vertical (orthotropic) stem

Analysis of radial growth for cross-sections taken at different basic heights (Fig. 4) demonstrate the increase in radial growth. Average tree-ring width increased by 0,08 mm, while going from O to OA. Obtained differences are statistically significant ($T=2,5$; $p=0,013\%$).

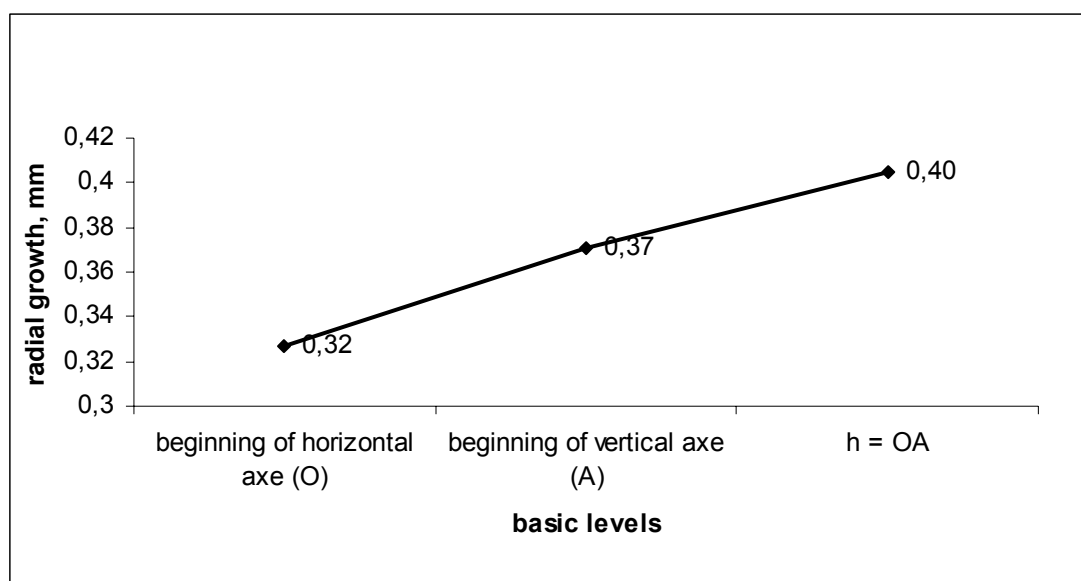


Figure 4: Average radial growth at different stem heights

Conclusion

Improvement of the thermal mode at the beginning of the 20th century caused the growth form change from plagiotropic to orthotropic for the studied samples of Siberian larch in the ecotone of the upper forest boundary at Polar Urals. Axial growth rate and radial growth for orthotropic stem parts are substantially higher than the corresponding characteristics of plagiotropic parts.

Acknowledgements

The work was performed with financial support of the grants RFFR 04-04-48687, INTAS 01-0052 and 04-83-3788.

Literature

- Goroshkevich, S.N., Kustova, E.A. (2002): Morphogenesis of the creeping life form of Siberian cedar at the upper limit of proliferation in West Sayan Mountains. *Ecology 4*: 243-249.
- Gorchakovskiy, P.L., Shiyatov, S.G. (1985): Phytoindication of the environmental conditions and natural processes in the alpine terrain. M. Nauka. 208 pp.
- Iroshnikov, A.I. (1984): Siberian larch at the northern boundary of proliferation: Materials proceedings of the session on the results of research activities at Archangelsk Institute of Forest and Dendrochemistry for 1983. Archangelsk. 93 p.
- Mazepa, V.S. (1999): Effects of precipitation on the radial growth dynamics for the coniferous is sub-Arctic regions of Eurasia. *Lesovedenie 6*: 15-22.
- Graybill, D.A., Shiyatov, S.G. (1992): Dendroclimatic evidence from the northern Soviet Union. In: Bradley, S., Jones, P.D., Climate since A.D. 1500. Routledge, London and New York: 393-414.

Dendroecological Analysis of Growth Anomalies in Walnut Forests in Southern Kyrgyzstan

D. Friedrichs¹, B. Neuwirth¹ & H. Gottschling²

¹Department of Geography, University of Bonn, Germany

²Department of Botany and Landscape Ecology, University of Greifswald, Germany

Email: d.friedrichs@giub.uni-bonn.de

Introduction

Kyrgyzsian walnut forests are characterized by a remarkable biodiversity and a worldwide exceptional volume expansion. Beside the walnut (*Juglans regia*), the forests consist of various fruit species, which contribute to the enormous genetical diversity.

Due to the political circumstances since the beginning of the nineties the ecological balance of the forests is endangered. The political breakdown of the Soviet Union 1991 leads to various socio-economical changes. One of the consequences is an increase of human influence on walnut forests. The local population depends on the agricultural sector; the forest regions are intensively farmed. Walnuts are harvested, firewood is lumbered and large areas are changed into pasture for cattle. The ecological consequences are a loss of forest area, a decrease of forest stand density, a loss of the genetical diversity and a loss of generative regeneration which leads to an ageing of the forests. Additionally, the forests lose their function as a shelter which leads to soil erosion, debris flows and floods. Further increase of utilisation pressure can end up in a breakdown of the ecosystem (Gottschling et al. 2005).

How the human activities in this region influence the forests is analysed within the research project "The Impact of the Transformation Process on Human-Environmental Interactions in Southern Kyrgyzstan" supported by the VW-foundation. Dendroecological analyses are made to find out how Kyrgyzsian walnut trees naturally grow, to what extent the climatological forcings influence tree-ring growth and how the anthropogenic utilisation changes the tree growth. Up to now the natural growth dynamics are investigated. The main subjects are:

- Age distribution: How old are Kyrgyzsian walnut forests?
- Analysis of growth variability i) internal site investigation ii) comparison of the sites

Material

For the dendroecological analyses tree cores from 20 sampling sites were taken.

The study sites are located in Southern Kyrgyzstan and belong to the Tien Shan Mountains, Fergana Range. The ecological conditions of the sampling sites differ in topographic characteristics such as elevation, exposition, inclination, and micro-relief, as well as in composition of species. Additionally, the degree of human influence varies between the sites, from non-utilised natural sites to completely farmed forests. In order to analyse the natural growth variabilities, four sampling sites are selected. The ecological settings are listed in

table 1. In all sites *Juglans regia* is the dominant tree species. The selected sites differ mainly in elevation.



Figure 1: map of Kyrgyzstan; with research area, Source: Microsoft Encarta

The Sary Tasch sites and Arpa Tökty belong to the lower forest step (1000-1400m.a.s.l.) and Daschman belongs to the middle forest step (1400-1750m a.s.l.). Further details about the classification of walnut forests depending on elevation can be found in Gan 1992 and Kolov 1997.

Table 1: Settings of investigated sites

Site location	Geogr. Coordinates	Elevation	Exposition	Inclination
Daschman	41.3409 N 73.0237 E	1730m a.s.l.	N	26°
Arpa Tökty	41.4049 N 73.0791 E	1370m a.s.l.	NNO	17°
Sary Tasch (1)	41.3124 N 73.1020 E	1260m a.s.l.	N	26°
Sary Tasch (2)	41.3138 N 73.1048 E	1160m a.s.l.	NNW	4°

In total, 81 walnut trees were sampled: 15 trees in Daschman, 18 in Arpa, 20 in Sary 1 and 28 in Sary 2.

Methods

The dendroecological analysis and interpretation follows conventional procedures. Ring width measurement was made by using a LINTAB measuring device including the program TSAP (Rinn 1996). Synchronisation of the tree-ring curves was carried out with TSAP and COFECHA software (Holmes 1999). Mean Gleichläufigkeit (GLK) (Schweingruber 1983),

interseries correlation r_{xy} (Bahrenberg et al. 1992) and NET (Esper et al. 2001) were calculated to describe the internal site homogeneity. NET characterises the signal strength by calculating the coefficients of variation and Gegenläufigkeit. Due to the low number of sample depth before 1900, the time interval chosen for the comparison of the sites comprises the period between 1900 and 2003. Some cores which consist of less than 50 rings were eliminated from the dataset.

The raw series (in mm) were standardized by a 5-year moving average and ratios were calculated to investigate the interannual signal. Event and pointer years were analysed following the method outlined by Schweingruber et al. (1990). Comparisons to further analyses in Kyrgyzstan and Pakistan (Esper 2000) were made to find out teleconnections. The 25-year moving average was calculated to search for the common signal between the four sites on a decadal to multi-decadal scale.

Results and Interpretation

Age distribution:

Daschman represents the longest cores going back to AD 1746 (Fig. 2). The mean segment length is 166 years, with a variation between 25 to 258 years. In contrast Arpa, whose longest core goes back to AD 1769, is characterized by the lowest mean segment length of all sites which is only 86 years. Sary 1 can be described by going back to AD 1866 and a mean segment length of 92 years. Sary 2, which has the highest sample depth, goes back to 1850 and has a mean segment length of 107 years.

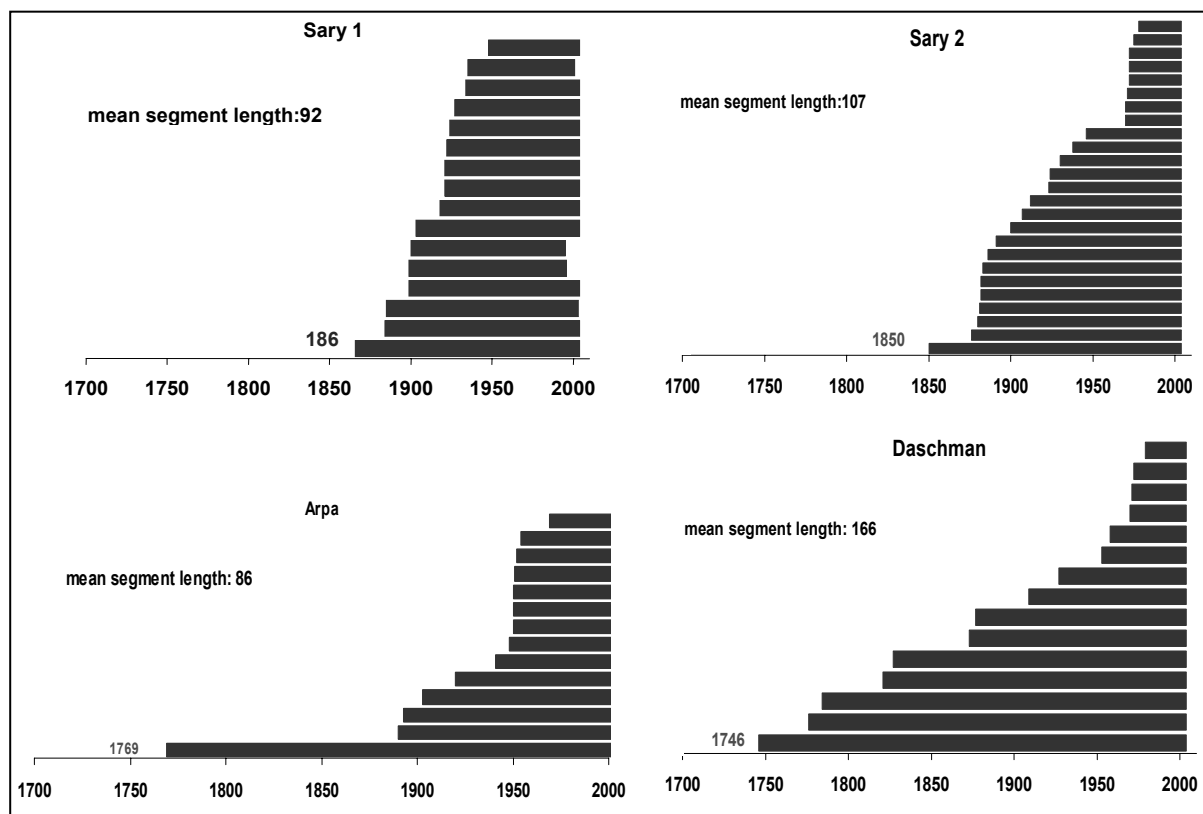


Figure 2: Age distribution and mean segment length of each site

Analysis of growth variability:

The internal site comparisons demonstrate a high level of similarity. The calculated statistical parameters are shown in Table 2. The mean GLK is very high and the significance in each site lies above the 95% level. Each NET value represents high signal strength, being below the defined threshold 0.8 (Esper et al. 2001).

Table 2: Statistical internal site comparison

Site	Mean GLK	Interseries correlation r_{xy}	NET
Daschman	80	0.50*	0.73
Arpa	77	0.41*	0.71
Sary 1	79	0.52*	0.70
Sary 2	80	0.45*	0.66

The mean tree-ring growth of Daschman, Sary1 and Sary2 is close to 1.5 mm/y. This value is very similar to European mean tree-ring growth which is described (defined) by 1.4 mm/y (Neuwirth 2005). In contrast to the other sites, Arpa has an exceptional high mean tree-ring growth of 2.4 mm/y. Thus, ring growth does not decrease with raising elevation. The ecological conditions in Arpa seem to be best for tree-ring growth in this region.

Comparing the different sites a site specific growth depression in Daschman for the period between 1917 and 1941 can be found. Ring growth of all individual series decreased during this strong depression (Fig. 3); the vertical ring growth dispersion is very low. The following increase of growth is not made by each series. To get detailed information about the interannual signal contained in the data, the 5-year moving average is calculated. Describing the ratios from the moving average, the dispersion of the values during the growth depression does not differ from the rest.

The years 1917/1918 can be defined as the beginning of the growth depression in Daschman. Regarding the increments of these years in all sites, they are characterised by small values and are therefore defined as pointer years. Other site overlapping negative pointer years are: 1912, 1931, 1932, 1947, 1965 and 1986. Positive pointer years are: 1972, 1995 and 2000. Comparison with further tree-ring analyses (*Juniperus spec.*) in Kyrgyzstan and Pakistan made by Esper (2000) confirm teleconnections. The years 1917 and 1965 in his data are defined as strong negative pointer years. Additionally, a one-year shift to our data exists in the years 1911, 1946 and 1948, which will be analysed in later investigations.

The 25-year moving average is calculated to find out the similarities in the decadal to multi-decadal scale. Apart from the influence of the growth depression on the moving average in Daschman, Arpa, which has no growth anomaly in the described time period, shows the same curve depression (Fig. 4).

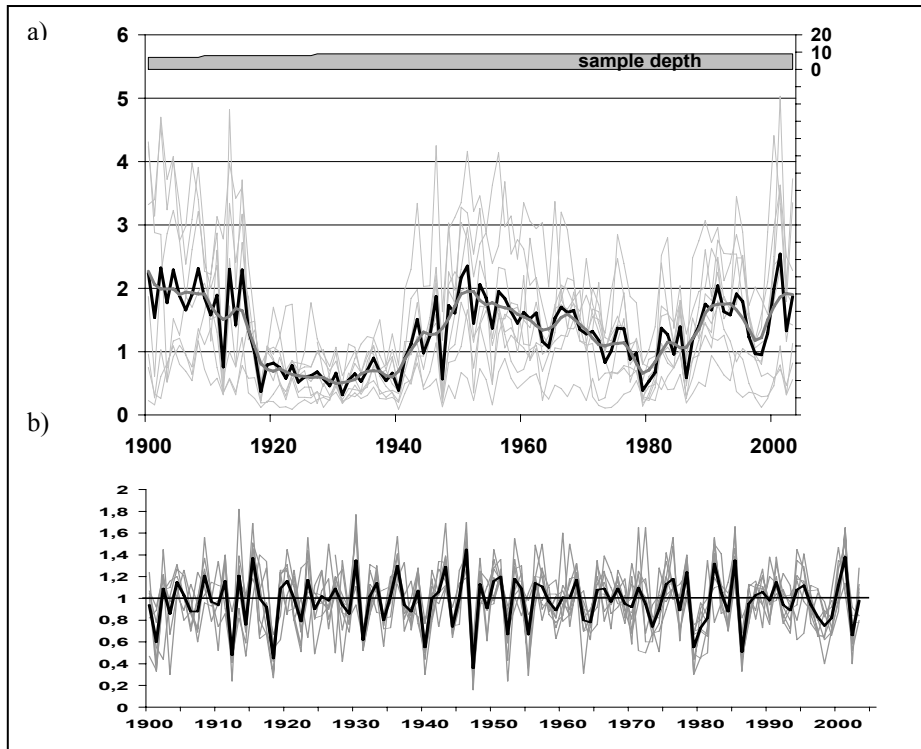


Figure 3: a) Daschman: grey: raw series, black: mean curve, dark grey: 5-year moving average; b) ratios from the 5-year moving average, grey: each series, black: mean curve

The whole curve progressions of Daschman and Arpa are very similar, but on a different level. Sary 1 and Sary 2 have similar curve progressions, too, whereas their behaviour in the time interval 1917-1941 differs from the other curves. All curves have an increase in the fifties ending up in peaks which vary in time. Since the end of the sixties, the curves rise temporally delayed.

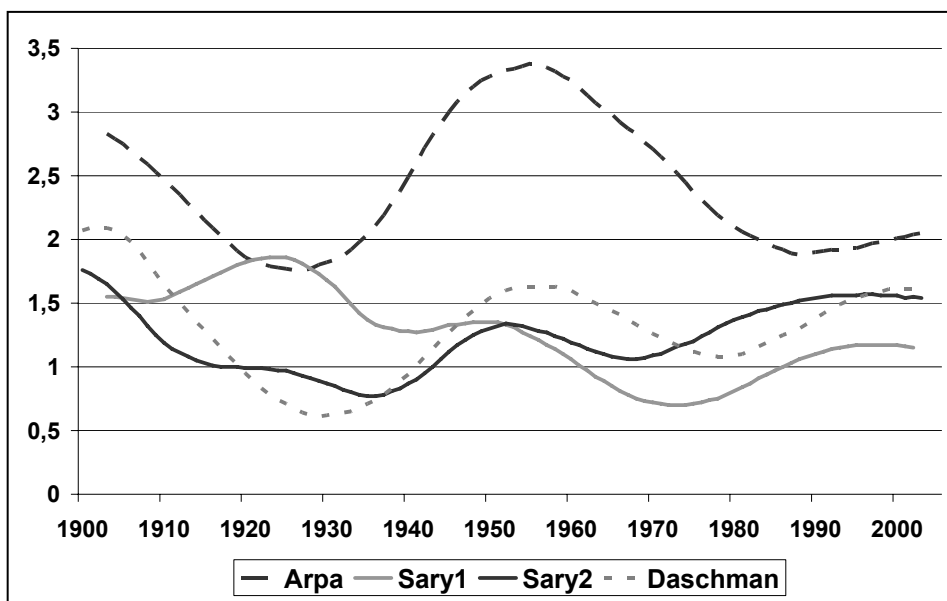


Figure 4: Calculated 25-year moving averages from the different sites

Conclusions and outlook

Our first results of dendroecological analyses in walnut forests in southern Kyrgyzstan confirm natural growth similarities between the different sites. Two groups of especially high similarities were found: Arpa – Daschman and Sary1 – Sary2. This grouping occurs due to the different levels of elevation. Arpa belongs to the lower forest step but due to its location in a v-valley, special climatological conditions are caused which are typical for the middle forest step. Hence, from a climatological point of view Arpa and Daschman belong to the middle forest step, whereas Sary1 and Sary2 belong to the lower forest step. The dividing line of elevation lies at the border of these elevation steps, which means at approximately 1400m a.s.l.. Therefore, we can interpret that elevation is more important for growth variabilities than exposition and inclination.

In later investigations, climate data will be used to estimate the influence of different climate forcings on tree-ring growth. These analyses will deliver further information for interpreting the growth depression in Daschman and the shift in time of the pointer years 1911/1912 and 1946/1947/1948. Additionally, tree-ring growth under anthropogenic influence will be investigated and compared with different natural growth behaviours in order to extract the ecological consequences of the increased utilisation pressure. These further analyses must be carried out under consideration of the above described different levels of elevation.

Acknowledgements

The whole dendroecological analysis is made within the research project “The Impact of the Transformation Process on Human-Environmental Interactions in Southern Kyrgyzstan”. This project is supported by the Volkswagen Foundation.

References

- Bahrenberg, G., Giese, E., Nipper, J. (1992): Statistische Methoden in der Geographie 1. Stuttgart.
- Esper J. (2000): Paläoklimatische Untersuchungen an Jahrringen im Karakorum und Tien Shan Gebirge (Zentralasien). *Bonner Geographische Abhandlungen* 103, p.137.
- Esper, J., Neuwirth, B., Treydte, K. (2001): A new parameter to evaluate temporal signal strength of tree-ring chronologies. *Dendrochronologia* 19 (1): 93-102.
- Gan, P.A. (1992): Orekhovo-plodovye lesa Yuga Kyrgyzstana. (Die Walnuß-Wildobst-Wälder des südlichen Kirgisistans). Teil I: Ilim, Bischkek.
- Gottschling, H., Amatov, J., Lazkov, G. (2005): Zur Ökologie und Flora der Walnuß-Wildobst-Wälder. *Archiv für Naturschutz und Landschaftsforschung* 44 (1): 85-130.
- Holmes, R.L. (1999): Users manual for program COFECHA. Laboratory of Tree-Ring Research, University of Arizona, USA.
- Kolov, O.V. (1997): Orekhovo-plodovye lesa Yuga Kyrgyzstana. (Die Walnuß-Wildobst-Wälder des südlichen Kirgisistans). Teil II: Bischkek.
- Neuwirth, B. (2005): Klima/Wachstums-Beziehungen zentraleuropäischer Bäume von 1901 bis 1971 - Eine dendroklimatologische Netzwerkanalyse. Dissertation, Geographisches Institut der Universität Bonn, p.151.

- Rinn, F. (1996): TSAP- Time Series Analysis and Presentation, Version 3 Reference Manual. Heidelberg
- Schweingruber, F.H., Eckstein, D., Serre-Bachet, F., Bräker, O.U. (1990): Identification, presentation and interpretation of event years and pointer years in dendrochronology. *Dendrochronologia* 8: 9-38.
- Schweingruber, F.H. (1983): Der Jahrring. Standort, Methodik, Zeit und Klima in der Dendrochronologie. Bern.

Impact of the drought in 2003 on intra- and inter-annual stem radial growth of beech and spruce along an altitudinal gradient in the Black Forest, Germany

H.P. Kahle

Institute for Forest Growth, University Freiburg, Tennenbacherstrasse 4, 79085 Freiburg, Germany

Email: Hans-Peter.Kahle@iww.uni-freiburg.de

Introduction

Measuring changes in stem dimension in high time-resolution is a suitable means to trace intra-annual diameter growth of trees as well as to monitor the hydrological status of tree stems. Tree growth rates vary considerably during a growing season and also from year to year (Mitscherlich *et al.* 1996, Abetz *et al.* 1993, Künstle 1995, Mäkinen *et al.* 2003). The term growth is defined as the increase in size by assimilation of material into the living organism (*c.f.*, Merriam-Webster 2005). Hence, changes in stem diameter due to growth are non-reversible, in contrast to the diurnal rhythm of contraction and expansion of tree stems which is due to shrinking and swelling processes associated with changes in trunk hydrology (Deslauriers *et al.* 2003, Zweifel *et al.* 2000). Continuous ongoing dendrometer measurements provide up-to-date insight into the current level of growth and the water status of tree stems. Recent studies focussing on the impact of the severe drought in the year 2003 on tree growth have shown the significant value growth monitoring based on dendrometer measurements can provide to the timely assessment of forest condition (Anders *et al.* 2004, Dietrich *et al.* 2004).

Drought resistance and resilience of European beech (*Fagus sylvatica* L.) in view of the anticipated climatic changes has recently been discussed controversially (e.g., Rennenberg *et al.* 2004, Kölling *et al.* 2005). With the comparison of intra- and inter-annual growth responses of beech and Norway spruce (*Picea abies* (L.) Karst.) during and after the severe drought conditions of summer 2003 this study aims at providing further empirical evidence to substantiate this discussion.

Material and methods

Dendrometer data

Beech and spruce sample trees have been continuously monitored over a several years period by means of point dendrometers (Fig. 1). Measurement data of sample trees on three sites along an altitudinal gradient at the western slope of the Black Forest are analysed (450 m, 750 m, and 1.250 m above sea level (asl), see figure 2).

Point Dendrometer (mounted on a beech stem)

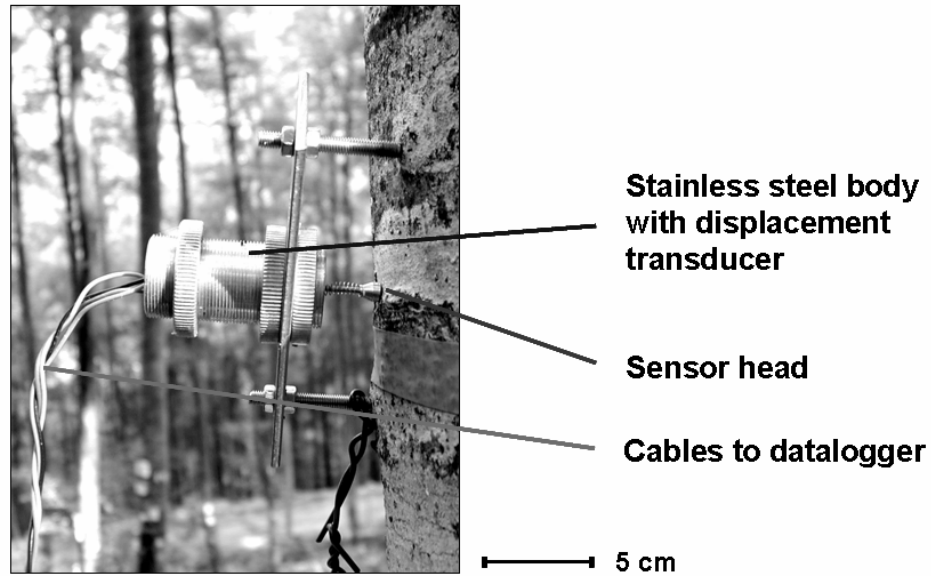


Figure 1: Point dendrometer, Model IWW. Sensor: linear displacement transducer. Height of measurement: 1.3 m (breast height).

Dendrometer Measurements - Field Sites

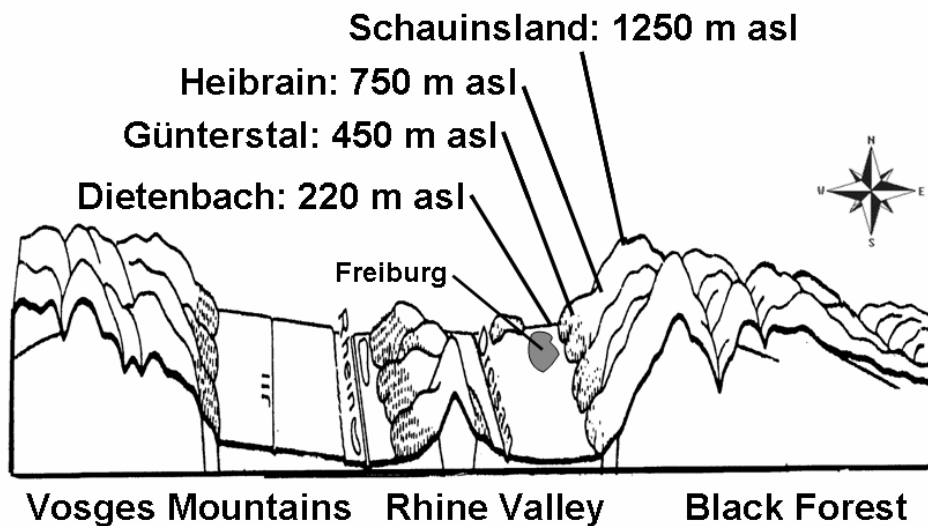


Figure 2: Sketch of the research area with locations of the four field sites in the Rhine Valley and at the western slope of the Black Forest running from 220 m to 1.250 m asl.

Data from an additional nearby site in the Rhine valley, Dietenbach (220 m asl) where beech and oak (*Quercus robur*) sample trees are monitored is as well included in the analyses.

The sites of the Black Forest altitudinal gradient are similar with respect to site type and aspect (northeast). All forest stands under study are mature, mixed-species stands. At each field plot several sample trees belonging to different crown classes are equipped with dendrometers. For the purpose of this study only sample trees that belong to the crown class pre-dominant and dominant are considered. The age of the sample trees is approximately 60-70 years at sites DIE, GUE, and SCH, and approximately 80 years at site HEI. For each site and species the number of sample trees included in the analyses is $n = 2$ trees. The dendrometer data time series span from 1999-2004 (Günterstal GUE, Heibrain HEI), 2000-2004 (Schauinsland SCH), and 2002-2004 respectively (Dietenbach DIE). The dendrometer measurement time interval ranges from 15 min (DIE) to 30 min. For the analyses the time series data have been aggregated to daily means. The presented mean time series are in each case based on a constant set of trees.

Climate data

Time series of measured daily average air temperature and daily precipitation sum of two measurement stations have been used for the analyses:

- Karlsruhe: Rhine Valley, 115 m asl, observation period: Jan 1895 - Sep 2004 (Deutscher Wetterdienst DWD)
- Schauinsland: Black Forest, 1205 m asl, observation period: Jan 1994 – Sep 2004 (Umweltbundesamt UBA).

Methods of data analysis

Besides radial/diameter growth dendrometer data reflect reversible changes due to stem hydrological changes. For this reason the data measured with point dendrometers are termed “radial displacement” (RadDisp), rather than “radial growth”. In order to suppress high frequency variation and to amplify medium- and long-term oscillations the individual tree time series of radial displacement were smoothed using a symmetric 11-day running average. For the analysis of the daily rate of change of radial displacement (Rate of RadDisp or RRD) the data on daily differences once more was smoothed using a cubic smoothing spline with a 50% frequency cut-off of 30 days.

Three cardinal points of the RRD time series are analysed and discussed:

- the beginning of radial growth is the date at which the RRD-curve crosses the zero line (from negative to positive) during the early growing season,
- the date of RRD culmination max is the date at which the maximum RRD occurs,
- the end of radial growth is the date at which the RRD-curve crosses the zero line (from positive to negative values) during the late growing season.

To investigate the radial growth response to the drought in the year 2003 the RadDisp data of the years 2003 and 2004 are related to the average course of RadDisp in a several year

lasting reference period comprising the data of all other available years in the specific data set.

Results

Baseline climatic conditions and anomalies of air temperature and precipitation in 2003

Data on mean air temperature and precipitation sum at the climate measurement stations Karlsruhe and Schauinsland for the common overlap period 1992-2002 are given in Table 1. Mean air temperature at the low elevation station Karlsruhe is 5.4 K and 6.4 K higher than at the high elevation site over the whole year and for the months May-September respectively. Precipitation sum at the high elevation site Schauinsland is 2.6 and 2.5 times larger over the whole year (Dec-Jan) and for the growing season (May-Sep) respectively.

Table 1: Climate data for the period 1994 to 2002 and for the year 2003 at climate stations Karlsruhe (data source: Deutscher Wetterdienst DWD) and Schauinsland (data source: Umweltbundesamt UBA) (top: mean air temperature (Tp), bottom: precipitation sum (Pr)).

Station	Season	Period/Year	Mean temperature		Tp-Anomaly	
			°C		K	
Karlsruhe (Rhine Valley, 115 m asl)	Jan-Dec	1994 - 2002	11.4			
		2003	11.9		0.5	
	May-Sep	1994 - 2002	18.1			
		2003	20.3		2.2	
Schauinsland (Black Forest, 1.205 m asl)	Jan-Dec	1994 - 2002	6.0			
		2003	7.2		1.2	
	May-Sep	1994 - 2002	11.7			
		2003	14.8		3.1	
			Precipitation sum		Pr-Anomaly	
			Mm		Mm	%
Karlsruhe (Rhine Valley, 115 m asl)	Jan-Dec	1994 - 2002	813			
		2003	561		252	31
	May-Sep	1994 - 2002	352			
		2003	245		107	31
Schauinsland (Black Forest, 1.205 m asl)	Jan-Dec	1994 - 2002	2142			
		2003	1488		654	31
	May-Sep	1994 - 2002	894			
		2003	532		362	40

The year 2003 was extraordinarily warm and precipitation records were far below average at both stations. At the Schauinsland site the increase in mean seasonal (May-Sep) air temperature reached a maximum with +3.1 K. At the same time precipitation was reduced to 30-40 % of normal.

A comparison of the weather conditions in the year 2003 with those of other years characterized by above average air temperatures and below average precipitation sums during the period 1895 to 2002 was possible for the Karlsruhe station (Fig. 3).

Weather in selected warm and dry years in 1895-2004

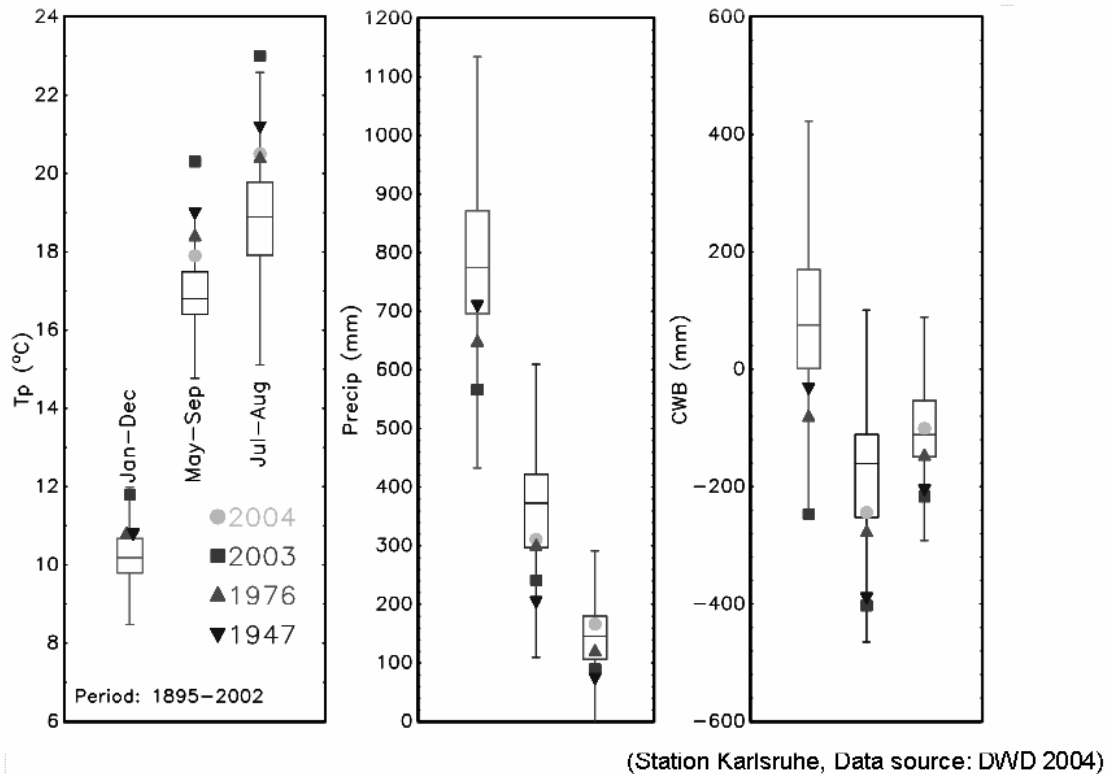


Figure 3: Box plots of weather conditions in selected warm and dry years at climate station Karlsruhe. Left figure: mean air temperature (T_p), centre figure: precipitation sum ($Precip$), right figure: climatic water balance (acc. to Thornthwaite and Mather 1955, 1957). The three boxes in each figure represent: left: Jan-Dec, centre: May-Sep, right: Jul-Aug. The boxes indicate the range of 50 % of the observations during the reference period 1895-2002 (horizontal line: median). The whiskers represent the empirical 95-percentil.

According to mean air temperature the year 2003 was unparalleled by the other warm years 1976 and 1947 for all three periods (Jan-Dec, May-Sep, Jul-Aug). Precipitation in the year 2003 was lower than in the other two years, however growing season and late summer precipitation in 1947 was slightly lower than in 2003. Due to the high air temperature anomalies and large precipitation deficits the climatic water balance (acc. to Thornthwaite, Mather 1955, 1957) was lower in 2003 than in the other two years, and reached a minimum with less than -400 mm when referred to the growing season.

Level of radial growth

Figures 4-6 show the time series of RadDisp (top) and of the rate of change of RadDisp (bottom) for spruce and beech at the three Black Forest sites.

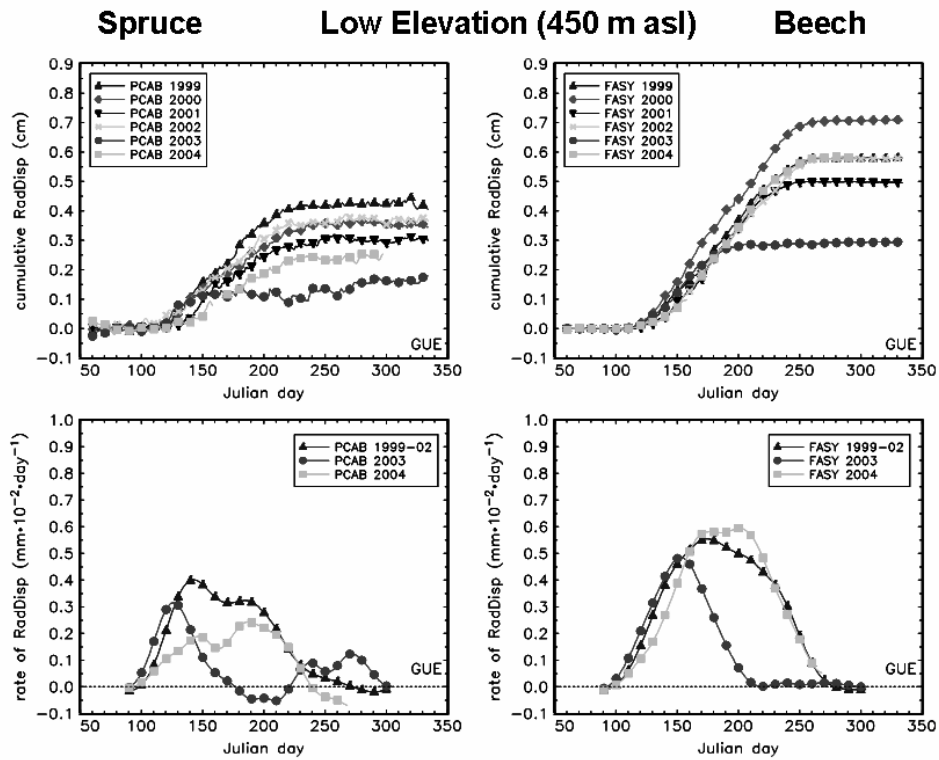


Figure 4: Smoothed (11-day running average) daily dendrometer data versus day of the year for the low elevation site Günterstal (GUE). Top: cumulative radial displacement (RadDisp), bottom: rate of change of radial displacement (smoothed with spline). Left: Norway spruce (PCAB), right: European beech (FASY).

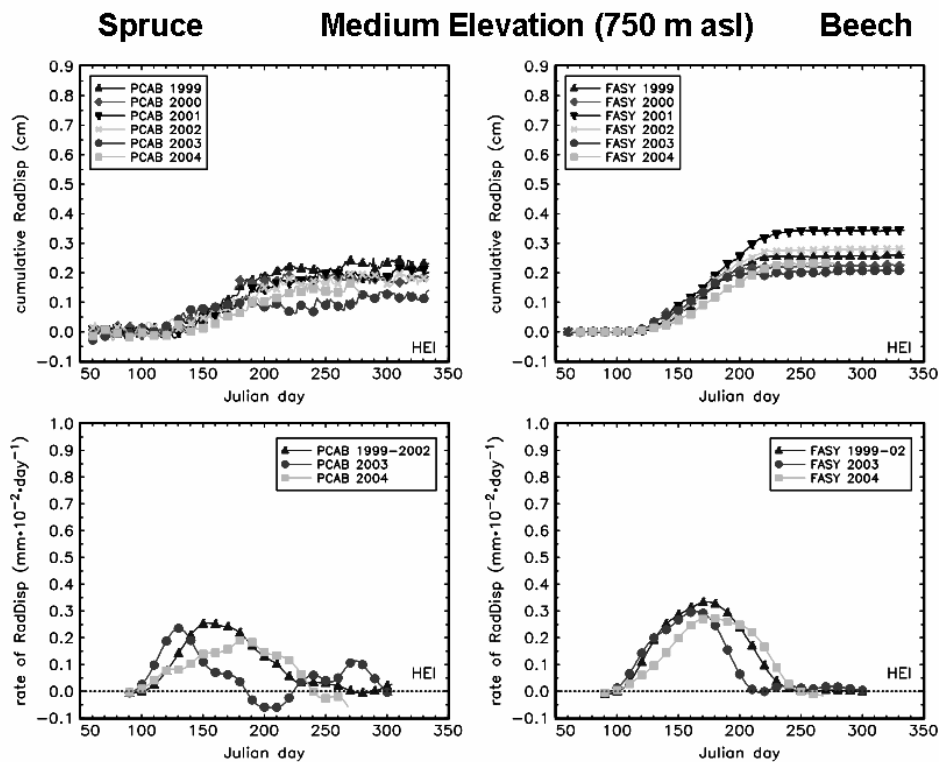


Figure 5: Dendrometer data, medium elevation site Heibrain (HEI). See explanation figure 4.

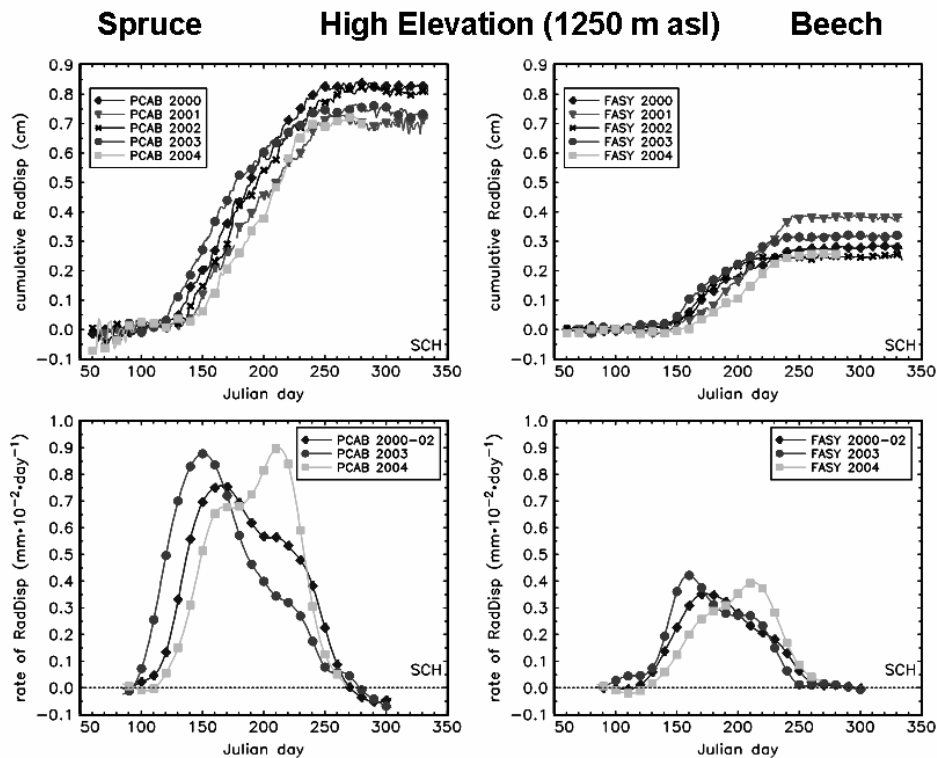


Figure 6: Dendrometer data, high elevation site Schauinsland (SCH). See explanation figure 4.

As can be seen in the upper plots of figures 4 to 6 there is considerable variation in the mean level or RadDisp between the sites and between the two species. Whereas at the low elevation site (GUE) the beech sample trees grew faster than the spruce sample trees (Fig. 4) the mean level of growth of the sample trees of both species was roughly equal at site HEI (Fig. 5). At the high elevation site (SCH, Fig. 6) the mean level of growth of the spruce sample trees was superior to that of beech.

Beginning, end and length of growing season

During the period 1999-2002 beginning of radial growth occurred in the spruce and beech sample trees simultaneously at day 98 at site GUE and at day 101 at site HEI respectively (Tab. 2). At the high elevation site (SCH) growth of the spruce sample trees was advanced compared to beech: growth started in the mean at day 98 and at day 103 respectively. End of radial growth of the beech sample trees at the medium and high elevation sites (HEI and SCH) occurred in the mean 20 days, and 4 days respectively earlier than that of the spruce sample trees. The growing season of the beech sample trees was at the low elevation site (GUE) 7 days longer, and at the sites HEI and SCH 20 days, and 9 days respectively, shorter than for the spruce sample trees (Tab. 3).

Date of maximum rate of radial displacement

In the mean over the period 1999-2002 the date of maximum rate of radial displacement for the spruce sample trees from the low to the high elevation site was day 142, 154 and 166

respectively. Nearly independent of elevation the beech sample trees reached their maxima around day 173/174 (Tab. 2).

Table 2: Date of begin and end of radial growth and of maximum rate of radial displacement.

Species	Site	Begin		Maximum rate		End	
		1999-2002	2003	1999-2002	2003	1999-2002	2003
day of year							
PCAB	GUE	98	91	142	126	272	177
	HEI	101	93	154	130	270	186
	SCH	98	93	166	151	269	278
FASY	GUE	98	93	174	153	279	214
	HEI	101	96	174	164	250	211
	SCH	103	92	173	159	265	252

Table 3: Number of growing days derived from dendrometer data.

Species	Site	Days		2003 rel. to 1999-2002 %
		1999-2002	2003	
PCAB	GUE	174	86	49
	HEI	169	93	55
	SCH	171	185	108
FASY	GUE	181	121	67
	HEI	149	115	77
	SCH	162	160	99

Level of radial growth in 2003

The increased temperatures accompanied by deficits in precipitation in 2003 severely affected radial growth of both species at the low and medium elevation sites: radial growth of the spruce sample trees was reduced by 57 % (GUE) and by 40 % (HEI) as compared to the mean level during the period 2000-2002, for the beech sample trees it was 51 % and 28 % respectively. At the high elevation site (SCH) radial growth of the spruce sample trees was only slightly reduced by 4 %, and for beech it was slightly increased by 5 % (Fig. 6). Reduction in radial growth is paralleled by a shortening of the growing season which was reduced to 49-55 % for the spruce and 67-77 % for the beech sample trees at sites GUE and HEI respectively (compared to the period 1999-2002) (Tab. 2). The level of radial growth in 2003 in relation to the one in 2002 is plotted versus altitude of the site in the upper half of figure 7.

Intra-annual course of growth in 2003

Radial growth of the Norway spruce and beech sample trees in 2003 started earlier at all research sites compared to the reference period. After initiation radial growth in 2003 is ac-

celerated especially in Norway spruce (Fig. 4 to 6). The date at which the maximum rate of RadDisp occurred is advanced in 2003 as compared to the reference period: in spruce by 15 to 24 days and in beech by 10 to 21 days (Tab. 1). The end of radial growth was in 2003 even more advanced: for the spruce sample trees at the medium and low elevation sites by 84-95 days, and for beech by 39-65 days respectively. However, the increase in the rate of RadDisp after day 220 at the medium and low elevations sites might indicate, that spruce has reactivated growth at the late growing season before growth finally ended. At the high elevation site cessation of radial growth of the spruce sample trees was delayed by 9 days.

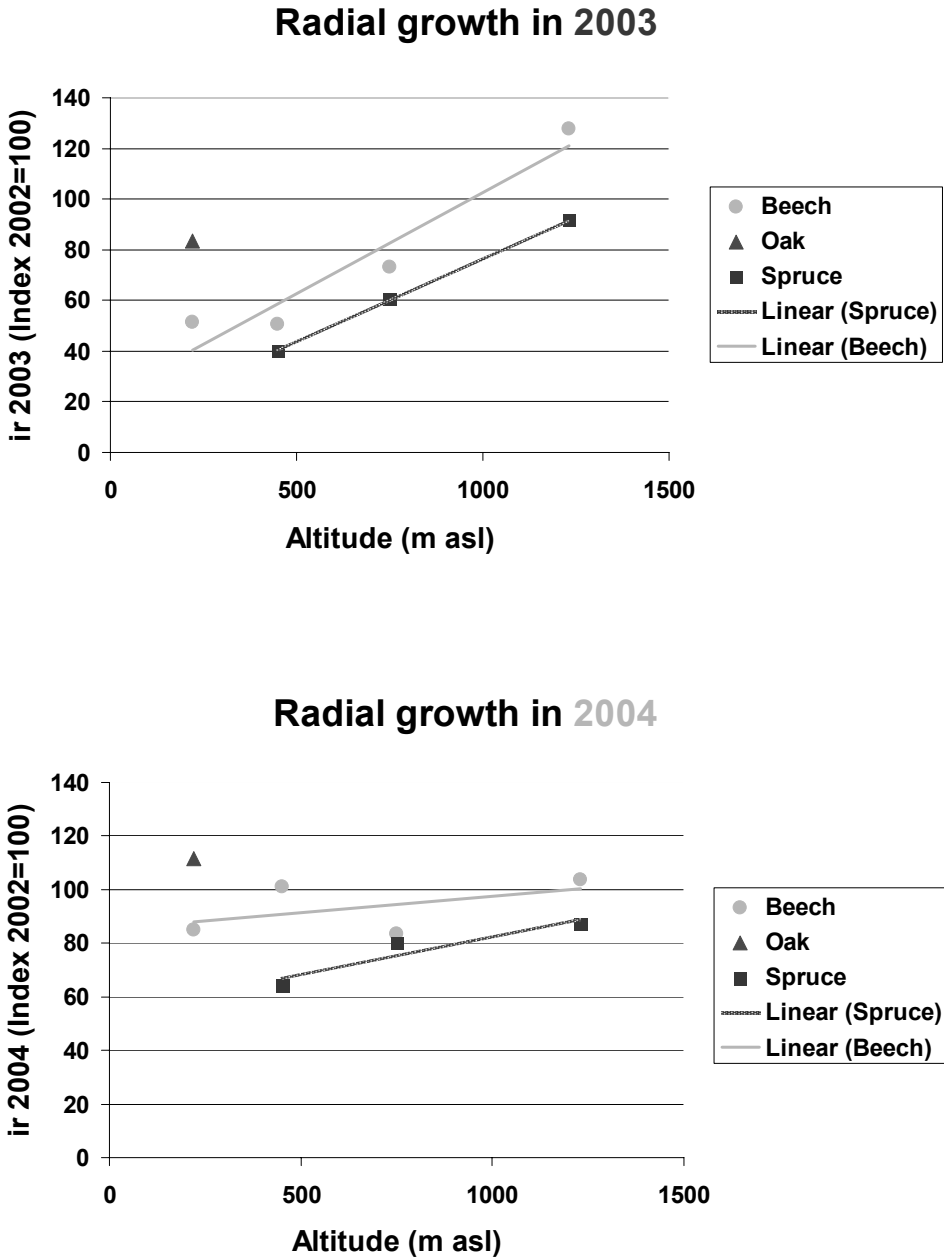


Figure 7: Indexed radial growth in 2003 (top) and 2004 (bottom) versus elevation of the site.

The rates of RadDisp expressed as percentage of the maximum rate during the reference period are displayed in figure 8. The reduction in mean level of growth in 2003 is mainly caused by the shortening of the growing season than by a reduction in the maximum rate of radial displacement.

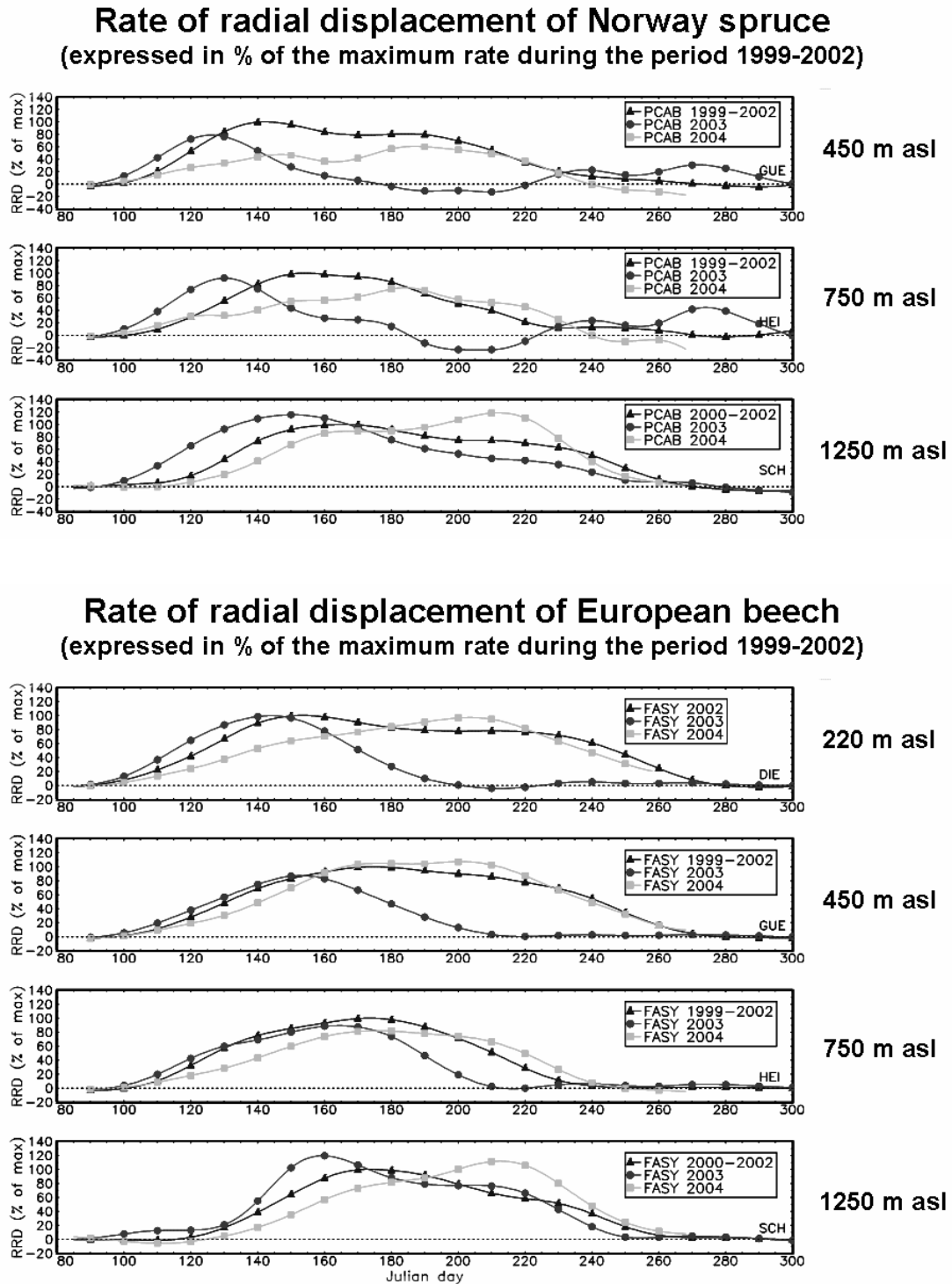


Figure 8: Rate of radial displacement (RRD) versus day of the year of Norway spruce (PCAB, top) and European beech (FASY, bottom) at the research sites.

Level of growth in 2004

Whereas beech radial growth recovered in the year following the severe drought at the low and medium elevation sites to 83-98 % of the reference level (mean of 2000-2002), spruce growth in 2004 was still reduced to a level of 70-79 %. The level of radial growth in 2004 in relation to the one in 2002 is plotted versus altitude of the site in the bottom half of figure 7.

Discussion

Critical evaluation of the data

The number of sample trees used in the analyses is quite low. Each presented curve is at least based on two sample trees. However, the weakness of lacking more replications in sample trees is attenuated by the high precision of the dendrometer data. Highly significant inter-series correlations among the individual tree dendrometer measurement time series indicate high precision of the assessed temporal signals.

Critical evaluation of the methods

The measurement data were pre-processed before the analyses by a one- respectively two-step smoothing procedure as described in the methods section. Whereas the symmetric running average filter applied in the first step only affects the signal amplitudes, the applied smoothing spline function could also produce unwanted phase-shifts. The flexibility of the spline function has been optimized so that most of the medium-term ($5 \text{ days} < x < 30 \text{ days}$) variations are preserved whereas high- as well as low-frequency variations are largely attenuated. The degree of phase-shift was visually checked so that it should not severely affect the results. Another aspect of the data pre-processing is related to end-fit problems of the applied smoothing filters. These could lead to distorted fluctuations at the beginning and end of the curves. The somewhat strange course of the RRD curves for spruce of the sites GUE and HEI in the year 2003 after day 260 (Fig. 8) could partially be due to this effect.

Critical evaluation of the results

The results concerning the dates of beginning and end of radial growth have been achieved by applying the respective definitions given in the methods sections. It is well known from literature that the cambial activity can hardly be tracked by dendrometer measurements (Mäkinen *et al.* 2003, Zweifel *et al.* 2000). A comparison of the results of this study with phenological data on the occurrence of May shoot of Norway spruce at site Schauinsland (Henhappi 2004, unpublished data) revealed a substantially earlier onset of radial growth according to the definition applied here than expected from the phenological data. However, by applying a different definition of beginning of radial growth Abetz *et al.* (1993) found at the same site (SCH) a close relation between the occurrence of May shoot and the beginning of radial growth derived from dendrometer data.

Since the precision of the temporal signal of the dendrometer data is high, the variation in level of growth between the different years of the observation period should be reliably represented. This also holds for the comparison of the performance in radial growth between the two investigated tree species, since these comparisons are based on the time series data.

Due to limitations in the data structure it was in this study not possible to evaluate the effects of and possible interactions between the factors tree age, growth level, and elevation of the site on inter- and intraannual radial growth, since these factors are confounded in the data base.

Summary

The main results of this study can be summarized as follows:

- The record year 2003 was extraordinarily warm over the whole year and especially during the growing season: air temperature anomalies (May-Sep) were as large as +2.2 K at the low elevation site and +3.1 K at the high elevation site. The warm weather in 2003 was accompanied by exceptionally large precipitation deficits: -69 % at the low elevation site and -60 % at the high elevation site (May-Sep). Water availability in the year 2003 as indicated by the climatic water balance was at the low elevation site distinctly lower than in the years 1947 and 1976.
- For the beech sample trees the period during which radial growth occurs is longer at the low elevation site than at the high elevation site, which is mainly due to delayed growth cessation in fall.
- Radial growth of the spruce sample trees at the low elevation site was more severely affected by the drought in the year 2003 than that of the beech sample trees (-60 % and -50 % respectively; reference: mean of 2000-2002). Reduction of radial growth in the year 2003 is paralleled by a shortening of the season of radial growth which was at the low and medium elevation sites reduced by ~50 % for the spruce and by ~30 % for the beech sample trees.
- At the high elevation site radial growth was only slightly affected by the exceptional weather conditions in the year 2003: -5 % for the spruce and +5 % for the beech sample trees (reference: mean of 2000-2002).
- Whereas beech radial growth recovered in the year following the severe drought at the low and medium elevation sites to 80-100 % of the reference level (mean of 2000-2002), spruce growth in 2004 was still reduced to a level of 70-80 %.

Acknowledgements

I am grateful to Ms Eberling and Mr Meinhard, both Umweltbundesamt Messstelle Schauinsland, for providing the climate data of the measurement station Schauinsland and to Felix Baab and Albert Fehrenbach, both Institute for Forest Growth University Freiburg, for the continuous maintenance of the field measurements.

References

- Abetz, P., Künstle, E., Wolfart, A. (1993): Jahrgang des CO₂-Gaswechsels und der Transpiration von solitären Fichten in den Hochlagen des Südschwarzwaldes in kontrollierter Standortluft mit und ohne Ozonbelastung. *KfK-PEF* 101: 155 p.
- Anders, S., Beck, W., Lux, W., Müller, J., Fischer, R., König, A., Küppers, J. G., Thoroe, C., Kätzel, R., Löffler, S., Heydeck, P., Möller, K. (2004): Auswirkung der Trockenheit 2003

- auf Waldzustand und Waldbau. Eberswalde, *Zwischenbericht, BMVEL 533-7120/1*, BFH Hamburg: 109.
- Deslauriers, A., Morin, H., Urbinati, C., Carrer, M. (2003). Daily weather response of balsam fir (*Abies balsamea* (L.) Mill.) stem radius increment from dendrometer analysis in the boreal forests of Québec (Canada). *Trees - Structure and Function* 17: 477-484.
- Dietrich, H.P., Raspe, S., Schubert, A. (2004): Trockenheit 2003 war nicht die einzige Ursache für starke Zuwachsverluste. Beobachtungen zur Reaktion von Baumkronen, Belaubung und Durchmesserzuwachs der Waldbäume im Jahr 2003. *LWF-Aktuell* 43: 14-16.
- Kölling, C., Walentowski, H., Borchert, H. (2005). Die Buche in Mitteleuropa: Eine Waldbaumart mit grandioser Vergangenheit und sicherer Zukunft. *AFZ/Der Wald* 60: 696-701.
- Künstle, E. (1995): Beginn, Verlauf und Ende des Dickenwachstums von Solitär-Fichten auf dem Schauinsland bei Freiburg in den Jahren 1989 bis 1993. *Forstliche Forschungsberichte München* 153: 24-39.
- Mäkinen, H., Nöjd, P., Saranpää, P. (2003): Seasonal changes in stem radius and production of new tracheids in Norway spruce. *Tree Physiology* 23: 959-968.
- Merriam-Webster Online (2005): <http://www.m-w.com/> (information retrieved July 10 2005).
- Mitscherlich, G., Moll, W., Künstle, E., Maurer, P. (1966): Ertragskundlich-ökologische Untersuchungen im Rein- und Mischbestand: VI. Zuwachsbeginn und -ende, Stärkeänderung und jährlicher Durchmesserzuwachs. *Allgemeine Forst- und Jagdzeitung* 137: 72-91.
- Rennenberg, H., Seiler, W., Matyssek, R., Geßler, A., Kreuzwieser, J. (2004): Die Buche (*Fagus sylvatica*) - ein Waldbaum ohne Zukunft im südlichen Mitteleuropa? *Allgemeine Forst- und Jagdzeitung* 175: 210-224.
- Thornthwaite, C.W., Mather, J.R. (1955): The water balance. *Publ. in Climatology - Drexel Inst. of Tech., Lab. of Climatology*, Vol. 8, No. 1: 104 p.
- Thornthwaite, C.W., Mather, J.R. (1957): Instructions and tables for computing potential evapotranspiration and the water balance. *Publ. in Climatology - Drexel Inst. of Tech., Lab. of Climatology*, Vol. 10, No. 3: 308 p.
- Zweifel, R., Item, H., Häsler, R. (2000): Stem radius changes and their relation to stored water in stems of young Norway spruce trees. *Trees - Structure and Function* 15: 50-57.

Dendroecological analysis of the influence of strong winds and snow accumulation on the growth of trees at the treeline in Vitosha Mountain, Bulgaria

M. Panayotov & S. Yurukov

University of Forestry, Dendrology Department, Kl.Ohridski 10 Blvd., Sofia, Bulgaria

Email: mp2@abv.bg

Introduction

As in other parts of Europe, the treeline position in the Bulgarian mountains has been affected by human action in the past. In certain regions such as the highest parts of Vitosha Mountain overexploitation and fires have destroyed a large part of the coniferous forests. In the 1940s their restoration has been started by afforestation. The forest authorities have taken the decision to use tree species that were found elsewhere in the Bulgarian subalpine forests. The most commonly used species were Macedonian pine (*Pinus peuce* Griseb.), Bosnian pine (*Pinus heldreichii* Christ), Scots pine (*Pinus sylvestris* L.), Norway spruce (*Picea abies* (L.) Karst.) and to a limited extent the dwarf form of Mountain pine (*Pinus mugo* Turra ssp. *mugo*).

Currently the condition of these species enables a study of the differences in their resistance to the limiting factors at the treeline.

The natural treeline of Vitosha Mountain is situated below the potential thermal treeline, which is marked by the position of the 10°C July isotherm (Dakov et al. 1980). For Vitosha Mountain this isotherm lies at approximately 2000m a.s.l. whereas the treeline is at 1850m a.s.l. This is a clear sign that there are other limiting factors besides temperature. Vitosha Mountain is the second windiest mountain in Bulgaria and is characterized by large snow accumulations as a result of wind transport activity (Vekilska 1966). Stem deformations observed in afforestations suggest that these two factors (i.e. wind and snow accumulation) may be of primary importance.

An obstacle to the research on the relative importance of limiting factors in the region is that forest managers do not have accurate data from observations in these forests. This necessitates the use of methods which allow restoration of past events and collection of information about their influence. Dendroecological methods are particularly useful because they provide the possibility to analyze the effect of natural conditions on tree growth and, specifically, on the structure of tree rings (Fritts 1976, Schweingruber 1996)

Study Area

The chosen study site is the treeline that borders with a wide treeless plateau near Aleko hut at an altitude of 1850 m a.s.l. Three plots with area of 2000 m² have been set in *Pinus peuce* forests (Fig.1) The first plot (plot N1) was set in an afforestation that is isolated in front of the treeline forests and thus is exposed to the action of winds from all directions. The second one is at the treeline (plot N2) and the third one is in the forest stand behind the treeline (plot

N3). The trees in all of the plantations are at about the same age (approximately 60 years). Because of their proximity, plots are exposed to similar general climate conditions. Therefore, this design allows the responses to other limiting factors that act locally to be distinguished. The region is generally flat and exposed to strong winds. The mean annual temperature is 2.58°C. It ranges from a mean monthly temperature of -6.04°C in January to +11.54°C in August. Prevailing strong winds are Northwestern, Western and Southwestern.



Figure 1: Study area and position of the study plots

Methods

In order to obtain more information about the influence of strong winds and snow accumulations on the growth of trees at the Vitosha Mountain treeline, and test whether these could be the most important limiting factors, we have chosen to use dendroecological analysis.

In the study plots, H, Dbh and crown dimensions of the trees have been measured. In the treeline sites, trees have been separated in the following groups according to their stem and crown state:

1. trees with normal stems and crowns;
2. trees with normal stems and crowns, but with broken tops;
3. trees with broken stems (Figure 2a);
4. trees with strongly bent stems (Figure 2c);
5. trees that were bent near the base of the stem and have horizontal growth (Figure 2b) and
6. trees with inclined stems;

In the treeline sites (plots N1 and N2) coordinates of the trees were recorded and digital maps were built with the use of ArcGIS 8.3 software package.

Cores for dendroecological analysis were taken from trees of the different groups. The directions of the extraction of the cores were from (a) the side of bending and from (b) the opposite side. A total of 90 trees were sampled, 58 of which had stem deformations.

Ring widths were measured in the Dendrochronology laboratory at the University of Forestry in Sofia. Special attention was paid to rings with a structure that differed from the normal one.

This was done because such rings might be very helpful in crossdating procedures and could carry valuable information about the growth of the tree (Fritts 1976, Schweingruber 1996)



Figure 2a



Figure 2b

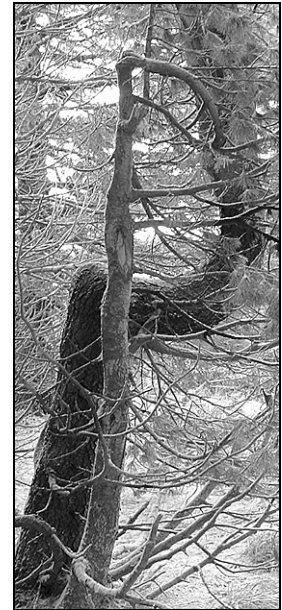


Figure 2c

Figure 2: Tree with a stem that was broken twice (2a); tree with a stem that was bent near the base and had consequent horizontal growth (2b) and tree with a strongly bent stem (2c)

The tree ring series were crossdated using the COFECHA software and visual clues in the ring structure (e.g. dated frost and light rings).

Cores that showed strong correlation were used for the composition of chronologies after a standardization procedure. For this process we used a modified exponential curve from the type $y = a \exp(-bx) + c$ (Cook et al. 1990). After the composition of the chronologies that carry the common signal of the climate influence, these chronologies were compared to the growth curves of trees with broken tops or stem damage. Thus we determined periods of stress, serious stem deformations, and the influence of top breakage on tree growth. Special attention was paid to the initiation of periods with formation of reaction wood for more than one year, which is considered an attempt by the tree to regain its vertical growth orientation after bending (Kwon et al. 2001). Data from plots with a significant number of trees with such response in a certain year were compared with climate data for winter precipitation to test for a possible relationship.

In 2003 and 2004, after storms, regular observations were carried in the plots in order to obtain more precise information for the influence of strong winds and snow accumulations. To obtain information for the snow accumulation and distribution in the winter of 2004 we carried out regular measurements of snow depths in plot N1 with the use of avalanche probe.

Results and discussion

Results from measurements of snow depths

The results from the measurements of snow depths in plot N1 in the winter of 2004 are shown on figure 3.

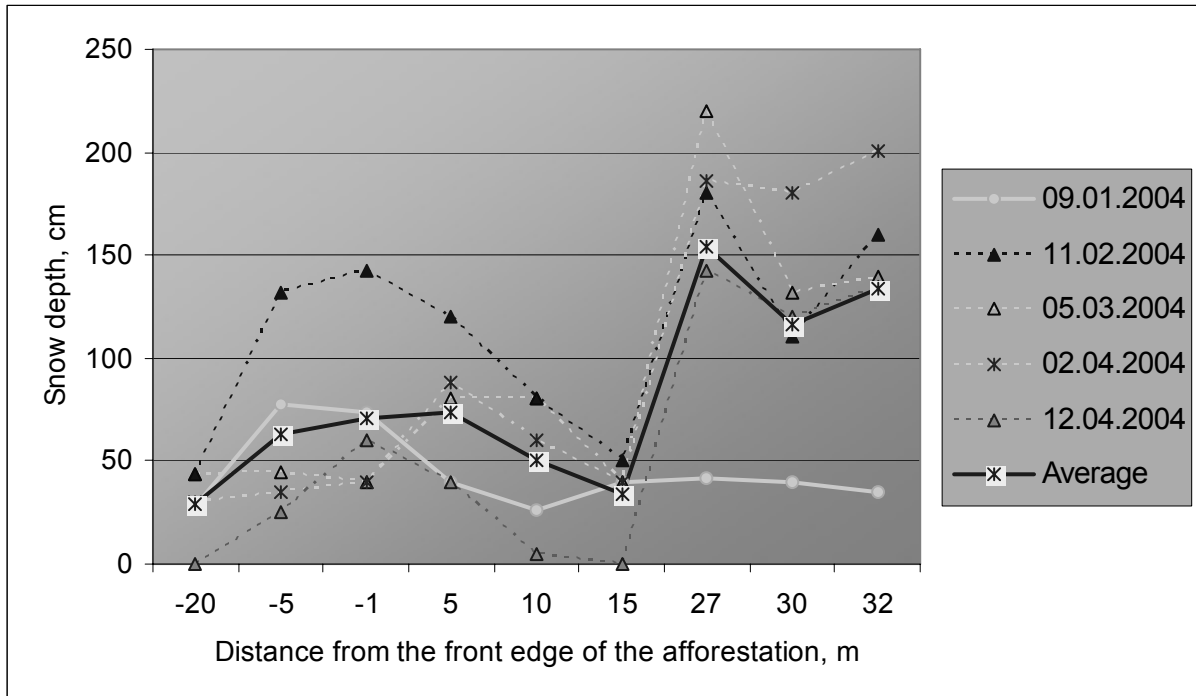


Figure 3: Snow depths in plot N1 in the winter of 2004.

As it can be seen from the figure above, at the beginning of the period of snow accumulation (09.01.2004), the snow cover is almost evenly distributed within the plot and in front of it. The next measurements show that there is a tendency of increase of the snow depth in proximity to the front edge of the plot and a slight decrease in the first 10m in the forest. Then at about 15m behind the front edge snow depths increase sharply to reach a maximum depth at a distance of about 25m behind the forest edge. The maximum snow depth, which was measured at the beginning of March, was 220cm. At the same time the snow depth on the flat plateau, 20m in front of the forest edge, was 50cm. This shows that snow transportation by wind plays a major role in distributing snow accumulation on Vitosha Mountain. Our results also show that snow accumulation is strongly influenced by the existing forest stands or groups.

Distribution of the trees in the plots according to their stem and crown form

As it has been shown on Figure 4 there is a zone with increased concentration of trees with broken, bent or horizontal stems and of dead trees in the middle of plot N1. Therefore we called that part of the plot "Mortality and disturbance zone". There is a relationship between the position of this zone and the distribution of snow accumulation. As discussed above, the snow depths start increasing sharply 15 m behind the front edge of the afforestation, which coincides with the border of the "Mortality and disturbance zone".

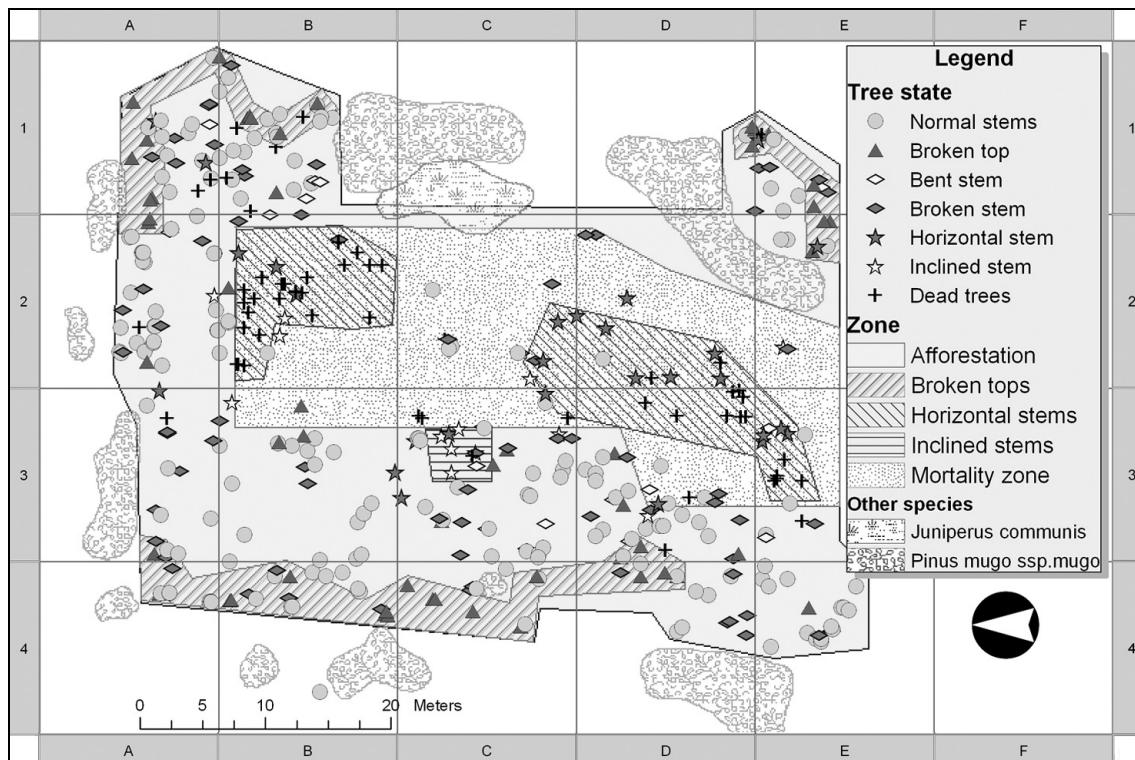


Figure 4: Map of the trees, stem, and crown deformation zones in plot N1

Almost the same distribution is observed in the other treeline plot – plot N2. Here, there is also a zone with increased concentration of trees with damaged stems and crowns, which starts at approximately 15m behind the forest edge.

It is known that dense forest borders decrease the speed of wind (Somerville 1980). Most probably, this causes increased snow deposition at a certain distance behind the edge. Snow loaded trees are more subject to stem damage during events of strong winds (Petty and Worrell 1981, Peltola et al. 1999). This, together with the large snow accumulations, explains the existence of the “Mortality and disturbance zones” in the plots.

Trees with broken tops are more frequently found at the forest edges (Figure 4). During field inspections, it was observed that very strong winds sometimes cause the breakage of the last 3 or 4 years of vertical increment. Thus, it is not surprising that there is an increased frequency of trees with broken tops in parts of afforestation characterized by highest wind speeds. Strong winds, or the combination of strong winds and snow or rime frost accumulation might also have caused the stem breakage of trees at the forest edge when they were younger. This is consistent with the existence near the forest edge of trees with stems that were broken once at height of up to 3m and then were successfully substituted by lower branches.

Influence of climate events on tree ring structure

During the observations and measurements of the tree rings, 13 types of tree ring structure were described which can be classified as differing from the normal one. Most frequent, and

therefore important for the current research, were frost rings, light rings and rings with different types of reaction wood.

Frost rings were first described by Ratzburg in 1871 (ex Schweingruber 1996). Usually their formation has been associated with events of spring frosts or water stress (Stockli 1996). In the study site the frost rings formed in 1952, 1955 and 1962 were very frequent. The 1952 frost ring has a wide zone of distorted cells and is found in 80% to 85% of the cores from the different plots. The 1955 frost ring is less distinct with narrower zone of distorted cells and is found in 50% to 85% of the cores. The 1962 frost ring is quite peculiar. It has most probably been formed after a late frost event, which was caused by an unusually cold storm event at the beginning of June 1962. Thus, the beginning of the ring has normal cells, followed by a very dark layer of thin, crushed cells and a wide zone of distorted cells. This frost ring is found in 85% to 92% of the cores. The recurrence of these rings was very helpful for the crossdating of the samples, especially in cases of dead trees and trees with missing rings.

Several different types of reaction wood were observed in the samples. Reaction wood formed in a narrow band or at the end of the ring was considered a sign of mechanical influence on the tree during the growing period (Kwon et al. 2001, Dunker and Spiecker 2004). It had most probably been caused by strong wind. Reaction wood formed at the beginning of the tree ring or in the whole ring was considered a sign of mechanical influence on the tree during the autumn and winter period. Therefore it had probably been caused by strong winds or snow accumulation. A special case with *Pinus peuce* wood is the presence of large quantities of resin in some rings ("rings with resin spills"). This has also most probably been caused by mechanical damage or injury of the tree, since it is known that after such events some coniferous trees tend to produce more resin in an attempt to protect themselves from further damage (Schweingruber 1996). In plot N1, about 23% of the trees with damaged stems had initiated the formation of reaction wood in the entire ring in 1963 (Figure 5). These years coincide with the beginning of the period with highest winter precipitation recorded by the adjacent Cherni vrah weather station (Figure 6).

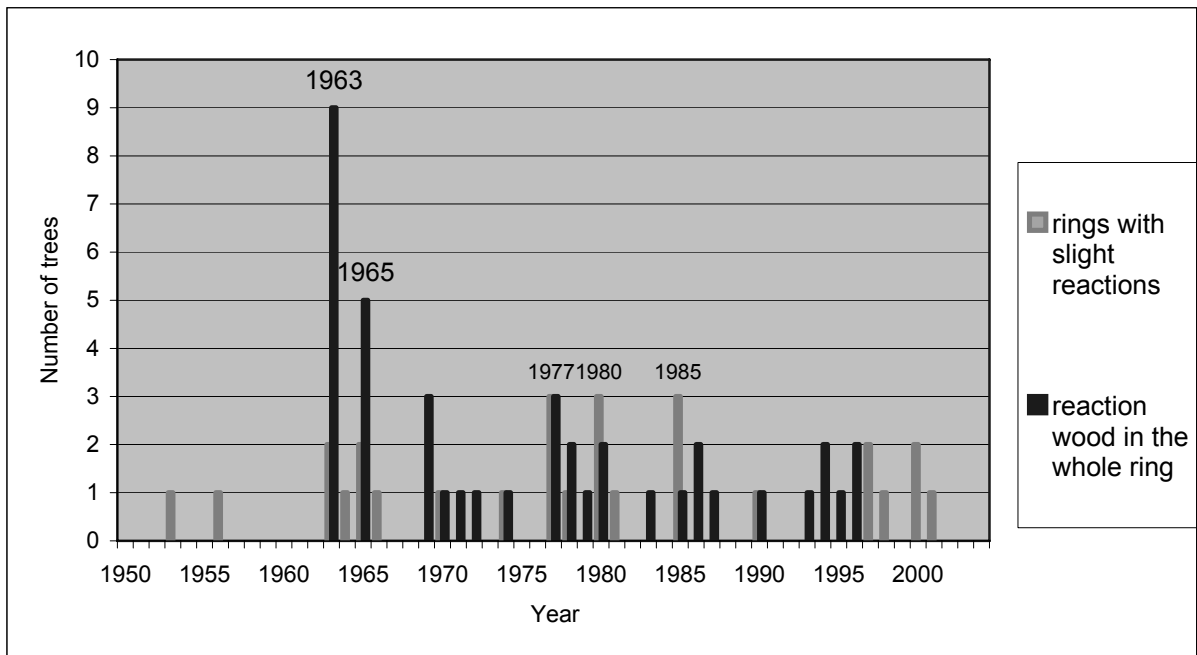


Figure 5: Initiation of periods with reaction wood in lee side cores from plot N1

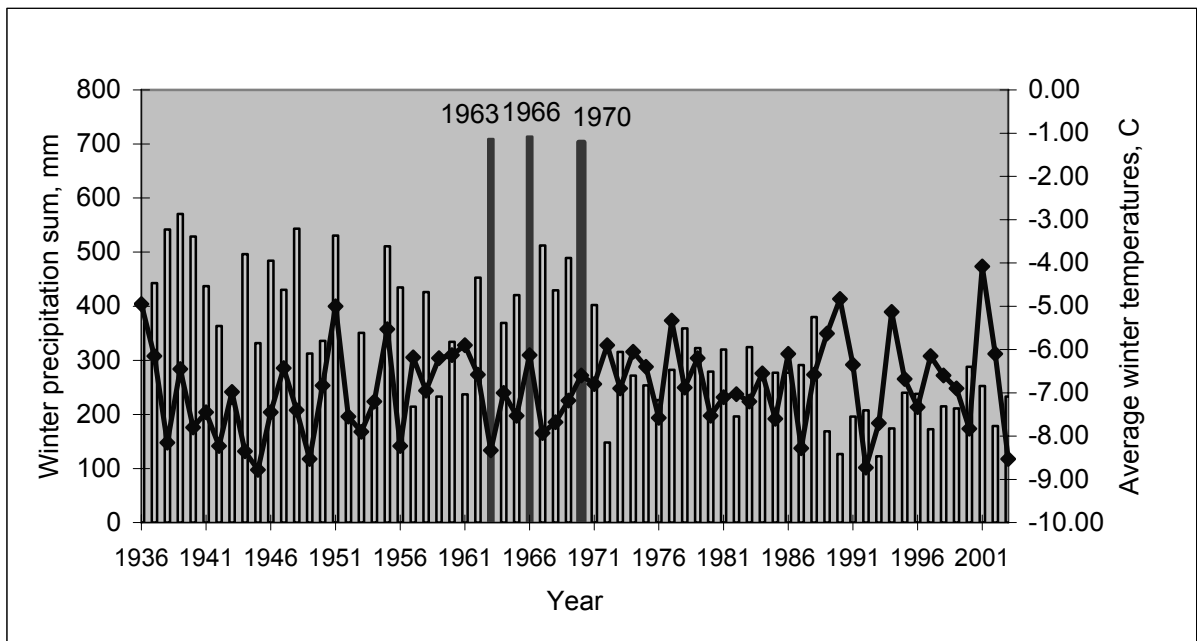


Figure 6: Average winter (December to March) precipitation (showed with columns) and winter temperatures (showed with line) recorded at the Cherni vrah weather station

In plot N2 the highest number of trees (40% of tested trees) that initiated the formation of reaction wood in the entire ring was also in 1963 (Figure 7). In plot N3, which is in the forest stand and is protected from higher snow accumulations due to wind transport, trees with reaction wood in the whole ring were just a few and there were no distinct years or periods with increase of this type of ring structure. This suggests that the observed situation in the treeline plots is closely related to the influence of extreme weather events such as strong gales, big snow and rime accumulations.

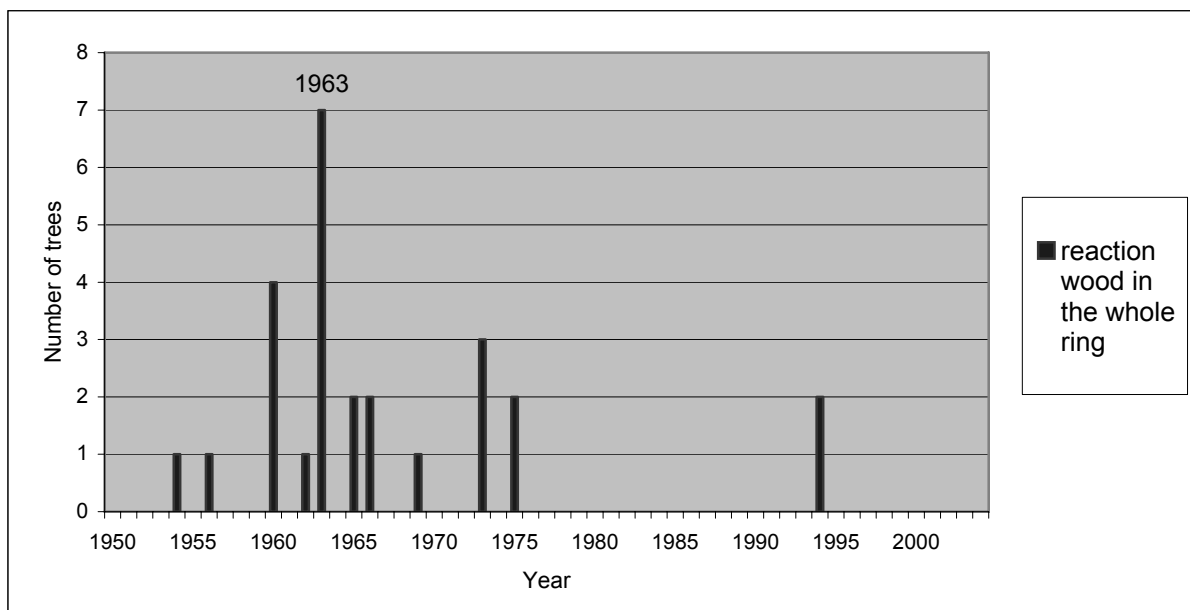


Figure 7: Initiation of periods with reaction wood in lee side cores from plot N2

It can be hypothesized that during the early development of the forest, when the trees in the “Mortality and disturbance zones” were small, their crowns and stems were damaged by large snow accumulations and strong winds. This disturbance has influenced their consequent development and these trees have grown inclined or even horizontally. The altered growth form has most probably been the reason for further damage in later years. Many of the trees in the “Mortality and disturbance zone” have been broken or bent repeatedly. This has caused the death of some of them, or at least has been the most important disturbance factor that has made the surviving trees susceptible to secondary fungal attacks. Currently, the existence of empty spaces at distances of one to two tree heights behind the forest edge contributes to additional snow accumulations and further stem damage of living trees.

Influence of top breakage on tree growth

Some studies (e.g. Larson 1964, Giertych 1964) show that cambial activity is dependent on the auxin production by the tree’s apical meristems (ex Fritts, 1976). Thus, it could be expected that after top breakage, a tree would decrease its radial growth for a certain period

of time. Keller and Lenz have observed this in a study of lopped spruce trees in 1970 (ex Schweingruber 1996).

The comparison of the individual growth curves of trees with broken tops (e.g. last 3 or 4 years of vertical increment) from plots N1 and N2 with the mean growth curves from trees with normal stems, showed that there is no serious radial growth decrease after the top breakage of *Pinus peuce* trees. We also did not find special reactions in the rings as indicators of the breakages, which is a further sign that they did not cause serious stress to the whole trees. This could be explained by the increased viability of young trees and the fact that Macedonian pine tends to rapidly substitute the broken top by a vertically orientated growth of a side branch (Dimitrov 1980).

Conclusions

The following major conclusions can be made from our results:

- Although *Pinus peuce* is one of the best-adapted species for the harsh growth conditions at the treeline zone in the highest Bulgarian mountains, some extreme climate events might have profound effect on the growth of certain individuals. In the region of Aleko hut in Vitosha mountain such events appear to be the strong winds and the large snow accumulations caused by wind transportation.
- In regions with strong winds and possibility for snow transportation it is not advisable to create afforestations with sharp forest edges, since this may be the reason for significant damage to the trees in a zone that begins at approximately 15m behind the forest edge.
- The breakage of the top of young *Pinus peuce* trees does not lead to a serious decrease in radial growth.
- Dendroecological methods might serve as a valuable tool in obtaining information for past events and their influence on the growth of trees, especially where there is limited historical information.

Acknowledgements

This work have been supported by the University of Forestry projects N47/17.02.2005 - "Studying of the growth and state of experimental afforestations from Pine tree species at the treeline zone" and N106/08.03.2004 – "Dendrochronological analysis of the influence of natural factors on the growth and development of tree species from Pine family (Pinaceae) at the treeline zone". The authors would like to thank Gancho Slavov, Peter Zhelev and George Lilianov for reviewing the manuscript.

References

- Cook, E., Briffa, K., Shiyatov, S., Mazepa, V. (1990): Methods of Dendrochronology. Applications in the Environmental Sciences" (Eds. Cook E. and L. Kairiukstis), Kluwer Academic Publishers. 391pp.
- Dakov, M., Dobrinov, I., Iliev, A., Donovan, V., Dimitrov, St. (1980): Raising the position of the treeline. Sofia, Zamizdat. 218pp (in Bulgarian)
- Dimitrov, M. (1980): The Macedonian pine. Sofia, Zemizdat. 217pp (in Bulgarian)
- Duncker, P. and H. Spiecker (2004): Compression wood formation and pith eccentricity in *Picea abies* L. depending on selected site-related factors: Detection of compression wood by its spectral properties in reflected light. *Proceedings of the TRACE Dendrosymposium 2004, 22-24.04.2004, Birmensdorf, Switzerland, Vol.3:150-158.*
- Fritts, H.C. (1976): Tree Rings and Climate, Academic Press. Lonon, Academic Press. 567pp
- Kwon, Mi, Bedger, D., Piastuch, W., Davin, L., Lewis, N. (2001): Induced compression wood formation in Douglas fir (*Pseudotsuga menziesii*) in microgravity. *Phytochemistry* 57: 847-857
- Peltola, H., Kellomacki, S., Vaisanen, H., Ikonen, V. (1999): A mechanistic model for assessing the risk of wind and snow damage to single trees and stands of Scots Pine, Norway Spruce and Birch. *Canadian Journal of Forestry research*, 29: 647-661
- Petty, J., Worrell, R. (1981): Stability of coniferous tree stems in relation to damage by snow. *Forestry*, vol.54, No.2: 115-128
- Schweingruber, F.(1996):Tree Rings and Environment. Dendroecology, Vienna, Haupt. 609pp
- Somerville, A. (1980): Wind Stability: Forest Layout and Silviculture. *New Zeland Journal of Forestry*, vol.10, No.3: 476-540
- Stockli, V. (1996): Tree rings as indicators of ecological processes: the influence of competition, frost, and water stress on tree growth, size and survival. Basel, 1996, 92pp
- Vekilska, B. (1966): Geography of the snow cover on Vitosha Mountain. *Yearly Book of the University of Sofia, Vol.60, book 2, Geography: 73-101* (in Bulgarian)
- Yurukov, S. (2003): Dendrology. Sofia, University of Forestry Press House. 212pp (in Bulgarian)

The use of dendroecological methods in a landscape-ecological approach on upper treeline fluctuations

O. Rößler¹, J. Löffler¹ & A. Bräuning²

¹Department of Geography, University of Bonn, Meckenheimer Allee 166, 53115 Bonn, Germany

Email: o.roessler@giub.uni-bonn.de; loeffler@giub.uni-bonn.de

²Department of Geography, Azenbergstr. 12, 70174 Stuttgart, Germany

Email: achim.braeuning@geogr.uni-stuttgart.de

Introduction

Treeline fluctuations were investigated vigorously during the last decades. In this context, dendrochronological and dendroecological methods were made use of relatively early (i.e. Kullman 1979, Treter 1984). The work of Müterthies (2003) showed the potential of dendrochronological methods in a vegetation ecological approach. In this paper we present a research program based on a combination of dendroecology with remote sensing, soil science, vegetation science and human geography. We have used this set of methods to study the influence of land use change and climate change on fluctuations of the upper treeline in central Norway. Climate and land use are supposed to be the superior factors influencing the position of the upper treeline. Both parameters have changed significantly in time. In central Norway, the annual mean temperature has increased during the last century by 0.08° per decade at most (Førland et al. 2000). The change of land use led to an extensification of less productive land like mountain areas. We assume that both, climate and land use changes led to a rise of the upper treeline. However, the exact extent of the influence of each factor is unknown. The qualitative and quantitative estimation of the impact of particularly temperature and land use on the treeline is the aim of the TRELAN – project, which started in 2002.

Study region

Four study areas were chosen along a climate gradient stretching from the western, oceanic part near Bergen (Bergsdalen, 60° 30' N; 5° 50' E) across two study areas in a transition zone (Gudmedalen, 60° 45' N; 7° 5' E and Geiranger, 62° 03' N; 7° 15' E) to the most continental area in the east (Vågå, 61°53'N, 9°15'E) (Fig. 2). According to the oceanic – continental climate differentiation and a subsidiary mountain mass elevation effect *Betula pubescens* s.l. dominated treelines rise from app. 700 m at Bergsdalen to app. 1050 m a.s.l. at Vågå.

Methods

We used tree-ring widths to obtain specific information about the age structure of forests stands at the upper treeline and to indicate possible responses to changing environmental conditions during the last century. Dendroecological methods were embedded in detailed site mapping including vegetation, soil, and winter snow depth. This data set was accomplished by results from bitemporal aerial photo interpretation, meteorological measurements, and

inquiries about the history of land use. All methods were applied using a nested hierarchical design at four spatial scales along different gradients in central Norway (Fig. 1).

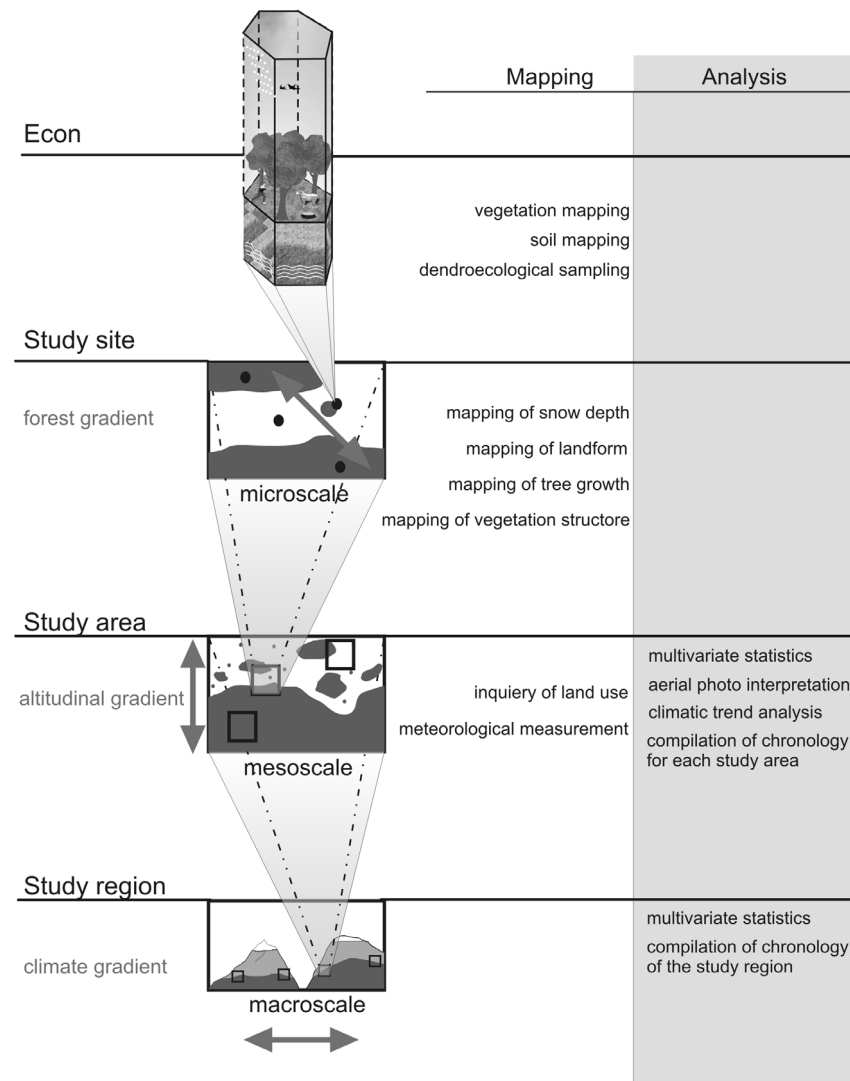


Figure 1: Mapping and analysis approach at different spatial scales.

Mapping Methods

In each study area, we investigated the upper treeline along an altitudinal gradient stretching from dense forest to the low alpine belt. Several representative study sites were selected, each comprising wooded and unwooded plots. The study sites were mapped and structured according to vegetation types, topography, and growth forms of trees. Increment cores of all present woody plants were collected.

Dendroecological Methods

Trees with a trunk diameter above 5 cm were drilled at the trunk basis, parallel and perpendicular to the slope and the length of the aslope trunk from the root to the drill-point was recorded. Cross-sections were taken from smaller trunks. Circumference and vertical height above ground were measured. Polycormic trees were sampled at different trunks.

Furthermore, we collected saplings. The cross-sections and increment cores were mounted and polished in the laboratory before tree rings were counted by using a stereomicroscope. To increase the contrast of the wood we used white chalk to fill the vessels as suggested by Iseli and Schweingruber (1989). Then, ring width was measured with a precision of 0.01 mm.

Remote Sensing

The development of the treeline was estimated by using bitemporal aerial photo interpretation. Since only limited aerial photos for the study areas were available, those of 1992 and 1993 were compared with the earliest photos existing (Vågå 1964, Geiranger 1976, Gudmedalen 1969, Bergsdalen 1972). Scales of the aerial photos differ from 1:15,000 to 1:40,000. The photos were transformed into orthophotos using a digital elevation model. Forests, solitary standing trees and woodless areas were distinguished. By comparison of the earliest and latest photos, the development of treeline was reconstructed. These results were combined with the dendroecological results of age structure.

Inquiries

We carried out inquiries about the current and the historical land use. Quantitative data about the numbers of grazing animals and the period when mountain summer farms had been utilised were obtained from official statistics (local and national scale), reports (e.g. *landbruksplan*), and archives. Inquiries of local administrative authorities (*community*) led to contact locals with relevant knowledge, e.g. farmers and landowners. The latter were interviewed by an informal and semi-structured approach about the present and former ways of land use (cp. Lundberg 2000).

Climate Analyses

Climate data derived from official meteorological stations in the valleys were analysed in terms of temperature and precipitation trend during the last decades. Moreover, these data served as a comparison with the ring width of trees.

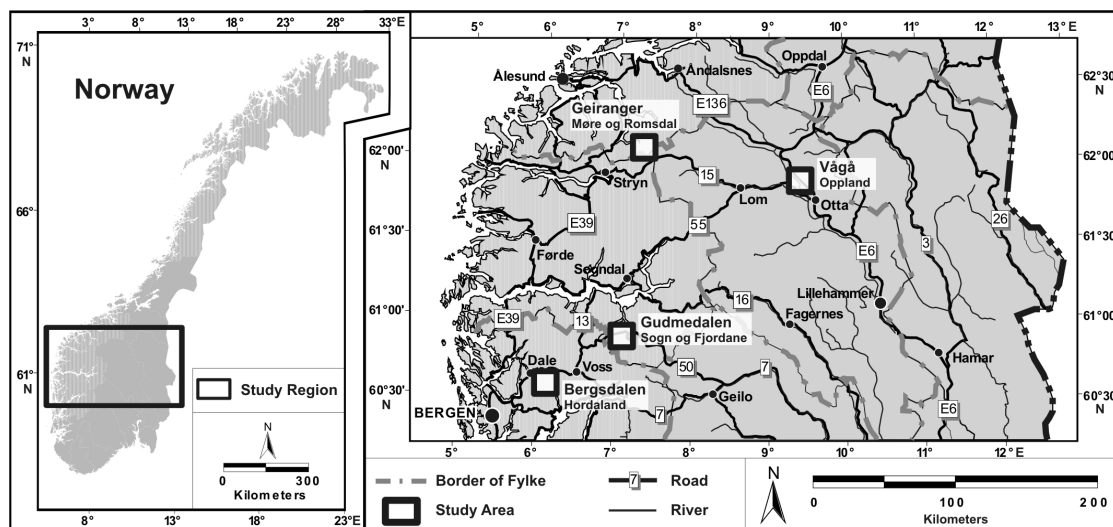


Figure 2: Map of the study region in central Norway and the location of the four study areas

Results and Discussion

We present the results by the example of the Gudmedalen area. The comparison of the aerial photo interpretation (1976 – 1992) revealed differences between the northern and the southern slope (Fig. 3). Only in the southern part of the area serious treeline changes occurred. The age determination of *Betula pubescens* trees at five study sites indicated a rising upper treeline in the southern part of the study area. Two distinct age classes were distinguished: old trees (average age 127 years) and only young trees (max. 47 years). This age structure indicated a recent rise to be interpreted as a regeneration process: old trees were found all over the treeline ecotone and form the present treeline, whereas young trees almost exclusively germinated between the older individuals (Fig. 3). Concerning the effect of changing climate on the treeline this rise might be interpreted as an effect of increasing temperature. Results of the trend analysis of climate data confirmed this hypothesis by a slightly significant increase of annual mean temperature (0.028°C/year, $p = 0.5$). But, intra-annual calculation of temperature trends showed an increase of temperature only in winter months.

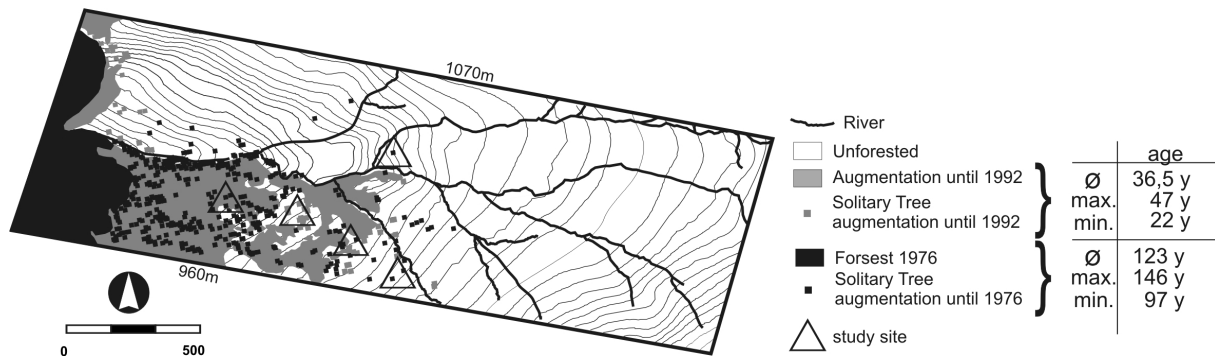


Figure 3: Comparison of bitemporal aerial photos and age structure of trees in the study area.

However, as the results of our inquiries proof, the local rise of the treeline has to be explained by changes in land use. While the northern part of the study area was continuously grazed by app. 300 goats, summer farming ceased in the southern part after 1953. Additionally, in the 1930s the former forest was rooted out apart from some solitary trees. Both incidents, abandoning and rooting could still be retraced today. As indicated by the age structure, old trees found in the area were left from the clear-cut, while young trees started to regrow in the former forest after abandonment by the summer farmers. Consequently, the recent dynamics of the treeline in this area were interpreted as a result of land use change. This finding generally holds true also for the other study regions. Moreover, similar results were published by Hofgaard (1997) and Löffler et al. (2004) for other areas in central Norway. Hofgaard (1997) even denied the sensitivity of anthropogenic treelines to recent climate changes. To test this hypothesis, we are currently working on the development of a local *Betula pubescens* tree-ring chronology covering approximately the last century.

References

- Førland, E., Roald, L. A., Tveito, O. E., Hanssen-Bauer, I. (2000): Past and future variations in climate and runoff in Norway. DNMI-Report 19/00 KLIMA. 77 p.
- Hofgaard, A. (1997): Inter-relationship between treeline position, species diversity, land use and climate change in the central Scandes Mountains of Norway. *Global Ecology and Biogeography Letters* 6, 419-429.
- Iseli, M., Schweingruber, F.H. (1989): Sichtbarmachen von Jahrringen für dendrochronologische Untersuchungen. *Dendrochronologia* 7, 145-157.
- Kullman, L. (1979): Change and Stability in the Altitude of the Birch Tree-Limit in the Southern Swedish Scandes 1915 – 1975. *Acta Phytogeographica Suecica* 65: 121.
- Löffler, J., Lundberg, A., Rößler, O., Bräuning, A., Jung, G. Pape, R., Wundram, D. (2004): The Central Norwegian Alpine Tree Line under a Changing Climate and Changing Land Use. *Norwegian Journal of Geography* 58: 183-193.
- Lundberg, A. (2002): The interpretation of culture in nature: landscape transformation and vegetation change during two centuries at Hystad, SW Norway. *Norwegian Journal of Geography* 56: 246–256.
- Müterthies, A. (2003): The potential timberline: Determination with dendrochronological methods. In: G. Schleser, M. Winiger, A. Bräuning, H. Gärtner, G. Helle, E. Jansma, B. Neuwirth, and K. Treydte, eds., *Tree Rings in Archaeology, Climatology and Ecology*, Volume 1. Proceedings of the Dendrosymposium 2002. Schriften des Forschungszentrum Jülich, Reihe Umwelt 33: 94-100.
- Treter, U. (1984): Die Baumgrenzen Skandinaviens: ökologische und dendroklimateische Untersuchungen. Franz Steiner Verlag, Weisbaden, 111p.

Hydraulic architecture of the mangrove *Rhizophora mucronata* under different salinity and flooding conditions.

N. Schmitz^{1,2}, A. Verheyden², F. De Ridder³, H. Beeckman² & N. Koedam¹

¹Laboratory for General Botany and Nature Management (APNA), Vrije Universiteit Brussel (VUB), Pleinlaan 2, 1050 Brussels, Belgium

²Laboratory of Wood Biology and Xylarium, Royal Museum for Central Africa (RMCA), Leuvensesteenweg 13, 3080, Tervuren, Belgium

³Laboratory of General Electricity and instrumentation, Vrije Universiteit Brussel (VUB), Pleinlaan 2, 1050 Brussels, Belgium

Email: nschmitz@vub.ac.be

Introduction

Mangroves are (sub)tropical forests occurring in the intertidal areas of coastal shorelines protected from wave action. This saline habitat implies that these trees experience a perpetual physiological drought. Consequently, mangrove trees are at risk of drought-induced cavitation. A question which immediately presents itself is “How do mangroves safeguard the water transport under these stressful conditions”. This question can be dealt with by studying xylem anatomy. In particular, vessel density and diameter are frequently mentioned in relation to cavitation susceptibility. High vessel density creates a redundancy in the transport system which increases the conductive safety. According to the air-seeding hypothesis, the advantage of small vessels is a high cavitation resistance due to the association with small pit pore diameters within a species (Tyree and Sperry 1989, Lo Gullo and Salleo 1990, 1993).

This study focuses on the mangrove species *Rhizophora mucronata* (Rhizophoraceae) from Kenya, in which annual growth rings were recently detected (Verheyden et al. 2004). The rings are formed by a gradual change in vessel density. A zone of low vessel density is produced during the rainy season (earlywood), while a zone of high vessel density was found to be associated with the dry season (latewood) (Verheyden et al. 2004). It is important to note that the identification of annual growth rings now enables us to account for the inter- and intra-annual variability when studying vessel characters in mangroves (see Verheyden et al. 2005). Although salinity is a determining factor for the regulation of the water transport in mangroves (Naidoo 1985, 1986, Clough and Sim 1989, Zimmermann et al. 1994, Ball et al. 1997), the influence of salinity on vessel density and diameter remains to be demonstrated.

Aims and methods

The aim of this study was to investigate the relationship between vessel features, in particular vessel density and diameter, and site-specific environmental conditions. Fifty wood discs from eight sites in Gazi Bay (39°30'E, 4°25'S), Kenya, differing in salinity (Salinity category 1-6, covering a salinity range from 26.4 to 49.2) and inundation class (class 1-4) were considered. In addition to vessel density, both tangential and radial diameter were measured directly on the sanded stem discs making use of digital image analysis software

(AnalySIS Pro v.3, Soft Imaging System GmbH, Münster, Germany). Moreover, inter-annual variability was excluded by focusing on one distinct year and intra-annual variability is considered by separating the early- and latewood (Fig. 1) (except for SAL5, in which growth rings were too narrow to differentiate early- from latewood).

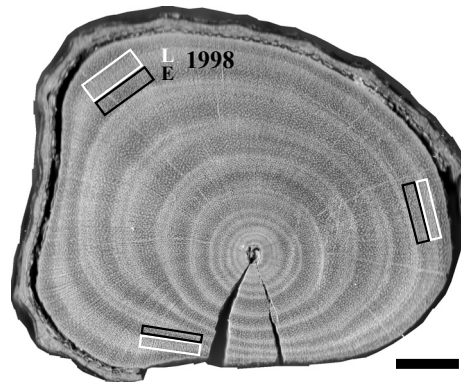


Figure 1: Wood anatomical measurements were carried out at three positions, chosen along a radius of high, moderate and slow growth rate. At each position two quadrats (size is exaggerated for clarity) covering earlywood (E) and latewood (L) of the year 1998 were studied. Scale bar: 1cm. Specimen number Tw56722, part of the Tervuren wood collection.

The effect of growth rate on the vessel features was examined by comparing vessel characters with ring width along three different radii per specimen. Finally, results were statistically analysed making use of a “repeated measures analysis of variance” and a t-test for dependent samples, carried out in STATISTICA 7.0 (StatSoft Inc., Tulsa, USA).

Results and discussion

The effect of salinity

A major correlation was observed between vessel density and salinity (Fig. 2), both in rainy (ANOVA: $F=3.45$, $p<0.05$) and dry season ($F=3.24$, $p<0.05$). In Fig. 2, (as well as in Fig. 3, see further) the use of the average of the three positions was appropriate since the analysis of variance did not show a growth rate effect for either salinity or inundation class, irrespective of vascular traits (rainy season: $F=2.57/0.69$, $0.11/0.095$, $1.52/1.87$; $p=ns$; dry season: $F=1.35/0.52$, $0.018/0.088$, $0.36/0.078$; $p=ns$, for respectively vessel density, tangential and radial vessel diameter). In addition, vessel density and seasons were shown to be tightly coupled ($t=13.31$, $p<0.0001$). A strong evaporation results in an increasing salinity, which leads to a higher vessel density at each site (Fig. 2).

In this way, the findings of the previous study on *R. mucronata* carried out at one site (Verheyden et al. 2005) are validated. It is hypothesized that the adjustment in vessel density allows *R. mucronata* to withstand the negative effects of a spatial as well as a temporal varying salinity, regarding an adequate water balance. Although water is not a limiting factor in the mangroves, the salt concentration causes a serious stress by creating a physiological drought (Clough and Sim 1989).

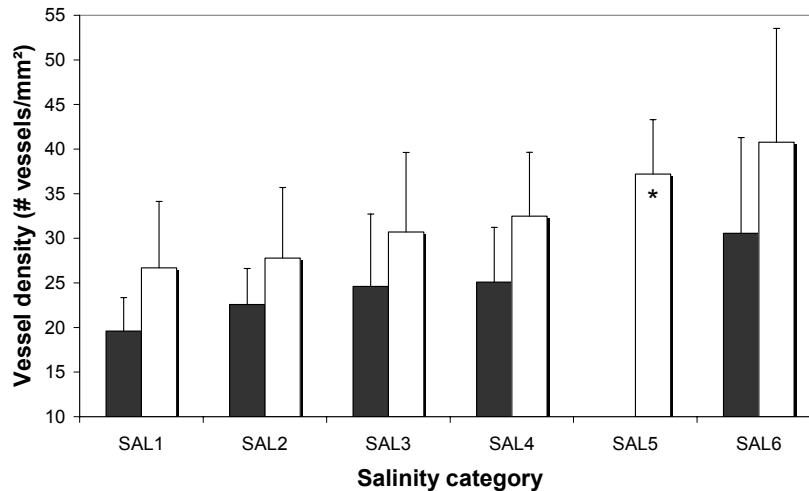


Figure 2: Mean vessel density in relation to salinity for both rainy season (dark bars) and dry season (light bars). * This category represents the annual average vessel density since growth rings were too narrow to differentiate between dry and rainy season (see also Aims and Methods). Error bars correspond to standard deviations.

Consequently, the water transport in mangroves is at risk of drought-induced cavitation. A high vessel density offers a double advantage with respect to conductive safety. First, when the same number of vessels is cavitated, a higher percentage of the transport system remains functional in high vessel density compared to low vessel density wood (Baas *et al.* 1983, Villar-Salvador *et al.* 1997). Second, a high proportion of vessels are in contact with each other via intervessel pits since vessels do not follow a straight line but twist along their path (Kitin *et al.* 2004). Therefore, embolized vessels can be circumvented by means of the high number of alternative routes for the water transport.

In contrast to vessel density, tangential vessel diameter was found to be extremely constant. Neither salinity ($F=0.41$ and 1.28 , $p=ns$, for rainy and dry season respectively), nor seasonal fluctuations ($t=1.85$, $p=ns$) turned out to have any impact. Moreover, the striking similarity between the frequency distributions for different salinity categories, stress the invariable nature of the tangential vessel diameter (Fig. 3a).

Interestingly, although not statistically significant ($F=1.11$ and 2.04 , $p=ns$ for rainy and dry season respectively), radial diameter does show a tendency to be smaller at sites with a high salinity (Fig. 4). This declining trend is supported by a slight shift in size distribution towards narrower vessels when salinity is increased (Fig. 3b). A difference between dry and rainy season was recorded but is not well expressed ($t=-2.5$, $p<0.02$).

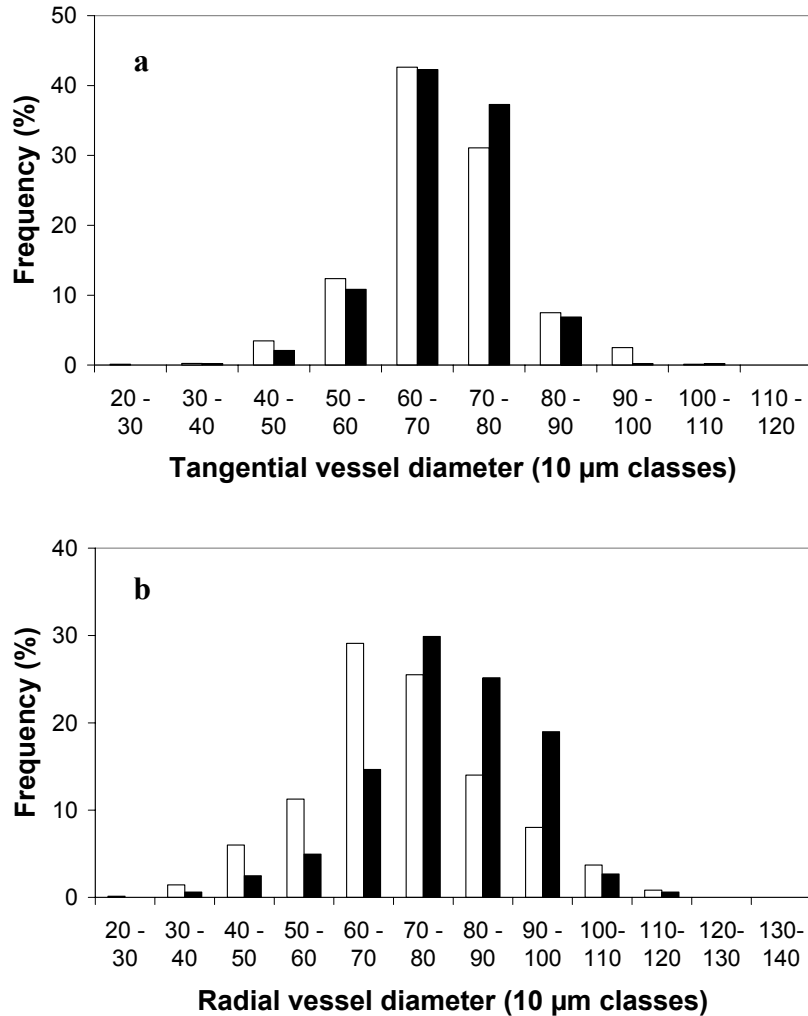


Figure 3: Frequency distribution of (a) tangential and (b) radial diameter of wood samples originating from sites with contrasting salinity (SAL2-SAL5) and inundation classes (class 1-class 4). Dark bars: SAL2, inundation class 1. Light bars: SAL5, inundation class 4.

Several studies report a link between drought and narrow conduits (e.g. Lo Gullo et al. 1995, Villagra and Roig Juñent 1997, Arnold and Mauseth 1999, Corcuera et al. 2004, Stevenson and Mauseth 2004), which was not found here. The presence of two diameter classes in the xylem vessels is a frequent observation of the arid flora (Baas et al. 1983, Baas and Schweingruber 1987, Villagra and Roig Juñent 1997) for it combines an efficient (large vessels) with a safe (small vessels) water transport system (Mauseth and Stevenson 2004). However, as the unimodal diameter distribution (Fig. 3) demonstrates, the absent trend with salinity and inundation class can not be attributed to the interference of a vessel dimorphism. Longer and wider vessels are usually produced in the lower parts of a tree with age, to maintain a favourable water balance when growing and increasing its leaf surface (Tyree and Ewers 1991, Hudson et al. 1998, Cruziat et al. 2002). Mangrove trees, with the smallest average diameter (SAL5, Fig. 3-4), are noted to have the highest cambial age. Vessel diameter is therefore shown to be influenced by salinity more than by age.

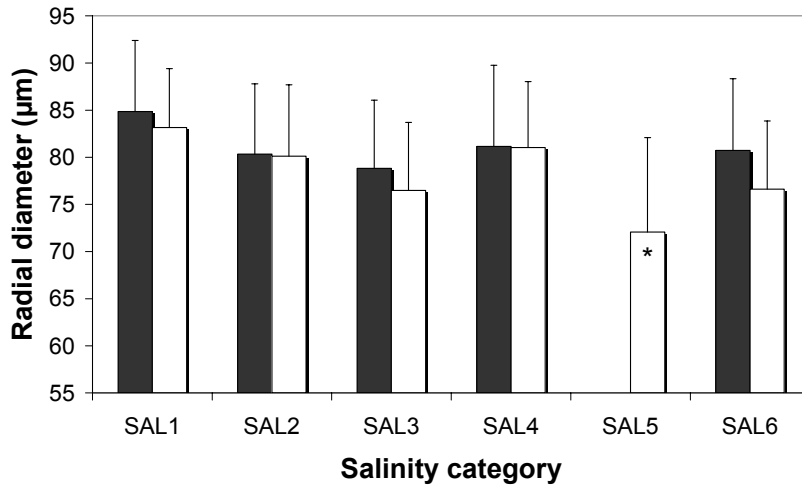


Figure 4: Mean radial vessel diameter in relation to salinity for both rainy season (dark bars) and dry season (light bars). * This category represents the annual average radial vessel diameter since growth rings were too narrow to differentiate between dry and rainy season (see also Aims and Methods). Error bars correspond to standard deviations.

The increased vessel density with salinity and inundation class, not coinciding with a pronounced decrease in vessel diameter, indicates a lack of a trade-off between conductive safety and efficiency. According to the air-seeding hypothesis, small vessel diameters can be associated with small pit pore diameters within a species, and thus to cavitation resistance (Tyree and Dixon 1986, Tyree and Sperry 1989, Lo Gullo and Salleo 1991, 1993). Therefore, declining vessel dimensions with an increase in water stress were expected. However, only a marked increase in vessel density was recorded, which possibly balances out the greater susceptibility to cavitation due to the almost steady diameters. However, the relationship between vessel and pit pore diameter is still subject of investigation, and cavitation susceptibility is generally dependent of the pore diameter of the pits (Sperry and Tyree 1988, Tyree and Sperry 1989, Jarbeau et al. 1995, Cruziat et al. 2002). In this context, a varying pit pore diameter, independent of vessel diameter, is proposed as an alternative explanation for the quasi-invariable vessel size.

The effect of inundation class

With respect to inundation class a positive relationship was found with vessel density ($F=7.91$, $p<0.002$ and $F=7.51$, $p<0.01$ for rainy and dry season respectively); similar to our findings for the salinity-effect. The highest vessel density occurred at inundation class four (Fig. 5), which can be explained by the associated poikilohaline conditions. The exposure to cavitation associated with a fluctuating salt concentration exceeds the one resulting from a constant salinity, of the average and in some cases even the maximum salinity value of the fluctuation (Lin and Sternberg 1993, Yáñez-Espinosa and Terrazas 2001).

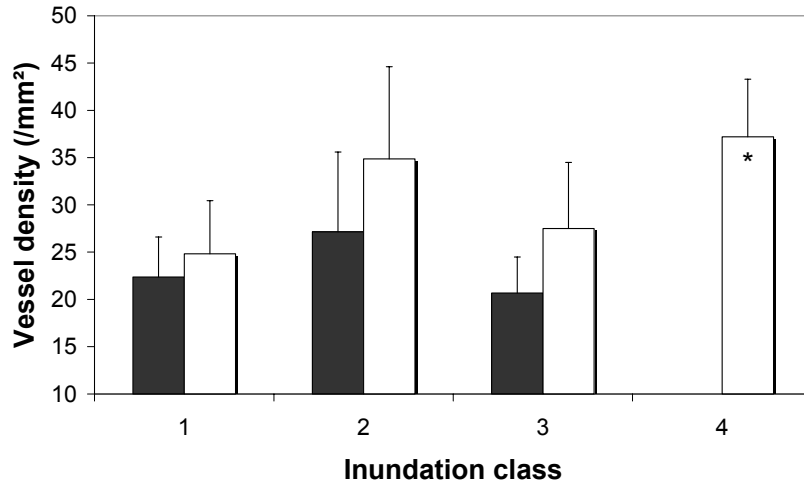


Figure 5: Mean vessel density in relation to inundation class for both rainy season (dark bars) and dry season (light bars). * This category represents the annual average vessel density since growth rings were too narrow to differentiate between dry and rainy season (see also Aims and Methods). Error bars correspond to standard deviations.

The positive trend in vessel density with inundation class is interrupted at inundation class three (Fig. 5). It is assumed that the low vessel density is a reflection of the low salinity (SAL1 and SAL2) at these sites. Concerning vessel diameter, only annual averages of radial diameter are significantly smaller at higher inundation class ($F=3.36$, $p<0.02$). However, a pronounced shift in size distribution is observed when SAL2 and SAL5 are compared (Fig. 3b), which can most likely be ascribed to the interplay with contrasting inundation classes (class 1 and 4).

Conclusion and perspectives

There has been much interest in the ecology of mangroves in general, but their hydraulic architecture received less attention. The plasticity in vessel characters of *R. mucronata* in response to the prevailing climate conditions was reported earlier by means of a time series analysis (Verheyden et al. 2005). In the present study, these findings have been validated on a larger sample size, representing different environmental conditions. In particular, the seasonal difference in vessel density was confirmed and the relation between salinity and vessel density was demonstrated. In addition, the absent growth rate effect strengthens its potential as an environmental proxy. Finally, our results are especially motivating for future studies concerning intervessel pits. We suggest variability in pore diameter can offer an explanation for the almost invariable nature of vessel dimensions. Investigation of the pits is unfortunately a delicate one. Several artefacts have to be taken into consideration (Choat et al. 2003, 2004), which may however not be a drawback but may encourage further efforts.

Acknowledgements

Research funded by a Ph.D. grant of the Institute for the Promotion of Innovation through Science and Technology in Flanders (IWT-Vlaanderen).

References

- Arnold, D.H., Mauseth, J.D. (1999): Effects of environmental factors on development of wood. *American Journal of Botany* 86(3): 367-371.
- Baas, P., Schweingruber, F.H., (1987): Ecological trends in the wood anatomy of trees, shrubs and climbers. *IAWA Bulletin n.s.* 8(3): 245-274.
- Baas, P., Werker, E. and Fahn, A. (1983): Some ecological trends in vessel characters. *IAWA Bulletin n.s.* 4(2-3): 141-159.
- Ball, M.C., Cochrane, M.J., Rawson, H.M. (1997): Growth and water use of the mangroves *Rhizophora apiculata* and *R. stylosa* in response to salinity and humidity under ambient and elevated concentrations of atmospheric CO₂. *Plant, Cell and Environment* 20: 1158-1166.
- Choat, B., Ball, M., Luly, J., Holtum, J. (2003): Pit membrane porosity and water stress-induced cavitation in four co-existing dry rainforest tree species. *Plant Physiology* 131: 41-48.
- Choat, B., Jansen, S., Zwieniecki, M.A., Smets, E., Holbrook, M. (2004): Changes in pit membrane porosity due to deflection and stretching: the role of vested pits. *Journal of Experimental Botany* 55(402): 1569-1575.
- Clough, B.F., Sim, R.G. (1989): Changes in gas exchange characteristics and water use efficiency of mangroves in response to salinity and vapour pressure deficit. *Oecologia* 79: 38-44.
- Corcuera, L., Camarero, J.J., Gil-Pelegrin, E. (2004): Effects of a severe drought on *Quercus ilex* radial growth and xylem anatomy. *Trees* 18: 83-92.
- Cruziat, P., Cochard, H., Améglio T. (2002): Hydraulic architecture of trees: main concepts and results. *Annals of Forest Science* 59: 723-752.
- Hudson, I., Wilson, L., Van Beveren, K. (1998): Vessel and fibre property variation in *Eucalyptus globulus* and *Eucalyptus nitens*: some preliminary results. *IAWA Journal* 19(2): 111-130.
- Jarbeau, J.A., Ewers, F.W., Davis, S.D. (1995): The mechanism of water-stress-induced embolism in two species of chaparral shrubs. *Plant, Cell and Environment* 18: 189-196.
- Kitin, P., Fujii, T., Abe, H., Funada, R. (2004): Anatomy of the vessel network within and between tree rings. *American Journal of Botany* 91(6): 779-788.
- Lin, G. en Sternberg, L. da S.L. (1993): Effects of salinity fluctuation on photosynthetic gas exchange and plant growth of the red mangrove (*Rhizophora mangle* L.). *Journal of experimental Botany* 44(258): 9-16.
- Lo Gullo, M.A. and Salleo, S. (1991): Three different methods for measuring xylem cavitation and embolism: a comparison. *Annals of Botany* 67: 417-424.
- Lo Gullo, M.A. and Salleo, S. (1993): Different vulnerabilities of *Quercus ilex* L. to freeze- and summer drought-induced xylem embolism: an ecological interpretation. *Plant, Cell and Environment* 16: 511-519.
- Lo Gullo, M.A., Salleo, S., Piaceri, E.C., Rosso, R. (1995): Relations between vulnerability to xylem embolism and xylem conduit dimensions in young trees of *Quercus cerris*. *Plant, Cell and Environment* 18: 661-669.

- Mauseth, J.D., Stevenson, J.F. (2004): Theoretical considerations of vessel diameter and conductive safety in populations of vessels. *International Journal of Plant Sciences* 165(3): 359-368.
- Naidoo, G. (1985): Effects of waterlogging and salinity on plant-water relations and on the accumulation of solutes in three mangrove species. *Aquatic Botany* 22: 133-143.
- Naidoo, G. (1986): Response of the mangrove *Rhizophora mucronata* to high salinities and low osmotic potentials. *South African Journal of Botany* 52: 124-128.
- Sperry, J.S., Tyree, M.T. (1988): Mechanism of water stress-induced xylem embolism. *Plant Physiology* 88: 581-587.
- Stevenson, J.F., Mauseth, J.D. (2004): Effect of environment on vessel characters in cactus wood. *International Journal of Plant Sciences* 165(3): 347-357.
- Tyree, M.T., Dixon, M.A. (1986): Water stress induced cavitation and embolism in some woody plants. *Physiologia Plantarum* 66: 397-405.
- Tyree, M.T., Ewers, F.W. (1991): The hydraulic architecture of trees and other woody plants. *New Phytologist* 119: 345-360.
- Tyree, M.T., Sperry, J.S. (1989): Vulnerability of xylem to cavitation and embolism. *Annual Review of Plant Physiology and Plant Molecular Biology* 40: 19-38.
- Verheyden, A., De Ridder, F., Schmitz, N., Beeckman, H., Koedam, N. (2005): High-resolution time series of vessel density in Kenyan mangrove trees reveal a link with climate. *New Phytologist* doi: 10.1111/j.1469-8137.2005.01415.x.
- Verheyden, A., Kairo, J.G., Beeckman, H. en Koedam, N. (2004): Growth rings, growth ring formation and age determination in the mangrove, *Rhizophora mucronata*. *Annals of botany* 94: 59-66.
- Villagra, P.E., Roig Juñent, F.A. (1997): Wood structure of *Prosopis alpataco* and *P. argentina* growing under different edaphic conditions. *IAWA Journal* 18(1): 37-51.
- Villar-Salvador, P., Castro-Diez, P., Pérez-Rontomé, C., Montserrat-Marti, G. (1997) : Stem xylem features in three *Quercus* (Fagaceae) species along a climatic gradient in NE Spain. *Trees* 12: 90-96.
- Yáñez-Espinosa, L., Terrazas, T. (2001) : Wood and bark anatomy variation of *Annona glabra* L. under flooding. *Agrociencia* 35: 51-63.
- Zimmermann, U., Zhu, J.J., Meinzer, F.C., Goldstein, G., Schneider, H., Zimmermann, G., Benkert, R., Thürmer, F., Melcher, P., Webb, D., Haase, A. (1994): High molecular weight organic compounds in the xylem sap of mangroves. Implications for long distance water transport. *Botanica Acta* 107: 218-229.

Dendroecological analysis of Scots pine (*Pinus sylvestris* L.) stands in Vitosha Mountain, Bulgaria

N. Zafirov

University of Forestry, Sofia, Bulgaria

Introduction

Current state

Scots pine (*Pinus sylvestris* L.) is one of the most widely distributed tree species in Europe, and the Balkan Peninsula is its southern tree limit. In Bulgaria pine stands cover one sixth of the woodland and more than 50 per cent of the land occupied by coniferous forests. It is also the main species that has been used in the large scale afforestation for the last 50 years. However, nowadays many of these plantations are affected by the widespread forest decline, and more than 20 per cent of them have already degraded. Unfortunately, the causes leading to the declining health condition of pine plantations are not fully clarified. Some of the scientists attribute it to fungal diseases, others – to insect infestations but most of them suppose that abiotic factors and mainly the ongoing climate change is the trigger leading to the worsening of plantations' condition (Innes, 1993).

The most precise way to investigate the influence of the variety of environmental factors on trees is by considering the dimension of time. The environmental situation is shown in true light only by tree rings (Schweinguber, 1996), which makes dendrochronological methods the most suitable for studying the impact of the factors affecting tree health.

Objective and research tasks

The objective of this study is assessing the state and dynamics of the condition of Scots pine plantations in Vitosha Mountain and evaluating the impact of climate conditions. For this purpose, several research tasks were planned to be achieved:

1. To establish mean index series for the radial increment of several pine plantations and to assess the impact of climate conditions, mainly mean monthly temperatures and monthly precipitation,
2. To analyze the dynamics of the mean indices during the growth periods of the stands and to ascertain the effect of the tree age, altitude and slope exposure on the health condition of the stands, and
3. To build models for the radial increment of the sites that show similar changes in the established series.

Materials and methods

Objects of this study are pine plantations in Vitosha Mountain which is located in the centre of the Balkan Peninsula near Sofia, the capital of Bulgaria. It has an area of 311 km² and an unusual, dome like shape which makes it suitable for studying the impact of the slope exposure on tree growth.

Samples were taken from seven pine plantations at different ages and growing under different ecological conditions. On the eastern slope at 1200 m altitude three stands were sampled, each at different age – 50, 70 and 90 years old. Samples were also collected from stands on the other slopes of the mountain at the same elevation and also from one stand at 1600 m altitude.

Twelve to seventeen trees per sample site were sampled and one or two cores per tree were extracted. Dendrochronological methods, as described by Fritts (1976), Cook and Kairiukstis (1990), were used for sampling the trees, processing and cross-dating the cores. Tree-ring widths were measured by using a tree-ring measuring table with Dendrostat computer program in the University of Forestry, Sofia. Exponential, modified exponential and power functions were used for detrending the increment series. For better visual analysis the mean index chronologies were smoothed with five-year moving average curves and were plotted on joint graphs.

After the autocorrelation of each index series was removed, a multiple regression analysis was performed for assessment of the climate impact on tree growth. As predictors in the model the following variables were used: mean monthly temperatures and monthly precipitation over a period of twelve months – from September of the previous year to August of the current year. Climatic data was provided for the Cherni Vrah meteorological station which is the nearest available for all of the stands. The period from 1955 to 2003 was used for developing the models because this is the common time span for the mean index series.

For building a model which can be used for prediction of the current year health condition of the trees, stepwise regression was used. The variables, which are used as predictors in such models, must precede the period of the growth season (Mirtchev *et al.* 2000). So the following variables were used: mean index for the previous year and mean monthly temperatures and monthly precipitation from September of the previous year to March of the current year.

Results and discussion

By cross-dating the cores, one missing and several partially missing rings were found which shows that the environmental conditions in the studied sites rarely became so unfavorable for Scots pine trees to cease their radial growth.

For establishing mean index series, between 20 and 30 cores per site were used. The calculated chronology signal (Expressed Population Signal) for the different stands has values between 0.85 and 0.92 which shows that the number of sampled trees was sufficient for establishing mean index series.

The multiple regression analysis, where monthly precipitations and mean monthly temperatures were included as predictors together, showed that there is a strong climatic signal in all of the series. The coefficients of determination (R^2) vary from 0.45 for the Northern site to 0.63 for the Southern site (Tab. 1).

Table 1: Coefficients of determination from multiple regressions with both mean monthly temperatures and monthly precipitations as predictors

Study site	East, 1200 m a.s.l., 90-year-old	East, 1200 m a.s.l., 70-year-old	East, 1200 m a.s.l., 50-year-old	East, 1600 m a.s.l.	North	West	South
R ²	0.60	0.62	0.54	0.62	0.45	0.62	0.63

In order to determine which climatic factor has greater effect on the increment of the trees, multiple regression analyses were performed separately with the mean monthly temperatures and with the monthly precipitations. Again, great difference between the reactions of the separate sites was not established (Tab. 2). Almost all index series showed greater correlation with the mean monthly temperatures than with the monthly precipitations. The age of the trees does not modify the climate-growth relationship. Minor differences were established for trees growing on differing slopes of the mountain. The Southern plantation is the most influenced by the temperature variation, and showed the same dependence upon both of the factors. Unlike it, the Northern plantation is the least influenced by the temperature variation, and has the highest difference in the dependence upon these factors. The absence of great differences in the impact of the two factors on the different sites is probably due to the fact that these plantations are neither at the high nor at the low tree line of the Scots pine distribution.

Table 2: Coefficients of determination from separate multiple regressions with only precipitations or only mean temperatures as predictors

	East, 1200 m a.s.l., 90-year-old	East, 1200 m a.s.l., 70-year-old	East, 1200 m a.s.l., 50-year-old	East, 1600 m a.s.l.	North	West	South
R ² (T)	0.40	0.45	0.32	0.44	0.37	0.44	0.37
R ² (P)	0.22	0.28	0.30	0.32	0.14	0.33	0.37

Through the graphical analysis of the smoothed index chronologies for the stands at different ages, several differences between them were established (Fig. 1). The two longer chronologies have a common stress period from the beginning of the 40-s to the beginning of the 50-s of the last century. Then an improvement in their condition is observed until the beginning of the 90-s when the index series steadily drop below average. The indices of the youngest trees vary around one during the 70-s, and after the beginning of the 80-s they reach their lowest level. The great differences between the sites are found when the stands reach an age of about 50 years. At that age their indices generally reach their highest values: for the 90-year-old stand – in the 60-s, for the 70-year-old stand – in the 80-s and for the 50-year-old stand – at the end of the century. It is very interesting that in spite of the unfavorable climatic conditions during the last decade that affected the two older stands, the youngest stand is in good condition. Clearly, Scots pine trees in this area are most vital at 50 to 60 years of age, when they are less affected by the adverse influence of the environmental

factors. After this period, they gradually become more vulnerable to adverse influences. This fact can be used in forestry practices for determining the age at which Scots pine trees have to be felled.

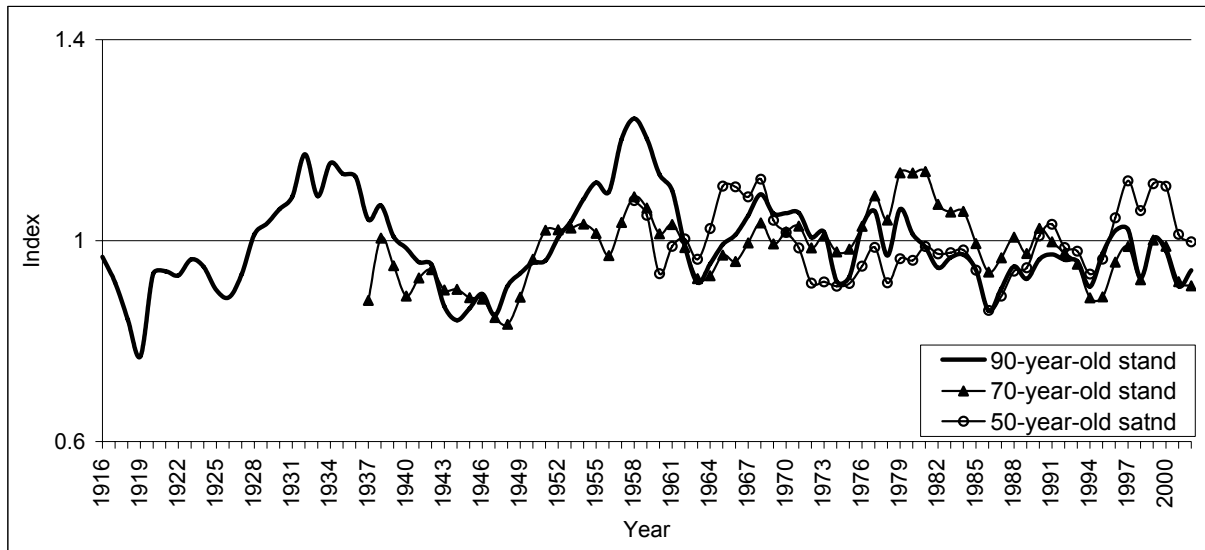


Figure 1: Mean indices dynamics of pine trees at different ages growing at 1200 m altitude on the eastern slope of Vitosha Mountain

The morphological analysis of the temperature-precipitation regime confirmed the conclusions made by the regression analyses. The established stress periods for the pine plantations at lower elevations, during the 40-s and after the 80-s of the last century, correspond to periods with mean monthly temperatures above average (Fig. 2). There is not clearly visible relationship between the dynamics of the mean indices and monthly precipitations, with the latter being above average for the first period and below average for the second one.

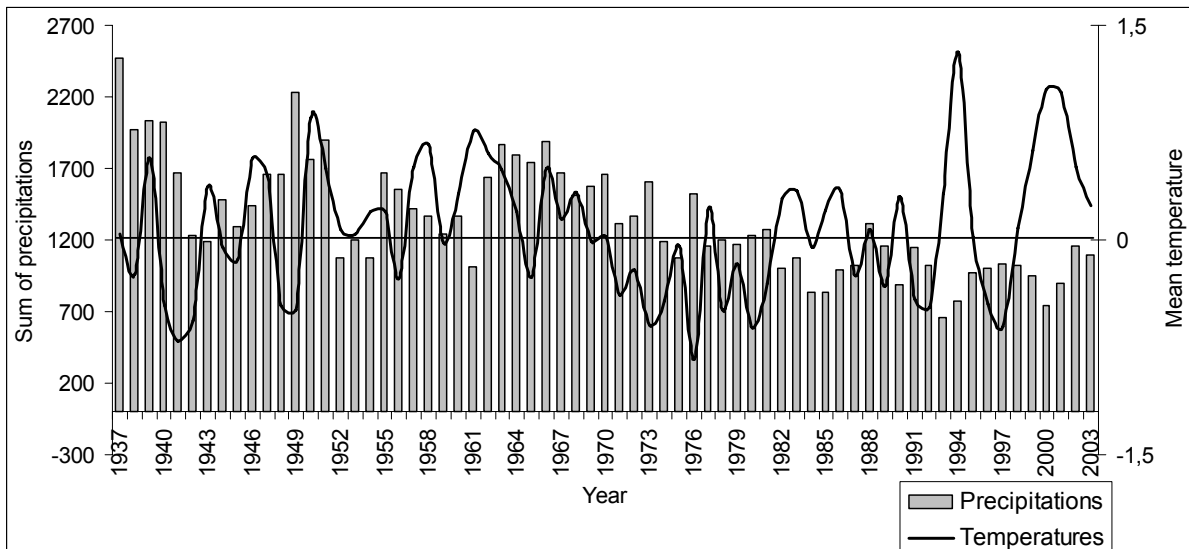


Figure 2: Monthly precipitation and mean monthly temperature dynamics for the Cherni Vrah Meteorological Station

The mean index series of the stand at high altitude, together with the series of the stand at low altitude at the same age are shown on Figure 3. It is noticeable that the two curves have opposite trends, with the periods below one for one of the chronologies corresponding to periods above one for the other. At 50 years of age only, both of the stands are in good condition, and the indices for the stand at a higher elevation reach their higher values. This shows that although the two stands are affected in the same degree by the climatic factors, as established by the regression analyses, the way in which they exert influence on them is probably opposite.

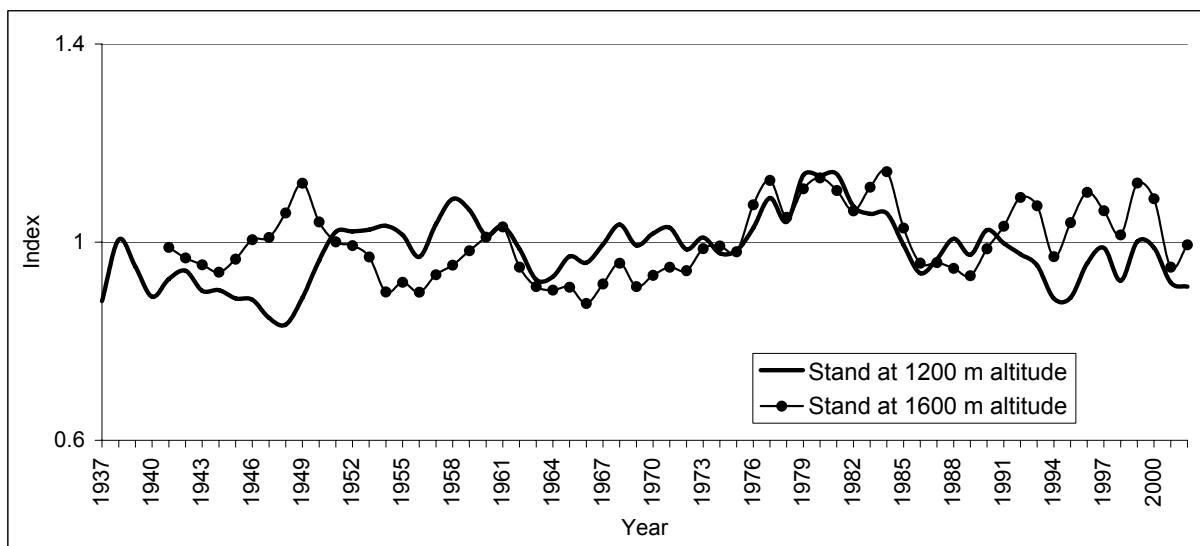


Figure 3: Mean indices dynamics of 70-year-old pine trees growing at different altitudes

The index chronologies for the western and southern stands have the same pattern as these for the eastern stands at 1200 m altitude. Nevertheless, the series for the stand on the

northern slope resembles more the one from the stand at a higher altitude. During the 40-s and after the 90-s its indices are above the average and between these periods they are below the average.

The same results were established using correlation analyses between the mean index series of the different stands. All of the chronologies, except the one at a higher altitude and the one on the Northern slope, have high correlation coefficients, ranging from 0.39 to 0.66 (Table 3). At the same time the two remaining index series have high correlation, with r being 0.56. These results allowed the mean indices for these two groups to be averaged for the further analysis.

Table 3: Correlation matrix for the mean index series of stands at 1200 m altitude at Eastern, Western and Southern slopes

Study site	East, 90-year-old	East, 70-year-old	East, 50-year-old	West	South
East, 90-year-old	1	0.57	0.41	0.57	0.62
East, 70-year-old		1	0.52	0.50	0.39
East, 50-year-old			1	0.62	0.50
West				1	0.66
South					1

In forestry and forest protection practices it is useful to have a model for predicting the increment of the trees for the next growth period. The most valuable models are those that include just several variables as predictors which are from the period before the growth season. Because of that, stepwise regression analysis was performed with the two built mean index series as dependent variables and the climatic factors until the beginning of the growth period as independent variables. Sufficient significance level (below 0.05) had only the increment of the previous year and the mean temperatures for two months for both of the chronologies and the precipitation for one month for the chronology of the lower sites. The models can be expressed as:

$$I_1 = 0.623 + 0.576 \times PrI_1 - 0.03 \times T_{\text{October}} + 0.038 \times T_{\text{March}} + 0.001 \times P_{\text{December}}$$

and

$$I_2 = 0.843 + 0.516 \times PrI_2 + 0.021 \times T_{\text{January}} + 0.035 \times T_{\text{March}},$$

where I_1 is the index for the radial increment of the trees growing on eastern, southern and western slopes of the mountain; I_2 is the index for the radial increment of the trees growing at 1600 m elevation and trees growing on the northern slope of the mountain; PrI_1 , PrI_2 are the indices for the radial increment of the previous year; T is the mean monthly precipitation for the previous October and the current January and March and P is the mean precipitation for the previous December.

The coefficients of determination for the models are high – 0.69 for I_1 and 0.59 for I_2 . However, these models can be used only for Scots pine trees, growing in the region of Vitosha Mountain. That is why, for prediction of the increment of the plantations in different areas, other models must be established.

Summary

The influence of the temperature-precipitation regime on the radial increment of Scots pine plantations in Vitosha Mountain is strong. However, at the studied sites the temperature affects the variability of the mean index series in a greater degree than the precipitation does.

The chronologies of trees at different ages, growing at similar ecological settings are well correlated among each other and show common stress periods for the stands. The trees are also identically affected by the climatic factors. However, differences in the trends of the radial increment at around 50 to 60 years of age of these trees were established. This shows that pine plantations in this region are most vital at this age, and prematurely felling of the trees is not needed. However, to determine the right age at which trees must be felled in different areas, such analyses must be done.

The relief is also an important factor, affecting the health condition of pine trees in the studied area. Trees growing at different elevations have opposite trends in their health condition. The periods of good health condition for the trees growing at a lower elevation correspond to periods of bad health condition for the trees growing at a higher elevation. The slope exposure also affects the health condition of the trees. Although trees growing on the Eastern, Western and Southern slopes of Vitosha Mountain have common stress periods, the ones growing on the Northern slope of the mountain differ from them and have a common signal with trees at a higher altitude.

References

- Cook, E.R., Kairiukstis, L.A. (eds.) (1990): *Methods of Dendrochronology: Applications in the Environmental Science*. Kluwer Academic Publishers, Dordrecht. 394 p.
- Fritts, H.C. (1976): *Tree rings and climate*. London, New York, San Francisco, Academic Press. 576 p.
- Innes, J. (1993): *Forest Health: Its Assessment and Status*. CAB International, Wallingford. 513 p.
- Mirtchev, St., Lyubenova, M., Schikalanov, Al., Simeonova, N. (2000): *Dendrochronology*. Pensoft, Sofia. 198 p. (in Bulgarian)
- Schweingruber, F.H. (1996): *Tree Rings and Environment. Dendroecology*. Berne, Stuttgart, Vienna: Paul Haupt, Birmensdorf, Swiss Federal Institute for Forest, Snow and Landscape Research. 609 p.

SECTION 4

GEOMORPHOLOGY

Reconstruction of Erosion Rates in Swiss Mountain Torrents

O. Hitz¹, H. Gärtner², I. Heinrich¹ & M. Monbaron¹

¹ University of Fribourg, Department of Geosciences, Geography, Switzerland

² Swiss Federal Institute for Forest, Snow and Landscape Research WSL

Introduction

Alpine areas are highly affected by various geomorphic processes, such as landslides or debris flows. Most of these processes can cause severe damage to existing infrastructure in the affected areas. Due to the effect of global change (IPCC 2001a,b) the potential risk of natural hazards occurring in alpine areas is expected to increase to an even higher risk-level than it has been recorded for the last century (PLANAT 2004). These global changes also have distinct influences on fluvial processes in torrents causing erosion on slopes and riverbanks even in forested areas.

In the last decades the Swiss federation has subsidised forest management procedures along mountain torrents which are characterised by intensive erosion and accumulation. Slow continuous as well as dramatic discontinuous erosion of forested riverbanks frequently cause structural destabilisation and finally the affected trees fall over. These fallen trees hold the potential to lead to a blockage of the fluvial system and in severe cases can cause dams to collapse resulting in a severe flooding or even debris-flow surges. Consequently, frequently a risk for a potential threat to human live and infrastructure caused by erosive processes exists and hence needs to be estimated (Böll et al. 1994). Based on the risk potential strategies need to be considered and expected costs calculated to evaluate the best solution for a cost-effective integral risk management (Wilhelm 1999, Böll et al. 1994, BUWAL 1994a,b 1998). It is common policy in Switzerland to find the most cost-efficient strategy to protect threatened areas against potential natural hazards. However, both politicians and foresters need to decide which protective actions at what risk level they should take (Böll 1997, Böll et al. 1999, BUWAL 2001). These protective actions in forests along alpine torrents have so far mostly concentrated on cutting down bigger trees growing along the riverbanks of the torrents to lower the risk of uprooting due to



Figure 1: Typical situation along the riverbank of the study site Steinibach

erosional events (Wasser and Frehner 1996). These actions also aim to reduce the risk of deadwood and consequential blockages within the torrents which might ultimately cause catastrophic flood waves in the case of a bursting dam. However, sparse knowledge exists about the effects of these forest management actions on the drainage zones of mountain torrents and the potential of the torrents to become a hazard. As the forest actions are very cost-intensive it is important to know, if they are necessary and efficient. In addition, new tools need to be developed to more precisely estimate the risk potential of threatened regions in order to supply politicians and foresters with more data and thus help them during the decision process.

The project presented here aims to evaluate the influence of riverbank erosion to the quantity of driftwood in alpine torrents. For the first time, a central focus is set on the analysis of wood anatomical features of exposed roots of deciduous trees for the reconstruction of erosional processes. Dating the time of root exposure along riverbanks in combination with common dendrogeomorphic analysis techniques applied to tree trunks allows the reconstruction of erosion dynamics also leading to a potential destabilisation of adjoining trees.

Study area

The project started with an evaluation of potential mountain torrents in Swiss alpine areas according to basic requirements such as high recent fluvial dynamics, the occurrence of exposed roots and forested riverbanks. Preferably, the forests examined should comprise a mixture of conifers and deciduous trees. Two mountain torrents were selected, the "Brüggwaldbach" (Gersau, Canton of Schwyz), managed for several decades and the "Steinibach" (Flühli, Canton of Luzern), unmanaged for more than 50 years, to also evaluate the effects of different forest management procedures (fig. 1 and 2).



Figure 2: Location of the study sites Brüggenwald-bach **B** (Schwyz), and Steinibach **S** (Luzern), in Switzerland.

Both torrents had caused damage to infrastructure through various flooding events in the last decades. Although both torrents have mostly steep slopes on both sides of the torrents (figure 1) and similar geological and climatic site patterns they show differences regarding the channel geometry, flooding potential, drainage areas, topography of riverine forests and structure of these forests (i.e., distribution of diameter and height, different species composition).

Material and Methods

At each torrent a sector spanning 1 km along the river banks was selected for comprehensive analyses. Within this sector detailed geomorphic mapping (scale 1:1000) was conducted. Besides the general dimensions of the riverbed specific zones showing signs of accumulation and erosion were documented as well as specific characteristics of the surrounding area such as slope angle and density of forest cover. Trees showing exposed roots obviously influenced by erosional processes along the riverbanks were of special interest for the analysis of the erosion dynamics at the sites.

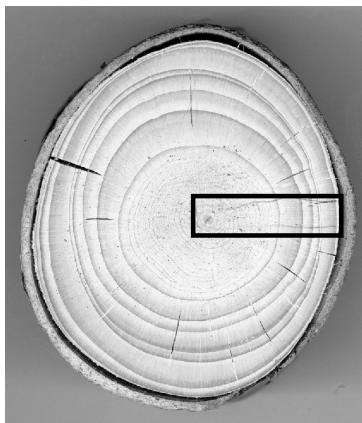


Figure 3: Sanded disc of a root, rectangle indicates the location of micro section sampling

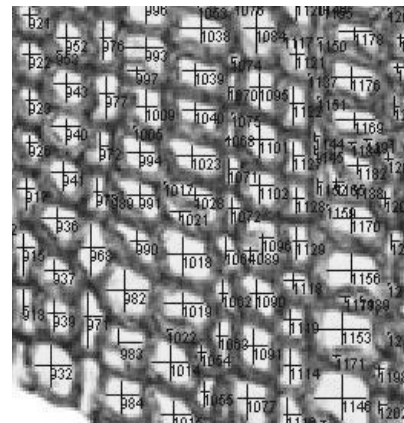


Figure 4: Micro section taken from a root showing cell measurements by WinCELL

All locations showing exposed roots within the sector were documented in detail. The geomorphic mapping (scale 1:100) included the measurement of profiles and a precise documentation of the position of the exposed roots related to the recent soil surface. Site locations containing exposed roots of both coniferous and deciduous trees were preferred because the anatomical reactions after exposure are already known for conifers (Gärtner et al. 2001) and hence can act as a reference during dating of the angiosperm root. Finally, disc samples were taken from the roots and their respective position was marked in the documented profiles. At each position two discs were sampled, one for macroscopical analysis of ring-width variations and the second for preparing micro slides to analyse anatomical variations (Gärtner 2003).

The surfaces of all discs were treated with a belt sander (400 grain) to prepare for general macroscopic analysis and to define the positions most suitable for the micro sections used for the following wood anatomical analysis (figure 3). The micro sections were cut with a

sledge microtome at a thickness of approximately 15µm, stained with Safranin and Astra blue and finally fixed in Canada balsam (Schweingruber 1978).

Finally micro photos were taken from the slides for further digital imagery. Cell dimensions (e.g., cell lumen, cell wall thickness) were measured using WinCELL software (figure 4) and following the measurement routines established for coniferous earlywood root cells (Gärtner 2003). Mean values of the various cell dimensions were calculated for each tree ring visible in the micro sections. The analysing procedure started with roots of coniferous trees followed by roots of angiosperms.

Preliminary Results and Discussion

Some of the exposed roots of coniferous trees analysed showed an abrupt reduction of cell lumen in the earlywood from one to another year. In addition, small scars and callous tissue also often appeared in the same year or in the year before (figure 5). This distinct change in cell size can be attributed to a sudden exposure of the root due to an intense erosional event at the specific location.

Based on former studies of anatomical changes of exposed roots it is known, that continuous erosion causes a continuous lowering of soil surface and with this a continuous reduction of cell sizes over many years, until a reduction of about 50% is reached once a large part of the root is exposed (Gärtner et al. 2001, Gärtner 2003).

In addition, the scars occurring in the previous year indicate, that the position of the root in the year before the event was near the soil surface. This information helps reconstructing the position of the soil surface before the exposure of the root (Gärtner et al. 2001).

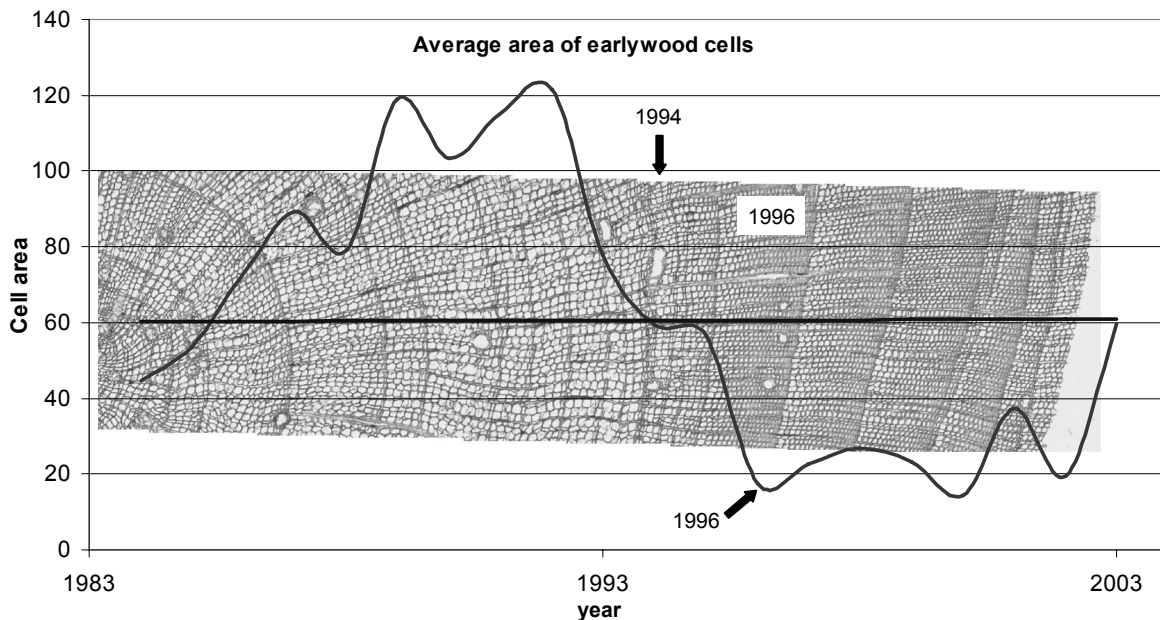


Figure 5: Micro section taken from a root disc (see figure 4) with an overlaying graph showing annually measured averages of the lumen area of earlywood cells. Note that the graph has linear annual steps (x-axis) as scaled below, due to the slide, which shows a normally grown ring width pattern without a scale).

From 1984 to 1994 the rings of this root (figure 5) consist of large cells with small cell walls and a large cell lumen in the earlywood. The ring boundary zones contain hardly more than

one row of latewood cells, which are flattened in radial direction, cell walls display only minor thickening. From 1996 onwards, the ring structures exhibit a more stem like structure, that is, cell sizes are reduced to about 50% with a continuous change of the cell dimensions at the earlywood / latewood boundary and a very distinct latewood portion. Consequently it can be determined, that the ring 1996 was formed after root exposure. Combining these findings with the reconstructed position of the former soil surface and the geomorphological mapping of the location, it is possible to determine local erosion rates since 1996.

A comparable procedure was then applied to various deciduous species. The anatomical structure of deciduous trees is more complex than the structure of coniferous trees and several cell types assume different functions. The analysis concentrated on possible variations in the anatomical structure of vessels and fibre cells as well as on differences in earlywood and latewood. So far, best results are found for ash (*Fraxinus excelsior* L.).

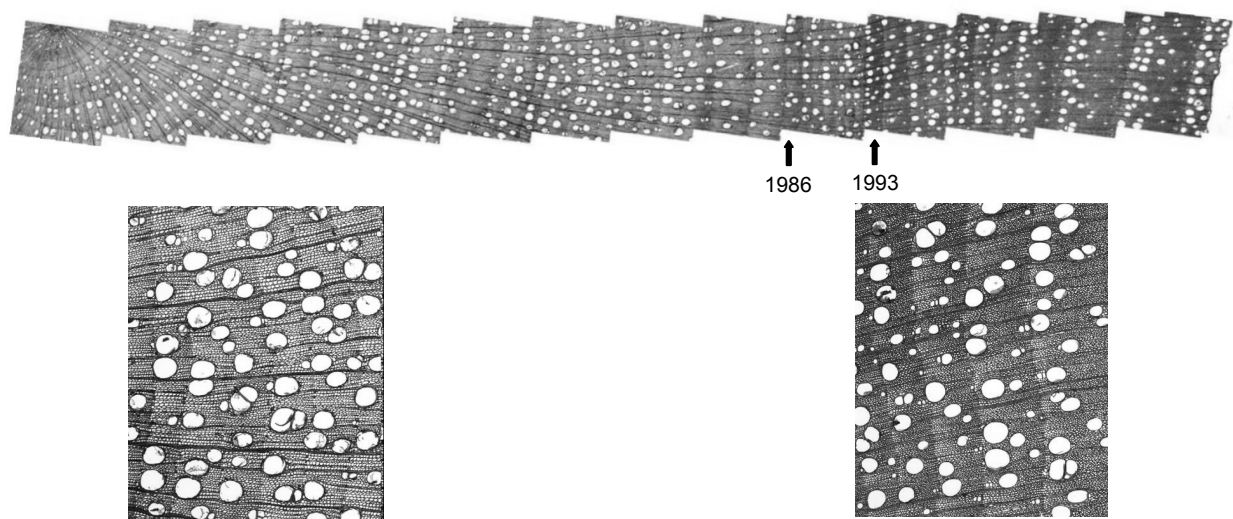


Figure 6: Top: Micro section taken from an exposed ash root. Lower left: Detail of the micro section near the centre. Right: Detail of the micro section near the bark. Note that the overall structure appears darker near the bark.

In figure 6, the presented micro section of an exposed root of an ash tree shows a change in the overall structure. The appearance of the outer rings is darker than near the centre of the root. In the innermost part of the root the fibre cells have thin cell walls and big cell lumen areas. In addition, it is very difficult to differentiate between earlywood and latewood. In the outer part of the root the cell lumen area is reduced and cell walls are thickened, hence the generally darker colour. In addition, the intra-seasonal structural variations within one ring are more distinct because last cells formed appear denser at the end of each ring. In contrast to the innermost rings, an obvious change from earlywood to latewood is detectable.

Furthermore, differences in regard to the vessel characteristics between the inner- and outermost rings are also discernible. Large vessels seem to concentrate along the tree-ring boundary in the earlywood part. Within the innermost rings the number of vessels is higher and the cell lumen area is bigger compared to the outermost part. Near the bark the latewood is dominated by small vessels which are missing in the inner part of the root.

To investigate these observations further sectors of about 0.5 mm² including one full tree ring with latewood and earlywood were selected. In these sectors the areas covered by fibre cells and vessels were measured separately (figure 7). In a second step only vessel lumen area was measured separated into latewood and earlywood zone.

All these measurements reveal similar trends with abrupt changes of the cell lumen area (figure 7), a reaction comparable to that found in coniferous roots. Figure 7 illustrates several reactions, e.g., the variations of the fibre cell dimensions (black graph) indicate that two reductions, the first in 1986 / 1987 and a second in 1993, have occurred. These reactions are paralleled by the values for the vessel lumen area (grey graph) which also suggests two lumen area reductions, one in 1987 and a second in 1993. The graphs are similar to the ones shown for the coniferous roots. After 1993 the reduction in cell size is about 50% which strongly suggest that 1993 indicates the first ring after root exposure. Nevertheless, further analyses need to be conducted to define more comprehensively the specific wood structural anomalies occurring during and after angiosperm root exposure.

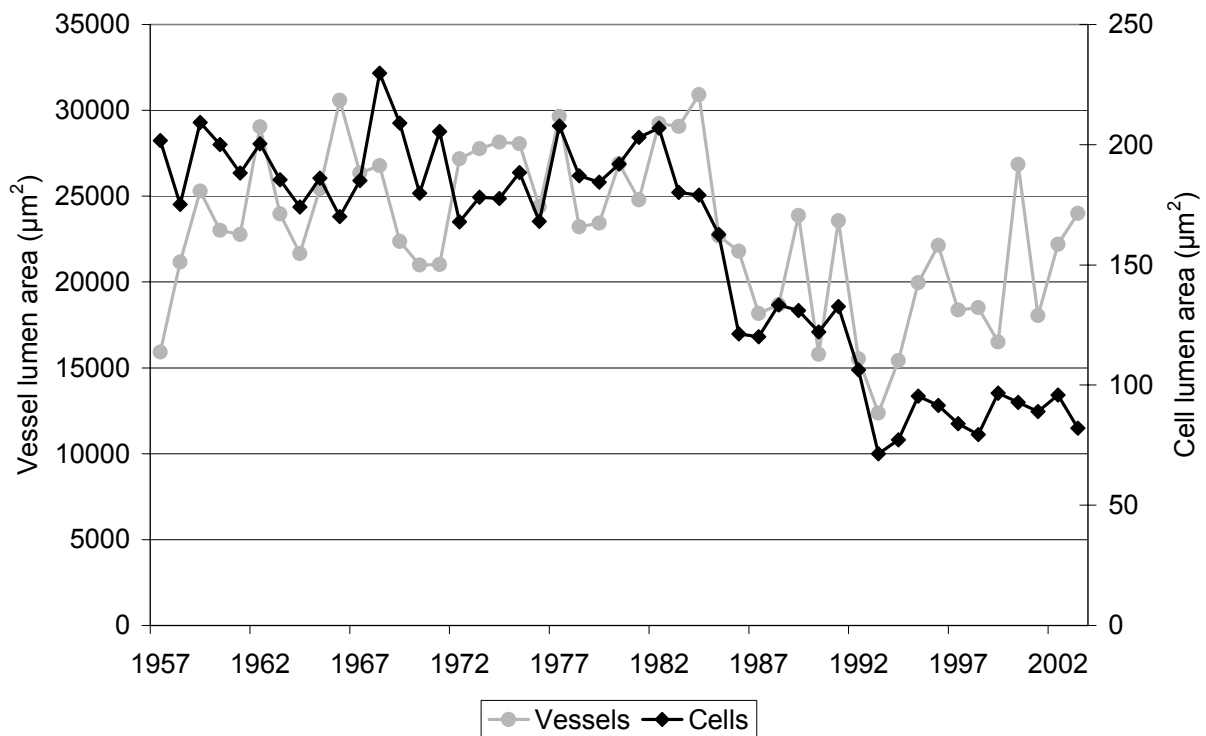


Figure 7: The Graph shows annual mean values of vessel and cell lumen area measured by WinCELL. Both vessel and cell lumen area show a distinct reduction of cell size of about 50%.

Generally, the results imply that it is possible to determine wood anatomical reactions in roots of broadleaf species due to root exposure. These reactions of roots can be used as a new dating tool to reconstruct the exact year of exposure and hence of erosional processes in vegetation zones dominated by angiosperms. Due to the complex and specialised structure of angiosperm wood it might also hold more information than coniferous wood and thus might deliver further details on the processes of root exposure and the different erosion processes (continuous or discontinuous erosion).

Acknowledgements

The authors wish to thank the Swiss Agency for the Environment, Forests and Landscape (SAEFL / BUWAL) for funding the project. Furthermore we wish to thank Christian Rickli, Hansueli Bucher and Raphael Holland for their support in the field.

References

- Böll, A. (1997): Wildbach- und Hangverbau. Berichte der Eidgenössischen Forschungsanstalt für Wald, Schnee und Landschaft.
- Böll, A., Gerber, W., Graf, F., Rickli, C. (1999): Holzkonstruktionen im Wildbach-, Hang- und Rensenverbau. Eidgenössische Forschungsanstalt für Wald, Schnee und Landschaft.
- Böll, A., Gerber, W., Rickli, C. (1994): Polykopien Kursunterlagen zum FAN-Kurs 1994.
- BUWAL (1994a): Kreisschreiben Nr. 20. Bundesamt für Umwelt, Wald und Landschaft, Eidgenössische Forstdirektion. 4.
- BUWAL (1994b): Anleitungsentwurf zur Durchführung einer Risikoanalyse. Bundesamt für Umwelt, Wald und Landschaft, Eidgenössische Forstdirektion. 7.
- BUWAL (1998): Methoden zur Analyse und Bewertung von Naturgefahren. Umwelt-Materialien Nr. 85. Bundesamt für Umwelt, Wald und Landschaft.
- BUWAL (2001): Kreisschreiben Nr. 13. Bundesamt für Umwelt, Wald und Landschaft, Eidgenössische Forstdirektion. 8.
- Gärtner, H. (2003): Holzanatomische Analyse diagnostischer Merkmale einer Freilegungsreaktion in Jahrringen von Koniferenwurzeln zur Rekonstruktion geomorphologischer Prozesse. *Dissertationes Botanicae* 378. 118.
- Gärtner, H., Schweingruber, F.H., Dikau, R. (2001): Determination of erosion rates by analyzing structural changes in the growth pattern of exposed roots. *Dendrochronologia* 19: 1-11.
- IPCC (2001a): Climate Change 2001. The Scientific Basis: A contribution of Working Group I to the Second Assessment Report of the Intergovernmental Panel of Climate Change. Cambridge University Press.
- IPCC (2001b): Climate Change 2001. Synthesis Report: A contribution of Working Group I, II and III to the Third Assessment Report of the Intergovernmental Panel of Climate Change. Cambridge University Press. 398.
- PLANAT (2004): Strategie Naturgefahren Schweiz Synthesebericht. 81.
- Schweingruber (1978): Mikroskopische Holzanatomie. Eidgenössische Anstalt für das forstliche Versuchswesen. Birmensdorf, Switzerland.
- Wasser, B., Frehner, M. (1996): Wegleitung Minimale Pflegemassnahmen für Wälder mit Schutzfunktion. Vollzug Umwelt. Bundesamt für Umwelt, Wald und Landschaft.
- Wilhelm, C. (1999): Kosten-Wirksamkeit von Lawinenschutzmassnahmen an Verkehrsachsen. Vorgehen, Beispiele und Grundlagen der Projektevaluation. Vollzug Umwelt, Praxishilfe. Bundesamt für Umwelt, Wald und Landschaft.

Extreme rainfall events as a triggering mechanism for erosion analysed by means of anatomical changes in exposed roots in permanent gullies (southern Poland)

I. Malik

Faculty of Earth Sciences, University of Silesia, Będzińska St. 60, Sosnowiec, 41-200, Poland,

Email: irekgeo@wp.pl

Introduction

One of the main factors conditioning gully erosion is the quantity and intensity of precipitation. According to (Stankowianski 2003) gullies are formed during periods of extensive forest clearance and expansion of farmland, but the triggering mechanisms of gully erosion are extreme rainfall events. Therefore, deforestation and the introduction of cultivated plants in areas covered with dust sediments are the only important factors causing gully erosion (Fanning 1999).

Studies of gully erosion rate are often based on the comparison of gully lengths on maps produced in different centuries or on aerial photos (Daba et al. 2003). Another method of measuring the rate of gully erosion includes continuous monitoring of headcuts (Malde, Scott 1976). Also a dendrochronological method has been used for estimating the rate of gully erosion, using in addition to root exposures, corrosion scars on exposed roots or on above-ground parts of fallen trees, exposed and dead root ends, root suckers, stems, branches and leading shoots of fallen trees and the age of trees within a gully (Vandekerckhove et al. 2001).

A tree ring analysis reflects geomorphic processes in the past, but it is concentrated mostly on the stem, and only to a lesser extent on roots (Alestalo 1971, Shroder 1980). There are few studies of erosion intensity conducted on the basis of exposed roots. They frequently only measure the length of an exposed part of the root and indicate its age, which allows one to estimate erosion volume (Carrara and Carroll 1979, Hupp 1990). An exception are studies conducted out in southern Spain, where, based on dendrochronological root analysis, the time of erosion episodes has been indicated together with an estimation of the rate of gully erosion (Vandekerckhove et al. 2001).

Research has been conducted for some time on the possibility of determining an erosion episode based on anatomical changes occurring in root wood after exposure (Gärtner et al. 2001). The research has shown that cells within tree rings become more numerous and smaller after exposure. One can clearly see the division into early wood and late wood within tree rings originating after exposure. In the process of exposure roots are often wounded. Scars frequently occur on the boundary between exposed and unexposed tree rings. They document one erosion episode that has led to their exposure. These anatomical changes in root tree rings allow one to date erosion episodes.

The aim of this study is demonstrate the possibility of dating gully erosion events by means of anatomical changes in tree rings in exposed roots and reconstructing the conditions of

incision occurring in the permanent gullies of the Proboszczowicka Plateau in southern Poland.

Study area

Studies were carried out on the Proboszczowicka Plateau, the northern part of which belongs to the Silesian Upland and the southern part of which falls in the Silesian Lowland (Fig. 1). A dense network of permanent gullies 10-15 meters deep dissects large areas of the summit surface at 270-300 above m. s. l. This gully network has been formed in loess sediments.

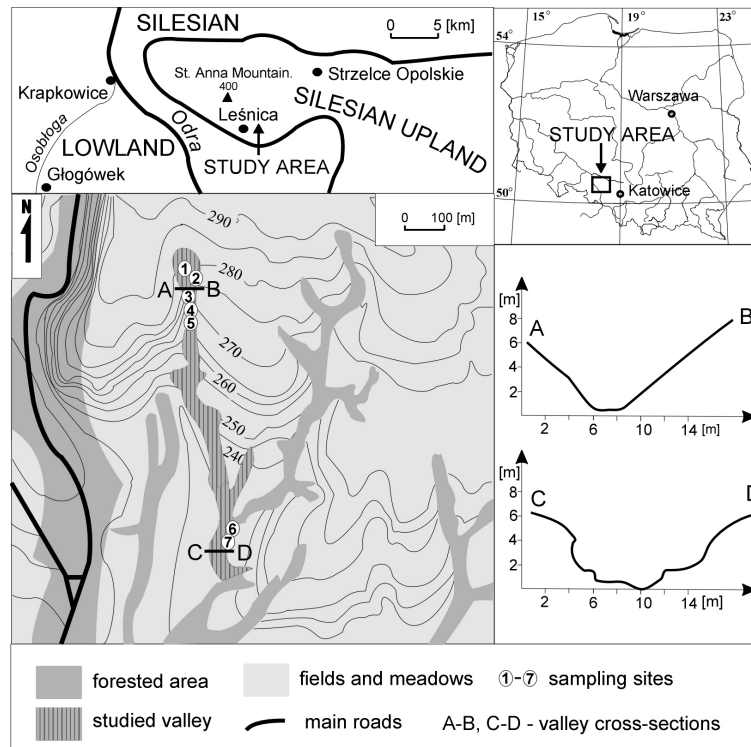


Figure 1: Location of study area and sampling sites.

The gullies in the area where research was conducted are covered with forest as opposed to the extensive areas of summit plateau used for agriculture. Arable land in the area under consideration constitutes 88% of the surface area, whereas forests only comprise 11%. In the gullies the predominant tree is mainly beech (*Fagus sylvatica*).

Average annual precipitation in the area studied amounts to about 680 mm. Maximum frequency of occurrence of storms in the area studied occurs at the beginning of June as well as at the end of June and early July. The biggest monthly precipitation reported in Leśnica is considerable and amounts to 200-260 mm in July (the precipitation gauge in Leśnica is situated about 1.5 km away from the gully studied). Daily precipitation exceeds 30 mm several times per decade; in the years 1970-2000 daily precipitation exceeded 60 mm as many as four times (Fig. 4).

During heavy downpours the run-off intensifies, which leads to the occurrence of new incisions in gullies. Erosion not only initiates dusty sediments, but also causes transportation and deposition of the limestones and dolomites underneath them.

The Commune of Lešnica, which covers the area of research, already had the character of an agricultural settlement similar to nowadays at the beginning of 13th century. On the basis of studies conducted in adjacent loess areas, one may assume that the change to agriculture occurred much earlier, since the land was already used in Neolithic times and deforestation relating to this was already occurring (Klimek 2002).

The research was conducted in a 900 m long gully whose upper part is narrow and V-shaped. The valley is wide, flat-bottomed and possesses terraces in the lower part (Fig. 1). Samples were collected at 7 sites. Three sites were located in the bottom of the upper part of the valley, two on each slope and two at its mouth (Fig. 1).

Material and methods

The height, width and length of incisions were measured by means of a rod and a measuring tape, while in the upper course and at the mouth cross-sections were made of the whole valley. Next, 10 cm fragments of exposed beech tree roots were collected by means of a handsaw. In 7 sites, 53 samples were collected from 28 roots. Between 1 and 3 samples were collected from each root, depending on the individual circumstances. In favourable conditions two samples were collected in places where the root connects with the soil and a third one from the middle of the exposed part of the root. In addition, samples were collected in places where roots were wounded. In order to date the initiation of incision, and not its deepening or extension, samples were collected from halfway through the length of exposed roots located in the surface parts of incised gully at sites number 1-5. The height of the root outcrop above the gully bottom and the distance from the beginning of the incision was also measured. All samples were cut with knives in order to show the structure of the wood in root cross-section. The moment of exposure was identified afterwards by means of a binocular microscope on the assumption that it is indicated by an obvious decrease in cell size and increase in their number, as well as a division of cells into early wood and late wood within each tree rings occurring after exposure. The exposure time was calculated by counting the number of tree rings with anatomical changes. In addition scars occurring on the boundary between anatomical differences in root wood were noted. They confirmed the year in which exposure of the roots occurred (Schweingruber 1996). In the case of 22 root samples, the number of tree rings after exposure was difficult to calculate by means of a binocular microscope. Microscopic sections were prepared from these samples in order to better show the wood structure of the roots. Slices of wood 15-20 μm thick were cut by means of a microtome and the number of tree rings occurring after exposure was then calculated under the microscope.

Results and discussion

Erosion dating based on the time of root exposure in the sites studied

The oldest exposure of roots in site 1 was reported in the upper part of the incision. Roots were exposed here from 1981 to 1984, whereas 1.5 m lower down the exposure of roots occurred in the years 1992-1997. Halfway through the incision it becomes older again: the exposure of root number 9 was dated to 1984 (Fig. 2). At the moment of collection of the samples, roots nos. 2 and 7 were dead, other roots were alive. Roots nos. 3 and 4 had erosion wounds.

Site number 2 is an incision running down the slope between espaliers of trees and along its gradient. In total 4 roots were sampled originating from different places in this incision. The exposure of roots in the lower part of the incision occurred in the years 1981 and 1984, whereas the exposure of roots in the upper parts of the incision occurred in the years 1998 and 2000 (Fig. 3). All of the roots examined were alive. Roots nos. 10 and 12 had wounds.

There is an oval niche at site 3 which is 0.5 m deep and has a diameter of 3.5 m. In total 2 roots were dated here: one of them situated within the niche was exposed in 1991. The other one, situated 2 m above the niche was exposed in the years 1999-2000 (Fig. 3). The roots were alive and did not have any wounds.

A 150-year old beech tree grows at site number 4, on the left hand slope and 2 m above the bottom of the valley. Roots are exposed at soil level within the bastion. They grow back into the soil below the place where they are partially exposed. At this site 3 roots were dated, all of them were partially exposed in the years 1994-1995 (Fig. 2). They were alive and did not have any wounds.

The incision at site 5 is situated in the bottom of the valley, about 10 m below the bastion. In total 4 roots exposed in the middle part of the incision were dated from this site. They were exposed at different times in the years 1982-1994 (Fig. 2). Roots nos. 15 and 16 were dead, but root no. 17 was alive. The roots had no wounds.

A beech tree growing on a slope about 200 m from the valley mouth was undercut at site 6. The niche is located 2.5 m above the bottom of the valley; it is 1.2 m deep, 2.5 m high and about 4 m long. Below the niche there are 2 terrace levels: 0.5-0.8 m and 1.2-1.7 m. In the niche 3 roots were dated which were exposed in the years 1984-1989 (Fig. 3). They were alive, root B4I had wounds.

At site number 7, situated on the left slope 120 m away from the mouth of the valley, there is an incision in the shape of a longitudinal niche. Below the niche there is a 1-1.5 m terrace. In the incision 5 roots were dated, the oldest of them, exposed in the years 1974-1978, are located in the middle part of the exposure. Roots on the sides of the exposure are younger, uncovered from sediments in the years 1988, 1990 and 1994 (Fig. 3). Apart from roots B6 and B10, all of the roots examined are alive and have no wounds.

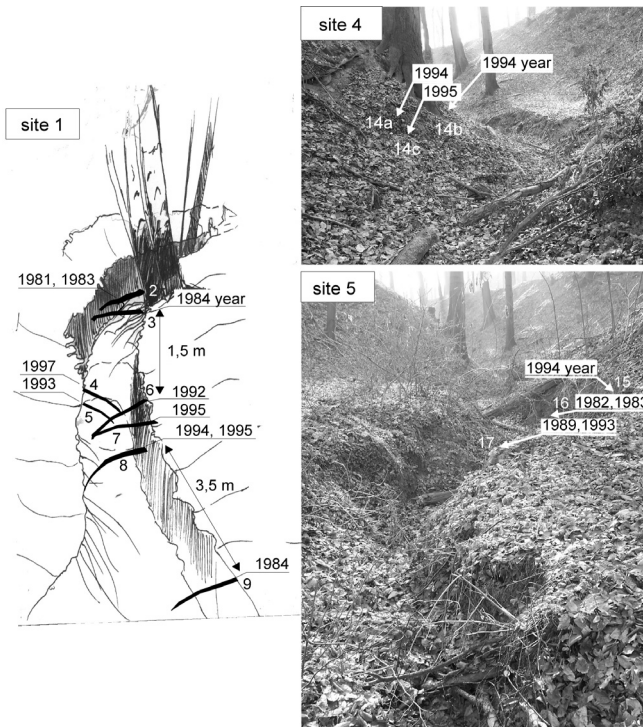


Figure 2: The years of root exposure at sites nos. 1, 4 and 5.

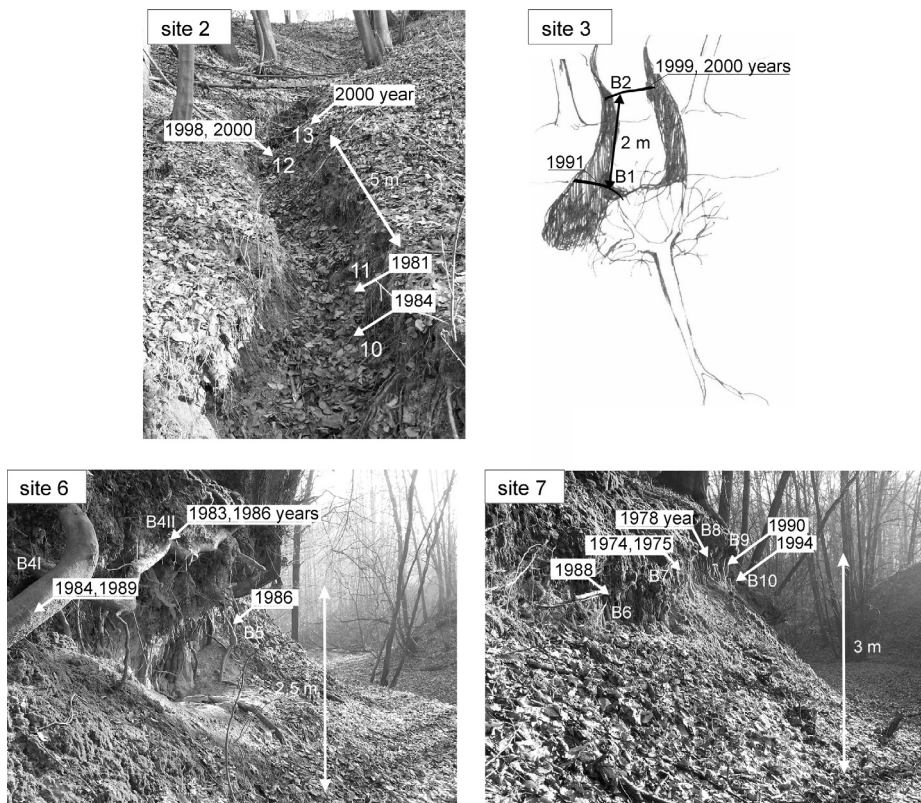


Figure 3: The years of root exposure at sites nos. 2, 3, 6 and 7.

Precision of dating of erosion episodes by means of exposed roots

In order to verify the accuracy of dating erosion events by determining the moment of exposure of roots, a figure has been developed to present the highest daily precipitation in the years 1946-2000 as recorded at the precipitation recording station in Leśnica. Following this, the timing of those events responsible for modelling the valley profile was documented dendrochronologically and added to the figure (Fig. 4). The years in which extreme rainfall events were reported are frequently not the same as the years in which markers of root exposure were reported. One of the reasons may be the fact that the data from the precipitation gauge describes daily precipitation of varying intensity. Some of the extreme precipitation episodes represent heavy local downpours of short duration e.g. a rainstorm in 1991, whereas some are continuous rainfall affecting extensive areas with long duration e.g. rainfall in 1997. The course of a precipitation event has a significant effect on gully erosion; that is why daily precipitation with a similar daily size does not necessarily have a similar impact on gully form (Starkel 2002).

The time of root exposure as identified from the analysis of anatomical changes within its tree rings is not always the same as the actual year of the exposure of that root. Tree rings are shaped in a moderate climate in the period from May to August (Krapiec, Zielski 2004). When a root is exposed at this time, anatomical changes are visible in the area of a tree ring. If the root exposure occurred from January to August, the tree ring may be changed in the same year as the exposure occurred. If the exposure occurred between September and December, the tree ring with anatomical changes will appear the following year. A marker of exposure may be thus recorded in roots one year after an erosion episode.

In the area being studied roots frequently include signs of exposure over one year after an extreme rainfall event (Fig. 4). This results from the fact that subsequent rainfall episodes may not be as intense to erosion continue as the one that initiated the incision. This is why numerous signs of erosion appear in several years following major rainfall episodes in spite of the fact that at that time no precipitation with high intensity was reported. Such a situation can be clearly seen in the case of a downpour in 1991, after which, in the years 1992-1995, as many as 12 roots were exposed (Fig. 5).

The moment of exposure can be dated precisely provided that a root is damaged by material being transported during a downpour. Such situations were observed in the case of roots nos. 3 and 4 at site 1, root no. 10 at site 2 and root B4I at site 6. All of the damaged roots indicated the year 1984 or 1997 as the moment of exposure.

The course of erosion may also be determined by comparing markers regarding exposure from the middle part of the exposed part of the root and the part adjacent to the soil. If the marker is identical, then the exposure occurred as a result of one episode. If the time of exposure recorded in the part of the root adjacent to the soil is younger, then the exposure occurred as a result of at least two erosion episodes. It appears from the research conducted that roots could have been exposed as a result of several erosion episodes, as in case of roots B4I and B4II at site 6 exposed in the years 1984, 1989, 1983, and 1986, respectively.

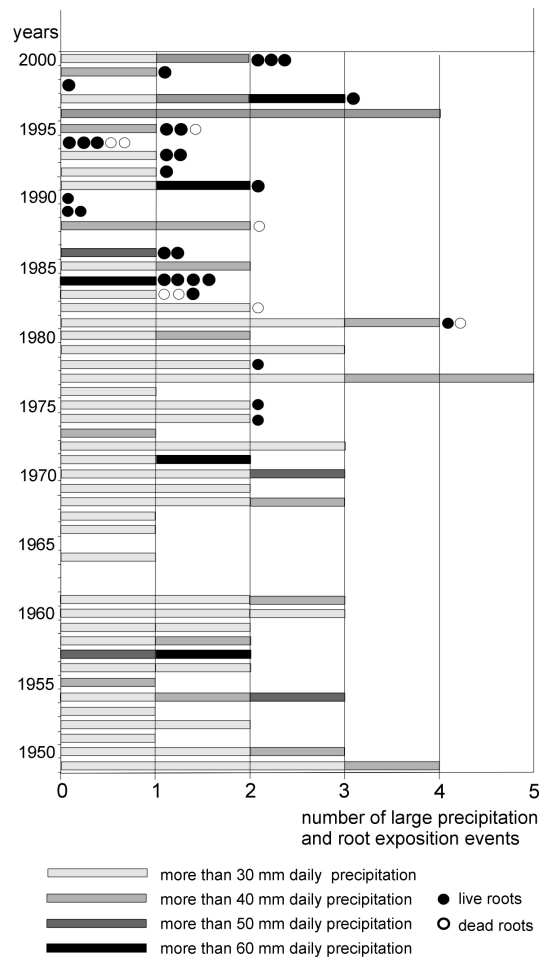


Figure 4: Comparison of root exposure dating and big daily rainfall events recorded at the Lešnica gauge in 1949-2000.

Reasons for erosion in the gully

The results obtained prove that intense erosion occurred at the beginning of 1970s in the gully studied. At the same time, the number of precipitation episodes has decreased since the 1970s, but they have become much more intense with time. This explains the revival of erosion processes in the gully studied.

The markers obtained by means of dating roots point to at least several erosion and deposition episodes shaping the valley under consideration. They may be divided into 4 main groups. In the first group there are 9 markers coming from the years 1974-1983. Probably the erosion the roots document took place in 1971. As many as half of the roots are dead, all of them document exposure in the years 1981-1983, and thus it was a relatively long time after a major precipitation episode in 1971 (Fig. 4). Therefore, they may be roots documenting erosion relating to a rainfall in 1971 or demonstrating an even older major precipitation episode. The second group of markers covers 10 roots exposed in the years 1984-1990. They are the effect of erosion relating to an intense rainfall in 1984. The third and the largest group of roots, including 12 markers, represents the years 1991-1996. They document a major rainfall episode in 1991. The last group constitutes 6 markers documenting the intense rainfall of July 1997.

It seems from root dating that the incision in the valley studied was shaped mainly during the extreme rainfall events in 1971, 1984, 1991 and 1997. A secondary role in shaping the valley studied was played by other precipitation episodes during which the total precipitation was 50% smaller than in the years with extreme rainfall events e.g. 1973, 1977, 1980, 1981, 1985, 1986, 1995, 1996, and 2000. It is surprising that there are no markers regarding erosion older than 1970. The years 1950-1960 had many large precipitation events, although there were not as many as within the last 35 years. Perhaps the relatively small number of sites resulted in no roots documenting erosion in that period being found. It is also possible that roots were exposed in the 1950's, but died since that time.

Course and rate of erosion

Erosion in the bottom of the upper part of the valley (sites 1,4,5) was most intense in the years 1981-1989 and 1992-1995 (Fig. 2). The precipitation episodes of 1971, 1984 and 1991 mainly account for the origin of incisions. The incision in the upper part of site 1 is older and is likely to have occurred during intense rainfall in 1971. In the middle part, the incision is younger and was initiated in 1991. Further down, halfway through the incision, it becomes older again and root no. 7 indicates erosion in 1984. Parts of roots nos. 3 and 4 which were collected from below sediments had wounds covered with earth dating from 1984 and 1997 respectively. This proves that those parts of the roots were initially exposed and later covered with earth again. Site 1 is located at a point where there is a significant increase in slope gradient below the boundary between a head valley and the beginning of a V-shaped gully. There is therefore a higher likelihood of erosion on this boundary between two forms of valley. It seems from the dating evidence that this occurs alternately with the deposition of material coming from the deforested summits. This alternate occurrence of erosion and deposition in the incision does not permit one to estimate the rate of erosion. However, we may state that this takes place slowly taking into account the small gradient of the bottom of the gully examined, so that the material can be transported for small distances. Roots at site number 5 included markers regarding exposure in the years 1982-1989 and 1993-1995. This site was composed of incised rocks in the bottom of the gully lying under dust-like material. This means that the incision was formed during precipitation episodes in 1971 and 1991, similar to the incision at site 1. Those episodes are responsible for the incision of the rocky foundation at this site. At site no. 4 roots were exposed during rainfall in 1991. Their location about 2 m above the bottom of the gully indicates high flow dynamics during the precipitation in 1991.

The incisions are relatively young at sites nos. 2 and 3, located on the valley slope. The vast majority of roots have given markers dating from 1998-2000 (Fig. 3). The incision at site number 2 was initiated in the lower part of the site and afterwards retreated. The lower part of the incision originated in 1984, whereas the upper part developed after rainfall in 1997. It is likely that the incision could also have been initiated during a precipitation episode in 1971 since the exposure of one of the roots in the lower part of the incision was dated to 1981. At a distance of about 5 m, the maximum age difference identified between roots is 19 years. This means that the incision retreats at least 2.6 m/year^{-1} . At site no. 3, the exposure of roots

in the niche took place as a result of a precipitation episode in 1991. Roots in the incision above it were exposed after extensive rainfall in 1997. This implies that the niche occurred as a result of a tree falling, which, at a later date, caused the erosion above the site. Erosion at site no. 4 amounted to 3 m/year^{-1} . The results obtained enable one to conclude that the rate of erosion is much faster in the area of very steep slopes than in the bottom of the upper part of the valley.

At sites nos. 6 and 7 situated at the mouth of the valley erosion markers are generally older than in the upper part of the valley (Fig. 3). The undercutting at site no. 6 was formed during a precipitation episode in 1984. The undercutting at site no. 7 is the oldest one in the middle part of the valley and a precipitation episode in 1971 was responsible for its origin or deepening. Its form was also further developed during freshets in 1984 and 1991. The distribution of areas of undercutting at a height of even 3 m above the valley bottom proves the existence of a water level at least this high during the precipitation episodes which modelled those incisions. Such a high water level in the valley results from catching significant amounts of water from the higher parts of the gully. A very small number of markers of erosion of areas of undercutting from the most recent precipitation episodes and terrace levels in the bottom of the valley prove that it was deepened during older erosion episodes, e.g. 1971 and 1984.

Conclusions

Erosion started in the valley studied within the last 35 years. That erosion has resulted from the occurrence of extensive precipitation episodes taking place since the 1970s. The observed erosion contributes to the deepening and headcut retreat of the valley, as well as to the origin of new incisions on slopes.

The bottom of the upper part of the valley was mainly formed during extensive precipitation episodes in 1984 and 1991. Sediments are being eroded there and the incisions thus formed may be filled with sediments again. The rate of bottom erosion in the upper parts of the valley is relatively slow. The slopes of the valley examined were intensely incised during rainfall in 1997, however, erosion was initiated during earlier precipitation episodes. The incisions on the slopes retreat with a rate of at least $2.5\text{-}3 \text{ m/year}^{-1}$. Erosion occurred at the mouth of the gully during extreme rainfall events in 1971, 1984 and 1991. The valley has deepened as a result of the incision of the bottom of the valley within the last 35 years. This has resulted in areas of undercutting becoming inactive.

References:

- Alestalo, J. (1971): Dendrochronological interpretation of geomorphic processes. *Fennia* 105: 1-140.
- Carrara, P.E., Carroll, T.R. (1979): The determination of erosion rates from exposed tree roots in the Piceance basin. Colorado. *Earth Surface Processes and Landforms* 4: 307-317.
- Daba, S., Rieger, W., Strauss, P. (2003): Assessment of gully erosion in eastern Ethiopia using photogrammetric techniques. *Catena* 50: 273-291.

- Fanning, P.C. (1999): Recent landscape history in arid western New South Wales, Australia: a model for regional change. *Geomorphology* 29: 191-209.
- Gärtner, H., Schweingruber, F.H., Dikau, R. (2001): Determination of erosion rates by analysing structural changes in the growth pattern of exposed roots. *Dendrochronologia* 19: 81-91.
- Hupp, C.R. (1990): A dendrogeomorphic approach to estimating slope retreat, Maxey Flats, Kentucky. *Geology* 18: 658-661.
- Klimek, K. (2002): Human-induced overbank sedimentation in the foreland of the eastern Sudety Mountains. *Earth Surface Processes and Landforms* 27: 391-402.
- Krapiec, M., Zielski, A. (2004): *Dendrochronologia*. PWN, Warszawa. pp. 1-328.
- Malde, H.E., Scott, A.G. (1976): Observations of contemporary arroyo cutting near Santa Fe, New Mexico, USA. *Earth Surface Processes and Landforms* 2: 39-54.
- Schweingruber, F.H. (1996): Tree rings and Environment. Dendroecology. Birmensdorf, Swiss Federal Institute for Forest, Snow and Landscape Research. Berne, Stuttgart, Vienna, Haupt: 222-226.
- Shroder, J.F. (1980): Dendrogeomorphology: review and new techniques of tree-ring dating. *Progress in Physical Geography* 4: 161-188.
- Stankowianski, M. (2003): Historical evolution of permanent gullies in the Myjava Hill Land, Slovakia. *Catena* 51: 223-240.
- Starkel, L. (2002): Change in the frequency of extreme events as the indicator of climatic change in the Holocene (in fluvial system). *Quaternary International* 91: 25-32.
- Vandekerckhove, L., Muys, B., Poesen, J., De Weerd, B., Coppé, N. (2001): A method for dendrochronological assessment of medium-term gully erosion rates. *Catena* 45: 123-161.

The role of flood events in mid-mountain river-bed transformation dated by anatomical changes in exposed roots

M. Matyja

University of Silesia, Department of Quaternary, Paleogeography and Paleoecology, Sosnowiec 41-200,
ul. Bedzinska 60, Poland; Email: marmat80@go2.pl

Introduction

There are three basic methods of estimating lateral erosion rates of a riverbed. The first of them is to compare large-scale maps and aerial photos from different periods. The second method consists of measuring distances from poles or marked trees to a riverbed. The poles or marked trees are stably located up to several or tens of meters from a riverbed. When a riverbed moves horizontally, the distance from poles/marked trees to a riverbed changes. Thus measurement of the distance from poles/marked trees to a riverbed repeated at equal time intervals permits the determination of erosion rates in the riverbed. The third method involves geomorphological mapping of particular sections of a riverbed, repeated at equal time intervals (Florek 1978). A new fourth method is described in this article. This method consists of estimating lateral erosion rates of a riverbed based upon anatomical changes in exposed roots.

In moderate climatic conditions, mountain rivers are supplied by precipitation and snowmelt. The Bilá Opava valley is V-shaped (Fig. 2), has steep slopes and an impermeable valley floor. As a result, there are brief freshets with high water levels during rainfall, during which bottom and lateral erosion occurs. During exceptional floods, discharge can be 150 times greater than during periods of mean flow (Klimek 2005). Floods on the High Jeseník area occur with a more or less constant frequency – about one flood per two years (Gába, Polách 1998). During flooding, spruce (*Picea spp.*) growing in the bottom of the Bilá Opava valley are undercut, and their roots are partly exposed. Roots and trunks are wounded by rocky and coarse woody debris flowing within the river during floods. Therefore, erosive events are recorded as scars on roots and trunks.

The aim of this study is to determine erosion rates in the upper regions of the Bilá Opava River and compare these erosion rates with precipitation and flood data.

Samples of exposed roots were collected in order to determine their dates of exposure.

In this research, anatomical changes of exposed roots were analysed. This method permits the estimation of the dates of erosive events (Gärtner et al. 2001). These dates were compared with recorded precipitation and flood data.

Study area

The High Jeseník is a mid-mountain massif in the Eastern Sudetes Mountains in the Czech Republic (Fig. 1). The High Jeseník massif is dissected by deep, V-shaped valleys (Fig. 2) formed by tributaries of the upper Odra River and upper Morava River. Between the valleys are dome-shaped ridges (Praded 1492 m a.s.l., Keprník 1423 m a.s.l.). There are variable

thickness slope regoliths on the valley slopes. Slopes regoliths are a product of weathering of rocky outcrops during the last glacial period (Klimek 2004). Slope regoliths in the valley bottoms are undercut during floods. When this occurs, the material from slope regoliths is added to the fluvial system and results in the formation of gravel and boulder bars.

Average precipitation in the High Jeseník massif reaches 1400 mm/year. The majority of this precipitation is connected with summer rainstorms. The intensity of precipitation can reach 260-300 mm per 5-12 h (Štekl et al. 2001). Heavy rainfall triggers floods. During floods the speed of running water in the river and intensity of erosion increase.

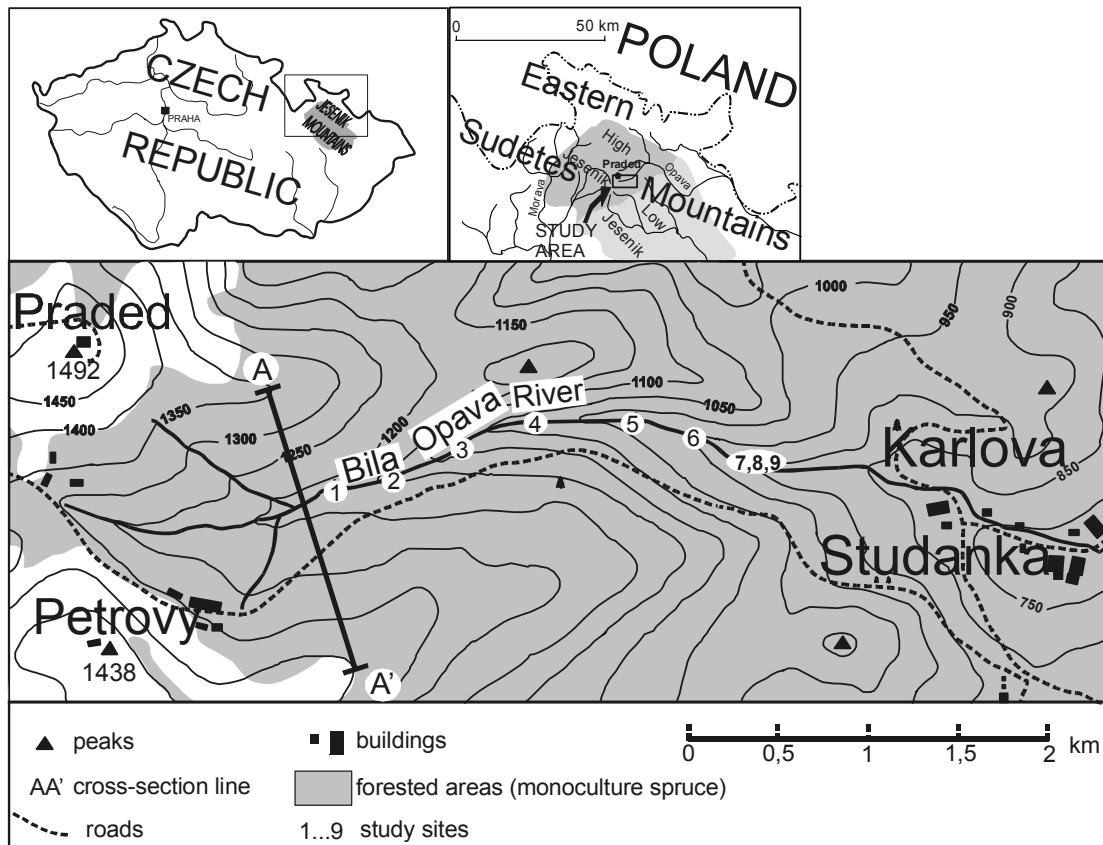


Figure 1: Location of study area.

The study area is located in the upper Bilá Opava Valley, between the sources of the Bilá Opava River and the community of Karlova Studánka. The sources of the river are located about 1360 m a.s.l., on the southern slopes of Praded mountain. Within 4.1 km of the reach of the Bilá Opava River studied, the gradient is about 100 m/km. The Bilá Opava valley is covered by spruce (*Picea spp.*) except for the highest parts of the Praded and Petrovy peaks.

Nine sites were sampled in the bottom of the Bilá Opava Valley, along the Bilá Opava River (Fig. 1).

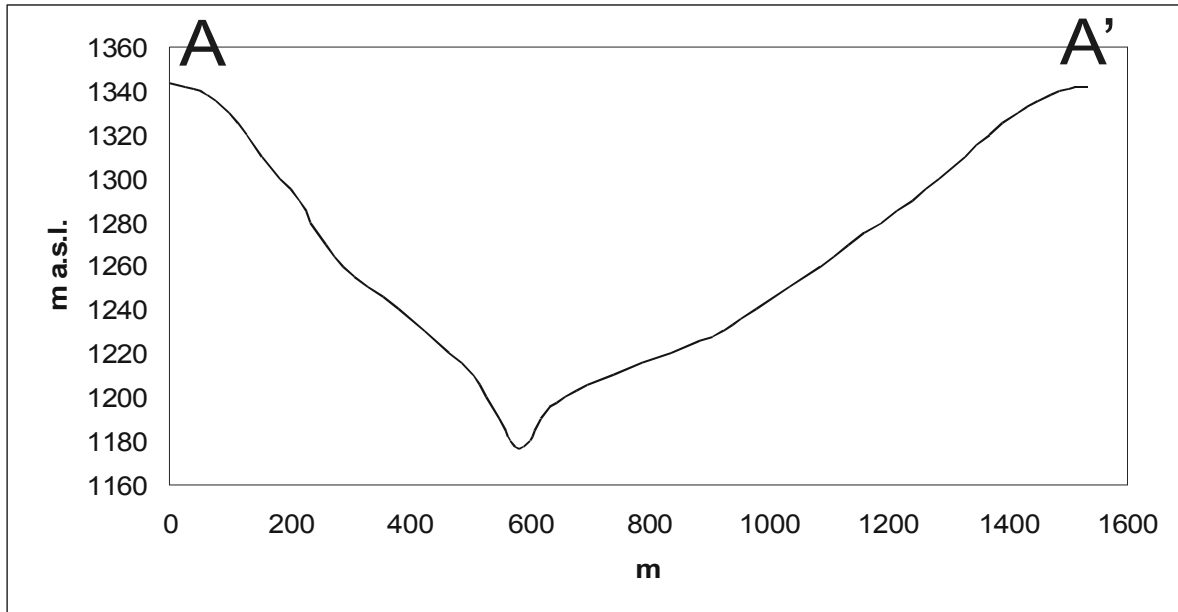


Figure 2: The cross-section through the Bilá Opava valley.

Methods

Transversal cross-sections of the riverbed were measured in the reaches studied. Next, samples of exposed roots were collected using a hand-saw. Distances from roots to the river channel and the difference in height between the root and the mean water level were measured. Samples of the roots were collected at a distance of up to 12 m from the river channel and from 0.2 to 3.6 m above the mean water level. Only samples of exposed roots, whose ends were in the soil, were collected. All of the roots were alive. The longer the exposed root was, the more samples were collected from it.

One sample was taken at the beginning of the exposed part of the root (closest to the trunk), and one at the end of the exposed part of the root (closest to the tip). The rest of the samples were taken between the beginning and the end of the exposed part of the root at regular intervals. Samples from particular roots were collected at distances of 10-60 cm from each other, depending on the root length (Fig. 3). All samples collected were about 7 cm long.

A total of 74 samples of exposed roots were collected from 19 roots (17 spruce roots, 2 beech roots) from 9 trees (each tree representing a separate sampling site).

All samples were cut into cross-sections 1-2 cm thick. These cross-sections were then cut with an upholsterer's knife to expose the wood structure. Samples were then analyzed using a binocular microscope. The analysis was to estimate the number and calendar dates of tree rings with anatomical changes (Fig. 4), as well as to estimate the number of tree rings that covered individual scars (that is, the number of years since the wound event). The anatomical changes investigated in exposed roots were (Fig. 4):

- increase in the width of tree rings
- increase in the width of late wood in relation to early wood
- decrease in the size of cells
- scars in the root wood

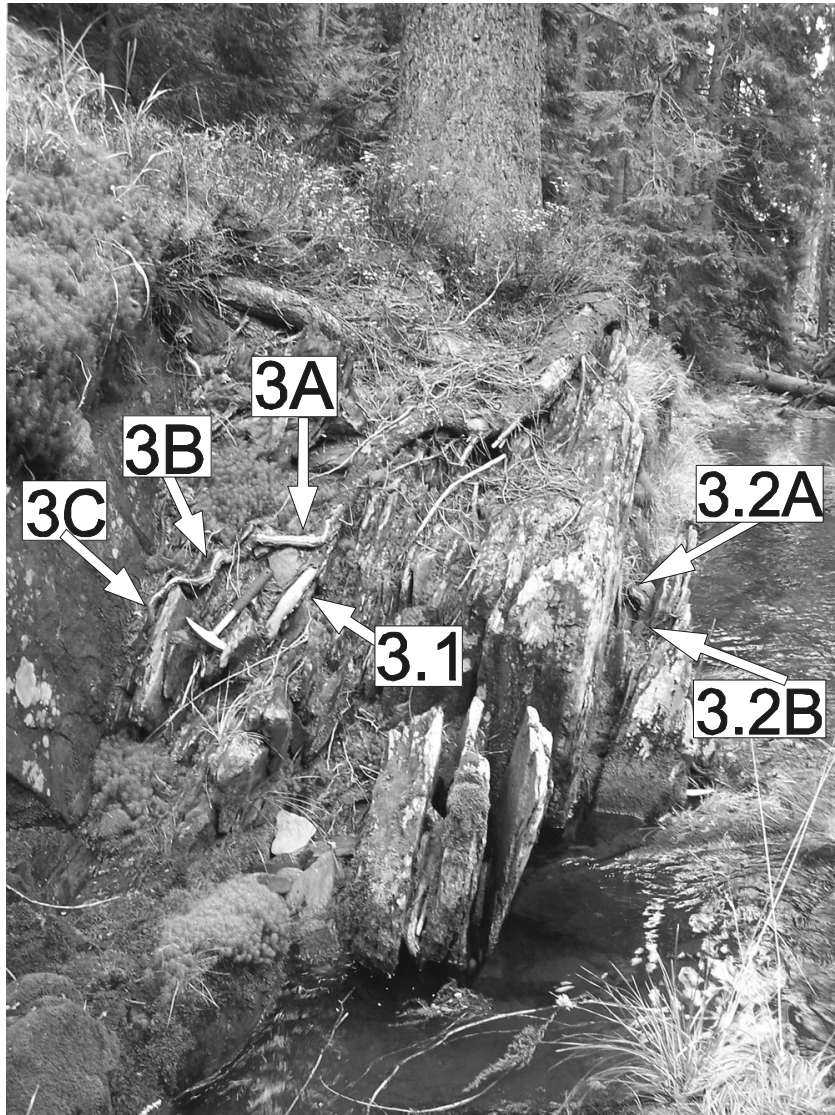


Figure 3: Example of an exposed root sampling site.

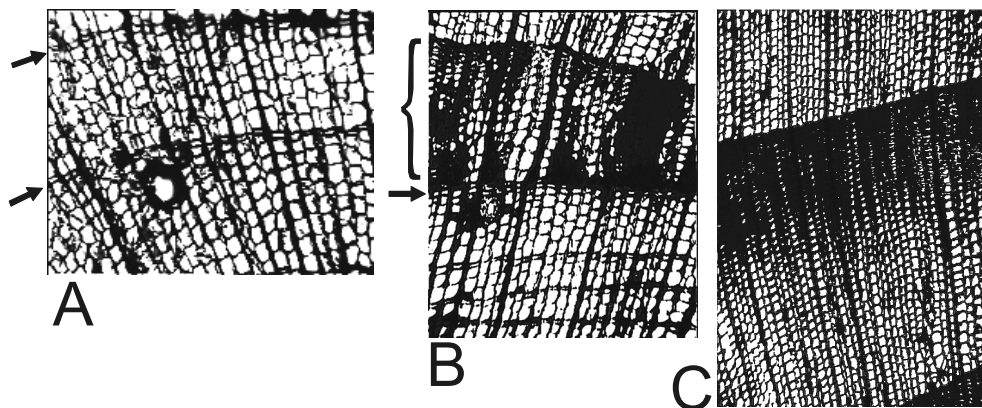


Fig. 4: An example of a slice of the root with anatomical changes. A) Fragment of the spruce root cross-section (sample 5A) with narrow latewood (marked with black arrows) before exposure. B) Fragment of the spruce root cross-section (sample 5A) with a considerable increase in the width of tree rings following exposure – indicated by a bracket. Exposure date marked with an arrow. C) Fragment of a spruce root cross-section (sample 5A) with a wide area of latewood – after root exposure.

The number of tree rings with anatomical changes marks the date the erosive event occurred. A microscope (Evolution ME 200B) with an attached digital camera permitted the taking of photographs of the root samples as well as a more precise estimate of tree rings in difficult cases (in which thin sections prepared using a sledge microtome were analysed). The date of exposure was recorded and rate of lateral erosion estimated as follows: The horizontal distance between fragments of root exposed at different times was determined. Next, the distance was divided by the difference in the date of root exposure, for example 50 cm/5 years = 10 cm/year. Only one sample from a particular sampling site was used to estimate the rate of lateral erosion.

The exposure and wound dates of roots so determined were correlated with their location in the longitudinal profile of the river. These dates were also correlated with their height above mean water level in the river.

Dates of root exposure and wounding were compared with precipitation and flood data. Flood data for the High Jeseník is comprised of a composite of archive data (Gába, Polách 1998) consisting of data from historical sources, museums, communal archives, meteorological and climatological annuals, for example. This data spans the period from 1472 AD to 1997 AD. In this article, data from 1900 to 1997 was used.

Precipitation data – maximum monthly precipitation – came from the Karlovice gauge station, situated about 15 km east of Karlova Studánka. These data span the period 1976 to 1997.

Results

From all 74 samples, 68 dates of exposure and wounding of roots were determined. Particular roots may simply be exposed (i.e. Sample 1A), or exposed and wounded simultaneously (i.e. Sample 1B), or exposed and wounded later during the next erosive event (i.e. Sample 3A) (Tab. 1).

Dates of root exposure and injury span almost the entire 20th century and the beginning of the 21st century. In this period, there were at least 35 erosive events in the Bilá Opava section under research (Tab. 1). The dates of root exposure and injury are not evenly distributed in time. More events are dated to the second half of the 20th century. The largest number of determined dates – 17 in total – comes from the year 1997. In July of this year there was a catastrophic flood in Central Europe (This flood covered a large part of Poland, Germany and the Czech Republic). The number of exposure dates from other years is considerably less and fluctuates between 1 and 4 (in 1990).

There is a connection between the date of exposure or root injury and root location along the longitudinal slope of the river. Most of the 1997 dates were recorded on sampling sites 1-6 (Tab. 1). The bottom of the Bilá Opava valley in this section is very narrow – not wider than 20 m. In many sites along this section the width of the bottom of the valley is the same as the width of the channel and amounts to only several meters. Thus the erosional force of the river is great. Within sampling sites 7-9 only three 1997 dates were recorded. Within these sampling sites the bottom of the valley is wider than 100 m, so the erosional force of the river during flooding is diffuse.

Table 1: Dates of exposure and wounding of roots on particular sites and their height above mean water level.

SITE NUMBER	SAMPLE NUMBER	TREE SPECIES	EXPOSED ROOT LENGTH [M]	HEIGHT ABOVE MEAN WATER LEVEL [M]	DATE OF EXPOSURE AND/OR WOUNDING OF THE ROOT. THE YEAR OF THE WOUND IS MARKED WITH A LETTER "S"
1	1A	SPRUCE	0,6	0,2	1997
	1B			0,4	S 1997
	1.1A		0,5	0,8	1997
	1.1B			0,8	1967
2	2A	SPRUCE	0,7	0,8	1912
	2B			0,8	1957
3	3A	SPRUCE	0,7	1,5	1991, S 1997
	3B			1,3	1991, S 1997
	3C			1	1986, S 1997
	3.1		0,35	1,3	S 1949, S 1951, S 1990, S 1997
	3.2A		0,7	0,8	1931, S 1997
	3.2B			0,8	1958, S 1997
	3.3			0,2	S 1964, S 1995
4	4A	SPRUCE	1,5	1	1988
	4B			1	1990
	4C			1	1992, S 2002
	4.1A		0,5	0,5	1961
	4.1B			0,4	S 1957, S 1969
5	5A	SPRUCE	1	0,8	1989
	5B			0,65	1997
	5C			0,5	1997
	5.1A		1,1	0,8	1997
	5.1B			0,8	1997
	5.1C			0,8	1997
6	6A	SPRUCE	1,2	1,3	1982
	6B			1,1	1983
	6C			0,8	1983, S 1994, S 2000
	6.1A		0,8	1	1974
	6.1B			0,9	1973
	6.1C			0,8	1977
7	7A	BEECH	0,8	0,7	NO INDICATION
	7B			0,7	NO INDICATION
	7C			0,7	NO INDICATION
	7.1A		0,7	1,7	1973
	7.1B			1,45	1977
8	8A	SPRUCE	3	3,5	1982
	8B			3,4	1997
	8C			3,2	2003
	8D			3	1997
	8E			2,6	S 1976, S 1987, S 1992
	8F			2,2	1983, S 1991, S 1997
	8G			1,8	NO INDICATION
	8.1A		0,8	3,5	1980
	8.1B			3,4	1986, S 1994
9	9A	SPRUCE	0,6	3	1980, S 1981
	9B			2,75	1979
	9C			2,5	1978
	9.1A		0,6	2,5	1998
	9.1B			2,2	NO INDICATION
	9.1C			2	NO INDICATION
	9.2A			1,1	3,5
	9.2B		3,5		1990
	9.2C		3,5		S 1979, S 1985
	9.2D		3,5		1973

There is no correlation between the date of exposure or wounding of the root and root height above the mean water level in the river (Tab. 2).

The height of the exposed roots above mean water level can be classified according to the water level during floods. The highest water level during floods – from 3.2 to 3.6 m above mean water level – took place in the years: 1973, 1979, 1980, 1982, 1985, 1986, 1990, 1994 and 1997. Root exposure and wounding in 1997 took place at almost all elevations above the mean river level – from 0 to 3.2 m (Tab. 2).

Exposed and wounded roots located highest above mean water level are on study reaches 8 and 9 – along the lower course of the Bilá Opava River. This is probably a result of the increase of the height of the flood wave down river during floods.

Roots growing on the channel can be wounded multiple times (e.g., sample 3.1 was wounded 4 times). The oldest date of exposure is 1912 for sample number 2. This root is located about 1 m from the channel and indicates the long-term horizontal stability of the riverbed. On the other hand, it seems that spruce tolerate the erosional activity of the river well. Spruce growing near the channel often envelope big boulders they are growing upon within their roots (fig. 3). Therefore, they are rarely undercut and felled into the channel. In the course of the study, the rate of lateral erosion of the river was determined for sampling sites 2,3,4,5,6 and 7 and fluctuated between 0.55 cm/year and 10 cm/year. The rate of lateral erosion was not determined for sampling sites 1,8 and 9. The exposed roots at the sampling site 1 were parallel to the riverbed. On sampling sites 8 and 9 the exposed roots were on a slump between a river terrace and gravel and a boulder bar at a distance of about 12 m from the river channel.

Table 2: Dates of exposure and wounding of the root and their height above the mean water level in the river.

HEIGHT ABOVE MEAN WATER LEVEL [M]	DATE OF EXPOSURE AND WOUNDING OF ROOT SAMPLES
(3,4-3,6)	1973, 1979, 1980, 1982, 1985, 1990, 1990
(3,2-3,4)	1986, 1994, 1997
(3-3,2)	2003
(2,8-3)	1980, 1981, 1997
(2,6-2,8)	1979
(2,4-2,6)	1976, 1978, 1987, 1992, 1998
(2,2-2,4)	- - -
(2-2,2)	1983, 1991, 1997
(1,8-2)	- - -
(1,6-1,8)	1973
(1,4-1,6)	1977, 1991, 1997
(1,2-1,4)	1949, 1951, 1982, 1990, 1991, 1997, 1997
(1-1,2)	1983
(0,8-1)	1973, 1974, 1986, 1988, 1990, 1992, 1997, 2002
(0,6-0,8)	1912, 1931, 1957, 1958, 1964, 1967, 1977, 1983, 1989,1994, 1995, 1997, 1997, 1997, 1997, 1997, 1997, 2000
(0,4-0,6)	1961, 1997
(0,2-0,4)	1957, 1969, 1997
(0-0,2)	1997

Comparison of exposure dates and wounding of roots in relation to flood and precipitation data

Double tree rings can appear within tree stems, e.g. caused by heavy ground frost shortly after the beginning of vegetation growth period. A missing tree ring can be the result of very unfavourable conditions, e.g. extremely cold winters or insects outbreaks (Krapiec, Zielski 2004). The roots growing under ground are in great part isolated from external influences. However, tree rings are created simultaneously in the trunk and in the roots. So double and missing tree rings can appear in the root tree rings. Exclusion (or confirmation) of the appearance of double or missing tree rings is only possible by analysing annual tree rings in the trunk. However in the course of these researches only roots were analyzed. Thus the comparison of exposure dates and wounding of roots with flood and precipitation data was done assuming ± 1 year accuracy (Tab. 3).

Table 3 shows the comparison of dates of root exposure and injury with archival flood data in the High Jeseník area (Gába, Polách 1998). Fig. 5 shows the comparison between dates of exposure or wounding of roots and precipitation data – maximum monthly precipitation – from the rain gauge station in Karlovice.

In total 32 dates only correspond with flood data (Tab. 3), 2 dates only correspond with precipitation data (Fig. 5), and 2 dates correspond with both of these sets of data (Fig. 5).

Table 3: Comparison between dates of exposure or wounding of roots and flood data in the High Jeseník area.

SAMPLE NUMBER	DATE OF EXPOSURE AND/OR DAMAGE	FLOOD DATA (FROM GÁBA, POLÁCH, 1998)
2A	1912	1911
3.2A	1931	1931
2B, 4.1B	1957	1958
3.2B	1958	
3.3	1964	1965
1.1B	1967	1966
6.1B, 7.1A, 9.2D	1973	1972
8E	1976	1977
6.1C, 7.1B	1977	
9C	1978	
1A, 1B, 1.1A, 3A, 3B, 3C, 3.1, 3.2A, 3.2B, 5B, 5C, 5.1A, 5.1B, 5.1C, 8B, 8D, 8F	1997	1997

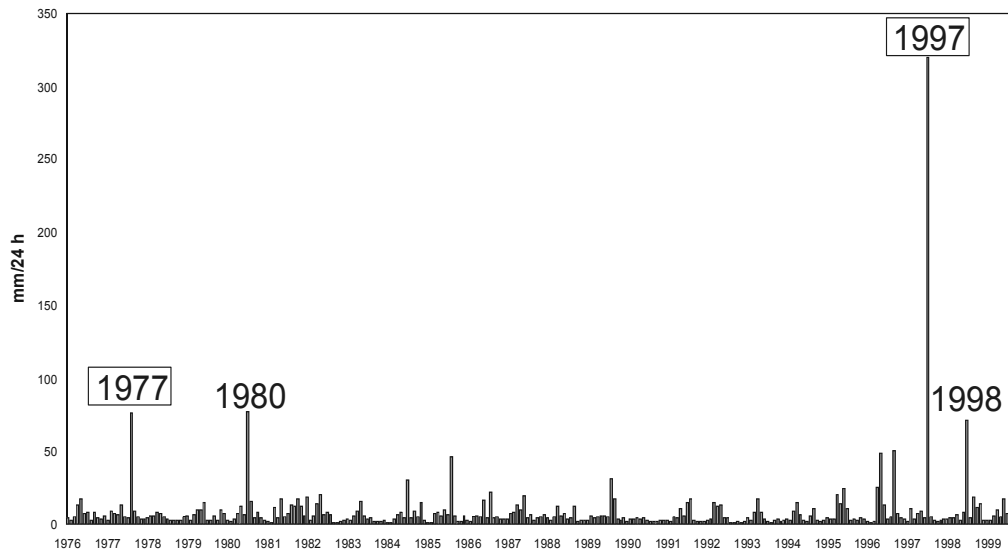


Figure 5: Comparison between dates of exposure or wounding of roots and precipitation data from the rain gauge station in Karlovice. Dates in black rectangles match flood data (see Table 3). Other dates which only match precipitation data – are: 1980 (samples 9B, 9.2C, 9A, 8.1A, 9A), 1998 (sample 9.1A).

In all, 36 dates (52,9 %) of exposed and wounded roots corresponded with flood and precipitation data. The rest of the events – 32 dates (47,1 %) – have no correspondence with extreme flooding or precipitation records. The conclusion can be drawn that local, unrecorded floods were also significant for the transformation of the Bilá Opava channel.

Conclusions

1. The dendrochronological method used in this study enabled investigations to be made on the erosion rates in rivers.
2. This method has the following limitations:
 - It is not always possible to estimate the date of exposure with precision to one year.
 - Ambiguity exists in estimating the year of occurrence of erosive events. This results from the lack of production of tree rings from September to April. For example, both the exposure of the root between September and December in the year 2004 and exposure of the same root between December 2004 and April 2005 will be recorded in the wood structure in the year 2005.
 - Gradual changes in wood structure are more difficult to interpret than rapid changes in wood structure.
 - Precision in the reconstruction of the erosive events in time and space depends on the number of samples of roots collected. The larger the number of samples collected, the more precise the reconstruction.
3. This method provides the following opportunities:
 - When the root net is dense, a large number of samples can be collected within in a small distance. This allows precise reconstruction of the history of root exposure.
 - All roots were investigated from transversal cross-sections in contrast to sampling with increment cores. This method is better able to avoid errors from missing or wedging rings.

- Scars within the root mark the time of exposure of the root beyond a shadow of doubt.
 - Several erosive events can be recorded in one root. The older and longer the root is, the more dates can be recorded in its structure.
4. Dates of exposure of roots noted in the Bilá Opava valley span almost the entire 20th century and the first years of the 21th century. This exposure is often caused by intense, dynamic floods. Through the decades the frequency with which flooding occurs is more or less constant. Most of the dates identified came from the year 1997 – in all 17 dates.
 5. The riverbed is fairly stable on all of the sections studied in this research.
 6. In the Bilá Opava valley, local floods significantly influence the geomorphological processes in the riverbed.

References

- Gärtner H., Schweingruber F.H., Dikau R., (2001): Determination of erosion rates by analysing structural changes in the growth pattern of exposed roots. *Dendrochronologia*, 19, 1: 81-91.
- Florek E., (1978): Wybrane metody badania współczesnych zmian koryta rzecznego na przykładzie dolnego odcinka Bobru. *Badania Fizjograficzne nad Polską Zachodnią, T. 31, Seria A, Geografia Fizyczna*: 348-359.
- Gába Z., Polách D., (1998): Historie povodni na šumperském a jesenickém okrese. *Severní Morava*, 75: 3-28.
- Klimek K., (2004): Transfer pokryw stokowych z NE skłonu Jesioników (Sudety Wschodnie) pod wpływem zdarzeń antropogenicznych i impulsów klimatycznych. [w:] *Geologiczne i środowiskowe problemy gospodarowania i ochrony doliny górnej i środkowej Odry. Państwowy Instytut Geologiczny*. Wrocław: 45-57.
- Klimek K., (2005): Terasy rolne w Górach Opawskich: rola rolniczej kolonizacji stoków w transformacji środowiska przyrodniczego. [w:] *Human Impact on Mid Mountain Ecosystems, vol. 1, Sosnowiec*: 9-13.
- Krapiec M., Zielski A., (2004): *Dendrochronologia*. PWN. Warszawa. 256-275, 239-242.
- Štekl J., Brazdil R., Kakos V., Jeř J., Tolasz R., (2001): Ekstremni denni sražkove uhrny na uzemi ČR v období 1879-2000 a jeich synoptyce příčiny. Praha. 127p.

Debris flow activity and relevant effects on the tree radial growth. An example from the Central Italian Alps

M. Santilli & M. Pelfini

*Dipartimento di Scienze della Terra "A. Desio", Sezione di Geologia e Paleontologia, Università di Milano,
Via Mangiagalli 34, 20133 Milano, Italia
Email: maurizio.santilli@unimi.it*

Introduction

Debris flows are one of the most frequent mass movements in the alpine environment and represent an important element of geomorphological hazards. Thus, dating the past events is important to estimate the evolution of their intensity and frequency (Corominas and Moja 1999, Santilli 2005). Classical dendrogeomorphological methods usually employ the analysis of corrasion scars, reaction wood and abrupt growth changes (Gärtner et al., 2003, Alestalo, 1971, Heikkinen 1994, Hupp 1984). However, while the first two types of signals are easily recognizable, growth variations are often more difficult to be interpreted.

In fact, the accumulation of sediments at the tree base due to depositional processes determines a change of the environmental conditions influencing the dimensions of annual growth rings masking the physiological age trend (for a quantification of the abrupt growth changes see, e.g., Z'Graggen 1987). Generally, when a considerable part of a tree stem is buried its radial growth abruptly slows down (Shroder 1978, Heikkinen 1994). However, when the burial is limited, growth can also increase if the tree benefits from a reduced competition for light, water and nutrients thanks to the destruction of other specimens, or the possible richness in nutrients coming from the deposited sediments (Heikkinen 1994). Moreover, also the decomposition of the buried herbaceous vegetation can release nutrients beneficial for the roots (Alestalo 1971).

The dating of depositional processes based on the interpretation of the ring-width variations is therefore often difficult just for the variability of the responses. Moreover, it is sometimes difficult to determine if some variations in the radial growth are really caused by geomorphological processes or by other factors (Heikkinen 1994). Hence, it is necessary to compare the radial growth of the affected trees with the one of undisturbed trees growing in the same area on a site, where the analysed process is definitely not present (Alestalo 1971, Gärtner et al. 2004). Finally, growth changes are not always so abrupt to be clearly identified and dated, since sometimes only gradual variations occur that cannot easily be recognized or quantified.

The presented work studies the Val Paolaccia fan, in the Valle del Gallo (upper Valtellina, Central Italian Alps), where both dendrochronological and geomorphological researches have been carried out on several fans occupying the valley bottom (Santilli et al. 2002, Santilli and Pelfini 2002, 2005, Pelfini and Santilli 2003, Santilli 2005, Pelfini et al. 2005a, b). This fan is characterized by some weak debris flows covering the vegetation and the tree stem bases with a gravel layer few tens of centimetres thick, without however causing

damages or inducing the development of compression wood. Consequently this situation makes it difficult to date some of the landslide events, since no clear suffering of the influenced trees is visible. Our aim is to study the effects of the burial of the stem base on radial growth and to use this response as a complementary dating method to the use of scars and compression wood for the reconstruction of the chronology of debris flows that affected the Val Paolaccia fan.

Also sheetfloods characterize the studied fan. They deposit silt layers few centimetres thick without causing mechanical damages to the trees. In this case, the analysis of the radial growth alterations has allowed us to date some sheetfloods, although different possibilities of the trees reaction to this disturbance have been identified (Pelfini et al. 2005a).

Study area

The Val Paolaccia fan (Fig. 1-2) is located at the head of the Valle del Gallo, connected with the Passo di Fraele (1952 m), which constitutes the watershed with the contiguous Valle di Fraele. The southern portion of the fan is turned towards the latter and it has been stable for a long time, while the northern one, facing towards the Valle del Gallo, is affected both by debris flows and by sheetfloods. A mountain pine forest (*Pinus montana* Miller) dominates the vegetation of the studied valley.

The fan has a maximum radius of approximately 1400 m and it extends until the base of the opposite slope at an altitude between 2050 and 1930 m. Normally, water flows on the surface only in the apex part. A single big main channel (A in Fig. 1) exists. It is delimited by numerous areas and terraces of various ages and with a various degree of vegetation cover. This channel, which is narrow and deep in its upper part, considerably widens in its distal part, where there are also groups of trees (Fig. 2) with a buried stem base.

From the hydrographical left of the main channel, a lateral channel (B in Fig. 1) originates and big trees grow on a debris surface.

The analysis of the aerial photos and field observations show that the activity of this fan has been rather intense in recent times, since several areas have been covered by debris layers some centimetres to few decimetres thick. These debris flows did not manage to destroy even very small trees, which are frequently found only partially buried. Moreover, the formation of some small erosion channels uncovered the herbaceous vegetation present on the original soil in a decomposition stage.

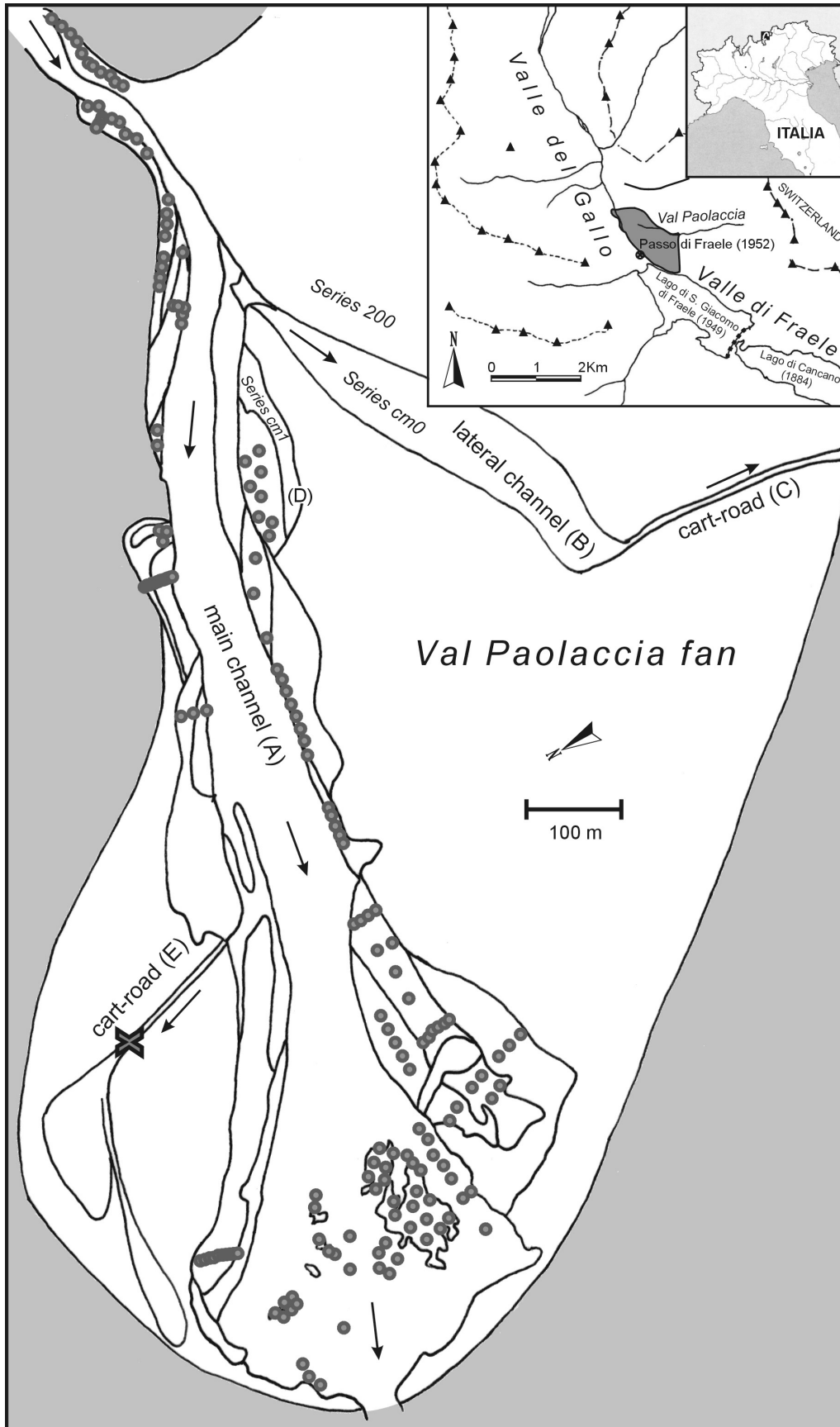


Figure 1: Location of the study area and morphologic outline of the Val Paolaccia fan. The grey circles indicate the position of the trees sampled for the debris flow dating. The X indicates the erosion of the cart-road showed in figure 8.



Figure 2: Panoramic view of the Val Paolaccia fan (photo by Santilli 1998)

Methods

In order to analyse the effects of the stem base burial on the radial growth, to be used as a debris flow dating method, a study along the lateral channel of the fan (B in Fig. 1) has been carried out. This channel does not cut the fan surface and it is not delimited by banks. It represents the new path of debris flows which have recently affected part of the forest previously undisturbed with the deposition of 20-30 cm of gravels. In fact, it is not visible in the aerial photographs of 1981 (flight TEM 1 Regione Lombardia). Debris simply overlap the herbaceous vegetation and the soil of the fan surface and cover the stem bases of the trees, many of which, however, survived the events and still show a vertical stem without clear damages. The surface is made of debris with no herbaceous vegetation which is a probable sign for a recent deposition. Locally, where the debris layer has been eroded, the dry herbaceous cover on the old surface can be seen. In this channel 24 trees have been sampled (called Series cm0, Fig. 1) taking three cores from every specimen approximately one meter from the ground.

Moreover, a marginal zone of the main channel (D in Fig. 1) has been identified, too. This zone is characterized by trees with buried stem bases as well, but they grow on a debris surface partially covered by herbaceous vegetation. Also in this case it is a debris accumulation, 10-20 cm thick, of recent deposition covering the base of the pine forest. However, this surface can be considered older compared with the lateral channel (B). 23 trees (called Series cm1, Fig. 1) have been sampled taking two cores from each specimen in this area.

The growth curves of all samples have been constructed measuring the ring width with program TSAP (Rinn 1996) and through image analysis by using software WINDENDRO. Cross-dating has been executed with program COFECHA (Holmes 1983). Individual chronologies of the single trees and a mean chronology of the population have then been

obtained. In this case the comparison of the mean chronologies, besides that of the individual ones, is justified since all the trees belonging to each of the two groups have been involved in the same event and therefore they should supply similar responses.

All the single tree curves and the mean chronologies have then been compared with two reference chronologies, one built in stable areas of the same fan (called Series 200, Fig. 1) and the other built outside the fan, on a slope not affected by debris flows (called Series 400). Chronology 200 is made up of 45 samples taken from 18 trees and spans 217 years from 1785 to 2001. Chronology 400 is composed of 59 cores extracted from 30 trees and spans 138 years from 1864 to 2001. The reference chronology built on the fan has been used to have a longer curve, since the trees living on the slope are decidedly younger than those living in the lateral channel (B).

Other comparisons have been made taking into consideration the growth variation percentage of each year compared to the average of the four previous ones (modified from Schweingruber et al. 1986), in the period 1960-2001, and the mean ring width relevant to the years following the identified variation compared to that of a same number of years preceding the event.

Once the effects of the burial on the mountain pine growth have been established, the sequence of debris flows occurred on the Val Paolaccia fan has been reconstructed. The dendrochronological dating has been carried out by sampling about 200 trees, 167 of which have been used, located along the main channel (Fig. 1). In particular, besides the alterations of the radial growth, based on the analyses of Series cm0 and cm1, the development of compression wood and the presence of corrosion scars have been examined. The accuracy of the dating of many samples has been verified through cross-dating with the reference chronologies.

Finally, an old cart-road dismantled by debris flows at the fan border has been analysed (E in Fig. 1). Four sections of exposed roots and five cores from stems of as many trees fallen from the banks of the formed channel have been taken in order to establish the age of the latter.

Results and discussion

Comparison between Series cm0 and reference chronologies

The mean chronology cm0 (Fig. 3) covers the period from 1783 to 2001. The curve shows oscillations synchronised with those of the reference chronologies. However, in 1991, it shows an increase contrasting with the decrease in the reference chronologies and this trend lasts until 2001.

The comparison of the growth variation percentages of every year with the average of the four previous ones (Fig. 4) indicates that, starting from 1960, they agree until 1990. For this year, all the chronologies show substantial reductions. On the contrary, in 1991, while the reference curves still endure reductions of approximately -20%, the decrease of chronology cm0 is only -3.4%.

The mean ring width in the period from 1991 to 2001 compared with the one in the period from 1980 to 1990 shows that the reference chronologies respectively decreases from 670 to 520 and from 560 to 510 microns, while Series cm0 increases from 530 to 720 microns. Results obtained indicate that the lateral channel (B) of the fan, which surely originated after 1981, was formed by a debris flow happened in the dendrologic year 1991 and that the burial of the stem base of trees which are not bent or wounded by the debris flows has caused an increase in the radial growth.

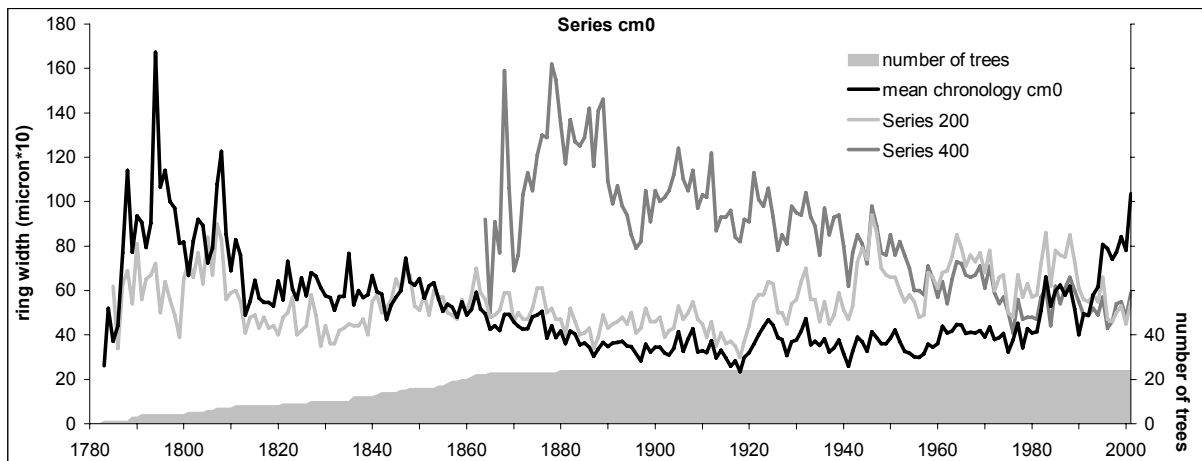


Figure 3: Comparison between chronology cm0 and reference chronologies. The number of trees composing the mean cm0 is also shown.

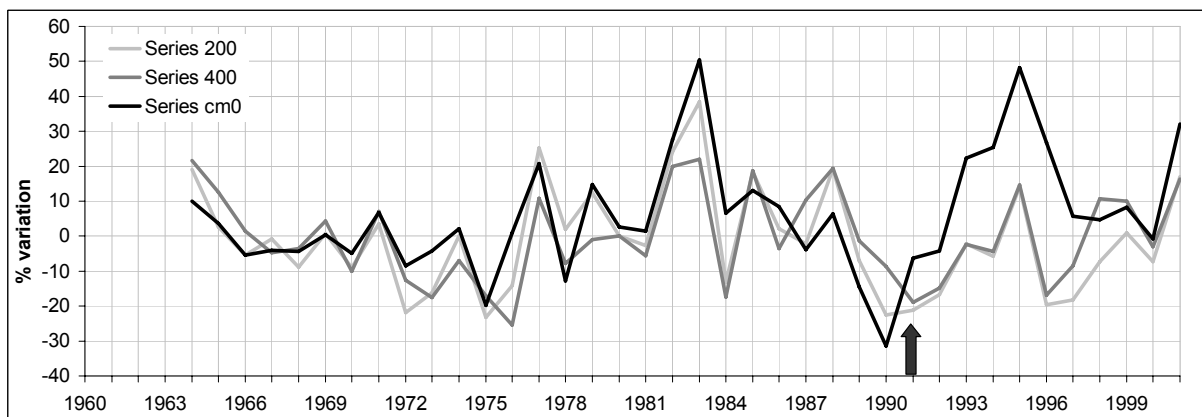


Figure 4: Comparison between the growth variation of one year and the average of the 4 previous years of chronology cm0 and of the reference chronologies.

Comparison between Series cm1 and reference chronologies

Also in the second analysed case (D area, Series cm1 in Fig. 1) the same comparison analysis has been carried out, but without having any information from the aerial photos.

The chronology cm1 (Fig. 5) spans the period from 1738 to 2001 and shows oscillations in phase with those of the reference chronologies until 1990, when the curve shows an increase in contrast with the decrease in the reference curves. This growth release lasts until 1995.

The comparison between the growth variation percentages of every year with the average of the four previous years (Fig. 6) shows that both the chronologies agree until 1989, while in 1990 Series cm1 endures a variation of +14.0%, while the reference ones reduce (-22,4% for Series 200 and -8,7% for Series 400).

The mean ring width in the period from 1990 to 2001 compared with the one of the period from 1978 to 1989 shows that the reference chronologies respectively decreases from 660 to 530 and from 550 to 510 microns while Series cm1 increases from 370 to 670 microns.

Therefore, we can deduce that the debris flow which has affected area (D) occurred in the dendrologic year 1990, confirming, moreover, the type of reaction of the trees to burial.

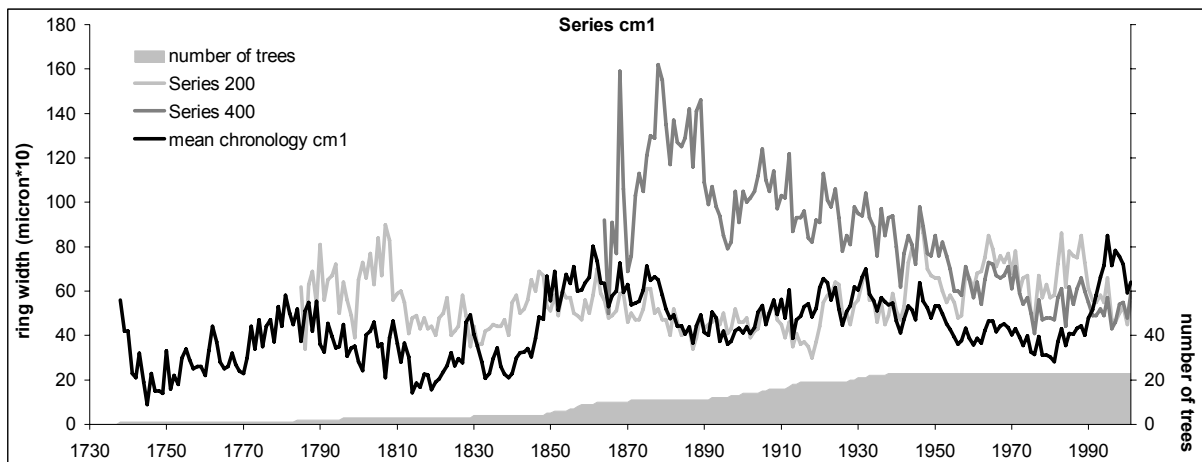


Figure 5: Comparison between chronology cm1 and reference chronologies. The number of trees composing the mean cm1 is also shown.

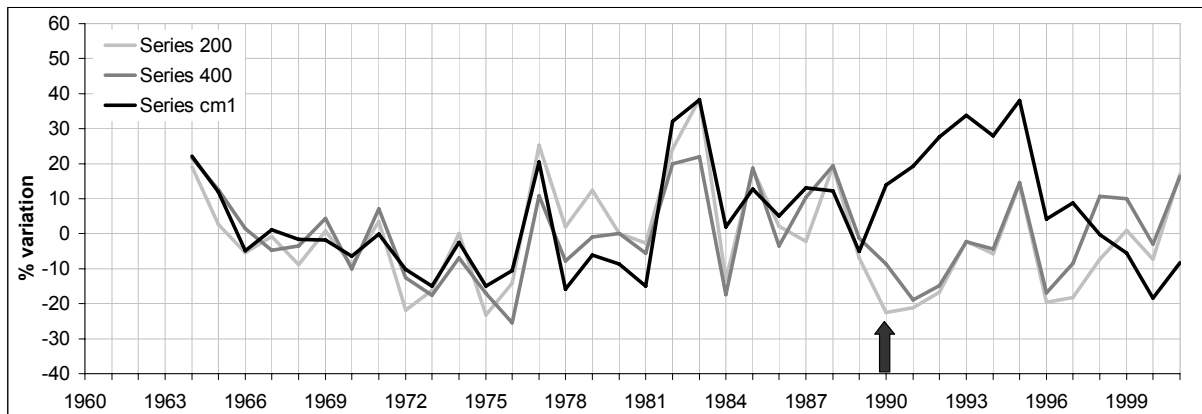


Figure 6: Comparison between the growth variation of one year and the average of the 4 previous years of chronology cm1 and of the reference chronologies.

Chronology of debris flows in the Val Paolaccia

The abrupt radial growth releases, emerged from the analysis presented above, have been used for the dendrochronological reconstruction of the other debris flows occurred on the Val Paolaccia fan, together with the other types of damage and disturbance caused by these processes and more easily recognizable (scars and compression wood).

Altogether, 35 possible debris flows occurred between 1875 and 2001 have been dated (Fig. 7), among which are also two events happened in 1990 and 1991, almost certainly corresponding to the ones dated with Series cm0 and cm1.

Since the characteristics of the debris and the vegetative cover indicate a more recent surface of the lateral channel (B) comparing to area (D), we can deduce that the first one has been affected by other debris flows (e.g. in 1997, 2000 or 2001). This can be suggested also by the fact that while the chronology cm1 shows a positive growth variation from 1990 to 1995 followed by a decrease, the growth release in the Series cm0 lasts until 2001.

Debris flows have repeated at 1 to 8-year intervals (3.5 years on average) and are grouped in time so that more events which have followed after 1-2 years are spaced out by some years of stasis.

Among all the identified debris flows, the one happened in 1951 particularly stands out. It has been recorded by 44 trees (about a quarter of the total), confirming itself as the event of greatest intensity among the dated ones. Moreover, the 1951-event has been identified in other fans located in the Valle del Gallo (Santilli 2005), too. Other debris flows with strong intensity occurred in 1899, 1917, 1948 and 1977.

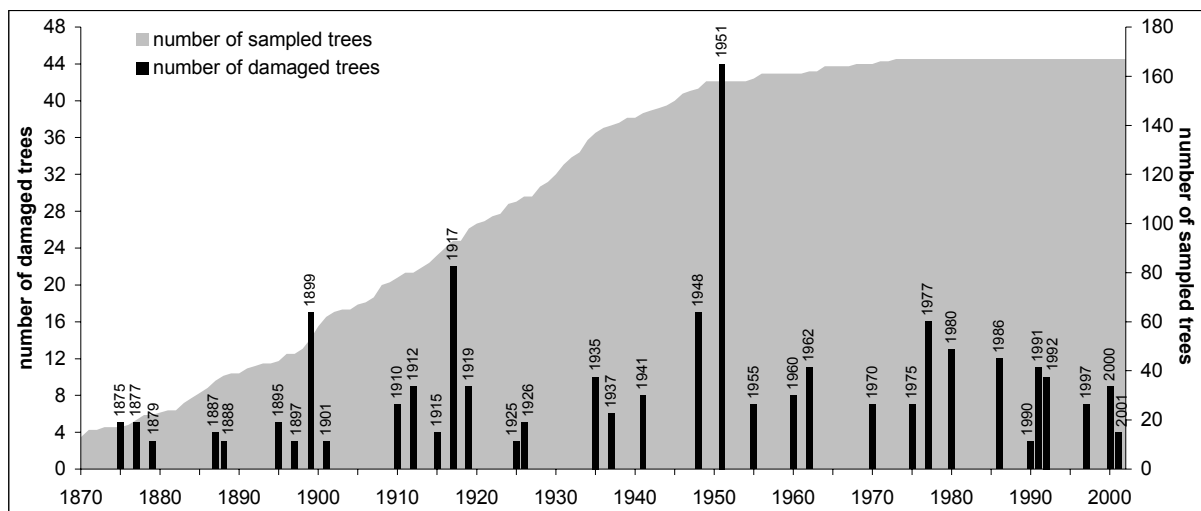


Figure 7: Chronology of the debris flows dated on the Val Paolaccia fan

Debris flows and processes of erosion at the fan border

The lateral channel (B) previously analysed meets one of the cart-road crossing the Val Paolaccia fan (C in Fig. 1). Starting from this point, the cart-road has been dismantled and dug from the erosion activity of debris flows to form a small channel that reaches the fan-toe. An analogous situation can also be found on the northern margin of the fan, on the hydrographical right of the main channel. In fact, some lateral flows have reached a cart-road (E in Fig. 1, Fig. 8) which is abruptly dug and forming a channel whose filling material is currently found on the pasture located at the fan margin. Also in this case the activity is very recent, since the accumulated material is not visible on the aerial photos of 1981, and it was observed in small part in 1999 and then progressively in a more extended way in 2002 and

2004. The recent activity of the channel is also documented from the freshness of the roots still exposed (Fig. 8).

The analysis of the exposed roots along the channel (Fig. 9) reveals the presence of corrosion scars on the upper part caused by the dismantling of the cart-road, while very wide rings, partially made of compression wood, have formed on the lower part since 2001.

The samples taken from the stems of the trees fallen from the channel sides show compression wood starting from 2001 (one tree), from 2002 (three trees) and from 2003 (one tree).

Therefore, the erosion event which caused the formation of this channel occurred in dendrologic year 2001 and in the following years some trees living on the banks tilt towards the channel, consequently beginning to produce compression wood. A debris flow happened in 2001 is also documented along the main channel (Fig. 7). Moreover, since the situation observed in 2004 is different from the one of 2002, we can deduce that the channel has also been active later on, probably in 2003.



Figure 8: Erosion channel formed in 2001 connected with an old cart-road (X in Fig. 1). Roots, still in life position, are visible (photo by Santilli 2002).

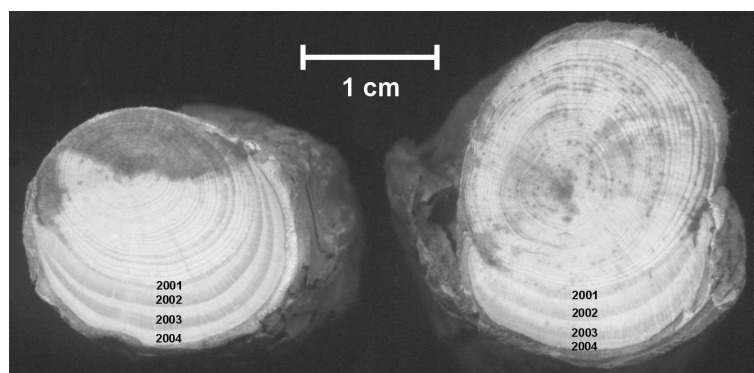


Figure 9: Sections of exposed mountain pine roots. The scars caused by the erosion have stopped the growth of the upper part. On the lower part we can see some very wide rings which have developed as a result of the exposure (photo by Santilli 2004).

Conclusions

Abrupt radial growth releases identified in the studied trees represent a useful dating method for low-energy debris flows which have deposited only thin debris layers without causing clear mechanical damages to the trees. The reasons of this positive growth reaction of the mountain pine can be attributed to the nutrients contribution both from the debris material, which is of carbonatic type, and from the buried herbaceous vegetation, which is later mineralized. Moreover, the inter- and intra-specific competition is also reduced.

However, it is better to analyse a great number of samples affected by the same event, since trees do not always react in the same way. Reactions depend on the entity of the burial that can vary locally, on the season in which it happens and on the individual sensitivity of each tree, and can even happen with delay from the time of disturbance.

The use of this method in addition to the other dendrochronological dating methods allowed us to reconstruct the detailed sequence of debris flows which have been affecting the Val Paolaccia fan since 1875. The event happened in 1875 is also the most ancient debris flow among those dated in the Valle del Gallo up to now. In regard to this, the potentialities of the mountain pine in this area are remarkable, if we consider that many trees analysed on the Val Paolaccia fan date back to the 18th century.

Finally, it has been documented that cart-roads crossing the fan constitute a line of weakness, a discontinuity in the pine forest that can become a line of preferential outflow for the debris flows, which can take material from the road itself and transport it to the fan border. A similar erosion process is also attributable to the sheetfloods coming from the Val Paolaccia itself. They have originated peculiar erosion morphologies characterized by small watersheds meeting in the Valle del Gallo torrent.

References

- Alestalo, J. (1971): Dendrochronological interpretation of geomorphic processes. Soc. Geographica Fennia, n. 105, pp. 140.
- Corominas, J., Moya, J. (1999): Reconstructing recent landslide activity in relation to rainfall in Llobregat River basin, eastern Pyrenees, Spain. *Geomorphology* 30: 79-93.
- Gärtner, H., Esper, J., Treydte, K. (2004): Geomorphologie und Jahrringe - Feldmethoden in der Dendrogeomorphologie. *Schweizerische Zeitschrift für Forstwesen* 155, 6: p. 198-207.
- Gärtner, H., Stoffel, M., Lièvre, I., Conus, M., Grichting, M., Monbaron, M. (2003): Debris-flow frequency derived from tree-ring analyses and geomorphic mapping, Valais, Switzerland. In: Rickenmann D. and Chen C. (eds.). Debris-Flow Hazard Mitigation: Mechanics, Prediction and Assessment. Proceeding of the 3rd International DFHM Conference, Davos, Switzerland, September 10-12, 2003. 2 vol. Millpress Rotterdam, Netherlands: 207-217.
- Heikkinen, O. (1994): Using dendrochronology for the dating of land surfaces. In: Beck C. (eds.). Dating in Exposed and Surface Contexts. University of New Mexico Press, Albuquerque: 213-235.

- Holmes, R.L. (1983): Computer-assisted quality control in tree-ring dating and measurement. *Tree-Ring Bull.* 43: 68-78.
- Hupp, C.R. (1984). Dendrogeomorphic evidence of debris flow frequency and magnitude at Mount Shasta, California. *Environ. Geol. Water Sci.*, vol. 6, n. 2: 121-128.
- Pelfini, M., Leonelli, G., Santilli, M. (2005a): The influence of debris flows and sheetfloods on tree-ring growth in upper Valtellina (Sondrio, Italy). European Geosciences Union. General Assembly, Vienna, Austria, 24-29 April 2005. Geophysical Research Abstract, Vol. 7, 2005. EGU05-A-07506.
- Pelfini, M., Santilli, M. (2003): Variabilità spazio temporale dei processi di versante in alta montagna negli ultimi secoli, indagati mediante tecniche dendrogeomorfologiche. In: Biancotti A., Motta M. (eds.). Proceeding of the Conference: Risposta dei processi geomorfologici alle variazioni ambientali. Bologna, Italia, 10-11 febbraio 2000: 345-364.
- Pelfini, M., Santilli, M., Merlini, C. (2005b): Determination of the erosion rate of escarpments at the debris flow fan toe. In: Gärtner H., Esper J., Schleser G.H. (eds.). TRACE, Tree Rings in Archaeology, Climatology and Ecology, Vol. 3, Proceeding of the Dendrosymposium 2004, Birmensdorf, Switzerland, 22-24 April 2004: 70-75.
- Rinn, F. (1996): TSAP: Time Series Analysis and Presentation. Version 3.0. Reference manual, pp. 262.
- Santilli, M. (2005): Debris flows ed erosione torrentizia in Valle Del Gallo (Valtellina - SO): analisi dendrocronologica e geomorfologica della distribuzione, frequenza e intensità dei processi. PhD Thesis in Natural and Environmental Sciences, Earth Sciences Department, University of Milan, Italy, pp. 265
- Santilli, M., Pelfini, M. (2002): Dendrogeomorphology and dating of debris flows in the Valle del Gallo, Central Alps, Italy. *Dendrochronologia* 20 (3): 269-284.
- Santilli, M., Pelfini, M. (2005): Forme di erosione regressiva originate da sheetfloods: un esempio in Valle del Gallo (SO). In: Bondesan A., Fontana A. (eds.). National Conference A.I.Geo "Montagne e Pianure, Recenti sviluppi della ricerca in Geografia fisica e Geomorfologia", Abstracts, Dipartimento di Geografia, Università di Padova, 15-17 February 2005, Padova, Italy: 148-150.
- Santilli, M., Pelfini, M., Caccianiga, M., Comolli, R., Ravazzi, C. (2002): Late Holocene environmental evolution of the upper Valle del Gallo (Central Alps): an interdisciplinary study. *Il Quaternario* 15 (2): 187-208.
- Schweingruber, F.H., Albrecht, H., Beck, M., Hessel, J., Joos, K., Keller, D., Kontic, R., Lange, K., Niederer, M., Nippel, C., Spang, S., Spinnler, A., Steiner, B., Winkler-Seifert, A. (1986): Abrupte Zuwachsschwankungen in Jahringabfolgen als ökologische Indikatoren. *Dendrochronologia* 4: 125-183.
- Shroder, J.F. (1978): Dendrogeomorphology: review and new techniques of tree-ring dating. *Prog. Phys. Geogr.* 4: 161-188.
- Z'Graggen, S. (1987). Dendrocronologia e moria del bosco nella regione alpina. Proceeding of the Conference: Dendrocronologia e moria del bosco in Europa, 10/10/1986, Verona: 21-31.

SECTION 5

ARCHAEOLOGY

Preliminary tree-ring dating of historical wood from Ust-Voykar settlement (15th-20th) Centuries), Northwestern Siberia

M. Gurskaya

Institute of Plant and Animal Ecology. 8 Marta, 202, Ekaterinburg, Russia, 620144

Email: mgurskaya@yandex.ru

Introduction

Calendar dates for archaeological monuments and environmental reconstruction in Northern Siberia are an important application of dendrochronology to the history of Siberia. Historical monuments from the northern taiga of Western Siberia represent a unique source of knowledge about people's past life in the harsh environment of the Russian North. Shiyatov and Hantemirov (2000) studied historical settlements, Nadym and Yarte IV in Western Siberia; they found that a great number of trees and other woody plants were used in their construction. Timber from these settlements was used to define building-period dates and the tree species used in construction were identified. This work revealed that long tree-ring chronologies could be developed from tree-ring series constructed from historical timbers from northern settlements. Tree-ring chronologies provide a proxy record of past climatic conditions (Kolchin 1963, Bailie 1982). However, there a limited number of long tree-ring chronologies from the northern part of Western Siberia exist. We believe that historical timbers, recovered from high latitude settlements especially those near the Russian Polar circle, are a great source of tree rings for developing long tree-ring chronologies. The subject of this paper, the Voykar settlement from North-Western Siberia, supplies one such chronology.

The Ust-Voykar settlement

The Voykar settlement, situated on the west bend of the Gornaya Ob River (65°41'N, 64°41'E), is one of the largest and best-known settlements of the XVI – XIX centuries. There are various myths and legends attached to the historical events that happened in this settlement. It was a trade centre for the native "Ostyak" and "Samoed" tribes from the vast territory of Siberia and a centre for the collection of tribute by the Russian Government.

Voykar is an exceptional settlement because of its location on the crossroads between the Russian West and the Ural region and North, East and South Siberia. The main migratory flows passed through Voykar. The first written record mentioning the settlement dates to the end of the XVI and the beginning of the XVII century (a letter of AD 1601 describes a siege of the town of Berezovo in AD 1595). Besides this letter, there are census records from the XVIII-XIX centuries. These records show that the Voykar settlement was a well-developed and flourishing town as far back as the 17th-18th Centuries, with the town only being abandoned at the beginning of 20th century. Today, the settlement is completely overgrown by grass and there are no accurate dates for its foundation or rebuilding phases.

The settlement, built on permafrost, is situated on the southern shore of Voykar lake (65°41'N, 64°41'E) on the northern taiga (Fig. 1). In 2003 the Yamal Archaeological Expedition carried out an excavation at this place. At the beginning of the excavation, the site looked like an 11-m high by 200-300 m diameter overgrown grass hill surrounded by a stand of spruce (*Picea obovata* Ledeb) established in the middle of the XIX century. Surrounding this hill is a mixed forest of larch (*Larix sibirica* Ledeb.) and pine (*Pinus sibirica* Du Tour).

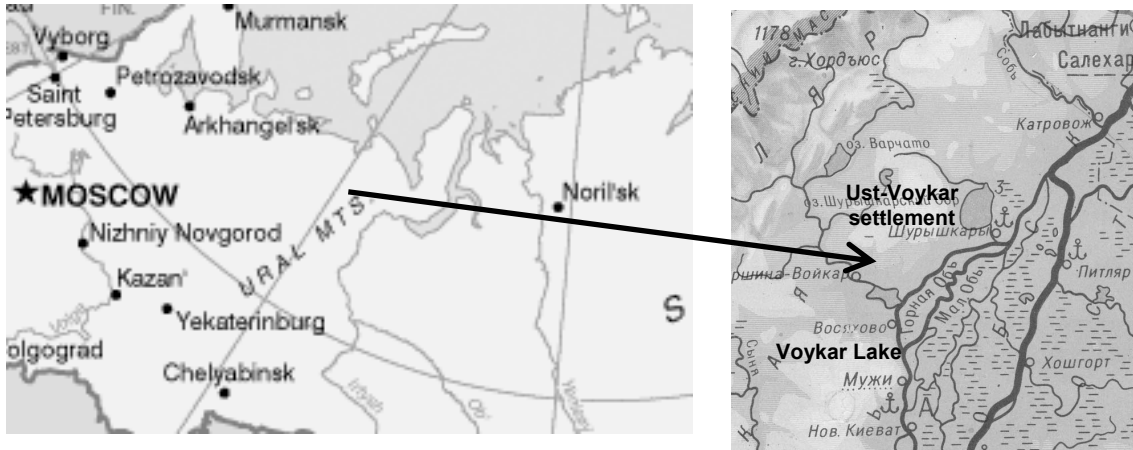


Figure 1: Research area

The Expedition identified a large number of construction timbers from which wood samples were taken for tree-ring analysis. The study's aims were as follows:

- To develop three tree-ring chronologies based on living trees, growing around of the site;
- To determine the species of collected archaeological samples;
- To establish calendar dates for the settlement's main buildings;
- To develop a long tree-ring chronology by overlapping tree rings from historical timbers with living trees.

Materials and methods

Living trees

We collected 18 cores from living spruce (termed the ELM chronology) and 12 cores from living larch (termed the LMY chronology) during the summers of 1997 and 2000. The trees grow on the southern side of Voykar Lake mixed with wild rosemary, sphagnum and pleurotium within 5-10 km of the Voykar site.

Archaeological wood

About 250 cross-sections were collected from 14 Voykar constructions and loose logs during two seasons of settlement excavation. From each construction not less than 5 wood samples were taken. Most of the samples were taken from fences, wattle fence posts and planking. Walls of buildings have few logs, because houses had only 1-3 or 1-3 joists per floor. The timbers were all well preserved in the permafrost. Bark rings were present in most samples

allowing precise identification of felling dates. All constructions were located at different heights on different parts of the Voykar hill.

Methods

We identified the tree species used in constructions at the Voykar settlement based on well-known anatomical features of spruce, larch, pine and birch (Benkova and Schweingruber 2004).

Numbers of tree rings in each cross section varied from 30 to 240 and it was possible to cross-date most of the samples found during the two years of our excavations. Samples were 'polished' using a blade and measured along two radii to reveal partial or false rings. Samples were dated with TSAP software (Rinn 1996) and the COFECHA program provided quality control for the calendar dates supplied by our new chronologies: generalised master chronologies were constructed using the ARSTAN negative exponential curve method (Holmes et al. 1986).

Samples from the Voykar settlement were crossdated with our living-tree chronologies. The spruce and larch master chronologies, 300 and 450-years-long respectively, were based on trees growing within a 5 km radius of the excavated site. In addition, earlier samples were cross-dated with a 1000-year-long larch master chronology constructed from buried wood from the South Yamal peninsula by Hantemirov (1995).

Results

Tree species of archaeological timberwood samples

Micro-anatomical examinations of the wood show that most of the ancient samples were spruce and larch, with spruce being the most common species in this archaeological monument (Fig. 2).

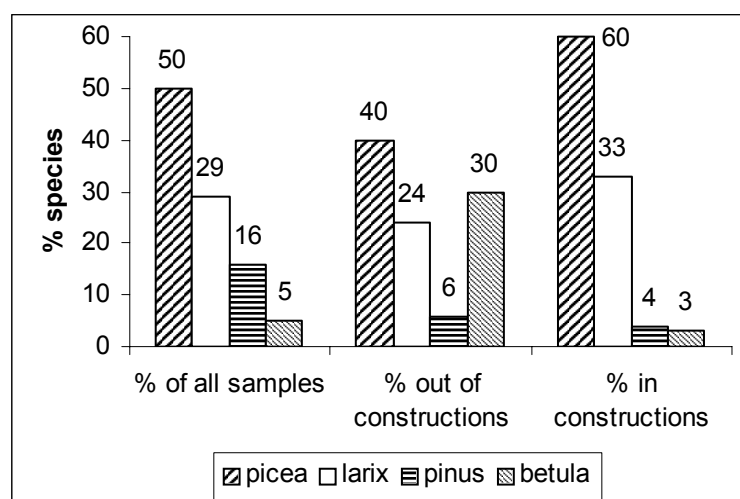


Figure 2: Ratio of tree species used for construction of the Ust-Voykar settlement

A total of 111 spruce samples were collected. Spruce was used to provide fences, banks, wicker-fence posts and floors. Spruce logs were found to be particularly abundant around

constructions. Unfortunately, these samples usually possessed few rings (<50) and many knots so they could not be cross-dated with any confidence.

Fifty-seven larch samples made up one third of all the samples collected over the two excavation seasons. Most of the larch samples (41) were taken from constructions, with this species used for main walls and floors in houses in the Ust-Voykar settlement. Sometimes larch logs were found mixed with spruce logs in fences.

A few floorboards in Voykar buildings were of Siberian pine, but pine wood was badly preserved. Unfortunately, we could not cross date even well preserved floor samples with 90-150 tree rings since the pine ring series showed very low sensitivity. It is a well-known fact that Siberian pine growing in the high latitudes of the Polar Urals is hard to cross-date (Shiyatov 1986). Consequently, individual pine chronologies are lacking from the dating result in this article.

Plenty of birch posts were found around later constructions in the top strata of our excavation site. However, birch was not used for main constructions i.e. houses and only a few posts were found in a wicker-fence. Unfortunately, the birch posts only had from 4 to 20 tree rings, so it was impossible to obtain tree-felling dates and, consequently, birch could not be used in further analysis. Thus, neither the pine nor the birch samples could be used and only the most numerous species, spruce and larch, were selected for further analysis.

Most settlement constructions were either of larch or spruce. Samples of other species such as birch or pine were seldom employed; although a mixture of species was present: for example, in wicker-fences and in-fillings requiring regular renovation.

Statistical characteristics of tree ring series

Numbers of tree rings in our archaeological wood samples varied from 30 to 150, with an average of about 90 rings (Tab. 1). The modern larch tree-ring widths, within 3 km of the site, are narrower than those found in the larch used for construction in the archaeological monument. A comparison of the coefficient of sensitivity between the archaeological and living trees shows that the average value of sensitivity of the ring series constructed from the archaeological samples is low compared with the sensitivity of living larch growing around Voykar Lake. Comparison of the median and maximum values of the coefficient of sensitivity shows that living larch trees are characterised by high sensitivity, because these two values are closely related. By contrast, there is a big difference between the median and maximum values of the ring series from the archaeological samples (the median value is 1.7 times less than the maximum one). However, mean and median values are equal meaning that half the samples are characterised by low sensitivity (below 0.28). This suggests that the larch trees used in the constructions were probably not growing in the vicinity of the settlement, but were brought from other areas characterised by more favourable conditions for larch growth.

By contrast, spruce rings from the archaeological timbers share very similar statistical characteristics, both as regards tree-ring width and series sensitivity, with the rings of living trees. The sensitivity of most spruce samples both from archaeological and living trees is low, with this being typical for the area. (Shiyatov 1986). This means that people used local spruce trees for building the settlement. Although most of the samples of spruce and larch

had enough rings for the construction of time series and show typical averages for this area and adequate coefficients of sensitivity for cross dating, the sensitivity of almost half the larch samples and most of the spruce samples is low; with this consequently reducing confidence in cross dating.

Table 1: The statistical characteristics of individual chronologies of samples. Med is median value. PAC1 is pooled auto correlation of the 1st order.

Ident	Total time span		Yrs	Mean years	Tree-ring width, mm				Sensitivity				PAC1
					Mean	Med	Min	Max	Mean	Med	Min	Max	
LMY	1538	1999	462	267,2	0,39	0,32	0	2,93	0,42	0,41	0,31	0,54	0,58
ELM	1717	1996	280	167,8	0,76	0,72	0,05	4,34	0,27	0,27	0,17	0,43	0,58
Larch	1111	1886	810	88,15	0,63	0,58	0	3,4	0,29	0,28	0,17	0,48	0,72
Spruce	1171	1887	716	87,5	0,61	0,56	0,06	3,4	0,25	0,24	0,14	0,43	0,72

Cross dating of archaeological samples

Calendar dates for tree ages were established with the help of TSAP and COFECHA software. Ninety four out of 111 spruce samples were successfully cross-dated, with a dating success of 82 % (it should be noted that 74 of the samples were from different constructions). The dating success of the larch samples reached 90 %: with the life span of 57 larch samples limited to 50 years: 41 of these samples were from constructions.

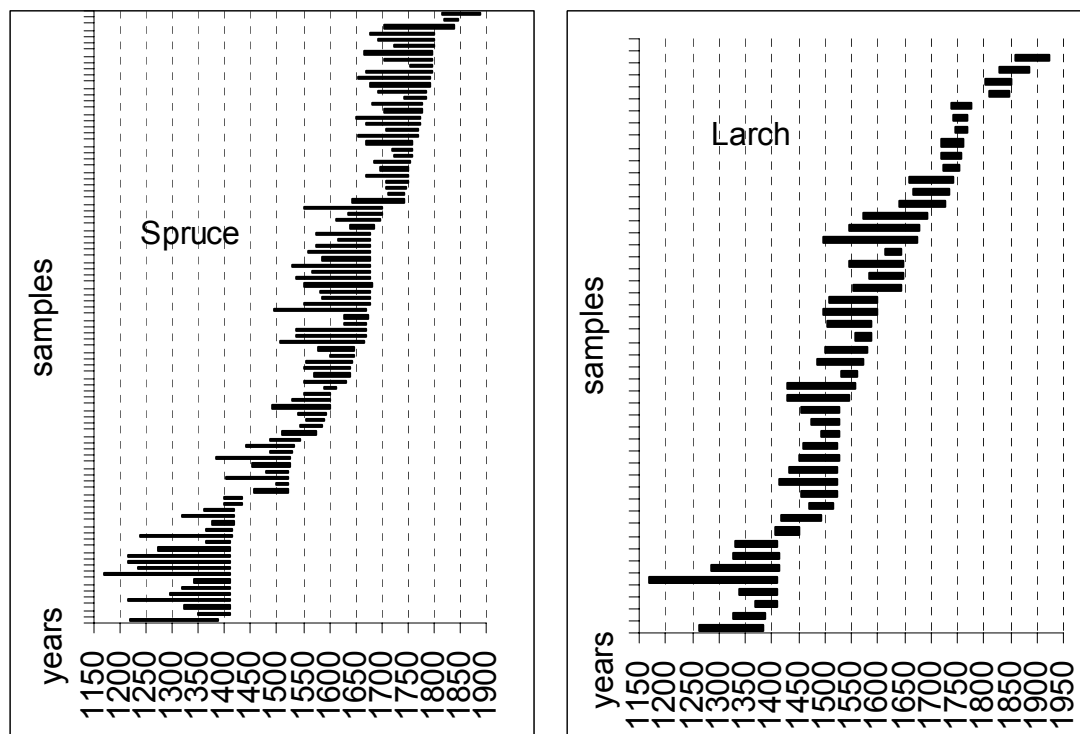


Figure 3: Life span of trees

The results of dating are shown in figure 3. Mass tree felling for settlement construction was carried out at the beginning of the XV century (flooring and fence posts located at the bottom of the research hill were cut in 1412); throughout the XVII and half the XVIII centuries (1600 to 1730). One construction framework was found at ground level 10 m from the archaeological monument for which the trees were felled in 1850. In addition, logs dated of the second half of the XIX century are trees with the latest felling dates being 1886 and 1887 (spruce and larch respectively). But these logs do not belong to any constructions of the settlement. Trees from the top strata of the excavated site were felled in the XX century. It was possible to develop and extend the spruce and larch tree-ring chronologies using the archaeological wood (fig. 4). The larch chronology covers 810 years, and the spruce chronology 716 years extending from the 12th to the 19th centuries. Comparisons of these chronologies with living tree chronologies show good agreement. The constructed tree-ring chronologies were overlapped with the chronologies from the living trees growing around of the Voykar settlement. The larch chronology, including living trees, covers 888 years with the archaeological samples prolonging the chronology by 427 years. The age range of the spruce chronology, including both living and archaeological samples, is 825 years. Thus, the spruce chronology is extended by 546 years.

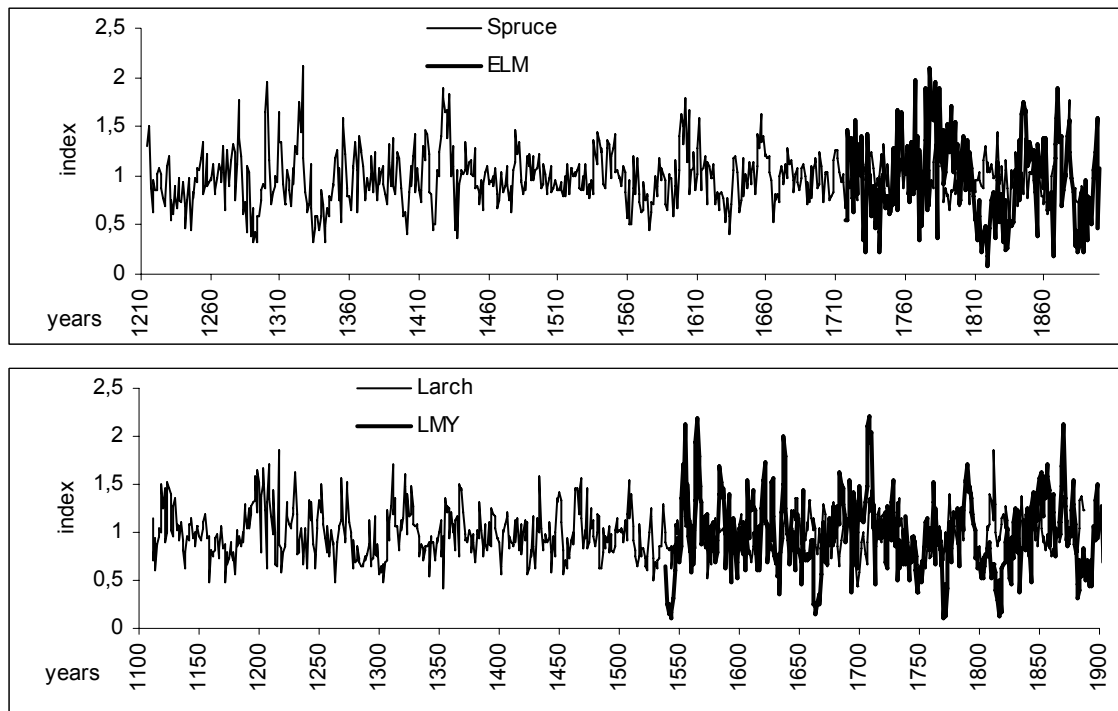


Figure 4: Averaged spruce and larch tree-ring chronologies

Micro anatomical analysis of the most recent ring structures shows that trees used in the construction of this archaeological monument were felled in different seasons. All the wood used for large constructions such as house walls had completely-formed latewood rings under their bark. Thus, the wood for the main walls of the Ust-Voykar settlement was cut during autumn or winter, between August and May.

Timber for flooring, fences, and wicker--fence posts was cut at the beginning of summer. These samples have a few earlywood cells in their last tree ring and latewood cells are absent.

The generalised characteristics of all 14 constructions at this site are combined in Table.2. Most of the excavated constructions were built in the XVII century, a period according to the chronicles during which Voykar was intensively expanded and developed. New constructions were built every 20-30 years, with intensive building continuing until 1730. In future excavations it is hoped that we will find even more and earlier constructions.

Table 2: Calendar dates of Voykar settlement constructions. C. - number of construction, L - Larix, P - Picea, B- Betula, S - summer (June-July), W- winter (August-May).

	Name of construction	Tree species	Felling year	Season of tree felling
1	Fence	P	1412	S
2	Flooring	L	1412	S, W
3	Filling of C.7	L, P	1542	S
4	Wall C.5	L	1600	W
5	Bank C.6	P	1640	S
6	Filling of C.4	L	1640	W
7	Wicker- fence C.4	L, P, B	1645	S, W
8	Framework C.7	P	1652	S
9	Framework C.6	L	1676	W
10	Fence	P	1678	S
11	Filling of C.6	L	1701	S
12	Filling of C.8	L, P, B	1730	S
13	Flooring	P	1799	W
14	Framework on the ground	L	1850	S

Conclusions

1. Four species including spruce, larch, Siberian pine and birch were used to build the Ust-Voykar settlement, with locally grown spruce being the most commonly used while larch was used more sparingly.
2. Chronologies were constructed for spruce and the larch, 825 and 880-years-long respectively. There were insufficient samples of Siberian pine and birch with enough tree rings for the development of chronologies. .
3. The settlement was established at least 200 earlier than is recorded in the chronicles. The oldest construction was found at the bottom of the hill. The settlement was regularly rebuilt every 20-40 years from 1412 to 1880.

Acknowledgements

The author wishes to thank Irina Panyushkina and Vanessa Winchester for their kind remarks and good advice on this article. This work was supported by the Russian Fund of Basic research (RFBR) No 05-06-80-233.

References

- Baillie, M.G.L. (1982): Tree-ring Dating and Archaeology. The University of Chicago press. Chicago. 265 p.
- Benkova, V.E., Schweingruber, F. H. (2004): Anatomy of Russian woods (an atlas for the identification of trees, shrubs, dwarf and woody lianas from Russia). Bern, Stuttgart, Wien. Haupt. 456 p.
- Brusnicyna, A.G. (2003): Gorodische Ust-Voykarskoe. Nachalo izucheniya. Ugry. Materialy VI Sibirskogo simposiuma " Kulturnoe nasledie narodov Zapadnoy Sibiri". Tobolsk: P. 45-52.
- Hantemirov, R.M. (1995): A 2,305 year tree-ring reconstruction of mean June-July temperature deviation in the Yamal Peninsula // International Conference on Past, present and Future Climate (Proceedings of the SILMU conference held in Helsinki, Finland, 22-25 August 1995). Ed. by Henkinheimo Pirkko. Publication of the Academy of Finland. Painatuskeskus 6/95.
- Holmes, R.L., Adams, R.K., Fritts, H.C. (1986): Tree-ring chronologies of western North America: California, eastern Oregon and northern Great Basin, with procedures used in the chronology development work, including users manuals for computer programs COFECHA and ARSTAN. Chronology Series VI. Laboratory of Tree-Ring Research, University of Arizona, Tucson.
- Kolchin, B.A. (1963): Dendrochronology of Novgorod. Novye metody v archeologii. Trudy Novgorodskoy archeologicheskoy ekspedicii. M. AN SSSR. No117. T3. 331 p.
- Rinn, F. (1996): TSAP - time Series Analysis and Precipitation, Version 3 reference Manual. Heidelberg.
- Shiyatov, S.G. (1986): Dendrochronologiya verchney granicy lesa na Urale. M. Nauka: 136 p.
- Shiyatov, S.G., Hantemirov, R.M. (2000): Dendrochronologicheskaya datirovka drevesiny kustarnikov iz archeologicheskogo poseleniya Yarte IV na poluostrove Yamal: drevnosty Yamala. Ekaterinburg-Salehard. Vypusk I.

2500 years from dendrochronology back to ancient French human biotopes. Trees studied: low altitude oaks

G. Lambert, S. Durost & J. Cuaz

*Laboratoire de Chrono-Ecologie, CNRS, University of Franche-Comté, 16 Route de Gray,
F-25030 CEDEX, Besançon*

Email: joellamb@club-internet.fr, sebastiendurost@yahoo.com, cuaz.jac.clim@wanadoo.fr

Introduction

We propose an experimental method, using curvilinear regressions, called corridor method, for dating and building a global useful signal based on oak ring widths in northern and eastern France. The resulting signal seems to be more useful than others to progress in the domains of ancient climate and ancient environments: dendrodating, dendroclimatology, dendroecology and, of course, human history (Lambert, 2002, Houbrechts and Lambert, 2004, Durost, 2005). However, we were lead to adapt or reconsider several basic mathematical functions, meteorological indexes or common dendrochronological definitions.

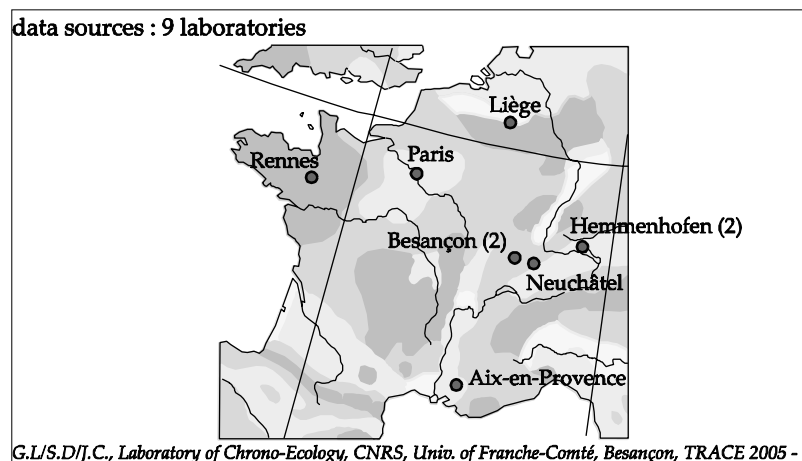


Figure 1: Contributing laboratories. The map gives a first idea of the concerned area.

We are currently working towards the publication of a large Data Base (web-DB). A first element of this DB can be consulted on the website of the ChronoEcology laboratory (French keywords: chrono-Ecologie, dendrochronologie). A discussion has opened about the participation of private contributors to such a public DB. The private contributors to this note agreed to show a part of their data without rights (money) and to justify explicitly their own dating procedures.

Data sources and dating method

Data source

A set of 142 synchronized historical site oak chronologies gave information about the last 1000 years. Another group of 74 site chronologies related to the late prehistoric and roman

periods. The studied area which lies within the points 51°N-3°E, 50°N-7°E, 45°N-6°E, 45°N-0°E corresponds to low altitude countries, under 500m, and covers a global area of about 300 000 km². 2500 years of chronologies were rebuilt with 500 missing years from the early medieval period. The oldest ring dates back to 546 BC, the latest ends the system at 1995 AD. The missing years are precisely between 194 AD and 671 AD. We will show how the resulting signal, obtained by the corridor method, is interesting for engaging climatologic researches on large areas. The material comes from 9 laboratories based in France, Belgium, Switzerland and Germany (Fig. 1 and acknowledgments). Samples come from living trees, old buildings and archaeological excavations. About 5000 trees (4.781) were selected from an original set of 10000 dated oaks. The average age of samples is about 90 years. The average depth of the resulting chronology is around 80 rings by year. The main prehistoric and roman sites, which provided more than 50 samples, are Tours (F-37), La-Pacaudière (F-42), Rouen (F-76), Brognard (F-25) (Durost, 2005). The most interesting medieval and modern sites are cathedrals of Paris (F-75), Beauvais (F-60), Amiens (F-80), Auxerre (F-89), Laon (F-02), Poitiers (F-88), abbay of Fontevraud (F-49), Landevennec (F-29), towns of Liège (B), Autun (F-71), Cluny (F-71) (Lambert, 2002, Houbrechts and Lambert, 2004). A site chronology was first built for each site for a given period. In a second phase, the signals of nearby locations were grouped to create coherent local chronologies. The properties of the two resulting data basis are listed below.

Reference system

Part 1: historic periods

Name: HistoricOaks-20050126
Period: from 672 AD to 1995 AD; duration: 1324 years
Location: North of France, South of Belgium, West Switzerland
Source: 9 laboratories; woods: several materials
Last version from: Laboratory of Chrono-Ecology (LCE-CNRS)
Registration: 26 January 2005 by Georges Lambert (GL)
Components: 142 chronologies; 2529 samples.

Part 2: prehistoric and roman periods

Name: ClassicOaks-20050101
Period: from -546 (BC) to 193 AD; duration: 739 years
Location: North of France, West Switzerland
Source: 7 laboratories; woods: archaeological excavations
Last version from: Laboratory of Chrono-Ecology (LCE-CNRS)
Registration: 01 January 2005 by Sébastien Durost (SD)
Components: 74 chronologies; 1252 samples.

Method: computing the corridor index

The raw data calibration by the corridor method is obtained after three steps (Fig. 2). The first step computes a triple polynomial regression, which draws for each tree a curving corridor

which follows the main movements of the growth. The first regression of computing data gives the trend of each series. The polynomial degree of the regression is chosen either by the operator or by the computer. The same degree is used for computing a regression with the lowest data (under the trend) and thus we draw the "floor" of the corridor. The last regression repeats the same operation with the highest data, which stands up the trend, and draws the "ceiling" of the corridor.

The second step modifies the corridor to give it the shape of a rectangle and at the same time, each point of the data series moves to keep its relative position between the top and the bottom of the corridor (morphing). Usually, choosing lower degrees for the polynomials is the best solution. Degrees between 3 and 6 are generally chosen. The computer program proposes to take degree 3 as default option. This degree 3 is a good tool for erasing the senility effect. However we must search for sufficient stability of the global signal in order to later apply calculations as the correlation coefficient (for instance). Therefore, the user is often led to raise the starting degree. However, we must be careful not to suppress all movements from the series: a minimum flexibility is necessary in order to get interesting information from the resulting calibrated series.

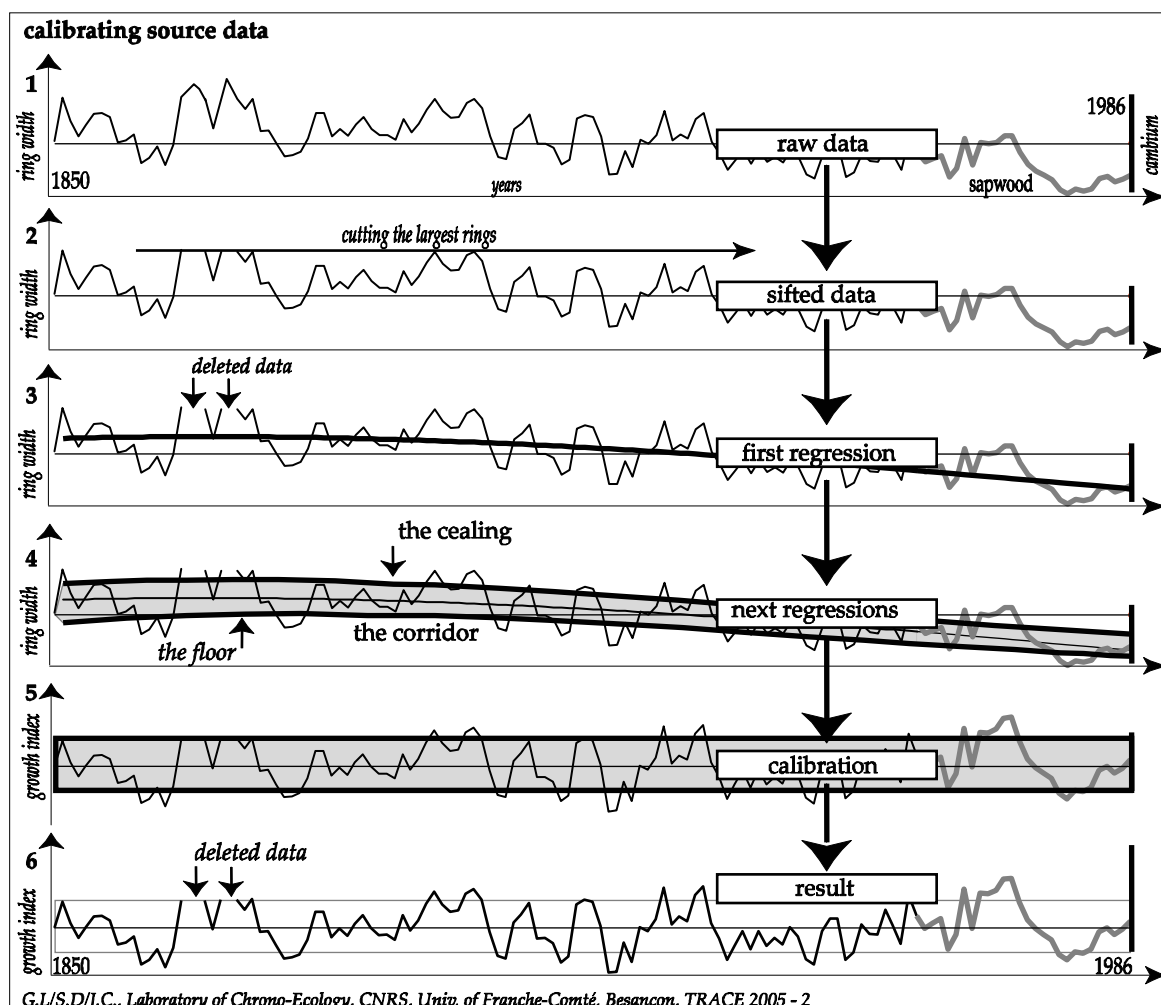


Figure 2: Dendrochronological data calibration by the corridor method using polynomial regressions

The third step is the computing of the dendrochronological average from a set of several individual calibrated series. A useful property of the resulting series is that it is comparable with other source series, which are not (or not yet) calibrated. In theory, this calibration authorizes mixing both raw data (if it is regular enough or does not show too much noise) with other indexed series to build experimental local averages. The global signal obtained is stable enough to allow a wide range of computations.

Consequences for dating

Significant changes were made compared to previous chronological propositions. About 40% of the original series was discarded because the dating could not be verified by the new calculations. Many of these series are too short or have problematical noise. A great part of this discarded series was probably correctly dated but we could not confirm the date through the mentioned method above.

The re-update was made in each local group. Some dates were changed. A new chronology is accepted as a new component of the system if it yields a set of pertinent correlations with the previously integrated items. Figure 3 shows correlations between a new eligible item and a potentially contemporary series, which has already been dated (chronology Cluny-GL51: Cluny is a well known medieval site in Burgundy; GL=operator's identifier; 51=version or number); the best correlations are grouped in the left part of the fan. Then, the set of resulting chronologies shows best correlations between contemporary sites, as the old data bank did.

The correlating system becomes coherent on a large geographical scale. Very good correlations through wide areas can be exhibited whatever the period (Fig. 3). The accuracy of a group of chronologies of a given century is expressed, through another method, by a symmetric matrix, which shows the correlations between all components.

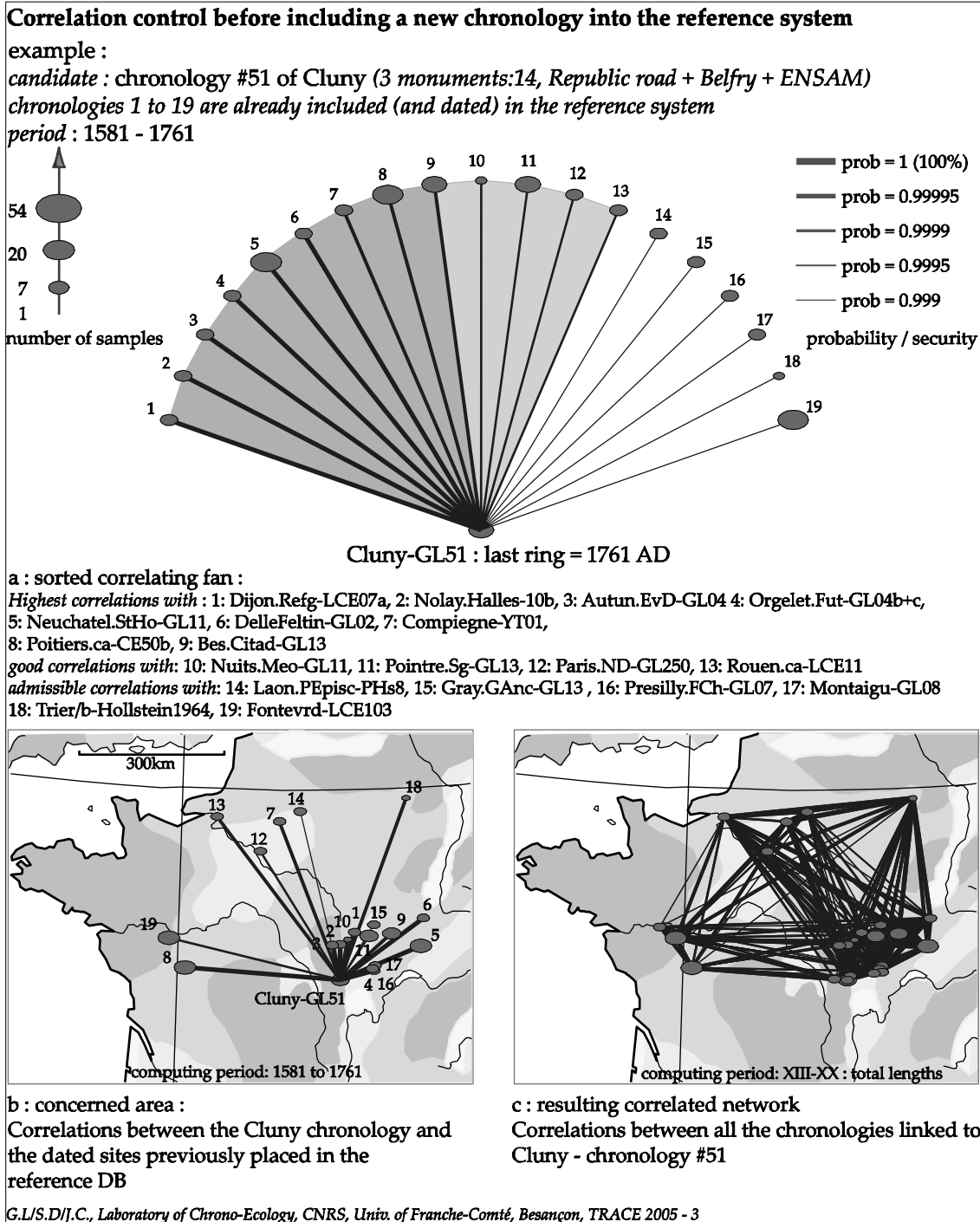


Figure 3: The new site chronology Cluny, version 51 –built or (re)built by GL - has to demonstrate his ability to be accepted in the existing reference system.

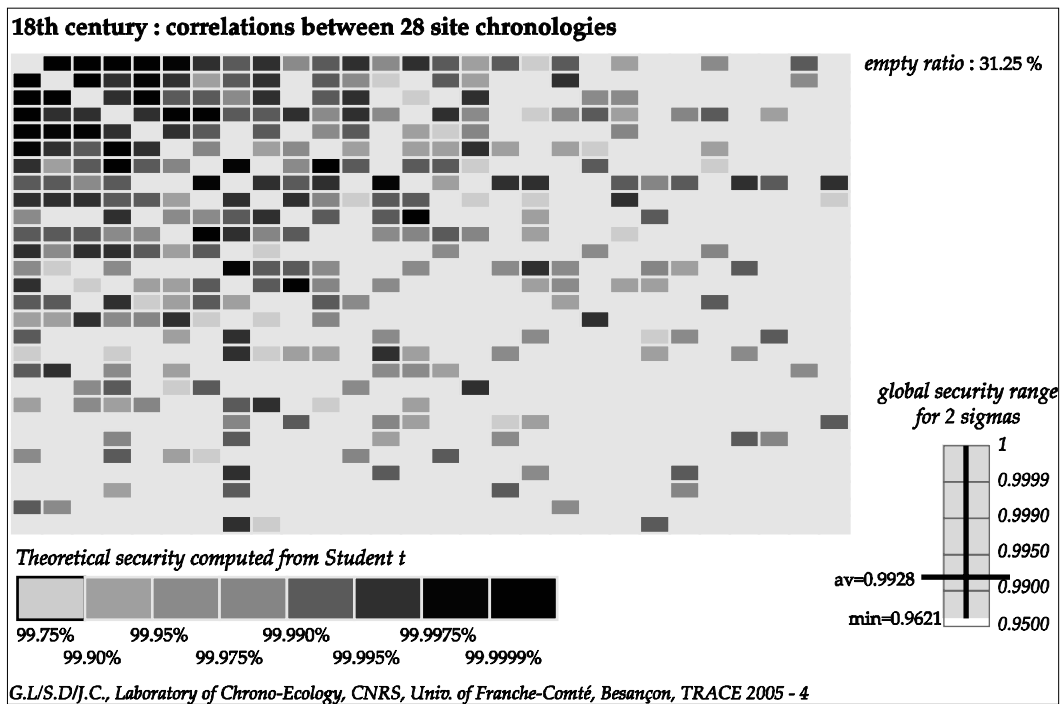


Figure 4: Matrix of inter-correlations between the site chronologies which pass through the 18th century.

The Student t is the used value for building the matrix. As for the fan graphic, the minimum shown t value corresponds to the theoretical risk 0.999. The best coefficients give a dark box in the figure (Fig. 4) and the lowest give a light box.

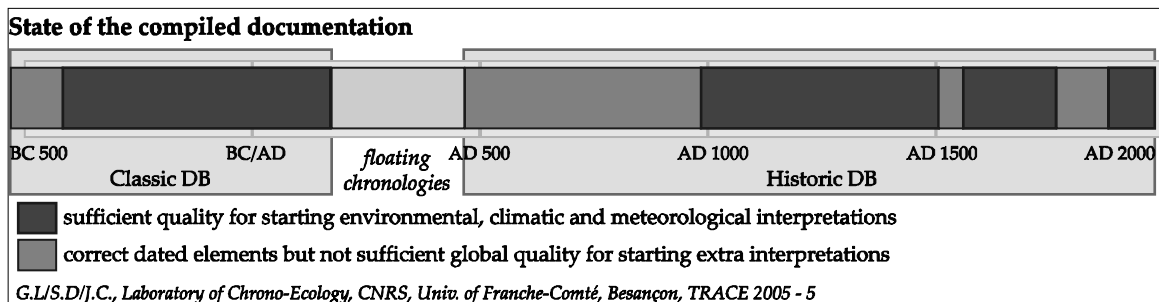


Figure 5: Prehistoric et historic bar of subjective credibility of the reference system Hist20050126

Finally, thousands of wood chronologies were connected for a 2500 years period except for the late Roman and Merovingian times for which we got some chronologies, still floating though. The credibility of the resulting system is summarized in the next figure (Fig. 5).

Climatic signification of the resulting signal

Aim

The goal was to find a method to build multi-proxy charts or matrices through time for trying meteorological or climatic reconstructions with the growth index discussed above. Therefore, we had to find a method which allowed the association of dendrochronological data,

meteorological data and, later, other information such as historical precisions for example. The necessary starting condition was to find enough sites or better, sectors - which group several sites - for a sufficiently long period (minimum 500 years) and for each sector to be able to build comparable data. It is very rare to find long ring chronologies and long enough meteorological records for the same location. The dendrochronological information in particular is spread over a large area but the internal structure of this area changes with time: buildings or sites used several times rarely give data over a long time and none of them give information for the whole of the period in question. Precise maps of known areas change from a century to another. As a result, site chronologies are not adequate to work from with such a process. We were therefore led to consider theoretical spaces, which yield dendrochronological and meteorological records. The previous discussion showed that the dendrochronological growth index is stable information through a relatively large area around a given point, so it authorizes us to try to create regrouping sectors. Starting from phytoclimatic studies (Choisnel et Payen 1989, Emberger 1930), we divided the French territory into 42 "natural" sectors and built an elementary geographical model. Our research sector encompassed about 30 of these sectors. In a second step, we built a new dendrochronological average chronology for each sector, which is a chronology that summarizes all the data of the sector. In a third step, a global regional chronology was built from the sector chronologies – not from the original samples. This regional chronology will provide some parameters for the following computing. Meanwhile, we collected as much meteorological data as we could from the stations which are - or were - located in the sector. After applying the dendrochronological methods, we summarized and averaged it to get a global yearly data for the sector: temperatures, precipitations and climatic indexes. This step in the collection of the meteorological data from a lot of little temporary old stations put to us the questions of data choice (not all compiled data is reliable) and of missing data reconstruction. Here we will ignore this point as it requires a long explanation. This way, we will be able to collect dendrochronological and meteorological data to build mixed charts for each sector and a global chart for a global zone: the North and East of France. In such a situation, the use of the response function poses a lot of questions. Before introducing these computations, we made a survey of the potential information located in the dendrochronological calibrated signal, compared with the meteorological information of the sector. Below are our findings for one of these sectors.

Tree ring and meteorology in middle Saône basin

We chose the middle Saône basin as the experimental sector and the 20th century as the experimental period. Six meteorological stations of the sector were selected:

1. Chalon-sur-Saône (F-71),
2. Bourg-en-Bresse (F-01),
3. Dijon (F-21),
4. Dole (F-39),
5. Lons-le-Saunier (F-39),
6. Besancon (F-25).

This way a coherent area of about 90 000 Km² was delimited. The last 120 meteorological years were re-built and we kept the synthetic trimester data of rains and temperatures. Thus, for precipitations and temperatures, we got respectively 4 annual series, one per season in which the autumn of the previous year is taken as the start of the concerned year (biological year: In the charts the autumn of the year 1900 i.e. is the period October-December 1899). A yearly meteorological index (ED7) derived from the bio-climatic index of Emberger (Emberger 1930, Lacoste and Salanon 1999) was added as a ninth climatic vector. This index expresses the notion of dryness and includes somehow the tree adaptation capacity through the winter. And, in order to introduce a meteorological index that does not include a division we tested an index, called GL2, which simply adds autumn temperature average, winter temperature average, spring precipitations and summer precipitations, after having made an elementary reduction. This index expresses the most part of the atmospheric energy usable by the tree during the biological year.

The ED7 and GL2 indexes are computed as follows,

$$ED7 = k * \ln(\text{som.p}) / (\text{som.t} - \text{win.t}) * (\text{som.t} + \text{win.t}).$$

$$GL2 = \text{red. aut.t} + \text{red.win.t} + \text{red.spr.p} + \text{red.som.p}$$

with:

\ln = natural logarithm;

for the global period (1879-1993):

per.aut.t = average of autumn temperatures

per.win.t = average of winter temperatures

per.spr.p = average of spring precipitations

per.som.t = average of summer temperatures

for each year:

aut.p = autumn precipitation average (previous year),

win.p = winter precipitation average,

spr.p = spring precipitation average,

som.t = summer temperature average,

aut.t = autumn temperature average,

win.t = winter temperature average,

spr.t = spring temperature average,

som.t = summer temperature average,

k = arbitrary factor for convenience (here k=100),

and

red. aut.t = aut.t / per.aut.t (previous year),

red.win.t = win.t / per.win.t,

red.spr.p = spr.t / per.spr.t,

red.som.p = som.t / per.som.t

The middle Saône basin (sectors 18 and 25: between 47.50N-5E, 47.40N-6.50E, 46N-5E, 46N-4.40E) lays under low altitudes (under 500 m) seven dendrochronological stations were selected:

1. Area of Luxeuil (F-70),
2. Chaux forest, between Dole and Besançon (F-39),
3. Oussières, old trees (F-39),
4. Several points in the West-Jura, in the South of Lons-le-Saunier, called "Petite Montagne" (little mountain, F-39),
5. Citeaux, forest in the South of Dijon (F-21),
6. La Ferté, forest in the South of Chalon-sur-Saône (F-71),
7. Forests in the neighboring of Cluny (F-71).

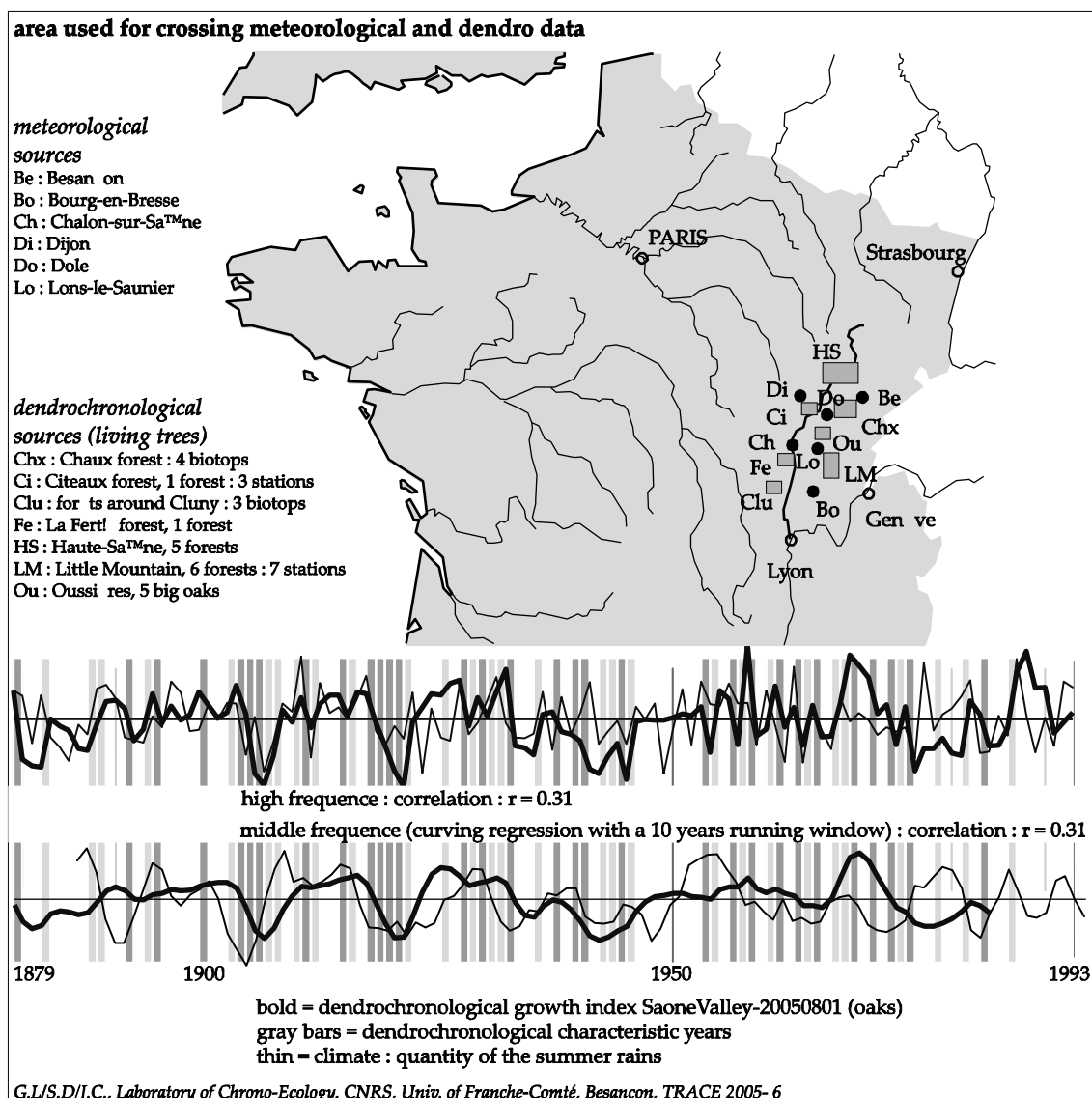


Figure 6: Dendrochronological signal and meteorology in the middle Saone Valley.

The "middle Saône-Valley" room, which represents about 20% of northern France (as defined above), is considered as a representative container of the global climatic energy on which the 300 living trees of the corpus depended (Fig. 6).

The resulting chronology is called SaoneValley20050801 (version of 08 August 2005, abbreviated below as SVoaks). Computations were drawn for the period 1879 AD - 1993. The correlations (r) between the oak chronology and the fifth meteorological data are summarized with a few numbers:

1879-1993:

- r (SVoaks, autumn prec) = 0,01
- r (SVoaks, winter prec) = 0,06
- r (SVoaks, spring prec) = 0,17
- r (SVoaks, summer prec) = 0,31
- r (SVoaks, autumn temper) = 0,09
- r (SVoaks, winter temper) = 0,1
- r (SVoaks, spring temper) = 0,16
- r (SVoaks, summer temper) = 0,13

Such results are not satisfactory. Only one correct correlation is given with the summer precipitations. We had hoped to find better correlations, especially with the climatic factors from spring and summer. A lot of other computations show that in this sector and for this period there are no direct correlations between spring and summer temperatures and the global growth of the oak. However, the indexes as ED7 and GL2 deliver better results:

1879-1993:

- r (SVoaks, ED7) = 0.37
- r (SVoaks, GL2) = 0.36

Combinations between factors give better results than direct correlations. At this point, we wanted to know what happens for typical years known for notable events like a hard winter or severe summer dryness. To choose the potentially most symptomatic years, we did not consider meteorological facts,- which are too diversified to allow an easy choosing procedure, but we looked at a dendrochronological indicator: the event year which carries a positive or a negative sign.

Event or signed years

The notion of dendrochronological event years or positive or negative signed years comes from old German researches (*Huber and Giertz-Siebenlist, 1969*) and is frequently used as an auxiliary of the dating procedures. An event year is defined, in a lot of woods - here, in a lot of site chronologies - by the common sign of growth difference (positive or negative) between the studied year and the previous one. If the minimum growth of 75% of a group of trees falls

between the years $y-1$ and y , B. Huber marked the year y as a characteristically negative year (a negative signed year) and, symmetrically, if the growth gets up in a minimum of 75% of the trees between the years $w-1$ and w , then year w is a positive characteristic year (a positive signed year). As other authors who tried to put the arbitrary floor of 75% in a probability evaluation (Schweingruber and coll. 1990), we used the probability notion to compute an event index, but starting from a floor of 70%. And, other change of usual, the synthetic chronology SVOaks was built with site chronologies as individuals (not with the tree chronologies). The Saône Valley chronology, calibrated by the corridor method, showed 62 event years in the period 1879AD-1993 (54%) in which we saw the known dry summers of 1904, 1911, 1959, 1976 (Fig. 6). The correlations computed with the meteorological data, only for the event years, gave the following results:

- $r(\text{SVOaks, autumn prec}) = -0,08$
- $r(\text{SVOaks, winter prec}) = 0,21$
- $r(\text{SVOaks, spring prec}) = 0,21$
- $r(\text{SVOaks, summer prec}) = 0,43$
- $r(\text{SVOaks, autumn temper}) = 0,13$
- $r(\text{SVOaks, winter temper}) = 0,12$
- $r(\text{SVOaks, spring temper}) = -0,32$
- $r(\text{SVOaks, summer temper}) = -0,21$

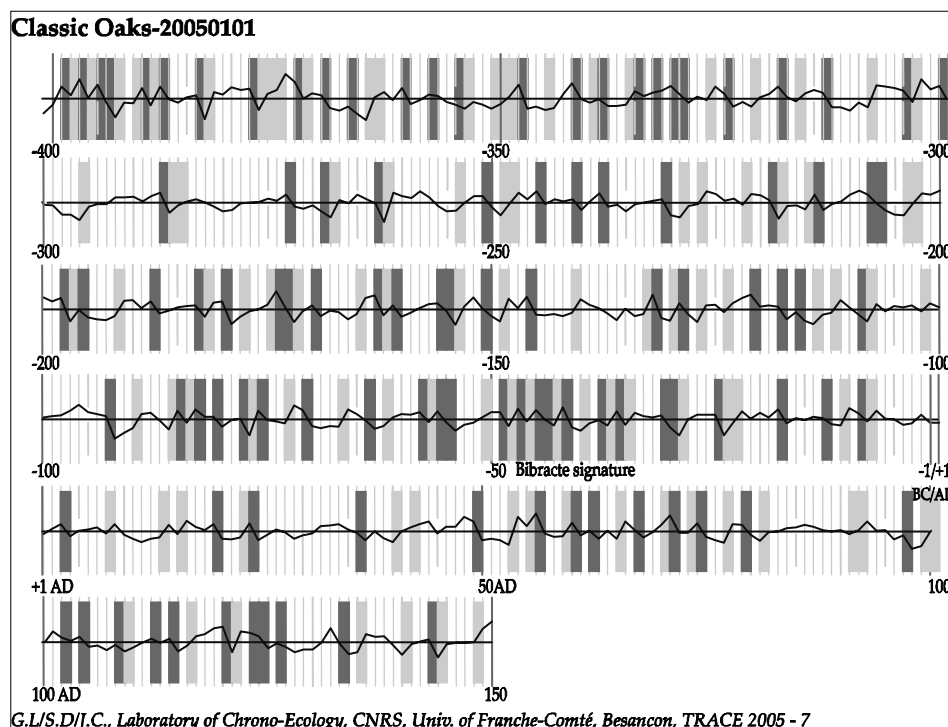


Figure 7: Event years of the classic period (400 BC – 150 AD) in northern France

The precipitations of the current year work as a positive factor of the tree ring growth. Instead we are led to consider a signed narrow ring as a sign of a potential dryness. There is but a

question about the negative correlations given by the spring and summer temperatures. Of course summer temperatures which are too high probably indicate dryness and in this case, a negative correlation between ring width and temperature is understandable; but according to the previous computations carried out on the whole period, it seems that in this sector of the Saône Valley the spring and summer temperatures do not influence directly the making of the current tree ring. The next correlations with indexes ED7 and GL2 show that we can be more optimistic. The correlations between tree growth and the combined meteorological indexes ED7 and GL2 clearly show that working with combined meteorological factors is better and the relationships between the ring growth and the immediate meteorology work efficiently:

62 event years between 1879 and 1993 give:

$$r(\text{SVoaks}, \text{ED7}) = 0.46$$

$$r(\text{SVoaks}, \text{GL2}) = 0.47$$

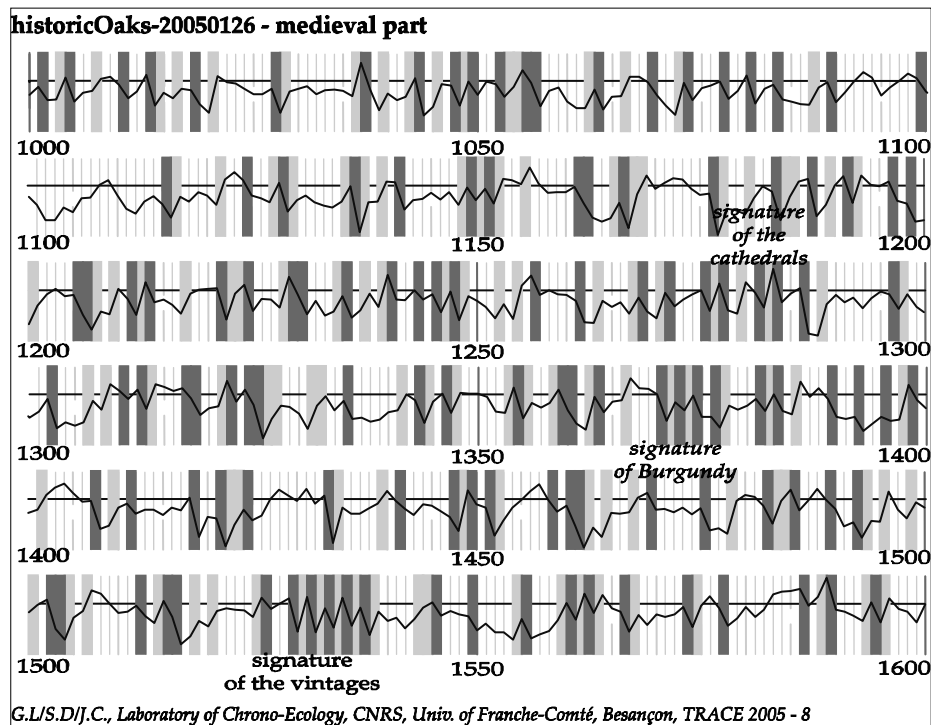


Figure 8: Event years of the late medieval period in northern France.

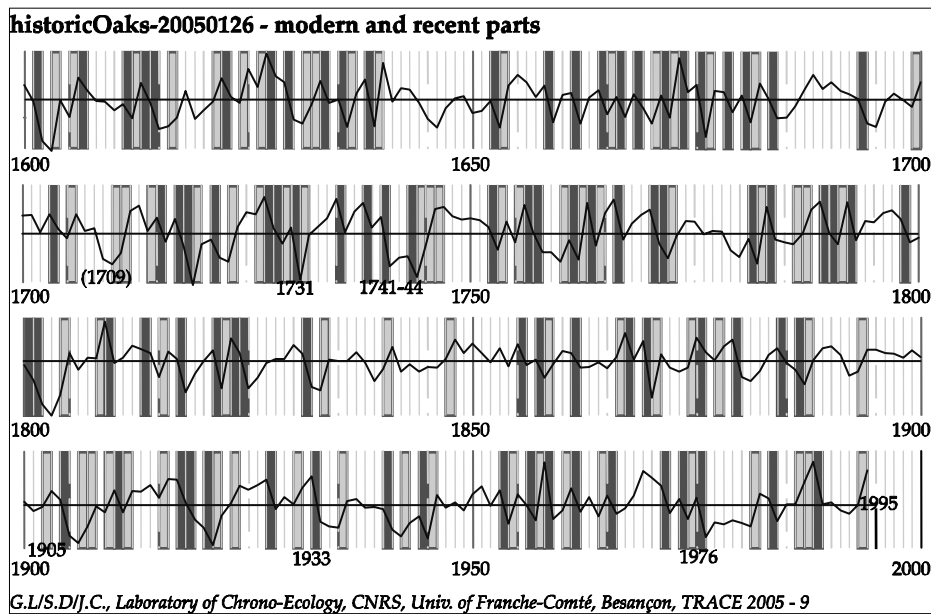


Figure 9: Event years of the modern and contemporary periods in northern France

Such good correlations encouraged us to look at the situation in other countries. In the direction of the historians, we note that most of the negative signed years (narrow ring) indicate, more or less, dryness. Negative event years highlight bad vegetal production, potentially bad harvests. This may be related to potential nutritional and social human problems. On the other hand, a global narrow ring is a possible indicator of good vintages in the northern half of France (Fig. 7, 8 and 9).

Then, for each event year, we thought about a mapping of the phenomenon. But, we had first to find a method for modeling the tree response of event years like 1904, 1911, 1959, 1976, etc.

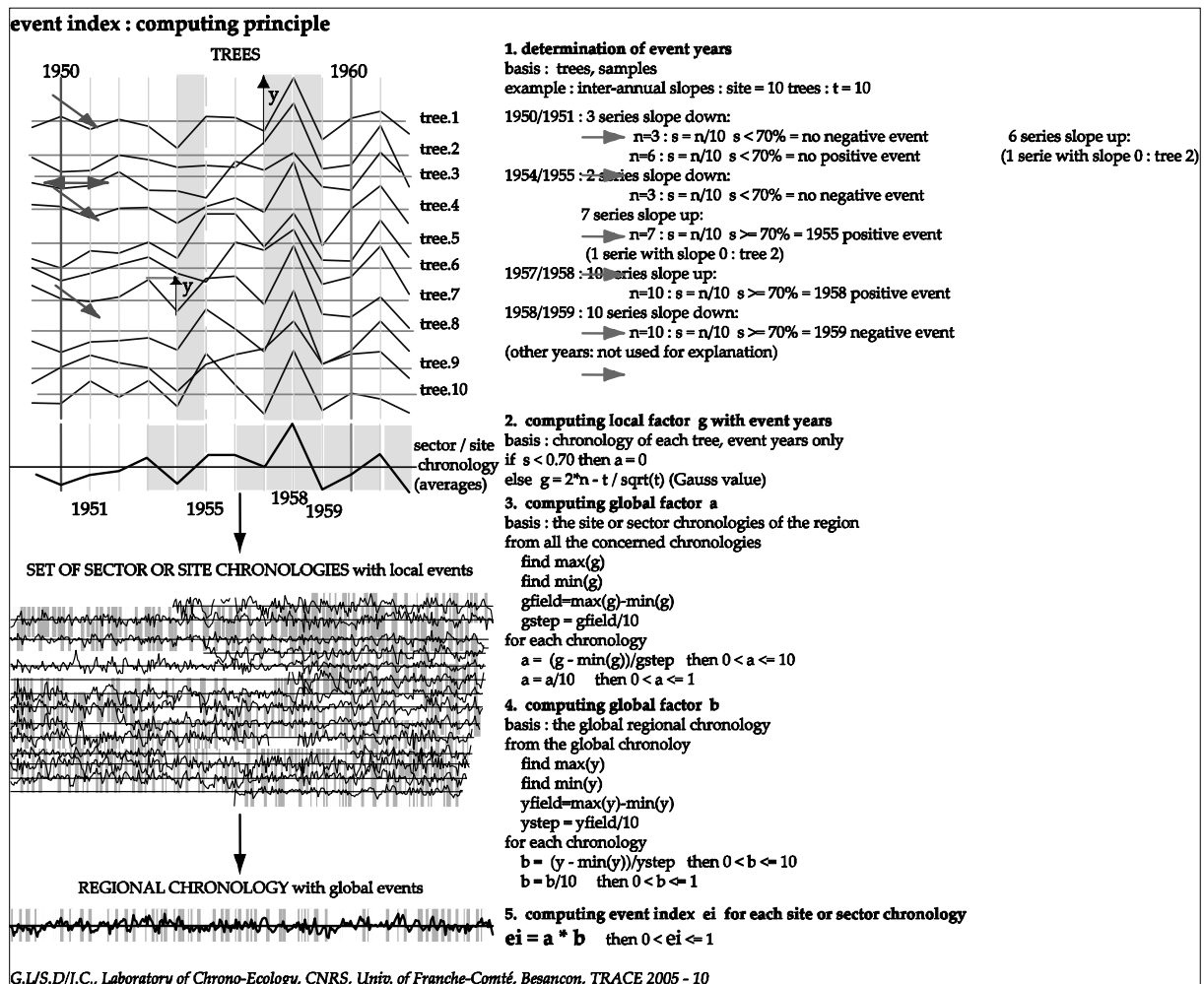


Fig. 10: Event index computing

Maps for prognostics back in the history: mapping the event years

We then looked at what happens over a large area with the event years. The starting model included 30 forests, more than 500 trees spread over 300 000 km² and the application field was the data basis HistOaks20050126 and ClassicOaks20050101. In order to be concise, we will only consider small rings.

Process

The trees of each site did not all respond in exactly the same way to hydric stress. For each year, the response of each region was evaluated according to the average size of the ring width and to the percentage of sensitive trees which show a typical narrow ring. All other trees were ignored. An index of this type of response was computed, associating both points of view. For the whole region, ring widths of the event years were divided into 10 classes (factor b); for each sector the Gauss value provided by the significant part of the trees contributing to the signature were also divided into 10 classes (factor a). The product of both results, $ei = a \cdot b / 100$, gives a number between 0 and 1 (Fig. 10). It is used as a percentage or a precise colour (or a shade of gray) for representing on a map the response degree of a sector. Here 0 is white (no tree response, neutral situation) and 1 totally black (best

sensitivity: sector with the narrowest rings). Four years (1959 (AD), 1976, 1928 and 1952) known for their summer hydric deficit and which give a very narrow ring on oak trees are shown (Fig. 9). The resulting maps are quite different from each other. Each year gives a typical image. Such an image is the result of global meteorological conditions which were interpreted by the trees over a 500 km area.

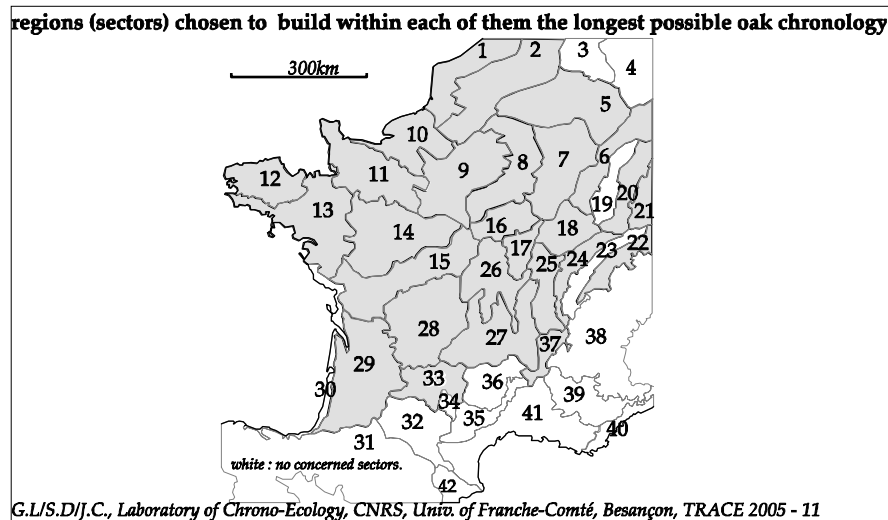


Figure 11: Initial territorial partition, potential stable biotopes

We think that a precise map could describe a global precise meteorological situation. The more extreme the meteorological conditions are - especially during spring and summer -, the stronger the relationship between them and map types are. Our goal is to classify these maps and to try and compare them over the time. Recent well known mapped situations could be used to explain historic or prehistoric years which are represented by the same type of map. Thus, for example, the 15th century is globally a bad century for trees - and harvests - (Fig. 8) and the exact opposite situation seems to characterize the first century before Christ (Fig. 7). The necessary condition is being to have got over the time dendrochronological information in comparable geographical sectors.

Taking phytogeographical studies as a basis, we divided the French territory into 42 areas. Each area represents a balance between several environmental parameters: latitude, altitude, distance from the ocean and geological ground. All the trees and woods of all the periods of each area were collected to build a regional chronology. 27 sector chronologies were re-built: zones 1-2, 5-18, 20-22, 24-29, 33 and 37. The Saône Valley region, which we previously discussed, groups sectors 18 and 25 (Fig. 11). As explained above, the event index values were computed and recorded in a 27-column chart. The year 1026 AD was taken as the starting point, the year 1995 as the ending point (970 years). Note however that not all chronologies are complete for the whole period and this work is a first draft.

First results

The chart was sorted according to the average value index of each year. Then the most typical 80 years were returned ahead in the chart and led to a factor analysis. To solve the

problem created by the missing data (no event years), a special linear distance was chosen instead of the classic Correlation coefficient r . The plot obtained shows a central group surrounded by scattered points (Fig.12).

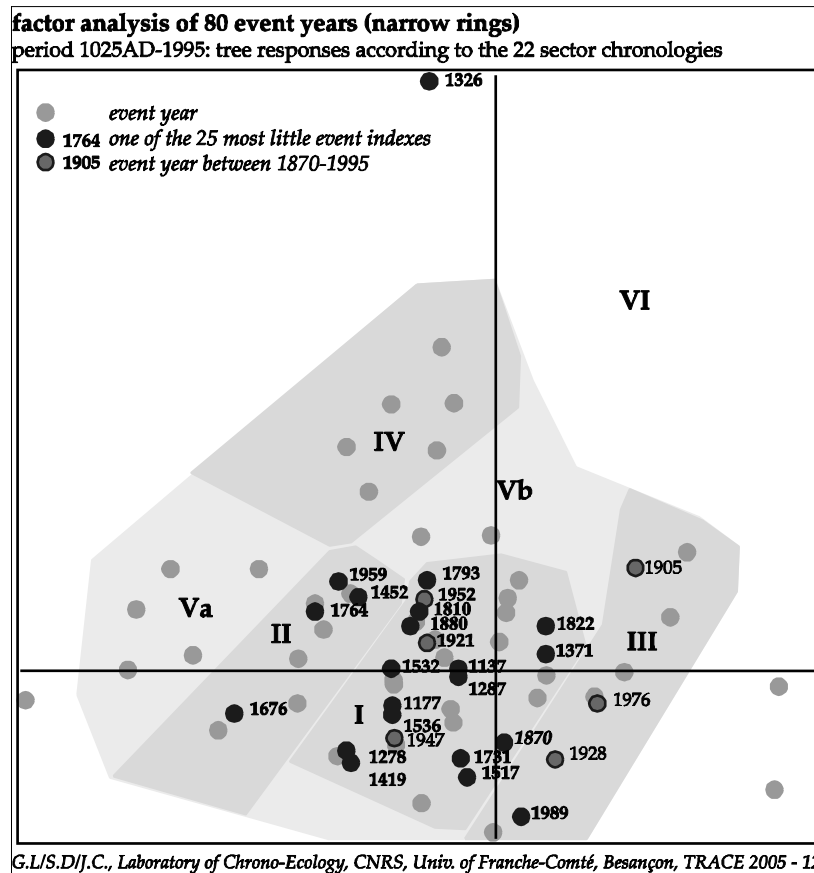


Figure 12: Factor analysis of 80 historical event years

20th century years fill the right part of the scatter plot. This is probably a wrong effect due to the set of living trees, which is making the best network of the basis. Nevertheless the points scattering shows definite evidence of the quality of the stress changes with the sector and the year. In fact, the most marked years (by the narrowest rings) tend to regroup around the center of the graph. Generally they are the warmest and driest years of the period. The right of the graph probably indicates the warm section and the left section indicates the colder part but still dry enough. We defined six temporary areas of sensibility within the plot. The maps, drawn from samples of zones I, II and III, show the diversity of the tree responses through the landscape. Such responses are possibly representative of cyclic or repeated climatic conditions. Zones IV to VI relate to more special or individual years and especially some parts of the original chart, which does not contain enough data.

The year 1976, marked by a strong spring-summer warm dryness, yielded laboriously a very narrow ring in all the territory. But the dryness of 1959 did not hit with the same strength the rings in the eastern part of the country. It looks as though the plain between Bordeaux and Paris recorded the worst climatic impacts. 1952 gives another view in which western countries clearly escaped the stress. Then, each map is linked to a particular meteorological

situation (Fig. 13), in which the dominant position of clouds and dominant direction of the winds work efficiently or not. We think that some types of map suggest the main direction of the winds in summer and then the positions of the anticyclones of the northern hemisphere around the Greenwich line. We will explain this later in another paper.

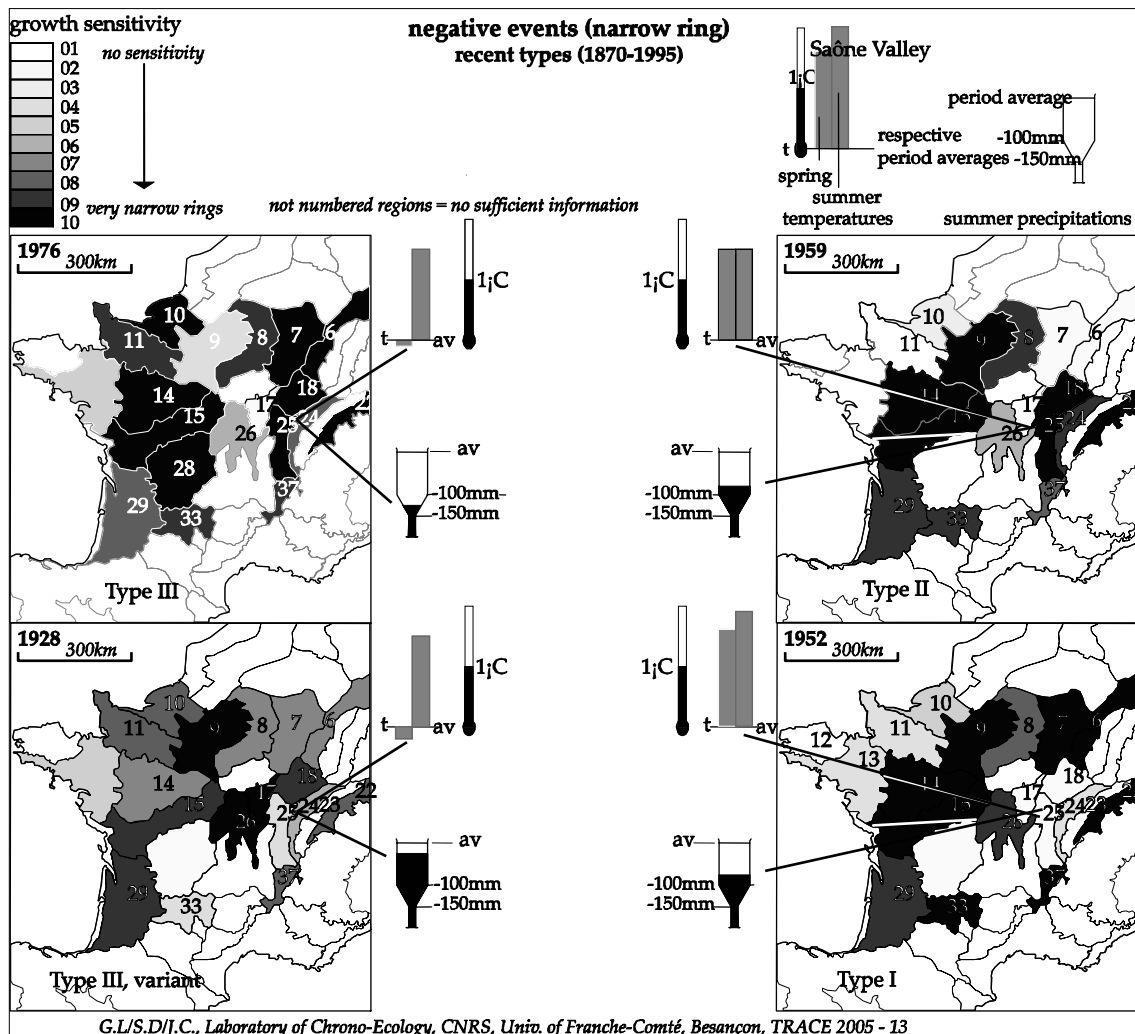


Figure 13: Narrow oak rings and dryness in France in the last century.

Conclusion: sensitive years

At this point, we are not able to lead the demonstration at this end because we did not get enough woods: treating 2500 years in such a small area as northern France would require about 10000 trees correctly chosen. Except for short periods (late roman /early medieval) they are in the backgrounds of our laboratories! We can however put forward a hypothesis about the weather of some past years, which concerned the life of the most important sites we had to study. The last figures (Fig. 14 and 15) show, firstly, noteworthy historic (event) years and secondly, other event prehistoric years about which we only know the figure. It is more difficult at this point and stage of this research, which requires lengthy controls of a lot of small sites, to draw complete maps of the historical period. Nevertheless we produced some maps, which suggest dendrochronological situations that would be workable. The year 1137, well known for its very narrow ring (sometimes invisible on the samples!) tends to

show a comparable situation to 1976. Potentially, the same climatic situation could be applied to year 1676. The meteorology of the summer of that year is described in ancient texts as exceptionally hot and dry. Year 1419 shows a situation similar to 1959. As a paradox, data from the late prehistory (late Gallic and early roman period) gives more results. Numerous excavations about this period delivered a lot of woods which were recently re-studied (Durost 2005). Samples of maps show the dendrochronological potential of these periods: The year 76 before Christ is probably the driest one in the Gallic period (as 1976).

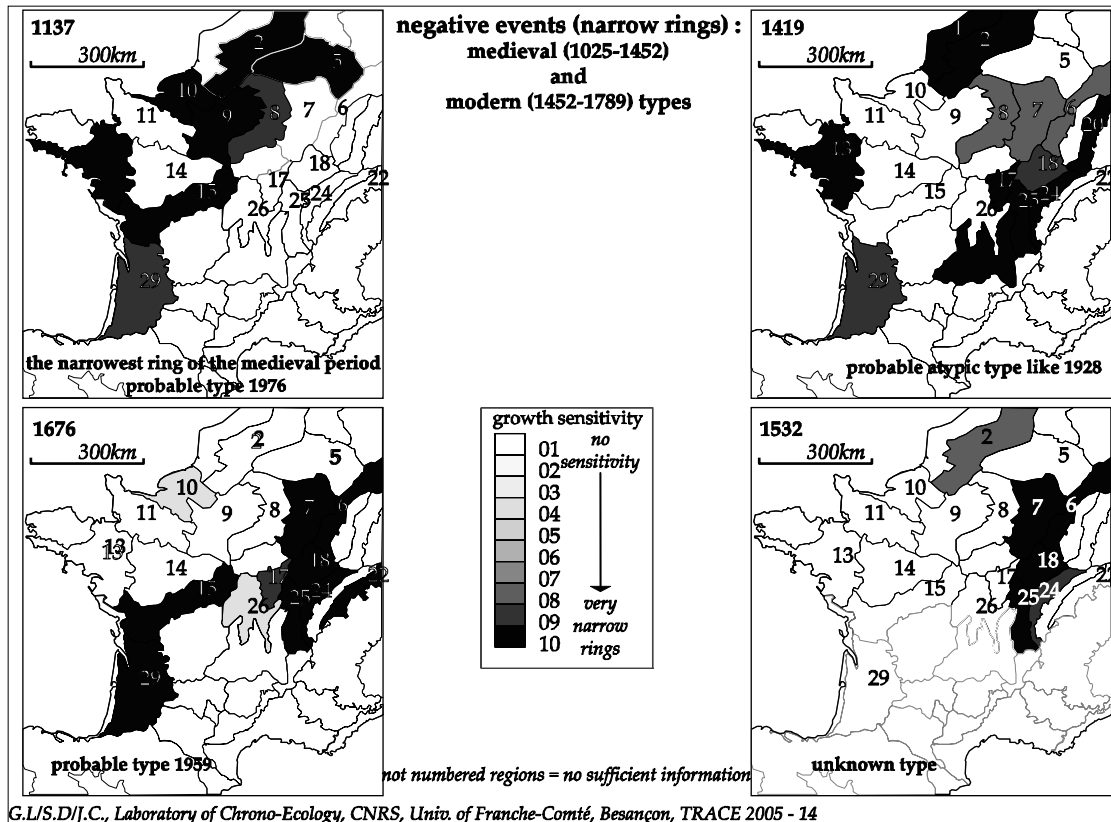


Figure 14: Medieval and modern narrow rings

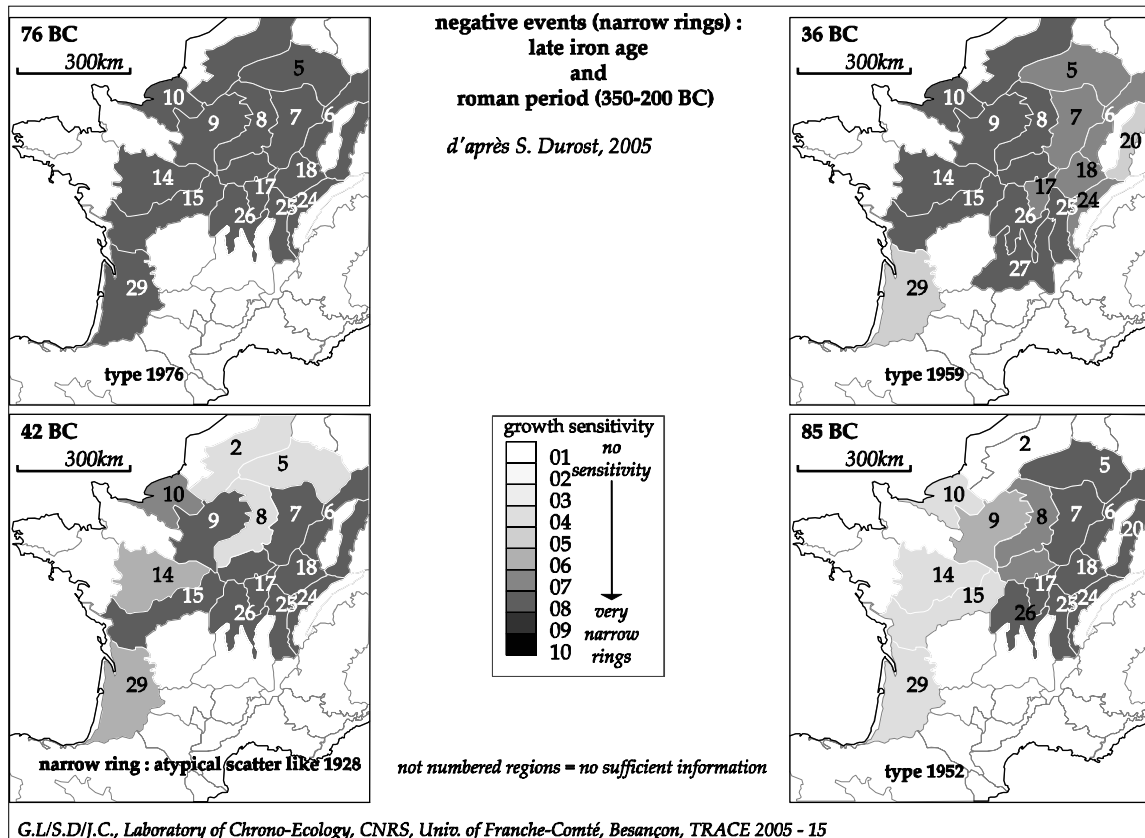


Figure 15: Late prehistoric narrow rings

But a suite of such years has been noted during the 300-year period before Christ and the whole of Gaul, which stretched under temperate climate. This leads us in two directions: firstly, that the human impact on trees, even on trees located in neighboring areas of human societies and used by men, is less than we thought – this is a subject for researches in archaeology - and, secondly, that the global climatic factors worked differently compared to the 20th century.

We give at the end a summary of years, which could be discussed with Historians (Fig. 16).

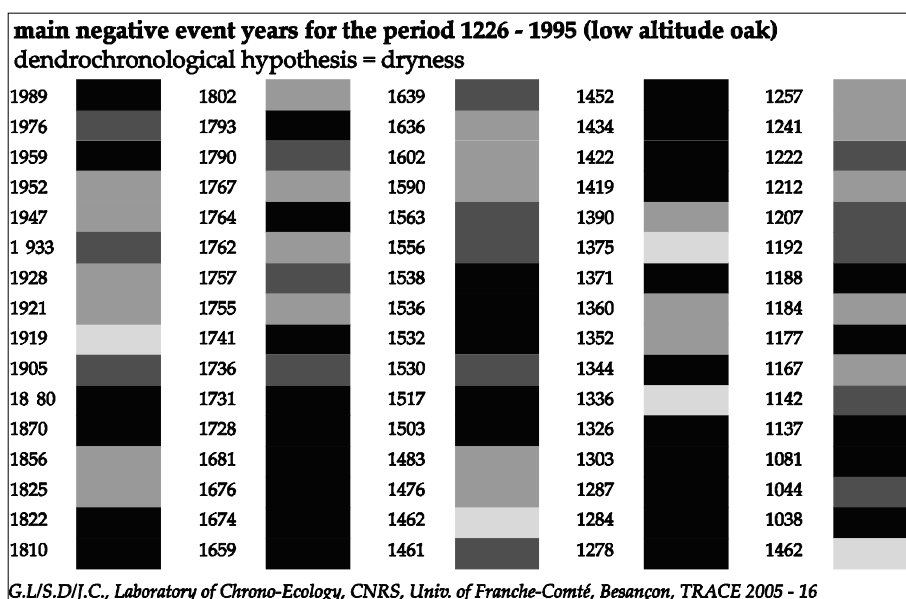


Figure 16: Ancient negative event years: dark = probable hard summer dryness; grays : opened hypothesis for discussion.

Acknowledgments

Centre Européen d'Archéométrie de l'Université, Liège (B);

Firm CEDRE, Besançon (F);

Firm Dendronet and Labor für Holzanalyse Singen-Böhlingen (D)

Laboratoire d'Archeosciences de l'Université de Rennes 1 et CNRS, Rennes (F)

Laboratoire de Chrono-Ecologie de l'Université de Franche-Comté et CNRS, Besançon (F)

Laboratoire de dendrochronologie du Laténium, Neuchâtel (CH);

and

André Billamboz, D-LBW, Hemmenhofen (D);

Frédéric Guibal, AO des Compagnons du Devoir du Tour de France et CNRS, Aix-en-Provence (F);

Mrs Yvonne Trenard, CTB, Paris (F).

Basic calendar : Ernst Hollstein 1980, Rheinisches Landesmuseum, Trier (D).

References

- Baillie, M.G.L., Pilcher, J.R. (1973): a simple Cross-dating Program for Tree-ring Research. *Tree Ring Bulletin* 37: 1-12.
- Choisnel, E., Payen, D. (1989) : L'agrométéorologie. In Brunn, A., Stephan, J.-M., Bonton, J.-C. (Eds) : *Le Grand Atlas de la France Rurale*. INRA, SCEES, JP de Monza, Paris: 410-425.
- Durost, S., (2005): Dendrochronologie et dendroclimatologie du second âge du fer et de l'époque romaine dans le nord et l'est de la France. Thesis, Besançon, manuscript, 297 p.
- Emberger, L. (1930): La végétation de la région méditerranéenne. Essai de classification des groupements végétaux. *Revue générale de Botanique* 42: 641-721.

- Hollstein, E. (1980): Mitteleuropäische Eichenchronologie. Trierer dendrochronologische Forschungen zur Archäologie und Kunstgeschichte II. Philipp von Zadern, Mainz. 273 p.
- Houbrechts, D., Lambert, G.-N. (2004): Les arbres, témoins du temps qui passe. In *Le Temps des Datations, Pour la Science, Dossier hors-série, janvier/mars*: 70-75.
- Huber, B., Giertz_Siebenlist, V., (1969): Unsere tausendjährige Eichen-Jahrringchronologie durchschnittlich 57 (10-150) fach belegt. Aus der *Sitzungsberichten der österreich. Akademie der Wissenschaften, Mathem. naturw. K1, Abt 1/78, Heft 1-4*: 37-42.
- Lacoste, A., Salanon, R. (1999): *Eléments de biogéographie et d'écologie - Une compréhension de la biosphère par l'analyse des composantes majeures des écosystèmes*. Nathan, Paris. 300 p.
- Lambert, G.-N, (2002): Datation dendrochronologique des charpentes, crédibilité et précision. In Patrick Hoffsummer et Jannie Mayer 2002, éd.: *Les Charpentes du XIème au XIXème siècles. Typologie et évolution en France du Nord et en Belgique*. Centre des Monuments Nationaux, Cahiers du Patrimoine, Editions du Patrimoine, série "Monum". Paris: 85-98.
- Schweingruber, F.H., Eckstein, D., Serre-Bachet, F., Bräker, O.U. (1990): Identification, presentation and interpretation of event years and pointer years in dendrochronology. *Dendrochronologia* 8: 9-38.

SECTION 6

ISOTOPES

The potential of stable isotopes to record aridity conditions in a forest with low-sensitive ring widths from the eastern Pre-Pyrenees

O. Planells¹, L. Andreu¹, O. Bosch¹, E. Gutiérrez¹, M. Filot², M. Leuenberger², G. Helle³
& G.H. Schleser³

¹University of Barcelona, Department of Ecology. Diagonal 645, 08028 Barcelona, Spain

²University of Bern, Climate and Environmental Physics Institute. Sidlerstrasse 5, 3012 Bern, Switzerland

³Forschungszentrum Juelich GmbH, Institute of Sedimentary Systems, ICG-V. 52425 Juelich, Germany

Email: octaviplanells@ub.edu

Background and objectives

The Mediterranean climate has a marked seasonality characterized by relatively cold winters, humid springs and autumns, and dry summers. The low water availability due to summer drought made species to develop special mechanisms for adaptation during their process of evolution. Independently, summer droughts have an unfavourable effect on tree growth. However, owing to topography, droughts are less frequent in some mountainous Mediterranean areas, and consequently plant growth is not that much limited in these areas by the lack of water. Tree rings of old trees are excellent climatic archives since they are sensitive to numerous environmental variables. The oldest trees around the Mediterranean basin are located close to the altitudinal tree line, far away from direct human activities.

In the present work, three different tree-ring chronologies covering 400 years were investigated with regard to ring widths (RW), $\delta^{13}\text{C}$ and $\delta^{18}\text{O}$. The corresponding trees originate from of an old sub-alpine forest that is not limited by summer droughts (Vigo et al., 2003). More specifically, the aim of this investigation was to (1) study whether stable isotopes of that region record climate variations, (2) explore whether a particular meteorological quantity is specifically recorded, and (3) estimate the climatic content of ring widths (RW) in relation to stable isotopes.

Study site

The study site is an east-facing sub-alpine forest of *Pinus uncinata* located in the Massís del Pedraforca, eastern Pre-Pyrenees (Fig. 1). *P. uncinata* forms the sub-alpine forests in the Spanish Pyrenees ranging from 1600 to 2500 m a.s.l. Previous studies performed at lower altitudes in the same mountain area (1680 m a.s.l.) showed a negative response of tree growth to July temperature, indicating a growth limitation by drought (Gutiérrez 1991). This is in contrast to the study site in this work (>2100 m a.s.l.), where rainfall is higher due to the advection of humid air masses coming from the Mediterranean Sea (annual precipitation higher than 1000 mm, June-September higher than 300 mm, mean annual temperature around 7 °C).

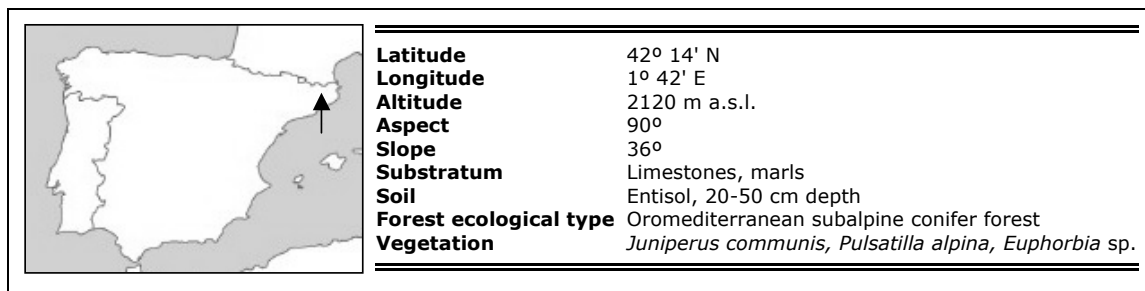


Figure 1: Map and description of the main features of the studied *P. uncinata* stand in Massís del Pedraforca mountain.

Methods

The individual power-transformed RW measurements were detrended by negative modified exponential or linear fitting in order to remove non-climatic trends related to tree age. Autocorrelation was also removed to get independent values and to enhance the climatic signal. The master chronology was computed with a biweight robust mean (Cook and Kairiukstis 1990).

For isotopic analyses, the whole annual rings from 4 trees (2 cores each were taken, resulting in 2 samples per year and per tree) were pooled, homogenized, and α -cellulose was extracted. $\delta^{13}\text{C}$ measurements were performed in 2 different laboratories following two different methods (combustion and pyrolysis). Although both types of measurements provide series with identical inter-annual patterns, i.e. equal relative variations, there is a shift in the absolute values of the series (Knöller et al., 2005). For correction, the difference between the means of both series was added to the annual measurements of one series. To remove the non-climatic $\delta^{13}\text{C}$ decrease observed in the raw data due to anthropogenic CO_2 emissions since industrialization, a correction was applied as suggested by McCarroll and Loader (2004). The corrected $\delta^{13}\text{C}$ series were averaged to reduce inhomogeneities of each individual record ($r = 0.765$). Finally, autocorrelation of averaged measurements was removed similar to the method for RW (Monserud and Marshall 2001). It was not applied any correction to the $\delta^{18}\text{O}$ series, however autocorrelation was also removed before statistical analysis.

Calibration of tree-ring proxies and climate was performed by bootstrapped correlation (95% significance level) and single Pearson correlation analysis. We used homogenized mean monthly temperature and total precipitation of a 25x25 km grid of regional climatic records covering the years from 1931 to 2003 (Spanish National Meteorological Institute). The relationships between tree growth and climate were computed with variables from July of the year prior to tree growth (small letters; Figure 3) to October of current year (capitals). Aridity, which was expressed by a certain combination of temperature and precipitation, was one particular quantity to look at. Calibration was performed by using a simple aridity index expressing the monthly deficit of rainfall versus temperature:

$$A = Std[T] - Std[\log_{10}(P+1)]$$

where T and P are monthly temperature and precipitation, respectively. P is expressed as logarithms to get normalized values (T records are supposed to follow normal distributions). Std represents a scaling of both variables, according to,

$$Std_t = \frac{x_t - \bar{x}}{SD}$$

with x_t being the observed value, \bar{x} the mean value of the climate records, including all the months, and SD its standard deviation.

Results and discussion

Figure 2 shows the standardized series. The RW chronology is statistically representative of the stand since the expressed population signal (EPS; Wigley et al 1984) for the period 1600-2003 is 0.88 (15 trees / 32 radii cover this whole period). The low mean sensitivity index and percent of variance explained by the first eigenvector (0.175 and 36%, respectively) point to a low sensitivity of RW to climate. In accordance with this result, bootstrapped correlation analysis (Fig. 3) shows only few significant relationships with temperature of the previous year (jul = 0.232; oct = 0.281; nov = 0.305), suggesting an important role of food storage on tree growth of following years. In addition, RW show some significant response to aridity, but values are very close to the significance thresholds (nov = 0.194; JUL = -0.228).

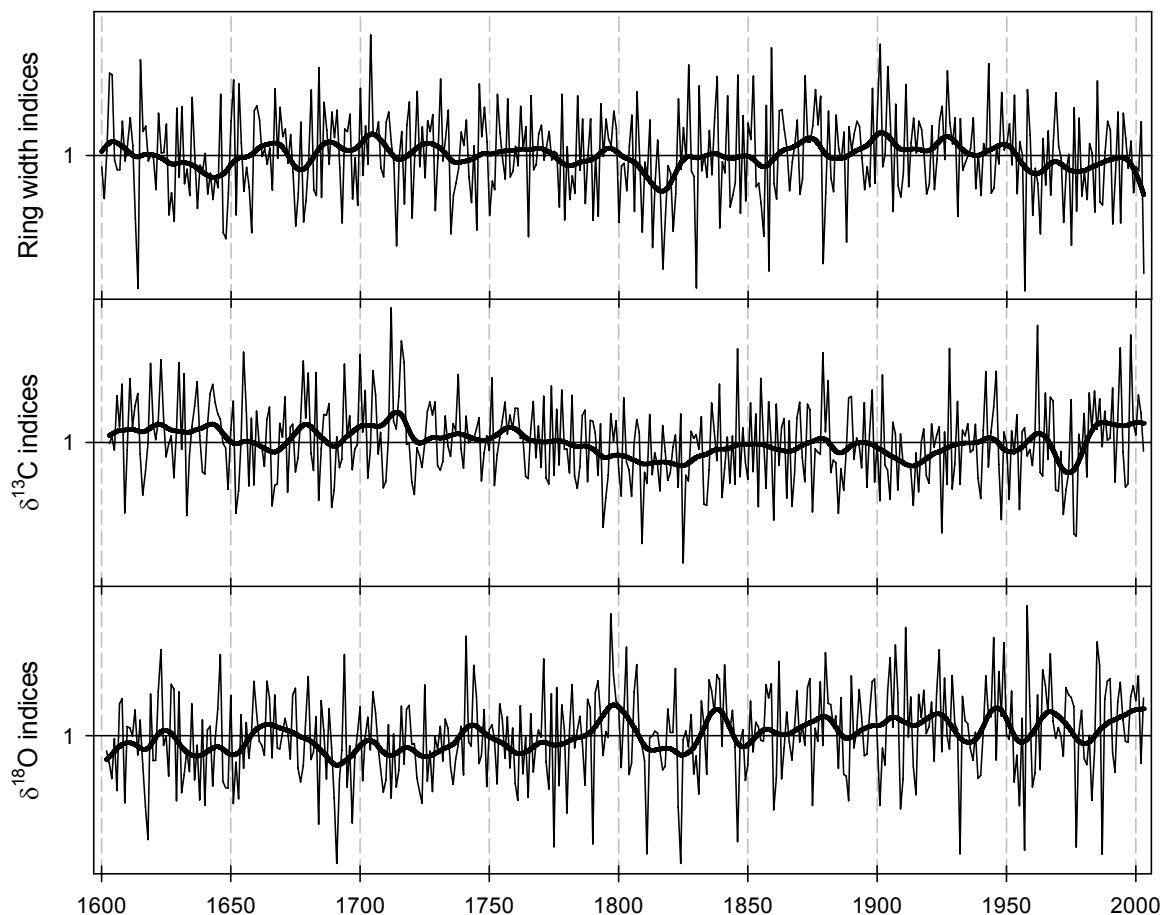


Figure 2: Ring width (top), $\delta^{13}\text{C}$ (middle) and $\delta^{18}\text{O}$ (bottom) chronologies of *P. uncinata* in Pedraforca. These are indexed series resulting from the different standardization procedures described in the text. The smoothed curves correspond to a 20-year spline fitting.

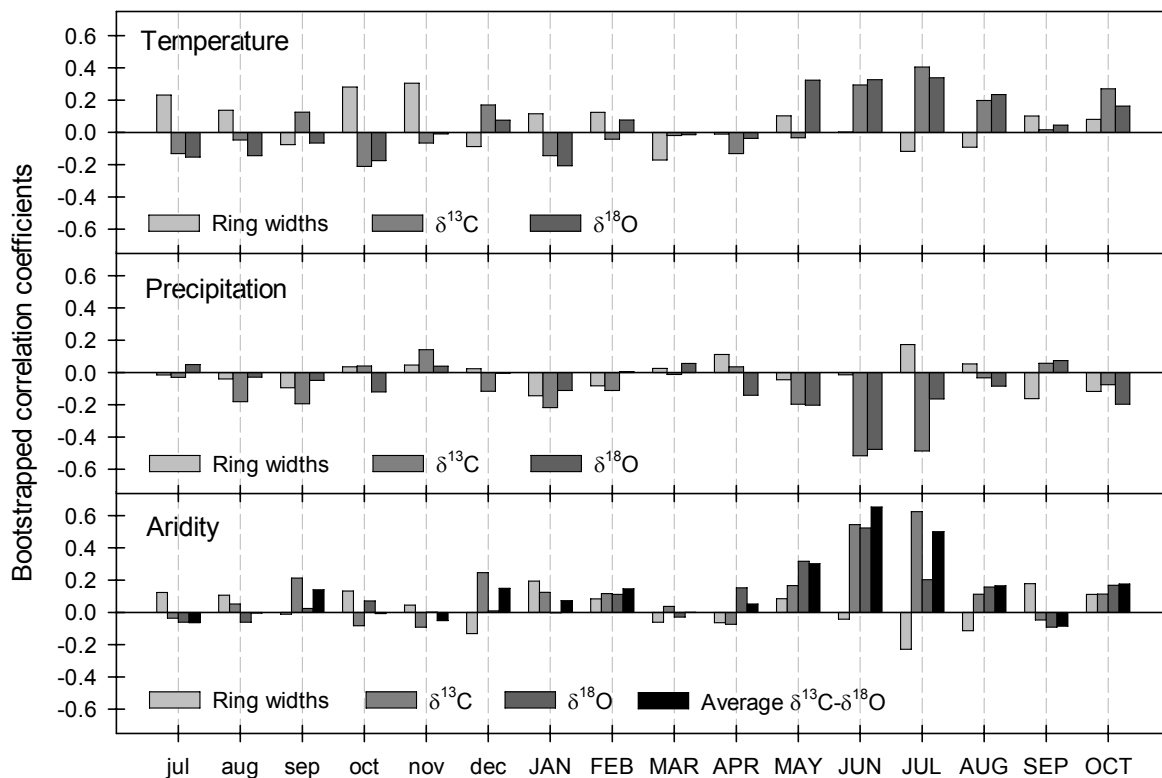


Figure 3: Bootstrapped correlation analysis performed with the different tree-ring proxies and mean temperature (top), total precipitation (middle), and aridity index (bottom) from July of the year prior to tree growth (small letters) to current year October (capitals). See text for explanation of calculations.

It is noteworthy to mention a slight negative response to current July aridity, which suggests a certain tree growth limitation due to summer water deficit. In contrast to RW, $\delta^{13}\text{C}$ data show a major response to summer climate. There is an important and significant positive relationship with temperature (JUN = 0.294; JUL = 0.405), and a negative response to precipitation (JUN = -0.516; JUL = -0.487). Correlations with summer aridity are even higher (JUN = 0.544; JUL = 0.624) and positive. These results are well in line with the Francey and Farquhar model of carbon isotope discrimination in plants (1982). This model is related to drought severity since it takes into account the stomatal aperture and the intercellular availability of CO_2 for the enzyme rubisco. According to the model, higher water stress (lower precipitation/higher temperature) results in stomatal closure and more positive $\delta^{13}\text{C}$, thus consistent with a positive sign of the regression equation for temperature and a negative sign for precipitation. There are some other relationships between $\delta^{13}\text{C}$ and monthly variables prior to the growing period, but their significance is very low. The role of reserves accumulated during the dormancy period could be an explanation of these relationships. However, most of them could be reached just by chance since their coefficients oscillate close around the significance thresholds.

Similar results as for $\delta^{13}\text{C}$ were obtained for $\delta^{18}\text{O}$. Temperature has a broader influence in terms of number of months exceeding the significance level (MAY = 0.344; JUN = 0.352; JUL = 0.340; AUG = 0.256). On the other hand, on a monthly basis, there is only one significant relationship with precipitation (JUN = -0.487). Response to aridity is also positive and

significant for early summer (MAY = 0.318; JUN = 0.524), indicating a response comparable to that of $\delta^{13}\text{C}$. However, there are some dissimilarities probably caused by the different fractionation processes driving the isotope ratios in tree rings. In contrast to the causes for $\delta^{13}\text{C}$ discrimination, $\delta^{18}\text{O}$ largely depends on the isotope ratio of soil water (which is related to $\delta^{18}\text{O}$ of rain water, residence time in the soil, evaporation rates, etc.) and the enrichment of leaf water due to evapotranspiration (Yakir and Sternberg 2000). In a further step, we looked for an optimisation procedure to extract the climatic signal contained in the isotope proxies. The similar results obtained with $\delta^{13}\text{C}$ and $\delta^{18}\text{O}$, in terms of response to summer conditions and the significance of this response, indicate that a common climatic signal could be recorded in both ($r = 0.200$). The averaging of $\delta^{13}\text{C}$ and $\delta^{18}\text{O}$ series could reduce the non-climatic noise contained in these records, possibly favouring the common climatic variability.

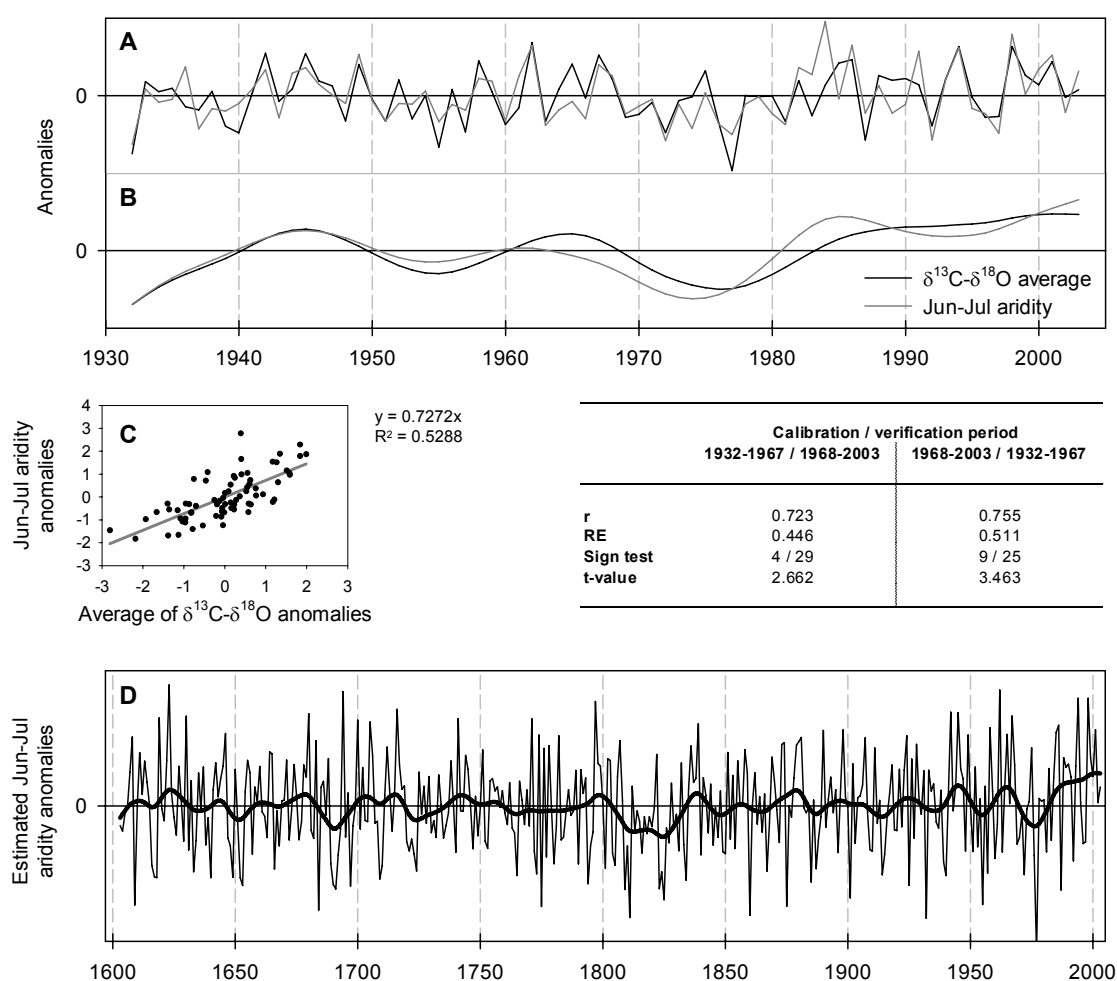


Figure 4: (A) Anomalies of June-July aridity and the averaged $\delta^{13}\text{C}$ and $\delta^{18}\text{O}$ series from 1932 to 2003. (B) 20-year smoothing spline of both. (C) Scatter plot and linear regression of the variables plotted in A. (D) Reconstruction of June-July aridity covering the last four centuries after the verification of the relationship described in C. All the verification statistics (see the table) are significant at 95% probability level. (Table) *r*, Pearson correlation coefficient; RE, reduction of error; sign test, disagreements / agreements; *t*-value of the product means test.

The bootstrapped correlation coefficients obtained for the averaged series and the aridity index, are also high (MAY = 0.302; JUN = 0.654; JUL = 0.501), but not notably higher than those obtained for $\delta^{13}\text{C}$ and $\delta^{18}\text{O}$ separately. However, after combining the climatic variables in clusters of months, the strongest relationship was found for the averaged $\delta^{13}\text{C}$ and $\delta^{18}\text{O}$ data. Combining June and July, computed as a mean of both months resulted in a very high correlation for the aridity index (JUN-JUL = 0.727; Fig. 4).

The high agreement shown in Figure 4 leaves the average of $\delta^{13}\text{C}$ and $\delta^{18}\text{O}$ as the best proxy record to reconstruct the summer climate of the sampled area. Strictly speaking is it, the trade-off between precipitation and temperature of June and July. The verification of these relationships for the sub periods 1932-1967 and 1968-2003 was successful in all the statistic tests. According to the relationship established with the instrumental records, the reconstructed June-July aridity anomalies show some long-term arid and humid periods. The most conspicuous anomaly is the rise of aridity that starts around 1940 and increasingly oscillates until the end of the 20th century. Noticeable is also a cool or humid period in the first half of the 19th century, and a long interval of climatic stability covering the time period from 1740 to 1800. The averaging of $\delta^{13}\text{C}$ and $\delta^{18}\text{O}$ does enhance climatic reconstructions in this region, but this method may not hold as a general rule, because in other site conditions often the two isotopes may not be influenced by the same factors.

The use of an aridity index, which integrates temperature and precipitation, makes it sometimes difficult to discern the causes of these anomalous climatic periods. In the present case, the information provided by the individual proxies is rather useful. For example, the increase of the late 20th century aridity index is also observed in the individual $\delta^{13}\text{C}$ and $\delta^{18}\text{O}$ series, being the amplitude of the oscillations slightly smaller in both records (Fig. 2). In contrast, the RW series show a slight decrease but with an abrupt decrease at the last decade, coinciding with the rise of aridity. RW showed a slight limitation by summer drought (Fig. 3).

Despite the fact that RW of the studied forest are not very sensitive to climate, the decrease in mean widths since 1930 to now coinciding with the increase of aridity could be understood as an increase in sensitivity to the changing climatic conditions.

Considering that stable isotopes respond positively to aridity, and RW negatively, coinciding trends can provide complementary information. This is e.g. the case of the negative aridity anomalies of the mid half of the 19th century. It coincides with notable tree growth suppression visible in the RW chronology. This suggests that the limitation of tree growth is not due to drought but due to the shortness of cold and wet growing seasons. This approach of combined analysis of RW and isotopes for understanding climatic changes would be worthwhile to study in more detail in a future study.

In conclusion, the results shown demonstrate that the information provided by different tree-ring proxies is complementary and sometimes can be combined to get better and more reliable climatic reconstructions. The interpretation of long-term trends and pointer years of reconstructions made with single proxies or a set of proxies, can occasionally be improved by defining indirect climate quantities such as the used aridity index being a combination of two meteorological variables.

Acknowledgements

The authors are grateful to Carlos Almarza, Javier Martín Vide and Mariano Barriendos for their help in providing meteorological resources. We also thank Henry Grissino-Mayer for supplying useful references. This research was funded by the EU project ISONET '400 years of Annual Reconstructions of European Climate Variability using a High Resolution Isotopic Network' (EVK2-2001-237).

References

- Cook, E.R., Kairiukstis, L.A. (1990): *Methods of Dendrochronology*. Kluwer, Dordrecht.
- Francey, R.J., Farquhar, G.D. (1982): An explanation of $^{13}\text{C} / ^{12}\text{C}$ variations in tree rings. *Nature* 297: 28-31.
- Gutiérrez, E. (1991): Climate tree-growth relationships for *Pinus uncinata* Ram. in the Spanish pre-Pyrenees. *Acta Oecologica* 12(2): 213-225.
- Knöllner, K., Böttger, T., Weise, S.M., Gehre, M. (2005): Carbon isotope analyses of cellulose using two different on-line techniques (elemental analysis and high-temperature pyrolysis) – a comparison. *Rapid Communications in Mass Spectrometry* 19: 343-348.
- McCarroll, D., Loader, N.J. (2004): Stable isotopes in tree rings. *Quaternary Science Reviews* 23: 771-801.
- Monserud, R.A., Marshall, J.D. (2001): Time-series analysis of $\delta^{13}\text{C}$ from tree rings. I. Time trends and autocorrelation. *Tree Physiology* 21: 1087-1102.
- Vigo, J., Soriano, I., Carreras, J., Aymerich, P., Carrillo, E., Font, X., Masalles, R.M., Ninot, J.M. (2003) *Flora del Parc Natural del Cadí-Moixeró i de les serres veïnes (Prepirineus orientals ibèrics)*. Monografies del Museu de Ciències Naturals 1, Institut de Cultura, Ajuntament de Barcelona, Barcelona, 407 pp.
- Wigley, T.M.L., Briffa, K. R., Jones, P.D. (1984): On the average value of correlated time series, with applications in dendroclimatology and hydrometeorology. *Journal of Climate and Applied Meteorology* 23: 201-213.
- Yakir, D., Sternberg, L.S.L. (2000): The use of stable isotopes to study ecosystem gas exchange. *Oecologia* 123: 297-311.

The European Isotope Network ISONET: First Results

K. Treydte¹, G.H. Schleser², J. Esper¹, L. Andreu³, T. Bednarz⁴, F. Berninger⁵,
T. Böttger⁶, C.D. D'Allessandro⁷, N. Etien⁸, M. Filot⁹, D. Frank¹, M. Grabner¹⁰,
E. Gutierrez³, M. Haupt⁶, G. Helle², E. Hilasvuori¹¹, H. Jungner¹¹, M. Kalela-Brundin¹¹,
M. Leuenberger⁹, N. Loader¹², V. Masson-Delmotte⁷, A. Pazdur¹³, O. Planells³,
R. Pukiene¹⁴, C. Reynolds¹⁵, K. Rinne¹⁶, M. Saurer¹⁵, E. Sonninen¹¹, M. Stievenard⁷,
R. Switsur¹⁶, M. Szczepanek¹³, L. Todaro⁷, J. Waterhouse¹⁶, M. Weigl¹⁰ & R. Wimmer¹⁰

¹Federal Research Institute WSL, Zürcher Str. 11, CH-8903 Birmensdorf, Switzerland

²Forschungszentrum Jülich GmbH, Leo-Brandt-Str., D-52425 Jülich, Germany

³Universitat de Barcelona, Av. Diagonal, 645, 08028 Barcelona, Spain

⁴Agricultural University, 29 Listopada 46 PL-31425 Krakow, Poland

⁵University of Quebec at Montreal, Montreal, Canada

⁶Umweltforschungszentrum Leipzig-Halle GmbH, Theodor-Lieser-Strasse 4, D-06120 Halle/Saale, Germany

⁷Università della Basilicata, v.le Ateneo Lucano, 10, 85100 Potenza, Italy

⁸Laboratoire des Sciences du Climat et de l'Environnement; L'Orme des Merisiers CEA Saclay; LSCE UMR
CEA/CNRS 1572 Bat 709; 91 191 Gif sur Yvette cedex, France

⁹University of Bern, Sidlerstrasse 5, 3012 Bern, Switzerland

¹⁰Universität für Bodenkultur, Gregor-Mendel-Strasse 33, A-1180 Wien, Austria

¹¹University of Helsinki, POB11, FIN-00014 Helsinki, Finland

¹²University of Wales, Singleton Park, Swansea, SA2 8PP, United Kingdom

¹³Silesian University of Technology, Boleslaw Krzywoustego 2, 44 –100 Gliwice, Poland

¹⁴Vytautas Magnus University, Kaunas Botanical Gardens, lab, Kaunas, Lithuania

¹⁵Paul Scherrer Institut, 5232 Villigen, Switzerland

¹⁶Anglia Polytechnic University, East Road, Cambridge, CB1 1PT, United Kingdom

Introduction

Within the EU-Project ISONET (co-ordinator: G. Schleser, <http://www.isonet-online.de>), 16 partner institutions collaborate to develop the first large-scale network of stable isotopes (C, O and H), integrating 25 European tree sites reaching from the Iberian Peninsula and southern Italy to Fennoscandia. Key species are oak and pine. The sampling design considers not only ecologically “extreme” sites, with a single climate factor predominantly determining tree growth, as required for ring width and wood density analyses (Bräuning and Mantwill 2005, Briffa et al. 2001, 2002, Frank and Esper 2005a, b), but also temperate regions with diffuse climate signals recorded in the ‘traditional’ tree ring parameters. This may enable expanding climatic reconstructions into regions not yet well covered.

In this project we aim to estimate temperature, humidity and precipitation variations with annual resolution, to reconstruct local to European scale climate variability over the last 400 years. Climate variability is addressed on three timescales, namely decade-century, inter-annual and intra-annual. This strategy allows understanding of both, high frequency (high resolution exploration of seasonality signals, and extreme events) and longer-term trends (source water/air mass dominance, baseline variability) in site specific and synoptic climate across Europe. Here we present results from initial network analyses considering first data of

carbon ($\delta^{13}\text{C}$) and oxygen ($\delta^{18}\text{O}$) isotopes, to evaluate (a) common patterns in these networks and (b) their potential for detailed climate reconstruction beyond the information commonly achieved from ring width and density analyses.

Material and Methods

Oxygen isotopes were measured at 18 sites, and carbon isotope analyses at 21 sites (several data sets provided independent from ISONET), ranging from the Iberian Peninsula and southern Italy up to Fennoscandia, as shown in figure 1.

Ring widths were measured using a semi-automated RinnTech system with a resolution of 0.01 mm and cross dated following standard procedures (Fritts 1976). 4 trees per site (2 cores per tree) were selected for isotope analysis. Criteria for sample selection were low numbers of missing rings and regular ring boundaries. Tree rings were then separated year-by-year using sharp knives or scalpels (for oak only late-wood was considered). For the majority of sites tree-rings grown in the same year were pooled prior to cellulose extraction to facilitate the development of this large network (Borella et al. 1998, Leavitt and Long 1984, Treydte et al. 2001). Cellulose was extracted following standard procedures (overview in McCarroll and Loader 2004) and burned to CO_2 or pyrolysed to CO , respectively, before mass spectrometer analysis (McCarroll and Loader 2004). $\delta^{18}\text{O}$ values are expressed as deviations from the VSMOW and $\delta^{13}\text{C}$ values as deviations from the VPDB standard (Craig 1957).

Carbon isotope records were corrected for the decrease of atmospheric $\delta^{13}\text{C}$ values due to fossil fuel burning since the beginning of industrialisation AD 1850 (Friedli et al. 1986, Francey et al. 1999).

Results and Discussion

In a first step, individual site chronologies of all records were calculated over the common period of AD 1913-1994. $\delta^{18}\text{O}$ means mirror the patterns of $\delta^{18}\text{O}$ values in precipitation, recorded by European GNIP-stations ("Global Network of Isotopes in Precipitation", IAEA), with distinct gradients from lower to higher latitudes, oceanic to continental regions, and low to high elevation (Fig. 1). These patterns are related to evaporation and condensation effects taking place as air masses move from oceanic source regions to higher latitudes, over continental land or from low lands to mountainous regions (Cole et al. 1999, Jouzel et al. 2000, Siegenthaler and Oeschger 1980, Rozanski et al. 1993). Corresponding mean values of the $\delta^{13}\text{C}$ chronologies reflect local water supply due to the physiological response and fractionation of trees under water stress and therefore are related to the regional atmospheric moisture distribution (Saurer et al. 1997b, Treydte et al. 2001) (Fig. 1).

Cluster and Principal Component Analyses (PCA) suggest that both $\delta^{18}\text{O}$ and $\delta^{13}\text{C}$ site chronologies show systematic spatial relationships independent of species, although the inter-site correlations are higher for $\delta^{18}\text{O}$ than for $\delta^{13}\text{C}$. Clusters are identified in western central, eastern, and southern Europe. The "network extremes", namely both Mediterranean sites in southern Spain and Italy and the Finnish site do not fit in any clusters, pointing to specific climate and/or site conditions.

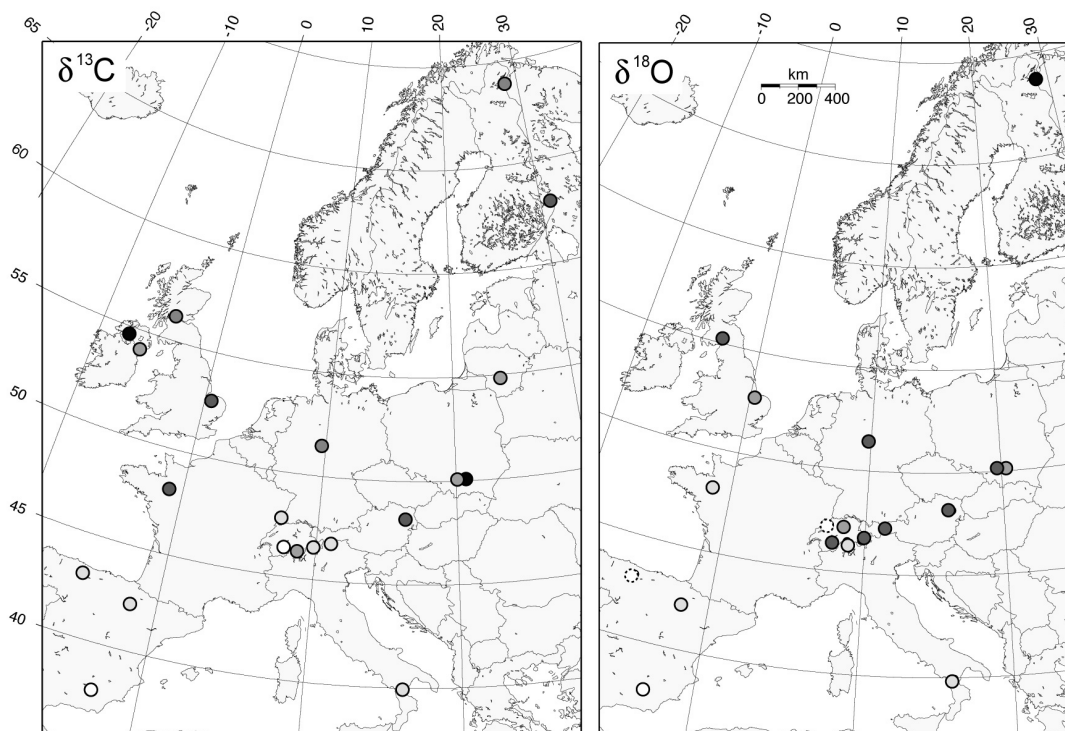


Figure 1: Sites used for preliminary network analysis (left: $\delta^{13}\text{C}$, right: $\delta^{18}\text{O}$). Light colours: high mean isotope values, dark colours: low mean isotope values, dotted signature: missing cellulose values for the common period, therefore excluded for comparison of mean values, but used for time series analysis.

Most of the $\delta^{18}\text{O}$ sites show positive loadings on the first principal component (PC1) (again except for the above mentioned sites), pointing to a common signal over the network (21% explained variance at PC1). In comparison, coherence within the $\delta^{13}\text{C}$ network is lower, likely resulting from differences in local ecological conditions, which have a greater influence on $\delta^{13}\text{C}$ than on $\delta^{18}\text{O}$ patterns (Saurer et al. 1997a, Treydte 2003). Both, PCA and cluster analysis prove the quality particularly of the $\delta^{18}\text{O}$ network through clear common signals, but also point to potential regionalisation of European climate reconstruction.

Parameter-specific analysis of low-frequency trends, using 200-year splines, suggests heterogeneous long-term behaviour in the oxygen records. In contrast, $\delta^{13}\text{C}$ long-term trends are rather common over the network pointing to the dominant impact of decreasing atmospheric $\delta^{13}\text{C}$ values induced by fossil fuel burning since industrialisation (Friedli et al. 1986, Francey et al. 1999). Correcting the records for this effect leads to heterogeneous long-term behaviour similar to the oxygen measurements. Differences could either be due to regionally differing low-frequency climatic trends over the study region, individual age-related long-term biases in the records, variable physiological response (e.g. reduction of stomatal conductance) to increasing CO_2 depending on differing site conditions, or currently unexplainable noise (Treydte 2003, Treydte et al. 2005). However, this finding has to be tested in the future using all records covering the full time span of 200-400 years.

After high-pass filtering from 200-year-splines, the oxygen records in particular reveal significant variance in the inter-decadal frequency domain. This signal seems to be common over the whole network.

The oxygen isotope network was used for initial climate calibration. Based on calculations with a 100-year (1901-2000) monthly European temperature and precipitation 0.5° gridded data set (New et al. 2002), months of significant correlation could be identified.

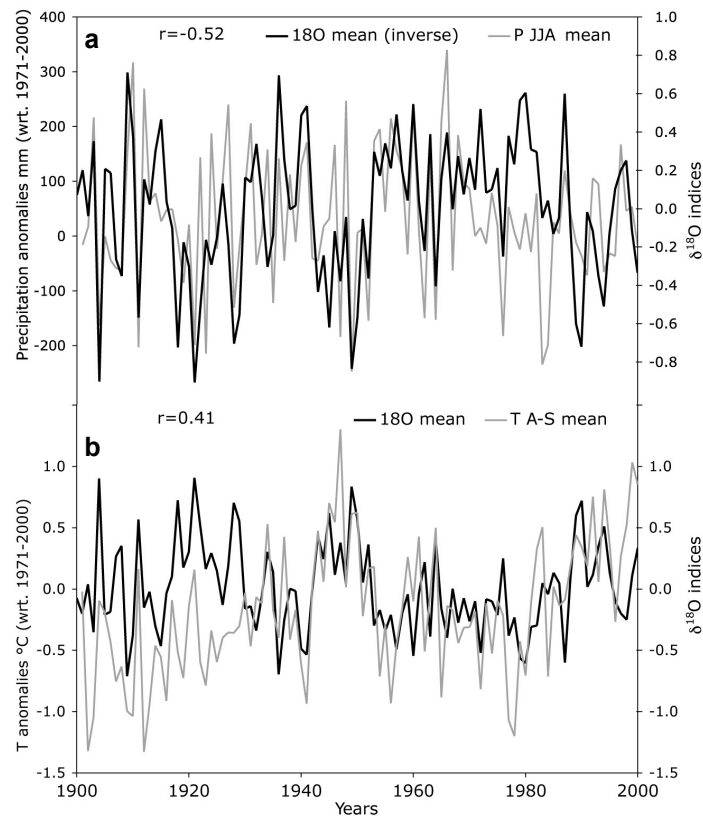


Figure 2: Comparisons between precipitation (a), temperatures (b) and a mean (European) $\delta^{18}\text{O}$ chronology for the 20th century (detrended from 200-year splines); The isotope chronology was developed by averaging $\delta^{18}\text{O}$ measurements from all available sites, the climate records by averaging all corresponding grid point data. P JJA mean is the mean summer precipitation from June to August; T A-S are the mean temperatures from April to September, both expressed as anomalies with respect to their 1971-2000 means.

At the majority of sites, tree ring $\delta^{18}\text{O}$ correlates positively with temperature and negatively with precipitation variations during the summer months. Averaging the $\delta^{18}\text{O}$ records of all sites and correlating them with similarly averaged meteorological data, leads to highly significant relationships for June to August precipitation (-0.52) and April to September temperature (0.41), indicating the potential for a “European” climate reconstruction. It should be noted, that in some cases the meteorological grid points do not ideally represent local site conditions. This holds particularly for precipitation conditions at high elevation sites, e.g. in Italy. Hence, using local meteorological station instead of grid point data could likely enhance the precipitation signal.

The rather coarse data treatment of averaging all sites and hence ignoring spatial details within the network provides already surprisingly good results. Obviously precipitation

variability is mirrored particularly in the short-term (year-to-year) domain (Fig. 2a), whereas temperature variability is fingerprinted particularly in the decadal scale domain (Fig. 2b). Differing temperature and isotope records in the early period (Fig. 2b) could be explained on the one hand through a too stiff de-trending of the isotope records, on the other hand through decreasing data replication in the instrumental records (Büntgen et al. 2005, this volume). Initial comparisons of the mean carbon and oxygen isotope chronologies averaged over the whole network (Fig. 3a) indicate significant correlation between these parameters (0.53 for the 20th century). This relationship seems to appear mainly between high-frequency variations, whereas on decadal scales some differences exist. Correlations between the first principal components of the carbon and oxygen data improve this relationship to 0.58.

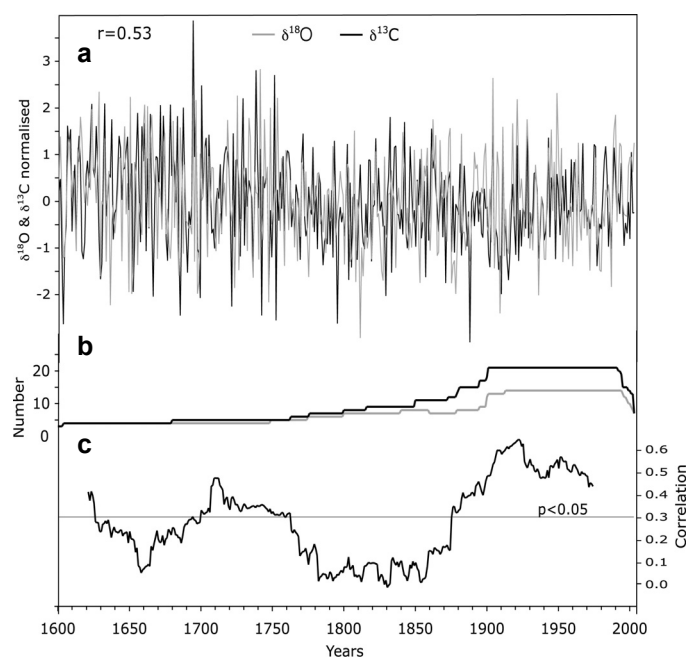


Figure 3: Relationship between the “European” $\delta^{18}\text{O}$ and $\delta^{13}\text{C}$ chronologies; Site data are de-trended using 200-year splines (a). The records correlate at 0.53. (b) Replication of the chronologies, and (c) moving correlation using 30-year time windows.

Moving correlations over a 30-year time window (Fig. 3c) indicate strongest relationships in the 20th century, being the period with highest replication (Fig. 3b). The changing sign of the correlation coefficient could indicate some change in the climate system (yet to be explored). High-frequency similarity between carbon and oxygen data is explained through variations in stomatal conductance, influencing the behaviour of both isotopes, due to the combined effect of varying temperature and precipitation conditions, which themselves are inter-correlated. Low stomatal conductance during dry/warm weather conditions causes high $\delta^{13}\text{C}$ values through weak discrimination against ^{13}C . Nevertheless transpiration increases compared to cool/wet conditions, resulting in higher leaf water enrichment and thus in higher $\delta^{18}\text{O}$ values (Anderson et al. 1998, 2002, Farquhar and Lloyd 1993, Leuenberger et al. 1998, Masson-Delmotte et al. 2005, Rafalli-Delerce et al. 2004, Roden et al. 2000, Treydte 2003, Treydte et al. 2004). Hence, both parameters should be mainly driven by summer moisture conditions.

Conclusion and Outlook

Preliminary tree ring $\delta^{13}\text{C}$ and $\delta^{18}\text{O}$ network analyses integrating data from about 20 European sites clearly demonstrate the potential for detailed European climate reconstructions over the last 400 years. Isotope datasets from temperate sites in Central Europe contain species-independent common signals, which enable to spatially extend climate reconstruction from tree rings which at present are mainly limited to “extreme” sites. Common signal strength on annual to multi-decadal timescales is higher in the oxygen isotope than in the carbon isotope network, pointing to a stronger external forcing. Nevertheless, the comparison of “European” $\delta^{13}\text{C}$ and $\delta^{18}\text{O}$ chronologies after averaging all sites indicates significant similarities on annual to decadal scales. We hypothesise that both parameters are mainly driven through summer moisture availability. This is important because currently detailed tree-ring reconstructions of precipitation are lacking for temperate regions. Centennial scale variation is, however, not yet understood in $\delta^{13}\text{C}$ and $\delta^{18}\text{O}$ data. Besides the incompleteness of the current data-sets, regionally differing synoptic conditions, age-related biases, and varying plant physiological reactions on changing atmospheric CO_2 concentrations could account for heterogeneities in the long-term behaviour between sites. Further investigations will be based on the use of complete and extended isotope datasets from all sites, covering the full period of 400 years where possible. Detailed wavelength analyses by separating the datasets into different timescales (high frequency, decadal, secular) will be employed to analyse the climate signal in tree ring data and to differentiate potential age- and site-related and anthropogenic noise from climate signals. Consideration of additional meteorological data such as vapour pressure, sunny hours, cloudiness, and particularly drought indices will be utilized to test the environmental information in the isotope records. Together with large-scale surface pressure data sets, such as NAO, and comparisons with new European temperature reconstructions (e.g. Luterbacher et al. 2004), detailed knowledge about European climate variation over the past few centuries will be derived.

Acknowledgements

Supported by the European Union, EVK2-CT-2002-00147 (ISONET).

References

- Anderson, W.T., Bernasconi, S.M., McKenzie, J.A. (1998): Oxygen and carbon isotopic record of climate variability in tree-ring cellulose (*Picea abies*): an example from central Switzerland. *Journal of Geophysical Research* 103: 31625-31636.
- Anderson, W.T., Bernasconi, S.M., McKenzie, J.A., Saurer, M., Schweingruber, F.H. (2002): Model evaluation for reconstructing the oxygen isotopic composition in precipitation from tree ring cellulose over the last century. *Chemical Geology* 182: 121-137.
- Borella, S., Leuenberger, M., Saurer, M., Siegwolf, R. (1998): Reducing uncertainties in $\delta^{13}\text{C}$ analysis of tree rings – pooling, milling and cellulose extraction. *Journal of Geophysical Research* 103: 19519-19526.

- Bräuning, A., Mantwill, B. (2005): Summer temperature and summer monsoon history on the Tibetan Plateau during the last 400 years recorded by tree-rings. *Geophysical Research Letters* 32, doi:10.1029/2004GL020793.
- Briffa, K.R., Osborn, T.J., Schweingruber, F.H., Harris, I.C., Jones, P.D., Shiyatov, S.G., Vaganov, E.A. (2001): Low-frequency temperature variations from a northern tree ring density network. *Journal of Geophysical Research* 106: 2929-2941.
- Briffa, K.R., Osborn, T.J., Schweingruber, F.H., Jones, P.D., Shiyatov, S.G., Vaganov, E.A. (2002): Tree-ring width and density data around the Northern Hemisphere – part 2, spatio-temporal variability and associated climate patterns. *The Holocene* 12: 759-789.
- Büntgen, U., Esper, J., Frank, D. C., Böhm, R. (2005): Influence of instrumental data on reconstructed Alpine temperature amplitudes. *TRACE, this volume*.
- Cole, J.E., Rind, D., Webb, R.S., Jouzel, J., Healy, R. (1999): Climatic controls on interannual variability of precipitation $\delta^{18}\text{O}$: Simulated influence of temperature, precipitation amount, and water source region. *Journal of Geophysical Research* 104: 14223-14235.
- Craig, H. (1957): Isotopic standards for carbon and oxygen and correction factors for mass-spectrometric analysis of carbon dioxide. *Geochimica et Cosmochimica Acta* 12: 133-149.
- Farquhar, G.D., Lloyd, J. (1993): Carbon and oxygen isotope effects in the exchange of carbon dioxide between terrestrial plants and the atmosphere. In: Ehleringer, J.R., Hall, A.E., Farquhar, G.D. (Eds.): *Stable Isotopes and Plant Carbon Water Relations*. Academic, San Diego, California: 47-70.
- Francey, R.J., Allison, C.E., Etheridge, D.M., Trudinger, C.M., Enting, I.G., Leuenberger, M.C., Langenfelds, R.L., Michel, E., Steele, L.P. (1999): A 1000-year high precision record of $\delta^{13}\text{C}$ in atmospheric CO_2 . *Tellus* 51B: 170-193.
- Friedli, H., Löttscher, H., Siegenthaler, U., Stauffer, B. (1986): Ice core record of the $^{13}\text{C}/^{12}\text{C}$ ratio of atmospheric CO_2 in the past two centuries. *Nature* 324: 237-238.
- Frank, D., Esper, J. (2005a): Characterization and climate response patterns of a high-elevation, multi-species tree-ring network in the European Alps. *Dendrochronologia* 22: 107-121.
- Frank, D., Esper, J. (2005b): Temperature reconstructions and comparisons with instrumental data from a tree-ring network for the European Alps. *International Journal of Climatology*, in press.
- Fritts, H.C. (1976): *Tree rings and climate*. New York: Academic Press, 567 S.
- IAEA/WMO (2004). *Global Network of Isotopes in Precipitation. The GNIP Database*. Accessible at: <http://isohis.iaea.org>.
- Jouzel, J., Hoffmann, G., Koster, R.D., Masson, V. (2000): Water isotopes in precipitation: data/model comparison for present-day and past climates. *Quaternary Science Reviews* 19: 363-379.
- Leavitt, S.W., Long, A. (1984): Sampling strategy for stable carbon isotope analysis of tree rings in pine. *Nature* 311: 145-147.

- Leuenberger, M., Borella, S., Stocker, T., Saurer, M., Siegwolf, R., Schweingruber, F.H., Matussek, R. (1998): Stable isotopes in tree rings as stress indicators. vdf Hochschulverlag Zürich. 200 S.
- Luterbacher, J., Dietrich, D., Xoplaki, E., Grosjean, M., Wanner, H. (2004): European seasonal and annual temperature variability, trends, and extremes since 1500. *Science* 303: 1499-1503.
- Masson-Delmotte, V., Raffalli-Delerce, G., Danis, P. A., Yiou, P., Stievenard, M., Guibal, F., Mestre, O., Bernard, V., Goose, H., Hoffmann, G., Jouzel, J. (2005): Changes in European precipitation seasonality and in drought frequencies revealed by a four-century-long tree-ring isotopic record from Brittany, France. *Climate Dynamics* 24: 57-69.
- McCarroll, D., Loader, N.J. (2004): Stable isotopes in tree rings. *Quaternary Science Reviews* 23: 771-801.
- New, M., Lister, D., Hulme, M., Makin, I. (2002): A high-resolution data set of surface climate over global land areas. *Climate Research* 21: 1-25.
- Raffalli-Delerce, G., Masson-Delmotte, V., Dupouey, J. L., Stievenard, M., Breda, M., Moisselin, M. (2004): Reconstruction of summer droughts using tree-ring cellulose isotopes: a calibration study with living oaks from Brittany (western France). *Tellus* 56B: 160-174.
- Roden, J.S., Lin, G., Ehleringer, J.R. (2000): A mechanistic model for interpretation of hydrogen and oxygen isotope ratios in tree-ring cellulose. *Geochimica et Cosmochimica Acta* 64: 21-35.
- Rozanski, K., Araguas-Araguas, L., Gonfiantini, R. (1993): Isotopic patterns in modern global precipitation. In: Swart KLLPK, McKenzie, J., Savin, S. (eds.): Climate change in continental isotopic records. AGU *Geophysical Monograph*: 1-37.
- Saurer, M., Aellen, K., Siegwolf, R. (1997a): Correlating $\delta^{13}\text{C}$ and $\delta^{18}\text{O}$ in cellulose of trees. *Plant, Cell and Environment* 20: 1543-1550.
- Saurer, M., Borella, S., Schweingruber, F.H., Siegwolf, R. (1997b): Stable carbon isotopes in tree rings of beech: climatic versus site-related influences. *Trees* 11: 291-297.
- Siegenthaler, U., Oeschger, H. (1980): Correlation of ^{18}O in precipitation with temperature and altitude. *Nature* 285: 314-317.
- Treydte, K., Schleser, G.H., Helle, G., Winiger, M., Frank, D., Haug, G., Esper, J. (2005): 20th-century precipitation maximum in western High Asia from 1000 years of tree-ring $\delta^{18}\text{O}$. *Nature*, in review.
- Treydte, K. (2003): Dendro-Isotope und Jahrringbreiten als Klimaproxis der letzten 1200 Jahre im Karakorumgebirge/Pakistan. Schriften des Forschungszentrums Jülich, Reihe Umwelt/Environment 38, 190 S.
- Treydte, K., Schleser, G.H., Schweingruber, F.H., Winiger, M. (2001): The climatic significance of $\delta^{13}\text{C}$ in subalpine spruce (Lötschental, Swiss Alps) – a case study with respect to altitude, exposure and soil moisture. *Tellus* 53B: 593-611.
- Treydte, K., Welscher, C., Schleser, G.H., Helle, G., Esper, J., Frank, D., Büntgen, U. (2004): The climatic signal in oxygen isotopes of junipers at the lower timberline in the Karakorum, Pakistan. *TRACE* 2: 100-106.

The reaction of $\delta^{13}\text{C}$, $\delta^{18}\text{O}$ and ring width on Larch Budmoth (*Zeiraphera diniana* Gn.) outbreaks in the European Larch (*Larix decidua* Mill.) - A case study in the Lötschental, Switzerland

K. Weidner^{1,2}, G. Helle², J. Löffler¹, B. Neuwirth¹ & G. H. Schleser²

¹Department of Geography, University of Bonn, Meckenheimer Allee 166, Germany

²Research Centre Jülich GmbH, Department of Chemistry and Dynamics of the Geosphere, ICG-V: Sedimentary Systems, Germany

Email: k.weidner@fz-juelich.de

Introduction

European Larch (*Larix decidua* Mill.) from the subalpine forest is commonly used for low-frequency temperature reconstructions (Büntgen et al. 2005). These subalpine forests form the habitat of the larch budmoth (LBM; *Zeiraphera diniana* Gn). Normally, the population of this insect strongly multiplies at intervals of 7-11 years. These outbreaks cause a red-brown discoloration of the crowns from larch trees due to the wasteful feeding of the 4th and 5th instar larvae and the drying out of the needles (Baltensweiler and Rubli 1999).

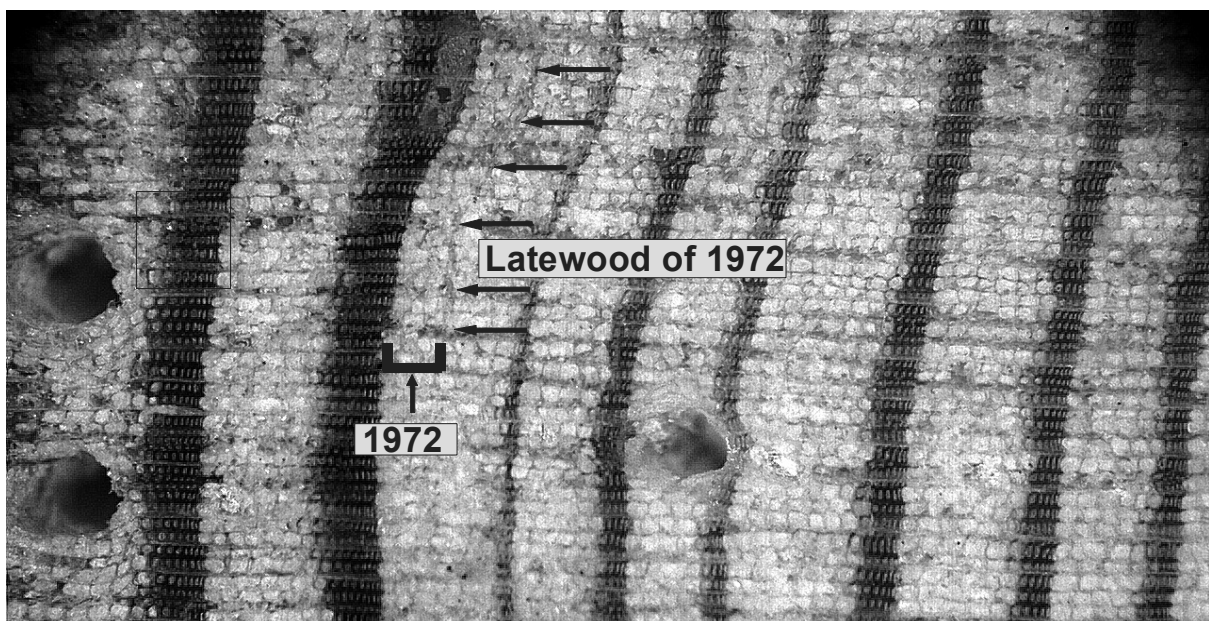


Figure 1: Typical tree-ring pattern due to a LBM outbreak. The 1970-1978 sequence is given showing the outbreak of 1972.

Figure 1 shows a typical pattern caused by these outbreaks which is characterized by an abrupt growth reduction in the year of the outbreak and a slow increase of ring width in the following years. The way trees recover depends on the intensity of the previous outbreak. Obviously a number of plant physiological reactions are disturbed in such a way that trees need a longer period to regain their normal activity. This typical tree-ring pattern causes problems in high-frequency climate reconstructions.

Stable isotopes usually provide better insight into plant physiological processes underlying tree growth. Therefore the aim of this study was to investigate to what extent LBM outbreaks modify the signature of the stable carbon and oxygen isotopes of the corresponding tree-rings. The study area chosen is located in the Lötschental, an inner-alpine dry valley in Valais, Switzerland.

Material and Methods

For inter-annual $\delta^{13}\text{C}$ and $\delta^{18}\text{O}$ analyses we took 6 cores of a tree located at 1900 m a.s.l. on the south exposed slope. After measuring the ring widths of the cores with a resolution of 0.01 mm, the cores were dated by synchronizing the ring widths with the corrected master-chronology of the Lötschental (Büntgen et al. 2004). The years of LBM outbreaks were identified by comparison of the tree-ring pattern with historical documentation which exists back to 1850. (Baltensweiler and Rubli 1999). Based on ring width, LBM outbreaks were identified in a quantitative and a qualitative way. For each ring width the relative width reduction was calculated by comparing the mean value of the 4 previous years. The threshold for LBM outbreaks was fixed at 40% of growth reduction. (Rolland et al. 2001). The qualitative way consisted in the visual detection of the typical pattern as described above. The historical documentation confirmed this ring width analysis. Each tree-ring of the time span 1900-1982 was separated from the cores and the wood of the separated tree-rings was pooled after Treydte (1998).

It is usual to extract cellulose to concentrate on one chemical compound because the different components of the wood have different isotopic signatures. Nevertheless, we analysed cellulose and wood for the time span 1950-1982, the idea being that similar results for cellulose and total wood could ease the workload considerably by concentrating on wood. The investigations resulted in a correlation coefficient of $r = 0.84$ for carbon and $r = 0.91$ for oxygen. Therefore, we decided to use only wood for the time period 1900-1950. The samples were measured by using an elemental analyser interfaced to a continuous flow isotope ratio mass spectrometer (Micromass Optima). The resulting δ -values are defined as the isotope ratio R of an element relative to the ratio of an internationally accepted reference material of this element. Thus, e.g.: $\delta^{13}\text{C} = [R_{\text{sample}}/R_{\text{reference}} - 1] * 1000$. These values are normally multiplied by 1000 and thus given as per mill deviation from the reference. The analytical error was $< \pm 0.1\text{‰}$ for carbon and $< \pm 0.35\text{‰}$ for oxygen.

For intra-annual $\delta^{13}\text{C}$ analyses a stem disk of a tree located at 1800 a.s.l. on the south-exposed slope was used. To obtain an intra-annual resolution we took a segment of this disc and prepared micro-slices of 15 μm for the years 1970–1974 including the LBM outbreak of 1972. The complementary climate data originate from the meteorological stations of Kippel (1370 m) and Ried (1480 m) in the Lötschental, extended by the data of Montana, 30 km west of Lötschental (Neuwirth 1998, Neuwirth et al. 2004).

Results and discussion

Outbreaks of LBM were identified for the years 1907, 1944, 1954, 1963 and 1972 on the basis of ring width, $\delta^{13}\text{C}$ and $\delta^{18}\text{O}$. As shown in figure 2, comparison with climate data did not

reveal any anomalies in these years. Therefore, the values of the identified years of LBM outbreaks do not result from particular climatic conditions.

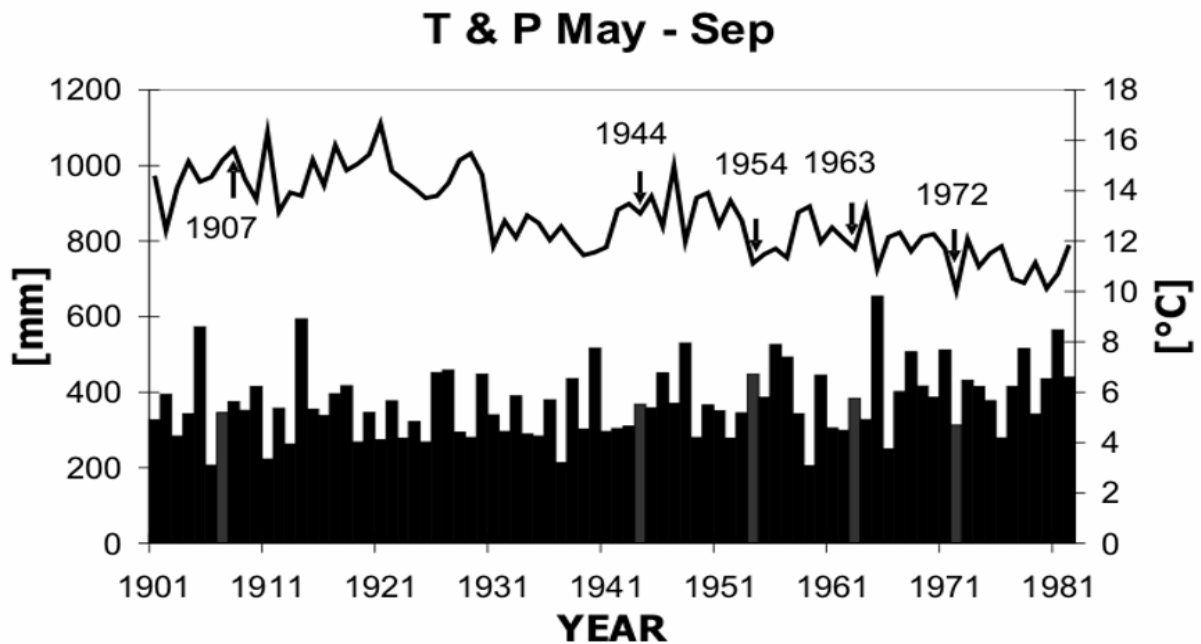


Figure 2: Temperature and precipitation records in the Lötschental during the growth period of the investigated larch. The years of LBM outbreaks are marked.

Tree-ring width, $\delta^{13}\text{C}$ and $\delta^{18}\text{O}$ records are summarized in figure 3. $\delta^{18}\text{O}$ -values are characterized by a strong decrease in the years of LBM outbreaks except for 1944. Both, ring width and $\delta^{18}\text{O}$ respond to LBM outbreaks with strongly decreasing values. Ring width does not indicate any LBM outbreaks between 1907 and 1944 contrary to $\delta^{18}\text{O}$. On the basis of $\delta^{18}\text{O}$ it cannot be ruled out that during the year 1931 an infestation occurred. Strong LBM outbreaks are related to defoliation (Baltensweiler and Rubli 1999). Generally, transpiration of leaf water leads to a loss of the lighter H_2^{16}O molecules in the intercellular air spaces and consequently to an enrichment in H_2^{18}O (McCarroll and Loader, 2004). The absence of the leaves leads to low $\delta^{18}\text{O}$ values because no transpiration takes place. In general carbon isotopes show a weaker decrease in the year of LBM outbreak as compared to $\delta^{18}\text{O}$ and a stronger decrease one year after the outbreak (Fig. 3). The chemical composition and morphological constitution of the needles is strongly dependent on nutrient reserves of the previous year (Baltensweiler and Fischlin 1988) As a reaction to LBM outbreaks the needle mass in the following year is lower. Therefore, the lower $\delta^{13}\text{C}$ -values in this year are possibly due to a lower photosynthesis rate which in turn results in a reduced isotope discrimination.

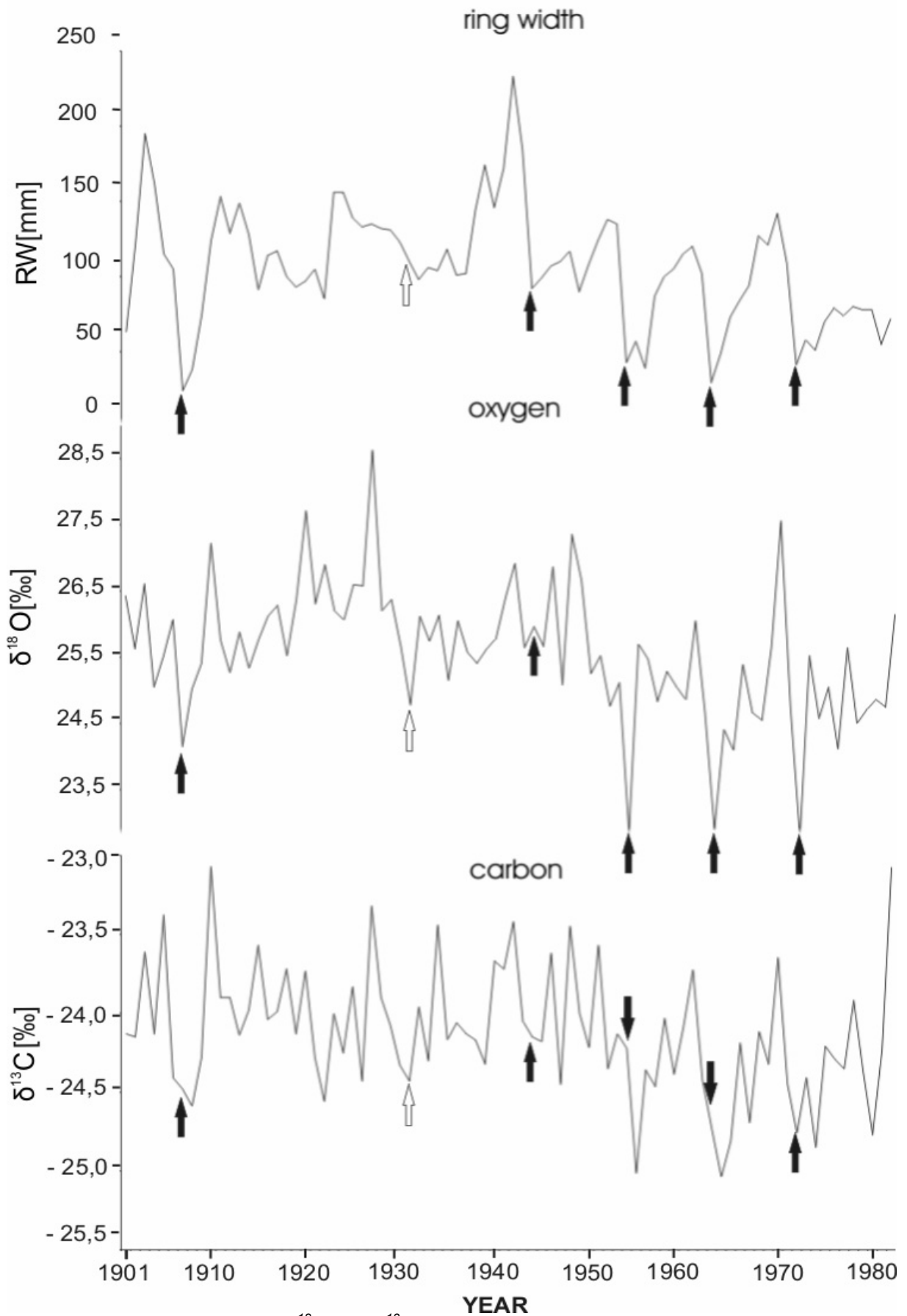


Figure 3: Records of ring width, $\delta^{18}\text{O}$ and $\delta^{13}\text{C}$ from total wood for the time period of 1900-1982.

Seasonal variations of $\delta^{13}\text{C}$ 1970-1974

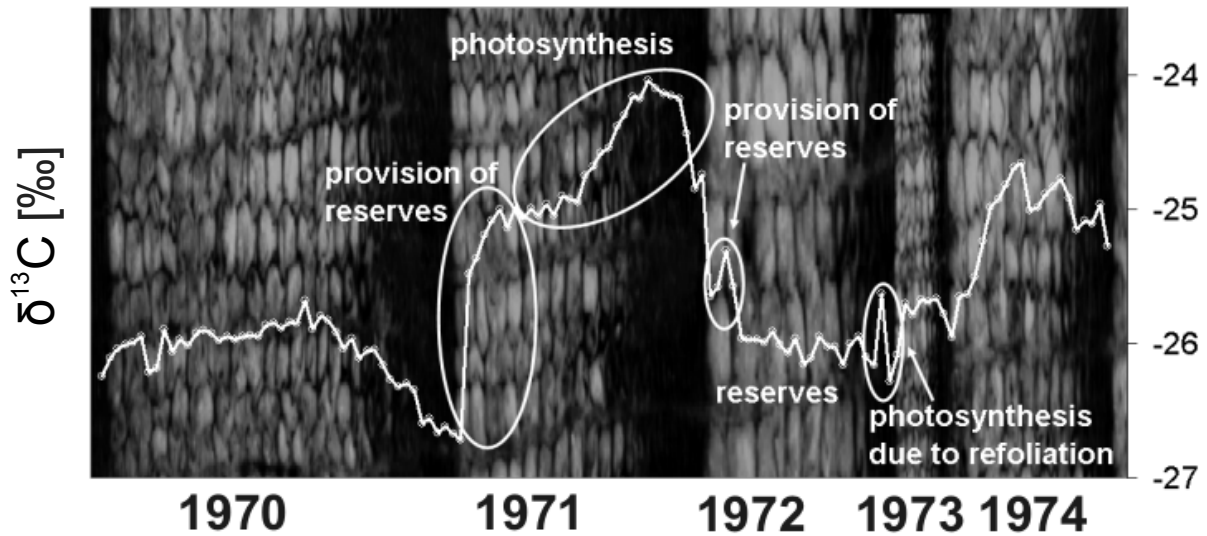


Figure 4: Seasonal variations of the carbon isotopes during the years from 1970-1974 including the LBM outbreak of 1972. (ring width not true to scale)

The seasonal carbon isotope pattern for the years of 1970, 1971, 1974 shows the normal $\delta^{13}\text{C}$ course to be expected. At the beginning of the growing season the $\delta^{13}\text{C}$ -values increase while a decrease is observed in latewood. The seasonality in $\delta^{13}\text{C}$ is due to seasonal changes in isotopic fractionation partly due to photosynthesis (Helle and Schleser 2004, Verheyden et al. 2004). The year of LBM outbreak, 1972, shows a different pattern. After a short increase at the beginning, indicating the standard year to year situation, $\delta^{13}\text{C}$ -values decrease abruptly and remain on a low level without any significant variation. In the latewood a slight increase is observed, however, only for a short time. The initial increase is due to the provision of reserves from the previous year with minor contributions of photosynthates of the current year. After the tree is defoliated, wood formation depends solely on remaining reserves with a lower $\delta^{13}\text{C}$ -value. The $\delta^{13}\text{C}$ -increase in latewood is possibly attributed to the refoliation of the larches. Larches which have been defoliated to more than 50% refoliate within 3-4 weeks (Baltensweiler and Fischlin 1988). Against the background of a decreasing needle mass in 1973, the low $\delta^{13}\text{C}$ -values are possibly caused by a lower photosynthesis rate which normally leads to a higher discrimination.

Conclusions

The results of this initial study revealed similar reactions for ring width and for inter-annual oxygen isotope values to LBM outbreaks. Carbon isotope signatures most likely reveal the influence of reserves. The reasons for the differences in the behaviour of the different parameters to LBM outbreaks are presently not fully understood. But they are due to different tree physiological (yet unknown) processes. Further investigations with more trees are necessary to substantiate the observed pattern. However, this study shows that multi-

parameter investigation bear a great potential for studying the influence of LBM outbreaks on trees. Cores of a site on the south-exposed slope at 2000 m a.s.l. in the Löttschental / Switzerland are currently prepared for inter-annual and intra-annual carbon and oxygen isotope analyses to investigate the reaction on LBM outbreaks of different intensities. This is to obtain more information on the mechanisms which are responsible for the observed behaviour.

Acknowledgement

The authors wish to thank the ICG-V laboratory staff of the Research Centre Juelich for their active assistance within this project.

References

- Baltensweiler, W. and A. Fischlin (1988): The Larch Budmoth in the Alps. In: Berryman, A. (ed.): Dynamics of forest insect populations: 331-349.
- Baltensweiler, W. and D. Rubli (1999): Dispersal: an important driving force of the cyclic population dynamics of the larch budmoth, *Zeiraphera diniana* Gn. *Forest Snow and Landscape Research* 74: 153.
- Büntgen, U., Esper, J., Frank, D. C., Nicolussi, K. and M. Schmidhalter (2005): A 1052-year tree-ring proxy for Alpine summer temperatures. *Climate Dynamics*.
- Helle, G. and G.H. Schleser (2004): Beyond CO₂-fixation by Rubisco – an interpretation of ¹³C/¹²C variations in tree-rings from novel intra-seasonal studies on broad-leaf trees. *Plant, Cell and Environment* 27: 367-380.
- McCarroll, D. and N.J. Loader (2004): Stable isotopes in tree rings. *Quaternary Science Reviews* 23: 771-801.
- Neuwirth, B. (1998): Dendroklimatologische Untersuchungen im Löttschental, Schweiz. Visuelle Jahrringparameter subalpiner Fichten in Abhängigkeit von Höhenlage, Exposition und Standortverhältnissen. Diploma Thesis. Geographical Institute, University of Bonn. Germany.97.
- Neuwirth, B., Esper, J., Schweingruber, F. H., M. Winiger (2004): Site ecological differences to the climatic forcing of spruce pointer years from the Löttschental, Switzerland. *Dendrochronologia* 21 (2): 69-78.
- Rolland, C., Baltensweiler, W. and V. Petitcolas (2001): The potential for using *Larix decidua* ring widths in reconstruction of larch budmoth (*Zeiraphera diniana*) outbreak history: dendrochronological estimates compared with insect survey. *Trees* 15: 414-424.
- Treydte, K. (1998): Dendroklimatologische Untersuchungen im Löttschental, Schweiz. d¹³C subalpiner Fichten in Abhängigkeit von Höhenlage, Exposition und Standortverhältnissen. Diploma Thesis. Geographical Institute, University of Bonn. Germany. 97.
- Verheyden, A, Helle, G, Schleser, G. H., Dehairs, F., Beekman, H. and N. Koedam (2004): Annual cyclicity in high-resolution stable carbon and oxygen isotope ratios in the wood of the mangrove tree *Rhizophora mucronata*. *Plant, Cell and Environment* 27: 1525-1536.

SECTION 7

NEW APPLICATIONS

Application of a 3D Laser scanning device to acquire the structure of whole root systems- A pilot study

H. Gärtner¹ & C. Denier²

¹Swiss Federal Research Institute WSL, Zürcherstrasse 111, 8903 Birmensdorf, Switzerland

Email: holger.gaertner@wsl.ch

²Terra Data AG, Mühlestrasse 9, 8840 Einsiedeln, Switzerland

Email: c.denier@geoterra.ch

Introduction

The analysis of entire root systems in tree stability studies as well as the estimation their role in the CO₂ budget of Swiss forests is confronted with multifaceted problems. Whereas the dimensions of the above ground parts of a tree are more or less easy to determine, measuring root dimensions and especially their spread is rather difficult.

Tree stability towards mechanical impacts has been research topics in forestry and tree-ring research for more than a century (e.g., Hegler 1893). Research has focused on growth reactions on a micro- and macroscopic level mostly due to the influence of wind (Jacobs 1954). Since then, various species-specific reaction mechanisms in stems due to mechanical stress have been analysed and used to date geomorphic processes (Alestalo 1971, Shroder 1980, Wiles et al. 1996, Gärtner et al. 2004). More recently, the focus has been set on physical parameters respecting the distribution of various mechanical pressures as well as the mechanical properties of stem wood (Burgert et al. 2004). Apart from studying specific tree parameters (e.g., tree and stem height, crown area) the effect of stand density and soil properties, which are important factors for the development of root systems are of special interest (Peltola et al. 2000) because tree anchorage is crucial for stability. Mattheck et al. (1997) have shown, that an optimised design of root systems would ensure an equal distribution of acting forces along the roots. Consequently, a uniform distribution of coarse roots around the stem might be expected on a shallow site with homogeneous site conditions. Root system development is controlled by various factors, which are determined by the main functions of a roots system: (i) anchorage, (ii) absorption of water and nutrients and (iii) transport of these substances to the stem (Sitte et al. 1998). Normally, these functions would be equally distributed within the root system, but specialisations of single roots due to e.g., varying soil properties specialisations frequently occur resulting in the dominance of one of the main functions. As a consequence a symmetric spread of roots rarely occurs and even ring-width variations along single roots are highly variable. Ring-width measurements and analysis of anatomical variations are techniques which have been applied to reveal the development and mechanical properties of a root at a given section (Gärtner et al. 2001, Gärtner 2003). For the analysis of the full complexity of a root system, it is desirable to attribute the properties of these sections to their position within the system. Due to the complexity of bifurcations within a root system, this mapping and the following analysis is highly complicated, often even impossible (Gärtner and Bräker 2004). Consequently, to

realise a detailed analysis of a whole root system, a high resolution model of the root structure is required. This model has to be even more detailed than it is realized using magnetic field devices, used to measure and represent root lengths and bifurcations in three-dimensional space (Nicoll and Ray 1996, Sinoquet and Rivet 1997, Danjon et al 1999, Di Iorio et al. 2005). At the Swiss Federal Research Institute WSL a ground based 3D- laser scanner was used for the first time to generate a three dimensional model of an exposed root system. The study presented here was accomplished to investigate the opportunities and limitations of this technology.

Material and methods

The work started on a separated part of the root system of a mature beech (Fig. 1), which was exposed for root biomass analysis (Gärtner and Bräker 2004).



Figure 1: Removal of the root system of a mature beech for further analysis in the lab. One part of the root system was used for the scanning procedure (lower picture)

This part consisted of two main roots (length 1.3 m) with hundreds of small lateral roots, many of them showing anastomosis. This rather dense network was chosen to identify problems resulting from expected shadowing effects caused by mutual maskings of the single roots within the complex system. For this pilot study, a Cyrax® HDS2500 scan device was used. It has a maximum 40° x 40° field-of-view (Leica Geosystems 2003), a single-point range accuracy of +/- 4mm, angular accuracies of +/- 60 micro-radians, and a beam spot size of 6mm from 0-50m range. Minimum vertical and horizontal point-to-point measurement spacing is 0.25mm referred to a distance of 50m. The root was scanned by 1.000 points/column and 1.000 points /row. The resulting data file contains 1.000.000 data points

(xyz-coordinates) representing the surface of the roots visible from the position of the scanner. However, all areas behind these visible surfaces do not deliver data (shadowing effect, Fig. 2). To prevent this effect, the root system was scanned from different positions to acquire the whole structure. Several tests had to be conducted to identify the most effective way of data acquisition to avoid shadowing effects.

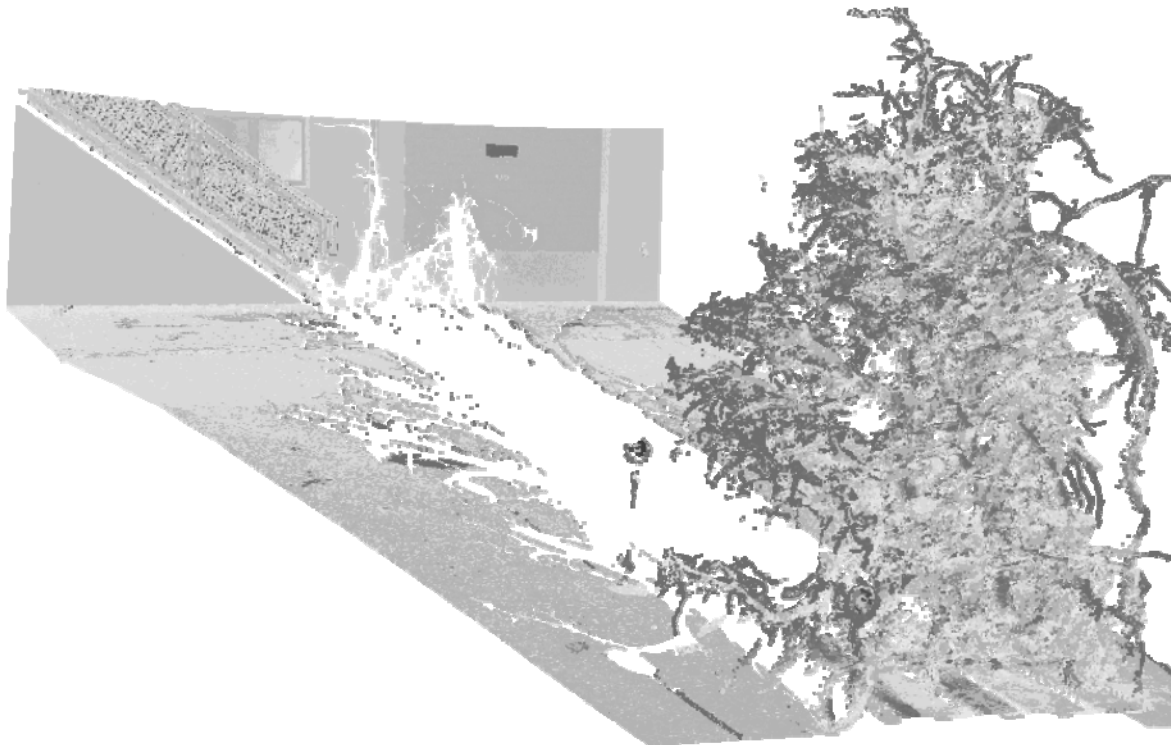


Figure 2: Perspective view of the scatter-plot resulting from one scan. White areas within the scan range represent the shadowing effects caused by the laser device and masking of roots resulting in no data.

The root was scanned from 4 directions to minimize the shadowing effects. To ensure correct orientation of each single scan, four stages with fixed points were placed around the root system. These four poles guaranteed the accurate positioning of each scan image while creating the three-dimensional model by combining the single scenes. At least two of the poles needed to be visible in each scan to enable a referenced combination of the scenes. Point-to-point measurement spacing was set to 2 mm to simplify data processing and to accelerate the procedure of the single scans for this preliminary study. With this set up, each single scan took 15 minutes. In total, it took about 1 hour for scanning and approximately 30 minutes for moving the scanner 4 times to acquire all data needed to finally represent the whole root system in the final scatter plot. The scanner detects all surfaces within its 40°x40° field-of-view. Thus, each resulting scene includes unnecessary data point areas. The first step in data processing was to extract the area representing the root system and the poles from the whole scatter plot of the area. To do this, non-target areas had to be cut out of the scenes.

Preliminary results

The resulting scenes of the root were combined to a three-dimensional scatter-plot of the entire root system (Fig. 3a). This scatter-plot consists of approximately 3 million xyz-coordinates representing the surface of the roots. A more detailed view of the individual roots of the scatter plot (Fig. 3b) illustrates a good data acquisition of roots as small as 4-5 mm, which are all well represented in the plot (black arrow in Fig. 3b). However, there are numerous scattered dots in some areas in vicinity of the coarse roots.

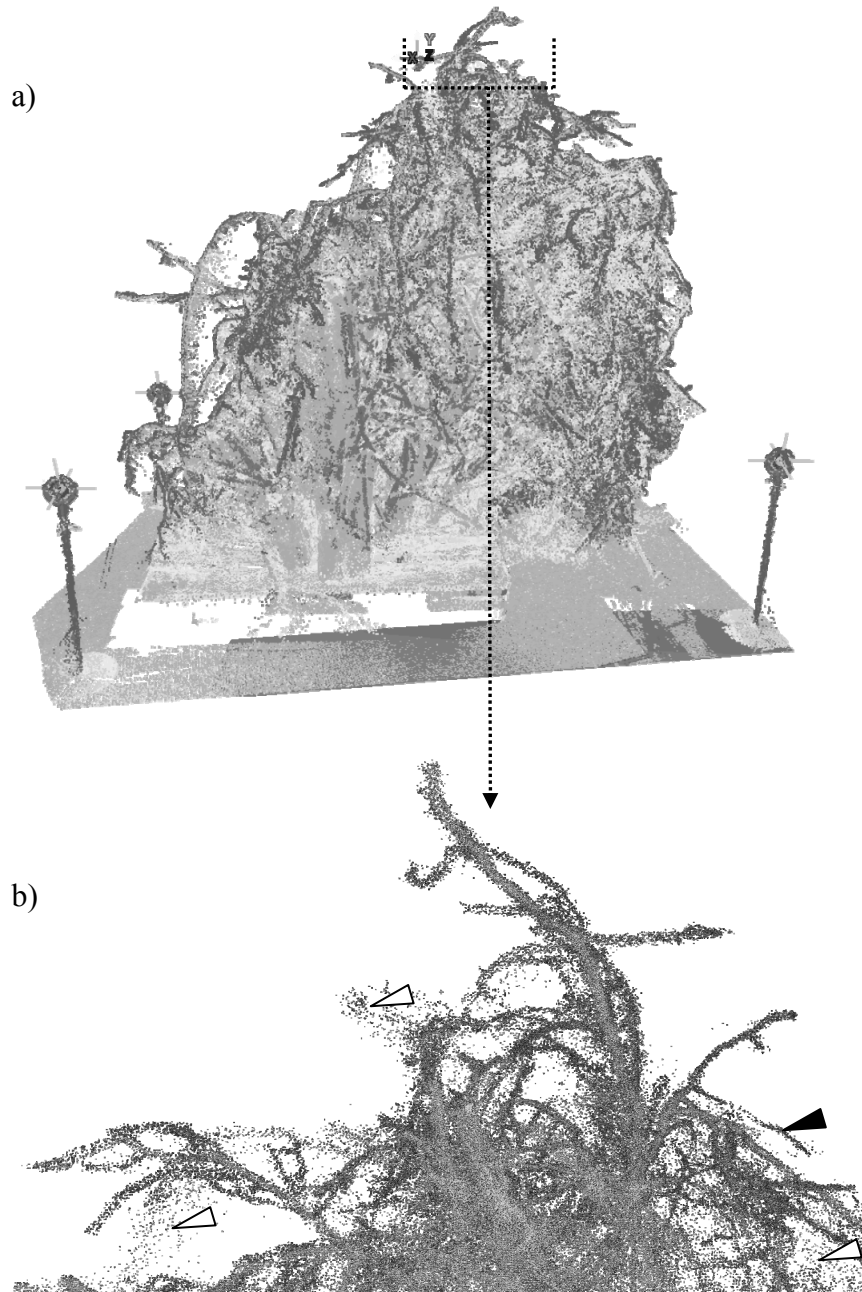


Figure 3: a) 3D-scatter plot of the root system consisting of 4 single images of the laser scanner. b) magnified view of the top section of the root system. Black arrow: Example for a root of 4-5mm in diameter; White arrows: cloud of reflected data points from fine roots smaller than 2 mm, not sufficient to represent the single roots entirely and therefore resulting in scattered areas in the scan view.

These dots are individual reflections of fine roots smaller than 2 mm, which were only partly scanned in the single scenes. The scattered areas (white arrows in Fig. 3b) are results of combining scenes with incomplete images of the respective fine roots. Nevertheless, the coarse root structure is clearly visible and single roots bigger than 5 mm in diameter can be differentiated. Consequently, the main aim of the pilot study to represent the three-dimensional structure of a complex root system in a computer has been achieved. This dataset can now be used to further analyse the root structure by creating the surfaces of the single roots and hence create a closed, three-dimensional model of the whole root system. To derive more detailed information on the structure of the root system without modelling the surfaces in detail, horizontal layers (thickness: 10 cm) were cut from the plot to generate volumetric bodies of the structure at different levels (Fig. 4).

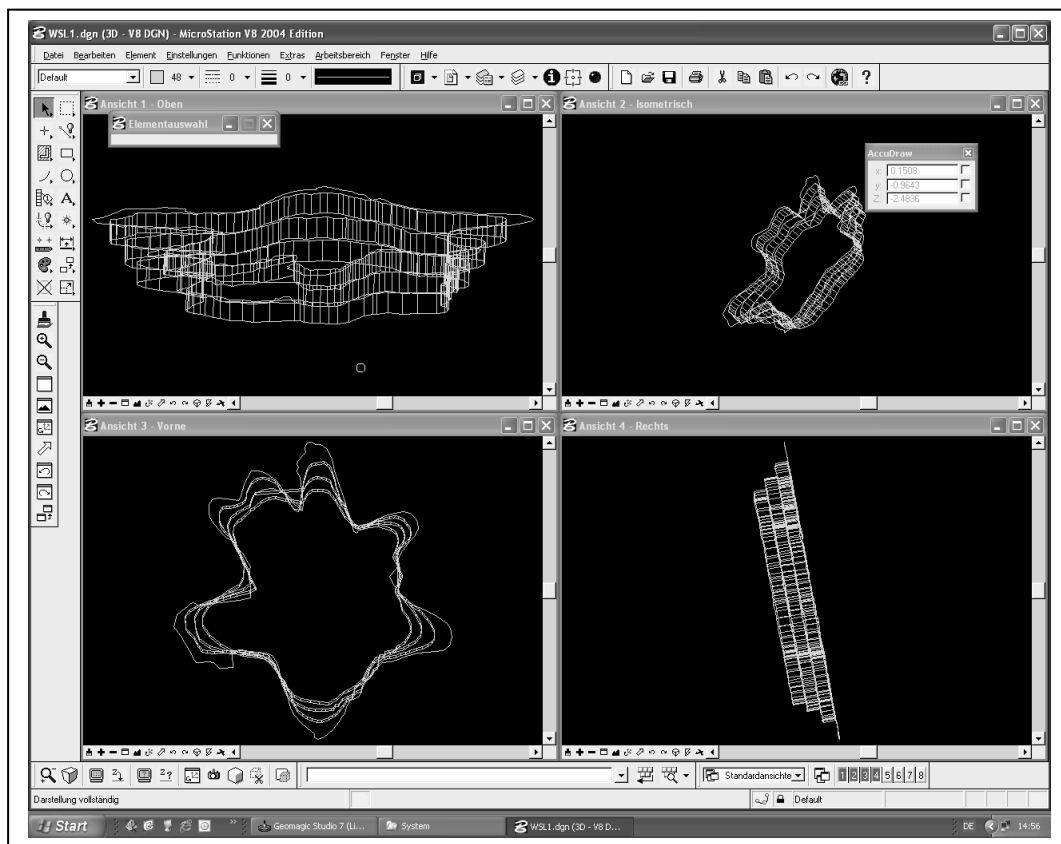


Figure 4: Illustration of composed 3D-slices of the root system (screenshot: visualized data output, CAD/CAE-Software "Bentley MicroStation"). The single volumetric bodies were created by using the section plane area and the height of the section.

The scan data of the lowermost data points girdling the surface texture of the root layer were then combined to closed contour lines. Finally the bodies were created by adding the height information of the layers using the CAD/CAE-software Bentley MicroStation. This procedure was conducted to evaluate the possibilities for a time and cost effective modelling of a three-dimensional body to e.g., estimate the biomass of a root system. This rather basic modelling worked well, but with an increasing complexity of the structure, manual data corrections became more important to accurately represent smaller roots within the structure.

Conclusions and perspectives

The of basic modelling procedure we presented here is effective and leads to more detailed information than can be achieved with other methods of root structure acquisition mentioned before. But with regard to the high resolution data of the scatter plot a more detailed modelling technique is required to fully use the potentials of the scanner data. The overall aim to analyse root system development in detail or mechanical properties of the system as a whole requires a more complex modelling and presentation of the surface of each single root within the system. This is required e.g., to enable the addition of ring-width data to the model.

Without anticipating forthcoming modelling techniques, it is obvious that data sampling for the tree(root)-ring analysis can start immediately after the scanning procedure. All samples taken from the root system will be tagged in the scatter-plot and then transferred to the 3D-model. Combining ring-width data with a 3D-model is the base for detailed future spatiotemporal analyses of the development of a mature root system. First steps towards this analysis procedure have recently been started at the Swiss Federal Research Institute WSL. The identical procedure can also be used to analyze the dimensions of stem and branches of trees. The detailed presentation of whole-tree dimensions using a 3D-Laserscanner in combination with dendrochronology in roots, stem and branches opens new perspectives in the analysis of biomass-distribution and tree-stability research.

Acknowledgements

The authors wish to thank Leica Geosystems AG, Switzerland for their interest in the project and for funding the use of the laser scanning device. We are also grateful to Dr. Ingo Heinrich (Department of Geosciences, Geography, University of Fribourg, Switzerland) for his helpful comments.

References

- Alestalo, J. (1971): Dendrochronological interpretation of geomorphic processes. *Fennia* 105: 140.
- Burgert, I., Frühmann, K., Keckes, J., Fratzl, P., Stanzl-Tschegg, S. (2004): Structure-function relationships of four compression wood types: micromechanical properties at the tissue and the fibre level. *Trees* 18: 480-485.
- Danjon, F., Sinoquet, H., Godin, C., Colin, F., Drexhage, M. (1999): Characterisation of structural tree root architecture using 3D digitising and AMAPmod software. *Plant and Soil* 211: 241-258.
- Di Iorio, A., Lasserre, B., Scippa, G.S., Chiatante, D. (2005): Root System Architecture of *Quercus pubescens* Trees Growing on Different Sloping Conditions. *Annals of Botany* 95: 351-361.
- Gärtner, H., Bräker, O.U. (2004): Roots - the hidden key players in estimating the potential of Swiss forest to act as carbon sinks. In: Jansma, E., Bräuning, A., Gärtner, H., Schleser, G. (Hrsg.) (2004): TRACE - Tree Rings in Archaeology, Climatology and Ecology 2: 13-18.

- Gärtner, H., Esper, J., K. Treydte (2004): Geomorphologie und Jahrringe - Feldmethoden in der Dendrogeomorphologie. *Schweizerische Zeitschrift für Forstwesen* 155, 6: 198-207.
- Gärtner, H. (2003): Holzanatomische Analyse diagnostischer Merkmale einer Freilegungsreaktion in Jahrringen von Koniferenwurzeln zur Rekonstruktion geomorphologischer Prozesse. *Dissertationes Botanicae* 378. 118.
- Gärtner H., Schweingruber F. H., Dikau, R. (2001): Determination of erosion rates by analysing structural changes in the growth pattern of exposed roots. *Dendrochronologia* 19, 1: 81–91.
- Hegler, R. (1893): Über den Einfluss des mechanischen Zugs auf das Wachstum der Pflanze. *Beiträge zur Biologie der Pflanze* 6: 383–432.
- Jacobs M. R. (1954): The effect of wind sway on the form and development of *Pinus radiata* D. Don. *Australian Journal of Botany* 2: 35-51.
- Leica Geosystems (2003): Leica HDS2500.
 Url: http://hds.leica-geosystems.com/products/hds2500_specs.html
- Mattheck, C., Teschner, M., Schäfer, J. (1997): Mechanical Control of Root Growth: A Computer Simulation. *Journal of theoretical Biology* 184: 261–269.
- Nicoll, B.C., Ray, D. (1996): Adaptive growth of tree root systems in response to wind action and site conditions. *Tree Physiology* 16: 891-898.
- Peltola, H., Kellomäki, S., Hassinen, A., Granander, M. (2000): Mechanical stability of Scots pine, Norway spruce and birch: an analysis of tree-pulling experiments in Finland. *Forest Ecology and Management* 135, 1-3: 143-153.
- Shroder, J.F. (1980): Dendrogeomorphology: Review and new techniques of tree-ring dating. *Progress in Physical Geography*, 4: 161-188.
- Sinoquet, H., Rivet, P. (1997): Measurement and visualisation of the architecture of an adult tree based on a three-dimensional digitizing device. *Trees* 11: 265-270.
- Sitte, P., Ziegler, H., Ehrendorfer, F., Bresinsky, A. (Hrsg.) (1998): Strasburgers Lehrbuch der Botanik. Fischer, Stuttgart.
- Wiles, G.C., Calkin, P.E., G.C. Jacoby (1996): Tree-ring analysis and Quaternary geology: Principles and recent applications. *Geomorphology* 16: 259-272.

Different forms of tension wood in alder and beech in relation to mechanical stress – preliminary results

I. Heinrich¹, H. Gärtner² & M. Monbaron¹

¹Department of Geosciences, Geography, University of Fribourg, 1700 Fribourg, Switzerland

Email: ingo.heinrich@unifr.ch

²Swiss Federal Research Institute WSL, Zürcherstrasse 111, 8903 Birmensdorf, Switzerland

Introduction

In the context of changing magnitudes and frequencies of natural hazards such as debris flows or snow avalanches caused by the current climate change a detailed understanding of tree reactions on growth stresses induced through different geomorphological forces is desirable. Macroscopic changes in wood formation (growth variations in trees) as reaction to external impacts have often been used for dating catastrophic events. Frequently, conifers have been used in dendrogeomorphology for reconstructions of geomorphic processes while similar studies with broadleaf species are rather rare. However, broadleaf species often occur in mixed forests together with conifer trees and are sometimes the dominant species in lower elevations. Furthermore, broadleaf species possess a more complex wood anatomy and offer structural features for further analysis not found in coniferous wood. Hence, it is essential to also examine the reaction wood of broadleaf species in more detail in order to enable dendrogeomorphological studies in vegetation zones dominated by them. It is suggested here that the additional application of wood anatomical techniques can harvest supplementary information about type, size and intensity of past hazardous impacts on tree growth. Long-term growth experiments imitating typical impacts of different geomorphic events are being conducted and their wood anatomical reactions monitored in order to study the likely varying reactions to a range of mechanical stresses, and first results are presented.

Study sites and methods

Growth experiments with European beech (*Fagus sylvatica*) and European alder (*Alnus glutinosa*) were set up near Krattigen (7° 45' / 46° 38', 840m asl, Bernese Oberland) and near Posieux (7° 08' / 46° 45', 600m asl, Canton of Fribourg), respectively, at the end of the tree winter dormancy in March 2004 (Fig. 1)



Figure 1: Location of experimental plots: Krattigen (dot), Posieux (star)

The treated specimens at both sites were mainly young trees. In Krattigen the forest stand contains beech regrowth following storm damage and the stand of European alder in Posieux was planted for re-vegetation purposes approximately ten years ago. At both sites ten groups containing four trees each were set up applying different treatments listed in table 1.

Table 1: List of groups with different treatments (four trees per group)

T1	Stem bent to 80° from the vertical
T2	Stem bent to 45° from the vertical
T3	Stem bent increasingly in time starting from small angles up to 80°
T4	Stem bent to 80°, but with the apex remaining vertical
T5	Stem bent to 80°, with apex cut
T6	Stem bent to 80°, but with the bark & cambium partly removed from the upper side
T7	Stem bent to 80°, but with the bark & cambium partly removed from the lower side
T8	Stem bent to 80° and sideways
T9	Stem and root system tilted to 80° from the vertical, with roots partly destroyed
T10	Reference group

After the commencement of tree growth at the beginning of the vegetation period 2004 the pinning method (Mariaux 1967, Wolter 1968) was applied to all trees and repeated afterwards every fortnight. In addition, puncher samples (Forster *et al.* 2000) of the tension wood side of one tree per group were taken. Thin sections of the puncher samples were cut for further microscopy and digital photos were taken. Wood anatomical structures, that is, cell wall and lumen area of all cells and lumen area of vessels were recorded by digital imagery and analysed utilizing the software programs Adobe Photoshop Elements and WinCELL Pro 2005a.

Results and discussion

Figure 2 illustrates the differences between typical tension wood and normal growth in beech. The tension wood contains much denser fibre cell tissue with fewer and smaller vessels. Furthermore, it shows no vessels in the early part of the tree ring. Obviously, then priority was given to stabilisation of the tree rather than to its supply with nutrients and water. This stands in direct contrast to the results gained for the two coniferous species (spruce and larch) which were also treated in the experiment (Gärtner *et al.* in prep.). The first cell rows formed by the conifers were normal earlywood tracheids with thin cell walls and large lumen. Hence, it seems as if conifers follow a different strategy when responding to heavy mechanical impact, *e.g.*, geomorphic processes. While they seem to secure water conductance at the beginning of the growing period the broadleaf species first respond to the mechanical stress by forming reaction wood cells and then ensure sufficient water supply. The visual impression is confirmed by the analysis results of the digital imagery. Both species display substantial differences between the treatment groups and the reference group (Fig. 3).

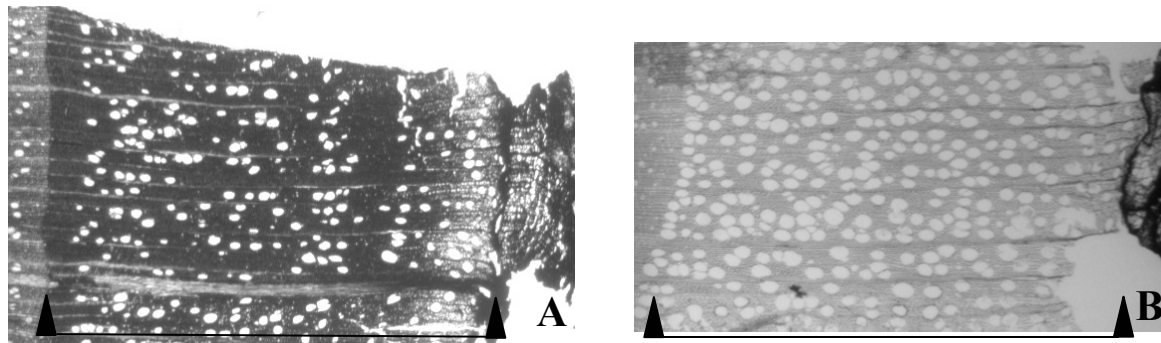


Figure 2: Light microscopy photos of microsections cut from a tilted beech (A) and an untreated reference tree (B) at site Krattigen; tree-ring width indicated by lines between arrows (mag.: 25x)

In alder, the largest percentage of cell-wall material are found in groups T1 and T9 in contrast to the smallest values in groups T2 and T6 and in the reference group. In beech, groups T1 and T7 exhibit the largest cell wall area percentages while the reference group and T3 have the smallest values. This shows that generally the treatments were successful in inducing tension wood in both species and that the quality of the tension wood varied between the groups due to the special treatments, e.g., cutting off the apex or partial removal of the cambium. The data reveal a differentiation into tension wood classes caused by the different treatments. Severe mechanical stress appears to result in more cell wall material, e.g., in groups T1 to T3 of alder the decreasing mechanical stress is paralleled by a diminishing amount of cell wall material. In both species, the more intensive treatments in T1 result in denser tension wood compared to group T3 with less mechanical stress present.

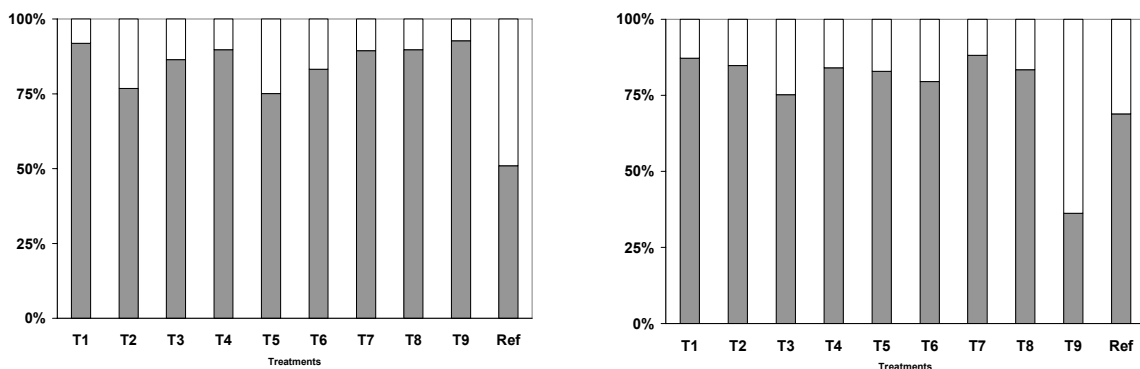


Figure 3: Percentage area covered by cell wall (grey) and cell lumen (white) per treatment (T1-9 & reference group) for alder (left) and beech (right)

The percentage area covered by cell wall material for both species is larger in T7 than in T6. In both treatment groups the trees were bent to 80° from the vertical. However, the difference between both groups is that in T6 bark and cambium were partly removed from the upper part of the stem above the bend while in T7 they were stripped off from the lower side below the bend. This result indicates that the reaction wood induction is controlled more from the upper part of trees because the removed tissue from the upper side probably hindered relatively stronger the flow of hormones and other substances responsible for stimulating the production of tension wood than did the removed tissue from the lower part.

The cell wall percentages of both species in T4 are smaller than in T1 but larger than in T5. This suggests that the intensity of the tension wood formation was weakened considerably in T5 when the apex was cut. In contrast, the apex remaining vertical in group T4 appeared to have less influence on the severity of the tension wood. The result implies that different conditions of an apex during a tree's reaction to mechanical stress can lead to dissimilar types of tension wood comparable to the differentiation in tension wood intensity due to the severity of the mechanical stress found in groups T1 to T3. The finding might also support the above result that tension wood formation is mainly controlled by the upper part of a tree. However, the very low cell wall percentages of beech in group T9 would suggest that the root system might be more important for the control of tension wood formation in beech than it is in Alder. In treatment T9 the root systems of the trees were partly destroyed and hence tension wood control by the roots might have been weakened in beech. The results suggest that the factor cell wall percentage can be used as an indicator of reaction wood intensity. However, attention needs to be paid when trees have not only been tilted or bent but also damaged in which case the intensity of the tension wood is likely to be altered.

Table 2: Analysis of variance (ANOVA) of vessel area for alder and beech

Species	F	P-value	F crit
Alder	18.99924	2.41E-25	1.954952
Beech	10.40234	8.39E-13	1.970619

(If $F > F_{crit}$, then variances between groups are larger than within groups, small P-values indicate high significance of results)

The wood anatomical feature vessel area seems to have been affected by the different treatments as well. The analysis of variance (Tab. 2) shows that the vessel area differs more between than within the treatment and reference groups. This suggests that the treatments were successful in inducing different vessel sizes embedded in changed densities of fibre cell tissue.

For a better comparison of the vessel-area variations between the treatment groups, box-whisker plots were created (Fig. 4). The vessel areas in both species declined significantly in group T1. However, they decreased less when the apex, as one of the main locations for a tree's ability to respond to gravitational forces (Strasburger *et al.* 2002), was cut (T5). This is comparable to the altered percentage area covered by cell wall material in this group shown in figure 3. In both species a progression from small to relatively large vessel areas in groups T1 to T3 is discernible indicating that tension wood can be classified in intensity classes with changed fibre cell and vessel features resulting from mechanical impacts of varying strength. In alder, treatment T6 resulted in significantly smaller vessel areas compared to those measured in T7, but in beech the vessel areas in the two groups do not differ distinctly. This might suggest that in alder both fibre cell and vessel formation are hindered by the removed tissue from above the impact zone while in beech the opposite seems to be true.

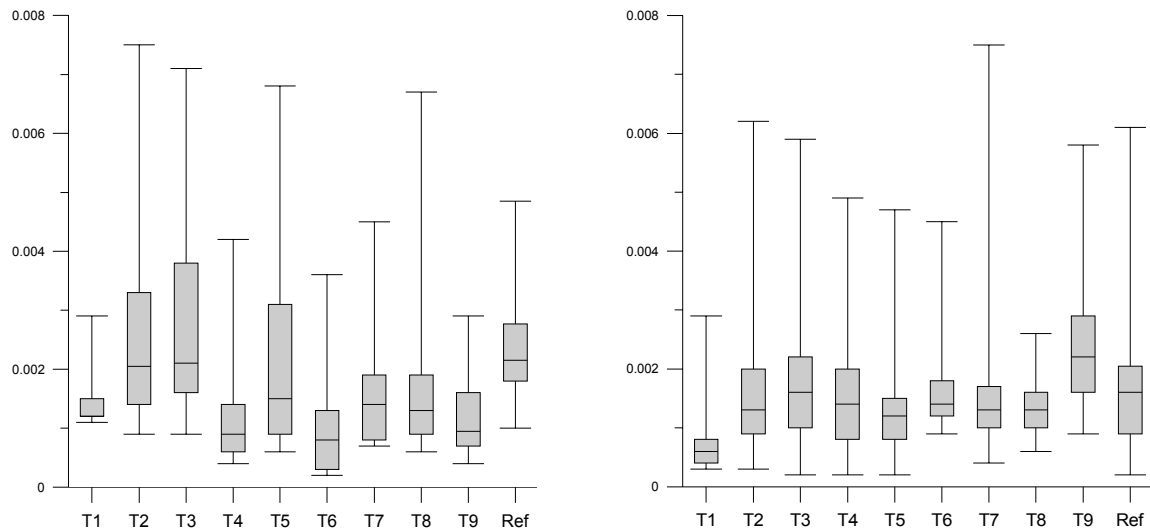


Figure 4: Vessel area per treatment (T1-9 & reference group) for alder (left) and beech (right)

When the root system is partly cut off in beech the species seems to produce less clear reaction wood, i.e., the cell lumen to wall ratio and the vessel area decrease less than in normal tension wood. However, before more reliable conclusions can be drawn all samples of the experiment need to be analysed.

Acknowledgements

The authors would like to express their gratitude to the local foresters Urs Andenmatten, Leo Jörger, Beat Zurbuchen and Jacques Galley for their help with the site selection and the sample collection. We are very grateful to Britta Eilmann, Jacqueline Bolli, Clarissa Zurwerra (Swiss Federal Institute for Forest, Snow and Landscape Research, WSL), Stefan Winter (Geography, University of Fribourg) and Raphael Holland (Geography, University of Bonn) for their help with the sample collection and preparation.

References

- Forster, T., Schweingruber, F.H., Denneler, B. (2000): Increment puncher: A tool for extracting small core of wood and bark from living trees. *IAWA Journal* 21: 169-180.
- Gärtner, H., Heinrich, I., Monbaron, M. (in prep.): Compression wood in two alpine tree species caused by different treatments – A validation of common features used for dating in dendrogeomorphology.
- Mariaux, A. (1967): Les cernes dans les bois tropicaux Africains nature et périodicité. *Revue Bois et Forêts des Tropiques* 114: 23-37.
- Strasburger, E., Sitte, P., Weiler, E. W., Kadereit, J. W., Bresinsky, A., Körner, C. (2002): Lehrbuch der Botanik für Hochschulen. Heidelberg, Berlin, Spektrum Akademischer Verlag, 1123 p.
- Wolter, K.E. (1968): A new method for marking xylem growth. *Forest Science* 14: 102-104.

Higher nutrient-levels in tree rings of *Eucalyptus grandis* following a wildfire

I. Heinrich

Department of Geosciences, Geography, University of Fribourg, 1700 Fribourg, Switzerland

Email: ingo.heinrich@unifr.ch

Introduction

Wet sclerophyll forest describes a narrow band of vegetation which, in northeast Queensland, occurs on the western edge of the rainforest above 600m. These forests grow in areas of high rainfall where rainforest would normally proliferate but the use of fire prevents the rainforest from invading. Scientists have documented a 50% loss of this forest type during the previous 50 years and many are worried that a complete take-over by rainforest could lead to the extinction of certain plant and animal species. With new evidence that rainforests are invading the wet sclerophyll forests at an alarming rate, scientists are assessing the impact of rainforest invasion on the wet sclerophyll flora and fauna.

The wet sclerophyll forest (WSF) of Far North Queensland describes a narrow band of vegetation stretching as a long narrow band on the northern tablelands 50 km inland parallel to the coast between Townsville and Cooktown adjacent to the western margin of the upland tropical rainforests above 600 m (Tracey and Webb 1975, Tracey 1982, Harrington and Sanderson 1994). These forests grow in areas of high rainfall where rainforest would normally proliferate but the use of fire by aboriginal people has prevented the rainforest from invading. Approximately 50% loss of this forest type during the previous 50 years have been documented (Harrington et al. 2000) which is of major concern to the local management authorities as the WSF has been part of the UNESCO World Heritage property Wet Tropics of Queensland since 1988. The cessation of aboriginal burning practices and an increase of non-aboriginal land use by the end of the 19th century paved the way for the invasion of rainforest into the WSF (Fautz 1984, Kohen 1995). Fire is also a vital part of the tall sclerophyll forests in the southern subtropical to temperate climate zones of Australia, which are in many aspects similar to the tropical WSF (Ashton and Martin 1996a, 1996b). Chambers and Attiwill (1994) ascribed the ash-bed effect in *Eucalyptus regnans* F. Muell. forests mainly to an increase in the availability of nitrogen and phosphorus.

Eucalypts, the dominant species in the WSF, possess a mobile sapwood pool, whereby nutrients are added through nutrient uptake and subsequently drawn on to maintain growth. At the sapwood-heartwood boundary nutrients are re-translocated into the living cells. In this way, nutrients, which would otherwise soon become a limiting growth factor, are recycled. This seems to be one of the main reasons for the adaptation of eucalypts to poor soils (Banks 1982). According to this concept of eucalypts adapted to growing on nutrient-poor soils, trees experiencing a post-fire ash-bed effect would not only exhibit a

higher nutrient level in the tree ring after the fire but in the whole sapwood usually consisting of several tree rings. More nutrients become available, and for a period of time when more nutrients are present the tree would not re-translocate nutrients as effectively as without the ash-bed effect and as a consequence an unusually high level of nutrients would remain in the dead cells of the most recently built heartwood ring. Thus the ash-bed effect, according to this “sapwood displacement effect” (Banks 1982), would not be detected in the tree ring directly formed in the year after the fire but in the heartwood cells created at that time. The extent of the displacement depends on the number of sapwood tree rings, which vary within and between species.

In his PhD thesis, Banks (1982) showed an increased ring width following a fire, and that this growth flush lasted five or more years in eucalypts. Chemical analysis of nutrient levels in pre- and post-fire tree-rings sometimes resulted in higher levels of some of the nutrients examined. He hypothesised that nutrient uptake associated with the ash-bed effect could be one of the factors involved. It has been demonstrated several times that the ash-bed effect only lasts approximately one year, and the nutrient level returns to pre-fire conditions quickly (Renbuss et al. 1973, Grove et al. 1986, Adams and Attiwill 1991a,b, Ashton and Martin 1996a, Attiwill et al. 1996).

Since fire may be a key factor for the expansion of rainforest into the WSF, Unwin et al. (1985), Stocker and Unwin (1986), Ash (1988), Unwin (1989), Harrington and Sanderson (1994) and Harrington et al. (2000) emphasise the need for more studies on the historical fire regime in that area. Furthermore, effective long-term management of tropical rainforests should always include the nearby sclerophyll forests as part of the whole ecological system (Janzen 1988). Therefore, the current study aimed to test a method useful for identification and dating of past fires by chemically analysing core samples of *Eucalyptus grandis* W. Hill ex Maiden (rose gum) for nutritional elements.

Materials and methods

The study site is located on a northern slope of Mt. Haig, (145° 36' E, 17° 06' N), Atherton Tablelands, altitude 1200m asl. An almost pure stand of *E. grandis* with a shrub-layer consisting of sclerophyll plants and young rainforest-trees had developed adjacent to rainforest (Harrington and Sanderson 1994). A controlled intensive fire burned the site in October 1996 killing the rainforest undergrowth. After the fire, only a grass layer consisting mainly of *Themeda triandra* Forssk., and some tussock sedges, for example *Gahnia aspera* (R.Br.) Spreng. and *Gahnia sieberiana* Kunth developed. Because large parts of the wet tropics in Far North Queensland are listed in the World Heritage cutting trees for cross sections was not an option but only two core samples per tree were extracted from 20 *E. grandis* stems at breast height. All tree size-classes ranging from 20 to 105 cm were included in the collection. The surface of each core was cut with a knife instead of using sand paper creating a smooth surface with visible rings but without contamination from dust particles. The samples were placed on holding devices without gluing them and the rings marked on the holder. The cores were oven-dried at 60°C for five days, cut at the boundary of each ring, ground to <0.2 mm and chemically analysed

for phosphorus (P) and nitrogen (N). Since eleven of the trees sampled did not supply enough ground material only nine *E. grandis* core samples were analysed. The single digestion method of Anderson and Ingram (1989) was used. Nitrogen was determined colorimetrically by the salicylate-hypochlorite method of Baethgen and Alley (1989), and phosphorus by an adaptation of Murphy and Riley's (1967) single solution method (Anderson and Ingram 1989).

Results

The samples exhibited relatively distinct tree rings in the parts formed in recent years. The wood is diffuse to semi ring porous with vessels decreasing in size towards the end of the growing season. In some years a small vessel free zone appears as a dark band within two tree rings probably marking an unusually dry season. Wedging rings and kino veins, large resin ducts caused by stress such as fire and drought, are typical features of this species. While wedging rings often hindered the identification of annual rings, kino veins were used as markers to identify event years and hence occasionally helped during the visual crossdating procedure.

Table 1: Nitrogen- and Phosphorus-levels in tree rings of E. grandis formed before (1996) and after the fire (1997)

Tree No	Size dbh	N ($\mu\text{g/g}$)		P ($\mu\text{g/g}$)	
		1996	1997	1996	1997
1	80cm	714.7	802.8	19.5	21.6
2	25cm	1045	1636	30.1	52
3	30cm	847	2184	19.7	40.5
4	50cm	1033.1	2932.2	50.6	79
5	100cm	567.7	1576.2	30	73.6
6	25cm	401.9	1272.2	40.4	42
7	60cm	797.4	915.2	25.3	47
8	30cm	647.6	726.5	23.7	31.3
9	40cm	622.6	980.3	21	22

Only the tree rings before and after the fire event located within the sapwood were analysed because their boundaries were most distinct in these outer parts of the samples. In table 1 the results of the chemical analysis are presented. For each tree nitrogen (N) and phosphorus (P) concentrations are presented for the year before and after the fire. All trees show an increase in both, N and P levels in the 1997 tree ring, the year after the fire with some trees exhibiting a near threefold increase in N (trees 3, 4, 5 and 6) but less distinct for the P-levels. No specific trends regarding age and size of the trees are recognisable.

Discussion and conclusions

As noticed in other studies (Bamber et al. 1969, Mucha 1979, Banks 1982, Brookhouse 1997, Smith 1997) the usage of disc samples is desirable when tree-ring analysis of Eucalypts is conducted. This was confirmed in this study with core samples unable to pick up false rings due to wedging ring patterns. However, these features can be detected in disc samples and then avoided by choosing the most appropriate radii. For the current study this problem was circumvented by examining only the most recent rings but for further investigations of longer periods cross sections are indispensable.

The results indicate that *E. grandis* has experienced an ash-bed effect directly after an intense fire. In the years before the 1996 fire a dense understorey consisting of sclerophyll and rainforest species had developed on the relatively fertile Mt Haig study site. Under those circumstances there would be an increase in soil fertility due to an increase in nitrogen fixing understorey plants, a change of the litterfall composition, a wetter micro-climate and a higher decomposition rate (O'Connell et al. 1981). Under the exclusion of fire the invasion of rainforest species into the site, according to Webb (1969), would also be an indication of the increased fertility of the soil.

Negi and Sharma (1996) have proposed two different eucalypt "ideotypes" regarding the efficiency of the re-translocation mechanism depending on the soil conditions. On fertile soils eucalypt species only partially re-translocate while on poor soils they possess a more efficient re-translocation mechanism. A similar suggestion comes from Keith (1997) who found a subgeneric difference in adaptation to soil nutrient concentrations and nutrient utilization. The two scenarios have been illustrated in figure 1. In one case there would be an opulent ash-bed uptake of nutrients on more fertile soils with a consequent waste of nutrients being not re-translocated from dying tissue such as old leaves and at the heartwood-sapwood boundary resulting in a reduced re-translocation of the nutrients from the heartwood to sapwood (Fig. 1, bottom).

In contrast, the other ideotype would occur on poor soils when the level of nutrients stored in the sapwood was not as high as in the first case. Those trees would not waste any nutrients but re-translocate most of them to ensure ongoing growth and survival in the harsh Australian environment (Fig. 1, top). Mulligan and Sands (1988) found that species adapted to low-nutrient soils had slower growth rates and stored as many nutrients as possible to enable longer survival on experimental soils with extremely low nutrient supplies.

The results presented here suggest that *E. grandis* at Mt. Haig, one of the fastest growing tropical Eucalypt species usually occurring on more fertile soils belongs to the bottom group in figure 1 because the nutrient levels in the tree-rings are higher in the year directly after the fire. It seems to have only a restricted ability to adapt to low nutrient supply or lost it gradually by adapting to more humid and fertile conditions. If *E. grandis* belonged to the ideotype growing on poor soils, one would expect little to no change of nutrient levels in the tree ring after the fire event.

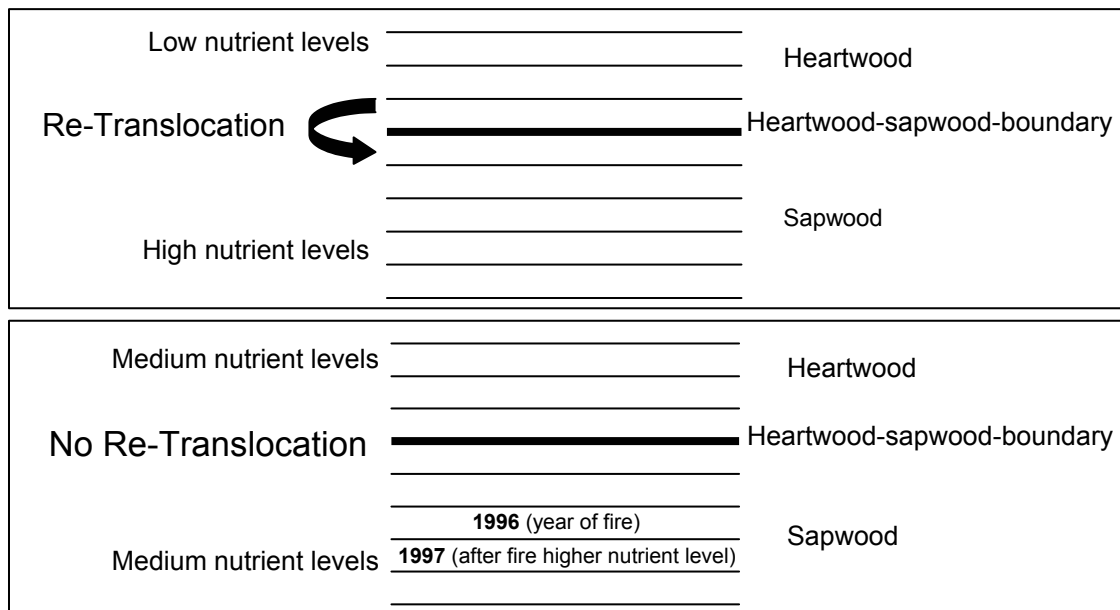


Figure 1. Diagram of the two potential types of nutrient distribution in eucalypts on a poor (top) and fertile soil (bottom)

Although this study was not able to fully examine the nutrient-level changes in the sapwood and heartwood of *E. grandis* it has indicated that on sites with soil types rich in nutrients, as is often the case in the ecotone wet sclerophyll forest between dry sclerophyll forests and rainforests, trees might not need to re-translocate the otherwise vital nutrients as strictly as on poor nutrient soil types. Dendropyrochronological ring studies have the potential to further investigate the fire regime of the wet sclerophyll forests of Far North Queensland where fire has always been a contentious point.

Although the dendrochronological part of the study has encountered similar problems (wedging and false rings) to those in Hickey et al. (1999) the construction of an approximate annual record of historical fire occurrences comparable to the results in Burrows et al. (1995) seems feasible. Future studies should also concentrate on sites with a known fire event in the more distant past to investigate whether the after-fire nutrient flush is also discernible in the heartwood. Furthermore, it is recommended to apply this method to other sites further south with a pronounced seasonal climate ensuring more reliable annual tree rings. Four instead of only two core samples per tree should be taken to obtain enough ground material for the chemical analysis. If possible, whole disc samples of the site should be used to ensure higher reliability during crossdating. Finally, it is recommended to expand the analysis of nutrients to other elements, e.g., potassium and magnesium.

Acknowledgments

Technical support came from Steve Turton, Department of Tropical Environment Studies and Geography, James Cook University, Cairns Campus, Laurence May, Department of Natural Resources, Atherton and the Department of Geography, University of Bonn. The chemical analysis was carried out by Robert Congdon, School of Tropical Biology, James

Cook University, Townsville. I would also like to thank Graham Harrington, Keith (Sandy) Sanderson and Matt Bradford, CSIRO Tropical Forest Research Centre, Atherton for their help. This research was funded by the German Academic Exchange Service (DAAD) Bonn.

References

- Adams, M.A., Attiwill, P.M. (1991a): Nutrient balance in forests of northern Tasmania. I. Atmospheric inputs and within stand cycles. *Forest Ecology Management* 44: 93-113.
- Adams, M.A., Attiwill, P.M. (1991b): Nutrient balance in forests of northern Tasmania. II. Alteration of nutrient availability and soil water chemistry as a result of logging, slash-burning and fertilizer application. *Forest Ecology Management* 44: 115-131.
- Anderson, S.E., Ingram, J.S.I. (1989): Tropical Soil Biology and Fertility: A Handbook of Methods. C.A.B. International, Aberystwyth.
- Ash, J. (1988): The location and stability of rainforest boundaries in north-eastern Queensland, Australia. *Journal of Biogeography* 15: 619-630.
- Ashton, D.H., Martin, D.G. (1996a): Changes in a spar-stage ecotonal forest of *Eucalyptus regnans*, *Eucalyptus obliqua* and *Eucalyptus cypellocarpa* following wildfire on the Hume Range in November 1982. *Australian Forestry* 59: 32-41.
- Ashton, D.H., Martin, D.G. (1996b): Regeneration in a pole-stage forest of *Eucalyptus regnans* subjected to different fire intensities in 1982. *Australian Journal of Botany* 44: 393-410.
- Attiwill, P.M., Polglase, P.J., Weston, C.J., Adams, M.A. (1996): Nutrient cycling in forests of south-eastern Australia. In: Attiwill, P.M., Adams, M.A. (Eds), Nutrition of Eucalypts, Collingwood: 191-227.
- Baethgen, W.E., Alley, M.M. (1989): A manual colorimetric procedure for measuring ammonium nitrogen in soil and plant Kjeldahl digests. *Communications in Soil Science and Plant Analysis* 20: 961-969.
- Bamber, R.K., Floyd, A.G., Humphreys, F.R. (1969): Wood properties of flooded gum. *Australian Forestry* 33: 3-12.
- Banks, J.C.G. (1982): The use of dendrochronology in the interpretation of the dynamics of the Snow Gum Forest. Unpublished PhD-Thesis, Australian National University, Canberra.
- Brookhouse, M.T. (1997): Identification and analysis of growth rings in *Eucalyptus obliqua* L'Hérit and *Eucalyptus cypellocarpa* L. Johnson. Unpublished Honours Thesis. Australian National University, Canberra.
- Burrows, N.D., Ward, B., Robinson, A.D. (1995): Jarrah forest fire history from stem analysis and anthropological evidence. *Australian Forestry* 58: 7-16.
- Chambers, D.P., Attiwill, P.M. (1994): The ash-bed effect in *Eucalyptus regnans* forest: chemical, physical and microbiological changes in soil after heating or partial sterilisation. *Australian Journal of Botany* 42: 739-749.
- Fautz, B. (1984): Agrarlandschaften in Queensland. *Geographische Zeitschrift* 65. Beilage. Wiesbaden.

- Florence, R.G. (1981): The biology of the eucalypt forest. In Pate, J.S., McComb, A.J. (Eds), *The Biology of Australian Plants*, University of Western Australia Press, Nedlands, 147-180.
- Florence, R.G. (1982): The Australian Forests. In Jahn, G. (Ed), *Handbook of Vegetation Science*, Dr W Junk, The Hague, pp. 73-95.
- Grove, T.S., O`Connell, A.M., Dimmock, G.M. (1986): Nutrient changes in surface soils after an intense fire in jarrah (*Eucalyptus marginata* Donn ex Sm.) forest. *Australian Journal of Ecology* 11: 303-317.
- Harrington, G.N., Sanderson, K.D. (1994): Recent contraction of wet sclerophyll forest in the wet tropics of Queensland due to invasion by rainforest. *Pacific Conservation Biology* 1: 319-327.
- Harrington, G.N., Thomas, M.R., Bradford, M.G., Sanderson, K.D., Irvine, A.K. (2000): Structure and plant species dominance in North Queensland wet sclerophyll forests. *Proceedings of the Royal Society of Queensland* 109: 59-74.
- Hickey, J.E., Su, W., Rowe, P., Brown, M.J., Edwards, L. (1999): Fire history of the tall wet eucalypt forests of the Warra ecological research site, Tasmania. *Australian Forestry* 62: 66-71.
- Janzen, D.J. (1988): Tropical dry forests: The most endangered major tropical ecosystem. In Wilson, E.O. (Ed), *Biodiversity*, Washington DC: 130-138.
- Keith, H. (1997): Eucalypts: an introduction. In Williams, J.E., Woinarski, J.C.Z. (Eds), *Eucalypt ecology – Individuals to ecosystems*, Cambridge University Press, Cambridge: 1-15.
- Kohen, J.L. (1995): *Aboriginal environmental impacts*. Sydney.
- Mucha, S.B. (1979): Estimation of tree ages from growth rings of eucalypts in northern Australia. *Australian Forestry* 42: 13-16.
- Mulligan, D.R., Sands, R. (1988): Dry matter, phosphorus and nitrogen partitioning in three *Eucalyptus* species grown under a nutrient deficit. *New Phytologist* 109: 21-28.
- Murphy, J., Riley, J.P. (1967): A modified single solution method for the determination of phosphate in natural waters. *Analytica Chimica Acta* 27: 31-36.
- Negi, J.D.S., Sharma, S.C. (1996): Mineral nutrition and resource conservation in Eucalyptus plantations and other forest covers in India. In Attiwill, P.M., Adams, M.A. (Eds), *Nutrition of Eucalypts*, Collingwood: 399-325.
- O`Connell, A.M., Grove, T.S., Lamb, D. (1981): The influence of fire on the nutrition of Australian forests. *Proceedings of the Australian Forest Nutrition Workshop productivity in perpetuity*. CSIRO, Melbourne, 277-289.
- Renbuss, M.A., Chilvers, G.A., Pryor, L.D. (1973): Microbiology of an ashbed. *Proceedings of the Linnean Society of N.S.W.* 97: 302-311.
- Smith, D. (1997): The relationship between ring-width and precipitation in subalpine *Eucalyptus pauciflora*. Unpublished Honours Thesis. Australian National University, Canberra.
- Stocker, G.C., Unwin, G.L. (1986): Fire. In Clifford, H.T., Specht, R.L. (Eds), *Tropical plant communities*, St. Lucia: 91-103.

- Tracey, J.G. (1982): The humid tropical region of North Queensland. CSIRO, Melbourne.
- Tracey, J.G., Webb, L.J. (1975): Vegetation of the humid tropical region of North Queensland. (15 maps at 1:100,000 scale + key.) CSIRO Aust. Long Pocket Labs: Indooroopilly, QLD.
- Unwin, G.L. (1989): Structure and composition of the abrupt rainforest boundary in the Herberton Highland, North Queensland. *Australian Journal Botany* 37: 413-428.
- Unwin, G.L., Stocker, G.C., Sanderson, K.D. (1985): Fire and the forest ecotone in the Herberton highland, north Queensland. *Proceedings of the Ecological Society of Australia* 13: 215-224.
- Webb, L.J. (1969): Edaphic differentiation of some forest types in eastern Australia. II. Soil chemical factors. *Journal of Ecology* 57: 817-830.

LIST OF PARTICIPANTS

Marc Abrams Email: agl@psu.edu	Penn State University	USA
Raphaël Bailly Email: rbailly@nancy.inra.fr	INRA EFPA	France
Annette Bär Email: annette_baer@web.de	University of Oldenburg	Germany
Timothée Barrelet Email: timothee.barrelet@dcb.unibe.ch	University of Bern	Switzerland
Warren Bentley Email: w.bentley@boltblue.com	University of Cambridge	UK
Marco Bezzi Email: marco.bezzi@ing.unitn.it	University of Trento	Italy
Joachim Block Email: jblock@geographie.uni-erlangen.de	University of Erlangen-Nürnberg	Germany
Michelle Bollschweiler Email: michelle.bollschweiler@unifr.ch	University of Fribourg	Switzerland
Achim Bräuning Email: achim.braeuning@geographie.uni-stuttgart.de	University of Stuttgart	Germany
Matthew Brookhouse Email: matthew.brookhouse@anu.edu.au	Australian National University	Australia
Sarah Brugger Email: brugger_sarah@hotmail.com	University of Zürich	Switzerland
Ulf Büntgen Email: buentgen@wsl.ch	WSL	Switzerland
Iris Burchardt Email: iris.burchardt@geographie.uni-stuttgart.de	University of Stuttgart	Germany
Filipe Campelo Email: fcampelo@ci.uc.pt	Universidade de Coimbra	Portugal
Adriana Carnelli Email: adriana.carnelli@epfl.ch	EPFL ECOS-ENAC	Switzerland
Alejandro Casteller Email: casteller@slf.ch	SLF	Switzerland
Anna Cedro Email: abcania@univ.szczecin.pl	Szczecin	Poland
Nadezda Devi Email: nadya@ipae.uran.ru	Russian Academy of Sciences	Russia
Linan Isabel Dorado Email: isabel.dorado@ua.es	Universidad de Alicante	Spain
Sébastien Durost Email: sebastiendurost@yahoo.com	CNRS	France
Britta Eilmann Email: britta.eilmann@wsl.ch	WSL	Germany

Jan Esper	WSL	Switzerland
Email: esper@wsl.ch		
Marc Filot	University of Bern	Switzerland
Email: filot@climate.unibe.ch		
Patrick Fonti	WSL	Switzerland
Email: patrick.fonti@wsl.ch		
Anthony Fowler	The University of Auckland	New Zealand
Email: a.fowler@auckland.ac.nz		
David Frank	WSL	Switzerland
Email: david.frank@wsl.ch		
Dagmar Friedrichs	University of Bonn	Germany
Email: dagmarfriedrichs@gmx.de		
Holger Gärtner	WSL	Switzerland
Email: gaertner@wsl.ch		
Edward Graham	University of Fribourg	Switzerland
Email: edward.graham@unifr.ch		
Jussi Grießinger	Research Centre Jülich	Germany
Email: j.griessinger@fz-juelich.de		
Marina Gurskaya	Institut of Plant and Animal ecology	Russia
Email: mgurskaya@yandex.ru		
Ingo Heinrich	University of Fribourg	Switzerland
Email: ingo.heinrich@unifr.ch		
Gerhard Helle	Research Centre Jülich	Germany
Email: g.helle@fz-juelich.de		
Erica Hendy	LDEO	USA
Email: ejhendy@ldeo.columbia.edu		
Angela Heule	University of Fribourg	Switzerland
Email: angela.heule@unifr.ch		
Oliver Hitz	University of Fribourg	Switzerland
Email: oliver.hitz2@unifr.ch		
Anna-Sofia Hug	University of Zürich	Switzerland
Email: annasofia@bluewin.ch		
Esther Jansma	University of Amsterdam	Netherland
Email: e.jansma@archis.nl		
Dominik Jungo	University of Fribourg	Switzerland
Email: dominik.jungo@unifr.ch		
Ryszard Jerzy Kaczka	University of Silesia	Poland
Email: kaczka@wnoz.us.edu.pl		
Hans-Peter Kahle	University of Freiburg	Germany
Email: Hans-Peter.Kahle@iww.uni-freiburg.de		
Klaus Felix Kaiser	WSL	Switzerland
Email: klaus.kaiser@wsl.ch		
Tiina Knoll	University of Tartu	Estonia
Email: tiinakn@ut.ee		
Brigitte Koffi	University of Fribourg	Switzerland
Email: brigitte.koffi@bluewin.ch		

Iryna Koval Email: koval@uriffm.org.ua	URIFFM	Ukraine
Georges Lambert Email: joellamb@club-internet.fr	CNRS	France
Astrid Leutwiler Email: astrid.leutwiler@unifr.ch	University of Fribourg	Switzerland
Ireneusz Malik Email: irekgeo@wp.pl	University of Silesia	Poland
Marcin Matyja Email: marmat80@go2.pl	University of Silesia	Poland
Michel Monbaron Email: michel.monbaron@unifr.ch	University of Fribourg	Switzerland
Burkhard Neuwirth Email: b.neuwirth@giub.uni-bonn.de	University of Bonn	Germany
Darko Ogrin Email: darko.ogrin@ff.uni-lj.si	Faculty of Arts	Slovenia
Sebastian Osenstetter Email: sebastian.osenstetter@stud.uni-regensburg.de	University Regensburg	Germany
Momchil Panayotov Email: mp2@abv.bg	University of Forestry	Bulgaria
Manuela Pelfini Email: manuela.pelfini@unimi.it	University of Milan	Italy
Octavi Planells Email: octaviplanells@ub.edu	University of Barcelona	Spain
Erhard Pressler Email: info@pressler-partner.de	Pressler GmbH	Germany
Andreas Rigling Email: andreas.rigling@wsl.ch@wsl.ch	WSL	Switzerland
Ole Rössler Email: o.roessler@giub.uni-bonn.de	University of Bonn	Germany
Vahid Reza Safdari Email: vahidsaf@hotmail.com	University of Teheran	Iran
Ingo Sahling Email: ingo.sahling@geo.uni-halle.de	Martin-Luther-Universität	Germany
Maurizio Santilli Email: maurizio.santilli@unimi.it	University of Milan	Italy
Gerhard Schleser Email: g.schleser@fz-juelich.de	Research Centre Jülich	Germany
Nele Schmitz Email: nschmitz@vub.ac.be	Vrije Universiteit	Belgium
Fritz Schweingruber Email: schweingruber@wsl.ch	WSL	Switzerland
Olga Sidorova Email: ovsidorova@forest.akadem.ru	Institute of Forestry	Russia

Michael Sigl Email: siglmich@yahoo.de	University Regensburg	Germany
Heinrich Spiecker Email: instww@uni-freiburg.de	University of Freiburg	Germany
Mike Staudinger Email: Mike.Staudinger@gmx.net	Regensburg University	Germany
Markus Stoffel Email: markus.stoffel@unifr.ch	University of Fribourg	Switzerland
Horst Strunk Email: horst.strunk@geographie.uni-regensburg.de	Regensburg University	Germany
Uwe Treter Email: utreter@geographie.uni-erlangen.de	University of Erlangen-Nürnberg	Germany
Kerstin Treydte Email: kerstin.treydte@wsl.ch	WSL	Switzerland
Anouk Verheyden Email: anouk.verheyden@africamuseum.be	Royal Museum for Central Africa	Belgium
Anne Verstege Email: a.verstege@uni-bonn.de	WSL	Switzerland
Ronald Visser Email: rm.visser@lycos.nl	Vrije Universiteit Amsterdam	Netherlands
Ralf Wagner Email: ralf.wagner@ufz.de	Environmental Research Centre	Germany
Gabrielle Weber Email: gweber@netwings.ch	WSL	Switzerland
Pascale Weber Email: pascale.weber@wsl.ch	WSL	Switzerland
Kathrin Weidner Email: kathrin_weidner@freenet.de	University of Bonn	Germany
Anny Weitner Email: weitner@nancy.inra.fr	INRA EFPA	France
Susanne Widmer Email: susanne.widmer@unifr.ch	University of Fribourg	Switzerland
Nikolay Zafirov Email: niki_zafirov@yahoo.com	University of Forestry	Bulgaria

SPONSORS

Credit Suisse
Avenue de la Gare 13
1700 Fribourg
Tel: 026 350 98 11
Fax: 026 350 94 99
<https://entry.credit-suisse.ch/csfs/p/rb/en/index.jsp>



REGENT INSTRUMENTS INC.
2672, Chemin Sainte-Foy
Ste-Foy, QC, G1V 1V4
Canada
<http://www.regentinstruments.com/>



Interprofession du Gruyère
Case Postale 12
1663 Gruyère – Pringy
Tel: 026 921 84 10
Fax: 026 921 84 11
<http://www.gruyere.com/>



KGV
Reichengasse 27
1702 Freiburg
Tel: 026 305 21 21
Fax: 026 305 21 46
<http://www.fr.ch/ecab/de/>



Banque Raiffeisen de Marly
Route du Chevalier 3
1723 Marly 1
Tel: 026 439 94 40
Fax: 026 439 94 41
<http://www.raiffeisen.ch>